学位論文

New Insights on Organic Reactions Explored in Water

（水中における有機反応の新展開）

平成 26 年 12 月博士(理学)申請

東京大学大学院理学系研究科

化学専攻

北之園　拓

Abstract

論文題目　New Insights on Organic Reactions Explored in Water

(水中における有機反応の新展開)

氏名　北之園　拓

　　　本論文は、地球上に遍在し、生命を育んできた「水」を反応溶媒とする有機化学を展開し、「水」にしかない特性を化学合成に組み込み、活用していく意義を実証する事を主たる目的とする。触媒的な不斉分子変換に於いて溶媒量の「水」が極めて巧緻で効果的に機能している例は、本論文中に多数抄録されている。有機溶媒中で涵養されてきた従来の有機化学では説明できない、未知の反応性や選択性を秘めた未曾有の化学変換を開発していく上で、「水」の活用は枢軸たり得る選択肢である。本論文が究極的には、「水」を積極的に化学変換に活用する為の新概念、次世代型有機合成を拓く事に繋がると考えている。

　　　第零章では、第一章から第六章までに抄録された数々の知見を理解すべく、「水」を中心として有機化学との関わりを歴史的に俯瞰している。その中で本論文中に抄録されている知見を基に、Sharpless の定義した"on-water" catalysis 及び乱立している機構モデルに対する徹底的な検証を行い、現状では"on-water" catalysis が極めて限定的な事象であることから溶媒量の「水」が何らかの形で関与し得る触媒作用に対する新表現創出の必要性に言及した。また、提唱されている機構モデルに対してもそれぞれの問題点を指摘し、より広く適用可能なモデル提唱を行った。

　　　第一章では、水系溶媒中で機能を発現する金属種、不斉配位子、添加剤より構成される 3 種の触媒系を使い分ける事によって、触媒的不斉向山アルドール反応に於いてこれまでになく幅広い基質一般性を実現した。1973 年の金字塔的発見以来、より温和な反応条件、広い基質寛容性を有する一種の"決定的"な触媒的アルドール反応の開発に多くの化学者が情熱を注いできたものの、従来の反応条件は厳密な無水条件や極低温を必要とする外、触媒系の多くは基質官能基の性質に影響され易い特性があった。開発に成功した反応系では、「水」は想定される触媒サイクルに於いて重要な役割を担っている。第一に、金属イオンの第一配位圏が置換活性となる事による Lewis 酸性の向上と反応加速効果。第二に、水分子の配位による脱シリル化促進によるアルドール体の直截変換と結果的な触媒回転の上昇。第三に、エントロピーを駆動力とする凝集効果による rigid な遷移状態の安定化。従来法と比較して、本手法は高い触媒活性、実験手順の簡便さ、広範な基質適用性の観点で優れている。各種分光学的測定によって金属周りの配位環境や添加剤の役割に関する知見を得ている。

　　　第二章では、それぞれ別個に機能している複雑系を単一構造中に効果的に組み込む事でより効果的な触媒作用が得られるとの仮定の下、最も単純な金属依存性アルドラーゼとも言うべき触媒系の完全な人工設計を行った。天然酵素の触媒活性を凌駕せんとする試みとして、タンパク質の人工改変、触媒抗体、ホスト分子を利用した"chemozymes"が一般的である。しかしながら、依然として活性部位の基本構造は天然酵素と大きく違わず、巨大な分子量やそれ故の構造改変の困難さ、苛酷な反応条件が必要とされる場合も多かった。上述の概念に基づいて合成した光学活性配位子は Sc^{3+} イオンを取り込んで水中で自己組織化し、目的の直截的アルドール反応を効率的に触媒した。集約されていない独立系と比較して、顕著な反応加速と熱的変化に強い不斉場の構築が確認された。これらの特性は必要最低限機能の適正な立体配置によって初めて発現するものであり、酵素様人工触媒の設計に於ける有益な指針になり得ると期待している。

　　　第三章では、酸化数の異なる銅触媒を用いた不斉ホウ素共役付加反応に関する知見を纏めた。アルケンに対するホウ素付加反応は、有機溶媒中、強塩基存在下に系中発生させる borylcopper(I)種を基盤として発展してきており、銅(I)を基調とする多くの(不斉)触媒系が報告されてきた。一方で銅(II)は銅(I)とは化学

的性質が大きく異なり、銅(II)を基調とする本格的な不斉触媒設計はなかった。銅(I)と較べて銅(II)は水中で安定であるのみならず、Lewis 酸性の観点から想定される O-エノラートを経由する機構により基質一般性を拡張できる可能性、四角錐型構造を基調とした柔軟な触媒設計が可能な事など、多くの利点がある。また、水中での効果的なプロトン化、第一配位圏の制御など「水」を溶媒として用いる利点と組み合わせる事で斬新な合成法の確立が期待された。検討の結果、不均一系触媒の $Cu(OH)_2$ と均一系触媒の $Cu(OAc)_2$ が、α,β-不飽和カルボニル化合物及びニトリルに対する不斉共役付加反応に対して幅広い基質適用性等の優れた触媒作用を示すことが見出された。「水」以外の溶媒は、たとえ水を含む混合溶媒系であったとしても、反応性と選択性両面に於いて機能しない。また、それぞれの触媒系は環状ジエノンを用いた反応系にて異なる位置選択性を与えるという興味深い知見も得られた。銅(II)を基調とする触媒系に続いて銅(0)触媒も適切な不斉配位子との組み合わせによって光学活性ホウ素付加化合物を与えた。すなわち、銅(0)、銅(I)、銅(II)孰れも不斉ホウ素共役付加反応に対する触媒活性を示すものの、反応性、選択性、基質適用性等は顕著に異なり、別々の反応機構で進んでいる事は明白である。

　　　　第四章では、溶媒量の「水」が綯う水素結合網を介した組織化されたプロトン移動に焦点を当て、プロトン付加段階での立体制御を試みた。最小単位であるプロトンの付加に対して立体制御を行うことは合成化学上、非常に挑戦的であるものの、アトムエコノミー等の観点から強く望まれる反応形式である。複数の触媒系を用いた実験結果を纏めており、本分野に於いて深遠なる洞察を与えるものである。

　　　　第五章では、第四章で得られた知見を拡張し、同位体による異性体合成に焦点を当てた。異なる同位体の存在がキラリティーを作っている鏡像異性体は、その僅かな違いにも拘わらず様々な特性を示す事から立体化学や生化学の分野に於いて極めて重要である。更に構造中の特定水素原子を重水素化した重薬に対して近年関心が高まっており、薬理活性構造の特定部位に重水素を導入する需要も高まっている。特に最小元素である水素の場合、多置換オレフィンに対するプロトン化や重水素化によって水素同位体不斉中心を構築する事は困難であり、構築法としては基本的にアルデヒドに対する不斉還元に依存するしかなかった。酵素の完璧な選択性を利用して不斉構築を伴う重水素導入法も知られているが、生成物の構造にはかなりの制約があった。確立した手法では、重水中、室温下という簡便なものであり、多分野での応用が期待される。

　　　　第六章では、水中で発現する触媒作用を更に改良する為の新規概念を提唱した。単独では触媒活性を示さない、若しくは副反応を優先的に触媒してしまう触媒系に望みの活性を付与する方法として、ナノ粒子化、二元金属(bimetallic)系、光照射(光触媒系)等があるものの、多くの場合、触媒設計の自由度や耐久性、汎用性、不斉反応への応用性に難があった。そこで高次構造物を足場として、金属を中心とする明確な反応場を構築し、凝集を含む金属被毒を防ぐと同時に、足場構造物を通じて金属の電子的性質を改変してしまう事で、未知の反応性を創出することを目指した。実際に、触媒活性の向上は様々な反応系に見られており、収率・選択性両面が劇的に改善された反応系も見出した。本触媒設計概念は、応用性や実用性、環境調和性において抜群に優れており、合成を必要とする様々な分野に強力なインパクトを与える事が期待される。

Contents

Preface

        Dew on the leek, as is often said, resembles the human life in its transitory.   A yearning for immortality has made the first Qin Emperor put all his eggs in one basket in order to procure an elixir of life.[1] Meanwhile, the King Zhaoxiang of Qin had once offered 15 cites to the State of Zhao in exchange for the He Shi Bi, a priceless jade artifact.[2] Thus, human beings have been obsessed with flawlessness down the ages; the deep-pocketed have been lavishing money on, whereas the poor have been sparing no effort to quest the exalted ideals.   No one is without ambitiousness; just in order to conquer so excellent a reputation as to be acclaimed 'being second to none', the courageous will attack the enemy encampment even at the risk of death and the intelligent will devote to becoming absorbed in the secrets through learning.   Merchants will aim at reaching at the zenith of their prosperity, and the lords will aspire to make their righteous government peaceful by reclaiming lands with the dreaming of the Shangri-La.   Likewise, researchers will be in pursuit of the acme of perfection, and yet they have been concurrently haunted with the fear of flawlessness in the recesses of the mind.   It is unrewarding for researchers to have ascended to the summit, where no further improvement can be made.   In general, one's awareness of something stimulates his or her curiosity further more.   The phenomena which remain unknown yet even after accumulation of enough information make us perceive the unenlightenment of human beings.   It is consummate happiness to seek the truth with singleness of mind on such an occasion and explore the field, which is not worth envying even the unequaled prosperity of lords or monarchs for the researchers.   Being usurped such an amusement would amount to the negation of living, incisively precepting that satisfaction should be something taken as a warning.

        For all that, never have I heard the completed knowledge or the undisputed research achievements.   The ruler of the universe will countenance nobody to provide perfect illustration of every phenomenon in the universe.   God enables nobody to be a man of complete virtue.   It has been divine providence that creek sometimes accepts the turbid rainwater, that forest sometimes fosters the poisonous insects or herbs, that gem sometimes contains minute defect and that monarch sometimes falls into contempt.[3] Who, however clever or powerful he is, can defy the rules in the universe?   Never has no nation been invaded by outside forces for thousands of years.   Making things prosper is such a herculean task as soaring into sky.   Although not worrying that the others didn't understand him, Confucius did care about his own incompetence.[4] A perpetually impeccable person would be neither more nor less than a saint.   Emperor Yu is said to have been flawless; for he presented offerings to ancestors and gods, and his diet was simple for that.[4] And he enacted formal dress for the ceremony, and he wore simple dress ordinarily for that.   Additionally he made efforts for irrigation and flood prevention works and he lived in a humble palace for that.   In the meanwhile, Laozi said that "the saint who knows 'the way' admits his faults and corrects them, and then he has no fault".[5] That is to say, researchers can be engrossed as they like, on the assumption that we will never reach the summit where we no longer has much scope left to improve.

        However, born in the progressive age, we believe even implicitly that Science is a panacea for the impossible, an emblem of perfection.   The evolution and transition in scientific technology up to today, even though in just one century, make us realize that we belong to another age. Especially in the era of Meiji in Japan, tradition has it that people were astonished to hear that

steamship can voyage hundreds of miles in one night once it moves.   In these days of ever-progressing science, the spacecraft can shake the ground on the moon and even can collect some tiny specks from a small asteroid as if it were the peregrine falcon.[6] We cannot help but express admiration for the fact that pipe dreams came true in only one century.   The impossible or the unattainable, never-ending quest for the impossible, was traditionally often portrayed as "blue rose" that presents blue pigmentation instead of the more common red, in English literature. Nevertheless, ironically enough, "blue rose" has been created by genetic engineering as a collaborative research by Australia and Japan.[7] In transition and evolution is Science "alive" undoubtedly.   The cutthroat competition for the advances in human intelligence will not afford enough time and composure to us in life of studying.   Science is also the only remedy which can expel gratuitous rumor or superstition.   As has been given "Truth shall make you Free" in the New Testament, researchers should indulge in a thorough investigation into the beauty of Nature and should enlighten the ignorant by ennobling human knowledge and wisdom.   In the era of Edo, Science such as *Wasan* (Japanese mathematics) unaffected by Western studies had been dominated by only an aristocracy, as learning for the sake of scholars.   Then with the enthusiasm for learning Western studies rising like a flood tide in Meiji period, Science has become "public".   Science has been defined as learning to probe into the cause of every phenomenon such as the motion of the planets, changes in the weather, the reason why we feel that fire is hot and ice is cold and the reason why we can boil the rice on fire and so on.[8] To perceive the phenomenon and try to know the principle of that makes human worthy of the name.   Given the universe, there has been a fixed rule in the motion of planets, physiological process of animal and vegetable life and deposition of geological stratum and so on.   What is more, it is a wonder that Nature has never erred in the usage of those rules.   Science can account for the reason why sky looks blue and sun turns red so far. And there exist these kinds of secrets all over the universe.   It is nothing short of true grace to divulge the secrets and lend spices to the secrets and how delectable it is!   Our daily life is constantly indebted to science.   For the transport as one example, we place our main reliance on the power of science; we rely on train when going out, car when coming back, escalator when going up and elevator when going down.   Hence not until the world is lit by the light of intellect, which means demonstrating what hath god wrought, is man freed from the yoke of ignorance.

All in all, truth is but one remove from religious faith.   It is described in "海から帰る日 (Day when we come back from the sea, 1931)", written by Niimi Nankichi, as follows; *My father believes that the striped mullet grows up into the fur seal.   He reiterates that faith whenever the striped mullet is served on a dish.   I explain on each occasion that it is impossible for the fish to grow up into the mammal.   He won't, however, assent to my explanation and says 'it may be theoretically right, but they **do** whatever may betide'.* (translated by T. Kitanosono)   The similar faith had been inserted in "巷街贅説 (Kougai-zeigetsu, 1829)", which describes rumors or ballads spread in Edo City approximately one hundred years before.   In Yin Dynasty, Qi people often talked anxiously about the sky falling down on their heads and lamented heaven, which is often used when rallying a groundless apprehensions.[9] The interpretation of history on Western national policy theory had ever been attributed to the authority of the Pope, resulting in the blind acceptance of the then biblical perspectives such as a geocentric theory.[10] The incomprehensible providence had been ascribed to *what hath God wrought* without exception; entertaining a few doubts had been regarded as a profanation to God, let alone refuting.   Now in the world of scientific expansionism,

unscientific truth was eradicated as the spread of scientific enlightenment.   After Charles Darwin turned up, his evolutionary theory has verified the fact that human beings are nothing but one of the creatures in other scientific fields and has compared skeletons, muscles, viscera, encephala and embryology.   Therefore it is faultless in proving that some belief in Christianity is too arbitrary to argue scientifically.[11] Thus the rampancy of science has made it a panacea.   The explanations disguised to be scientific, whether they are falsehoods or strained interpretations, can go unchallenged and are accepted as indisputable facts.   Explanation is required to be only scientifically clear and broken meter were not permitted.   It is as if the genius endowed by nature was inferior to monkey in fine clothes.   We, children of Science, worship Science with adoration and without suspicion, hastening under the banner of scientific expansionism.   On the steady path of evolution were we involuntarily proponents of the *Myth of Progress*.

On March 11th, 2011 the earth has roared abruptly in the Sanriku distinct and has undulated irregularly.   A ruinous earthquake also struck the University of Tokyo, although very far from hypocenter; the pubic was terrified, and glassware fell down and was inflicted one after another. Not long after, raging billows went upstream, brimmed over and engulfed the land.   A too extensive land was afloat, although hundreds or thousands kilometers away from the original coastline, to discriminate the land from the see.   A tsunami swallowed up all plains and roads in a moment.   Almost all possessions and rice plants were submerged, blood relatives to rely on were lost and the dwellings were floated on the sea.   One stood by unhelpfully as an idle onlooker, another was shaken by the incident and wailed over.   The sight of Kesen-numa in the dark, where the buildings were sunken under the sea and reduced to ashes, has been indelibly etched on my mind.   The rushing tsunami swept the seashore towns and there was something weird irresistibly carried to the sky.   All artifacts such as national oil stockpiling base, power plants, airports and railroads were swept away.   Normal backup cooling apparatus failed after tsunami broke the reactors' connection to the power grid, which lead the reactors to experience a meltdown.   The rampant Nature has smashed the fruit of hundreds of years' knowledge on the human part at one day, and the consequent diffusion of radioactive substances confused the people.   It was uneasy to dare face such a horrible sight and Japan was in imminent peril.   This disaster seemed to be unparalleled in history; whose fierce destruction is beyond our assumption.   None can deny that it will take ten or fifteen years to be restored.

Now, almost four years have passed since those nightmarish dark nights.   Nevertheless, time was mercilessly reluctant to heal grief; to the contrary, the consecutive obituary had devastated to me in the ensuring year.   Two consanguineous souls summoned to Heaven were upright, self-sacrificing, full of benevolence, full of virtues of fortitude and temperance, exemplary and sublime to the bare bones.   They enlightened me about a lot and were always on my side. Although seized by a sense of helplessness, I was unable to take any measures, other than awaiting their death.   We are surrounded by irrationalness.   As Agamedes and Trophonius did, whom the gods love will be often unable to outlive the other.   I was overwhelmingly impressed with what a large attendant is at funeral.   I fully realized that except for family funeral, the human nobility is evaluated posthumously.   That irrationalness was nothing else but despair for me, which is related to my glass roots. — A meditation has been the unequaled rejoicing for me since my childhood. Such euphoria is beyond description when immersed in my own world, which is alienated from the lapse of time and where I often have a flash of inspiration like a bolt out of the blue.   There had I

thought of abstruse mathematical problems, social landscape, philosophical problems and historical phenomena.　All things are consistent with logic but are unwilling to expound themselves to us. Able to find out neither their truth nor the meaning of my existence, I had felt a certain malaise with my heart enveloped in mist.　I had been, I think, lacking the volition to penetrate into everything's disguise and to give serious consideration to my days of life in those days; I had just escaped to compulsory education as the established road and have lived in idleness.　And going on to university just in these times without thoughtful consideration had made me stray into endless road. I had been constantly in agony about the meaning of life in the free atmosphere of university.　The inconsistency between stationary ego and the society changing hour by hour had brought about feeling of despair rather than desolateness.　When I had incidentally poked around books of biochemistry, I had perceived what the world is and the cause of all things.　All things are in a state of flux, but continue to exist in all ages.　All metamorphoses and all disparities are generally prescribed by differences in atomic units.　Hence it is concluded that the cause of natural truth and profoundness formed through severe evolution from time immemorial and the principle of creatures are accordingly atoms.　All phenomena brought about all over the universe are, to sum up, prescribed by chemistry.　It might be dim light in a lantern, but the pent-up mist was dispersed all of a sudden.　Impressed intensely by such truth, I was moved to tears and blessed the Creator. Since the era of the myth and alchemy, chemistry has been the only measure to grasp the mysteries of Nature which God only knows.　In the introduction of "化學入門 (the ABC of chemistry, first published in 1867)", Katsuragawa Hosaku, professor at Kaiseijo (the School of Western Learning) is stating as follows; *The power of chemists can be compared to the power of Nature.　They can create water, fire, soap and stone if required and they can also quench them if not required.　They can generate or decompose them at will and they acquire power to manipulate the substances as it wished.　Generally speaking the cause of the world is only sixty odd.　Combining them in accordance with the law constructs everything.　Chemists analyze such law and create many kinds of creations.　How mysterious they are!* (translated by T. Kitanosono)　It might be a high-flown rhetoric, but how sacred chemistry is!　I had soothed almost into a dreaming slumber.

　　　Thus, my intoxication and idealism had burst.　A scene of kaleidoscopic changes from their former selves to their ice-cold bodies is a humiliation as well as a loathsomeness for me; all my remembrances such as a wreck lying down on the bed, a delirium and a dropsy as side-effect of anticancer agent and a prostration caused by dysphagia were always so sharp and cruel that I felt like my heart was being gouged out.　The disconsolate days followed incessantly on the heels of lamentation.　We can identify the diseases and symptoms based upon the statistic and medical knowledge; however we could not retell the tragic ending prospective in the future.　The wretchedness I confessed is well-expressed in a poem "God of the universe, nonexistent or existent I wonder in this scourge" composed by Hirata Atsutane, which is evocative of mental conflict sealed in my heart.　It appears that every effort, we have made and will make, would prove fruitless forevermore.　I wondered to myself why we have to learn science for all that, seeing us unable even to strive against fate.　It is no exaggeration to say that our unenlightenment, conceit and incompetence massacred the innocent people.　"Nemo ante mortem beatus."　We witnessed the rage of Nature, our ineluctable destiny and evanescence of life with dismay.　What kind of warning did those give us?　Although we human have had faith in Science of hundred years, human knowledge cultivated through hundreds of years was completely incompetent in front of

Nature.　We could but lament our shallow knowledge and be overwhelmed in despair, anguish and enervation.　We can't be relieved of the denunciation that it was the result of our disgraceful conceit through the indulgence of material culture and eulogizing our Science to be omnipotent. Fukuzawa Yukichi, a famous scholar born in my birthplace, was said to have cherished opinions such as "与造化争境" and "束縛化翁是開明", which describes how profound the secrets of Nature is; *Nature is apt to disturb human activity, say, by making its fury to be rampant.　Hence human built the house to shelter from a storm and built a ship to go on the waves.　Further pursuit of safety will compel the houses or ships to be steadfast and offer a resistance to Nature.　In addition, Nature is inclined to be secretive about herself; She will be loath to teach us those secrets. Tormenting people with many kinds of diseases or epidemic, Nature will be unwilling to initiate us into the remedies.　Nature has concealed the existence of steam or electrical power for a long time since the dawn of history; it is only recently that we can divulge a part of those secrets.　This example seems enough to know the will of Nature.　Thus human, self-proclaimed emperor of every soul on the earth should deal proficiently with the meanness of Nature without any wonder.　And we should strive to disclose the secrets and absorb them.　It is of grave importance to pursue the pleasure by extension of human knowledge.　(Omitted)　Even in the era of enlightenment all over the world, Nature still has inestimable power and infinite secrets.　It is our mission to prevent their rampancy by control the Natural power everlastingly and to harness the secrets to our pursuit of convenience.* ("Fukuo hyakuwa", One Hundred Discourses of Fukuzawa, 1897; translated by T. Kitanosono)　There is no unlearning that pandemonium reigned throughout Japan.　We all are being haunted with the fear of recurring ignominious defeat of human.　Now Fukuzawa's motto "与造化争境" can I understand.　Even though we understand the impossibility of reaching the stage of perfect, we are apt to become conceited.　The remarkable progress of scientific civilization will provide us with an illusion as if we could twist Nature around our finger. However science, human knowledge accumulated assiduously, was revealed to be so incompetent that it could but leave vast plain, innocent people and many artifacts to be trampled down by Nature. The misery made us moan in despair and dismay; we were compelled to bewail the transitoriness of everything including our lives.　Nature is still beyond mortal control, which seems never to rival Nature eternally.　Now the thought of divine punishment once advocated by Viscount Shibusawa[12] isn't accepted unqualifiedly anymore; nevertheless even if human have profound wisdom, what can we do?　Fully worked-out stratagem couldn't preclude innocent people from deceasing in vain; an impotence of science once engendered an atmosphere of desperate and pessimistic resignation.

　　　However, the overwhelming power of Nature didn't pay any heed to futile resistance of scientific civilization.　Dr. Einstein said "***Raffiniert ist der Herrgott, aber boshaft ist er nicht***".[13] The reaction systems in all lives are the culmination of chemists' ideal and we can only sigh over the absoluteness of Creator.　No wonder Nature is the culmination of beauty as the emblem of God. And human may well be awed by majesty of Nature.　The creation of all things is anything but the acts of human being.　Here my resolution has gotten firmer.　Even in the era that material civilization was blossomed, all people are equally exposed to the severe struggle for existence regardless of their social standings.　We are all the weakest, vulnerable and timid, having neither a weapon to contain enemy's attack nor a defensive mechanism in our body, even nor a paranormal ability beyond scientific explanation.　In spite of our disability, we human have been dominating the earth at least within the memory of men.　How come?　According to neural Darwinism,[14]

some species acquire "learning" capacity through a functional development of the cerebrum. Among them, we alone can predict and prepare for threats from enemy through putting every engine of experience and knowledge in force, every trick that ingenuity can devise and rascality execute. That is, our trepidation caused by a lack of physical ability enables us to experience a continuous process of trial and error and to acquire such sapience. A Solomon can "learn" from setbacks.[15] It is only immutable that world-shaking inventions are generally created by the enthusiasm for childlike dream and preposterous fantasy. My dream is not only artificial re-construction of natural elaboration cultivated through the eternal times but also understanding what is existence and creation of new systems superior to natural systems. Nothing is more pleasant than being excited at thinking of the days when we will be able to generate even protoplasm, the fountainhead of creatures as if I were a child. It is said that the daughter of Sugawara Takasue had made and worshipped a life-size Yakushi-butsu (the healing Buddha) at home in order to fulfill her wish of reading tales as long as there are.[16] The curiosity amplifying increasingly is our vitality. I'm willing to lay down my life for the realization of my dream with a great appetite for frontier spirit without being caught up in my small pride. The haunting yearnings will scoff even at extreme difficulties. A fragile and dwarf spirit will be eager for solid evidence or insurance. However ambitiousness can be established on extraordinary tribulations, self-sacrifice and steady improvement. Herein I throw down the gauntlet against Almighty Divine toward Numinous world explored in water.

---

[1] The *Records of the Grand Historian* (*Taishi gong shu* 太史公書; currently known as the *Shiki* 史記 – "Historical Records"), Vol. 6, ca. **BC91**.

[2] a) The *Han Feizi* (韓非子), Chapter XIII, ca. **BC234**; b) The *Records of the Grand Historian*, Vol. 81, ca. **BC91**.

[3] The *Zuo Zhuan* (*Chunqiu Zuo Zhuan* 春秋左氏伝).

[4] The *Analects* (*Lunyu* 論語; also known as the *Analects of Confucius*).

[5] The *Tao Te Ching*, *Daodejing* (*Dao De Jing* 老子).

[6] H. Yano, T. Kubota, H. Miyamoto, T. Okada, D. Scheeres, Y. Takagi, K. Yoshida, M. Abe, S. Abe, O. Barnouin-Jha, A. Fujiwara, S. Hasegawa, T. Hashimoto, M. Ishiguro, M. Kato, J. Kawaguchi, T. Mukai, J. Saito, S. Sasaki, M. Yoshikawa, *Science* **2006**, *312*, 1350-1353.

[7] Y. Katsumoto, M. Fukuchi-Mizutani, Y. Fukui, F. Brugliera, T. A. Holton, M. Karan, N. Nakamura, K. Yonekura-Sakakibara, J. Togami, A. Pigeaire, G. –Q. Tao, N. S. Nehra, C. –Y. Lu, B. K. Dyson, S. Tsuda, T. Ashikari, T. Kusumi, J. G. Mason, Y. Tanaka, *Plant Cell Physiol.* **2007**, *48*, 1589-1600.

[8] Y. Fukuzawa, The *Gakko-no-setsu* (学校之説), **1870**.

[9] The *Liezi* (列子).

[10] In 1992, Pope John Paul II expressed regret for how the Galileo affair was handled and formally and publicly cleared Galileo of any wrongdoing; "Vatican admits Galileo was right" New Scientist, 1992/11/7.

[11] In 1996, Pope John Paul II declared the evolutionary theories of Charles Darwin to be fact, tacitly acknowledging that human being evolved from the apes, and reducing the biblical account of Genesis to that of mere fable; *The Quarterly Review of Biology* 72.4, **1997**.

[12] a) A bulletin issued by *Tokyo Chamber of Commerce* (東京商業会議所報) Vol. 6, No. 10, Nov. **1923**, pp19; b) Evening edition of the *Hochi Newspaper* (報知新聞) dated Sep. 10th, **1923**.

[13] "***Subtle is the Lord, but malicious He is not***", which made during Einstein's first visit to Princeton University in 1921.

---

[14] a) R. Dawkins, *Nature* **1971**, *229*, 118-119; b) G. M. Edelman, "*Neural Darwinism: The Theory of Neuronal Group Selection*", Basic Books, Inc. **1987**, New York.

[15] "Nur ein Idiot glaubt, aus den eigenen Erfahrungen zu lernen. Ich ziehe es vor, aus den Erfahrungen anderer zu lernen, um von vorneherein eigene Fehler zu vermeiden." by Otto Eduard Leopold, Prince of Bismarck, Duke of Lauenburg.

[16] The *Sarashina Nikki* (更級日記), Heian-period.

General Introduction

Numinous World Explored in Water

0-1   Background: Water and Dawn of Chemistry

Organic reactions have been long deemed to be conducted in organic solvents, owing to the compatibility and immiscibility between water molecules and many reagents or reactive species.[1] In addition to the concerns surrounding water-sensitive reagents or reactive species, solubility is believed to be an absolute requirement for reactivity.   Therefore, typically, the traditional organic reactions requires anhydrous and anaerobic conditions; when we conduct fundamental reactions in textbook, we will dry up all glass apparatus and reagents to remove water and use anhydrous solvents in gallon jugs and big metal canisters sometimes without thinking deeply.   Removal of water in organic reactions has been an "unspoken rule" and a "prevailing notion" among chemists. Great pains have been taken to construct strictly anhydrous conditions (Figure 1).
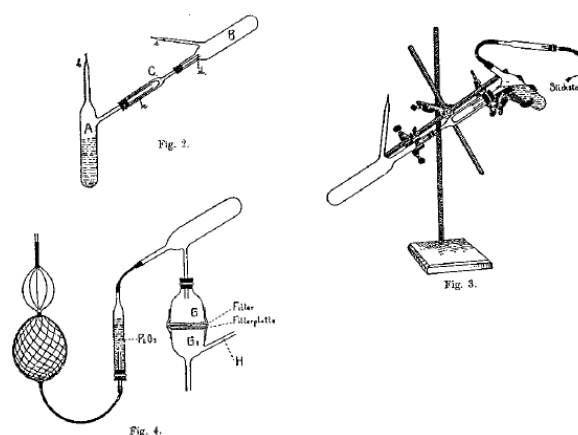
Figure 1. Schlenk glassware[2]

Nevertheless, biochemical reaction relies on an aqueous environment, which embodies the indispensability of water.   It is sometimes even called the "matrix of life", as referred to by Nobel Laureate Albert Szent-Györgyi.[3] Water was regarded as originally overspreading all things in Genesis: "The earth was without form, and void; and darkness was upon the face of the deep.   And the Spirit of God moved upon the face of the waters."   The pre-Socratic philosophy commenced with the preoccupation with the origin of the universe, seeking natural explanations for phenomena without reference to a supernatural power such as gods or other mythological forces.   There was the principle of all things, which is an immortal divinity and persists through changes.   Thales of Miletus (624-ca. 546 BCE), the first philosopher in the Greek tradition and the father of science claimed that "arché", the ultimate underlying substance was water, from which the universe is composed and on which the earth floated.   The belief in "arché" is commonly referred to monistic materialism; he is the first of its long line, extending all the way to the present day.   The originality of his theory does not lie on the notion that the whole universe emerged from primeval water, which is underlying Near Eastern and Greek mythology.   It is of great significance that water had

emerged from personified pantheon to become a natural phenomenon. His water-centered perception seems to rely on the biological view that all animate things benefit from water and environmental aspect that a never-ending global process of water circulation. His understanding of water was handed down to Empedocles' four-element theory, where any substance is defined by a fixed proportion of one or more among four elements: earth, water, air and fire.

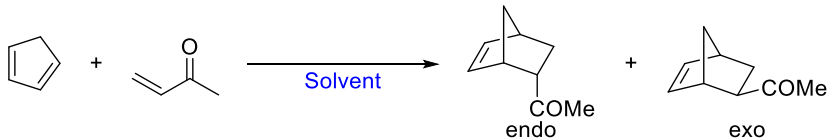Until the end of nineteenth century, the scientific community has been cultivated on the basis of an adage, *"Corpora non agunt nisi fluida (or liquida) seu soluta"*.[4] The Dutch physician Hermannus Boerhaave (1688-1738) accentuated that solvent should be considered to be the most essential part of chemistry itself. In the remote times, the Greek alchemists speculated about the nature of solution and dissolution and interpreted a liquid which is chemically active as "Divine water", bearing in mind that the term "water" was used to refer to anything liquid. Despite the conceptual incompatibility between "alkahest" and the other being such as the vessel to contain it, many alchemists toiled away on the fanciful search for the hypothetical universal solvent, which some called "alkahest θειον νδωρ" and others referred to as "menstruum universale", coined by Paracelsus (1493-1541). Since then, the concept of "alkahest" has been evaluated as an esoterica during the period of obscurantism. An eager pursuit of fantastic "alkahest" dreamed by alchemists led to numerous discoveries such as new solvents, reactions and compounds. Although discovering quite strong acids, including *aqua fortis* (concentrated nitric acid), and *aqua regia* (king's water, a 1:3 mixture of nitric and hydrochloric acids) which could dissolve even noble metals, gold and platinum, Alchemists could not but agree bitterly that the closest thing to a universal solvent was the primordial thing, water. The earliest chemical rule that "similia similibus solvuntor" which means "like dissolves like", a popular aphorism used for predicting solubility is among the tangible results in alchemy. Contemporary interpretation of solution or dissolution was, however, equal to all operations leading to a liquid. The polysemy of the "dissolution" did not make a conceptual distinction between the physical dissolution and the chemical change by dissolution. That erroneous equation between the physical dissolution, fusion, melting and even chemical transformation and the misdirected belief that the nature of a substance was fundamentally lost upon dissolution often led the alchemists down the collateral garden path. For instance, Hermann Boerhaave (1688-1738) asserted that the combustion was accompanied by an increase of weight because the burned substance interacted with the "particles" of fire, on the basis of the "dissolution" theory where the dissolution was dependent on the mutual affinities between both substances. This fallacy underlay the superstitious existence of fire, heat and light as material substances. Jan Baptista van Helmont (1580-1644) opposed such contention by defending that the dissolved substance had not disappeared, but remained in the solution as an aqueous form, being possible to recover.[5] Meanwhile, he also engaged in the fanciful search for "alkahest" and claimed to have found it. As irony would have it, his "alkahest" was identified as "sweet oil", glycerol 300 years before DuPont patented it. Not until the end of 1700s when French chemist Joseph Proust (1754-1826) rolled up a law of definite proportions was chemical reaction experimentally differentiated with dissolution. Although about to buried in oblivion, "alkahest" connotes the implicit belief that solubility is requisite to reactivity whether it is high or low. In spite of a myriad of failures stacked in the laboratories, the superstitious conviction has been survived gloriously until the middle of 18th century because of the absence of convincing theory alternative to alchemical one.

The role played by solvents in the chemical equilibrium or in the rates of chemical reactions was unraveled in 19th century.   In 1862, Berthelot and Péan de Saint-Gilles argued about the influence of some solvents on the rate of esterification between acetic acid and ethanol.[6] The participation of the solvent was thus systemized in some chemical reactions through a simple electrostatic model, for instance Hughes-Ingold rule.[7] The correlation between the solvent and chemical equilibrium was first reported in 1896, coinciding with the discovery of keto-enol tautomerization.[8] In the childhood of organic chemistry beginning with Wöhler's urea synthesis, water was the solvent of choice, although not popular, in many reactions such as Baeyer-Villiger oxidation, Wolff-Kishner reduction and so on.[9] The modern view of water as pariah in organic chemistry was engendered not long ago, along with the flourishing study of organometallic chemistry entailing strict exclusion of water and with the improved availability of traditional solvents through the technical progress in petrochemical industry.   However there are a few turning points toward the reinstatement of water in organic chemistry.

In the earlier stage, some pioneers proved that water was not just detrimental contaminant as an alternative solvent or an additive.   However the use of water was based on negative inducement as such roles and the chemistry still belonged to traditional organic chemistry.   I believe that Breslow's seminal rediscover on the rate acceleration of Diels-Alder reactions recorded in water is undoubtly one of historical watersheds (Table 1, left).[10] He also emphasized the benefits from water on the *endo-exo* selectivity (right).[11] The rate constant recorded in water was one- to two-order-magnitude larger than that in organic solvents, in spite of the relative immiscibility of those components in water.   Addition of "antichaotropic" salts such as lithium chloride was found to be effective for rate acceleration.   It must, however, be annotated that a connection of Diels-Alder reaction with water is not attributed to Breslow.   The original reaction between furan and maleic acid displayed by Diels and Alder was performed in aqueous media, including one article and two patents.[12] In 1973, intensive study of this reaction was reported and the beneficial influence of water on the rate of this reaction was described for the first time.[13] In addition, the characteristic change in *endo-exo* selectivity between the reaction in water and that in other solvents was already disclosed by Diels and Alder.   Considering the solubility of CpH in water (ca. 0.01 M),[14] stronger preference toward *endo*-product was obtained along with the rate acceleration when the reactants were distributed homogeneously throughout the solution.

Table 1. Diels-Alder reaction in water[10]

Solvent	$10^5 k_2$ (M^{-1} s^{-1})	Solvent	*endo/exo*
Isooctane	5.94	Cyclopentadiene	3.85
MeCN	15.2	EtOH	8.5
MeOH	75.5	0.15 M CpH in H_2O	21.4
H_2O	4400	0.007 M CpH in H_2O	22.5
LiCl in H_2O (4.86 M)	10800		
$(NH_2)_3CCl$ in H_2O (4.86 M)	4300		

The potentialities of performing organic reactions in water have thus stimulated chemists' ingenuous curiosity.   The extensive investigations with an eye to the beneficial effect of water have led to unexpected and unpredicted results, such as the reaction rate acceleration and enhancement of selectivity (Table 2).   In all examples, water provided significant rate acceleration over organic solvent.   Not only Claisen rearrangement[15] whose transition state was postulated to have substantial polar character but multicomponent reactions[16] yielding insoluble products could be accelerated in water.   The Michael addition of primary amines with α,β-unsaturated compounds furnished only monoaddition products unlike alternative methods which generally afforded mixtures of mono- and bis-addition products.[17]
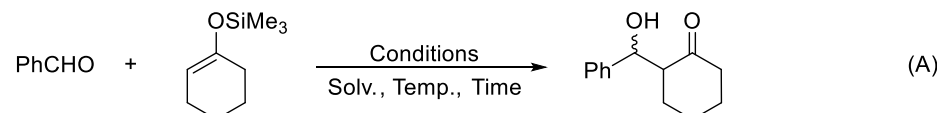
Table 2. Rate acceleration in water: (A) Claisen rearrangement[15]; (B) Passerini Reaction[16]; (C) Aza-Michael reaction[17]

(A)

$$k_{H2O}/k_{MeOH} = 22.8$$

(B)

Solvent	Time (h)	10^{-2} (M^{-2} s^{-1})
DCM	18	1.0
H$_2$O	3.5	18
LiCl in **H$_2$O** (1.0 M)	0.8	286

(C)

Solvent	Time (h)	Yield (%)
THF	10	40
DCM	10	70
H$_2$O	0.5	90
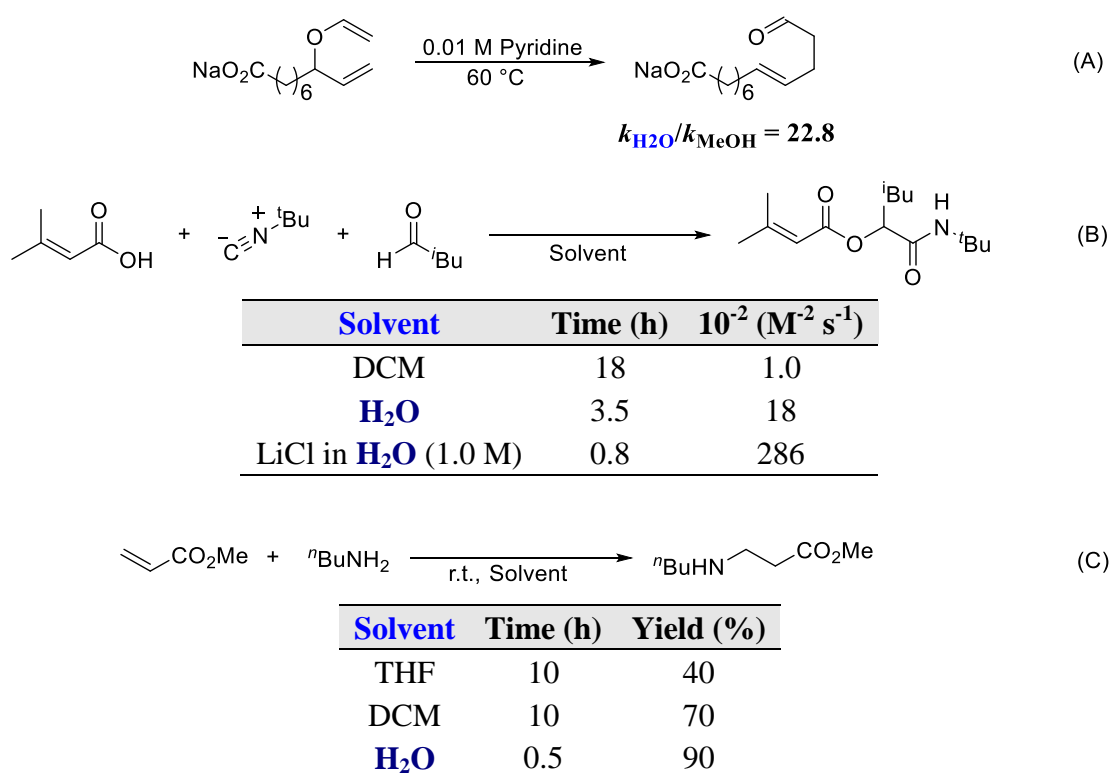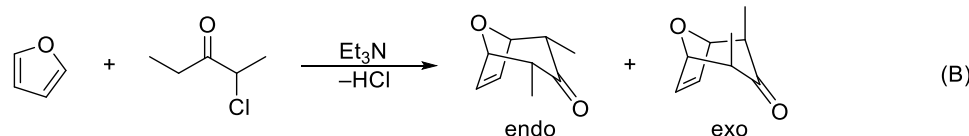
The curtain rises to exploit water positively as a solvent.   Subsequently, Lubineau *et al.* have demonstrated the Mukaiyama aldol reaction in water to be feasible. (Table 1, above).[18] While the same reaction carried out in the presence of a stoichiometric amount of TiCl$_4$ in dichloromethane (DCM) proceeded rapidly (82% yield after 2 h), the reaction in water proceeded more slowly (43% yield after 5 d).   The stereoselective preference of the product was reverse in comparison with conventional TiCl$_4$-catalyzed reaction (entry 1).[19] Although the reaction proceeded rather slowly, obvious rate acceleration was observed in water because no reaction occurred in DCM without any Lewis acids.   Intriguingly, the rate acceleration and the stereochemical outcome recorded in pure water bore a striking resemblance to that recorded under high pressure (entry 2).[20] The opposite between "in water"[21] and "at low pressure"[22] observed in

[4+3] cycloaddition was synonymous phenomenon (Table 3, below). A curious coincidence between in water and under high pressure has been observed in many reactions ever since (e.g. Passerini[23] and Ugi[24] reactions), which makes "water" an enigmatic solvent.[25] More conspicuous rate acceleration was observed in the Mukaiyama aldol reactions using ketene silyl acetals; the reaction of 2-pyridinecarboxyaldehyde in water was approximately 4-fold faster than that in organic solvents (Scheme 1, above).[26] Exhibiting *anti*-selectivity irrespective of the *E/Z* ratio of starting enolate, the water-promoted reaction can be interpreted through an open-transition-state model (Scheme 1, below).[27] The scope of the catalyst-free water-based Mukaiyama aldol reaction was explored through its application to the site-selective functionalization of *N*-terminal aldehydes of peptides and proteins.[28] As shown in the case of myoglobin, the reaction could be carried out without disturbing either the tertiary structure or the enzymatic activity of the protein.

Table 3. "In water" versus "under high pressure": (A) Mukaiyama aldol reaction; (B) [4+3] Cycloaddition

Entry	Solvent	Temperature	Conditions	Time	Yield (%)	Dr (*syn/anti*)
1[19]	DCM	20	TiCl$_4$ (1 equiv.)	2 h	82	25/75
2[20]	DCM	60	1000 MPa	9 d	90	75/15
3[18]	**H$_2$O**	20		5 d	23	**85/15**

Entry	Solvent	Temperature	Conditions	Time	Yield (%)	*Endo/exo*
1[22]	CF$_3$CH$_2$OH	60-80	0.4 Torr	6 h	82	19/81
2[21]	**H$_2$O**	20		5 h	88	**90/10**

THF : 22% yield
CH$_2$Cl$_2$: 23% yield
H$_2$O : 95% yield

(*Z*): *Z/E* = 72/28
(*E*): *Z/E* = 25/75

(**Z**): 95% yield, *syn/anti* = 35/65
(**E**): 84% yield, *syn/anti* = 33/67
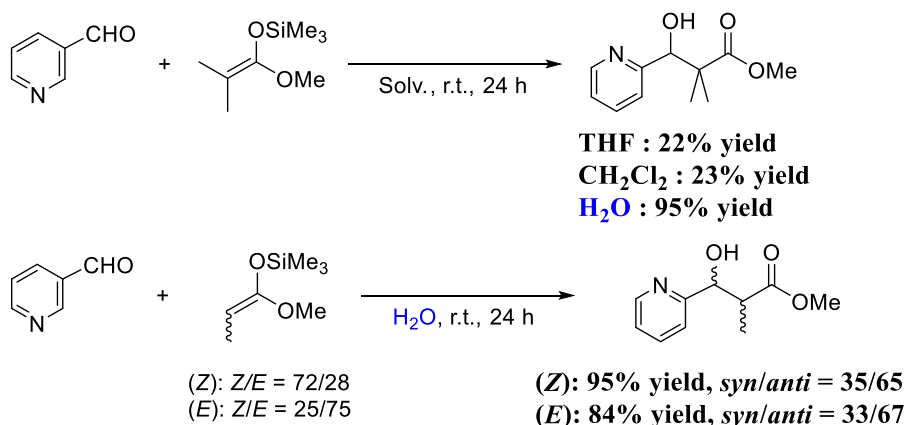
Scheme 1. Water-promoted Mukaiyama aldol reactions of ketene silyl acetals

The Mukaiyama aldol reaction of electron-rich Rawal's diene with carbonyl compounds proceeded without any activator in pure water (Scheme 2).[29] ^{1}H NMR analyses indicated that the solvents influenced the reaction pathway and the aldol adducts were obtained in water, while the cycloadduct was obtained through the Diels–Alder pathway in other protic solvents.[30] It should be noted that water offered the opportunity for variegating the reaction with different pathway from that adopted in organic solvents.
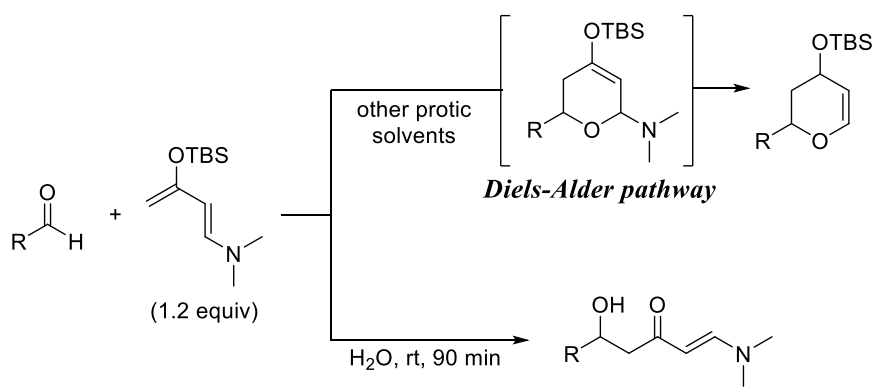
Scheme 2. Reaction of Rawal's diene in water[29]

As mentioned above, *in vivo* catalysis has been cultivated in water. Despite tremendous efforts dedicated by chemists, enzymes still exhibit overwhelmingly superior catalysis to artificial catalysts. Among many mysteries left in nat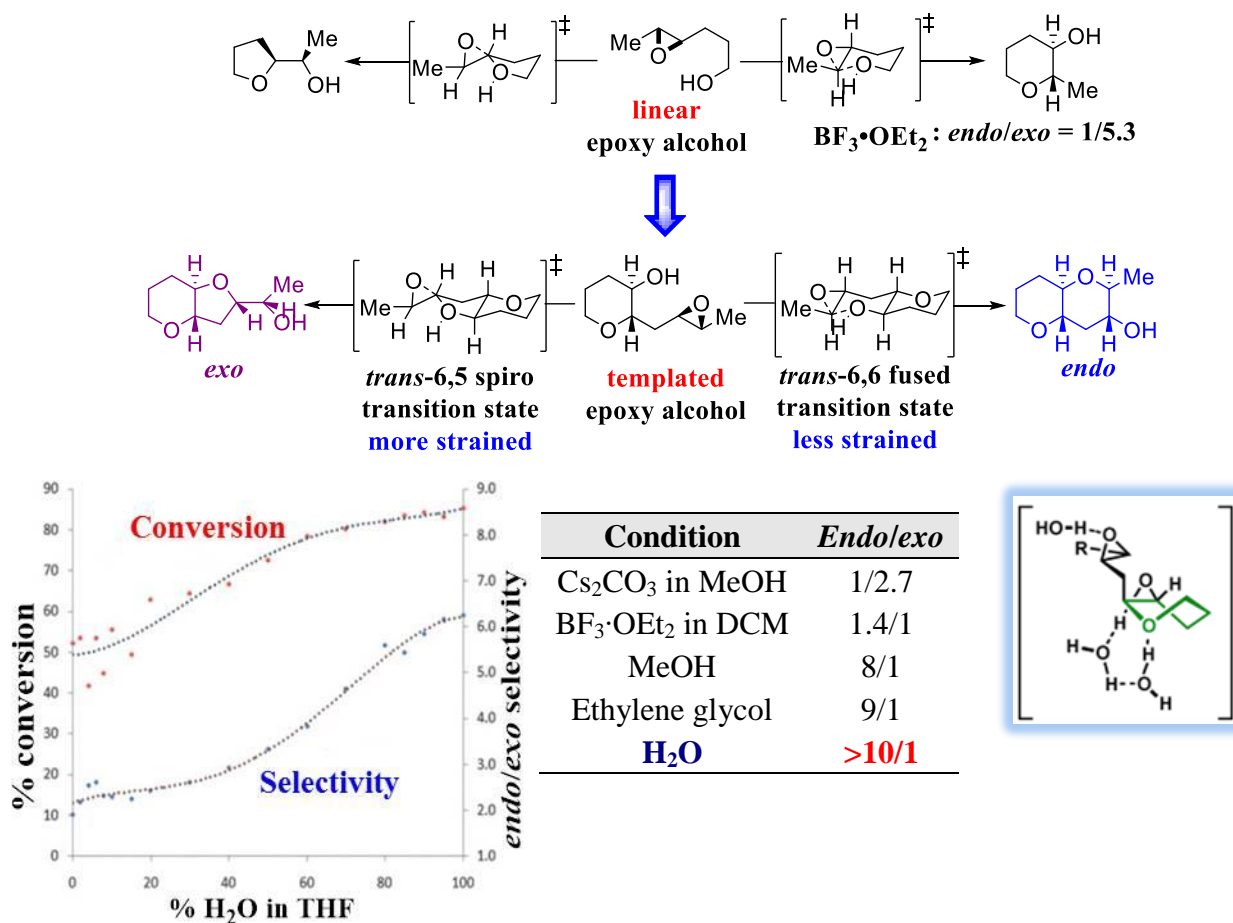ure, biosynthesis of ladder polyether, such as brevetoxin, gymnocin, ciguatoin and so on is of great concern, that are assumed to be synthesized from terpene derivatives. All ladder polyethers possess a structural pattern and stereochemical regularity involving a backbone of repeating O-C-O units and THP tetrad, along with *trans-syn* topography. On the basis of these speculation and earlier carbon-labeling and feeding experiments, Nakanishi *et al*. suggested the two-step conversion of polyenes to polyethers.[31,32] The mechanism invokes a disfavored *6-endo-tet* cyclization via an all-fused and regioselective epoxide-opening events against Baldwin's rule. From the standpoint of organic chemistry, one-pot assembly would streamline the synthesis and it scores remarkably high in terms of atomeconomy. However, chemists had to confront Baldwin's rule toward the *in vitro* emulation of biomimetic cascade synthesis. Jamisons' speculation was relied on the attachment of template as the potential factor governing the regioselectivity. Kinetic investigations disclosed the pivotal role of water in promotion of the epoxide-opening cyclization reaction forming the anti-Baldwin six-membered ring product (Table 4).[33] The reaction in aqueous tetrahydrofuran (THF) manifested a significant increment of both conversion and regioselectivity with increasing amount of water. The reaction in neutral water produced the best results. Water-promoted epoxide-opening cascades proceeds via stepwise mechanism. In contrast to the vacillating nature of the first cyclization step, the second cyclization step displayed substantially higher endo selectivity in neutral water, greater than 20:1. Other templates, such as a cyclohexane or oxepane were unsuccessful in overcoming the inherent *exo* preference. A more powerful template effect of THP diad and the combination with water could deliver the anti-Baldwin *endo* product. They assumed that the effect of water underlay charge stabilization and exerting conformational changes to the template, through a

stabilized twist-boat conformer shown in Table 4.

Table 4. Synergism between water and THP template (graph was excerpted from original paper with slight modification)[33]

linear
epoxy alcohol

$BF_3 \cdot OEt_2$: *endo/exo* = 1/5.3

exo

***trans*-6,5 spiro transition state** **more strained**

templated
epoxy alcohol

***trans*-6,6 fused transition state** **less strained**

endo

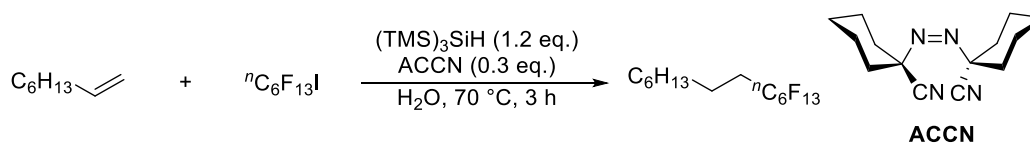| Condition	*Endo/exo*
Cs_2CO_3 in MeOH	1/2.7
$BF_3 \cdot OEt_2$ in DCM	1.4/1
MeOH	8/1
Ethylene glycol	9/1
H_2O	**>10/1**

In living cell free radicals or excited-state species generate constantly by breathing, playing a key role in basic biological function, such as aging.   In contrast to classical radical reactions entailing toxic and moisture-sensitive irritant tin hydride and aromatic solvent bearing π-system, free radical chemistry in water is expected to expand the versatility and flexibility of homolytic C-H, C-C, C-X (halogen), C-N bond formations through much milder process.   The remarkably beneficial effect of water was unearthed in triethylborane-induced atom-transfer radical cyclization (Scheme 3).[34] Treatment of allyl iodoacetate with Et_3B/O_2 system did not deliver the desired lactone in benzene or hexane, whereas the reaction proceeded smoothly in water to afford the corresponding γ-lactone efficiently.   Since iodine transfer is quite rapid, the cyclization is known to be the rate-determining step.[35] Calculations with the SCRF/CPCM option indicated that water lowers the activation barrier both in rotation process from C to A and in 5-*exo* cyclization from A to E.   The relatively low activation energy in rotation would facilitate the conversion of the *E*-rotamer A to the more stable *Z*-rotamer C, prohibiting topologically from cyclizing.   The large dielectric constant of water would lead to a relative accessibility to cyclization process constructing the γ-lactone framework.   In addition, the author concluded that the high cohesive energy density of water forced a decrease in the volume of the reactant, accelerating the cyclization pathway.
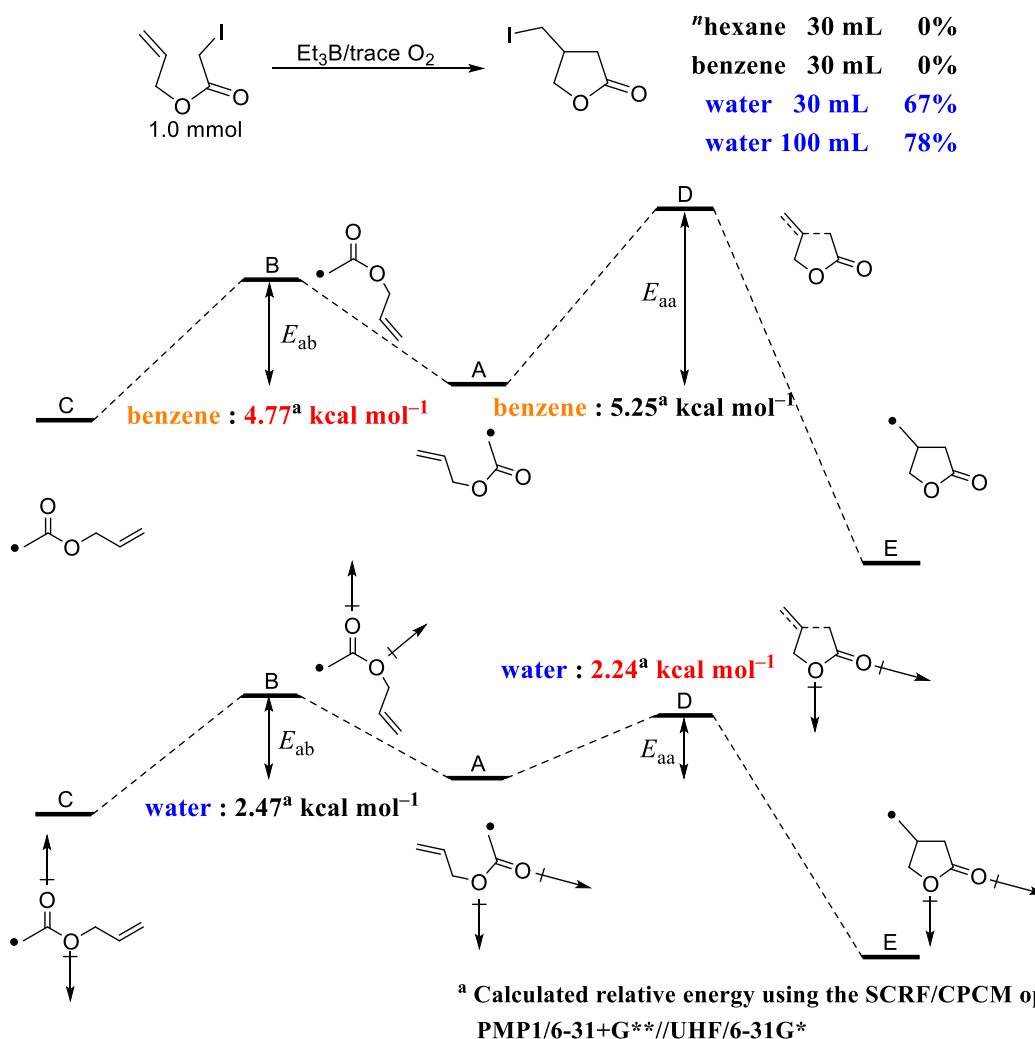
Scheme 3. Water-induced radical reaction in water[34]

The substantial progress has been made in the last decade to "tame" the reactive free radical species in aqueous phase reactions, leading to their application in total synthesis, DNA structural probing, and isotope labelling, living polymerization and so on.   For instance, indium(0) is often employed in water to induce radical reactions as a single-electron-transfer (SET) radical initiator.[36] Tris(trimethylsilyl)silane (Me₃Si)₃SiH is also applicable in water.   Treatment with a radical initiator the radical often triggers radical-based events.[37] The combination of (Me₃Si)₃SiH and 1,1'-azobis(cyclohexanecarbonitrile) ACCN enabled the perfluoroalkyl radical addition with electron-rich alkenes in water (Scheme 4).[38] In classical nucleophilic substitution process the lone pairs of the fluorine atoms result in the theoretical preclusion of S_N2 substitution event due to its repulsion against the invasion of other reactant, whereas the utilization of the corresponding perfluorinated radicals is highly expected.   They were, however, were known to be ca. 6-fold more reactive with hydride such as (Me₃Si)₃SiH than alkene in organic solvents.[39] The use of water as a solvent accelerated the reaction of perfluoroalkyl radical with the alkene to render the perfluoroalkylated radical adduct, followed by rapid hydrogen abstraction from the silane.

C_6H_{13}—CH=CH$_2$ + $^nC_6F_{13}$I $\xrightarrow[\text{H}_2\text{O, 70 °C, 3 h}]{\substack{\text{(TMS)}_3\text{SiH (1.2 eq.)} \\ \text{ACCN (0.3 eq.)}}}$ C_6H_{13}—$^nC_6F_{13}$

ACCN

**Scheme 4**. Radical C-C bond formation in water[38]

Nowadays, increased environmental awareness within the synthetic organic chemistry community has led to a soaring attraction toward water as a solvent in chemical transformations. Not only is water nontoxic, inexpensive, environmentally benign and inherently safe, but it also offers many advantages such as simplicity of reaction conditions and high efficiency in reactions that involve water-soluble substrates or reagents. Independently-developed "chemistry in water" cannot be written by the traditional organic chemistry cultivated in organic solvents. In addition, organic chemistry in an aqueous environment will provide us a potential for construction of the innovative artificial catalytic systems in living cell toward construction of "in vivo catalysis". Throughout a sagacious exploitation of water, we can even retell an existing organic chemistry cultivated through hundred years of history.

Figure 2. The increasing attention toward the use of water as a solvent
(Reprinted and modified from Cover Picture of *Green Chem.* **2014**, *16*, 3645.)

## 0-2 Milestone: Discovery of Water-Compatible Lewis Acids

In spite of the observation of surprising rate-enhancement in several chemical reactions in water, low yields and low reaction rates were often observed without activation by Lewis acids among them *e.g.* the Mukaiyama aldol reactions. In the meanwhile, traditional Lewis acids such as Al(III), Ti(IV), and Sn(IV) significantly accelerate the Mukaiyama aldol reaction in organic solvents, whereas these Lewis acids decompose rapidly in the presence of water. Indeed, Lewis acids were believed to be incompatible with water for a long time. It was, however, discovered in 1991 that rare earth trifluoromethanesulfonates (triflates)[40] such as $Sc(OTf)_3$, $Y(OTf)_3$ and $Ln(OTf)_3$ are water-compatible Lewis acids and accelerate the Mukaiyama aldol reaction significantly in aqueous media (water/organic solvents).[41] For example, $Yb(OTf)_3$, a representative rare-earth triflate, was revealed to exhibit superior performance in the Mukaiyama aldol reaction of various silicon enolates with aqueous formaldehyde in water–THF (Scheme 5) or in water–ethanol–toluene cosolvent systems.[42]
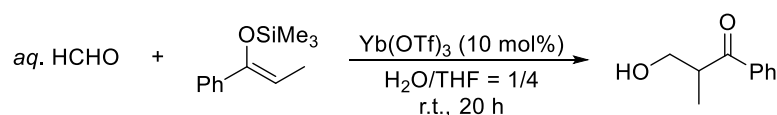
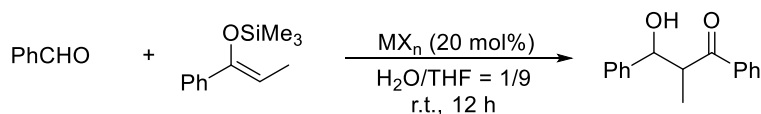**Scheme 5**. $Yb(OTf)_3$-catalyzed Mukaiyama aldol reaction in aqueous media

Likewise, a wide variety of aldehydes other than formaldehyde could be activated successfully by lanthanide triflates to deliver the corresponding cross-aldol adducts; even the water-soluble aldehydes such as acetaldehyde, acrolein and chloroacetaldehyde or coordinating aldehydes such as salicylaldehyde and 2-pyridinecarboxyaldehyde were reacted successfully.[43] The reactions carried out without water failed to give the corresponding aldols, thus verifying the intriguing nature of water in these catalysts.[44] In that sense, this method has many advantages over traditional $TiCl_4$-promoted reaction performed under strictly anhydrous conditions. Especially this method enabled us to use aqueous formaldehyde as C1 source. Generally speaking, hydroxymethylation reactions using formaldehyde as one of the most-valuable C1 electrophiles have received immense attention in organic synthesis.[45] Even though user-unfriendly toxic formaldehyde gas and paraformaldehyde in organic solvents can be employed as C1 electrophile for the reactions, tedious and harmful procedures to generate formaldehyde monomer from oligomers[46] are the main disadvantages. $Yb(OTf)_3$-catalyzed hydroxymethylation has been employed to construct a complex molecule in the total synthesis of various natural compounds such as A-seco taxane[47], (-)-sclerophytin A[48] and so on. More practical attachment of hydroxymethyl function on α-carbon adjacent to carbonyl group has been enlisted in total synthesis of biologically active compounds such as diazonamide A[49], (-)-strychnine[50], acutifolone A[51] and so on, in which the initial *in situ*-formation of a silyl enol ether (TMSCl, Et_3N) served to create a latent nucleophile that was subsequently unleashed upon reaction with $Yb(OTf)_3$ or $Sc(OTf)_3$ to engage the excess amount of aqueous formaldehyde in solution. This two-step, one-pot procedure was developed by Toyota *et al.* as a δ-lactone synthesis protocol in 2006.[52] Furthermore, this aqueous protocol impedes a seriously destructive desilylation pathway. For instance, seriously facile desilylation in Mukaiyama aldolization in a total synthesis of taxanes could be overcome by utilization of this

methodology.[53] The formation of undesired desilylated ketone was often the sole pathway when attempting Mukaiyama aldol reactions with conventional methodology. A thorough screening of Lewis acids or other catalysts under strictly anhydrous conditions was eventually in vain. Gratifyingly, the desired reaction of the TMS enolate with acrolein proceeded smoothly with $Gd(OTf)_3$ in water-ethanol-toluene system (1 : 10 : 4) to afford the corresponding keto-enone **15** as a 2 :1 mixture of diastereomers after subsequent oxidization with Jones' reagent (Scheme 6). Their endeavor bears eloquent testimony to the overwhelming ascendancy of aqueous $Ln(OTf)_3$ system as a powerful catalyst for Mukaiyama aldol reaction.
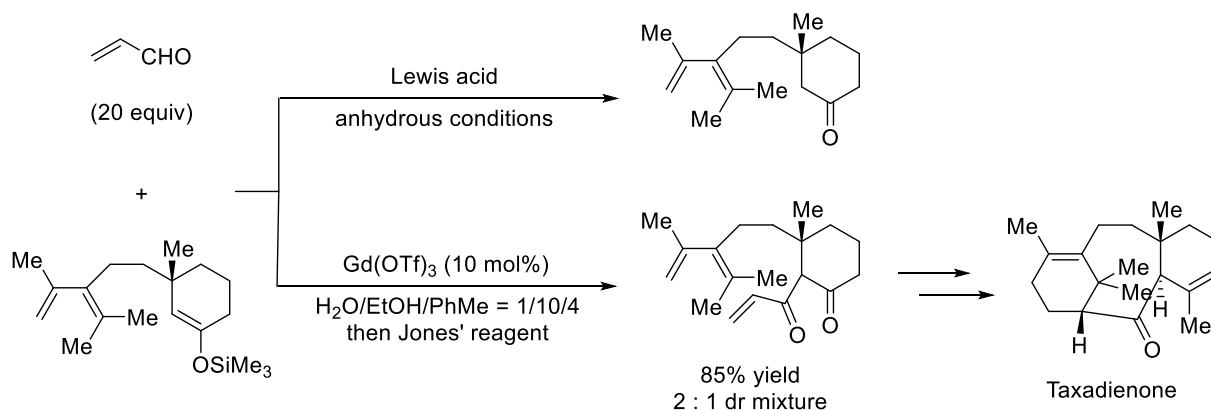
Scheme 6. Baran's example applying the aqueous Mukaiyama aldol reactions[53]
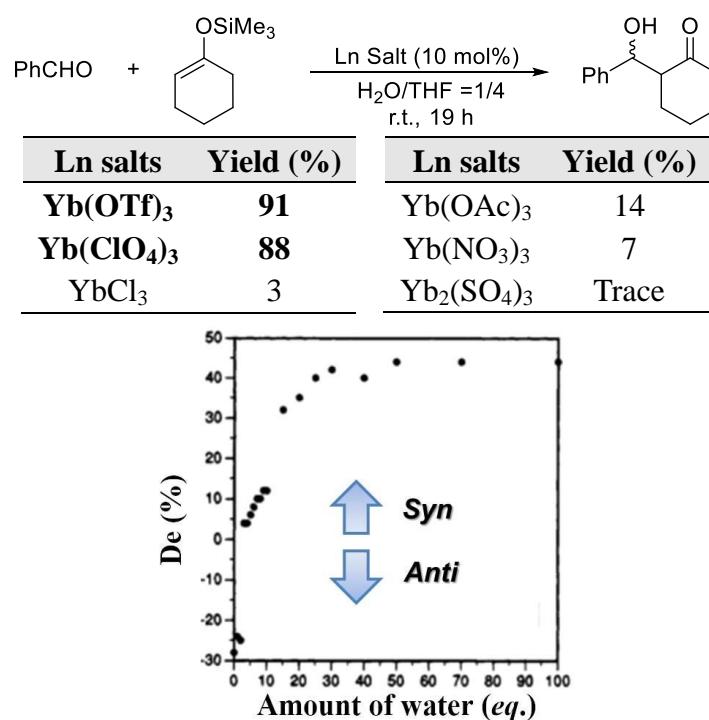
Thus the emergence of water-compatible Lewis acid catalysts has definitely broken down the wall of traditional prejudice that water is a detrimental contaminant in organic synthesis, and also offered industrially beneficial methodologies which facilitate recovery and reuse of the catalysts. One then wonders why rare-earth triflates, in contrast to conventional Lewis acids, are compatible with water. The Lewis acidity of group 1–15 metal chlorides, perchlorates and triflates was evaluated in a water–THF cosolvent system.[54] In addition to rare-earth metal cations, Fe^{II}, Cu^{II}, Zn^{II}, Cd^{II}, and Pb^{II} were disclosed to function as efficient and promising Lewis acids in an aqueous medium. Superior catalytic activity was observed in the presence of the metal cations surrounded by red square in Table 5. The reaction catalyzed by other metal salts hardly provided any of the desired product. Extensive research enabled us not only to expand the availability of water-compatible Lewis acids but also to establish empirical criteria with which we can assimilate "Lewis acidity" in an aqueous environment. Given the correlation between metal cations and their catalytic activities, hydrolysis constants (K_h) and exchange rate constants for the substitution of inner-sphere water ligands (water exchange rate constants (WERCs)) were suitable factors for estimating catalytic activities (Table 5).[55] These active metal compounds were found to have pK_h values in the range from about 4.3 (for Sc^{III}) to 10.08 (for Cd^{II}) and WERC values greater than 3.2×10^6 $M^{-1}s^{-1}$. Cations with large pK_h values do not generally undergo efficient hydrolysis. In the case of pK_h values being less than 4.3, cations are readily hydrolyzed to produce protons in sufficient number to cause rapid decomposition of silicon enolates. On the other hand, when pK_h values are higher than 10, Lewis acidities of the cations are too low to catalyze the aldol reaction.

Table 5. Hydrolysis constants and exchange rate constants for substitution of inner-sphere water ligands.[54]

$$PhCHO \ + \ \underset{Ph}{\overset{OSiMe_3}{\diagup\!\!\diagup}} \ \xrightarrow[\substack{H_2O/THF = 1/9 \\ r.t., \ 12 \ h}]{MX_n \ (20 \ mol\%)} \ \underset{Ph}{\overset{OH \quad O}{\diagdown\!\!\diagup\!\!\diagdown}} Ph$$

Legend box: M^{+n} / $pK_h{}^a$ / WERC^b

Group 1	Group 2	Group 3	Group 4	Group 5	Group 6	Group 7	Group 8	Group 9	Group 10	Group 11	Group 12	Group 13	Group 14	Group 15
Li^{+1} 13.64 4.7×10^7	Be — —											B^{+3} — —	C — —	N — —
Na^{+1} 14.18 1.9×10^8	Mg^{+2} 11.44 5.3×10^5											Al^{+3} 4.97 1.6×10^0	Si^{+4} — —	P^{+5} — —
K^{+1} 14.46 1.5×10^8	Ca^{+2} 12.85 5×10^7	Sc^{+3} 4.3 4.8×10^7	Ti^{+4} ≤2.3 —	V^{+3} 2.26 1×10^3	Cr^{+3} 4.0 5.8×10^{-7}	Mn^{+2} 10.59 3.1×10^7	Fe^{+2} 9.5 3.2×10^6	Co^{+2} 9.65 2×10^5	Ni^{+2} 9.86 2.7×10^4	Cu^{+2} 7.53 2×10^8	Zn^{+2} 8.96 5×10^8	Ga^{+3} 2.6 7.6×10^2	Ge^{+4} — —	As — —
Rb — —	Sr — —	Y^{+3} 7.7 1.3×10^7	Zr^{+4} 0.22 —	Nb^{+5} (0.6) —	Mo^{+5} — —	Tc — —	Ru^{+3} — —	Rh^{+3} 3.4 3×10^{-8}	Pd^{+2} 2.3 —	Ag^{+1} 12 $>5\times10^6$	Cd^{+2} 10.08 $>1\times10^8$	In^{+3} 4.00 4.0×10^4	Sn^{+4} — —	Sb^{+5} — —
Cs — —	Ba^{+2} 13.47 $>6\times10^7$	Ln^{+3} 7.6-8.5 10^6-10^8	Hf^{+4} 0.25 —	Ta^{+5} (-1) —	W^{+6} — —	Re^{+5} — —	Os^{+3} — —	Ir^{+3} — —	Pt^{+2} 4.8 —	Au^{+1} — —	Hg^{+2} 3.40 2×10^9	Tl^{+3} 0.62 7×10^5	Pb^{+2} 7.71 7.5×10^9	Bi^{+3} 1.09 —

La^{+3}	Ce^{+3}	Pr^{+3}	Nd^{+3}	Pm	Sm^{+3}	Eu^{+3}	Gd^{+3}	Tb^{+3}	Dy^{+3}	Ho^{+3}	Er^{+3}	Tm^{+3}	Yb^{+3}	Lu^{+3}
8.5	8.3	8.1	8.0	—	7.9	7.8	8.0	7.9	8.0	8.0	7.9	7.7	7.7	7.6
2.1×10^8	2.7×10^8	3.1×10^8	3.9×10^8	—	5.9×10^8	6.5×10^8	6.3×10^7	7.8×10^7	6.3×10^7	6.1×10^7	1.4×10^8	6.4×10^6	8×10^7	6×10^7

[a] $pK_h = -\log K_h$, Reference 55a,b. [b] Exchange rate constants for substitution of inner-sphere water ligands, Reference 55c.

When a certain metal cation has high catalytic activity, large WERC value may be necessary to allow sufficiently fast exchange between the water molecules coordinated to the metal and the aldehyde substrate. "Borderline" species such as Mn^{II}, Ag^{I}, and In^{III}, whose pK_h and WERC values are close to the criteria limits, produced the aldol adduct in moderate yields. Although the precise activity of Lewis acids in aqueous media cannot be quantitatively predicted by pK_h and WERC values, this heuristics has been instrumental in the identification of promising metal compounds as water-compatible Lewis acid catalysts,[56] and has also provided mechanistic insights into Lewis acid catalysis in aqueous media. Taking a high coordination number of these effective metals into account, the remarkable rate acceleration by water seems to arise from the predominant ionic properties in the interaction between the Lewis acidic metals and counter anion. Indeed, the catalysis of ytterbium salts with more-nucleophilic counter anions such as Cl^-, OAc^-, $NO_3{}^-$ and $SO_4{}^-$ were lower by far, compared with the effective catalysis of ytterbium salts with less-nucleophilic counter anions such as OTf^- (91% yield, *syn/anti* = 73/27) or $ClO_4{}^-$ (88% yield, *syn/anti* = 76/24) (Table 6, above).[43b] The best yields were obtained when the ratios of water were 10-20 %. Water seems to be prone to desterilize silyl enol ethers through hydrolysis of ytterbium salts.[57] The amount of water governed the stereochemical outcome as well as the consequent catalytic turnover in aqueous THF solution. While the reaction of benzaldehyde with cyclohexanone-derived silyl enol ether proceeded with *anti*-preference in the absence of water, the stereochemistry of the product underwent a change toward *syn* conformations in accordance with the increasing amount of water. The selectivity became, however, unchanged (up to *syn/anti* = 73/27) when more than 15 equivalent of water was added (Table 6, below).

Table 6. Effect of Yb salts and correlation between product stereochemistry and the amount of water

Ln salts	Yield (%)	Ln salts	Yield (%)
Yb(OTf)₃	**91**	Yb(OAc)₃	14
Yb(ClO₄)₃	**88**	Yb(NO₃)₃	7
YbCl₃	3	Yb₂(SO₄)₃	Trace

(graph was excerpted from original paper with slight modification)[43]

An unequivocal interrelation between the coordination environment of lanthanide triflate and steady state reaction rate on Mukaiyama aldol reaction was also proved through luminescence-decay measurements in combination with high-performance liquid chromatography analyses, suggesting the relationship between the coordination numbers (CN) of ytterbium center and the amount of water (Figure 2).[58] These phenomena can be explained as follows. The predominant coordination of THF molecule to Yb(OTf)₃ stabilizes the cyclic six-membered transition state to lead to the lower activity and *anti*-selectivity in the reaction that none or small amount of water was added.[59] On the other hand, when the equivalents of water are gradually increased, coordination of water molecules produces the naked active ytterbium cation with high water-exchange rate constant[60] to activate aldehydes effectively and catalyze the reaction *via* an acyclic transition state.[61] The structural fluctuation of coordinating water molecules around lanthanide ions determines favorable transition states (TS) in terms of entropy, promoting hydration of silicon enolate and proton transfer to aldehyde and subsequently activating both substrates. This model was confirmed by the AFIR method by Morokuma *et al.*[62] Thus, the elaborate exploitation of the unique properties of water in irreversible Mukaiyama aldol reactions is expected to facilitate the catalytic turnover with simultaneous desilylation as a direct access to aldol adducts, while in conventional acid- or base-catalyzed aldol reactions, the reaction yields of the aldol adducts are destined to depend upon their thermodynamic stabilities because of the reversibility of the reactions.
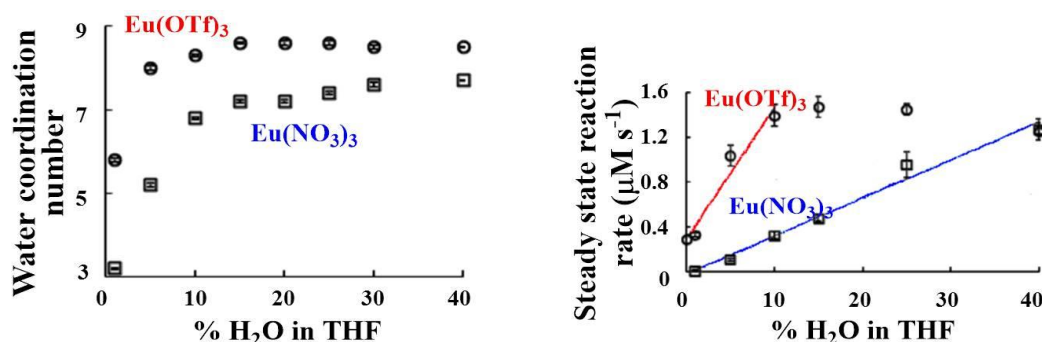
Figure 2. Correlation between CN and the amount of water (graph was excerpted from original paper with slight modification)[58]

It was also disclosed that the aza Diels-Alder reactions were efficiently catalyzed by AgOTf in water (Scheme 7).[63] Although the reaction hardly took place without any catalyst, AgOTf activated imines efficiently toward the cycloaddition with Danishefsky's dienes in water. The catalyst system with the aid of a non-ionic surfactant Triton X-100 was also applicable to one-pot three-component reactions where the imine was formed *in situ* from the corresponding amine and aldehyde.

83% yield
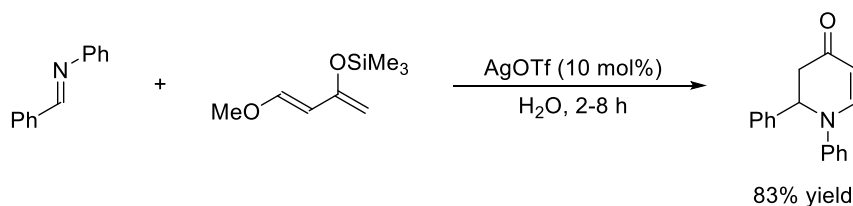
Scheme 7. Silver-catalyzed aza Diels-Alder reaction of Danishefsky's diene in water.[63]

To make the desired catalytic pathway dominant over the competitive hydrolysis, a possible approach is to enhance the hydrophobicity of the reaction environment. The addition of a catalytic amount of surfactant was found to increase the yield in $Sc(OTf)_3$-catalyzed Mukaiyama aldol reactions in 100% water. Micellar systems containing anionic or nonionic surfactant have led to remarkable enhancements of reactivity, even with ketene silyl acetals.[64] Sodium dodecylsulfate (SDS) was the most effective. Only cetyltrimethylammonium bromide (CTAB) was found not to be an effective surfactant because of the possibility of hydrolysis of the silicon enolate. A major disadvantage of Lewis acid catalysis aided by surfactants was that semi-catalytic use of the surfactants was required to achieve good results. There were also problems with separation. Because of the high affinity of water-compatible Lewis acids with water, the relative concentration of the catalyst in the hydrophobic micelles is low. Hence, there were severe substrate limitations in the Lewis acid-SDS system; very labile silicon enolates such as cyclohexanone-derived silyl enol ether decomposed rapidly. In 1998, a Lewis acid–surfactant combined catalyst (LASC) emerged as an innovative catalyst, in which a Lewis acid possessed ligands with surfactant properties to construct an efficient hydrophobic environment surrounding a Lewis acidic cation (Scheme 8).[65,66]
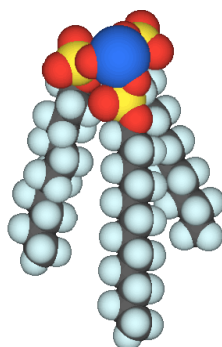
Scheme 8. Schematic representation of scandium tris(dodecylsulfate) (STDS).

Scandium tris(dodecylsulfate) (STDS, Sc(DS)$_3$ [DS = OSO$_3$C$_{12}$H$_{25}$]) was shown to dissolve in water and after the addition of organic substrates, a white dispersion formed. These oily particles, consisting of the organic substrates and STDS, were stabilized and dispersed in water to promote Mukaiyama aldol reactions. Because Sc(OTf)$_3$ *does not* react with SDS to form STDS *in situ*, the catalytic efficiency of STDS was superior to that of the Sc(OTf)$_3$-SDS system.[65a,67] Indeed, the Sc(OTf)$_3$-SDS system makes a kind of micelle (not a dispersion). The use of STDS to construct highly reactive microenvironments in water enlarged the substrate scope in the Mukaiyama aldol reaction to include quite labile silicon enolates. Indeed, the Mukaiyama aldol reaction was found to proceed 5×10^3 times faster in water than in dichloromethane.[65a] It was also shown that multifarious LASCs were applicable to various reactions in water.[68,69] In aqueous solution, surfactants aggregate into micelles, where the hydrophobic portions of the molecules are protected from water.[70] Normally, micelles in aqueous solution form with the surfactant molecules orienting themselves into spherical or elliptical structures with their hydrophobic tails oriented toward the center and their hydrophilic heads oriented toward the surrounding water.

The exploitation of insoluble metal hydroxides is worthy of mention. Since metal hydroxides except alkali metal and thalium(I) are almost insoluble in any solvent, they have never been regarded as a catalyst for organic synthesis. The preliminary implication of their potentiality in organic synthesis was disclosed in catalytic asymmetric allylation reactions of hydrazonoesters with allylboronates in aqueous media by using catalytic amounts of zinc fluoride and a chiral diamine.[71] The postulated mechanism involving transmetalation step suggested that zinc hydroxide might be generated in situ and work as a catalyst in aqueous media. Indeed, Zn(OH)$_2$ exhibited the identical catalytic performance as ZnF$_2$ and was considered to behave as a heterogeneous catalyst. The combination of Zn(OH)$_2$ with 2,9-dimethyl-1,10-phenanthroline was disclosed to catalyze the allylation of aldehydes (Scheme 9, above).[72] It is to be noted that the allylation of aldehydes using allylboronates generally undergo γ-addition *via* six-membered transition state, whereas the reaction furnished α-addition products preferentially in water. The catalyst system is also responsible for high *syn*-preference. In addition, Ag$_2$O was revealed to have an activity toward *anti*-selective allylation of aldehydes using allyltin reagent in water (Scheme 9, below).[73] A high level of *anti*-selectivity and a much higher catalytic turnover (0.01 mol%) resulting from Ag$_2$O were demonstrated in allylation in water using allylsilanes.[74]
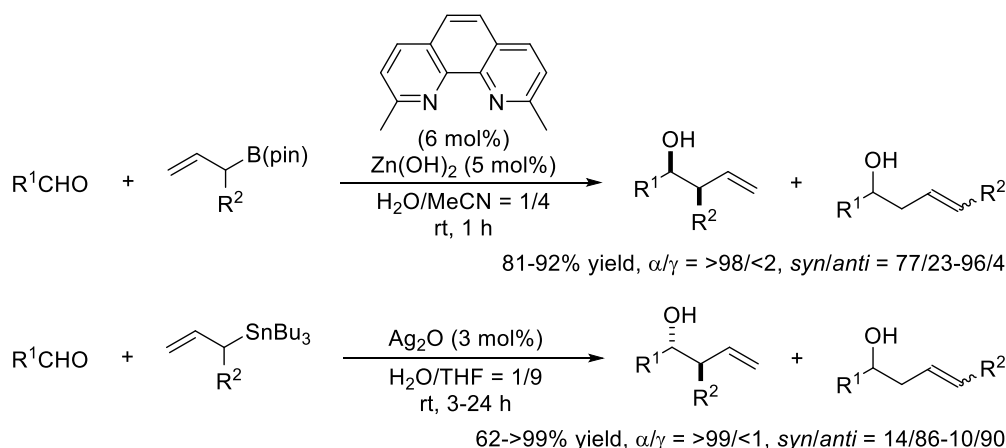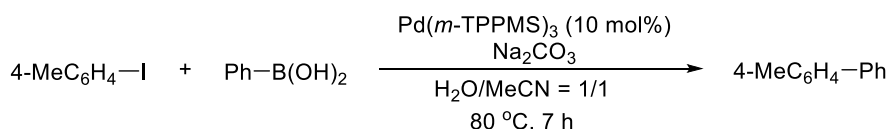
Scheme 9. Allylation of aldehydes in water.

The intriguing nature of allylation in water was extended to the reaction with allenylboronates in aqueous media (Scheme 10). [75] The reaction of hydrozonoester with allenylboronates in the presence of bismuth hydroxide underwent α-addition in aqueous DMF, whereas copper hydroxide switched the selectivity toward γ-addition producing propargylated product within 5 min.
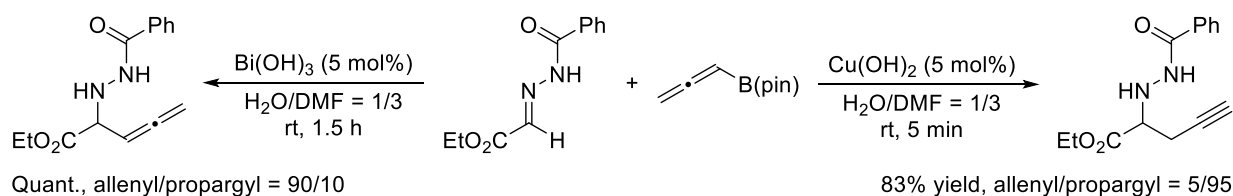

Scheme 10. Allenylation of benzoyl hydrazine in aqueous media.

As mentioned above, the discovery of water-compatible Lewis acids contributed significantly to an explosive advance in organic synthesis relying on Lewis acid catalysis.[76] A number of key enzymatic reactions in biological activity such as photosynthesis, nitrogen fixation, biodegradation, digestion and so on rely on a catalytic action of transition metals in an aqueous environment, which invoked the exploitation of carbon–metal (C–M) bond for the formation of C–C bond even in aqueous media. An elegant argument on the reactivity of C–M bonds involving p-block metals toward water arrived at the conclusion that the reinforcement of its covalent nature resulted in a dramatic decrease in their sensitivity toward water,[77] whereas the participation of d-orbitals in C–M bonds would become more complicated. The C–M bonds involving late transition metals such as organotin, organoboron, and organosilicon reagents are tolerant of water. As a result, there have been a number of reports on rate-acceleration of cross-coupling reactions of hydrophobic substrates in water.[78] Aqueous-phase cross-coupling has been demonstrated using metals with hydrophilic ligand, converting to hydrophobic products that can then be separated by simple decantation. The sulfonated triphenylphosphines were the first water-soluble ligands explored in aqueous media. The palladium combined with *m*-TPPMS (= sodium diphenyl(3-sulfonatophenyl)phosphine) was applied to the Suzuki, Sonogashira, and Heck coupling of aryl iodides and bromides in aqueous acetonitrile (Scheme 11).[79] The more water-soluble

m-TPPTS led to wide application to Heck, Sonogashira, Suzuki, and Tsuji-Trost reactions of aryl and alkenyl iodies or bromides.[80]

$$4\text{-MeC}_6\text{H}_4\text{—I} \quad + \quad \text{Ph—B(OH)}_2 \quad \xrightarrow[\substack{\text{H}_2\text{O/MeCN} = 1/1 \\ 80\ ^{\circ}\text{C, 7 h}}]{\substack{\text{Pd}(m\text{-TPPMS})_3\ (10\ \text{mol\%}) \\ \text{Na}_2\text{CO}_3}} \quad 4\text{-MeC}_6\text{H}_4\text{—Ph}$$

Scheme 11. Cross-coupling in aqueous media using hydrophilic catalyst.

The use of aryl chlorides in aqueous media became possible with *in situ* formation of a catalyst from NiCl$_2$(dppe) and 5 equivalent of *m*-TPPTS, with an aid of zinc.[81] In order to achieve the reaction progree under milder conditions, a great deal of endeavor has been devoted so far, producing a number of Pd or Rh catalyst with modification of sulfonated phosphines, cationic ammonium- or guanidinium-substituted phosphines, carbohydrate-modified phosphines, water soluble NHC ligands and so on.[82] Harnessing surfactants is also a well-recognized prescription. Lipshutz et al. has pioneered the use of the nonionic polyoxyethanyl β-tocopheryl sebacate (PTS) amphiphile, which was applied to palladium-catalyzed Suzuki-Miyaura,[83] Sonogashira,[84] Negishi,[85] and Buchwald‑Hartwig[86] cross-coupling reactions with a wide range of substrate coverage, including those previously inapplicable in aqueous environments. Subsequently, in order to achieve better catalytic efficiency, they made their amphiphilic molecule evolve, naming TPGS-750-M (Scheme 12).[87] It is composed of tocopherol (vitamin E), succinic acid, and methyoxy poly(ethylene glycol). It forms nanomicelles with 50-100 nm diameter in water, resulting in increased reaction rate. It is quite useful technology to transition organic synthesis based on precious-metal catalysis from organic solvents to water.[88]
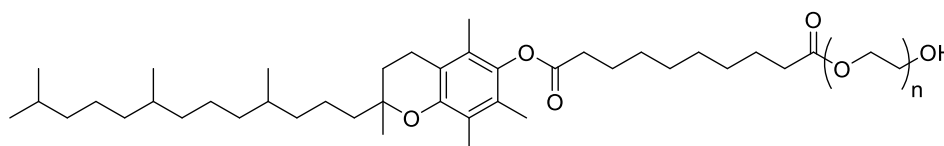
PTS
First Generation Amphiphile
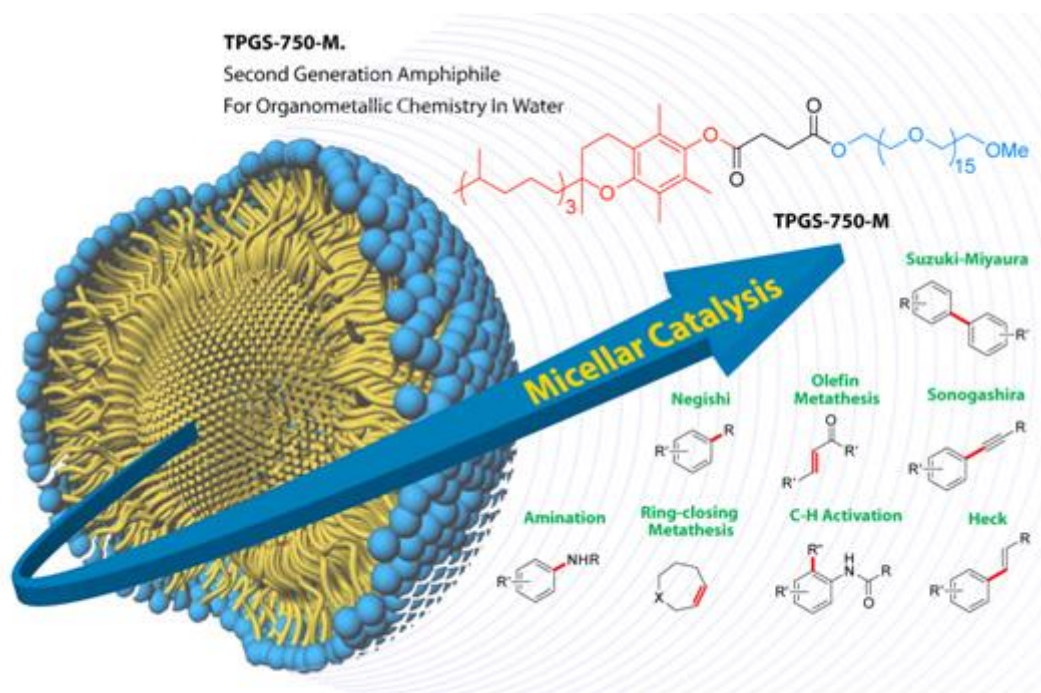
Scheme 12. Lipshutz's surfactants
(excerpted from the Aldrich homepage)

The nucleophilic addition of terminal alkynes to various unsaturated electrophiles is one of the Grignard-type reaction. Fine-tuning of the activity of metal acetylide with ligand resulted in a highly efficient palladium-catalyzed addition of terminal alkynes to unsaturated compounds in water, under an air atmosphere.[89]

91% yield
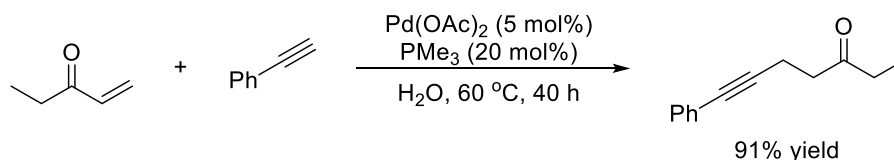
Scheme 13. Palladium-catalyzed nucleophilic addition of alkyne in water.

It was shown that small clusters of gold atoms are excellent inorganic catalysts with record-breaking efficiency in water (Scheme 14).[90] The clusters exhibited catalytic turnover frequencies of up to 100,000 per hour at room temperature for hydration of alkynes. The recorded catalytic activity is nearly five orders of magnitude higher than that previously reported.
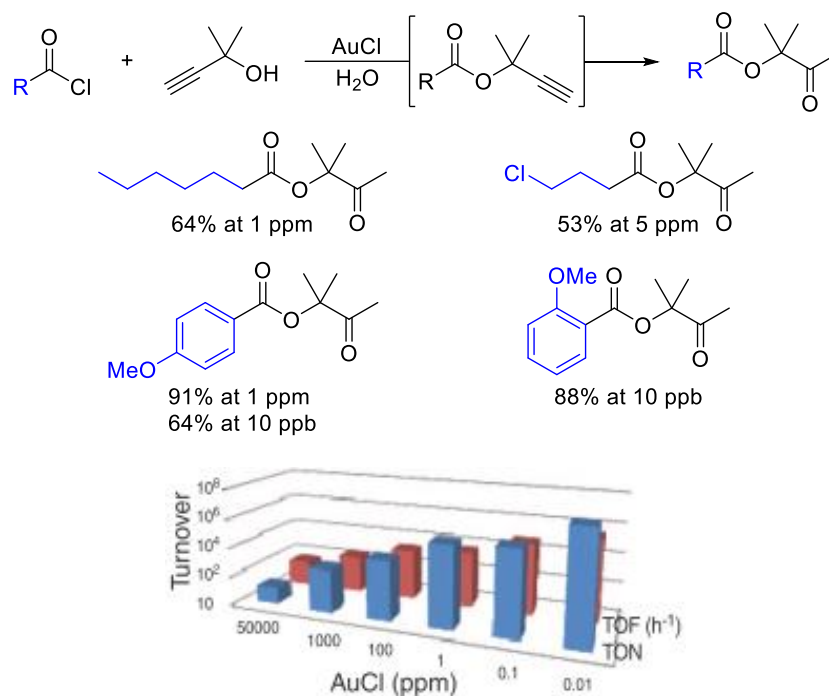
Scheme 14. High catalytic turnover recorded by gold clusters in water.
(Table was excerpted from the original paper)

Compared with imines, the increased reactivity of iminium ions renders the opportunity ot explore the catalysts for direct nucleophilic addition of terminal alkynes. Gold(III) catalysis is widely recognized as an efficient activator of alkynes in water (Table 7).[91]

Table 7. Au(III)-catalyzed aldehyde-alkyne-amine coupling reaction in water.
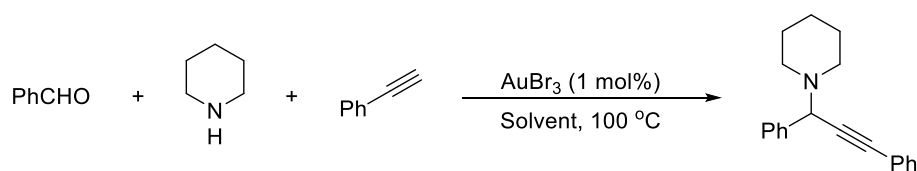
Solvent	Time (h)	Yield (%)
DMF	12	62
Toluene	12	78
H$_2$O	5.5	Quant.

The significant rate-acceleration in water has contributed to exploration of aqueous transfer hydrogenation.[92] Performing transfer hydrogenation reactions in water is potentially expected to be pH-dependent, allowing for fine-tuning of selectivity and inhibiting side reactions using relatively safe reductants. All of reported systems based on Ru or Ir or Rh use formic acid or formates as the hydride donor, since they produce only CO_2 as by-product. Aqueous transfer hydrogenation reactions emerged in 1989, where water-soluble complex $Ru^{II}Cl_2$(TPPMS) [TPPMS = 4-(diphenylphosphino)benzenesulfonic acid] catalyzed the hydrogenation of unsaturated hydrocarbons.[93] The rhodium salt in the presence of TPPTS (= tris(3-sulfonatophenyl)phosphine)

was reported for hydrogenation of functionalized olefins.[94] As a rare example, a range of unprotected indoles were selectively hydrogenated to their corresponding indulines in high yields over a heterogeneous Pt/C catalyst with p-toluenesulfonic acid under 30-50 bar H_2 at room temperature.[95] Rhodium and ruthenium complexes are generally responsible for selective hydrogenation of α,β-unsaturated aldehydes; the former favor the reaction at C=C double bonds, whereas the latter prefer C=O bond saturation.[96] In the case of hydrogenation of ketones, aldehydes and imines, the well-recognized piano-stool aqua complex $[Ir^{III}Cp*(H_2O)_3]^{2+}$ [Cp* = pentamethylcyclopentadienyl] bearing an aromatic π-acceptor ligand and three labile σ-donors followed thereafter.[97]

0-3 *Theoretical Elucidation on the Role of Water in Chemical Reactions*

Breslow interpreted the beneficial role of water to be an attribution to hydrophobic effect and he ruled out all other possibilities.[98] He illustrated that the successful rate acceleration by addition of "antichaotropic" salts such as lithium chloride in contrast to the retardation by "chaotropic" salts such as guanidium chloride could support his suggestion (Table 1, left).[99] He explained that the addition of lithium chloride "salted out" the reactants due to a decreased solubility and enhanced the hydrophobic effect, leading to the rate increase. Though, as pointed out by Dailey, the involvement of lithium chloride as a Lewis acid in the reaction was disregarded in his considerations.[100,101] The stereochemical switch induced by solvent can be comprehended as the force to minimize the total volume of the transition state, which apparently seems to be a quite large loss of the conformational entropy. Even if we focus on Mukaiyama aldol reaction in water, the pressure studies shown by Yamamoto *et al.*[102] definitely indicate that the transition state for the *syn*-selective pathway is more compact (see Table 3). As mentioned above, a curious coincidence between "in water" and "under high pressure" has been observed in many reactions. In order to comprehend the "hydrophobicity" or "hydrophobic effect", three types of solvation can be considered in water (Scheme 5). Thermodynamic understanding of "dissolution" is based on enthalpy-entropy compensation.
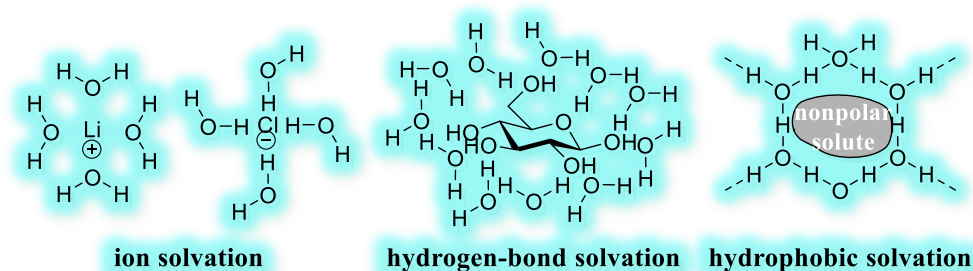

ion solvation   hydrogen-bond solvation   hydrophobic solvation

Figure 3. Aqueous solvation[103]

Compared with ionic and hydrogen-bond-based solvation, hydrophobic molecules are generally inclined to aggregate in water, in order to minimize their surface contact, and associated surface energy with water. When a hydrophobic molecule is immersed into water, hydrogen bonds are disrupted in a focal manner to lose structural entropy significantly, and the exothermicity of forming clathrates or cages of water molecules leads to an enthalpic loss. A hydrophobic molecule can interact with neighboring water molecules with multiple water-solute van der Waals interactions, due to the smallness of water molecules and flexibility in their spatial arrangement. On the other hand, there should be a gain in the translational entropy of water molecules originating from their highly-oriented structure. When two hydrophobic molecules are mixed, fewer water molecules are in direct contact with them due to their contact. In spite of destructuring the hydration shells around them, their contact is energetically advantageous in terms of Gibbs energy, thus leading to an entropy-driven aggregation between them. Now we wonder how surrounding water molecules are related to the thermodynamic dynamics of hydrophobic molecules. When water molecules are absorbed on the surface of branched oligosaccharides, their conformational spaces are explored

successfully by a stable isotope- and lanthanide-assisted NMR spectroscopic approach in conjunction with the replicaexchange MD simulations (Figure 4).[104] It was noted that a lack of one terminal mannose residue expanded the overall conformational freedom.
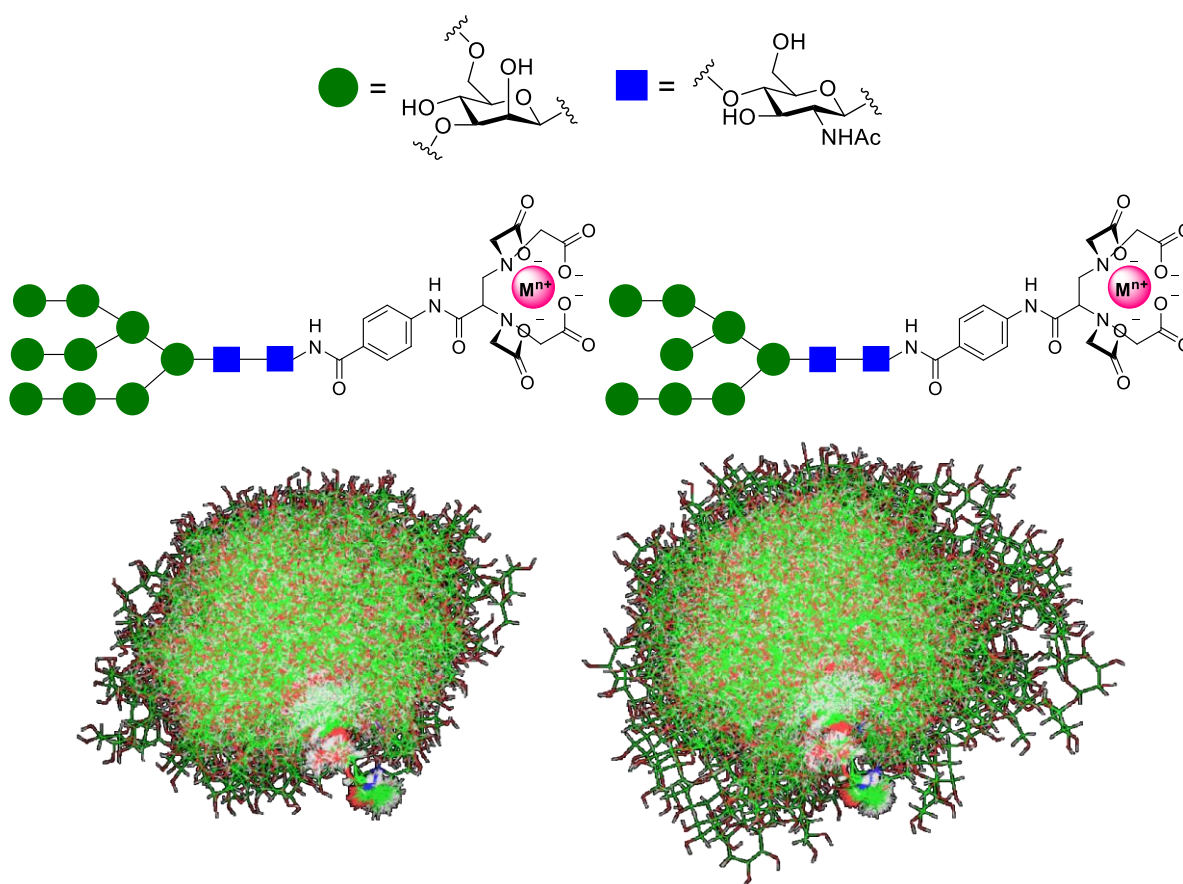

Figure 4. The extent of flexibility illustrated by superimposition of 240 conformers extracted at equal intervals from REMD trajectory of two oligosaccharides.[104]

Another intelligible example is the hydration of protein. Unlike the bulk water, water molecules adsorbed on the surface of protein do not freeze until temperature is below –38 °C.[105] It means that a percolating layer of water molecules on the surface of protein has thermodynamically specific properties based upon their structural reorganizations, thereby affecting the dynamics of protein. In the reactions where the reactivity and selectivity are governed by the unique properties of water, a relationship with entropic factors has been also pointed out. For instance, the epoxide-opening reaction in water reported by Jamison *et al*. (see Table 4) is revealed to be unusually *endo* selective. It is noteworthy that the substrates that can interact with water through hydrogen bonding tend to give the product with high selectivity. Comparing the activation parameters obtained for *exo* versus *endo* cyclization of such substrate and nonselective cyclization of substrate that cannot interact with water, the reaction was turned out to be governed by entropy (Figure 5).[106] With the exception of water, the absolute rate constants of *endo* and *exo* cyclization is roughly correlated to the acidity of the solvents. It is indicated that the reaction behavior in water is more consistent with a synchronous proton transfer.
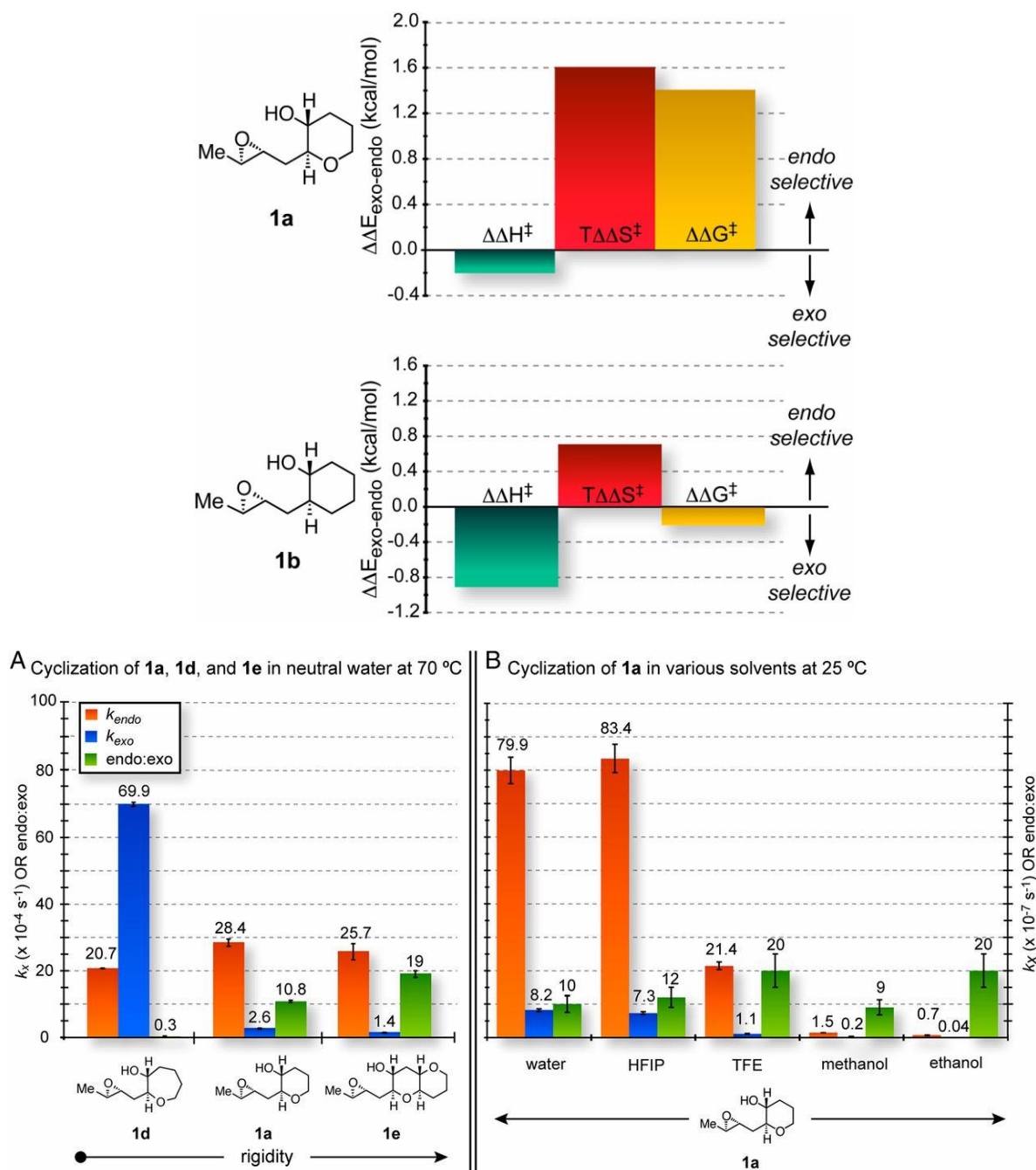
Figure 5. Comparison of activation parameters (above) and solvent effect (below). (excerpted from the original paper)[106]

We would be then wondering what an index of "hydrophobicity" is. Among several parameters which characterize water such as solvent polarity, Hildebrand solubility parameter, relative permittivity (dielectric constant), surface tension and so on, cohesive energy density (ced) is experimentally known to be proportional to "hydrophobicity".[107] The ced is defined as the amount of energy required for complete removal of unit volume of molecules from their neighbors to infinite separation. Water is known to have the high cohesive energy density (estimated 22 kbars) relative to conventional organic solvents.[108,109]

ced: defined as $\Delta E/Vm = (\Delta H_{vap} - RT)/Vm$

Likewise, the water network would force the clathrate of the transition state to be smaller volume than the combined clathrates of the starting materials, resulting in an entropic payoff because the neighboring water molecules are released into aqueous solution and re-incorporated into the intermolecular network.[110] In other words, the reaction between hydrophobic molecules in water has a negative molar volume of the transition state, which is determined as a measure of dependence of the reaction rate on pressure.

Sharpless *et al.* noticed a large rate enhancement in [2σ+2σ+2π] cycloaddition of quadricyclane and dimethylazodicarboxylate (DMAD) carried out in water relative to toluene as originally reported and in order to express this phenomenon the term "on-water" catalysis was coined (Table 5).[111] They made several observations characterizing "on-water" catalysis as below. First, heterogeneous reaction mixture should be formed that consists of oil-water interface as a consequent of vigorous stirring. The addition of small amount of methanol had little influence on the reaction rate, whereas the reaction retarded considerably in aqueous methanol enough to make the reaction mixture homogeneous (entries 2-6). And the reaction accelerated relative to the neat reaction (entry 8). Since the pronounced rate enhancement was not observed under heterogeneous conditions formed with organic reactants and perfluorous solvent, the interface formed with water should be privileged (entry 9). Second, solvent isotope effect should appear (entry 7). Though, "on-water" was not defined distinctly in the original paper.

Table 5. Solvent effect on the reaction of quadricyclane with DMAD[111]
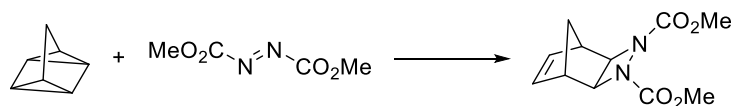
Entry	Solvent	Concentration [M][a]	Time to completion
1	Toluene	2	>120 h
2	MeOH	2	18 h
3	MeOH/**H₂O** = 3/1, homogeneous	2	4 h
4	MeOH/**H₂O** = 1/1, heterogeneous	4.53	**10 min**
5	MeOH/**H₂O** = 1/3, heterogeneous	4.53	**10 min**
6	**H₂O**	4.53	**10 min**
7	**D₂O**	4.53	45 min
8	neat	4.53	48 h
9	C₆F₁₄	4.53	36 h

[a] Concentrations of the neat and heterogeneous reactions are calculated from the measured density of a 1:1 mixture of two components.

Although a wave of enthusiasm was generated from their report, only a few models were put forward regarding the rationales to account for the rate enhancement. The "hydrophobic effect" seems to be an inadequate expression to convey the exact meaning of this phenomenon. This is because it does not contain foregoing *sine qua non* condition such as the pivotal involvement of water and the observation of solvent isotope effect. Though, multifarious explanations relying on

higher viscosity or reduced surface tension of D_2O is feasible, that may complicate mixing operation and may offer better solubility to nonpolar solute (*vide infra*).[112] Focusing on the unnoticed experiments performed by Shen *et al.*, Marcus and Jung invoked an alternative model in 2007.[113] Shen *et al.* applied IR-visible sum frequency generation (SFG) spectroscopy to direct-observation of water molecules at the interface with hydrophobic surface.[114] As a result, they revealed that "oil-water" interface extended into the hydrophobic phase with 25% of the water molecules protruding as a free hydrogen atom that was not involved in hydrogen bonding. The QM/MM simulation study of Claisen rearrangement also suggests that the site-specific stabilization of the transition state as well as the destabilization of the reactants allows the accessibility of the organic molecules to the water surface.[115] The free OH peak completely disappeared when even 11% of methanol was contaminated in bulk water. The "protagonist" in the Marcus-Jung model is these dangling hydrogen atoms that were predisposed to participate in the transition-state through hydrogen bondings (Figure 6).
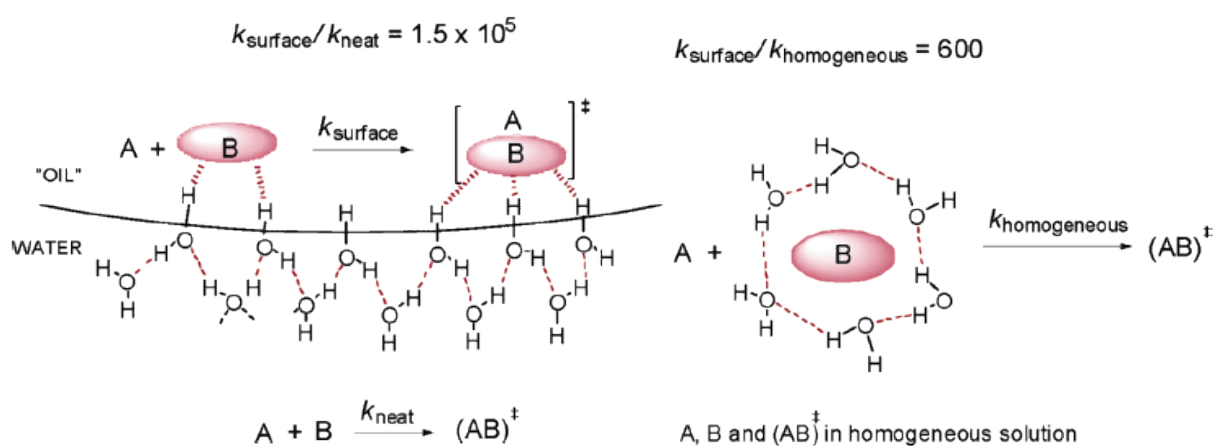

Figure 6. Cartoon summary of Marcus-Jung model and the comparison between neat and homogeneous catalysis (excerpted from the original paper)[113]

The transition-state structure would be, thus, stabilized and the consequent lowering of activation energy would be responsive for the rate enhancement. The *in silico* study based on the theoretical calculation of the reaction using three explicit water molecules bolstered their working hypothesis (Figure 7). It should be annotated that Jorgensen *et al.* reached a totally opposite conclusion through quantum mechanical/molecular mechanical calculations (QM/MM) approach to a series of three Diels-Alder reactions using a vacuum/water interface and more than 1200 water molecules, being skeptical about the "catalyzing" power of the dangling OH groups (Figure 9).[116] Although in the earlier stage, they relied on the classical explanation[117] using the variation of polarization presumably due to remarkably high dielectric constant of water (Figure 8),[118] they viewed water as a weak Brønsted acid catalyst in analogy to Lewis acid catalysis for Diels-Alder reactions. It should, however, be pointed out that the solvent makes the geometry undergo changes from that optimized by the QM calculations in a vacuum. Indeed, Hori *et al.* adopted the quantum mechanical/Monte Carlo/free-energy perturbation (QM/MC/FEP) method for the same Diels-Alder reaction as that described in Table 1.[119] According to a comparison with experimental data, they concluded that the reaction could not be described using too large numbers of solvent molecules

since only a few solvent molecules were responsible for large portions of the solute-solvent interaction energies at the reaction centers. Their *in silico* results for a droplet sizes with a various number of water molecules ranging from 34 to 106 were consistent with the experimental results. The explanation using Marcus-Jung model is, however, inconsistent with two observations. First, solvent isotope effect should be small since the hydrogen bonding at interface does not involve the breaking or the forming of any bond. It is known that Diels-Alder reaction between hydrophobic components in water varies in solvent isotope effect values from 1.2 to 4.5.[111] Although quantum mechanical tunneling can be invoked to account for this inconsistency with a donor-acceptor model of a proton transfer, they fail to elucidate the difference in isotope effect between one reaction and another similar reaction where one of component is different.[120] Second, addition of methanol should not have deleterious influence on the reaction rate whether the reaction mixture is homogeneous or heterogeneous (see entries 2-6 in Table 5).
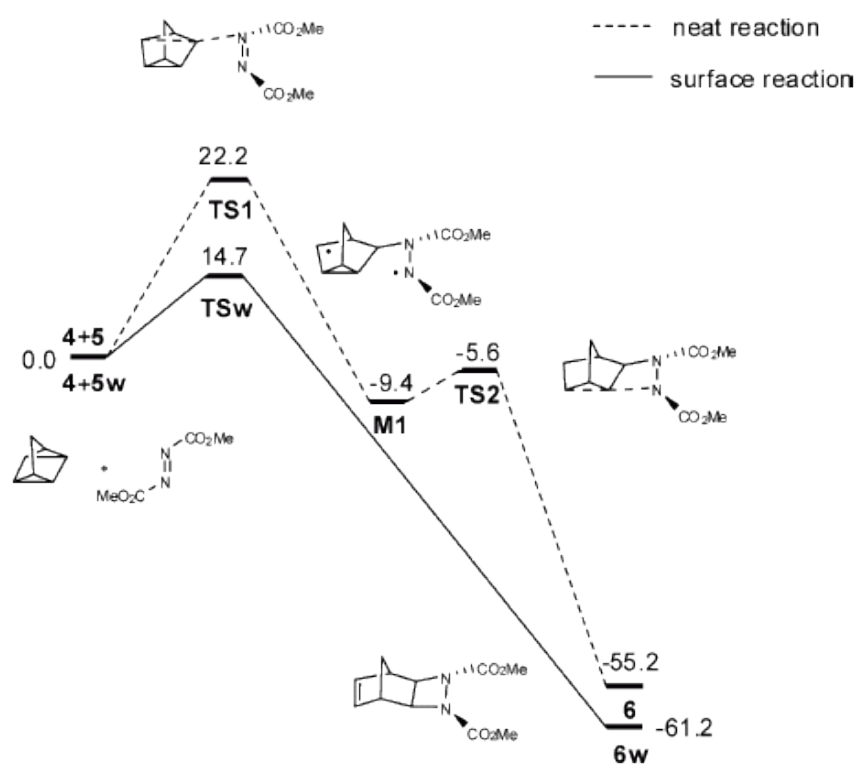

Figure 7. Energy diagram (kcal mol^{-1}) of the reaction under the neat and surface conditions using DFT calculation at the levels UB3LYP/6-31+G(d) (excerpted from the original paper)[113]
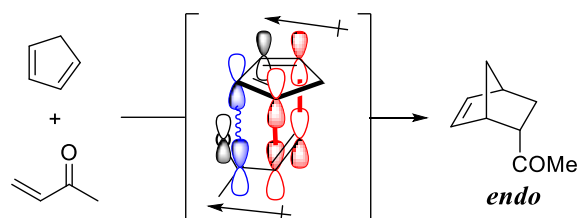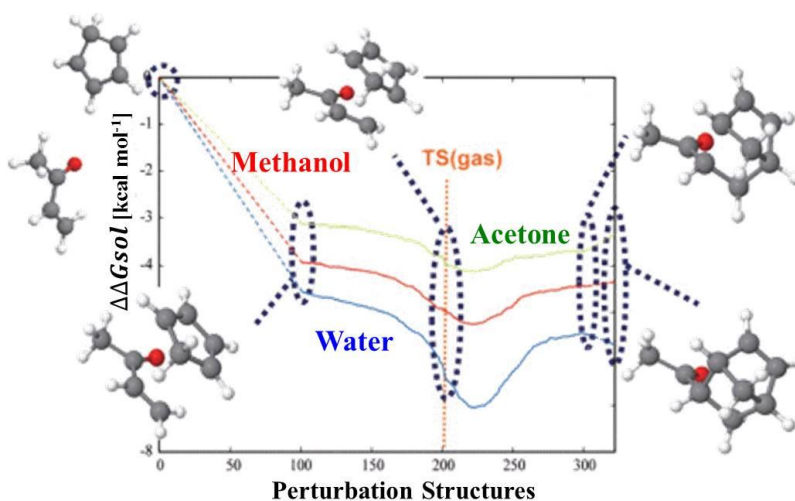

Figure 8. Classical model using the electric dipole moment

Method	H$_2$O	MeOH	Acetone
QM/MC/FEP	20.1 (–0.9)	21.4 (–0.2)	22.4 (–0.8)
SCRF	21.5 (–2.3)	20.4 (–1.2)	25.9 (–2.7)
Experiment	19.2	21.6	23.2

Figure 9. Calculated $\Delta\Delta G_{sol}$ curves along the IRC of the Diels-Alder reaction between methylvinylketone and CpH (excerpted from the original paper with slight modifications)[119] The table shown below represents activation free energies together with those from SCF calculations and experiments.

Another model has its inception in theoretical prediction where the surface of water at hydrophobic interfaces should be positively charged due to the preferential adsorption of proton.[121] Though, in this field there are conclusions on the pros and cons of this prediction. Carruthers noted that a suspension of *n*-octadecane in water shows a gradual increase in pH value up to 9 in the electrophoresis experiment, reasoning that the surface was saturated with hydroxide.[122] Graciaa *et al*. measured ζ-potential of an air bubble in deionized water with more justifiable measurement than previous method.[123] The result (–65 mV) supports the adsorption of hydroxide at the interface. With these experimental results in hand with Jorgensen's proposed on acting as a weak Brønsted acid catalyst, Beattie and McErlean insisted the *acid catalysis* model including promoted dissolution of water molecules and strong adsorption of hydroxide at interface.[124] They asserted that the independence of the reaction rate from the pH of aqueous medium (pH5.6 & pH9.0) denoted inefficacy of the partial dissolution of the reactants into acidic bulk solvent, which also appears to denote the irrelevance of "acid" on the reaction rate. Although able to cover all of the deficiencies made by Marcus-Jung model, this model adumbrates the impossibleness of rate acceleration in water when the reaction is catalyzed by base or involves the basic reactant. Incidentally, they demonstrated the aza-Claisen rearrangement of *N*-prenylated naphthylamines based upon their model.[125] If this model implicates a quite weak level of proton transfer, "acid catalysis" gives an erroneous impression. In the meanwhile, their comparison between the reaction with vigorous stirring, with gentle stirring and with homogenizing is noteworthy (Figure 10). Although a study of a slow reaction will be, as they mentioned, required to discuss the effect of droplet on the reaction quantitatively, the results are quite implicative when we consider other
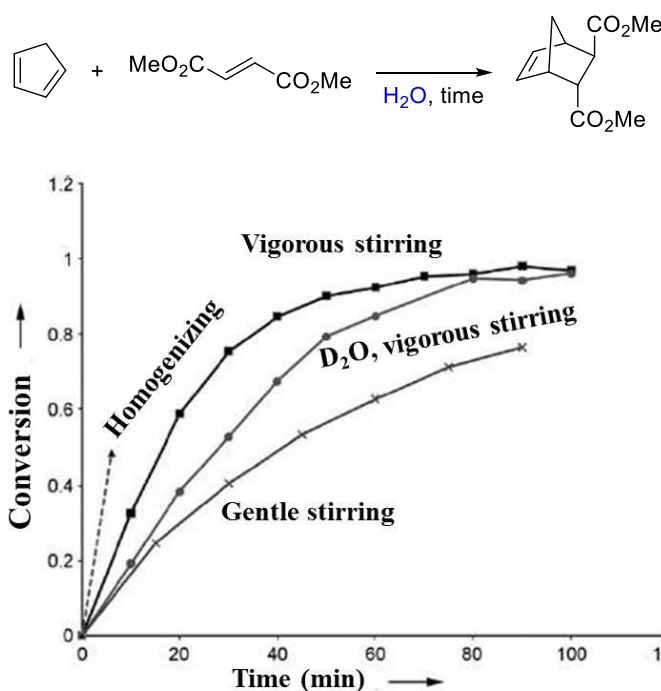
report on microdroplet described below.

Figure 10. Comparison of reaction rates in the reaction of dimethylfumarate with cyclopentadiene (excerpted from the original paper with slight modifications)[124]

Baret *et al*. noted that politer volume droplets were responsible for the rate enhancement despite the inherent thermodynamic unfavorability of the reaction.[126] Their model is based upon the simple reaction-adsorption mechanism coupling bulk and surface reactions that requires only relatively low binding energies of a few van der Waals interactions between reactants and the droplet interface. To begin with, they focused on the reversible reaction of a non-fluorescent amine with weakly fluorescent aldehyde to form a fluorescent imine (Figure 11). The reactants were first put in freestanding water, and then enclosed in tiny droplets, from 2.5 picoliters to 160 picoliters in volume (radius R from 8 to 34 μm). In contrast to the exponential kinetics in bulk, the reaction follows slightly sigmoidal kinetics in droplets, indicating a few-step mechanism. The apparent k_1 was inversely related to the droplet radius, with 45-fold higher in 2.5 pL droplets than that in bulk. The calculated standard Gibbs free energies of the reactants, transition state and product indicated that the reaction became more thermodynamically favorable in droplets. Based upon the mathematical analysis of the observed kinetics, they speculated the reaction-diffusion -adsorption mechanism with reaction thermodynamics being shifted in favor of product formation in droplets (~10 kJ mol^{-1} equilibrium shift in 2.5 pL droplets). Since the energy to form the interface of the 2.5 pL droplets is the same order of magnitude as the chemical energy, the rate enhancement in droplets attributes to the mechanical energy for droplet-formation. The thermodynamic cycle in droplets is governed by four reversible processes containing (1) reaction in bulk, (2) interfacial binding of reactants on the droplet, (3) reaction at interface, and (4) release of product from the interface into bulk.
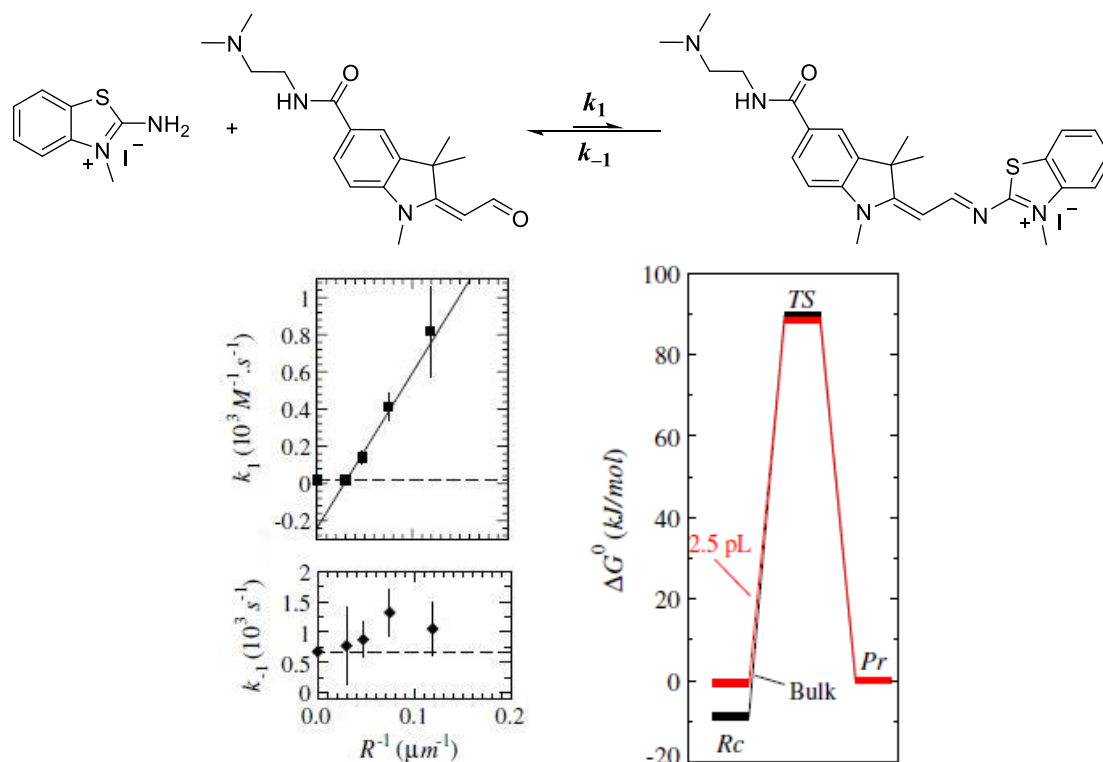
Figure 11. Model reaction and kinetics and thermodynamics studies (rate constant vs reciprocal radius of droplets) (excerpted from the original paper with slight modifications)[126]

The so-called "on water" catalysis still remains unsolved.[127] Indeed, a vigorous exploration of chemical reactions in water led to multifarious new findings incorporated in this dissertation. For instance, chapter 3 describes copper(II)-catalyzed asymmetric boron conjugate additions in water, where two solids reacts with each other successfully, leading to overwhelmingly high catalytic turnover despite the immiscibility of all solid materials (both substrates, copper(II) hydroxide and chiral ligand). While the use of organic solvents ruined the catalysis, the reaction failed to give the desired adduct completely when performed without any solvent (neat conditions). Water is, therefore, *sine qua con* for the reaction progress with high turnover. Incongruous with the aforementioned observations regarding "on-water", the reaction seems, however, to be disqualified for being catalyzed "on-water". First, the reaction is classified as a solid-solid reaction catalyzed by an insoluble solid. The heterogeneity or insolubility of actual catalyst was verified by a lack of catalytic activity in the filtrate. An ICP analysis of the filtrate revealed that Cu content in the filtrate was below the detection limit of the ICP equipment (0.005 ppm). Only a slight drop in reactivity was obtained in the homogeneous aqueous solution (H_2O/THF = 1/4) with almost same level of enantioselectivity as obtained in water, whereas the reaction did not proceed at all in non-aqueous homogeneous solution (THF only). Second, solvent kinetic isotope effect was not observed in this reaction (KIE = 1.01). If chemical society would like to conceptualize the rate-enhancement of chemical reactions sometimes observed in water systematically as "on-water" catalysis, a neologism alternative to "on-water" should be coined at least to be expressive of water-centered views in these reactions.

In biology, a surface on biomacromolecules are said to be surrounded by the collection of one to two layers of water molecules and is known to be an "asymmetric" hydrogen-bonding

environment.   Some evidences indicates that the majority of water molecules in bulk water exhibit a significant asymmetric in the strength of their hydrogen-bondings at any instantaneous time. The O–H stretching vibrational modes of water molecules, a sensitive probe for their hydrogen-bonding environment was calculated at several situations (Figure 12).[128] The higher frequency splitting of water molecules at the water/CCl_4[129] or water/^{n}alkane[130] interface revealed the vibrational asymmetry of water molecules at the interface.   Kumar *et al*. also concluded that the ease of the hydrogen bonding at the interface should be figured out through the preferential solvation of polarizable ions at the water surface and enthalpic and entropic modifications at the interface during a heterogeneous reaction.[131]
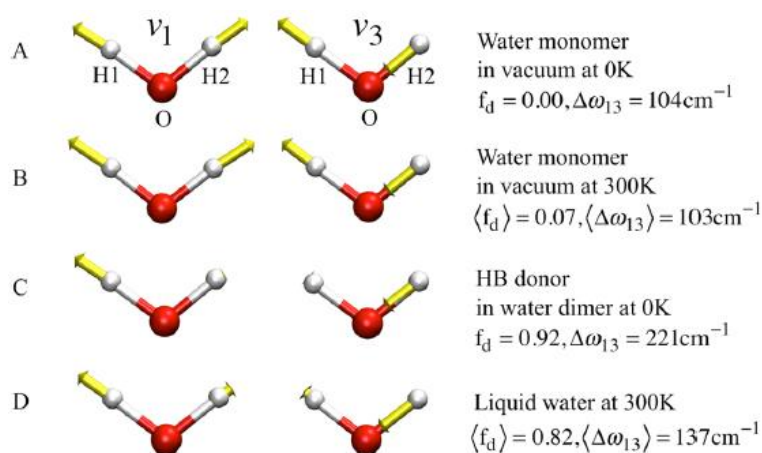
Figure 12. The symmetric and asymmetric stretching modes of a water molecule
(A) In vacuum at 0 K, (B) in vacuum at 300 K, (C) the water dimer at 0 K, acting as a hydrogen-bond donor, (D) in bulk water at 300 K
(excerpted from the original paper with slight modifications)[128]

Throughout the investigations so far, I assume that the rationale of the rate-enhancement in chemical reactions observed in water can be interpreted through a modified mechanism combining Marcus-Jung model, Baret model and Grotthus theory.   The interfacial water molecules liberated from hydrogen-bonding network should play a prominent role in the phenomena.   Although "acid-catalyzed" mechanism may be valid in a sense or in one aspect, it is puzzling and it is a little bit far from the scientific truth.   The irrelevancies of this model are embodied in enantioselective "control" of proton described in Chapter 4.   It is not the case that I am incredulous of electrochemical analysis.   Extraordinal high acidity of interfacial water molecules and the Stern layer surrounding hydrophobic components would result in apparent basicity.   In droplets, protruding water molecules would give an internal layer which adheres to the water-hydrophobe interface.   The "specified" proton of interfacial water molecules would "move around" orderly in this internal layer at high speed, stabilizing the hydrophobic species including the transition state. The systematic transportation of proton in the internal layer would be understood by Grotthus proton-hopping mechanism.   The total reaction progress would be classified into reaction, diffusion and adsorption as Baret *et al*. proposed.   That is, the specific effect of water on chemical reactions is assumed to be characterized by an interior polarized layer formed at interface where protons would be highly transferred.   The acidic property of the water surface is also contended by

the rate-enhancement on the nucleophilic substitution with the series of benzyl alcohols invoking carbocation intermediate[132] and enantioselective protonation in water (Chapter 4).

0-4 Outlook

The water-centered view of organic chemistry was historically arranged in chronological order. In this dissertation a number of new findings on the reaction in water were presented along with some peculiarities such as successful synergistic effect between Lewis acid and Lewis base (Chapter 1), rate-enhancement induced by functional compaction (Chapter 2), overwhelmingly high catalytic turnover (Chapter 3), enantioselective control of proton/deuteron (Chapter 4 & 5) and rate-enhancement induced by metal d-π integration (Chapter 6). It is noteworthy that water is always a prerequisite to these distinguishing qualities. Now is the time to give a shout of victory against "legitimate" organic chemistry that has regarded water as a pariah. These findings would emphasize the need for more suitable conceptualization and coinage for fruits obtained when chemical reactions are performed in water. To understand the rationale of such fruits, a modified mechanism combining Marcus-Jung model, Baret model and Grotthus theory was advocated.

[1] a) P. Grieco Ed. *Organic Reactions in Water*, Chapman & Hall, **1998**; b) C. –J. Li, T. –H. Chan, *Organic Reactions in Aqueous Media*, Wiley: New York, **1997**; c) A. Lubineau, J. Augé, Y. Queneau, *Synthesis* **1994**, 741-760; d) H. –U. Reissig, In *Organic Synthesis Highlights*, H. Waldmann Ed. VCH: Weinheim, **1991**, pp 71; e) C. Einhorn, J. Einhorn, J. Luche, *Synthesis* **1989**, 787-813.

[2] W. Schlenk, A. Thal, *Ber. Dtsch. Chem. Ges.* **1913**, *46*, 2840-2854.

[3] "Water is life's matter and matrix, mother and medium. There is no life without water."

[4] "The substances do not react unless fluid or if dissolved", quoted by Aristotle (384–322 BCE).

[5] F. Szabadváry: *Geschichte der Analytischen Chemie*, Vieweg, Braunschweig, and Akadémiai Kiadó, Budapest, **1966**, p38.

[6] M. Berthelot, L. Péan de Saint-Gilles, *Ann. Chim. Et Phys., Ser. 3*, **1862**, *65*, 385-422; **1862**, *66*, 5-110; **1863**, *68*, 225-359.

[7] E. D. Hughes, C. K. Ingold, *J. Chem. Soc.*, **1935**, *244*, 255-258.

[8] L. Claisen, *Liebigs Ann. Chim.*, **1896**, *291*, 25-137.

[9] U. M. Lindstrom Ed. *Organic Reactions in Water*, Blackwell Publishing, Oxford, **2007**.

[10] D. C. Rideout, R. Breslow, *J. Am. Chem. Soc.* **1980**, *102*, 7816-7817.

[11] R. Breslow, U. Mitra, D. C. Rideout, *Tetrahedron Lett.* **1983**, *24*, 1901-1904.

[12] a) O. Diels, K. Alder, *Justus Liebigs Ann*. **1931**, 490, 243-257; b) R. B. Woodward, H. Baer, *J. Am. Chem. Soc.* **1948**, *70*, 1161-1166; c) H. Hopff, C. W. Rautenstrauch, US Patent **1942**, 2,262,002; d) L. C. Lane, C. H. J. Parker, US Patent **1948**, 2,444,263.

[13] T. A. Eggelte, H. De Koning, H. O. Huisman, *Tetrahedron* **1973**, *29*, 2491-2493.

[14] A. Streitwieser Jr., L. L. Nebenzahl, *J. Am. Chem. Soc.* **1976**, *98*, 2188-2190.

[15] E. Brandes, P. A. Grieco, J. J. Gajewski, *J. Org. Chem.* **1989**, *54*, 515-516.

[16] M. C. Pirrung, K. D. Sarma, *J. Am. Chem. Soc.* **2004**, *126*, 444-445.

[17] B. C. Ranu, S. Banerjee, *Tetrahedron Lett.* **2007**, *48*, 141-143.

[18] a) A. Lubineau, *J. Org. Chem.* **1986**, *51*, 2142-2144; b) A. Lubineau, E. Meyer, *Tetrahedron* **1988**, *44*, 6065-6070.

[19] T. Mukaiyama, K. Banno, K. Narasaka, *J. Am. Chem. Soc.* **1974**, *96*, 7503-7509.

[20] Y. Yamamoto, K. Maruyama, K. Matsumoto, *J. Am. Chem. Soc.* **1983**, *105*, 6963-6965.

[21] A. Lubineau, G. Bouchain, *Tetrahedron Lett.* **1997**, *38*, 8031-8032.

[22] R. Herter, B. Föhlisch, *Synthesis* **1982**, 976-979.

[23] G. Jenner, *Tetrahedron Lett.* **2002**, *43*, 1235-1238.

[24] T. Yamada, T. Yanagi, Y. Omote, T. Miyazawa, S. Kuwata, M. Sugiura, K. Matsumoto, *J. Chem. Soc., Chem. Commun.* **1990**, 1640-1641.

[25] A. Lubineau, J. Augé, *Top. Curr. Chem.* **1999**, *206*, 1-39.

[26] T. –P. Loh, L. –C. Feng, L. –L. Wei, *Tetrahedron*, **2000**, *56*, 7309-7312.

[27] Investigation on transition state geometry of the aldol reaction in aqueous media, see: S. Denmark, W. Lee, R. Adams, *Tetrahedron Lett.* **1992**, *33*, 7729–7732.

[28] J. Alam, T. Keller, T. Loh, *J. Am. Chem. Soc.* **2010**, *132*, 9546–9548.

[29] M. D. Rosa, A. Soriente, *Tetrahedron* **2011**, *67*, 5949–5955.

[30] a) Y. Huang, V. H. Rawal, *Org. Lett.* **2001**, *2*, 3321–3323; b) Y. Huang, V. H. Rawal, *J. Am. Chem. Soc.* **2002**, *124*, 9662–9663.

[31] a) Y. –Y. Lin, M. Risk, S. M. Ray, D. V. Engen, J. Clardy, J. Golik, J. C. James, K. Nakanishi, *J. Am. Chem. Soc.* **1981**, *103*, 6773-6775; b) K. Nakanishi, *Toxicon* **1985**, *23,* 473-479; *c.f.* Stork-Eschenmoser hypothesis: G. Stork, A. W. Burgstahler, *J. Am. Chem. Soc.* **1955**, *77*, 5068-5077.

[32] Recent study on enzymatic catalysis: K. Hotta, X. Chen, R. S. Paton, A. Minami, K. Swaminathan, I. I. Mathews, K. Watanabe, H. Oikawa, K. N. Houk, C. –Y. Kim, *Nature* **2012**, *483*, 355-358;

[33] a) I. Vilotijevic, T. F. Jamison, *Science* **2007**, *317*, 1189-1192; b) C. J. Morten, J. A. Byers, T. F. Jamison, *J. Am. Chem. Soc.* **2011**, *133*, 1902-1908

[34] H. Yorimitsu, T. Nakamura, H. Shinokubo, K. Oshima, K. Omoto, H. Fujimoto, *J. Am. Chem. Soc.* **2000**, *122*, 11041-11047.

[35] M. Newcomb, D. P. Curran, *Acc. Chem. Res.* **1988**, *21*, 206-214.

[36] The first ionization potential of indium is 5.8 eV; First example on the use of indium(0) as a radical initiator, see: H. Miyabe, M. Ueda, A. Nishimura, T. Naito, *Org. Lett.* **2002**, *4*, 131-134.

[37] A. Postigo, S. Kopsov, C. Ferreri, C. Chatgilialoglu, *Org. Lett.* **2007**, *9*, 5159-5162.

[38] S. B. –Vallejo, A. Postigo, *J. Org. Chem.* **2010**, *75*, 6141-6148.

[39] X. X. Rong, H. –Q. Pan, W. R. Dolbier Jr., *J. Am. Chem. Soc.* **1994**, *116*, 4521-4522.

[40] They are reported to be prepared in aqueous solution: (a) K. F. Thom, U.S. Patent 3615169, **1971**; CA 1972, 76, 5436a; (b) J. H. Forsberg, V. T. Spaziano, T. M. Balasubramanian, G. K. Liu, S. A. Kinsley, C. A. Duckworth, J. J. Poteruca, P. S. Brown, J. L. Miller, *J. Org. Chem.* **1987**, *52*, 1017-1021.

[41] a) S. Kobayashi, *Chem. Lett*. **1991**, 2187-2190; b) S. Kobayashi, Lanthanide Triflate-Catalyzed Carbon–Carbon Bond-Forming Reactions in Organic Synthesis. In *Lanthanides: Chemistry and Use in Organic Synthesis*; S. Kobayashi, Ed.; Springer: Heidelberg, **1999**; c) S. Kobayashi, *Eur. J. Org. Chem.* **1999,** 15-27; d) S. Kobayashi, *Synlett* **1994**, 689-701; e) S. Kobayashi, M. Sugiura, H. Kitagawa, W. W.-L. Lam, *Chem. Rev*. **2002**, *102*, 2227-2302; f) S. Kobayashi, C. Ogawa, *Chem. Eur. J*. **2006**, *12*, 5954-5960.

[42] S. Kobayashi, I. Hachiya, Y. Yamanoi, *Bull. Chem. Soc. Jpn*. **1994**, *67*, 2342-2344.

[43] a) S. Kobayashi, I. Hachiya, *Tetrahedron Lett*. **1992**, *33*, 1625-1628; b) S. Kobayashi, I. Hachiya, *J. Org. Chem*. **1994,** *59*, 3590-3596; c) S. Kobayashi, *Synlett* **1994**, 689-699.

[44] The aldols were obtained only in ca. 10% yields.

[45] a) T. A. Geissman, *Org. React*. **1944**, *2*, 94-113; b) T. Neilsen, A. T. Houlihan, *Org. React*. **1968**, *16*, 1-438.

[46] For example, paraformaldehyde and trioxane.

[47] S. Arseniyadis, Q. Wang, D. V. Yashunsky, T. Kaoudi, R. B. Alves, P. Potier, *Tetrahedron Lett*. **1995**, *36*, 1633-1636.

[48] P. Bernardelli, O. M. Moradei, D. Friedrich, J. Yang, F. Gallou, B. P. Dvck, R. W. Doskotch, T. Lange, L. A. Praquette, *J. Am. Chem. Soc.* **2001**, *123*, 9021-9032.

[49] (a) K. C. Nicolaou, X. Huang, N. Giuseppone, P. B. Rao, M. Bella, M. V. Reddy, S. A. Snyder, *Angew. Chem. Int. Ed.* **2001**, *40*, 4705-4709; (b) K. C. Nicolaou, J. Hao, M. V. Reddy, P. B. Rao, G. Rassias, S. A. Synder, X. Huang, D. Y. –K. Chen, W. E. Brenzovich, N. Giuseppone, P. Giannakakou, A. O'Brate, *J. Am. Chem. Soc.* **2004**, *126*, 12897-12906.

[50] T. Ohshima, Y. Xu, R. Takita, S. Shimizu, D. Zhong, M. Shibasaki, *J. Am. Chem. Soc.* **2002**, *124*, 14546-14547.

[51] J. Shiina, M. Oikawa, K. Nakamura, R. Obata, S. Nishiyama, *Eur. J.Org. Chem.* **2007**, 5190-5197.

[52] a) N. Kagawa, M. Ihara, M. Toyota, *Org. Lett.* **2006**, *8*, 875-878; b) N. Kagawa, M. Ihara, M. Toyota, *J. Org. Chem.* **2006**, *71*, 6796-6805.

[53] A. Mendoza, Y. Ishihara, P. S. Baran, *Nature Chem.* **2012**, *4*, 21-25.

[54] S. Kobayashi, S. Nagayama, T. Busujima, *J. Am. Chem. Soc.* **1998**, *120*, 8287–8288.

[55] a) C. F. Baes, Jr., R. E. Mesmer, *The Hydrolysis of Cations*, John Wiley & Sons: New York, **1976**; b) K. B. Yatsimirksii, V. P. Vasil'ev, *Instability Constants of Complex Compounds*; Pergamon: New York, **1960**; c) A. E. Martell, Ed.; *Coordination Chemistry*; ACS Monograph 168; American Chemical Society: Washington, DC, **1978**; Vol. 2.

[56] Fringuelli and co-workers reported use of Al^{III}, Ti^{IV}, and Sn^{IV} as Lewis acids for epoxide opening reactions in acidic water whose pH is adjusted by adding H_2SO_4. F. Fringuelli, F. Pizzo, L. Vaccaro, *J. Org. Chem.* **2001,** *66*, 3554-3558.

[57] The pHs of $Yb(OTf)_3$ solutions were measured as follow: 5.90 ($1.6*10^{-2}$ M, H_2O/THF = 1/4), 6.40 ($8.0*10^{-2}$ M, H_2O).

[58] D. J. Averill, P. Dissanayake, M. J. Allen, *Molecules* **2012**, *17*, 2073-2081.

[59] C. H. Heathcock, In *Asymmetric Synthesis, Vol. 3, Part B*; J. D. Morrison, Ed.; Academic Press: New York, 1984, 111.

[60] $8×10^3$ according to ref. 26.

[61] S. Murata, M. Suzuki, R. Noyori, *J. Am. Chem. Soc.* **1980**, *102*, 3248-3249.

[62] M. Hatanaka, S. Maeda, K. Morokuma, *J. Chem. Theo. Comp.* **2013**, *9*, 2882–2886.

[63] C. Loncaric, K. Manabe, S. Kobayashi, *Adv. Synth. Catal.* **2003**, *345*, 475-477.

[64] S. Kobayashi, T. Wakabayashi, S. Nagayama, H. Oyamada, *Tetrahedron Lett.* **1997**, *38*, 4559–4562.

[65] a) S. Kobayashi, T. Wakabayashi, *Tetrahedron Lett.* **1998**, *39*, 5389–5392; b) S. Kobayashi, K. Manabe, In *Clean Solvents*, ACS Symposium Series, **2002**, *819*, 151–1665; c) M. Shiri, M. Zolfigol, *Tetrahedron* **2009**, *65*, 587–598.

[66] The rate acceleration by copper(II) bis(dodecylsulfate) $Cu(DS)_2$ in Diels–Alder reactions in water was described previously, see: S. Otto, F. Bertoncin, J. B. F. N. Engberts, *J. Am. Chem. Soc.* **1996**, *118*, 7702–7707.

[67] Y. Mori, K. Kakumoto, K. Manabe, S. Kobayashi, *Tetrahedron Lett.* **2000**, *41*, 3107-3111.

[68] a) K. Manabe, S. Kobayashi, *Synlett* **1999**, 547–548; b) S. Kobayashi, K. Manabe, *Acc. Chem. Res.* **2002**, *35*, 209–217.

[69] For example, Mannich-type reactions: K. Manabe, S. Kobayashi, *Org. Lett.* **1999**, *1*, 1965–1967; Diels–Alder reactions: K. Manabe, Y. Mori, S. Kobayashi, *Tetrahedron* **1999**, *55*, 11203–11208; Michael reactions: Y. Mori, K. Kakumoto, K. Manabe, S. Kobayashi, *Tetrahedron Lett.* **2000**, *41*, 3107–3111.

[70] T. Dwars, E. Paetzold, G. Oehme, *Angew. Chem. Int. Ed.* **2005**, *44*, 7174–7199.

[71] M. Fujita, T. Nagano, U. Schneider, T. Hamada, C. Ogawa, S. Kobayashi, *J. Am. Chem. Soc.* **2008**, *130*, 2914-2915.

[72] S. Kobayashi, T. Endo, U. Schneider, M. Ueno, *Chem. Commun.* **2010**, *46*, 1260-1262.

[73] M. Ueno, A. Tanoue, S. Kobayashi, *Chem. Lett.* **2010**, *39*, 652-653.

[74] M. Ueno, A. Tanoue, S. Kobayashi, *Chem. Lett.* **2014**, *43*, 1867-1869.

[75] a) S. Kobayashi, T. Kitanosono, M. Ueno, *Synlett* **2010**, 2033-2036.

[76] E. Klijn, J. B. F. N. Engberts, *Nature* **2005**, *435*, 746-747

[77] H. W. Roesky, M. G. Walawalkar, R. Murugavel, *Acc. Chem. Res.* **2001**, *34*, 201-211.

[78] a) B. Li, P. H. Dixneuf, *Chem. Soc. Rev.* **2013**, *42*, 5744-5767; b) R. N. Butler, A. G. Coyne, *Chem. Rev.* **2010**, *110*, 6302-6337.

[79] A. L. Casalnuovo, J. C. Calabrese, *J. Am. Chem. Soc.* **1990**, *112*, 4324-4330.

[80] a) C. Dupuis, K. Adiey, L. Charruault, V. Michelet, M. Savignac, J. –P. Genêt, *Tetrahedron Lett.* **2001**, *42*, 6523-6526; b) J. –P. Genêt, A. Linquist, E. Blard, V. Mouries, M. Savignac, M. Vaultier, *Tetrahedron Lett.* **1995**, *36*, 1443-1446; c) J. –P. Genêt, E. Blard, M. Savignac, *Synlett* **1992**, 715-717.

[81] J. –C. Galland, M. Savignac, J. –P. Genêt, *Tetrahedron Lett.* **1999**, *40*, 2323-2326.

[82] K. H. Shaughnessy, *Metal-Catalyzed Cross-Couplings of Aryl Halides to Form C–C Bonds in Aqueous Media*, In "*Metal-Catalyzed Reactions in Water*" Ed. by S. Kobayashi, **2013**.

[83] a) B. H. Lipshutz, A. R. Abela, *Org. Lett.* **2008**, *10*, 5329-5332; b) B. H. Lipshutz, T. B. Petersen, A. R. Abela, *Org. Lett.* **2008**, *10*, 1333-1336.

[84] B. H. Lipshutz, D. W. Chung, B. Rich, *Org. Lett.* **2008**, *10*, 3793-3796.

[85] a) A. Krasovskiy, I. Thomé, J. Graff, V. Krasovskaya, P. Konopelski, C. Duplais, B. H. Lipshutz, *Tetrahedron Lett.* **2011**, *52*, 2203-2205; b) A. Krasovskiy, C. Duplais, B. H. Lipshutz, *Org. Lett.* **2010**, *12*, 4742-4744; c) A. Krasovskiy, C. Duplais, B. H. Lipshutz, *J. Am. Chem. Soc.* **2009**, *131*, 15592-15593.

[86] B. H. Lipshutz, D. W. Chung, B. Rich, *Adv. Synth. Catal.* **2009**, *351*, 1717-1721.

[87] a) B. H. Lipshutz, S. Ghorai, A. R. Abela, R. Moser, T. Nishikata, C. Duplais, A. Krasovskiy, R. D. Gaston, R. C. Gadwood, *J. Org. Chem.* **2011**, *76*, 4379-4391; b) B. H. Lipshutz, S. Ghorai, *Aldrichimica Acta* **2008**, *41*, 59-88.

[88] Recent examples, see: a) N. A. Isley, M. S. Hageman, B. H. Lipshutz, *Green Chem.* **2015**, *17*, 893-897; b) E. D. Slack, C. M. Gabriel, B. H. Lipshutz, *Angew. Chem. Int. Ed.* **2014**, *53*, 14051-14054; c) S. Handa, D. J. Lippincott, D. H. Aue, B. H. Lipshutz, *Angew. Chem. Int. Ed.* **2014**, *53*, 10658-10662; d) R. T. H. Linstadt, C. A. Peterson, D. J. Lippincott, C. I. Jette, B. H. Lipshutz, *Angew. Chem. Int. Ed.* **2014**, *53*, 4159-4163; e) S. Handa, J. C. Fennewald, B. H. Lipshutz, *Angew. Chem. Int. Ed.* **2014**, *53*, 3432-3435; f) B. H. Lipshutz, M. Haqeman, J. C. Fennewald, R. Linstadt, E. Slack, K. Voiqtritter, *Chem. Commun.* **2014**, *50*, 11378-11381; g) S. R. K. Minkler, N. A. Isley, D. J. Lippincott, N. Krause, B. H. Lipshutz, *Org. Lett.* **2014**, *16*, 724-726.

[89] L. Chen, C. –J. Li, *Chem. Commun.* **2004**, 2362-2364.

[90] J. Oliver–Meseguer, J. R. Cabrero-Antonino, I. Domínguez, A. Leyva-Pérez, A. Corma, *Science* **2012**, *338*, 1452-1455.

[91] C. Wei, C. –J. Li, *J. Am. Chem. Soc.* **2003**, *125*, 9584-9585.

[92] A. Robertson, T. Matsumoto, S. Ogo, *Dalton Trans.* **2011**, *40*, 10304-10310.

[93] a) A. Bényei, F. Joó, *J. Mol. Catal.* **1990**, *58*, 151-163; b) F. Joó, A. Bényei, *J. Organomet. Chem.* **1989**, *363*, C19-C21.

[94] C. Larpent, R. Dabard, H. Patin, *Tetrahedron Lett.* **1987**, *28*, 2507-2510.

[95] A. Kulkarni, W. H. Zhou, B. Torok, *Org. Lett.* **2011**, *13*, 5124-5127.

[96] X. Wu, J. Xiao, *Hydrogenation and Transfer Hydrogenation in Water*, In "Metal-Catalyzed Reactions in Water" Ed. by S. Kobayashi, **2013**.

[97] S. Ogo, N. Makihara, Y. Watanabe, *Organometallics* **1999**, *18*, 5470-5474.

[98] R. Breslow, *Acc. Chem. Res.* **1991**, *24*, 159-164.

[99] a) R. Breslow, T. Guo, *J. Am. Chem. Soc.* **1988**, *110*, 5613-5617; b) R. Breslow, C. J. Rizzo, *J. Am. Chem. Soc.* **1991**, *113*, 4340-4341.

[100] M. A. Forman, W. P. Dailey, *J. Am. Chem. Soc.* **1991**, *113*, 2761-2762.

[101] Breslow made insightful comments in Ref. 98: "…simply seeing an increased rate of reaction in water does not establish that a hydrophobic effect is involved."

[102] Y. Yamamoto, K. Maruyama, K. Matsumoto, *J. Am. Chem. Soc.* **1983**, *105*, 6963-6965.

[103] M. C. Pirrung, *Chem. Eur. J.* **2006**, *12*, 1312-1317.

[104] T. Yamaguchi, Y. Sakae, Y. Zhang, S. Yamamoto, Y. Okamoto, K. Kato, *Angew. Chem. Int. Ed.* **2014**, *53*, 10941-10944.

[105] J. A. Rupley, G. Careri, *Adv. Protein Chem.* **1991**, *41*, 37-172.

[106] J. A. Byers, T. F. Jamison, *PNAS* **2013**, *110*, 16724-16729.

[107] G. Graziano, *J. Chem. Phys. Soc.* **2004**, *121*, 1878-1882.

[108] Review on the effect of water, see: M. Pirrung, *Chem. Eur. J.* **2006**, *12*, 1312-1317.

[109] Investigation on transition state geometry of the aldol reaction in aqueous media, see: S. Denmark, W. Lee, R. Adams, *Tetrahedron Lett.* **1992**, *33*, 7729-7732.

[110] S. Otto, J. B. F. N. Engberts, *Org. Biomol. Chem.* **2003**, *1*, 2809-2820.

[111] S. Narayan, J. Muldoon, M. G. Finn, V. V. Fokin, H. C. Kolb, K. B. Sharpless, *Angew. Chem. Int. Ed.* **2005**, *44*, 3275-3279.

[112] D_2O has a 3% higher cohesive pressure and a 23% higher viscosity than H_2O.

[113] Y. Jung, R. A. Marcus, *J. Am. Chem. Soc.* **2007**, *129*, 5492-5502.

[114] a) Q. Du, R. Superfine, E. Freysz, Y. R. Shen, *Phys. Rev. Lett.* **1993**, *70*, 2313-2316; b) Q. Du, E. Freysz, Y. R. Shen, *Science* **1994**, *264*, 826-828; c) Y. R. Shen, V. Ostroverkhov, *Chem. Rev.* **2006**, *106*, 1140-1154.

[115] O. Acevedo, K. Armacost, *J. Am. Chem. Soc.* **2010**, *132*, 1966-1975.

[116] L. L. Thomas, J. Tirado-Rives, W. L. Jorgensen, *J. Am. Chem. Soc.* **2010**, *132*, 3097-3104.

[117] J. A. Berson, Z. Hamlet, W. A. Mueller, *J. Am. Chem. Soc.* **1962**, *84*, 297-304.

[118] J. F. Blake, W. L. Jorgensen, *J. Am. Chem. Soc.* **1991**, *113*, 7430-7432.

[119] K. Hori, T. Yamaguchi, K. Uezu, M. Sumimoto, *J. Compt. Chem.* **2011**, *32*, 778-786.

[120] For instance KIE for the reaction of quadricyclane with dimethylazodicarboxylate is 4.5, whereas that for the reaction with diethylazodicarboxylate is 1.2, see Ref. 111.

[121] M. Mucha, T. Frigato, L. M. Levering, H. C. Allen, D. J. Tobias, L. X. Dang, P. Jungwirth, *J. Phys. Chem. B.* **2005**, *109*, 7617-7623.

[122] J. C. Carruthers, *Trans. Faraday Soc.* **1938**, *34*, 0300-0307.

[123] A. Graciaa, G. Morel, P. Saulner, J. Lachaise, R. S. Schechter, *J. Colloid Interface Sci.* **1995**, *172*, 131-136.

[124] J. K. Beattie, C. S. P. McErlean, C. B. W. Phippen, *Chem. Eur. J.* **2010**, *16*, 8972-8974.

[125] K. D. Beare, C. S. P. McErlean, *Org. Biomol. Chem.* **2013**, *11*, 2452-2459.

[126] A. F. –Araghi, K. Meguellati, J. –C. Baret, A. El Harrak, T. Mangeat, M. Karplus, S. Ladame, C. M. Marques, A. D. Griffiths, *Phys. Rev. Lett.* **2014**, *112*, 028301-1-028301-5.

[127] R. Stahl, In *Unsolved Problems in Chemistry*.

[128] C. Zhang, R. Z. Khaliullin, D. Bovi, L. Guidoni, T. D. Kühne, *J. Phys. Chem. Lett.* **2013**, *4*, 3245-3250.

[129] L. Scatena, M. Brown, G. Richmond, *Science* **2001**, *292*, 908-912.

[130] M. Brown, D. Walker, E. Raymond, G. Richmond, *J. Phys. Chem. B* **2003**, *107*, 237-244.

[131] A. Manna, A. Kumar, *J. Phys. Chem. A* **201**3, *117*, 2446-2454.

[132] For instance, see: a) C. D. Ritchie, *Acc. Chem. Res.* **1972**, *5*, 348–354; b) S. Shirakawa, S. Kobayashi, *Org. Lett.* **2007**, *18*, 311-314; b) P. G. Cozzi, L. Zoli, *Angew. Chem. Int. Ed.* **2008**, *47*, 4162-4166.

Chapter 1 : Development of Catalytic Asymmetric Mukaiyama Aldol Reactions in Aqueous Environments

Section 1.1 Asymmetric Mukaiyama Aldol Reactions in Aqueous Media

1.1-1 Introduction & History of Asymmetric Mukaiyama Aldol Reaction

The aldol reaction provides one of the most fundamental and reliable methods for stereoselective C–C bond formation in organic chemistry.   Despite its potential versatility, classical aldol reactions performed under basic conditions have suffered from generally low yields and selectivities owing to their reversibility and many competitive side pathways such as dehydration, dimerization, polymerization, and self-condensation.[1] The emergence of $TiCl_4$-mediated aldol reactions of silicon enolates (silyl enol ethers) with aldehydes in 1973—the renowned Mukaiyama aldol reactions—has allowed us to avoid these competitive processes.   Being unresponsive towards aldehydes under ambient conditions, silicon enolates react with aldehydes *via* Lewis acid catalysis.   Aldehydes possess more acidic α-protons and are apt to undergo unproductive homo-aldol reactions.   In addition, the desired β-hydroxycarbonyl product is more basic than the starting substrates, resulting in a quite low catalyst turnover.   Such limitations can be circumvented by combining preformed silicon enolates and Lewis acid catalysis, because the dimerization of aldehydes can be suppressed under mild conditions and the resulting silylated aldol adducts allow for catalyst turnover.

Following the stoichiometric use of chiral sources for chiral induction, the age of catalytic asymmetric synthesis had dawned.   However, almost all successful examples of catalytic asymmetric Mukaiyama aldol reactions reported for organic solvents since 1990[2] have entailed absolutely aprotic anhydrous conditions and quite low reaction temperatures (e.g., –78 °C). Meanwhile, it has been reported that aqueous environments sometimes lead to rate enhancement and unusual selectivity in several reactions including Mukaiyama aldol reactions.[3] Facile, convenient, and environmentally benign methodologies without tedious operation are desirable. The discovery of water-compatible Lewis acids in 1991[4] contributed significantly to an explosive advance in this field.   A major difficulty in the construction of asymmetric environments in aqueous conditions is the weakness of noncovalent interactions between substrates, chiral ligands, and metal ions under competitive polar conditions.   Conversely, it is anticipated that undesired unselective side reactions can be inhibited and stereochemical regulation stricter than that for other organic solvents can be imposed employing a hydrogen bond network, specific solvation, and hydrophobic interactions, if such processes can be strictly controlled.   Herein, recent attempts at this challenging endeavor are highlighted.   The underlying strategies in common are **1) the chiral aqua complex being stable**, **2) rapid and facile replacement of the coordinated water molecule by an aldehyde molecule**, and **3) one enantioface of a coordinated aldehyde carbonyl being shielded effectively**.
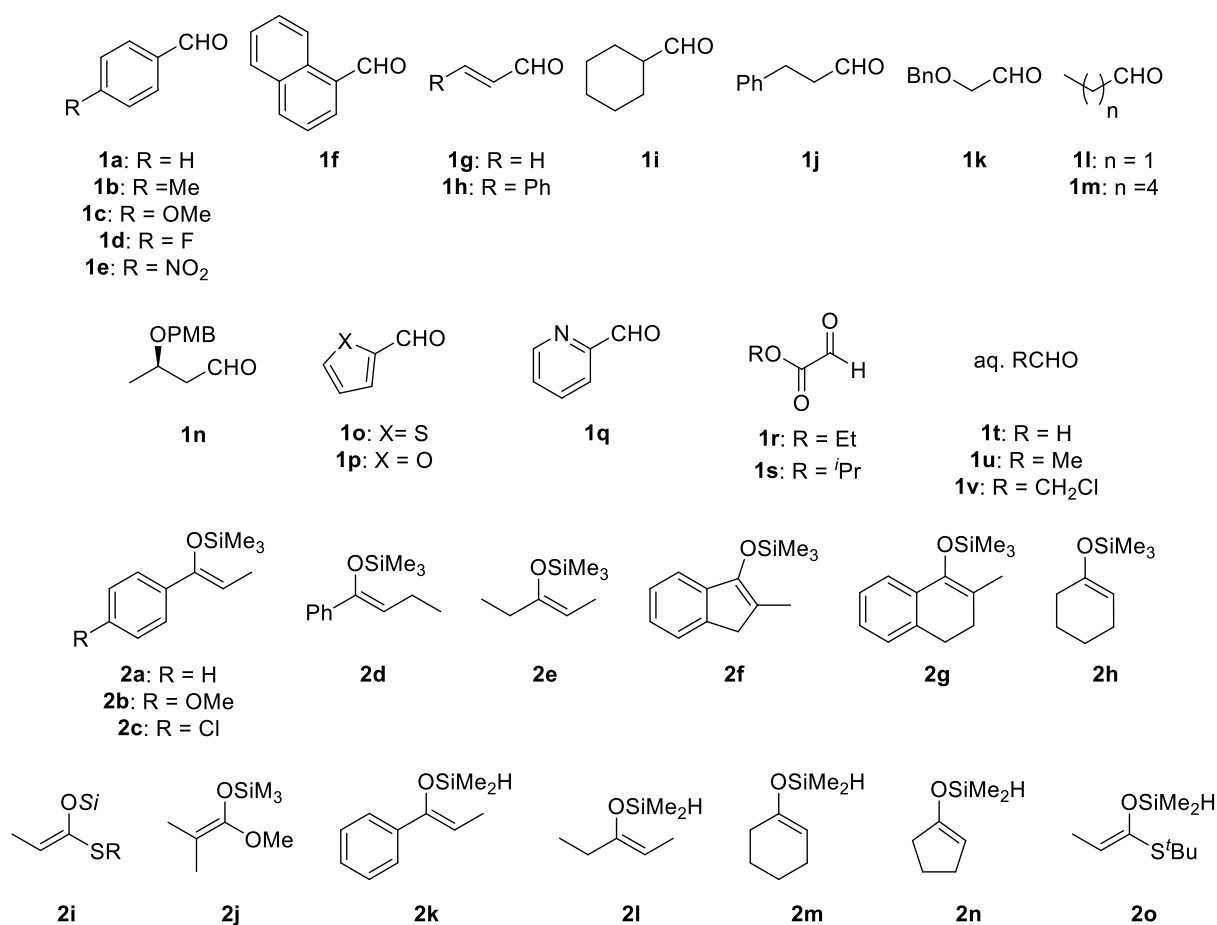
Figure 1. Aldehydes (**1**) and silicon enolates (**2**) employed in asymmetric Mukaiyama aldol reactions.
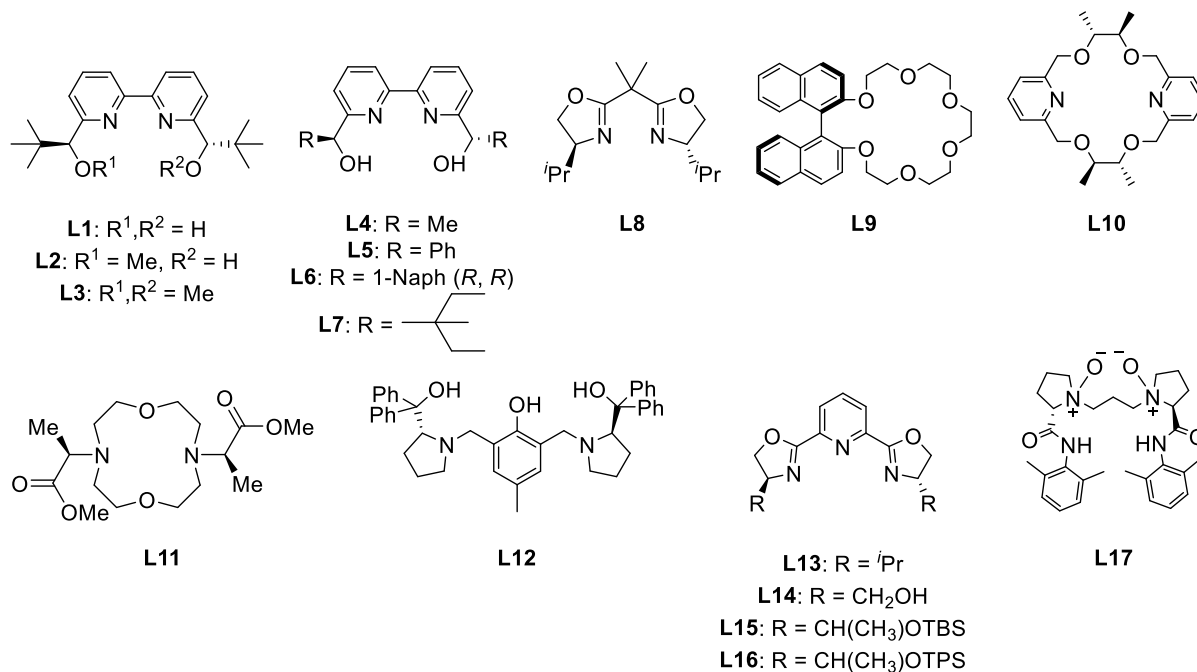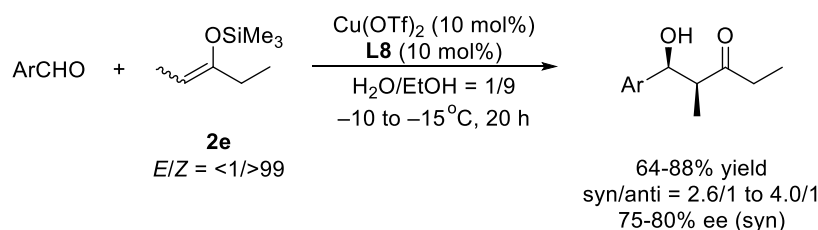

Figure 2. Ligands employed in catalytic asymmetric Mukaiyama aldol reactions in aqueous media

Among water-compatible Lewis acids investigated so far, copper(II) aqua structures formed with chiral bis(oxazoline) templates were depicted in many reports even though they are normally prepared under anhydrous conditions.[5,6] These results allude to the latent stability of copper(II)-bis(oxazoline) **L8** (for all ligands, **L**, see Figure 2) complex in an aqueous environment. That is why the first example of an asymmetric Mukaiyama aldol reaction in aqueous media relied on copper(II)-bis(oxazolines) complexes.[7] The Mukaiyama aldol reactions of (*Z*)-enolate **2e** with aldehydes were catalyzed by a chiral copper(II) complex efficiently in aqueous ethanol (H$_2$O/EtOH = 1/9) to afford the desired aldol adducts with moderate to good yields and enantioselectivities (Scheme 1). A (*Z*)-isomer provides higher yield and diastereo- and enantioselectivities than an (*E*)-isomer. It is noteworthy that much lower yields and selectivities are observed without water. The catalytic system was applied to the first example of Lewis acid-catalyzed asymmetric aldol reactions in pure water as the combination of Cu(DS)$_2$ (DS = OSO$_3$C$_{12}$H$_{25}$) with chiral **L8**.[8] Given the dominance of *Lewis acid–Lewis base interactions* over other interactions and the resulting loss of acidity upon coordination to chiral ligands, Lewis acid-catalyzed asymmetric reactions in water using hydrophilic substrates are recognized as highly challenging even though chiral induction can be achieved in aqueous media.[9]

ArCHO + (OSiMe$_3$ enolate) **2e** *E/Z* = <1/>99 → Cu(OTf)$_2$ (10 mol%) **L8** (10 mol%), H$_2$O/EtOH = 1/9, −10 to −15 °C, 20 h → aldol product (OH O, Ar) 64-88% yield, syn/anti = 2.6/1 to 4.0/1, 75-80% ee (syn)

Scheme 1. First example of an asymmetric Mukaiyama aldol reaction in aqueous media.

Another prescription to overcome the instability of chiral metal complexes in an aqueous environment is exploitation of multi-coordination systems. The detailed inspection of the combination of chiral crown ethers **L9** and metal triflates on the basis of ionic radii[10] and the hole sizes[11] led to the discovery of an efficient chiral lead(II) catalyst for asymmetric Mukaiyama aldol reactions in aqueous media (Scheme 2).[12,13,14] Compared with chiral copper(II) catalyst, the diastereo- and enantioselectivity of the desired adduct improved. Furthermore, this system could be applied to thioester-derived silicon enolates as nucleophiles. The complex between Pb(OTf)$_2$ and chiral crown ether **L9** was quantitatively recovered by simple extraction. The chiral lead(II) complex was characterized by one longer bond between Pb and the oxygen connected to the naphthalene rings, which would be ascribed to the dihedral angle between the two naphthalene rings. It was assumed that the water molecule at the apical position was replaced by an aldehyde, facilitating the catalyst turnover. A kinetic study performed for an asymmetric reaction and a Pb(OTf)$_2$-catalyzed achiral reaction resulted in the observation of almost comparable reaction rates and the same levels of diastereoselectivity.
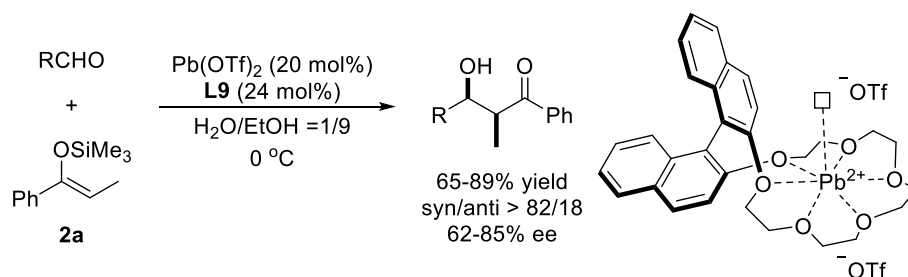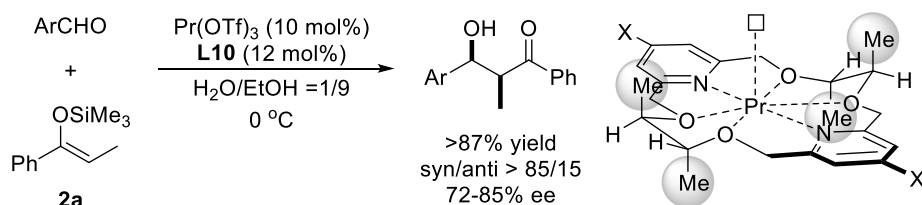
Scheme 2. Chiral lead(II) catalyst for enantioselective Mukaiyama aldol reactions.

Unlike the case for early transition metals, precise control of lanthanides is difficult owing to their large ionic radii, coordination numbers, and WERCs. The lanthanide coordination takes place predominantly via ionic interactions, leading to a strong preference for negatively charged donor groups. Since lanthanides are known to promote epimerization between *syn-* and *anti-*adduct via keto-enolization, presumably owing to their greater Lewis acidity in aqueous media (Scheme 3),[15] multicoordination systems would also play a prominent role in reactions between hydrophobic substrates.

Scheme 3. Plausible epimerization induced by lanthanides.

Indeed, a chiral complex comprising $Ln(OTf)_3$ and chiral bis-pyridino-18-crown-6 **L10** was found to be effective for the asymmetric Mukaiyama aldol reactions (Scheme 4).[16,17] Although ^{1}H NMR studies revealed the strong binding of **L10** to lanthanide cations, the asymmetric reaction with lanthanide complexes slightly decelerated the reaction rate compared with the corresponding achiral pathway without the chiral crown ether. In organic solvents, the coordination of heteroatoms generally leads to the loss of Lewis acidity of a metal, owing to the behavior of the heteroatoms as Lewis bases. In contrast, it seems that subsequent coordination of water molecules generates a naked metal cation, which functions as a Lewis acid in an aqueous environment. In the structure, the Pr cation is located almost in the plane of the crown ring and the methyl groups of the chiral ligand are all in axial positions. A vacant site at the apical position of the Pr cation was suggested to be crucial for catalytic activity as a recipient of an aldehyde molecule.

Scheme 4. Chiral praseodymium catalyst for enantioselective Mukaiyama aldol reactions.

Highly selective stereocontrol was attributed to the size-fitting between the crown ethers and the metal cations; the larger cations such as La, Ce, Pr, and Nd yielding the aldol adduct with

high diastereo- and enantioselectivities, while the smaller cations such as Dy, Ho, Yb, Y, and Sc resulted in lower selectivities. Introduction of an electron-donating (MeO) group at the 4 position of the pyridine rings afforded high selectivities for the larger cations and lower selectivities for the smaller cations. In the case of an electron-withdrawing (Br) group, although a similar tendency was observed, the effect of ionic radii was more significant. Allen *et al.* engaged in the modification of macrocyclic gadolinium-containing polyaminopolycarboxylate-based contrast agents for magnetic resonance imaging,[18] and Eu(III) or Nd(III) complexes formed with **L11** were applied to asymmetric Mukaiyama aldol reactions in aqueous media (Scheme 5). Unfortunately, these complexes possessed lower catalytic activities and the activities were highly dependent on the substrates.[19]
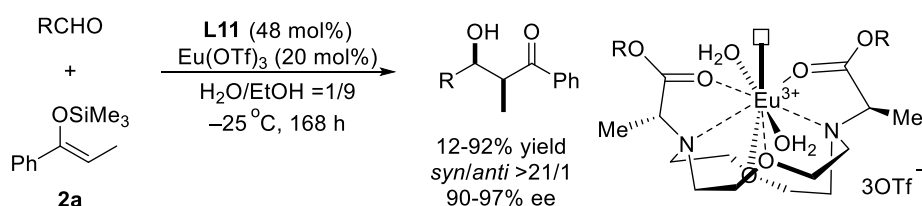
Scheme 5. Chiral lanthanide catalysts for enantioselective Mukaiyama aldol reactions.

The Pr-**L9** complex was applicable to the catalytic asymmetric hydroxymethylation reaction, albeit with low selectivity (Scheme 6a).[20] This is the first report of the catalytic asymmetric hydroxymethylation of silicon enolates. Contemporaneously, a bifunctional system of (*R*)-BINAP-AgOTf complex with a fluoride source was applied as a Lewis-base catalyst for the asymmetric hydroxymethylation of trimethoxysilyl enol ethers derived from cyclohexanone (31% yield, 57% ee) or α-tetralone (18% yield, 57% ee) in aqueous tetrahydrofuran, albeit in low yield (Scheme 6b).[21]
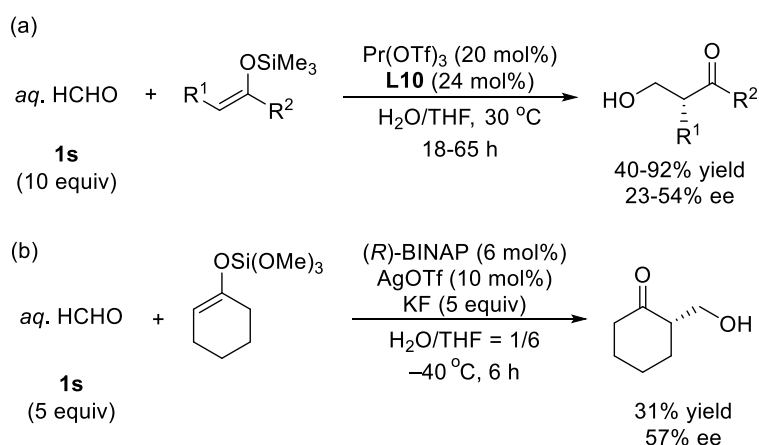
Scheme 6.   (a) Praseodymium- and (b) silver-catalyzed asymmetric hydroxymethylation in aqueous media.

In 2004, an excellent new catalytic system based on a chiral scandium complex was devised. Chiral 2,2′-bipyridine **L1**[22] was chosen as a ligand candidate for its coordination potentiality as the N_2O_2 cavity. The reaction proceeded smoothly to afford the hydroxymethylated

product with higher yields and enantioselectivities when compared with previous systems (Scheme 7).[23] The chiral scandium complex formed with **L1** turned out to function most effectively in a H$_2$O/dimethoxyethane (DME) solution. Under optimal conditions, asymmetric quaternary carbons can be obtained with high selectivities, and this methodology can be extended to various substrates such as thioester-derived silicon enolates. In some cases, there is competitive hydrolysis of silicon enolates, which can be resolved by the addition of 2,6-di-*tert*-butylpyridine as a proton scavenger.[24] Judging from X-ray crystallographic analysis, the chiral scandium complex adopts a pentagonal bipyramidal structure where the chiral ligand is bound to the central scandium in a tetradentate manner.
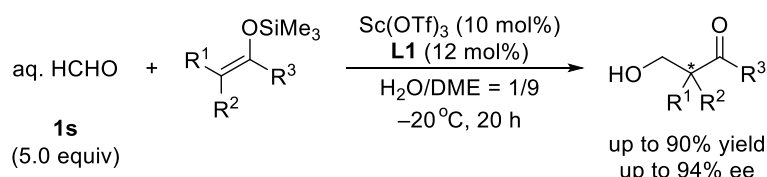
Scheme 7. Scandium-catalyzed asymmetric hydroxymethylation in aqueous media.

Catalytic asymmetric hydroxymethylation reactions without the use of any organic solvent were successfully carried out with 10 mol% of Sc(DS)$_3$ and 12 mol% of chiral 2,2′-bipyridine **L1** in the presence of Triton X-705 or with 10 mol% of Sc(OSO$_2$C$_{12}$H$_{25}$)$_3$ and 12 mol% of chiral *N*-oxide ligand **L16**[25] in the presence of C$_{12}$H$_{25}$SO$_3$Na to afford the desired aldol adducts in high yields and with high enantioselectivities (Scheme 8).[26] A wide range of silicon enolates including thioketene silyl acetals reacted smoothly and high enantioselectivities were attained. The centrifugation of the reaction mixture (3000 rpm, 20 min) led to successful separation of the colloidal dispersion into three phases: upper, middle, and bottom phases corresponding to the water, surfactant, and organic layers, respectively.
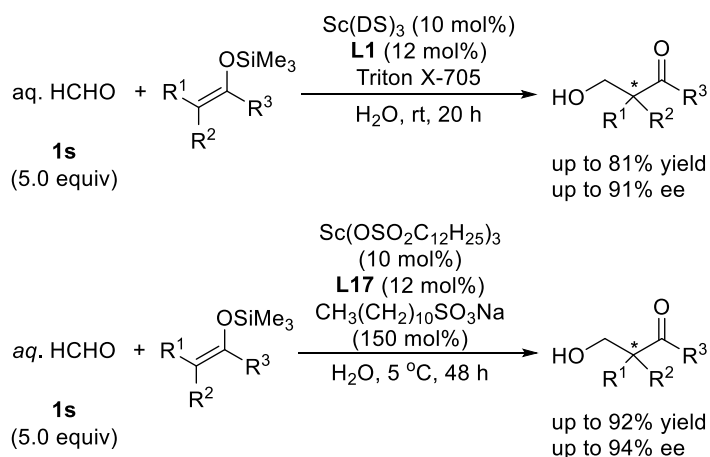
Scheme 8. Asymmetric Mukaiyama aldol reactions using formaldehyde in water.

An extensive effort dedicated to the asymmetric hydroxymethylation in aqueous media led to the discovery of a new catalytic system composed of Bi(OTf)$_3$ and chiral 2,2′-bipyridine **L1** (Scheme 9).[27] Given the ease of hydrolysis in the presence of water,[28] as well as the great

discrepancy in the ionic diameters between bismuth (2.34 Å for 8-coordination) and scandium (1.74 Å for 8-coordination), this unexpected result offered an interesting insight into asymmetric catalysis in an aqueous environment. Indeed, only a trace amount of hydroxymethylated adduct was obtained using Bi(OTf)$_3$ in the absence of **L1**, owing to rapid decomposition of the silicon enolate promoted by TfOH generating readily from Bi(OTf)$_3$ in water. The ligand acceleration effect of **L1** suggests that the stabilization of Bi(OTf)$_3$ is due to the coordination of **L1** in water. A chiral bismuth catalyst comprising 1 mol% of Bi(OTf)$_3$, 3 mol% of **L1**, and 5 mol% of 2,2′-bipyridyl was shown to afford the desired product in high yields with high enantioselectivities. Fundamental elucidation of the catalyst structure through NMR spectroscopy indicated that two equivalents of Bi(OTf)$_3$ and one equivalent of **L1** formed complex **A**, and that complex **B** consisting of one equivalent of Bi(OTf)$_3$ and one equivalent of **L1** was generated when an excess amount of **L1** was added (Scheme 10). It is noted that complex **B** is stable even in the presence of 2,2′-bipyridine, and that **B** readily forms from Bi(OTf)$_3$-2,2′-bipyridine complex and **L1**.
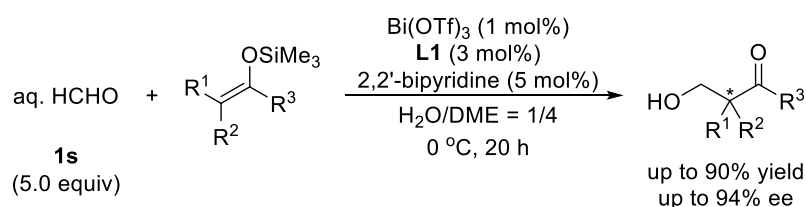
Scheme 9. Bismuth-catalyzed asymmetric hydroxymethylation in aqueous media.
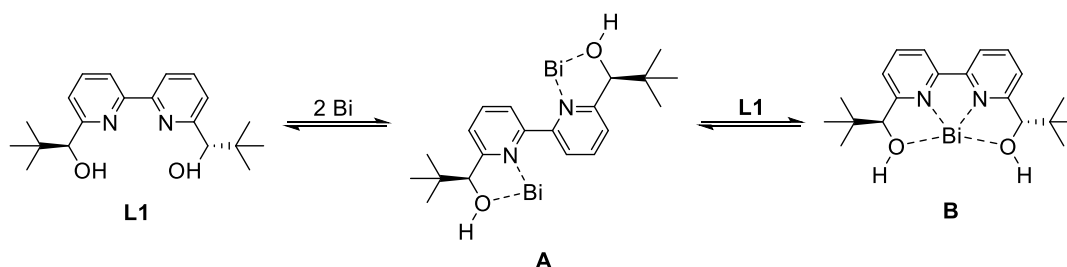
Scheme 10. Equilibrium between bismuth-2,2′-bipyridine **L1** complexes.

In 2002, Ga(OTf)$_3$ with chiral Trost-type semi-crown ligand **L11**[29] was reported as an efficient catalyst for asymmetric Mukaiyama aldol reactions in aqueous media (Scheme 11).[30] The substrate scope containing thioketene silyl acetals was comparably wide, except for the use of aliphatic aldehydes resulting in a significant loss of enantioselectivity. UV-vis titration and ESI-MS analysis confirmed this gallium complex to be a 1:1 complex.[31] Control experiments performed without the ligand suggested that it played a key role in accelerating the reaction and suppressing the hydrolysis of the silicon enolates.
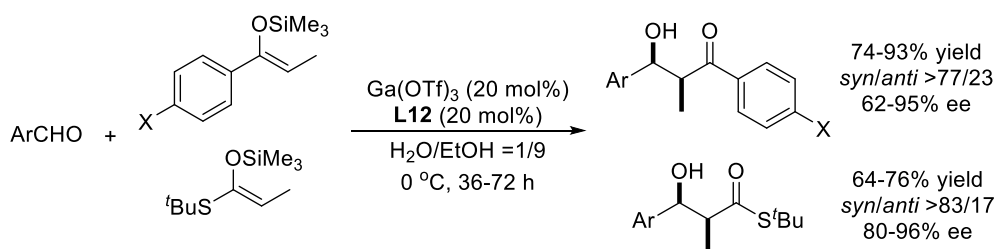
Scheme 11. Chiral gallium catalyst for enantioselective Mukaiyama aldol reactions.

The C_2-symmetric bis(oxazolines) disubstituted with two Fréchet-type polyether dendrimers exhibited similar reactivities and enantioselectivities (up to 78% yield, *syn/anti* = 2.2/1, 64% ee [*syn*]) for the asymmetric Cu(II)-catalyzed aldol reaction in aqueous media in comparison with Kobayashi's previous work (98% yield, *syn/anti* = 2.6/1, 61% ee [*syn*]) (Scheme 12).
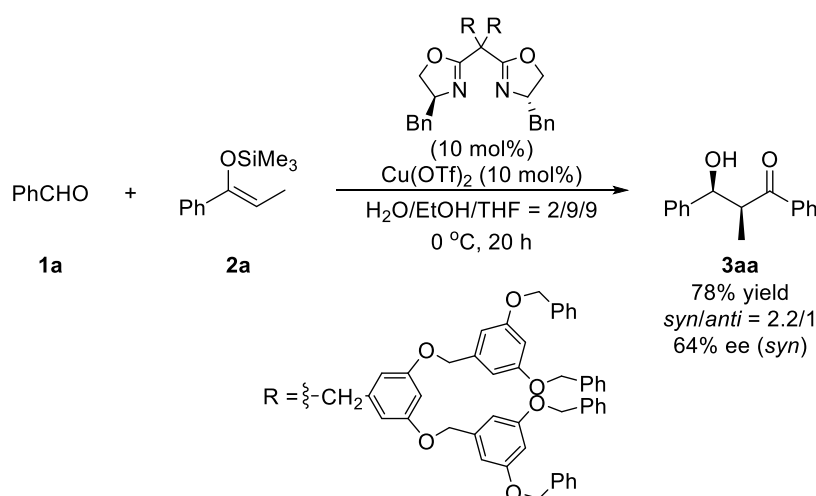

Scheme 12. Chiral dendritic copper(II) catalyst for enantioselective Mukaiyama aldol reactions.

Chiral catalysts formed with Zn(OTf)$_2$ and ^{i}Pr-pybox ligand **L12**[32] or FeCl$_2$ and hydroxymethyl-pybox ligand **L13**[33] were also reported for the asymmetric Mukaiyama aldol reactions in aqueous media (Scheme 13). Although both aliphatic and aromatic aldehydes were applicable with moderate selectivity, aldehydes bearing heteroatoms and aqueous aldehydes were apt to be unsuccessful in the former catalytic system. Meanwhile, the latter catalyst was effective for the reactions of aromatic aldehydes, having one example using aliphatic aldehyde with low enantioselectivity (23% ee). To overcome the instability, capriciousness, and sensitivity of chiral iron(II) and zinc(II) complexes in response to many reaction factors, tuned and lipophilic pybox ligands **L14** and **L15** were developed.[34] Although the selectivity improved comparatively in the reactions of some substrates, the reactions of aliphatic aldehydes still suffered from a significant drop in reactivity and selectivity.
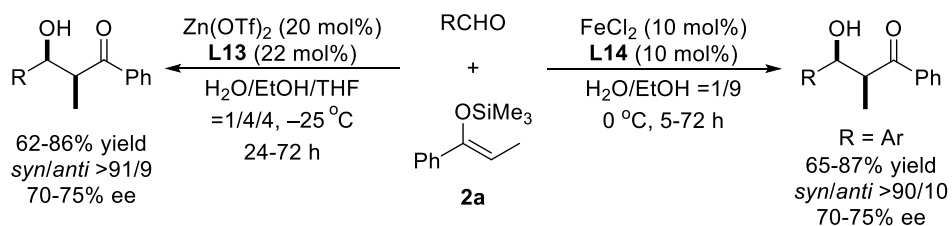
Scheme 13. Chiral zinc(II) and iron(II) catalysts for asymmetric Mukaiyama aldol reactions.
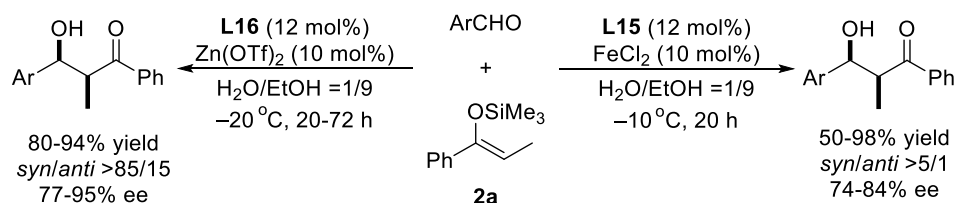
Scheme 14. Designed chiral iron(II) and zinc(II) catalysts.

In spite of these vigorous explorations pursuing efficient catalytic systems, there are still two insurmountable limitations in catalytic activity and substrate scope: **1) almost all catalytic systems entail 10–20 mol% of Lewis acids and 12–48 mol% of chiral ligands**, and **2) the methodologies possess limited substrate scope; some substrates such as aliphatic aldehydes, for which a remarkable drop in enantioselectivity** is commonly observed.

1.1-2 Construction of Asymmetric Environment in Water for Lewis Acid -Catalyzed Mukaiyama Aldol Reactions in Aqueous Media

Among the effective Lewis acids reported so far, the activities of Cu^{II}, Pb^{II}, Ln^{III} (e.g., Sc^{III}, La^{III}, Pr^{III}), Fe^{II}, and Zn^{II} as Lewis acids are in accord with the Lewis acid series predicted in 1998. The catalytic activities of Ga^{III} and Bi^{III} are, however, contrary to that prediction. Both Ga^{III} and Bi^{III} themselves are inclined toward hydrolysis in water to form gel-like polymeric hydroxide species. Despite their inherent weak Lewis acidities due to their ease of hydrolysis,[35] they exhibit the pronounced ligand acceleration in the presence of an appropriate ligand. It means that the electrostatic tuning of Ga^{III} or Bi^{III} center through leveraging appropriate ligands impede the cumbersome hydrolysis pathway and make them stable even in water. This result is suggestive of the latent ability of inactive metal cations, which should be exerted only in the presence of ligands. It appears that the coordination environment of metal cations should play a prominent role in uncovering their latent activity.

Taking the specific nature of forming complexes with almost all metals into consideration, 2,2'-bipyridine is an efficient candidate for a "privileged" structure of chiral ligand which can function in an aqueous environment. Indeed due to their coordinative potentiality as N_2O_2 cavity, crystallographic investigations on the complex formed with metal cation was succeeded in $Cu(I)$[22b], $Sc(III)$[23], $Bi(III)$[27], $In(III)$[36], $Y(III)$[37], $Cu(II)$[38], $Zn(II)$[39] and $Fe(II)$[40] either in a tetradentate or in a tridentate manner. In addition, several pioneering reports revealed that the combination of **L1** or derivatives and a few metal cations exhibits efficient performance in an aqueous environment for aforementioned enantioselective hydroxymethylation reactions[23,27,26], ring-opening reactions of *meso*-epoxides[38,41,42], Nazarov cyclizations,[43] α-alkyl- or α-chloroallylation of aldehyde[39] *etc*. The outstanding power of **L1** in aqueous environments directed our interest into the comprehensive and comparative studies of metal-**L1** complex. In order to expand the potentiality of metal-**L1** complexes as chiral Lewis acid catalysts, the Mukaiyama aldol reaction of benzaldehyde **1a** with propiophenone-derived silyl enol ether **2a** was carried out in the presence of 10 mol% of several Lewis acids and 12 mol% of **L1** in aqueous media (Table 1, defined as System A). Metal trifluoromethanesulfonates (triflates) or metal perchlorates were chosen as Lewis acids, because previous studies in water proved that the generation of naked metal cations is crucial for attainment of high Lewis acidity in an aqueous environment. The reaction suffered from low yield when any metal was used except Sc^{III}, whereas relatively high enantioselectivities were obtained by using Al^{III}, Sc^{III}, Fe^{II}, Cu^{II}, Cd^{II}, Sn^{II}, Yb^{III}, Lu^{III}, Hg^{II}, Pb^{II}, and Bi^{III}. In the case of rare earth metals, Y^{III} gave almost the same level of selectivity as Sc^{III}, whereas the late lanthanides afforded the product in a good selective manner. Former lanthanides such as Ce^{III} are known to be prone to promote the epimerization between *syn*-**3aa** and *anti*-**3aa** via keto-enolization presumably due to their greater Lewis acidity. In asymmetric hydroxymethylation, a dramatic improvement of yield and selectivity has been previously attained when $Bi(OTf)_3$ and **L1** were combined in the ratio of 1:3.[27] To bring the hidden Lewis acidity to light, a 3-fold excess of **L1** with 3 mol% of Lewis acids was also examined (Table 2, defined as System B). Indeed, throughout the screening, the excessive use of **L1** has turned out to be effective for several Lewis acids.

Table 1. Evaluation of Lewis Acidity in Asymmetric Mukaiyama Aldol Reaction 1.

PhCHO + (2a, Ph–C(OSiMe₃)=CH₂) → [L1 (12 mol%), MX$_n$ (10 mol%), H₂O/DME = 1/9, 0 °C, 24 h] → *syn*-**3aa** (2*S*,3*S*) + *anti*-**3aa** (2*R*,3*S*)

1a   **2a** (1.2 equiv.)

Legend: M^{n+} / yield^a(dr^b) / %ee^c

^{a} Isolated yield (%).
^{b} Determined by ^{1}H NMR analysis (*syn/anti*).
^{c} Determined by HPLC analysis (*syn/anti*).

G1	G2	G3	G4	G5	G6	G7	G8	G9	G10	G11	G12	G13	G14	G15
Li⁺ NR	Be²⁺ – / –											B³⁺ – / –	C – / –	N – / –
Na⁺ NR	Mg²⁺ NR											Al³⁺ 4(61/39) –51/3	Si⁴⁺ – / –	P⁵⁺ – / –
K⁺ NR	Ca²⁺ NR	Sc³⁺ 52(64/36) 24/1	Ti⁴⁺ – / –	V⁵⁺ – / –	Cr³⁺ 7(67/33) –4/23	Mn²⁺ NR	Fe²⁺/³⁺ NR	Co²⁺ 17(90/10) –7/<1	Ni²⁺ 2(68/32) –11/42	Cu²⁺ 8(82/18) –41/4	Zn²⁺ NR	Ga³⁺ 4(71/29) –11/9	Ge⁴⁺ –	As³⁺/⁵⁺ –
Rb⁺ tr(87/13) 5/27	Sr²⁺ – / –	Y³⁺ 9(65/35) 24/4	Zr⁴⁺ 12(74/26) –16/24	Nb⁵⁺ –	Mo⁶⁺ –	Tc⁴⁺ –	Ru³⁺ –	Rh³⁺ –	Pd²⁺ –	Ag⁺ NR	Cd²⁺ 11(89/11) 3/13	In³⁺ 8(89/11) 26/–9	Sn²⁺ 14(84/16) 1/22	Sb³⁺/⁵⁺ –
Cs⁺ – / –	Ba²⁺ NR	Ln³⁺	Hf⁴⁺ 6(71/29) 42/10	Ta⁵⁺ –	W⁶⁺ –	Re⁴⁺ –	Os⁴⁺ –	Ir⁴⁺ –	Pt²⁺ –	Au⁺ –	Hg²⁺ 27(98/2) 66/77	Tl⁺ 3(88/12) –3/26	Pb²⁺ 28(89/11) –32/78	Bi³⁺ 10(95/5) 69/17

Hg⁺ 3(65/35) –5/31

La³⁺	Ce³⁺ / Ce⁴⁺	Pr³⁺	Nd³⁺	Pm³⁺	Sm³⁺	Eu³⁺	Gd³⁺	Tb³⁺	Dy³⁺	Ho³⁺	Er³⁺	Tm³⁺	Yb³⁺	Lu³⁺
59(55/45) –3/7	38(52/48) –1/3 ; Ce⁴⁺ 10(56/44) –2/18	74(51/49) –1/6	41(49/51) 0/5	–	27(53/47) –6/4	97(53/47) 2/6	18(56/44) –4/–1	11(59/41) 7/2	79(63/37) 25/32	62(67/33) 29/19	28(71/29) 43/40	80(76/24) 44/28	66(79/21) 60/23	55(79/21) 62/6

Table 2. Evaluation of Lewis Acidity in Asymmetric Mukaiyama Aldol Reaction 2.

PhCHO + (2a, Ph–C(OSiMe₃)=CH₂) → [L1 (9 mol%), MX$_n$ (3 mol%), H₂O/DME = 1/9, 0 °C, 24 h] → *syn*-**3aa** (2*S*,3*S*) + *anti*-**3aa** (2*R*,3*S*)

1a   **2a** (1.2 equiv.)

Legend: M^{n+} / yield^a(dr^b) / %ee^c

^{a} Isolated yield (%).
^{b} Determined by ^{1}H NMR analysis (*syn/anti*).
^{c} Determined by HPLC analysis (*syn/anti*).

G1	G2	G3	G4	G5	G6	G7	G8	G9	G10	G11	G12	G13	G14	G15
Li⁺ NR	Be²⁺ – / –											B³⁺ – / –	C – / –	N – / –
Na⁺ NR	Mg²⁺ 2(85/15) –37/26											Al³⁺ 5(73/27) –7/1	Si⁴⁺ – / –	P⁵⁺ – / –
K⁺ NR	Ca²⁺ 4(84/16) –4/29	Sc³⁺ 23(80/20) 59/4	Ti⁴⁺ – / –	V⁵⁺ – / –	Cr³⁺ 6(76/24) –7/14	Mn²⁺ 4(91/9) –2/45	Fe³⁺ 15(96/4) 1/4 ; Fe²⁺ 70(97/3) 75/43	Co²⁺ 6(87/13) 3/6	Ni²⁺ 12(87/13) 24/2	Cu²⁺ 5(88/12) –57/0	Zn²⁺ 27(73/27) –4/2	Ga³⁺ 3(77/23) 0/11	Ge⁴⁺ –	As³⁺/⁵⁺ –
Rb⁺ NR	Sr²⁺ – / –	Y³⁺ 7(85/15) 29/0	Zr⁴⁺ 20(52/48) <1/10	Nb⁵⁺ –	Mo⁶⁺ –	Tc⁴⁺ –	Ru³⁺ –	Rh³⁺ –	Pd²⁺ –	Ag⁺ 6(88/12) 25/4	Cd²⁺ 36(88/12) –32/66	In³⁺ 67(59/41) –8/17	Sn²⁺ 5(85/15) 75/6	Sb³⁺/⁵⁺ –
Cs⁺ – / –	Ba²⁺ 4(78/22) –21/6	Ln³⁺	Hf⁴⁺ 5(58/42) 0/5	Ta⁵⁺ –	W⁶⁺ –	Re⁴⁺ –	Os⁴⁺ –	Ir⁴⁺ –	Pt²⁺ –	Au⁺ –	Hg²⁺ 2(49/51) –5/4	Tl⁺ 4(84/16) –2/0	Pb²⁺ 22(90/10) –1/25	Bi³⁺ 17(>99/<1) 91/31

La³⁺	Ce³⁺ / Ce⁴⁺	Pr³⁺	Nd³⁺	Pm³⁺	Sm³⁺	Eu³⁺	Gd³⁺	Tb³⁺	Dy³⁺	Ho³⁺	Er³⁺	Tm³⁺	Yb³⁺	Lu³⁺
38(60/40) 0/<1	26(54/46) –1/4 ; Ce⁴⁺ 16(58/42) –2/12	60(51/49) 0/2	62(50/50) 0/<1	–	68(51/49) 1/3	64(54/46) 1/<1	69(54/46) –8/14	62(57/43) 7/5	57(61/39) 24/8	66(64/36) 9/15	61(68/32) 19/21	56(75/25) 47/13	63(76/24) 38/28	19(81/19) 53/9

The results are summarized in Table 3. Although all reactivities were low except for those of lanthanides, Al^{III}, Yb^{III}, Lu^{III}, and Hg^{II} afforded higher selectivities in the presence of 1.2 equivalents of **L1**. In addition, an excessive use of **L1** could bring out the hidden activities of Fe^{II}, Cu^{II}, Sn^{II}, and Bi^{III} in a higher stereoselective manner, providing much lower selectivities in the presence of 1.2 equivalents of **L1**. However, the yields were low using Al^{III} and Cu^{II} in both System A and B. As for Cd^{II} and Pb^{II}, relatively high enantioselectivities were observed for only minor diastereomers. While System A gave higher enantioselectivities for Yb^{III} and Hg^{II}, System B showed higher enantioselectivities for Sc^{III}, Fe^{II}, and Sn^{II}. Both System A and B showed high enantioselectivities for Lu^{III} and Bi^{III}. Among them, it is noted that Bi^{III} showed very high selectivities (*syn/anti* = >99/<1, 91% ee (*syn*)) in System B. Moreover, while no reaction took place using Fe^{II} in System A, an outstanding level of product yield and promising selectivity (70% yield, dr 97/3, 75% ee (*syn*)) were obtained in System B.

Table 3. Summary of Metal Screening for Asymmetric Aldol Reaction in Aqueous Media.

Scheme: PhCHO (**1a**) + Ph–C(OSiMe₃)=CH–CH₃ (**2a**, 1.2 equiv.), with **L1** (y mol%), MX_n (x mol%), $H_2O/DME = 1/9$, 0 °C, 24 h → *syn*-**3aa** (2S,3S) + *anti*-**3aa** (2R,3S).

Legend:
- M^{n+}, yield[a](dr[b]), %ee[c], L/M = 1.2
- M^{n+}, yield[a](dr[b]), %ee[c], L/M = 3
- [a] Yield of isolated product (%).
- [b] Determined by ^1H NMR analysis (*syn/anti*).
- [c] Determined by HPLC analysis (*syn/anti*).
- [d] X = OTf, ClO₄

Each cell: element — yield(dr) — %ee (syn/anti)

Element	yield(dr)	%ee (syn/anti)
Li⁺	NR	
Na⁺	NR	
K⁺	NR	
Rb⁺	tr(87/13)	5/27
Cs⁺	–	–
Be²⁺	–	–
Mg²⁺	2 (85/15)	–37/26
Ca²⁺	4 (84/16)	–4/29
Sr²⁺	–	–
Ba²⁺	4 (78/22)	–21/6
Sc³⁺	23(80/20)	59/4
Y³⁺	7 (85/15)	29/0
Ti⁴⁺	–	–
Zr⁴⁺	12(74/26)	–16/24
Hf⁴⁺	6 (71/29)	42/10
V⁵⁺	–	–
Nb⁵⁺	–	–
Ta⁵⁺	–	–
Cr³⁺	6 (76/24)	–7/14
Mo⁶⁺	–	–
W⁶⁺	–	–
Mn²⁺	4 (91/9)	–2/45
Tc⁴⁺	–	–
Re⁴⁺	–	–
Fe³⁺	15 (96/4)	1/4
Fe²⁺	70 (97/3)	75/43
Ru³⁺	–	–
Os⁴⁺	–	–
Co²⁺	17(90/10)	–7/<–1
Rh³⁺	–	–
Ir⁴⁺	–	–
Ni²⁺	12(87/13)	24/2
Pd²⁺	–	–
Pt²⁺	–	–
Cu²⁺	5 (88/12)	–57/0
Ag⁺	6 (88/12)	25/4
Au⁺	–	–
Zn²⁺	27(73/27)	–4/2
Cd²⁺	36(88/12)	–32/66
Hg²⁺	27(98/2)	66/77
Hg⁺	3 (65/35)	–5/31
B³⁺	–	–
Al³⁺	4 (61/39)	–51/3
Ga³⁺	4 (71/29)	–11/9
In³⁺	8 (89/11)	26/–9
Tl⁺	4 (84/16)	–2/0
C	–	–
Si⁴⁺	–	–
Ge⁴⁺	–	–
Sn²⁺	5 (85/15)	75/6
Pb²⁺	28(89/11)	–32/78
N	–	–
P⁵⁺	–	–
As³⁺/⁵⁺	–	–
Sb³⁺/⁵⁺	–	–
Bi³⁺	17(>99/<1)	91/31

Lanthanides (Ln^{3+}):

Element	yield(dr)	%ee (syn/anti)
La³⁺	38(60/40)	0/<1
Ce³⁺	26(54/46)	–1/4
Ce⁴⁺	16(58/42)	–2/12
Pr³⁺	60(51/49)	0/2
Nd³⁺	62(50/50)	0/<1
Pm³⁺	–	–
Sm³⁺	68(51/49)	1/3
Eu³⁺	64(54/46)	1/<1
Gd³⁺	69(54/46)	–8/14
Tb³⁺	62(57/43)	7/5
Dy³⁺	79(63/37)	25/32
Ho³⁺	62(67/33)	29/19
Er³⁺	28(71/29)	4/40
Tm³⁺	80(76/24)	44/28
Yb³⁺	66(79/21)	60/23
Lu³⁺	55(79/21)	62/6

Regarding ionic radii of various six-coordinated metal cations (Table 4),[44] these results have shown that chiral 2,2′-bipyridine **L1** formed complexes with a wide variety of metal cations; ionic radii of those cations have a minimum of 53.5 pm (Al(III)) and a maximum of 119 pm (Pb(II)). Metal cations which produced the enantioselectivity exceeding 10% *ee*, obviously not within an instrumental error range, were painted pinkish.

Table 4. Ionic radii of elements.

Li^+ 76	Be^{2+} 45											B^{3+} –	C –	N –
Na^+ 102	Mg^{2+} 72											Al^{3+} 53.5	Si^{4+} –	P^{5+} –
K^+ 138	Ca^{2+} 99	Sc^{3+} 74.5	Ti^{4+} 60.5	V^{5+} 54	Cr^{2+} 73^b / Cr^{3+} 61.5	Mn^{2+} 67^b	Fe^{2+} 61^b / Fe^{3+} 55^b	Co^{2+} 65^b / Co^{3+} 54.5	Ni^{2+} 69	Cu^{2+} 73	Zn^{2+} 74	Ga^{3+} 62	Ge^{4+} 53	As^{3+} 58
Rb^+ 152	Sr^{2+} 118	Y^{3+} 90	Zr^{4+} 72	Nb^{5+} 64	Mo^{6+} 59	Tc^{4+} 64.5	Ru^{3+} 68	Rh^{3+} 66.5	Pd^{2+} 86	Ag^+ 115	Cd^{2+} 95	In^{3+} 80	Sn^{2+} 73-119	Sb^{3+} 76
Cs^+ 167	Ba^{2+} 135	Ln^{3+}	Hf^{4+} 71	Ta^{5+} 64	W^{6+} 60	Re^{4+} 63	Os^{4+} 63	Ir^{3+} 68	Pt^{2+} 80	Au^+ 137	Hg^{2+} 102	Tl^+ 150	Pb^{2+} 119	Bi^{3+} 103

La^{3+} 103.2	Ce^{3+} 101 / Ce^{4+} 87	Pr^{3+} 99	Nd^{3+} 98.3	Pm^{3+} 97	Sm^{3+} 95.8	Eu^{3+} 94.7	Gd^{3+} 93.5	Tb^{3+} 92.3	Dy^{3+} 91.2	Ho^{3+} 90.1	Er^{3+} 89	Tm^{3+} 88	Yb^{3+} 86.8	Lu^{3+} 86.1

Legend: M^{n+} ionic radii (ppm)^a *known (reported or unreported)* · M^{n+} ionic radii (ppm)^a *plausible complexation (major : >10% ee)* · *tetra- or tridentate* · ^{a} definition: CN = 6 · ^{b} *low spin*

Since easily available salts were tested for the screening, the effect of counteranion on Lewis acid catalysis was examined. For instance, comparatively high level of selectivity have been achieved when 10 mol% of Hg(OTf)$_2$ and 12 mol% of **L1** were employed (Table 1 or 3 or Run 1 in Table 5). In contrast, moderate diastereoselectivity and low enantioselectivity was observed when Hg(ClO$_4$)$_2$ was employed instead of Hg(OTf)$_2$ (Entry 4). And HgClO$_4$ provided almost same level of selectivity as Hg(ClO$_4$)$_2$ (Entry 3). The Frost diagram of Hg

Frost diagram of Hg

species clearly denies the possibility of disproportionation of Hg_2^{2+} species or reduction of Hg^{2+}. Therefore the difference between Entry 1 and Entry 4 was indicated to derive from the stability of Hg salts in an aqueous environment.

Table 5. Effect of counteranion in Hg^{II}-**L1** system.
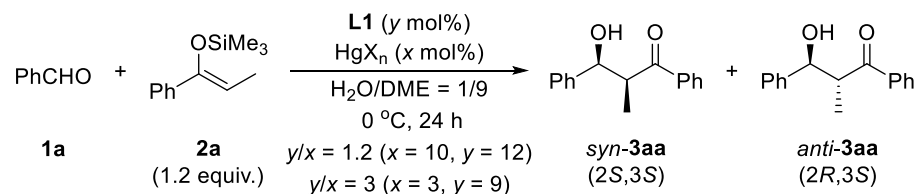
Entry	Hg salt (*y/x* ratio)	Yield (%)	Dr (syn/anti)[a]	Ee (%)[b]
1	$Hg(OTf)_2$ (1.2)	27	98/2	66/77
2	$Hg(OTf)_2$ (3)	2	49/51	–5/4
3	$HgClO_4$ (1.2)	3	65/35	5/31
4	$Hg(ClO_4)_2$ (1.2)	4	68/32	4/31

[a] Determined by ^{1}H NMR analysis.   [b] Determined by HPLC analysis, *syn/anti*.

The remarkable drop in selectivity caused by excessive use of chiral ligand can be explained by the loss of Lewis acidity (Entry 2).   Among tested metal cations, cobalt(II) was turned out to make an interesting difference by a type of counteranion, albeit low enantioselectivity (Table 6).

Table 6. Effect of Counteranion in Co^{II}-**L1** system
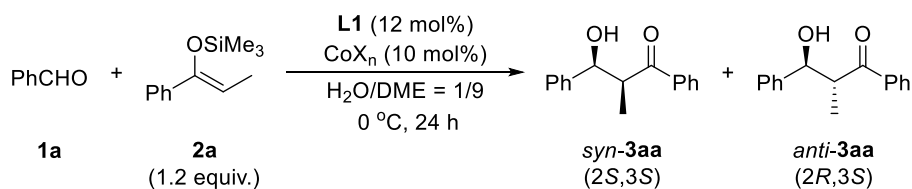
Entry	Co salt	Yield (%)	Dr (*syn/anti*)[a]	Ee (%)[b]
1	$Co(OTf)_2$	17	90/10	7/–1
2	$Co(ClO_4)_2$	10	84/16	0/27
3	$Co(BF_4)_2$	11	88/12	–6/19

[a] Determined by ^{1}H NMR analysis.   [b] Determined by HPLC analysis, *syn/anti*.

1.1-3 Effect of Additives

In order to enhance the performance of catalysts composed of promising Lewis acid and **L1**, addition of additives have been explored. Since having a long history on the investigation of Mukaiyama aldol reactions in aqueous media, our laboratory possesses many rewarding knowledge about additives effective for those. For instance, the beneficial assistance of benzoic acid to catalysis was observed in the Mukaiyama aldol reaction using a catalytic amount of a boron source (diphenylboronic acid), leading to an improvement of both yield and stereoselectivity (Scheme 15).[45] Only a trace amount of the product was obtained in organic solvents and much lower yield than that in water was obtained under neat conditions (24% yield, *syn:anti* = 90:10). When stronger acids such as hydrochloric acid or *p*-toluenesulfonic acid (PTSA) were employed, the yield decreased because of competitive hydrolysis of the silicon enolate and the diastereoselectivity was also lowered, presumably because of a Brønsted acid-catalyzed reaction pathway. A careful tuning of the diarylboronic acid structure led to the discovery that introducing a trifluoromethyl group at the *para* position brought about significant rate acceleration compared with the unsubstituted molecule. Introduction of an electron-donating group at the *para* position reduced both the yield and selectivity, whereas high selectivity was maintained with electron-withdrawing substituents. The first-order kinetics with respect to the amount of silicon enolate supported the boron–enolate mechanism rather than the Lewis-acid mechanism. The exchange from silicon to boron was assumed to be the rate-determining step. A significant dependence of the diastereoselectivity on the enolate geometry implied the formation of a chair-like six-membered transition state in the aldol condensation step. Although traditional boron-mediated aldol reactions required lower temperatures and strictly anhydrous conditions, a combinational use of diphenylboronic acid and Brønsted acid enabled the aldol reaction to be performed in water at ambient temperature.
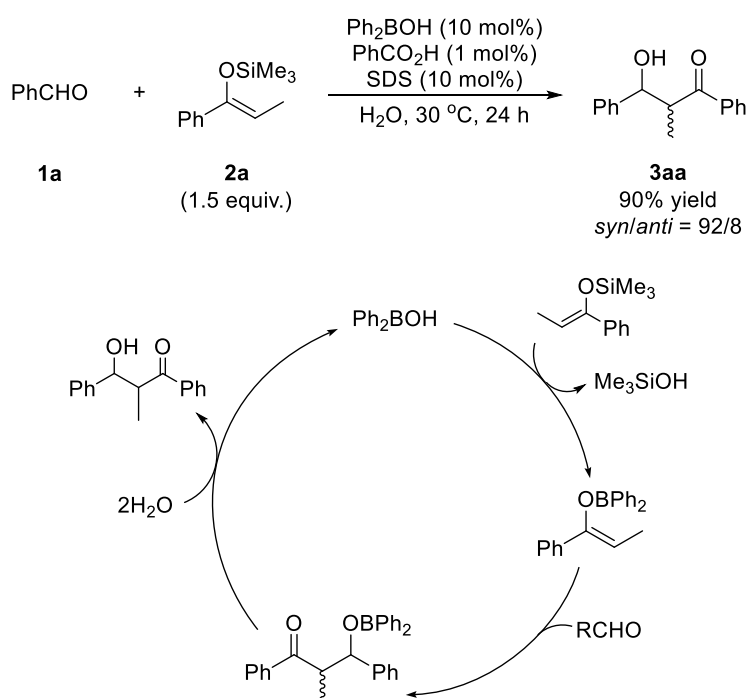
Scheme 15. Diastereoselective Mukaiyama aldol reaction using diphenylboronic acid in water.[45]

In addition, a remarkable enhancement of reactivity by an addition of Brønsted acids was also observed in aldol reactions mediated by Lewis acid-surfactant-combined catalysts in water.[46] This LASC/Brønsted acid system has further extended to a catalytic asymmetric Mukaiyama aldol reaction in an aqueous environment (Table 7).[47,48] Benzoic acid and lauric acid as additives were effective not only for reactivity but also for enantioselectivity (up to *syn/anti* = 2.8/1, 69% *ee* [*syn*]). Neither a strong Brønsted acid (10-camphorsulfonic acid, abbreviated as CSA) nor a weaker one (phenol) could improve the yield and the selectivity. Even with a stoichiometric amount of the scandium salt, the Brønsted acid was also found to accelerate the reaction. This implied that the rate-determining step accelerated by the Brønsted acid was not the catalyst turnover step, but the nucleophilic addition step.[49,50] These examples imply the collaborative assistance of Brønsted acids in Lewis acid-catalyzed Mukaiyama aldol reactions in water.[51,52] Although, from a mechanistic point of view, little is known about the real catalytic function of metal cation and proton, these effects will provide us a new methodology for efficient catalytic system in synthetic chemistry.

Table 7. Chiral Cu(II) dodecylsulfate-catalyzed asymmetric Mukaiyama aldol reactions in water[47].
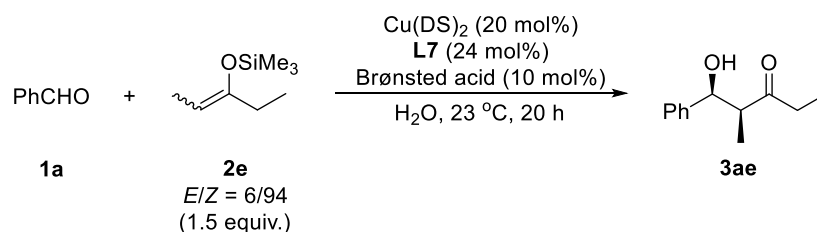
Entry	Brønsted acid	Yield (%)	Dr (*syn/anti*)[a]	Ee (%, *syn*)[b]
1	None	23	3.2/1	58
2	PhCO$_2$H	76	2.7/1	63
3	(+)-CSA	34	3.0/1	63
4	PhOH	15	2.7/1	60
5	4-NO$_2$C$_6$H$_4$CO$_2$H	63	2.4/1	64
6	4-MeOC$_6$H$_4$CO$_2$H	73	3.0/1	61
7	Lauric acid	76	2.8/1	69

[a] Determined by ^{1}H NMR analysis.   [b] Determined by HPLC analysis.
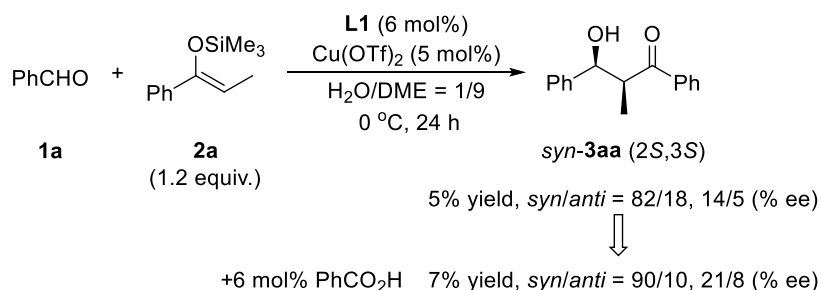
Scheme 16. Addition of benzoic acid to chiral Cu(II) catalyst

Therefore the knowledge of such collaborative assistance seems to be of tremendous attraction to explore organic chemistry in an aqueous media, especially based upon Lewis acid

catalysis. Referred to such enhancement of catalysis mentioned above, addition of benzoic acid was tested when Cu[II] was employed as Lewis acid (Scheme 16). As a result, an addition of a benzoic acid led to only the slight improvement of reactivity and selectivity, but not a satiable level. In order to examine the effect of additives and optimize the reaction conditions, Sc[III]-**L1** system which has low catalytic activity in the first screening was chosen for conducting control experiment. First of all a number of Brønsted acids or Brønsted bases were added (Table 8).

Table 8. Effect of additives in chiral Sc[III]-catalyzed Mukaiyama aldol reaction

PhCHO + Ph–C(OSiMe$_3$)=CH$_2$ →[L1 (6 mol%), Sc(OTf)$_3$ (5 mol%), Additive (10 mol%), H$_2$O/DME = 1/9, 0 °C, 24 h] Ph–CH(OH)–CH(Me)–C(O)–Ph (*syn*-**3aa**, (2S,3S)) + Ph–CH(OH)–CH(Me)–C(O)–Ph (*anti*-**3aa**, (2R,3S))

1a   **2a** (1.2 equiv.)
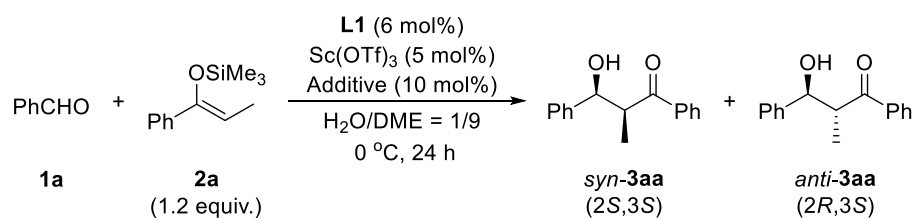
Entry	Additive	Yield (%)	Dr (*syn/anti*)[a]	Ee (%)[b]
1	–	32	59/41	7/0
2	AcOH	20	62/38	10/3
3	TfOH	33	57/43	8/0
4	TFA	21	57/43	3/–2
5	PhOH	30	58/42	10/1
6	PhPO(OH)$_2$	2	61/39	10/2
7	TsOH	15	59/41	3/<1
8	PhCO$_2$H	26	59/41	8/0
9	C$_6$F$_5$CO$_2$H	22	58/42	3/<1
10	**Pyridine**	36	68/32	27/1
11	2,2'-bipyridine	27	59/41	10/2

[a] Determined by ^{1}H NMR analysis. [b] Determined by HPLC analysis, *syn/anti*.

Addition of Brønsted acids such as acetic acid, trifluoromethanesulfonic acid, phenol and benzoic acid slightly contributed to improving diastereoselectivity of the desired aldol product and they had almost no effect in enantioselectivity (entries 2-9). Contrary to a reported acceleration influence exerted by Brønsted acid, it was counterproductive as for the reactivity in this reaction system. 2,2-Bipyridine used as additive produced almost the same result (entry 11), whereas pyridine used as an additive positively contributed to the successful improvement of all three factors containing the reaction yield, diastereo- and enantioselectivity (entry 10). Able to scavenge TfOH generated easily from metal trifluoromethanesulfonate in water, Brønsted base generally causes the stabilization of silicon enolate and concomitant slow reaction rate. On the contrary, it resulted in the slight enhancement of the chemical reactivity of Sc(OTf)$_3$-**L1** system. Taking significant enhancement of diastereo- and enantioselectivity into consideration, there is no doubt as to the cooperative interaction between Sc(OTf)$_3$ and pyridine. The effect of pyridine derivative additives on Lewis acid catalysis was then surveyed in order to clarify the minute mechanism on a catalytic assistance of pyridine toward Lewis acid catalysis (Table 9). The pyridine derivatives can function not only as a Brønsted base but also as a Lewis base. A Lewis base donates its electron pair to an

existing Lewis acid, thus theoretically ruining its Lewis acidity. Therefore a Brønsted base should enhance the reactivity as a protic acid scavenger, while a Lewis base should lower the reactivity as a Lewis acid scavenger. As expected, the catalytic activity increased a bit when hindered bases such as DTBP were employed as an additive (entries 8, 9). On the other hand, higher diastereo- and enantioselectivity were recorded basically in the coexistence of less hindered base, especially α-substituted pyridine (entries 3, 4). Sterically more hindered substituent at α-position is, however, comparatively less effective for selectivity (entries 5, 7). The highest enantiomeric excess was attained in the coexistence of 2,6-lutidine (entry 6). These experimental facts strongly indicate that the coordination of Lewis base on scandium atom plays a crucial role in the precise stereocontrol in an aqueous environment (*vide infra*). It is also noteworthy that the reaction did not proceed at all in the presence of additive alone.

Table 9. Effect of pyridine derivatives as additives in chiral Sc^{III}-catalyzed aldol reaction.

Entry	Additive		Yield (%)	Dr (*syn/anti*)[a]	Ee (%)[b]
1		R = H	36	68/32	27/<–1
2		R = Me	35	68/32	32/–1
3		R = Et	37	70/30	40/–4
4		R = CH$_2$OH	36	70/30	39/–9
5		R = OMe	37	63/37	25/<–1
6	2,6-lutidine		40	71/29	45/<–1
7	2,6-diphenylpyridine		38	62/38	22/<–1
8		R = H	46	61/39	22/–1
9		R = Me	47	64/36	28/–5

[a] Determined by ^{1}H NMR analysis. [b] Determined by HPLC analysis, *syn/anti*.

The coordination of Lewis base and Lewis acid disturbs the catalytic activity in organic solvent, due to the significant drop of Lewis acidity. In that sense, a role of water in enantioselectivity seems to be the most fundamental and the most elusive question. In this viewpoint, the effect of water-DME ratio on reactivity or selectivity was then examined (Table 10). The reaction run in dimethoxyethane (DME) in the absence of water didn't lead to the formation of desired aldol adduct.[53] The higher the ratio of water to DME, the lower reaction yield and the higher diastereo- and enantioselectivity was observed. Hence it was verified that water exerts an influence on steric interaction between active scandium complex and reactant.

Table 10. Effect of water in Sc-**L1**-2,6-lutidine ternary system.
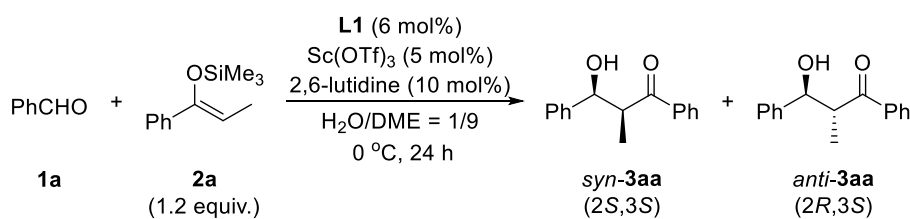
Entry	H$_2$O/DME ratio	Yield (%)	Dr (*syn/anti*)[a]	Ee (%)[b]
1	0/10	NR	–	–
2	1/9	40	71/29	45/<–1
3	2/8	36	74/26	47/<–1
4	3/7	34	78/22	56/–2
5	4/6	23	82/18	66/–5
6	5/5	21	86/14	74/–4
7	6/4	18	88/12	78/–10
8	7/3	10	83/17	70/–4

[a] Determined by ^{1}H NMR analysis.   [b] Determined by HPLC analysis, *syn/anti*.

Based upon the knowledge that has been obtained in Sc-**L1** system, a number of additives have been also explored in the presence of 3 mol% of Fe(OTf)$_2$ and 9 mol% of **L1** (Table 11).   The amount of additives was set to 6 mol%.

Table 11. Effect of additives in chiral Fe^{II}-catalyzed Mukaiyama aldol reaction.
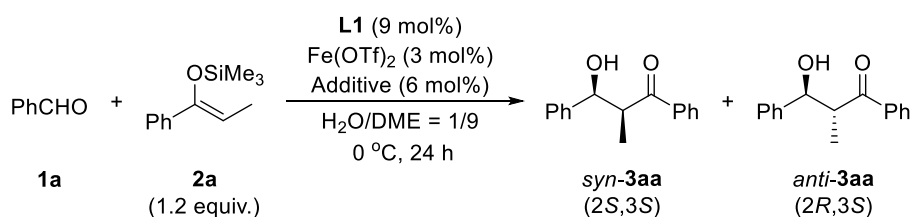
Entry	Additive	Yield (%)	Dr (*syn/anti*)[a]	Ee (%)[b]
1	–	70	97/3	75/43
2	**AcOH**	77	98/2	89/13
3	TfOH	21	98/2	25/6
4	PhOH	37	98/2	83/0
5	TsOH	13	98/2	15/12
6	**PhCO$_2$H**	71	97/3	88/16
7	**Pyridine**	68	97/3	87/–48
8	**2,2'-bipyridine**	76	97/3	86/26
9	Imidazole	7	85/15	0/0
10	*N*-MeIm	26	97/3	73/–31

[a] Determined by ^{1}H NMR analysis.   [b] Determined by HPLC analysis, *syn/anti*.

A Brønsted acid used as an additive has backfired on enantioselectivity when Sc(OTf)$_3$ was employed as Lewis acid, whereas some of them worked well and the desired aldol adduct was produced with high diastereoselectivity and significantly improved enantioselectivity in the presence of Fe(OTf)$_2$.   In particular acetic acid and benzoic acid were found as effective additive for Lewis acid catalysis (entries 2, 6).   Strong acids such as TfOH or *p*-toluenesulfonic acid (TsOH), however, impeded the function of catalyst which operates the precise stereocontrol (entries 3, 5).   Furthermore the significant enhancement of enantioselectivity was also observed in the presence of Brønsted base (entries 7, 8).   Such unprecedented assistance of these additives in Lewis acid catalysis, whether it is Brønsted acid or base unless strong, intrigues us.   The amount of additives were then optimized (Table 12).   Regardless of its nature, all additives exhibited best performance when employed 6 mol%, twice amount of Fe(OTf)$_2$.

Table 12. Optimization of the additive amount.
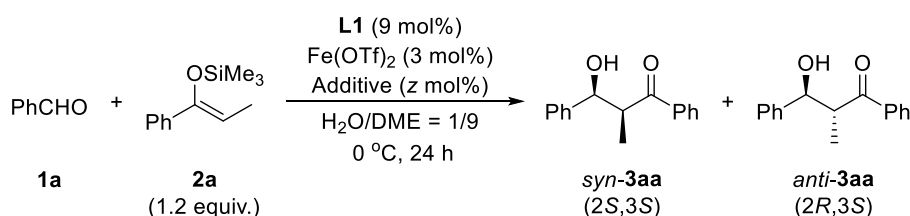
Entry	Additive	z (mol%)	Yield (%)	Dr (*syn/anti*)[a]	Ee (%)[b]
1		3	65	97/3	76/18
2	**AcOH**	6	77	98/2	89/13
3		9	55	97/3	76/13
4		3	46	96/4	83/–16
5	**Pyridine**	6	68	97/3	87/–48
6		9	7	96/4	53/–12
7		12	5	97/3	23/4
8		3	71	97/3	80/19
9	**2,2'-bipyridine**	6	76	97/3	86/26
10		9	68	97/3	79/10

[a] Determined by ^{1}H NMR analysis.   [b] Determined by HPLC analysis, *syn/anti*.

Throughout these investigations, the effect of additives in iron(II) catalysis is suggested to differ from that in Sc(III) catalysis.   In order to gain the insight on the interaction between Fe(II) and additive, several pyridine derivatives were examined as additive (Table 13).   Slowing down of the reaction rate and higher level of enantioselectivity were brought about in the coexistence of less hindered base, especially α-substituted pyridine (entries 3, 4).   Coordinative substituent should be avoided to obtain higher selectivity, too (entries 5, 6).   2,6-Lutidine used as additive afforded the aldol adduct in high enantiomeric manner (entry 7).   In contrast to Sc^{III}-**L1** catalytic system, enantioselectivity of desired aldol adduct was unaffected by the use of strongly hindered bases (entries 8-10).   Interesting influence on enantioselectivity was observed between imidazole and *N*-methylimidazole, presumably due to competitive coordination to iron(II) center with chiral ligand (entries 11, 12).   Such unprecedented assistance of these additives in Lewis acid catalysis, whether

it is Brønsted acid or base unless strong, intrigues us. Regardless of its nature, all additives exhibited best performance when employed 6 mol%, twice amount of Fe(OTf)$_2$.

Table 13. Effect of pyridine derivative additives in chiral Fe^{II}-catalyzed aldol reaction.
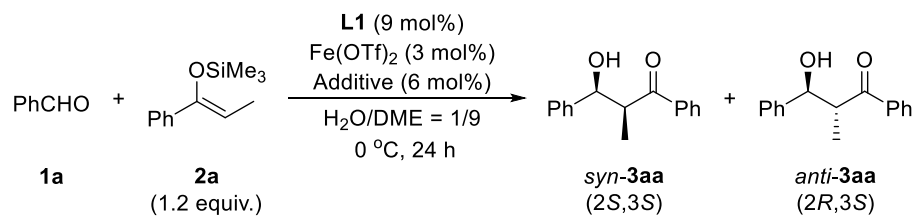
Entry	Additive		Yield (%)	Dr (*syn/anti*)[a]	Ee (%)[b]
1	-		70	97/3	75/43
2		R = H	68	97/3	87/–48
3		R = Me	27	97/3	93/–9
4		R = Et	31	97/3	92/–33
5		R = CH$_2$OH	46	95/5	7/7
6		R = OMe	60	98/2	77/14
7	2,6-lutidine		18	98/2	91/19
8	2,6-diphenylpyridine		58	97/3	76/39
9		R = H	69	97/3	77/38
10		R = Me	67	98/2	77/28
11	Imidazole		7	85/15	0/0
12	*N*-Methylimidazole		26	97/3	73/–31

[a] Determined by ^{1}H NMR analysis.   [b] Determined by HPLC analysis, *syn/anti*.

Table 14. Summary on the effect of additives on Lewis acid-catalyzed Mukaiyama aldol reaction in aqueous media.

To summarize, the effect of additive in enantioselectivity is outlined in Table 14.   Since Brønsted acid can promote the hydrolysis of silyl enol ether, addition of Brønsted acid has been avoided for Mukaiyama aldol reaction except for LASC/Brønsted acid system.   In fact it had no effect in enantioselectivity in the case of Sc^{III}, but amazingly weak Brønsted acid worked well in the case of Fe^{II}.   Brønsted base, known to make silyl enol ether stable in water, affected enantioselectivity positively both in the case of Sc^{III} and Fe^{II}.   As for pyridine derivatives hindered bases as proton scavenger had no effect in enantioselectivity in the presence of Fe^{II}, whereas did positive effect in the case of Sc^{III}.   α-substituted pyridine afforded the aldol adduct with so high enantioselectivity in both cases.   While coordinative substituents such as alcohol or ether were comparatively effective in the case of Sc^{III}, those were not effective in the case of Fe^{II}.   And it is noteworthy that bidentate-type additives such as acetic acid, benzoic acid and 2,2'-bipyridine was as effective as pyridine.   Being unaffected of a proton scavenger strongly suggests the coordination between Fe(II) and additive as a key in the reaction.

Table 15. Examining effect of pyridine with metal triflates.
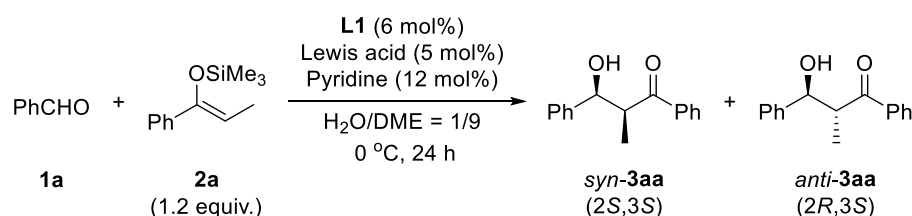
Entry	Lewis Acid	Pyridine	Yield (%)	Dr (*syn/anti*)[a]	Ee (%)[b]
1	Cu(OTf)$_2$	–	8	82/18	41/4
2		+	7	91/9	20/–1
3	Y(OTf)$_3$	–	9	65/35	–24/4
4		+	26	50/50	–6/16
5	Sn(OTf)$_2$	–	14	84/16	–1/22
6		+	14	89/11	0/0
7	Lu(OTf)$_3$	–	55	79/21	–62/6
8		+	49	72/28	–47/2
9	Hg(OTf)$_2$	–	27	98/2	–66/77
10		+	2	69/31	–10/4
11	Bi(OTf)$_3$	–	10	95/5	–69/17
12		+	21	97/3	–77/0

[a] Determined by ^{1}H NMR analysis.   [b] Determined by HPLC analysis, *syn/anti*.

This efficient assistance of Lewis base in Lewis acid catalysis is one of the most intriguing phenomena in this catalytic system.   The co-localization of Lewis acid and base has been providing numerous excellent examples in conventional organic chemistry.[54] Unlike in aprotic organic solvent, the basicity of Lewis base promotes the hydrolysis of Lewis acid so easily in an aqueous environment.   Indeed, an excessive use of a Lewis base has led to a sharp drop both in the chemical yield and the enantioselectivity of the products in Table 12.   Therefore it is postulated

that this cooperative effect in the coexistence of Lewis acid and Lewis base depend upon the nature of each metals. In order to investigate the congeniality between Lewis acids and pyridine, the catalytic activity of several metal triflates which have been found to produce promising and effective enantioselectivity was examined in the coexistence of pyridine (Table 15). As a result, addition of pyridine was negatively affected in the case of Cu(II), Y(III), Sn(II), Lu(III) and Hg(II). The enantioselectivity of aldol adduct decreased unexpectedly when yttrium(III) and lutetium(III) elements were employed as Lewis acid, while it affected positively in the case of scandium(III). The two criteria for the Lewis acidity of metal cations in aqueous media (pK_h and WERC values) cannot provide the clear illustration to these results. Therefore the positive catalysis exerted by addition of pyridine should be regarded as a specific and qualifying example. In addition to Sc^{III} and Fe^{II}, the catalytic activity of Bi^{III} was improved by addition of pyridine in terms of the reaction yield, diastereo- and enantioselectivity. Given the previous report[28] that the excessive use of chiral 2,2'-bipyridine and addition of 2,2'-bipyridine have led to the dramatic enhancement of enantioselectivity, pyridine used as additive *must* play a key role in the rigid formation of complex with chiral 2,2'-bipyridine **L1** and activation of substrate in an aqueous environment.

1.1-4　Substrate Scope

1.1-4-1　Optimization of three catalytic systems

In addition to Sc(III) and Bi(III) catalysis developed hitherto in enantioselective hydroxymethylation, Fe(II) catalysis seemed to be a promising candidate.　Intensive investigations on the optimization of the reaction conditions have led to a discovery of two distinct catalytic systems respectively including Brønsted base (pyridine, defined as **Condition A**) and acid (benzoic acid, defined as **Condition B**) (Scheme 17).　These additives, in spite of their antithetic nature, could assist Lewis acid catalysis exerted by chiral iron(II) complex formed with **L1** to afford the product in a higher enantioselective manner in an aqueous environment, which designates that this powerful assistance cannot be explained by the adjustment of pH value in the reaction solution. The acidity of these ternary catalytic solutions was manifested by the statistically robust measurement of pH value in these catalytic systems.　The Pourbaix diagram, calculated from redox potential of various iron species or water, the equation described by Nernst and hydrolysis constants, attests that Fe(II) is unmistakably active species in these catalytic systems (Figure 3).　Indeed, Fe(III) exhibited inferior performance in Table 1.　However, it is noteworthy that the reaction proceeded smoothly and enantioselectivity even under Argon atmosphere.
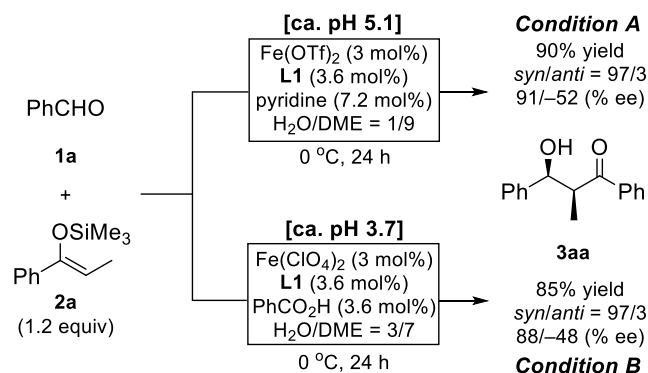
Scheme 17. The optimal conditions for Fe(II)-catalyzed Mukaiyama aldol reaction.
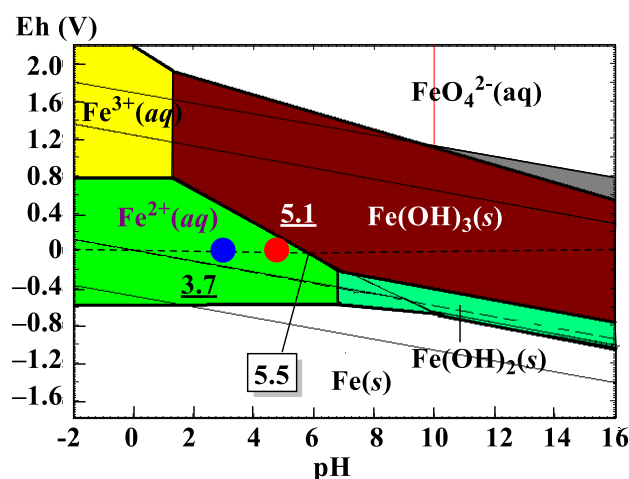
Figure 3. Pourbaix diagram of iron (298.15K).

A part of optimization is described below.　It turned out that the enantioselectivity of desired product leveled off irrespective of the amount of pyridine and it exerts an influence on only

the reaction rate (Table 16). These results were considered to result from the superb dispersion of the catalyst, too. It should be noted that a prolongation of the reaction time resulted in full consumption of benzaldehyde to afford the product in high yield in all cases. The best yield was obtained in $H_2O/DME = 1/9$ and the highest selectivity was obtained in $H_2O/DME = 3/7$ (Table 17).

Table 16. Amount of pyridine (*Condition A*).

Entry	Pyridine (*y* mol%)	Yield (%)	Dr (*syn/anti*)[a]	Ee (%)[b]
1	6	77	97/3	90/−53
2	**7.2**	**90**	**97/3**	**91/−52**
3	9	60	97/3	90/−44
4	10.8	58	97/3	90/−32
5	12	57	97/3	90/−51

[a] Determined by ^{1}H NMR analysis. [b] Determined by HPLC analysis, *syn/anti*.

Table 17. Effect of water (*Condition A*).

Entry	H$_2$O/DME ratio	Yield (%)	Dr (*syn/anti*)[a]	Ee (%)[b]
1	0/10	NR	–	–
2	1/9	90	97/3	91/−52
3	2/8	48	98/2	91/−55
4	3/7	22	96/4	93/−48
5	4/6	6	96/4	78/−34
6	5/5	6	97/3	72/−27
7	6/4	6	97/3	71/−26
8	7/3	5	96/4	70/−19
9	8/2	5	95/5	59/−10
10	9/1	7	95/5	37/−9
11	10/0	9	95/5	43/−10

[a] Determined by ^{1}H NMR analysis. [b] Determined by HPLC analysis, *syn/anti*.

Table 18. Effect of Fe^{II} salts and chiral 2,2'-bipyridines (*Condition A*).

PhCHO + (2a, OSiMe₃/Ph) →(L1 (3.6 mol%), Fe(OTf)₂ (3 mol%), Pyridine (7.2 mol%), H₂O/DME, 0 °C, 24 h)→ syn-3aa (2S,3S) + anti-3aa (2R,3S)

1a   2a (1.2 equiv.)
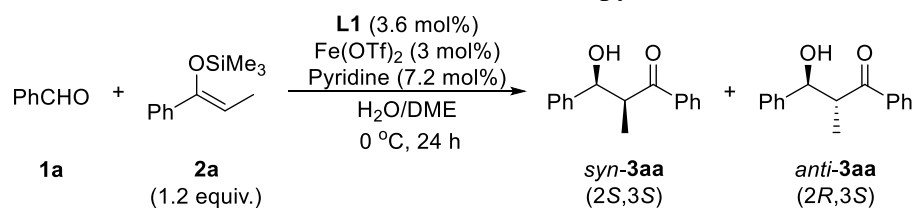
Entry	Ligand	Fe Salt	Yield (%)	Dr (*syn/anti*)[a]	Ee (%)[b]
1		Fe(OTf)₂	90	97/3	91/52
2[d]		Fe(OTf)₂	48	97/3	91/51
3[e]		Fe(OTf)₂	29	95/5	91/25
4		Fe(ClO₄)₂	66	97/3	92/35
5	**L1**	Fe(BF₄)₂	89	98/2	74/0
6		FeCl₂	7	81/19	5/0
7		FeSO₄	3	64/36	3/0
8		Fe(OAc)₂	3	94/6	88/5
9		FeC₂O₄	4	85/15	23/–10
10	**L4**	Fe(OTf)₂	25	97/3	22/11
11	**L5**	Fe(OTf)₂	21	92/8	39/0
12	**L6**	Fe(OTf)₂	25	90/10	–58/1
13	**L7**	Fe(OTf)₂	93	97/3	92/59
14	**L2**	Fe(OTf)₂	49	92/8	0/0
15	**L3**	Fe(OTf)₂	52	94/6	0/0

[a] Determined by ^{1}H NMR analysis.   [b] Determined by HPLC analysis.

[c] With lower catalyst loading (2 mol% Fe(OTf)₂).

[d] With lower catalyst loading (1 mol% Fe(OTf)₂).

Influence of a counteranion and a ligand structure on *Condition A* was summarized in Table 18.   Among tested Fe(II) species, in particular iron(II) triflate and iron(II) perchlorate promoted the reaction in a highly enantioselective manner exceeding 90% ee.   Iron(II) perchlorate afforded lower reactivity but higher enantioselectivity than iron(II) triflate (entry 4).   Iron(II) tetrafluoroborate also afforded the product with high enantioselectivity (74% ee, entry 5).   In contrast, when iron(II) chloride or sulfate was used as a catalyst, the rate acceleration of the reaction was hardly observed and the product was almost racemic (entries 6, 7).   Iron(II) acetate or oxalate afforded the small amount of product with lower selectivity (entries 8, 9).   The definite distinction between the former three counteranions ($^-$OTf, $^-$ClO₄ and $^-$BF₄) and the other ones is characterized by Lewis acidity strength on Fe(II) atom.   Theoretically the highly electronegative atoms such as fluorine, oxygen and so on causes the embrittlement of the interaction between Fe^{II} and low-coordinating counteranions ($^-$OTf, $^-$ClO₄ and $^-$BF₄) and the consequent enhancement of Lewis acidity.   Namely the ionic character plays a momentous role in determining both reactivity and stereoselectivity.   Highly coordinating anions might impede the coordination with hydroxy groups of **L1** in the solution.   As regards a prospective practical application, the requirement of modern asymmetric synthesis is now not only high-yielding with high regio-, chemo- and stereoselectivity but also minimal use of catalyst, in particular chiral ligand which is costly and laborious to

synthesize.   Eventually, the reaction was carried out with 3 mol% catalyst loading to attempt a highly dispersion of the catalyst.   The significant influence of ligand structure on the stereochemical outcome suggests the importance of a stereochemical environment around Fe(II) center (entries 10-13).   Introduction of aromatic substituents in the side chain structure resulted in rate retardation, presumably due to the increased heterogeneity of the reaction system and the resultant influence on an equilibrium between free Fe(II) cation and a formed complex.   The pivotal role of OH group in the structure of **L1** is strongly emphasized when **L2** or **L3** was used as a ligand (entries 14, 15).

The prototype of ***Condition B*** was released in 2012 as a chiral iron(II) complex comprising 5 mol% of $Fe(ClO_4)_2$, 3-fold excess of **L1** and benzoic acid, where both aromatic and aliphatic aldehydes were applicable in the reaction of **2a** with the limited substrate scope (Scheme 18).[55] An excessive use of **L1** could enhance the catalytic activity of iron(II) salt as well as the stereoselectivity of the desired products.

Table 19. Catalyst loading (***Condition B***).

Entry	Catalyst loading (x mol%)	Yield (%)	Dr (*syn/anti*)[a]	Ee (%)[b]
1	5	98	97/3	88/1
2[c]	5	89	97/3	95/–43
3	3	97	98/2	88/–10
4	1	82	97/3	81/–25
5[c]	1	>99	96/4	85/–30

[a] Determined by ^{1}H NMR analysis.   [b] Determined by HPLC analysis, *syn/anti*.
[c] A 3-fold excess of **L1** was used.
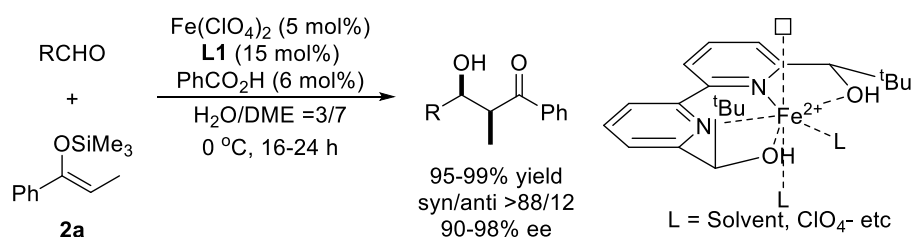
Scheme 18.   Chiral Fe(II) catalyst for enantioselective Mukaiyama aldol reactions.[55]

The supreme performance of Bi(III) catalysis exhibited in aforementioned asymmetric hydroxymethylation[27] also makes us harbor expectations about the further evolution of this catalytic system to enlarge the substrate generality.[56] Furthermore, the availability of bismuth due to its affordability, abundance and ubiquity is comparable to iron.   The reaction proceeded smoothly in the presence of Brønsted base to afford the product with the same level of enantioselectivity.   The

best performance was displayed when 12 mol% of pyridine was added to 3 mol% chiral bismuth complex formed with 3-fold excess of **L1** (Scheme 19).

Table 20. Additive screening (*Condition C*).

Entry	Additive (*y* mol%)	Yield (%)	Dr (*syn/anti*)[a]	Ee (%)[b]
1	–	17	>99/<1	91/–31
2[c]	–	10	95/5	69/17
3	PhCO$_2$H (6)	22	97/3	75/–4
4[c]	PhCO$_2$H (6)	22	96/4	69/–2
5	Pyridine (12)	84	98/2	79/38
6[c]	Pyridine (12)	21	97/3	77/0
7[c]	Pyridine (24)	63	98/2	79/58
8[c]	Pyridine (36)	59	98/2	74/64
9	2,2'-Bipyridyl (6)	57	97/3	75/–22
10[c]	2,2'-Bipyridyl (6)	33	97/3	63/–29
11	DTBP (12)	40	98/2	76/–1

[a] Determined by ^{1}H NMR analysis.   [b] Determined by HPLC analysis, *syn/anti*.
[c] Bi(OTf)$_3$ (5 mol%), **L1** (6 mol%).
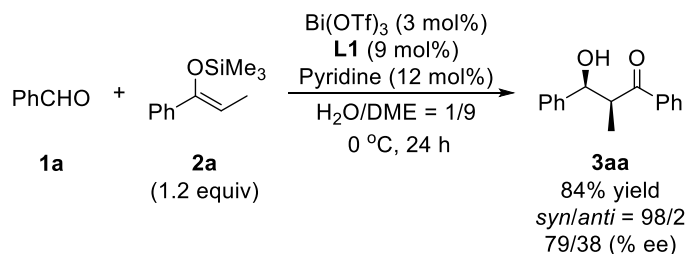
Scheme 19. The conditions for the Bi(III)-catalyzed Mukaiyama aldol reaction (*Condition C*).

1.1-4-2　Evaluation of Substrate Generality

　　　　Although the diversified optimization of three each reaction conditions were carried out, the detailed description is left out here.　As mentioned above, two insurmountable limitations in catalytic activity and substrate scope are still lying in a previous methodologies even including achievements developed in organic solvents: **1) almost all catalytic systems entail 10–20 mol% of Lewis acids and 12–48 mol% of chiral ligands**, and **2) the methodologies possess limited substrate scope for some substrates, such as aliphatic aldehydes, for which a remarkable drop in enantioselectivity** is commonly observed.

　　　　The substrate generality was evaluated under the optimized reaction conditions.　The intriguing assistance by two distinct additives suggests the possibility that the sagacious selection of additives can enlarge the substrate generality.　Based on such perspective, the general tendency was investigated in regards to the correlation between effective additive and substrate (Table 21). It was found out thus far that pyridine additive was more effective in the Mukaiyama aldol reaction of benzaldehyde **1a** with propiophenone-derived silyl enol ether **2a** (entry 1).　First of all, electronic effect resulting from the substituent on aromatic ring in the structure of propiophenone-derived silyl enol ether was surveyed.　The substitution of an electron-donating group (OMe) resulted in the definite drop in the reaction rate.　Extending the reaction time allowed almost complete consumption of aldehyde to afford the product **3ab** with excellent diastereo- and enantioselectivity in the presence of pyridine.　However, the reaction hardly proceeded when benzoic acid was employed as additive (entry 2).　An electron-donating group on aromatic ring can contribute to the stabilization of O–Si bond, thus slowing the rate of hydrolysis after the nucleophilic attack.　The substitution of an electron-withdrawing group (Cl) led to an imperceptible decrease in the reaction rate.　Addition of pyridine took effect in stereochemical outcome of the corresponding product, irrespective of the substituent on the aromatic ring (entry 3). However, the reaction of 4-fluorobenzaldehyde **1d** or 1-naphthaldehyde **1f** proceeded in higher enantioselective manner when benzoic acid was used as additive (entries 4, 5).　The optimal conditions could be applied to aliphatic aldehydes, which have been often poor electrophiles for Lewis acid-mediated asymmetric processes due to both electronic and steric difficulties in enantiofacial differentiation.　The reaction of **1j** or **1l** proceeded more smoothly to afford the desired product in higher yield with higher selectivity when pyridine was added (entries 9, 10).　It was also confirmed that the use of iron(II) perchlorate instead of iron(II) triflate or replacing the water-DME ratio to 3/7 retarded the catalytic turnover.　On the other hand, benzoic acid additive exhibited a superior performance in the reaction of cyclohexanecarboxyaldehyde **1i**, thiophenecarboxyaldehyde **1o** or α,β-unsaturated aldehydes **1g**, **1h** (entries 6-8, 11).　In the reaction of water-soluble aldehydes, the evaluation should be deferred to the discussion below (entries 12, 13).　As reported in Ref. 55, the use of almost double-amount of iron(II) and a 3-fold excess of **L1** allowed us to get better enantioselectivities for some substrates (**3da**: 98% ee *vs.* 89% ee, **3fa**: 98% ee *vs.* 91% ee, **3oa**: 98% ee *vs.* 91% ee).

Table 21. Effect of additives on substrate scope.

R^{1}CHO + [enol ether with OSiMe$_3$, R] $\xrightarrow[\text{H}_2\text{O/DME, 0 °C}]{\text{Conditions}}$ [product R^1 with OH O and R]

(1.2 equiv.)
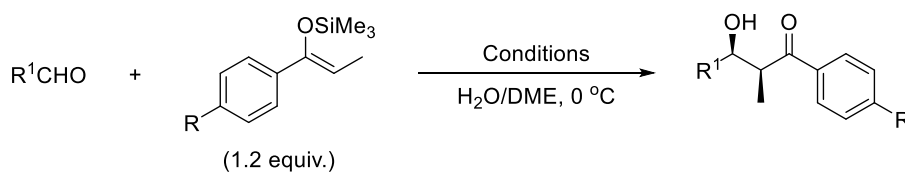
Entry	Additive R^1		Enol Ether R		Condition[a]	Yield (%)	Dr (*syn/anti*)[b]	Ee (%)[c]
1	Ph	1a	H	2a	A	90 (3aa)	97/3	91/52
					B	85	97/3	88/48
2	Ph	1a	OMe	2b	A	91 (3ab)	97/3	85/21
					B	6	>99/<1	49/nd
3	Ph	1a	Cl	2c	A	87 (3ac)	93/7	89/66
					B	70	95/5	65/40
4	4-FC$_6$H$_4$	1d	H	2a	A	76 (3da)	92/8	65/33
					B	99	96/4	89/39
5	1-Naphthyl	1f	H	2a	A	55 (3fa)	98/2	88/82
					B	Quant.	96/4	91/40
6	CH$_2$=CH	1g	H	2a	A	82 (3ga)	88/12	84/61
					B	94	88/12	95/73
7	PhCH$_2$=CH	1h	H	2a	A	82 (3ha)	88/12	84/61
					B	94	88/12	95/73
8	*c*-C$_6$H$_{11}$	1i	H	2a	A	40 (3ia)	>99/<1	69/4
					B	90	95/5	95/87
9	PhCH$_2$CH$_2$	1j	H	2a	A	82 (3ja)	94/6	99/25
					A[d]	25	94/6	98/12
					A[e]	37	93/7	99/14
					B	75	94/6	96/25
10	CH$_3$CH$_2$	1l	H	2a	A	93 (3la)	94/6	89/75
					A[d]	90	94/6	90/75
					B	71	87/13	66/37
11	2-C$_4$H$_3$S	1o	H	2a	A	1 (3oa)	–	–
					B	70	98/2	91/31
12	CH$_3$	1u	H	2a	A	72 (3ua)	93/7	74/68
					B	14	96/4	82/–
13	ClCH$_2$	1v	H	2a	A	98 (3va)	91/9	87/>99
					B	69	92/8	85/>99

[a] Condition A: Fe(OTf)$_2$ (3 mol%), **L1** (3.6 mol%), Pyridine (7.2 mol%), H$_2$O/DME = 1/9.
　　Condition B: Fe(ClO$_4$)$_2$ (3 mol%), **L1** (3.6 mol%), PhCO$_2$H (3.6 mol%), H$_2$O/DME = 3/7.
[b] Determined by ^{1}H NMR analysis.　　[c] Determined by HPLC analysis.
[d] Fe(ClO$_4$)$_2$ was employed instead of Fe(OTf)$_2$.　　[e] The ratio of H$_2$O/DME was replaced to 3/7.

Condition A. It was found out that a pyridine additive was generally more effective in the Mukaiyama aldol reaction. ***Condition A*** was thus set as a standard condition in the initial examining the substrate generality (Scheme 20). Addition of pyridine took effect in enantioselectivity of the product, irrespective of the substituent on the aromatic ring in silyl enol ether. Not only aliphatic aldehydes (**1j**, **1l**, **1m** and **1v**) but also aromatic aldehydes bearing electron-donating group (**1b** and **1c**) could react with silyl enol ether in a highly stereoselective manner.
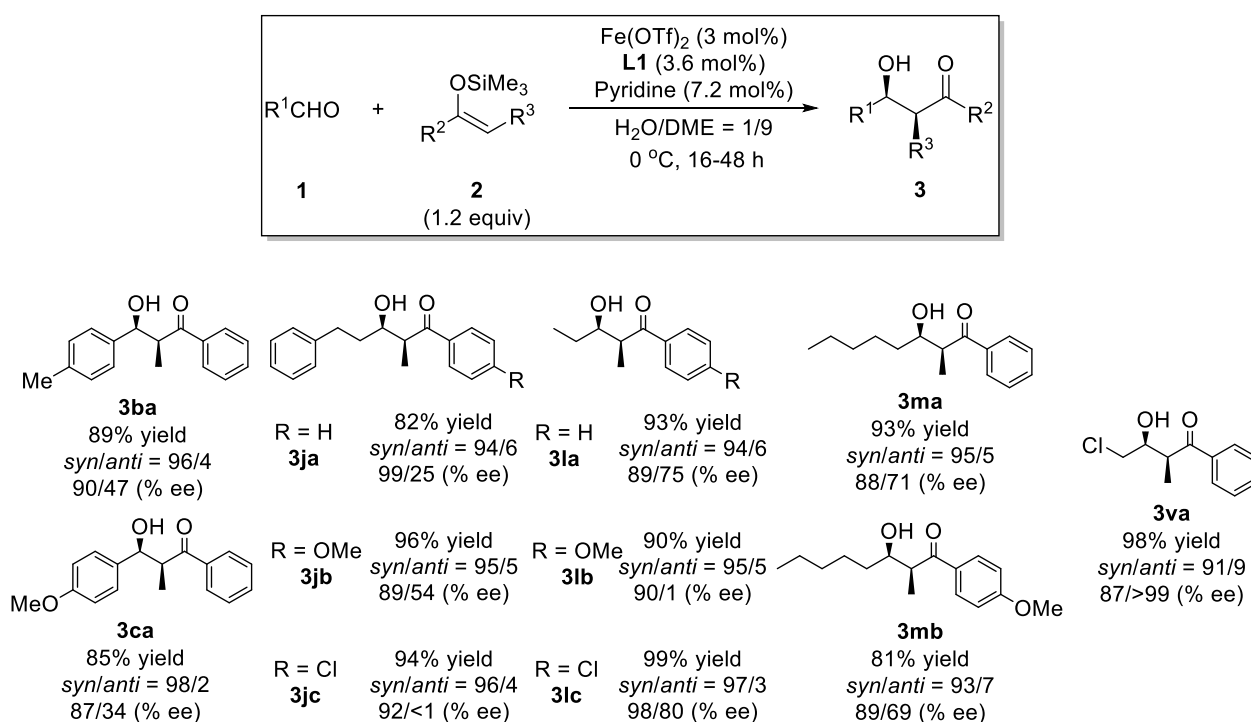
[a] DTBP (3 equiv.) was added.

Scheme 20. Substrate Scope – *Condition A*.

Condition B. When benzoic acid was employed as an additive, a superior effect was obtained in the reactions of electron-deficient aromatic aldehydes (**1d**, **1e**, **1f**), secondary aliphatic aldehyde **1i**, thiophenecarboxyaldehyde **1o**, and α,β-unsaturated aldehyde **1h** (Scheme 21). Introduction of an electron-withdrawing (chloro) group on the aromatic ring in the silicon enolate led to a slightly lower but satisfactory level of selectivity in high yield (**3hc**). The combination of Fe(II) and benzoic acid could also be applied to the reaction of **1a** with the silicon enolate derived from 3-pentanone (**2e**).

$$R^1CHO + \underset{R^2}{\overset{OSiMe_3}{\diagup}}R^3 \xrightarrow[\substack{H_2O/DME = 3/7 \\ 0\ ^\circ C,\ 16\text{-}48\ h}]{\substack{Fe(ClO_4)_2\ (3\ mol\%) \\ L1\ (3.6\ mol\%) \\ PhCO_2H\ (3.6\ mol\%)}} \underset{R^3}{\overset{OH\quad O}{R^1}}R^2$$

1   **2**   **3**
(1.2 equiv)

3da
99% yield
syn/anti = 96/4
89/39 (% ee)

3ea[a]
Quant.
syn/anti = 91/9
92/22 (% ee)

3fa
Quant.
syn/anti = 96/4
91/40 (% ee)

3ha
94% yield
syn/anti = 88/12
95/73 (% ee)

3hc
86% yield
syn/anti = 85/15
83/68 (% ee)

3hd
Quant.
syn/anti = 96/4
88/57 (% ee)

3ia
90% yield
syn/anti = 95/5
95/87 (% ee)

3oa
84% yield
syn/anti = 98/2
91/19 (% ee)

3ae
84% yield
syn/anti = 91/9
80/- (% ee)

[a] Fe(ClO_4)_2 (3 mol%), L1 (9 mol%), PhCO_2H (3.6 mol%).

Scheme 21. Substrate Scope – *Condition B*.

Benzaldehyde, 3-phenylpropanal, aliphatic aldehydes and so on afforded the desired product in high yield with high diastereo- and enantioselectivity in the presence of pyridine as additive irrespective of the kind of substituents on aromatic ring.   In contrast, the reactivity and selectivity depended upon the substituents on aromatic ring in propiophenone-derived silyl enol ether when benzoic acid was used as an additive.   Especially the introduction of methoxy group on aromatic ring suppressed the catalytic reaction pathway dramatically, leading to a quite low selectivity.   When chloro group was substituted, enantioselectivity of the desired adduct decreased slightly.   In that sense, a significant drop in enantioselectivity was observed in the case of electron-donating groups substituted on aromatic ring.   Meanwhile, when cinnamaldehyde, thiophenecarboxyaldehyde, cyclohexanecarboxyaldehyde and so on was chosen as a reactant, pyridine did not function as an effective additive and benzoic acid was more effective. Introduction of electron-withdrawing (chloro) group on the aromatic ring in the silicon enolate or employment of butyrophenone-derived silyl enol ether led to a slightly low but a satisfactory level of selectivity in high yield.   In contrast, introduction of electron-donating (methoxy) group led to a dramatic drop in both the reactivity and enantioselectivity.   In the co-existence of pyridine, the chemical reactivity enhanced along with much lower selectivity.   The electric influence of aldehydes or silyl enol ethers on iron(II)-based catalytic system was summarized in Table 22.

Table 22. Tendency on correlation between aldehydes and additive
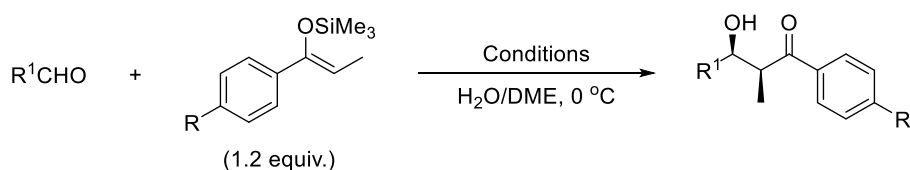
R	Condition A		Condition B	
	Electron-rich aldehyde	Electron-poor aldehyde	Electron-rich aldehyde	Electron-poor aldehyde
H	Yield ◎ Ee ◎	Yield × Ee △	Yield ○ Ee ○	Yield ◎ Ee ◎
OMe (ED)	Yield ◎ Ee ◎	—	—	Yield × Ee ×
Cl (EW)	Yield ◎ Ee ◎	—	—	Yield ◎ Ee ○

Condition C. Chiral Bi(III) catalyst (defined as *Condition C*) was also found to be an attractive choice as an alternative toolbox for asymmetric Mukaiyama aldol reactions (Scheme 22). In Bi(III)-catalyzed asymmetric hydroxymethylation, 2,2′-bipyridyl was selected as an effective additive. In that system, only a trace amount of product was obtained using Bi(OTf)$_3$ without **L1**, presumably because of the rapid decomposition of silicon enolates promoted by TfOH generated readily from Bi(OTf)$_3$ in water. Water-soluble aldehydes such as aqueous formaldehyde **1t**, acrolein **1g**, *etc*., reacted with silicon enolates to afford the corresponding aldol adducts in high yields with high enantioselectivities. The aldol reaction of acetaldehyde **1u** is regarded as difficult because acetaldehyde has high reactivity as both a nucleophile and an electrophile, causing a self-aldol reaction. Therefore, until recently, no asymmetric reactions using acetaldehyde have been reported.[57] The chiral Bi(III) complex catalyzed the reaction of **1u** with **2a** to afford the desired product in good yield with high diastereo- and enantioselectivities. The Bi(III) complex was also applicable to the reactions of aldehydes bearing functional groups (**1e**, **1k**, **1p**, **1s**, and **1r**). When 2-pyridinecarboxaldehyde **1q** was used as a substrate, most Lewis acid catalysts were poisoned for chiral induction (Table 22, metal/ligand ratio is corresponding to the superior result shown in Table 3). The similar tendency was observed in the reaction of ethylglyoxylate **1r** (*Condition A* [47% yield, *syn/anti* = 39/61, 18/8 (% ee)], *Condition B* [41% yield, *syn/anti* = 33/67, 14/7 (% ee)] , Sc(OTf)$_3$ (5mol%) [73% yield, *syn/anti* = 43/57, 73/84 (% ee)]). It is noteworthy that asymmetric quaternary carbons were constructed with high selectivities. Silicon enolate **2b** bearing an electron-donating group was not applicable to *Condition B*, whereas the chiral Bi(III) complex catalyzed the reactions with **2b** in high yields with high selectivities. That is, *Condition C* exhibited a superior catalysis in the reaction of electron-poor aldehydes with electron-donating silyl enol ether (e.g. **3eb**, **3hb**). For instance, the reaction of **1h** with **2b** under *Condition A* afforded **3hb** in high yield with moderate selectivity [95% yield, *syn/anti* = 74/26, 56/20 (% ee)], whereas it suffered from low yield under Condition B [15% yield, *syn/anti* = 81/19, 69/62 (% ee)]. The increased selectivity is also noteworthy in reaction of **1j** with **2d** compared with *Condition A* [95% yield, *syn/anti* = 98/2, 81/10 (% ee)]. It is of great interest that *Condition C* is also effective

in the chiral induction in the reaction with **2g** (***Condition A*** [72% yield, *syn/anti* = 98/2, 49/15 (% ee)], ***Condition B*** [65% yield, *syn/anti* = 98/2, 30/24 (% ee)], Sc(OTf)$_3$ (5mol%) [22% yield, *syn/anti* = 89/11, 20/30 (% ee)]).   Although water-soluble aldehydes seemed to be catalyzed efficiently under ***Condition C***, the reactivity difference between acetaldehyde **1u** with chloroacetaldehyde **1v** (NR) implies the effect of steric bulkiness.   In the presence of Sc-**L1** complex (5 mol%), the difference between acetaldehyde **1u** [83% yield, *syn/anti* = 66/34, 62/− (% ee)] with chloroacetaldehyde **1v** [66% yield, *syn/anti* = >99/<1, 91/31 (% ee)] was remarkable.

[a] Bi(OTf)$_3$ (1 mol%), **L1** (3 mol%), 2,2′-bipyridyl (5 mol%), in H$_2$O/DME = 1/4. See ref. 27.

[b] DTBP (3 equiv) was added.   [c] Sc(OTf)$_3$ (10 mol%), **L1** (12 mol%).   [d] Without pyridine.

Scheme 22. Substrate Scope – ***Condition C***.

The Mukaiyama aldol reaction of 2-pyridinecarboxyaldehyde led to the racemic adduct with high *anti*-selectivity in all cases unfortunately (Table 23).   The structure of this aldehyde can be regarded to be equivalent to half in the structure of 2,2'-bipyridine ligand **L1**, which seems to cause the suppression of complexation between metal and **L1** by the competitive coordination. Then the combinations of **L1** and some metal triflates were examined.   As a result, chiral bismuth complex formed with **L1** exhibited the highest enantioselectivity.   However the enantiomeric excess value is moderate, 74% ee and the reaction was *anti*-selective.   Since the *syn*-adduct and *anti*-adduct can be easily separated, optically active aldol adduct can be obtained anyway.

Table 23. The reaction of 2-pyridinecarboxyaldehyde (***Condition C***).
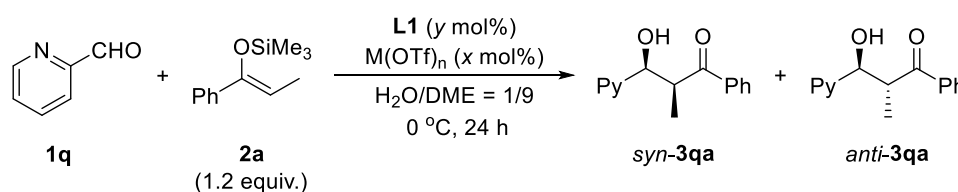
Entry	Lewis acid	Yield (%)	Dr (*syn/anti*)[a]	Ee (%)[b]
1	Fe(OTf)$_2$	41	18/82	2/0
2[c]	Fe(OTf)$_2$	54	18/82	2/0
3[d]	Fe(OTf)$_2$	Qunat.	12/88	2/0
4	Cu(OTf)$_2$	50	8/92	<1/2
5	Yb(OTf)$_3$	40	32/68	43/24
10	Lu(OTf)$_3$	57	33/67	39/26
11	Bi(OTf)$_3$	75	36/64	74/34

[a] Determined by ^{1}H NMR analysis.   [b] Determined by HPLC analysis, *syn/anti*.

[c] 7.2 mol% of pyridine was added as an additive.

[d] 3.6 mol% of PhCO$_2$H was added as an additive.

1.1-4-3   Complementary System.

Improved systems could avoid an excessive use of **L1** and could enlarge the substrate generality by interweaving *Condition A* and *B* with *Condition C*.   The effect of choice of ternary catalytic systems and the substituent effects obtained are summarized in Table 24.   It is noted that introduction of electron-withdrawing groups on the aromatic ring in the structure of benzaldehyde preferred *Condition B* as the best condition.   In contrast, electron-donating aromatic aldehydes preferred *Condition A*, indicating that the difference between pyridine and benzoic acid as the additive may lie in electronic effects through coordination with Fe(II).   The substituents on the aromatic ring in the structure of the propiophenone-derived silicon enolates affected neither reactivity nor selectivity, except for *Condition B*.   The reaction with butyrophenone-derived silicon enolate, which led to a significant loss in enantioselectivity in the presence of a chiral gallium catalyst with a Trost-type ligand, also led to an excellent result.   Introduction of a methoxy group on the aromatic ring of the silicon enolate led to a significant drop in both reactivity and stereoselectivity under *Condition B*, whereas the reaction proceeded quantitatively to afford the product with excellent selectivities under *Condition C* (e.g., **3eb**, **3hb**).   In addition, *Condition C* was effective for the reaction of less bulky aldehydes, including water-soluble aldehydes as well as aldehydes that can chelate with metals.   Stereoselective construction of asymmetric quaternary carbons was also displayed.

Table 24. Tendency on correlation among aldehydes, aromatic ketone-derived silicon enolates, and catalytic systems.

R	Aldehyde (R^1CHO)		
	More Bulky		Sterically Small, Chelate-type
	Electron-rich	Electron-poor	
H	**Condition A**	**Condition B**	**Condition C**
OMe (ED)	**Condition A**	**Condition C**	**Condition C**
Cl (EW)	**Condition A**	**Condition B**	**Condition C**

1.1-4-4　Match/Mismatch Effect

　　　　The reaction of a chiral β-alkoxy aldehyde bearing potential directing ability was surveyed to offer a rationale for the stereocontrol (Scheme 6).　Exposure of aldehyde **1n** and silicon enolate **2a** to the chiral Bi(III) complex formed with (*S*,*S*)-**L1** exhibited exclusive diastereofacial preference with high enantioselectivity. The use of Fe(II) instead of Bi(III) improved the reactivity with a high level of stereoselection. In contrast, the "mismatched" case using (*R*,*R*)-**L1** resulted in lower enantioselectivity, albeit the same level of yield and *syn*-selectivity because of the chelation.

Fe(OTf)$_2$ or Bi(OTf)$_3$
(3 mol%)
(*S*, *S*)-**L1** (3.6 or 9 mol%)
Pyridine (7.2 or 12 mol%)
H$_2$O/DME = 1/9
0 °C, 24 h

1n　　　　**2a**
　　　　(1.2 equiv.)

3na
(2*S*,3*R*,5*R*)

Bi(OTf)$_3$: 50% yield, *syn/anti* = >99/<1, 88% ee (*syn*)
Fe(OTf)$_2$: 74% yield, *syn/anti* = >99/<1, 91% ee (*syn*)

Fe(OTf)$_2$ (3 mol%)
(*R*, *R*)-**L1** (3.6 mol%)
Pyridine (7.2 mol%)
H$_2$O/DME = 1/9
0 °C, 24 h

1n　　　　**2a**
　　　　(1.2 equiv.)

3na
(2*R*,3*S*,5*R*)

79% yield, *syn/anti* = 96/4, 56% ee (*syn*)
91% ee (*anti*)
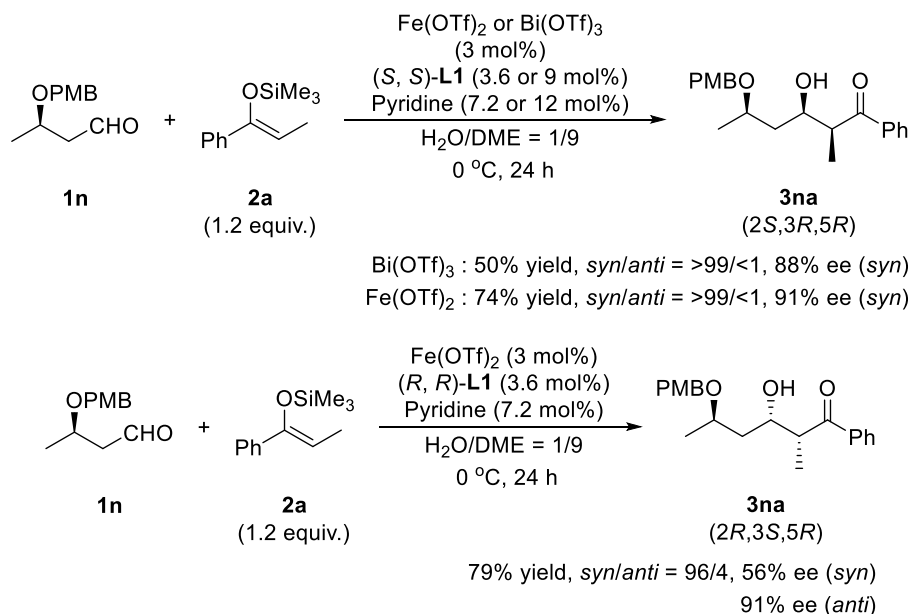
Scheme 23. Match/Mismatch Effect.

1.1-4-5 Application and Comparison with Reported Variants: Complementarity in Chemical Synthesis.

The Mukaiyama aldol reaction of benzyloxyacetaldehyde with propiophenone-derived silyl enol ether **2a** was then carried out using the optimal catalytic systems. The desired aldol-adduct is known to be a key intermediate in a total synthesis of various natural compounds. For instance the total synthesis of bafilomycin A_1, an inhibitor of vacuolar H^+–ATPase in vitro, has four steps to control stereogenic centers; one of them is asymmetric aldolization.[58] In conventional method, the product was prepared in three steps from 2-(benzyloxy) acetic acid (Scheme 24). After treatment with benzotriazole in the presence of DCC, the lithium enolate of propiophenone was added to afford the desired diketone. This diketone was then reduced under asymmetric transfer hydrogenation conditions with chiral ruthenium complex. Thus desired β-hydroxyketone was obtained in a ratio of 68/32 diastereoselectivity in total 62% yield (3 steps). The major isomer was formed in an enantiomeric excess of 93%.
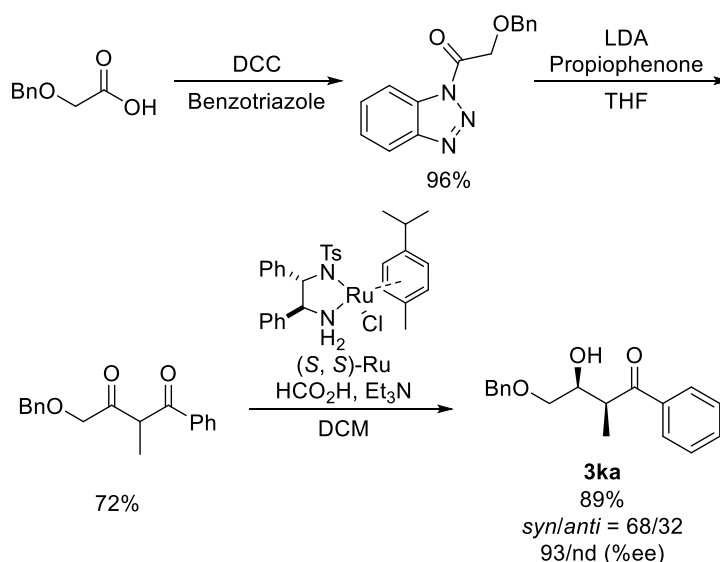
Scheme 24. Conventional synthesis of β-hydroxyketone.[58]

On the other hand, employment of chiral bismuth catalyst (only 3 mol%) led to the best result; the reaction proceeded quantitatively with excellent diastereo- and enantioselectivity (Scheme 25). Even though considering the preparation of silicon enolate and chiral 2,2'-bipyridine **L1**, this synthetic method *must* be much more useful than the conventional methods. Given chiral ligand **L1** could be synthesized readily in three steps,[22,59] the superiority and the utility of the new catalytic systems are evident.
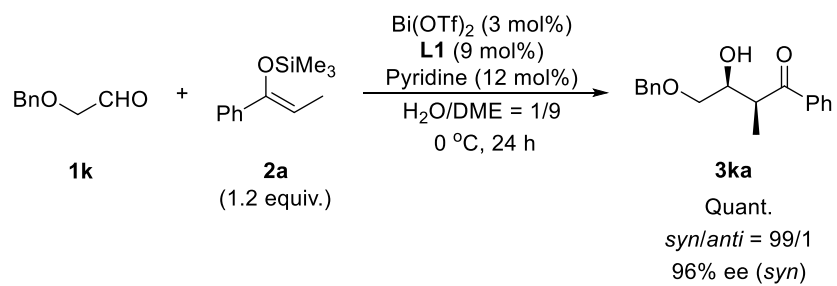
Scheme 25. Bismuth(III)-mediated synthetic methodology for β-hydroxyketone.

1.1-5 Mechanistic Elucidation

1.1-5-1 Historical debates

In Mukaiyama aldol reactions under kinetic control, the significant correlation between aldol configuration and enolate geometry has been observed. A large number of intensive contributions[60] following the seminal investigations reported by Dubois[61] have revealed that (*Z*)-configured enolates furnish mainly *syn*-aldols, whereas *anti*-aldols arise predominantly from (*E*)-enolates. Several transition-state hypotheses have been formulated to explain the stereochemical outcome of the Mukaiyama aldol reactions. Three kinds of explanation seem to be suitable for rationalizing stereochemistry. One of them is the Zimmerman-Traxler model, which was originally developed in order to offer a rationale for the stereochemistry in Ivanoff and Reformatsky reaction.[62] They proposed that some aldol reactions have six-membered transition states which involve a chair-like assembly of the reactants. The requirement of rationalization for more complicated phenomena (for instance, higher *syn*-selectivity of (*Z*)-enolates than *anti*-selectivity of (*E*)-enolates) led to various modification of this model (pericyclic-like transition state,[63] chair & twist-boat transition state[64] and so on). Another rationale relies on open-transition-state models which involve antiperiplanar orientation of enolate and carbonyl group (Figure 3).
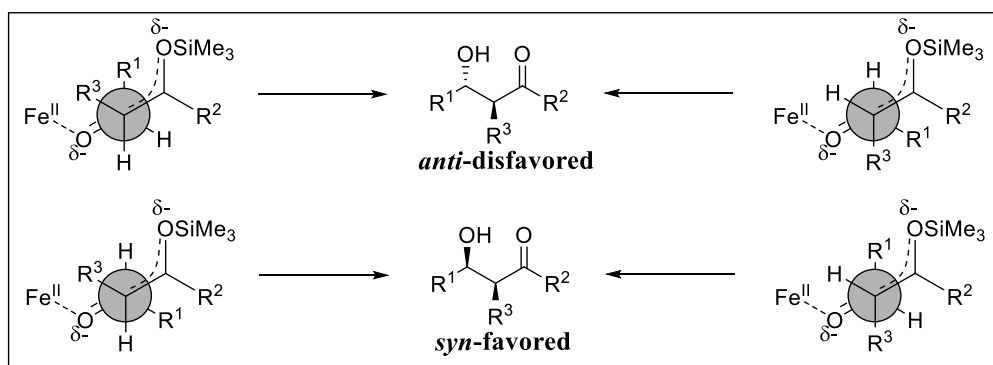
Figure 3. Open-transition-state models

Open-transition state structures have been invoked in order to comprehend the aldol reactions that give predominantly *syn* products, irrespective of enolate geometry.[65] This outcome has been observed in aldol reactions in tin and zirconium enolates. Synclinal transition-state structures are disfavored because of the dipole-dipole interactions between the two carbon-oxygen bonds. Both transition states that provide the *anti*-selective aldol are disfavored, due to the steric repulsion of substituents oriented in a *gauche* conformation. Third hypothesis involves transmetalation of silicon to a Lewis acid catalyst. The initial mechanistic hypothesis in Mukaiyama's landmark report in 1973 has involved the formation of titanium enolate *via* transmetalation. Although the resulting titanium enolate was believed to react with an aldehyde to afford a stable titanium aldolate *anti*-selectively, no structural evidence could be supplied at the time. The application of an INEPT (insensitive nuclei enhanced by polarization transfer) ^{29}Si NMR study was quite emphatic in denying the transmetalation.[66] Nevertheless, the reaction of pre-isolated

titanium enolates with aldehydes was amazingly *syn*-selective.[67] And the role of counterion in determining the stereochemistry of the aldols has become more evident.
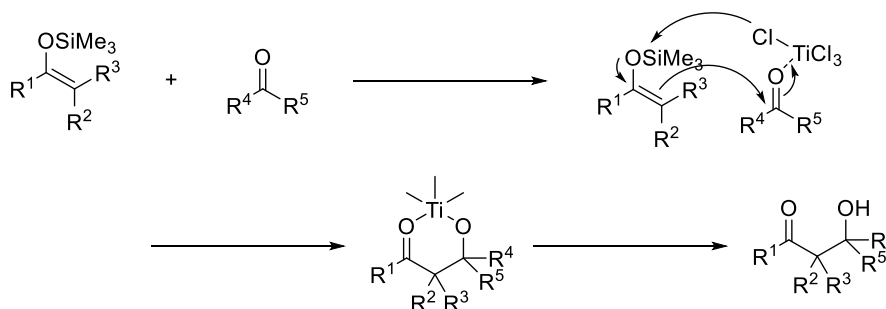
Scheme 26. Revised mechanism for TiCl$_3$-promoted aldol reaction.

Some complexes between Lewis acids and carbonyl compounds have been theoretically characterized by spectroscopic and crystallographic investigations, providing sufficient electrophilic activation to allow the enoxysilane derivative to add to the carbonyl group to afford the titanium-chelated aldolate and trimethylsilyl chloride. Either chair & twist-boat closed or open-transition-state hypothesis is convenient to explain the origin of diastereoselectivity in Lewis acid-mediated Mukaiyama aldol reactions. The validity of closed transition state model can be questioned, because the strongly electropositive metals might form ionic rather than covalent bonds to the enolate oxygen atom. On the other hand, the closed transition state hypothesis has been underscored by computational chemistry and the closed transition state model which does not involve transmetalation was also proposed.[68] To date, the actual mechanism has not been determined conclusively.

1.1-5-2   Mechanistic Insight based upon Stereochemical Outcome.

In order to gain an insight into the possible reaction mechanism for Lewis acid-catalyzed Mukaiyama aldol reactions, the kinetics for hydroxymethylation reaction using aqueous formaldehyde with **2a** in the presence of Sc-**L1** complex was examined in 2011 (Figure 4).[69] To find out the dependence of the *in situ* generated chiral scandium catalyst on the reaction rate, the catalyst concentration was varied whilst maintaining **L1** to Sc(OTf)$_3$ ratio at approximately 1.2 to 1.   The formation of **18** with time has turned out to proceed with a linear increase.   A first-order dependence of silyl enol ether **2f** and catalyst with **K** $_{sub}$ = 0.31 h^{-1} and **K** $_{Cat}$ = 5.10 h^{-1} represents an overall rate-law of: ***Rate** = k **[2f][Catalyst]***.   The observation of first-order dependence on both silyl enol ether and the catalyst negates the possible formation of scandium enolate as an intermediate and the involvement of discrete molecules of catalyst. Moreover, no observation of saturation kinetics also denies the direct bond-formation between chiral scandium catalyst and silyl enol ether.
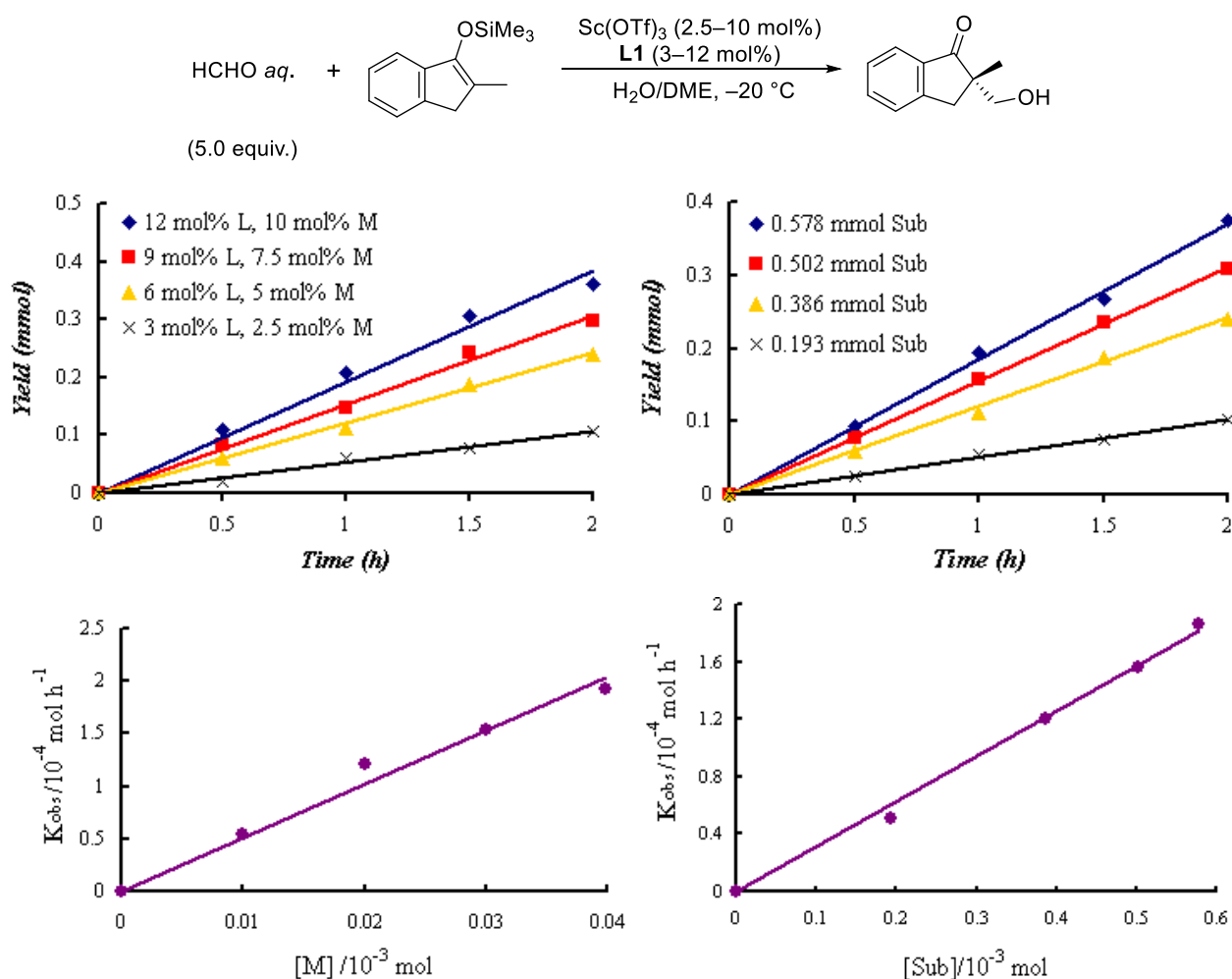
Figure 4. Plots of yield vs time (top) and rate vs concentration (bottom)

Open transition state model is more suitable when performed in an aqueous environment. This is because water can disturb a weak interaction between metals and oxygen atom of silyl enol

ether.   The (*E*)-enolate has reacted *syn*-selectively in the presence of iron(II) salt and **L1**. The direct comparison on the effect of enolate geometry was undergone by using 3-pentanone-derived enolate (Scheme 27).   The reaction of (*Z*)-enolate followed the same stereochemistry, which was in accord with my speculation.   The independence of stereochemistry from enolate geometry was also confirmed in the case of chiral bismuth complex (***Condition C***).
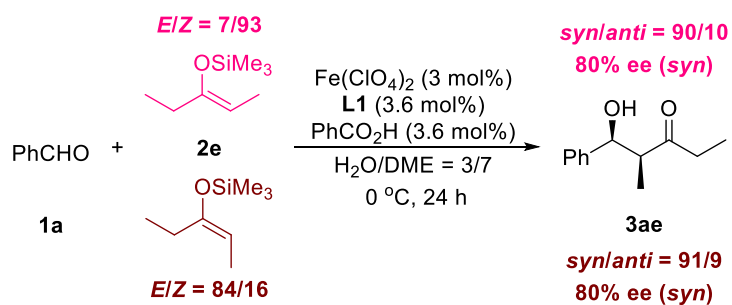
Scheme 27. Correlation between stereochemical outcome and enolate geometry.

1.1-5-3   Scandium Catalyst

The chiral scandium complex formed with **L1** has been characterized previously by using X-ray crystallography.[26] Crystallographic investigations have revealed the complex core to be a mono-positive species with the chelation of one tetradentate protonated ligand (**L1**) to the central scandium ion in an almost square-planar fashion.   The two axial positions of the pentagonal bipyramidal scandium complex are occupied by two bromide ions and the fifth equatorial position is occupied by a water molecule.   Two *tert*-butyl groups are situated opposite to each other compared to the basal plane formed by the central scandium ions and equatorial donor atoms.   In the complex, the central scandium ion has a d^0 configuration, and thus no crystal-field stabilization energy.   Therefore the scandium center is irrelevant to the nature of its coordinating ligands. Namely, water molecule, both reactants and additive have the identical preference for attachment to the scandium ion's coordination environment as ligands.   The position of ligating species to the scandium ion in the complex might be affected by steric crowding exerted by the two *tert*-butyl groups from **L1**.   As two *tert*-butyl groups are directed towards the axial positions, a ligand that is smaller in size would be preferred to be in the axial positions in the coordination sphere of scandium ion.

Chiral scandium catalyst formed with **L1** has also been reported to catalyze asymmetric ring-opening reactions of *meso*-epoxide of *cis*-stilbene oxide with aniline and indole derivatives. In the reaction with aniline in water, a good linear relationship was observed between the enantiopurity of chiral ligand **L1** and that of the product.   On the other hand positive nonlinear effects appeared in DCM (Figure 5).[38b,41]
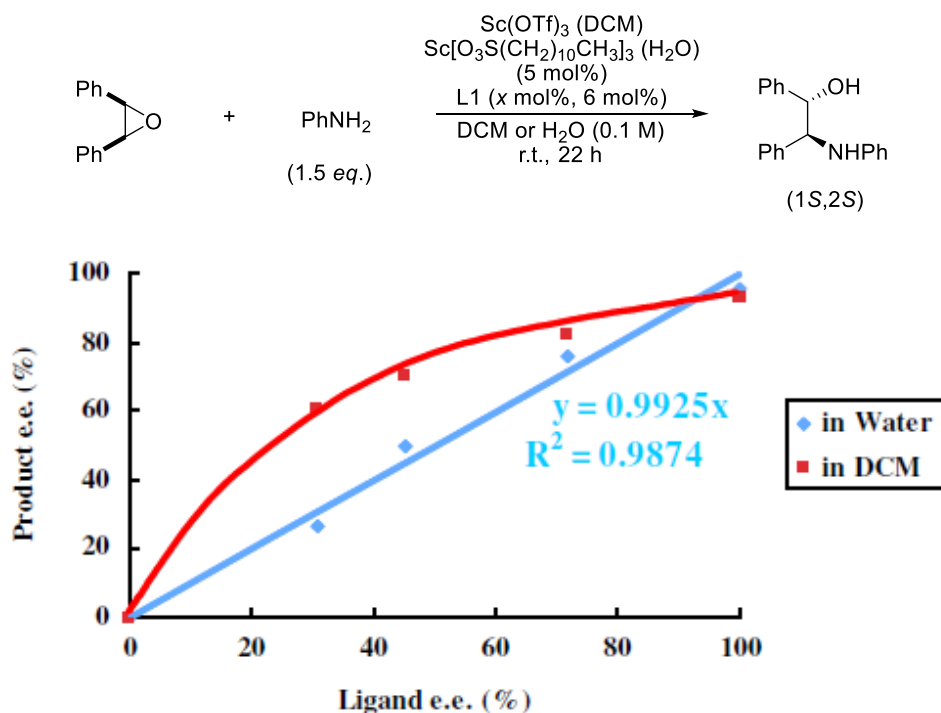
Figure 5. NLE experiments using chiral Sc catalyst in water and in DCM[38b,41]

When Sc-**L1** and Sc-(*R,R*)-**L1** (opposite conformation) were prepared independently and combined appropriately to make catalysts with low enantioselectivity in DCM, a nonlinear relationship between the enantiopurity of ligand and that of product disappeared (Figure 6). [38b,41] It was assumed that Sc-**L1** complex would not dissociate after the formation of the complex in DCM and the formation of such dimeric or oligomeric structure would be suppressed successfully in water. The exhibition of the same level of enantioselectivity both in water and in DCM suggests the predominant involvement of a monomeric conformation during the reaction.
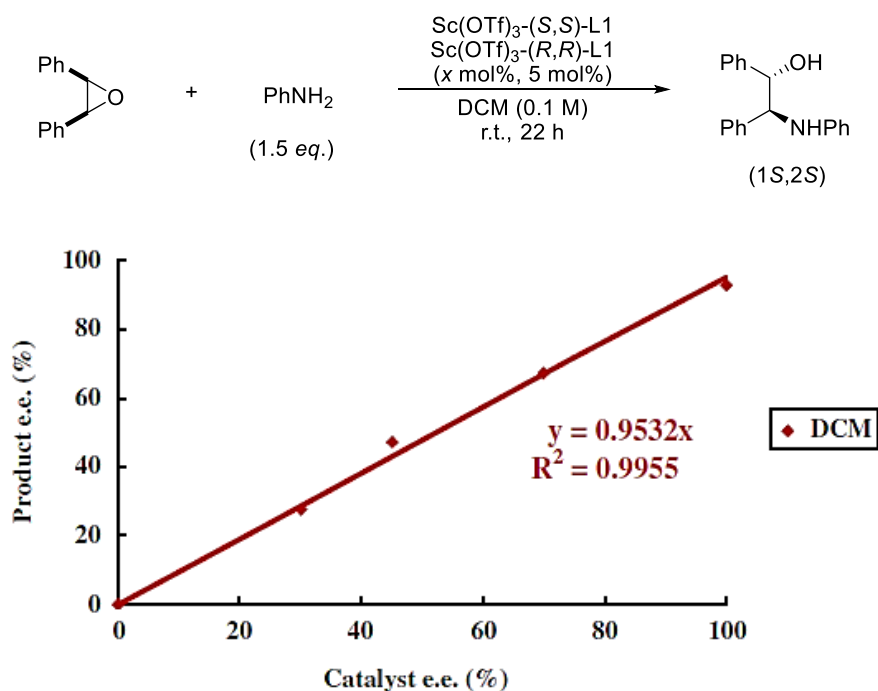
Figure 6. NLE experiments using premixed catalysts in DCM[38b,41]

The combination of Lewis acid catalyst and additive has opened up a new aspect in the history of Lewis acid catalyst. The powerful assistance of Lewis acid catalysis by additive is difficult to understand, due to the paucity of information on the catalyst structure. The elucidation of reaction mechanisms entails a profound insight into the coordination environment around the central metal ion in water, which renders the precise comprehension one of the most formidable tasks. In order to accumulate the knowledge on the catalyst structure, the relationship between the enantioselectivity of **L1** and that of product was examined in asymmetric Michael addition of benzylmercaptan with benzalacetone in water (Figure 2, refer to Chapter 4.2-3). The catalysis assistance by pyridine as additive was so high-potency that as low as 1mol% of scandium catalyst was enough to obtain high yield and high enantioselectivity. The existence of chiral scandium complex oligomer may be suggested by the positive nonlinear effects. Detection of chiral scandium complex in the reaction solution through NMR analysis was also conducted. The homogeneous catalyst solution is amenable to NMR analysis. In order to clarify the coordination environment around the central metal, ^{45}Sc NMR *must* be the most suitable choice. ^{45}Sc is a spin 7/2 and is therefore quadrupolar. As a result, the signal width increases with asymmetry of the environment. Scandium has, however, a limited chemistry due to its rareness and there has been

little knowledge on ^{45}Sc NMR spectrum. As a reaction model, Sc(OTf)$_3$ and **L1** were mixed with a ratio of 1 : 1.2 in D$_2$O/CD$_3$CN (1/9) solution and the subsequent catalyst solution was directly submitted to NMR analysis. The aqueous solution of ScCl$_3$ (Sc(H$_2$O)$_6^{3+}$) served as the external standard (δ = 0) for ^{45}Sc NMR. The observation of a single peak (δ = 51.9) denotes the quantitative formation of complex with **L1** (Figure 7).

d 54.52

Sc(OTf)$_3$ + **L1** + *aq.* HCHO

d 51.90

Sc(OTf)$_3$ + **L1**

250   200   150   100   50   0 **ppm**
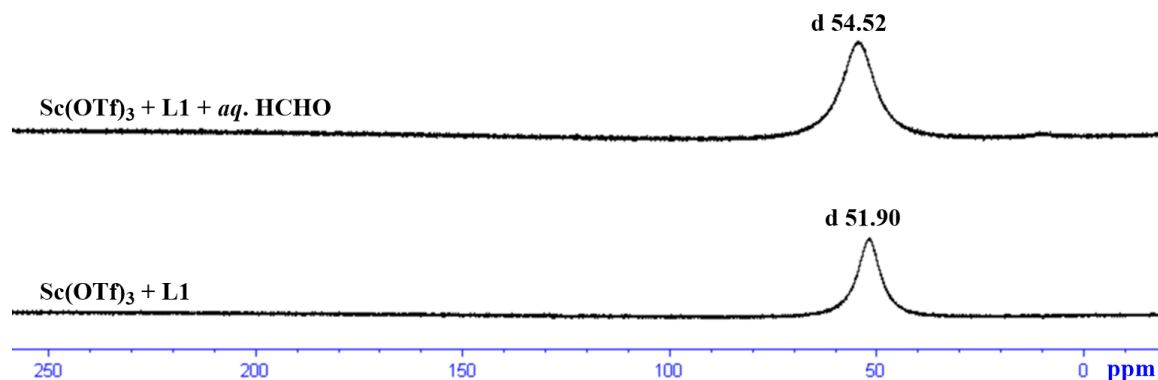
Figure 7. ^{45}Sc NMR spectrum in D$_2$O-CD$_3$CN (1/9) solution

Although the subsequent addition of aqueous formaldehyde had no influence on the complexation with **L1**, the subtle change in chemical shift will come from the enhancement of Lewis acidity on scandium through the coordination of formaldehyde as Lewis base. An equimolar complex formed from Sc(OTf)$_3$ and **L1** was also identified by ^{1}H NMR spectroscopy (Figure 8).

Sc(OTf)$_3$ + **L1**

L1

9   8   7   6   5   4   3   2   1   0 **ppm**
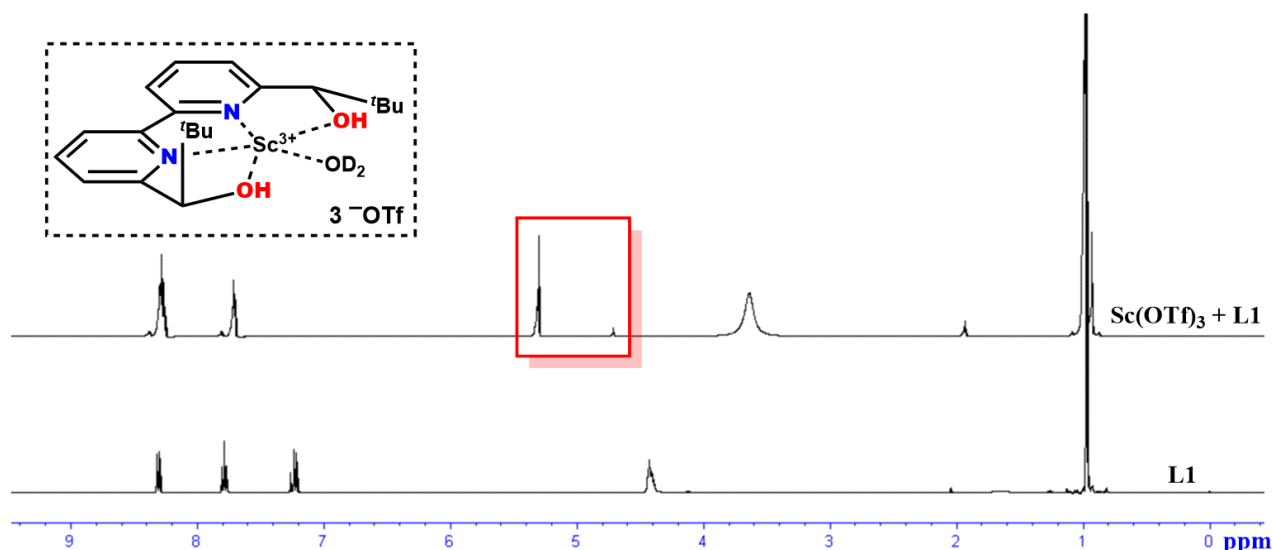
Figure 8. ^{1}H NMR spectrum in D$_2$O-CD$_3$CN (1/9) solution

Since 1.2 equivalents of **L1** were added to scandium triflate, the spectrum corresponding to excessive 0.2 mol% of **L1** was still observed. The influence of coordination with scandium was reflected clearly in a methyne proton spectrum. In addition, three signals corresponding to bipyridine moiety came to be recognized as two signals after the complexation. The effect of additives on the catalyst structure was then investigated through NMR analysis. It is noteworthy

that triflate anion exists constantly as ionic form even after the addition of various kinds of additives, which was verified by ^{19}F NMR spectroscopy. First of all, a preliminary NMR investigation has been explored in order to clarify the interaction between scandium and each additive. Given the chiral scandium complex with chiral 2,2'-bipyridine **L1**, 2,2'-bipyridine can behave as a ligand for scandium. The significant peak shift was observed when scandium triflate was added, although 2,2'-bipyridine itself is almost insoluble in water or deuterium oxide (Figure 9).
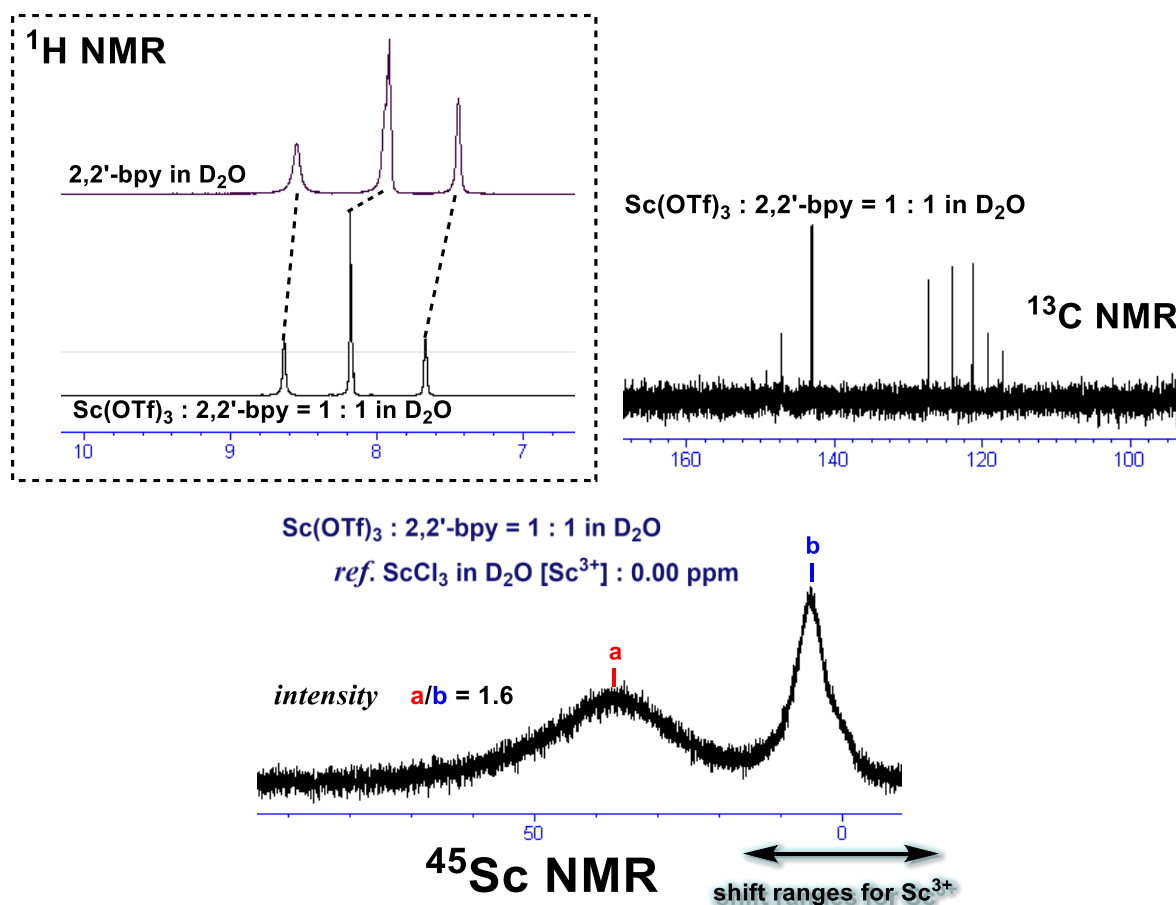
Figure 9. ^{1}H and ^{13}C NMR (above) and ^{45}Sc (below) NMR analysis of Sc-bpy mixture

Since four pairs of protons are recognized independently in organic solvent dependent on the chemical environment, 2,2'-bipyridine partially dissolves in water as ionic form. Two kinds of signals were detected in ^{45}Sc NMR spectrum (peak **a** [δ (^{45}Sc) = 36 ppm] & **b** [δ (^{45}Sc) = 5.96 ppm]). Aqueous solutions of scandium salts contain, in the pH/D range of *ca*. 2 – 4, the species $Sc(H_2O)_6^{3+}$, $Sc(OH)(H_2O)_5^{2+}$ and $Sc_2(OH)_2(H_2O)_8^{4+}$ in fast exchange with each other.[70] And at pH > 4, a slowly exchanging trinuclear complex, $Sc_3(OH)_5(H_2O)_n^{4+}$ [δ (^{45}Sc) = 36 ppm] is also present. Therefore it is considered that sharp peak **b** corresponds to $Sc(OH)(H_2O)_5^{2+}$ referred to the reported chemical shift corresponding to $[Sc(OH)(H_2O)_5]_2Cl_4 \cdot 2H_2O$ [δ (^{45}Sc) = 6.04 ppm].[71] And the pH value in this solution was less than 4, the peak **a** probably corresponds to $Sc(bpy)_m(H_2O)_n^{3+}$ complex. Although an involvement of a nitrogen function in coordination to scandium typically appears at *ca*. 70 ppm with respect to $Sc(H_2O)_6^{3+}$, the deshielding contributions caused by a decrease of symmetry are possible enough. The significant shift in ^{1}H NMR spectrum might result

from the interaction between scandium ion and 2,2'-bipyridine. Similarly in the case of pyridine, the remarkable change in ^{1}H NMR spectrum was observed in the presence of scandium triflate. Notably, the identical spectrum was recorded irrespective of the ratio of scandium to pyridine (Figure 10) [exception: more than 3-fold excess of pyridine will lead to the complete hydrolysis of scandium triflate]. It was confirmed that these signals corresponded to pyridinium trifluoromethanesulfonate. When Sc(OTf)$_3$ and pyridine were combined in the ratio of 3 : 1, hardly any interaction was observed and the dwarf and broad peak was detected at approximately 36 ppm (peak *c*). The 2-fold excess of pyridine eliminated free scandium cation and instead two broad peaks were obtained (peak *c* [δ (^{45}Sc) = 36 ppm] & *d* [δ (^{45}Sc) = 16 ppm]).
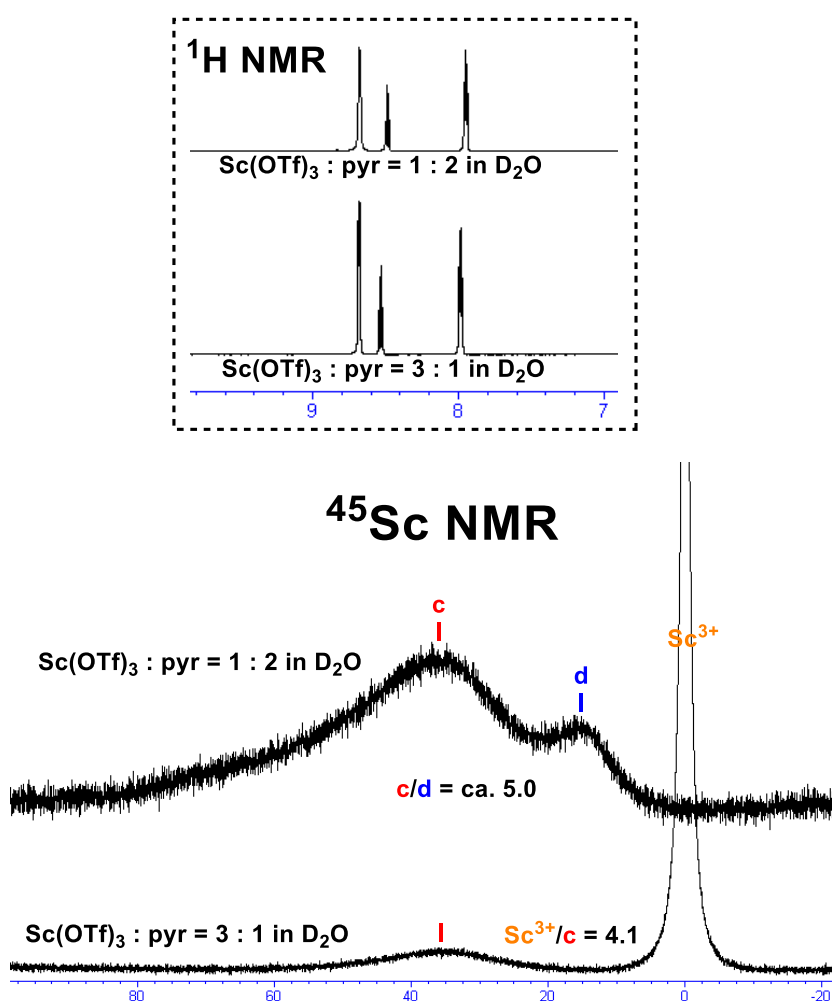
Figure 10. ^{1}H NMR (above) and ^{45}Sc (below) NMR analysis of Sc-py mixture

Due to its d^0 configuration, the scandium ion was not fastidious in whether it coordinates with solvent molecule or pyridine. Therefore the coordination through weak interaction should be in dynamic equilibrium with non-coordinating scandium ion. On the basis of these considerations, dominant peak *c*, which was detected even in the presence of small amount of pyridine, probably corresponds to Sc(py)(H$_2$O)$_5$$^{3+}$ species (Simple hydroxo-complex *must* correspond to a sharp signal). And Sc(py)$_2$(H$_2$O)$_4$$^{3+}$ or Sc(py)(OH)(H$_2$O)$_4$$^{3+}$ was the odds-on candidate for the peak *d*. The chiral pyridine **22**, the half structure of **L1**, was also verified to form a complex completely with scandium

ion from the evident changes in the chemical shift, especially at methyne proton (Figure 11). A pyridine moiety in the structure seems to behave as pyridinium cation. Therefore the signal at 39 ppm should correspond to an equimolar complex of scandium and **22** (peak **e**). And it is indicated that rather sharp signal at 11 ppm corresponds to Sc(**22**)(OH)(H$_2$O)$_3^{3+}$ (peak **f**).

Figure 11. ^{1}H NMR (above) and ^{45}Sc (below) NMR analysis of Sc-**A** mixture

Aqueous solution (D$_2$O) of chiral scandium complex formed between scandium triflate and **L1** was then amenable to NMR instruments (Figure 12). Owing to the complete insolubility of chiral 2,2'-bipyridine **L1** itself in water, the single chemical species seemed to be reflected in ^{1}H NMR spectrum. The strong acidity of an aqueous solution of Sc-**L1** mixture (pH 2.8) excludes the consideration on scandium hydroxo oligomer. An equimolar complex of scandium and **L1** is, therefore, detected undoubtedly as peak **g** [δ (^{45}Sc) = 46 ppm]. Judging from the ratio of their integrated values, the half amount of scandium triflate would be involved in the formation of the complex with **L1** and the other half would behave as a free cation. As the solubility of **L1** itself increase, the peak corresponding to a free scandium cation disappears in aqueous acetonitrile with a slight deshielding. The following addition of pyridine was disclosed to induce the structural changes in scandium complex formed with **L1** through ^{1}H NMR spectrum (Figure 13). When used as additive, a pyridine forms a pyridinium cation in this system. Approximately a half amount of scandium formed the complex with **L1** without additive, whereas a free scandium cation amazingly did not exist anymore in the presence of pyridine [δ (^{45}Sc) = 80 ppm]. The observation of remarkable downshielding implies the coordination of pyridine on scandium. In order to gain

an insight into the coordination environment surrounding to scandium cation, the influence of the coordinating ligand attached on the chemical shift was examined (Figure 14).   The chemical shift is strongly affected by the presence of electronegative ligands as can be seen in ^{45}Sc NMR shifts of Sc-**L1** complexes.   The planarity of tetradentate coordination of **L1** with Sc^{3+} would restrict the site of additional coordination. Although Sc^{3+} have no electron in its *d* orbital, the hybridization of *s*, *p* orbitals of **L1** with a vacant *d* orbital could produce the electronic change in the coordination environment, specifying the coordination at apical position.   An electron donating at the apical position would shorten the bond length, leading to a change in an electronic property of a given complex.

Figure 12. ^{1}H NMR (above) and ^{45}Sc (middle, below) NMR analysis of Sc-**L1** mixture

Figure 13. ^{1}H NMR (above) and ^{45}Sc (below) NMR analysis of Sc-**L1**-pyr mixture

Figure 14. Influence of apical ligand on ^{45}Sc NMR spectrum

The result of ^{45}Sc NMR analysis of scandium complex in aqueous solution was summarized in Table 25.

Table 25. Summary of NMR studies (structural changes).

$$Sc^{3+} \quad + \quad 3OTf^- \quad + \quad \text{(pyridine with } R^1, R^2) \quad \xrightarrow{D_2O} \quad \text{NMR analysis}$$

Additive		^{1}H NMR of pyridine moiety	^{45}Sc NMR
2,2'-bipyridine		Changed **_Cation form_**	40% Sc(OH)(H$_2$O)$_5$$^{2+}$ (6.4 ppm)[70] 60% Sc(bpy)$_m$(H$_2$O)$_n$$^{3+}$ (36 ppm)
pyridine	Sc : py = 1 : 2	Changed **_Cation form_**	85% Sc(py)(H$_2$O)$_5$$^{3+}$ (36 ppm) 15% Sc(py)$_2$(H$_2$O)$_4$$^{3+}$ or Sc(py)(OH)(H$_2$O)$_4$$^{3+}$ (16 ppm)
	Sc : py = 3 : 1		80% Sc(H$_2$O)$_6$$^{3+}$ (0.0 ppm) 20% Sc(py)(H$_2$O)$_5$$^{3+}$ (36 ppm)
(pyridine ^{t}Bu OH)		Changed **_Cation form_**	75% Sc(**A**)(H$_2$O)$_4$$^{3+}$ (39 ppm) 25% Sc(**A**)(OH)(H$_2$O)$_3$$^{3+}$ (11 ppm)
L1		Unchanged **L1** itself is insoluble	45% Sc(H$_2$O)$_6$$^{3+}$ (-1.7 ppm) 55% Sc(**L1**)(H$_2$O)$_n$$^{3+}$ (46 ppm)
L1 (with pyridine)			100% Sc(**L1**)(py)$_m$(H$_2$O)$_n$$^{3+}$ (80 ppm)
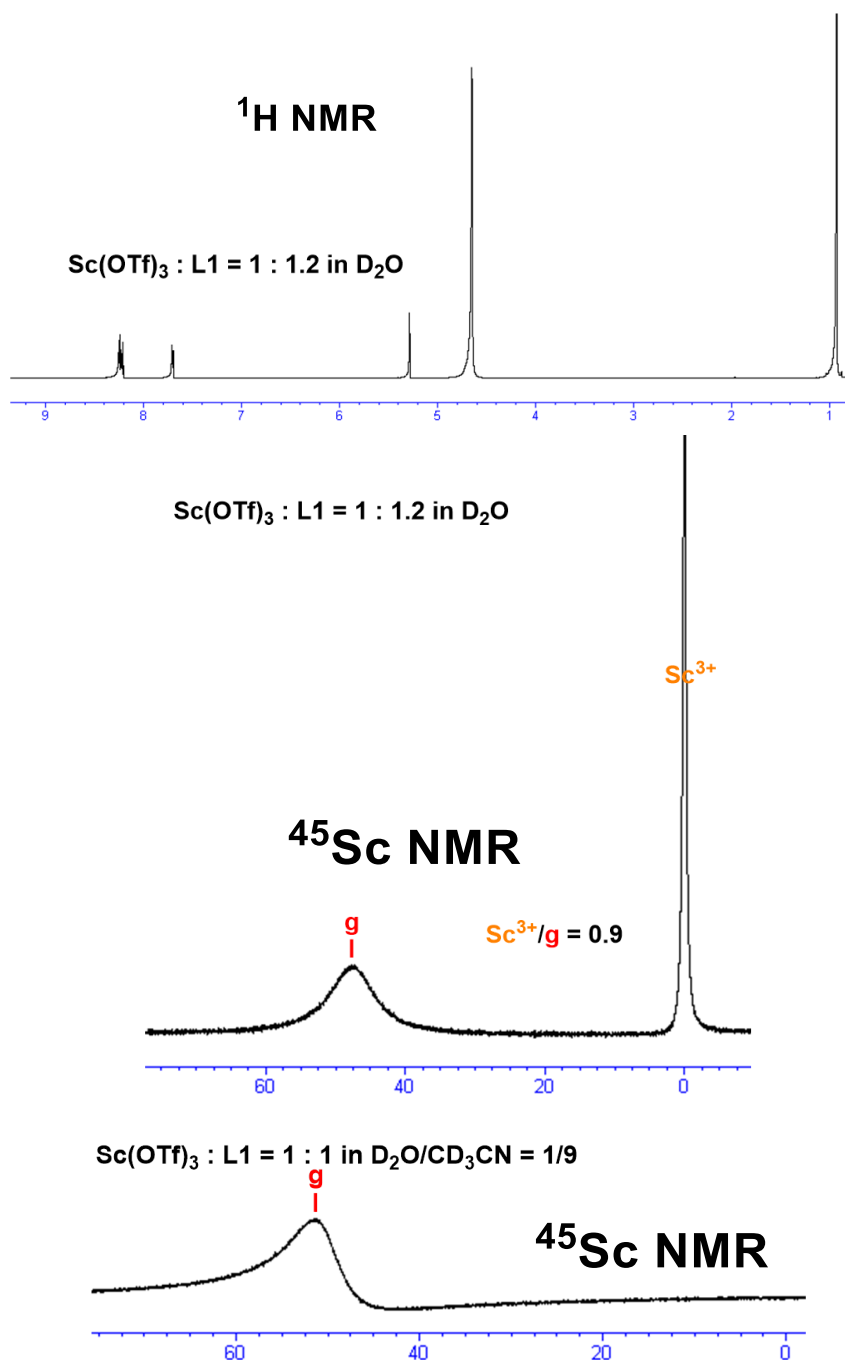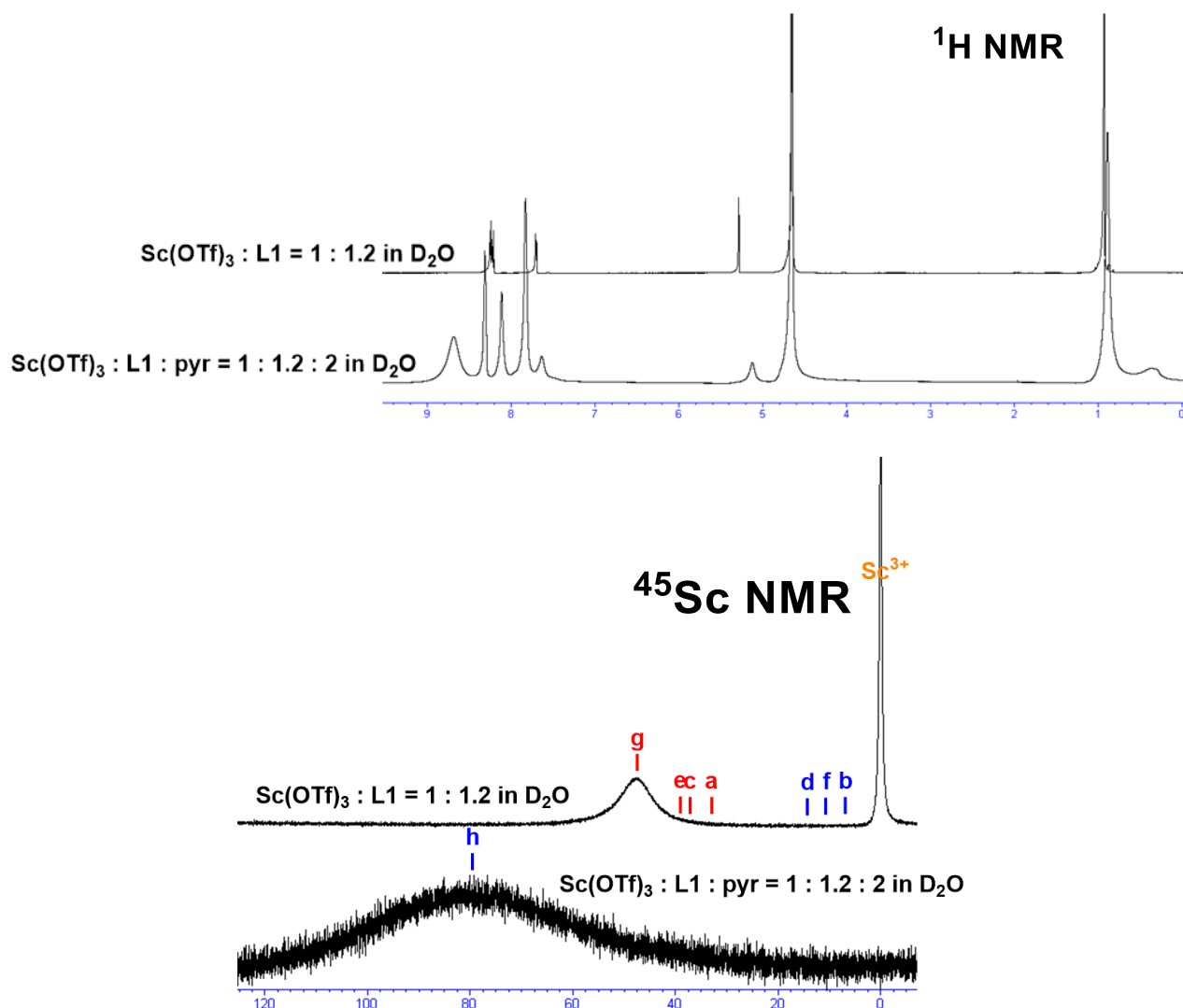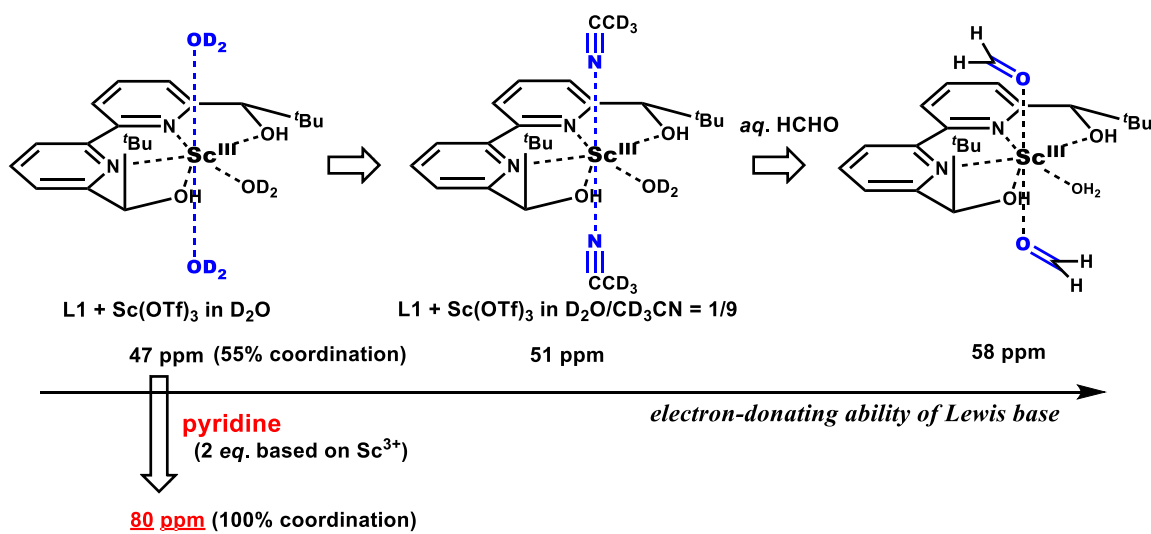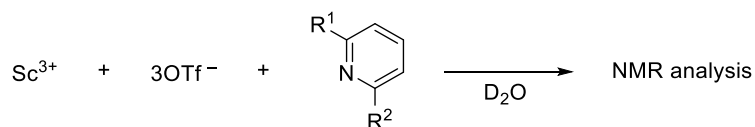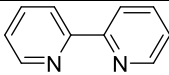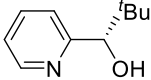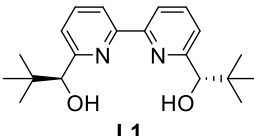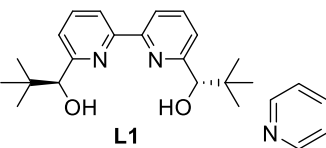
1.1-5-4 Bismuth Catalyst

Similarly, it was revealed that the active catalyst was formed from an equimolar mixture of Bi(OTf)$_3$ and **L1**.   X-ray crystal structure and the simple NMR experiment of a bismuth complex in aqueous environments are also reported, as mentioned above.   The complex adopts a pentagonal bipyramidal structure in which the tetradentate ligand occupies four of the equatorial sites.   The structure of the BiBr$_3$ complex formed with **L1** is closely related to that of the corresponding ScBr$_3$ complex.   Concerning a fundamental elucidation on the catalyst structure through NMR spectroscopy, the signal at 5.49 ppm was dominant when Bi(OTf)$_3$ and **L1** were combined in the ratio of 1 : 0.5.   An increase in the ligand/Bi(OTf)$_3$ ratio resulted in the appearance of another signal at 4.72 ppm and the concomitant decrease in intensity of the peak at 5.49 ppm until, at a ligand/Bi(OTf)$_3$ ratio of 3:1, it disappeared completely (Figure 15).   These results indicate that two equivalents of Bi(OTf)$_3$ and one equivalent of **L1** formed complex **A** (refer to Scheme 10), and that complex **B** consisting of one equivalent of Bi(OTf)$_3$ and one equivalent of **L1** was generated when an excess amount of **L1** was added.   The stability of complex **B** even in the presence of 2,2'-bipyridine was confirmed by the following experiments.   When Bi(OTf)$_3$ (1 mol%) and **L1** (3 mol%) were combined in DME at room temperature for 30 min and then 2,2'-bipyridine was added at 0 °C, the hydroxymethylation reaction proceeded at 0 °C within 21 h to afford the corresponding adduct in 93% yield with 91% ee.   On the other hand, the yield and the enantioselectivity decreased (73% y, 85% ee) when Bi(OTf)$_3$ and 2,2'-bipyridine were combined at room temperature for 30 min and then **L1** was added and the mixture was stirred at room temperature for 30 min. However, when the mixture was stirred at room temperature for 1 h, the enantioselectivity was improved (81% y, 91% ee).   NMR analysis also suggested that the formation of complex **B** was not impeded by addition of 2,2'-bipyridine as additive (Figure 16).   If anything, the peak intensity at 4.72 ppm identified as complex **B** increased significantly in the presence of 2,2'-bipyridine.   It is noted that complex **B** is stable even in the presence of 2,2'-bipyridine, and that **B** is readily formed from Bi(OTf)$_3$-2,2'-bipyridine complex and **L1**.
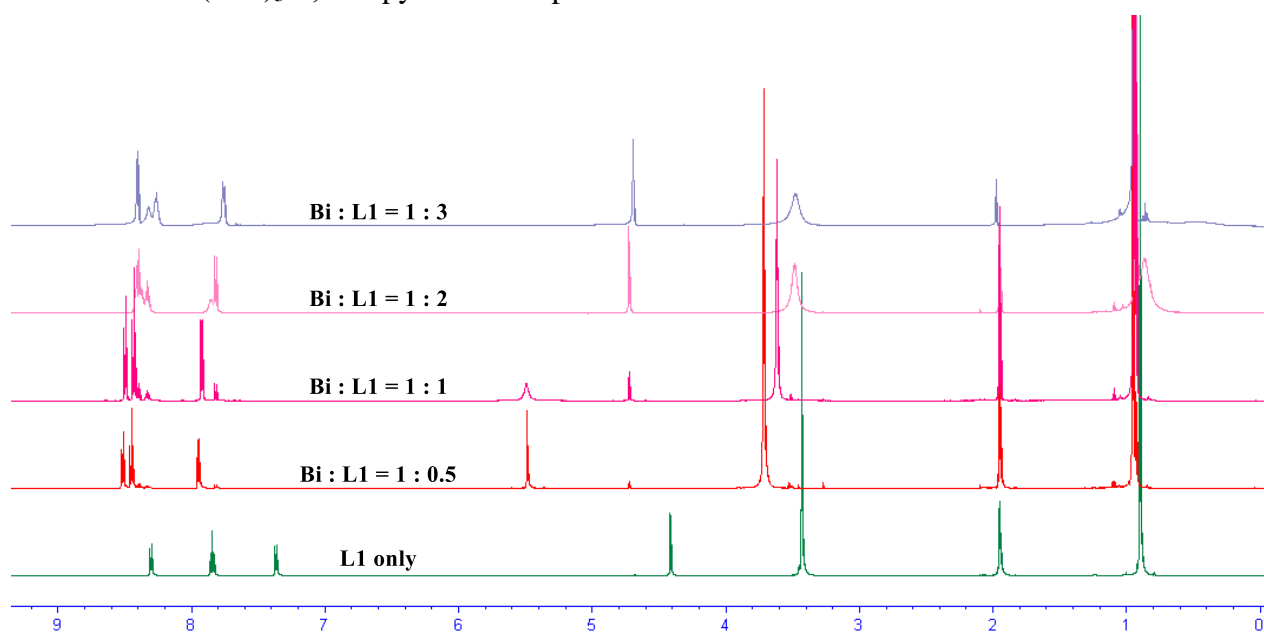
Figure 15. ^{1}H NMR analysis of bismuth complexes with a various mixing ratio
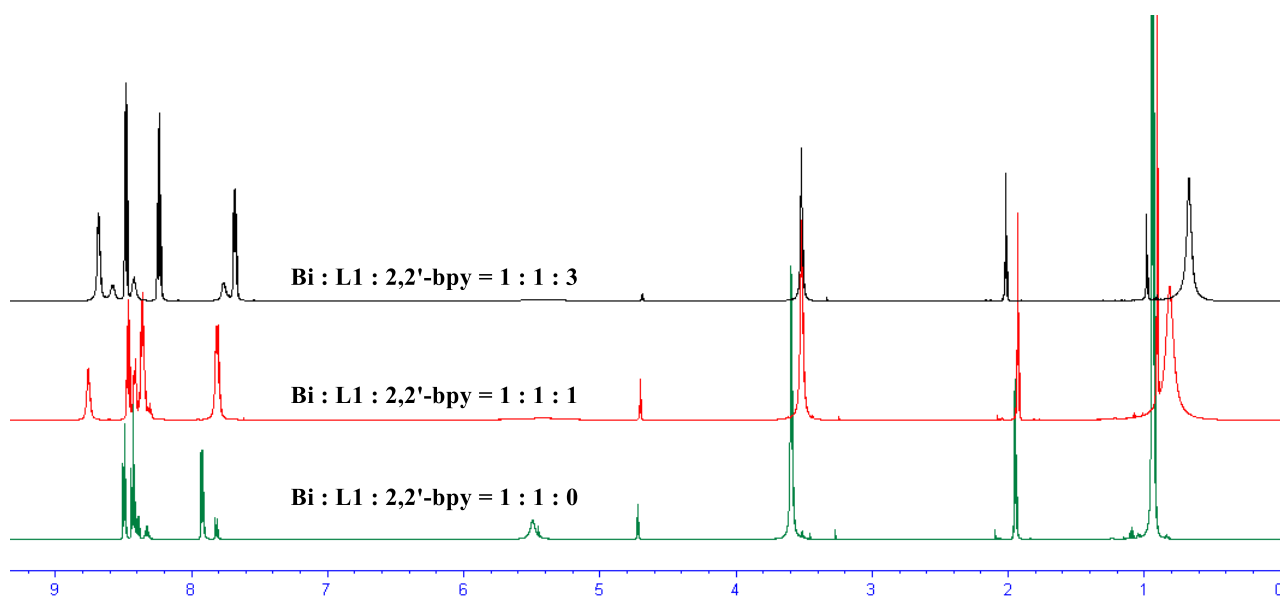
Figure 16. ^{1}H NMR Analysis of Bismuth Catalyst Structure 2
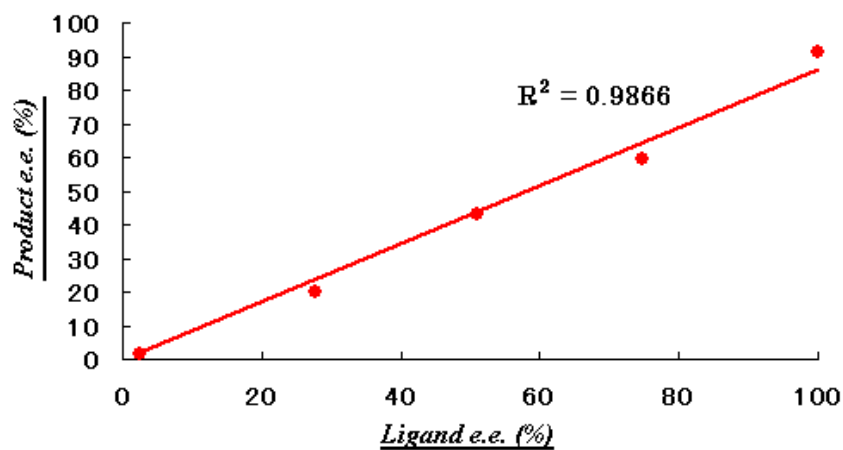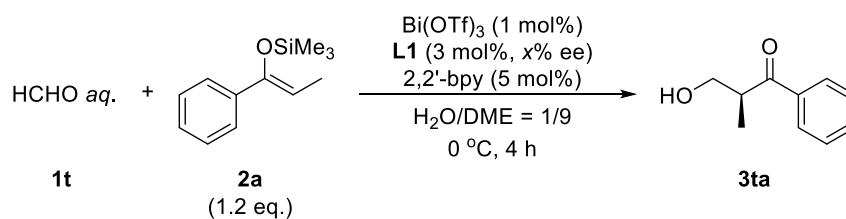
Entry	Ligand ee (*x*)	Yield (%)	Ee (%)[a]
1	2.5	81	1.6
2	27.8	79	20.2
3	50.9	80	43.2
4	74.8	82	59.6
5	>99.9	94	91.3

[a] Determined by HPLC analysis.

Figure 17. Correlation of ee values between product and ligand

In order to verify that complex B is real active species in asymmetric Mukaiyama aldol reaction in an aqueous environment, the correlation between enantiopurity of chiral ligand and that of product was investigated (Figure 17). Asymmetric hydroxymethylation of silyl enol ether **2a** provided enantioenriched product with linear correlation with enantiopurity of **L1**. This linear correlation implies that 2,2'-bipyridine contributes to the formation of bismuth monomeric complex.

1.1-5-5 Iron(II) Catalyst

The complex formed with Fe(II) salt and **L1**, reported in 2012,[40] adopts a pentagonal bipyramidal structure where the tetradentate ligand occupies four of the equatorial sites. It resembles that of the corresponding Sc(III) and Bi(III) complexes. Several examples[72] on the hepta-coordination mode of Fe(II) ion was reported and X-ray crystals of three kinds of Fe(II)-**L1** complexes[73] were obtained all in a hepta-coordination fashion. Thermogravinetric analyses, performed by Ollevier *et al.*,[74] imply that the chiral complex can behave in a hepta-coordination fashion under the reaction conditions. Apical binding of aldehydes is favored due to its least basicity, its ability to form stereoelectronically favored hydrogen bonding with alcohol moieties of **L1** and relatively greater *trans* effect of pyridine ligand.[75] The dependence in a choice of an additive on an electronic nature of aldehydes intimates the coordination of an additive to Fe(II) center. On the other hand, the behavior of Bi(III) as a naked cation is inferred from the fact that 2,6-di-*tert*-pyridine, a proton scavenger, could be an efficient additive. In order to procure fundamental insights into the catalyst structure, a model reaction of **1a** with **2a** was carried out in the presence of enantiomerically impure 2,2'-bipyridine **L1** and the results are depicted in Figure 2.In order to procure the fundamental insights into the catalyst structure, a model reaction of **1** with **2a** was carried out with enantiomerically impure 2,2'-bipyridine **L1** and the results are depicted in Figure 18. Subtle erosion of enantioselectivity in the product **3aa** was observed in the absence of additive; however the nonlinearity disappeared in the presence of the additive. The observation of negative nonlinear effects in the absence of additive can be rationalized by the changes of the catalyst structure into a monomeric form by mixed aggregate formation, which might be the actual catalytic species that result in the high enantioselectivity and reactivity. For details on these data, see below (Table 26).
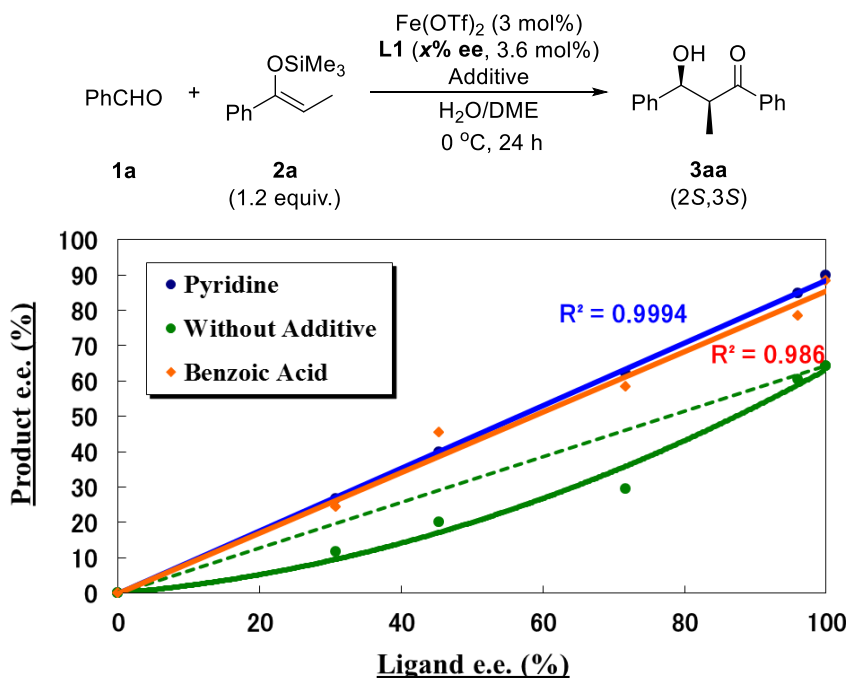
Figure 18. Nonlinear experiments

Table 26. NLE experiments.

Entry	Ligand ee (*x*)	Yield (%)	Dr (*syn/anti*)[a]	Ee (%)[b]
1	30.7	73	96/4	11.8/0
2	45.3	68	96/4	24.2/-12
3	71.7	56	96/4	29.5/-6
4	96.0	82	97/3	60.3/-30
5	>99.9	84	97/3	64.3/-28

Run	Ligand ee (x)	Yield (%)	Dr (syn/anti)	Ee (%)
1	30.7	83	97/3	26.6/4
2	45.3	82	97/3	39.8/-5
3	71.7	85	97/3	62.3/-20
4	96.0	87	97/3	84.8/-21
5	>99.9	91	97/3	89.8/-53

Run	Ligand ee (x)	Yield (%)	Dr (syn/anti)	Ee (%)
1	30.7	63	97/3	24.5/-20
2	45.3	67	97/3	45.5/-27
3	71.7	70	97/3	58.5/-45
4	96.0	70	97/3	78.6/-47
5	>99.9	85	97/3	88.4/-48

In order to gain insights on catalyst structure, the direct observation of iron(II) complexes with additives was carried out (Figure 19). It was confirmed that the observed spectrum was not dependent upon the counterion. Contrary to expectations, almost the same signals were observed even in the presence of pyridine. When benzoic acid was added, you can see small changes in the spectrum. However it seems that such small changes stem not from the drastic transformation in the structure of the iron(II) complex, but from just reinforcement of the interaction between iron(II)

and **L1**.   Any other conformations were not observed irrespective of additives, which is different from in the case of scandium and bismuth.

Fe(OTf)$_2$ + L1 + Pyridine (1 : 1.2 : 2.4)

Fe(ClO$_4$)$_2$ + L1 + PhCO$_2$H (1 : 1.2 : 1.2)

Fe(OTf)$_2$ or Fe(ClO$_4$)$_2$ + L1 (1 : 1.2)
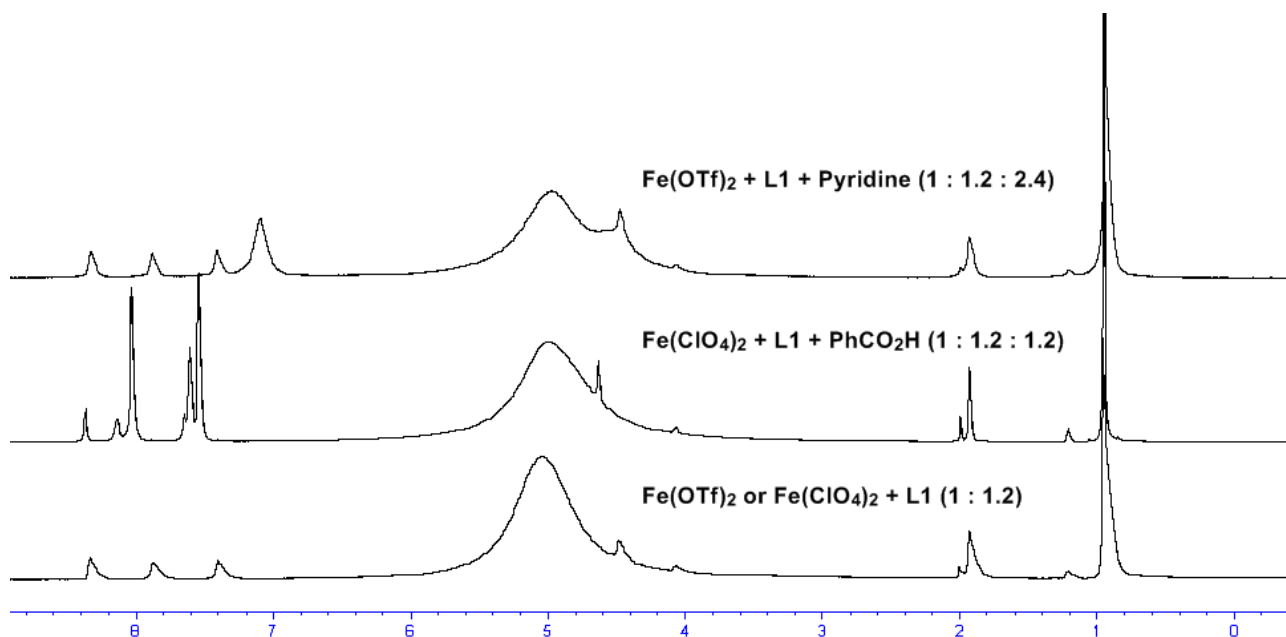
Figure 19. NMR study for Fe-**L1**-additive catalytic systems

Similarly, the powerful assistance of additive on Lewis acid catalysis is of tremendous attraction.   In order to rationalize these attractive effects, similar reaction systems have been surveyed.   Of course the similar phenomenon was not found in the field of chemistry.   In particular I focused upon the points as follow: 1) a complex formed from iron(II) and nitrogen-containing ligand, 2) iron(II) complex is much more reactive than iron(III) complex, 3) coordination of some functional groups at the apical position is crucial.   The nature has been exploiting the right iron (II) complex, iron(II)-porphyrin system (Figure 20).
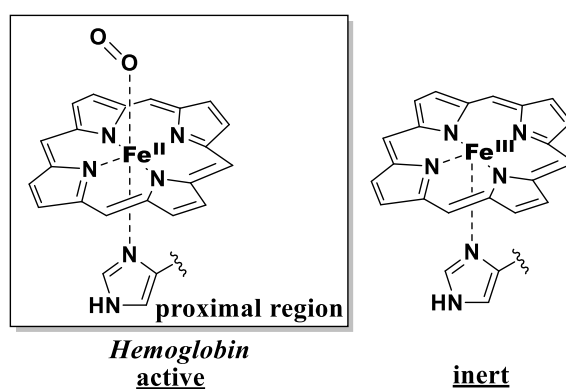
Figure 20. Natural example of iron(II) complex

It is well known that hemoglobin (Hb) can transport oxygen and carbon dioxide in the vascular systems of animals.   Heme, which has been considered as the active site of Hb, is constructed form at least one iron-porphyrin complex.   Both a donation to $3d_z2$ and a

back-donation from $3d_{yz}$ are suppressed by the imidazole ligand. Thus the donation from imidazole induces the suppression of both donation and back-donation between Fe and O_2 and the reinforcement of the O=O double bond. Without imidazole moiety, the catalytic activity was lost significantly. In addition iron(III) complex is known to have no activity of oxidation. Considering coordination chemistry on iron(II), chiral 2,2'-bipyridine **L1** and aldehyde seem to behave as a π-acceptor ligand (Figure 21).
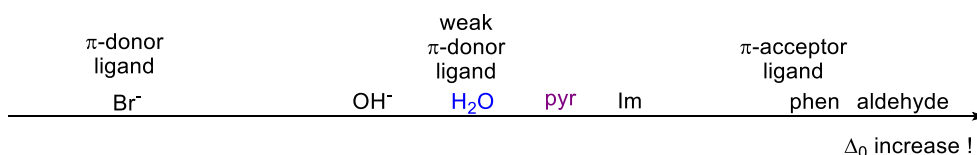
Figure 21. π-Acidity of ligands

In the meanwhile, pyridine or imidazole work as a weak π-acceptor and water does as a π-donor ligand. The length of the bond between iron and aldehyde therefore reflects a Lewis acidity of a given complex. Theoretically axial coordination of a Lewis base would decrease the Lewis acidity of metal complex through back-donation from π* orbitals of aldehyde and subsequent delocalization of an electron. When iron(II) locates in-plane, $d_{z}2$ orbital cannot interact with π orbitals of **L1** due to symmetry. However, when iron(II) locates out of plane, $d_{z}2$ orbital can interact with π orbitals of **L1** due to the broken symmetry. This stabilizes $d_{z}2$ orbital because π-electron of **L1** flows into $d_{z}2$ orbital. Therefore the interaction between $d_{z}2$ orbital and π* orbitals becomes weaker. Destabilization of $d_{z}2$ orbital is also caused by the coordination of water molecule due to the donation of π-electron. The coordination of another aldehyde molecule or pyridine have lower π* orbital than water molecule would stabilize $d_{z}2$ orbital through a donation to π* orbital, thus leading to a spin transition between the triplet and singlet states. This spin transition would overcome the deactivation due to the coordination of Lewis base, since there is no electron in the $d_{z}2$ orbital in the singlet state and the coordinative interaction between iron(II) and aldehyde would become more robust. It is reasonable to consider that the closer approaches of the substrate to the central metal enhance enantioselectivity of the product. The similar spin transition was reported in hetero Diels-Alder reaction and so on.[76] The effectiveness of a few kinds of π-acids in new catalytic system was examined. Pyridine gave the effective result, whereas the reaction was suppressed considerably and racemic product was obtained in the case of imidazole moiety. The strong coordinative nature of imidazole moiety compared with pyridine will be poisonous to the tetradentate iron(II) complex.
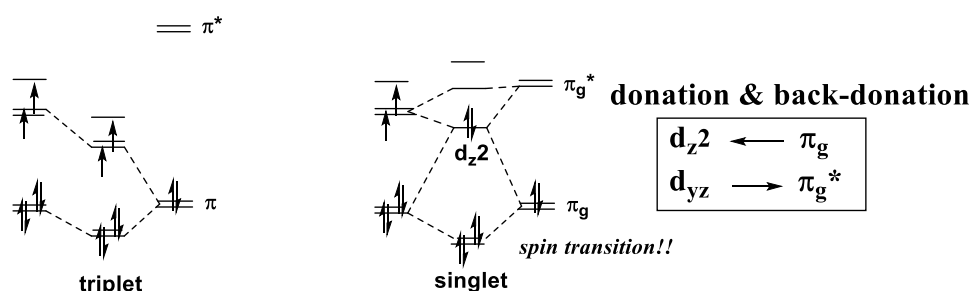
Figure 22. Coordination Effect of Pyridine and Aldehyde

1.1-5-6   The Interaction between Metal and Additives.

Fe(II),[40] Bi(III)[27] and Sc(III)[23] complexes formed with **L1** were reported all in a hepta-coordination fashion.   They exhibited the similar molecular geometry in terms of bond angles and torsional angles.   Since molecular geometry is determined by the quantum mechanical behavior of the electrons, significant differences are unlikely between these metal cations.

[Fe·L1·H₂O·DME]²⁺·2ClO₄⁻   **[BiBr₃·L1]**   **[ScBr₂·L1·H₂O]⁺·H₂O·Br⁻**

	Fe[40]	Bi[27]	Sc[23]
Angle	145.5	164.7	150.7
Torsion	16.6	27.5	19.0
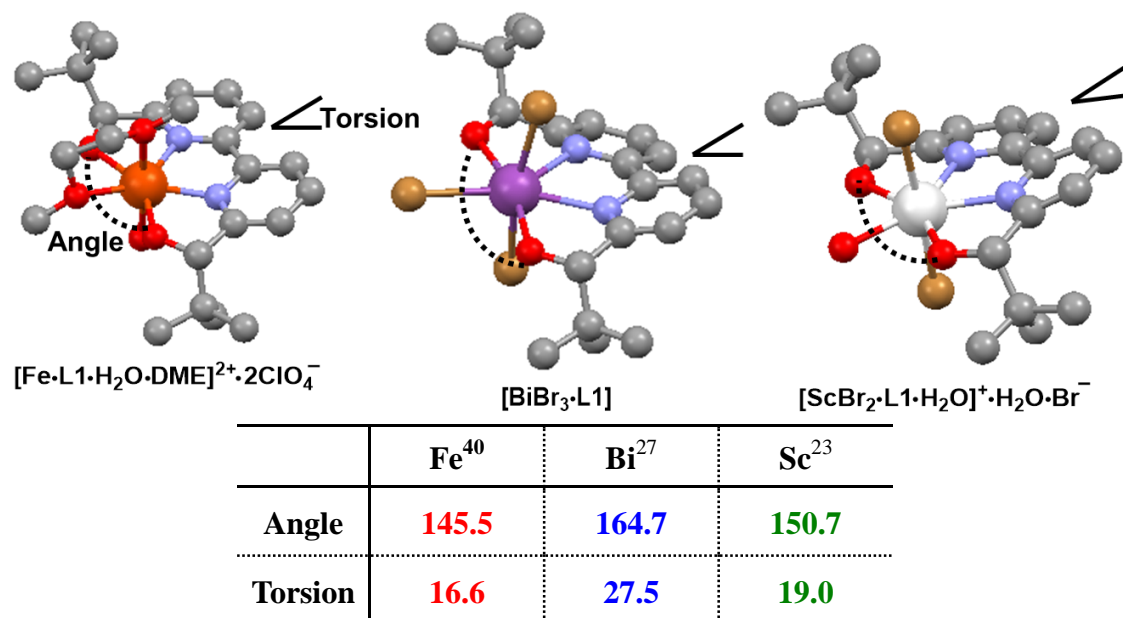
Figure 23. Comparison of metal-**L1** complexes based on molecular geometry.

In order to gain an insight on catalyst structures, the reaction solution was directly submitted to several spectrometric investigations.   Chiral iron(II) complex formed with **L1** did not give rise to massive changes in NMR analysis, in contradistinction to chiral Sc(III) and Bi(III) complexes ($D_2O/CD_3CN = 1/9$, Figure 24).   The methyne proton was affected by the catalyst structure most prominently.   And the differences in the slitting pattern corresponding to bipyridine moiety between iron(II) and other metals might imply that ^{1}H NMR spectrum did not reflect iron(II)-**L1** complex.   If so, it means that the real active species formed from iron(II) salt and **L1** is insoluble.   The profound consideration on NMR spectrum of iron(II)-**L1** complex aqueous solution is now under debate.   Likewise, the changes in an additive were not observed through NMR or UV-vis analyses.
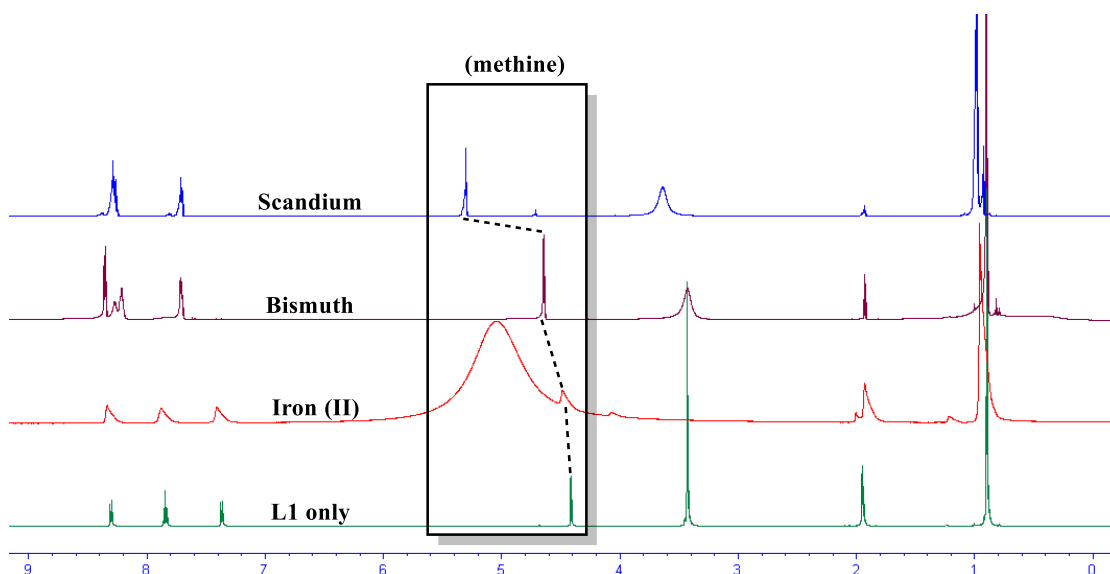
Figure 24. Various metal-**L1** complexes in $D_2O/CD_3CN = 1/9$

Meanwhile, ESI-MS experiments could shed light on the differences. In the absence of additive, two types of mono-iron(II) complexes $[Fe^{II}(\textbf{L1})(OTf)]^+$, $[Fe^{II}(\textbf{L1})(OTf)(DME)]^+$ were observed. One is coordinated by a DME molecule and the other is not. Some amount of iron(II) complex composed of two molecules of chiral ligand was also identified. When pyridine was added as additive, triflate anion was not identified as a counter anion. Instead of triflate, the formation of hydroxide $[Fe^{II}(\textbf{L1})(OH)]^+$ was verified. The major peak corresponded to iron(II) benzoate complex $[Fe^{II}(\textbf{L1})(O_2CPh)]^+$ formed with **L1**. The surroundings around Bi cation, known to be dependent upon metal to ligand ratio, were also proved to be a naked cation without any ligand.
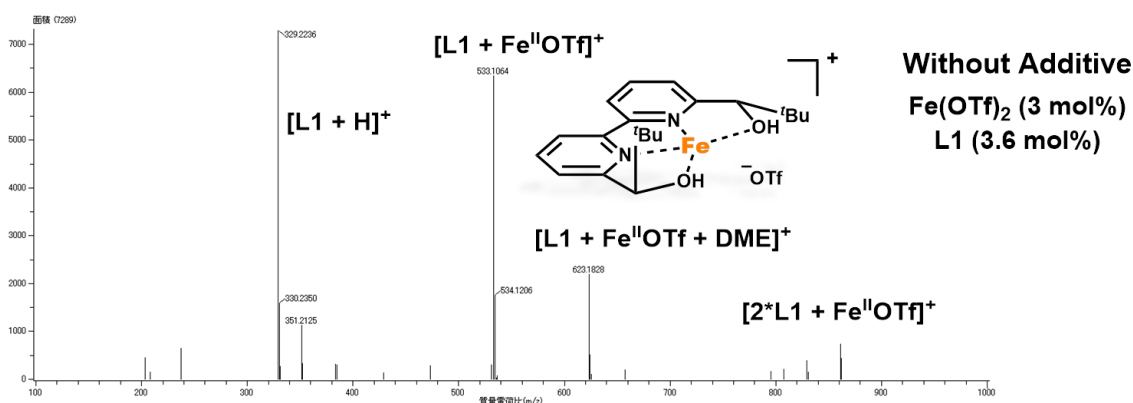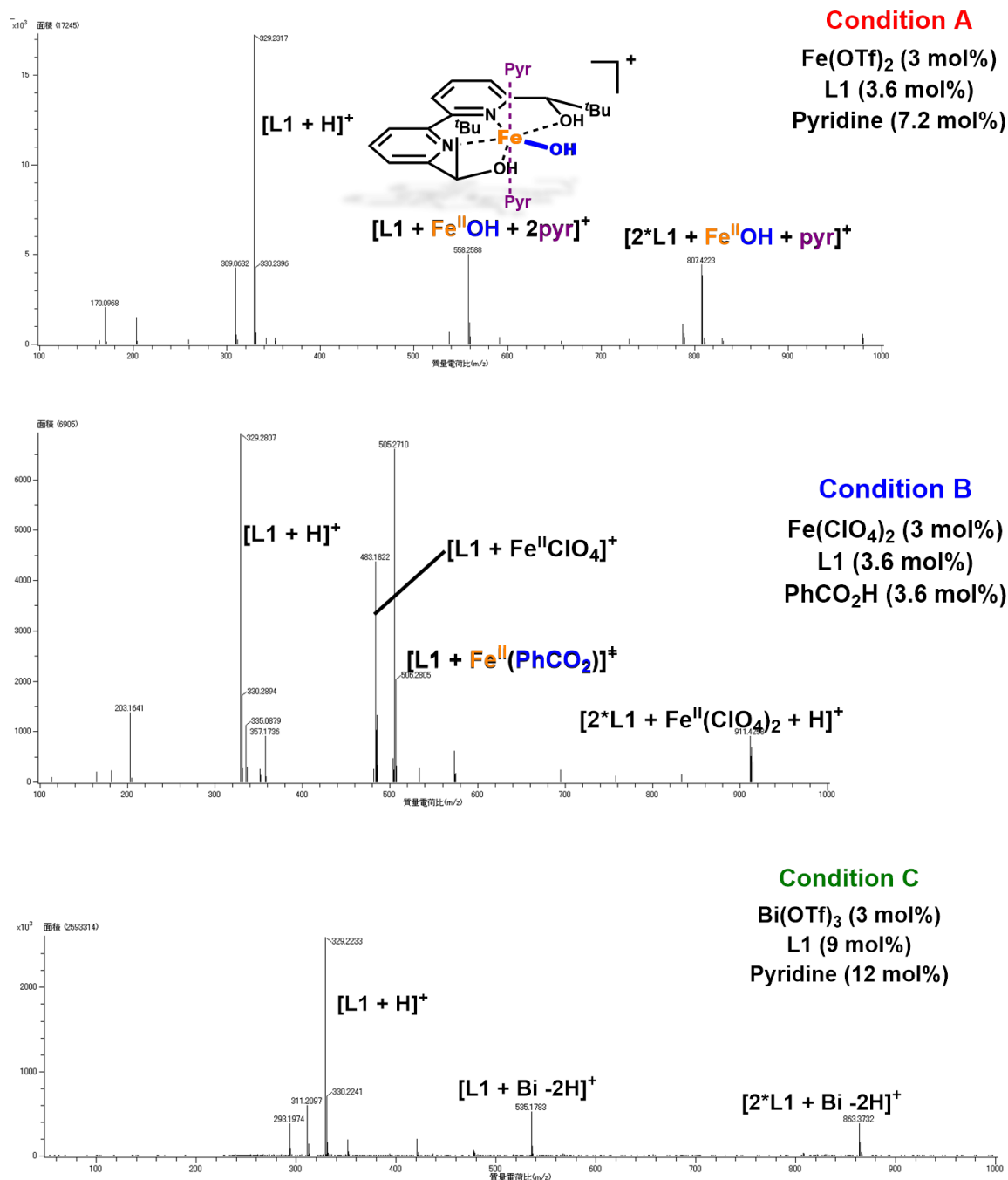
Figure 25. ESI-MS analysis of the reaction solutions.

Ligand Field Theory (LFT) is subservient to deepening our understandings on the effect of additives. The donation of electrons by σ-donor ligands to d orbitals and some weak bonding and anti-bonding interactions with s and p orbitals of an iron(II) center should be plausible. Compared with non-bonding orbitals consisting of d_{xz} and d_{yz}, the anti-bonding orbital between $4s$, $4p$, d_{xy} and $d_{x^2-y^2}$, and that between $4s$, $4p_z$ and d_{z^2} would become destabilized. When pyridine is added as an additive, OH ligand at equatorial position or pyridine at apical position would make the former bonding orbital unstable and the latter stable. The consequent spin transition in HOMO orbital would overcome the deactivation by the coordination of a Lewis base[76] and the lower HOMO would destabilize the π* orbital of aldehydes. Given the intriguing equilibrium shift observed in the case

of Sc-**L1** complex, the stabilization of pentagonal bipyramidal structure even in an aqueous environment is expected.   In contrast, bidentate coordination of benzoate anion to iron makes the latter unstable.   The resultant HOMO-LUMO gaps between aldehydes and silyl enol ethers correspond to the experimental tendencies shown in Table 24.   The strength of interactions between iron and both substrates governs the stereoselectivities on the assumption of some interaction between iron and π-orbital of silyl enol ether.[77]
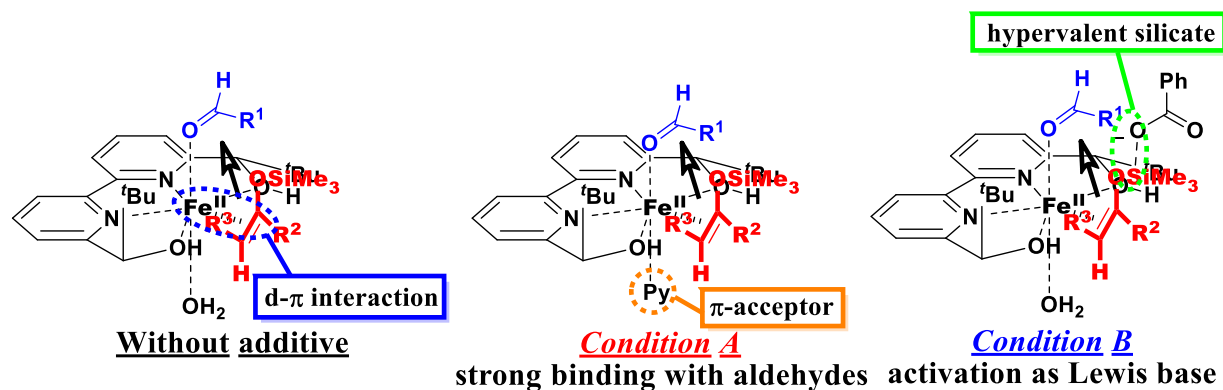
Scheme 26. Mechanistic elucidation of key complexes

1.1-5-7   The Effect of Additives on Silicon Enolates.

Due to the ability of silicon atom to adopt higher coordination states, promoting the Mukaiyama aldol reaction under basic conditions is known to be possible.   In that sense, an additive can function as a Lewis base in newly developed catalytic systems.   In order to examine whether a nucleophilic attack takes place at silicon or not, the Mukaiyama aldol reaction using dimethylsilyl enol ether was carried out (Table 27).   Throughout the enhancement of the reaction rate, almost quantitative amount of product was obtained under **Condition A**; however it also led to a significant drop in selectivity.   In the case of chiral bismuth catalyst, it was turned out that enantioselectivity remained definitely the same level; however the reactivity did not enhance at all. These results imply somewhat involvement of silicon enolate activation by a Lewis base in Fe(II)-catalyzed mechanism and no involvement in Bi(III)-catalyzed mechanism.   In the latter case, pyridine additive is assumed to be swamped with the elimination of *in situ* generated triflic acid. Due to the heterogeneity of the reaction solution, ^{29}Si NMR was not applicable.

Table 27. Effect of silicon enolates.

	Si = SiMe$_3$	**Si = SiMe$_2$H**
Condition A [Fe(OTf)$_2$]	72% yield *syn/anti* = 93/7 74% ee (*syn*)	95% yield *syn/anti* = 84/16 28% ee (*syn*)
Condition C [Bi(OTf)$_3$]	76% yield *syn/anti* = 98/2 90% ee (*syn*)	70% yield *syn/anti* = 96/4 90% ee (*syn*)

In order to investigate the role of benzoate anion as a Lewis base, the electronic effect on the additive was investigated (Table 28).   When 4-methoxybenzoic acid was used as additive, the reaction proceeded smoothly to produce almost same results as those when benzoic acid was used. On the other hand in the case of 4-nitrobenzoic acid both the reaction yield and enantioselectivity suffered from significant drop.   The enantioselectivity of a *syn*-isomer was almost same level as that in the absence of any additive.   As mentioned above, the substituents on the aromatic ring in the structure of silyl enol ether affected drastically to the reactivity and selectivity.   Similarly, Mukaiyama *et al.* reported that 10 mol% of metal carboxylates could function as a Lewis base catalyst to catalyze the reaction between benzaldehyde and ketene silyl acetal at –45 $^{\circ}$C in DMF/H$_2$O = 50/1.[78] They assumed that the role of the carboxylate in the catalytic cycle was the formation of a lithium aldolate, *via* a hexa-coordinated hypervalent silicate, that undergoes rapid hydrolysis and subsequent neutralization to re-generate lithium acetate catalyst.   The dependence

of reactivity on the electrophilicity of aldehydes to support their hypothesis was in accord with the results shown in Table 26.

Table 28. Effect of additives on silicon enolates.
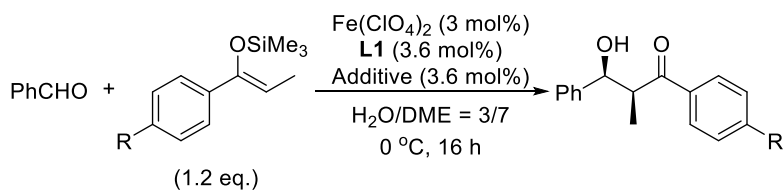
Entry	R	Additive	Yield (%)	Dr (*syn/anti*)[a]	Ee (%)[b]
1	H	-	70	97/3	75/43
2	H	$PhCO_2H$	85	97/3	88/48
3	H	$PhCO_2K$	NR	–	–
4	H	$4\text{-}MeOC_6H_4CO_2H$	80	97/3	84/43
5	H	$4\text{-}NO_2C_6H_4CO_2H$	52	96/4	73/47
6	MeO	$PhCO_2H$	6	97/3	49/nd
7	Cl	$PhCO_2H$	70	93/7	65/40

[a] Determined by ^{1}H NMR analysis.   [b] Determined by HPLC analysis, *syn/anti*.

To sum up, there are two functions in the role of additives; coordination to iron(II) ion and coordination to silicon.[79] Two kinds of additives can regulate the balance between two interactions to afford the desired aldol in high yield with high diastereo- and enantioselectivity.

1.1-5-8   Reaction pathways & transition states, the role of water

First of all, water is a sine qua non for *in situ* generation of active hydroxide species in the presence of pyridine and that of benzoate anion to coordinate with iron in the presence of benzoic acid. Besides, the reaction run in dimethoxyethane (DME) in the absence of water did not lead to the formation of desired aldol adduct.[80] The higher the ratio of water to DME was, the lower reaction yield, the higher diastereo- and enantioselectivity were observed. The amount of water governed the stereochemical outcomes as well as the consequent catalytic turnover, although water is prone to destabilize silicon enolates through hydrolysis of metal triflates. The profound correlation between the amount of water and the results has been observed in the incipient reports on the catalysis of $Yb(OTf)_3$ in aqueous media.[81] Hence it was verified that water exerts an influence on steric interaction between metal complex and reactants.   A plausible catalytic cycle for this Mukaiyama aldol reaction in aqueous media is shown in Scheme 27.   An aldehyde coordinates to the pentagonal bipyramidal Fe(II) consisting of Fe(II), **L1**, and an additive in the axial position.   One of the ligands, pyridine, benzoic acid, or water, may be replaced by the aldehyde.   Water coordinated with Fe(II) is willing to exchange and may help the replacement. One face of the aldehyde is shielded by the *t*-butyl group of **L1**.   The enantiofacial differentiation of an aldehyde carbonyl group was trivial due to the relative preference of the carbonyl coordinated by a Lewis acid toward (*E*)-conformation.   One face of the aldehyde is shielded by the *t*-butyl group of **L1** and the orientation of the aldehyde might be fixed through hydrogen bond formed between the aldehyde and the hydroxyl moieties of **L1**.   The formyl C-H⋯O hydrogen bond was known to be important for fixing an aldehyde in chiral Lewis acid-catalyzed reactions including the Mukaiyama aldol reaction.[82] A silicon enolate then attacks the aldehyde *via* an antiperiplanar acyclic transition state.   Water also plays a key role here to coordinate to the silicon of the silicon enolate to assist the reaction.   The additive, pyridine or benzoic acid, is also suggested to play the same role (***Condition A***, ***Condition B***).   In the Bi(III)-catalyzed reaction (***Condition C***), it was shown that the coordination of pyridine to the silicon atom was not significant; however, water coordination was assumed to be crucial there.   Having almost no influence on the reaction selectivity (e.g. for **3aa**, see Table 20, for **3ga**, without pyridine [Quant, *syn*/*anti* = 98/2, 91/69 (% ee)], for **3ja**, without pyridine [46% yield, *syn*/*anti* = 98/2, 91/43 (% ee)] *vs*. [66% yield, *syn*/*anti* = 98/2, 91/–15 (% ee)], for **3ua**, without pyridine [66% yield, *syn*/*anti* = 98/2, 90/– (% ee)]), pyridine seemed to play a role as a proton scavenger rather than as a coordinating ligand.   Carbon–carbon bond formation then occurred with high diastereo- and enantioselectivities, and the resulting Fe(II) alkoxide reacts with water to afford the desired aldol adduct along with regeneration of the Fe(II) catalyst.   The silicon moiety is quenched with water to decrease Lewis acidity (Me_3Si–O–$SiMe_3$) to prevent undesired Si-catalyzed achiral pathways, which often reduce diastereo- and enantioselectivities in asymmetric Mukaiyama aldol reactions.   It is noted that here water also plays an important role.   In newly-developed reaction systems, water is a *sine qua non* for in situ generation of active species in the presence of pyridine or benzoic acid.   Indeed, the reaction in DME in the absence of water did not lead to the formation of the desired aldol adduct.   The higher the ratio of water to DME, the lower the reaction yield and the higher the observed diastereo- and enantioselectivity.   The amount of water governs the stereochemical outcomes as well as the consequent catalytic turnover, although water is prone to destabilize silicon enolates through

hydrolysis of metal complexes. The profound correlation between the amount of water and the results were observed in the incipient reports on the catalysis of $Yb(OTf)_3$ in aqueous media.
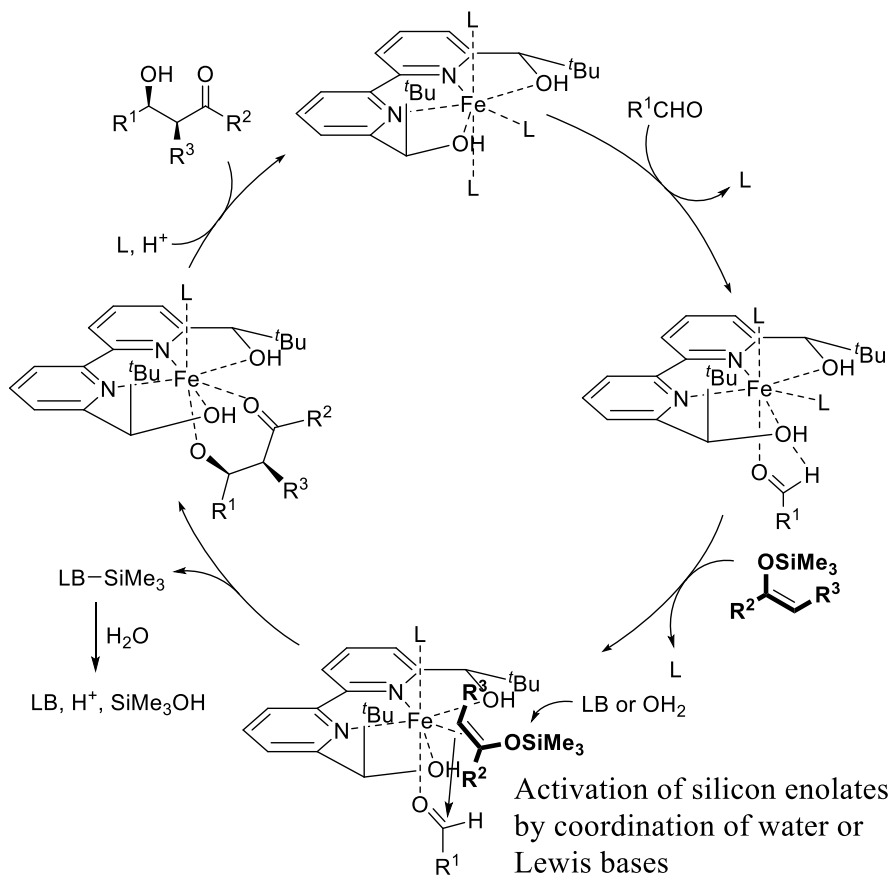
Scheme 27. Plausible catalytic cycle.

Activation of silicon enolates by coordination of water or Lewis bases

1.1-6   Conclusions

Extensive screening of Lewis acids with chiral 2,2'-bipyridine **L1** has revealed effective and promising Lewis acidity of Fe(II) and Bi(III) species.   The employment of 3–fold excess of the chiral ligand with respect to metal cation promoted the reaction in the most highly enantioselective manner to afford the *syn*-aldol adduct as a major product.   It is noted that the reaction didn't proceed at all in the absence of water.   The sagacious selection of three catalytic systems has enlarged the substrate generality.   An exquisite set of catalysts comprising metal, chiral ligand and additive has thus reinforced organic chemistry in aqueous media.   While previous reactions often required relatively harsh conditions, such as strictly anhydrous conditions, very low temperature (−78 °C), *etc*., the present systems work well in aqueous environments at 0 °C.   A wide variety of silicon enolates and aldehydes reacted under these conditions to afford the desired aldol products in high yields with high diastereo- and enantioselectivities.   The superiority of this methodology over conventional reactions has also been proved by high catalytic activity, simplicity of experimental procedures, wide substrate range including aqueous aldehydes that have been regarded to be difficult to govern the stereochemistry.   Coordination environments around Fe(II) and Bi(III) and the effect of additives in the chiral catalysts have been elucidated by mechanistic studies.   It is noted that both Brønsted acids and bases worked as efficient additives in Fe(II)-catalyzed reactions.   Extensive mechanistic elucidation through ^{1}H NMR analysis, NLE (non-linear effect) experiments and some experimental results on the catalyst structure suggested that the catalytic system is in dynamic equilibrium between multiple aggregated structures, and that a soluble monomeric catalyst complex is predominant in the presence of additives.   The assumed catalytic cycle and transition states have clarified the important roles of water,[83] a) producing the active metal complexes with high water-exchange rate constant (3.2×10^6) to activate substrates effectively and to catalyze the reaction via acyclic transition states, b) facilitating the catalytic turnover with simultaneous desilylation as direct access to aldol adducts or facile recovery of active metal complexes, and c) stabilizing rigid transition states composed of metal complexes and reactants through entropy-driven aggregation derived from its highest cohesive energy density (ced). Forty years after the discovery of the Mukaiyama aldol reaction, we have established a definitive catalytic asymmetric variant using Fe(II) and Bi(III) with chiral bipyridine **L1** in aqueous media.

Section 1.2 Applications of LASCs for Asymmetric Mukaiyama Aldol Reaction in Water

1.2-1   Introduction

   As mentioned above, a fundamental challenge of performing catalytic asymmetric Mukaiyama aldol reactions in aqueous environments is the construction of efficient asymmetric environment under polar conditions and the competitive hydrolysis of silicon enolates, lowering the product yield and narrowing the substrate scope. In antecedent section, a definitive catalytic asymmetric variant using chiral iron(II) and bismuth(III) complexes was established in aqueous media. These complementary catalytic systems, as the most distinguished catalyst ever reported, could enlarge the substrate generality considerably. The superiority of this methodology over conventional methods was marked by high catalytic activity, expedience, and broad coverage of substrates including aqueous aldehydes, for which the stereochemistry has been regarded as difficult to govern. Thus, a relationship between the Mukaiyama aldol reactions and water passes by degrees to a more mature stage. The intimate dependence of the catalyst structure on the substrate in highly selective Mukaiyama aldol reactions, a great problem for chemists, is nearly surmounted. The catalytic system hitherto admits of improvement in using organic solvents and low temperature. Given the dominance of *Lewis acid–Lewis base interactions* over other interactions and the resulting loss of their acidity upon coordination to chiral ligands, Lewis acid-catalyzed asymmetric reactions in water using hydrophilic substrates are recognized as highly challenging, even though chiral induction can be achieved in aqueous media.[84] Furthermore, the application to the reaction of ketene silyl acetals in water is desirable.

   Micellar systems containing anionic[85] or nonionic surfactant[86] have often improved reactivity in Lewis acid-catalyzed Mukaiyama aldol reactions.[87] A major disadvantage of Lewis acid catalysis aided by surfactants was semi-catalytic use of the surfactants to achieve good results, leading to the difficulty in separation. Another drawback arises in the substrate tolerance. Since the relative concentration of the catalysts in the hydrophobic micelles is low due to their high affinity with water, quite labile silicon enolates, such as cyclohexanone-derived substrate and thioketene silyl acetals, decompose rapidly. In 1998, a Lewis acid–surfactant-combined catalyst (LASC) emerged as an innovative catalyst, in which a Lewis acid possessed ligands with surfactant properties to construct an efficient hydrophobic environment surrounding a Lewis acidic cation.[88,89] The use of scandium tris(dodecylsulfate) ($Sc(DS)_3$ [DS = $OSO_3C_{12}H_{25}$]) to construct highly reactive microenvironments in water enlarged the substrate scope in the Mukaiyama aldol reaction to include quite labile silicon enolates. The reaction was found to progress 5×10^3 times faster in water than in dichloromethane.[88a] LASCs have been applied to various reactions in water hereafter.[90,91]

   The successful application of LASC for asymmetric Mukaiyama aldol reactions in pure water was reported in 1999, where the combination of $Cu(DS)_2$ and chiral bis(oxazoline) ligand was described.[47] Chiral disulfonated binaphthyl dialkyl ethers with $Ga(OTf)_3$ and $Cu(OTf)_2$ catalyzed the asymmetric Mukaiyama aldol reactions more efficiently than did $Sc(OTf)_3$ in water with moderate selectivities (Scheme 28).[92] The chiral amphiphile, which has been mainly used in

enantiomer separation by capillary electrochromatography,[93] formed micelles in water and the changes in the torsion between two naphthyl rings might result in chiral induction.
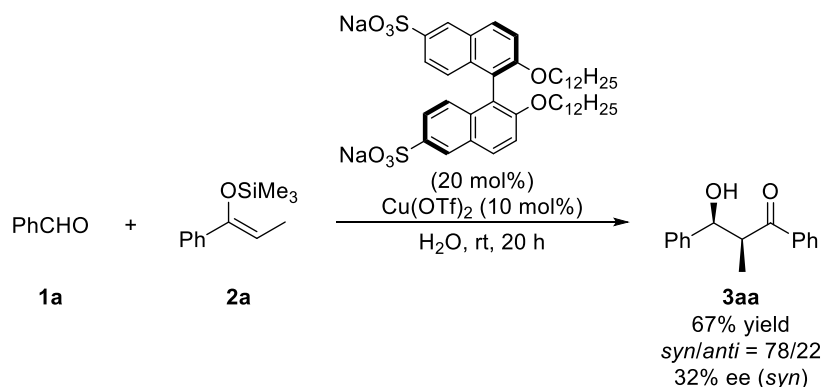
Scheme 28. Chiral surfactant for enantioselective Mukaiyama aldol reactions.

PEG- or Triton®-supported chiral bis(oxazoline) has been employed in combination with copper(II) salts as a catalyst for the Mukaiyama aldol reactions of ketene silyl acetal derived from methyl isobutyrate with aldehydes in water (Scheme 29).[94]
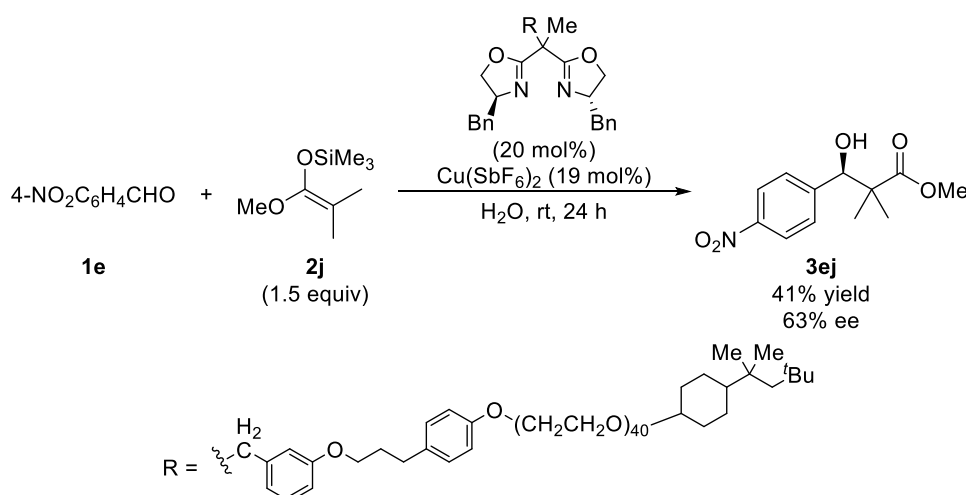
Scheme 29. Triton®-supported chiral copper(II) complex for enantioselective Mukaiyama aldol reactions.

A moderate level of yield, diastereo- and enantioselectivity as well as the narrow substrate scope are still a critical issue, except asymmetric hydroxymethylation in water (see Scheme 8). Herein the potentiality of LASCs for asymmetric Mukaiyama aldol reactions was demonstrated in water, especially toward the reaction with quite labile silicon enolates.

1.2-2 *LASC Catalysis for Asymmetric Reactions of Ketone-Derived Silicon Enolates*

At the outset, several LASCs were prepared and evaluated in the reaction of benzaldehyde **1a** with propiophenone-derived silyl enol ether **2a** performed in water (Table 29). Although the Sc(DS)$_3$-**L1** complex which is known to be an efficient catalyst in asymmetric hydroxymethylation reactions of silicon enolates[95] provided comparatively high enantioselectivity, the reaction suffered from a low yield of **3aa** unlike the reported hydroxymethylation catalyzed by the Sc(DS)$_3$-**L1** complex (entry 1). In contrast, another type of Sc^{III}-based LASC[96] gave poor results in terms of both reactivity and enantioselectivity (entry 2). Not only Sc^{III} but Cu^{II} and Fe^{II} were turned out to be efficient catalysts and they catalyzed the reaction in a comparatively high diastereo- and enantioselective manner (entries 3-6). In the meanwhile, Fe(OSO$_2$C$_{11}$H$_{23}$)$_2$ exhibited the almost same catalytic activity as that of Fe(DS)$_2$ but the enantioselectivity decreased slightly. The use of μ-oxo-dinuclear Fe^{III}-based LASC[97] instead of Fe^{II}-based LASC resulted in much lower reaction yield and lower diastereo- and enantioselectivity (entries 7, 8). The importance of ferrous ion as an efficient Lewis acid catalyst in this reaction is noteworthy. The LASCs prepared from the heavy metals exhibited low enantioselectivity in water (entries 9-11).

Table 29. LASC-catalyzed asymmetric Mukaiyama aldol reaction in water.

PhCHO + [2a structure: Ph, OSiMe$_3$] → **L1** (12 mol%), LASC (10 mol%), H$_2$O, rt, 48 h → *syn*-**3aa** (2S,3S) + *anti*-**3aa** (2R,3S)

1a   **2a** (1.2 equiv.)

Entry	LASC	Yield (%)[a]	Dr (*syn/anti*)[b]	Ee (%)[c]
1[d]	Sc(DS)$_3$	18	81/19	−72/−29
2	Sc(OSO$_2$C$_{11}$H$_{23}$)$_3$	8	77/23	−34/−33
3	Cu(DS)$_2$	22	71/29	−65/−7
4	Cu(OSO$_2$C$_{11}$H$_{23}$)$_2$	18	71/29	−66/−1
5	Fe(DS)$_2$	50	91/9	65/18
6	Fe(OSO$_2$C$_{11}$H$_{23}$)$_2$	53	91/9	58/14
7	Fe$_2$O(DS)$_4$	24	78/22	26/0
8	Fe$_2$O(OSO$_2$C$_{11}$H$_{23}$)$_4$	21	72/28	36/1
9	Sn(OSO$_2$C$_{11}$H$_{23}$)$_2$	13	74/26	−39/1
10	Hg(OSO$_2$C$_{11}$H$_{23}$)$_2$	26	82/18	0/0
11	Pb$_2$(OH)(OAc)(DS)$_2$	8	80/20	25/1

[a] Isolated yield. [b] Determined by ^{1}H NMR analysis.

[c] Determined by HPLC analysis; minus values indicate opposite enantioselectivity.

[d] DS = OSO$_3$C$_{12}$H$_{25}$.

In order to examine the assistance of Fe^{II} catalysis by additives and to enhance diastereoselectivity, a number of additives have been explored (Table 30). As reported under

co-solvent conditions described in Section 1.1, a successful aid by both Brønsted acids and bases was probed even in pure water. The use of 2,2'-bipyridyl or α-substituted pyridine derivatives, which were more effective for stereoselective control in aqueous media, were much less effective than simple pyridine (entries 1-5). Nevertheless, the effect of pyridine went to be negative when lowering the catalyst loading. Meanwhile, the effective combination between Lewis acid and Brønsted acid has been previously reported in Mukaiyama aldol reaction or allylation.[46,52] As shown in such pioneer investigations,[47] hydrophilic acid (*i.e.* acetic acid), weaker acid (*i.e.* phenol) and more hydrophobic acid (*i.e.* CSA) did not have any positive effect (entries 6-8). The addition of lauric acid was also ineffective (entry 9). The effect of substituents on the aromatic ring in benzoic acid was quite similar to a discussion in section 1.1-5-7 (entries 10-12). To date, yet one cannot elucidate how Brønsted acid assists LASC catalysis in water. As discussed in antecedent section, the formation of a hypervalent silicate by Lewis base function seems to be feasible. That is, carboxylate anion would serve as two types of Lewis base: coordination to Fe(II) ion and coordination to the silicon of silicon enolates for activation. The bidentate coordination of benzoate anion to Fe(II)-**L1**-aldehyde complex would destabilize the antibonding orbitals between $4s$, $4p_z$, and d_z^2 and stabilize the orbitals between $4s$, $4p$, d_{xy}, and $d_{x^2-y^2}$. Although the spin transition in the HOMO orbital overcomes the deactivation by the coordination of a Lewis base at the opposite site of aldehyde, the coordination of benzoate anion would bring the aldehyde close to Fe(II) center, distorting the exquisite transition state for chiral induction. By contrast, the latter coordination could activate the nucleophile, having almost no adverse effect on open-transition-state model. Although $Fe(OSO_2C_{11}H_{23})_2$ exhibited lower reactivity than $Fe(DS)_2$ without addition of any additive (Table 27), the combination of $Fe(OSO_2C_{11}H_{23})_2$ with benzoic acid resulted in significant enhancement of reactivity while retaining high level of enantioselectivity (entry 13). The reaction at lower catalyst loading was neither retarded nor less stereoselective, except for 1 mol% catalyst loading (entries 14-16).

Table 30. Effect of additives on Fe(II)-based LASC-catalyzed asymmetric Mukaiyama aldol reaction in water.

Entry	Additive	Yield (%)[a]	Dr (*syn/anti*)[b]	Ee (%)[c]
1	2,2'-bipyridyl	27	66/34	7/1
2	Pyridine	53	92/8	80/13
3	α-Picoline	36	88/12	64/54
4	2-Ethylpyridine	45	90/10	78/50
5	2,6-Lutidine	60	90/10	76/48
6	AcOH	21	89/11	78/52
7	PhOH	39	79/21	52/19
8	CSA	15	50/50	15/<1

9	Lauric acid	49	78/22	63/59
10	PhCO$_2$H	49	91/9	84/39
11	4-MeOC$_6$H$_4$CO$_2$H	68	88/12	84/59
12	4-NO$_2$C$_6$H$_4$CO$_2$H	64	86/14	81/55
13[d]	PhCO$_2$H	73	92/8	84/46
14[d,e]	PhCO$_2$H	73	94/6	81/36
15[d,f]	PhCO$_2$H	74	94/6	80/26
16[d,g]	PhCO$_2$H	78	91/9	43/7

[a] Isolated yield. [b] Determined by ^{1}H NMR analysis.   [c] Determined by HPLC analysis.
[d] Fe(OSO$_2$C$_{11}$H$_{23}$)$_2$ was employed instead of Fe(DS)$_2$.
[e] The reaction with 5 mol% catalyst loading. [f] The reaction with 3 mol% loading.
[g] The reaction with 1 mol% catalyst loading.

A number of LASCs derived from Fe(II) were screened anew in the co-existence of benzoic acid (Scheme 30).   Besides the steric or electronic influences inherent to a monomer structure itself, an interesting facet of the relationship between structure and reaction outcome lies in the micelle formation during the reaction.   When LASC was prepared from linear-type dodecylbenzenesulfonic acid, the formed micelle was assumed to differ from that formed by other LASCs because of the aromatic ring contiguous to the hydrophilic head.   The conceivable structural alternation of the micelle hardly affected the stereochemical outcome in this reaction. When the catalyst possesses a lower CMC, for instance Fe(OSO$_2$C$_{14}$H$_{29}$)$_2$, the reaction proceeded a bit less smoothly.   The insufficient micelle formed when chain length was too short resulted in a dramatic fall in the reaction yield.
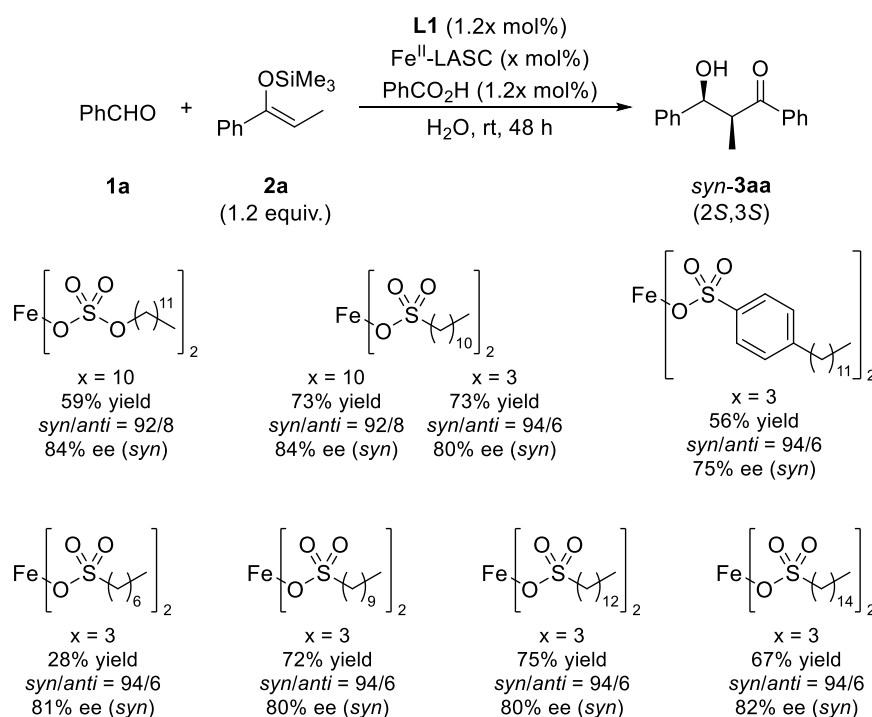
Scheme 30. The screening of several Fe(II)-based LASCs.

The substrate scope was then examined by using Fe(II)-LASC with benzoic acid. Aromatic aldehydes seem to be reacted with silyl enol ether efficiently under optimal conditions to afford the desired product with high enantioselectivity. However when aliphatic aldehydes were employed as substrates, the reaction suffered from a dramatic decrease in reactivity or enantioselectivity. The absolute configuration of the desired aldols obtained from aliphatic aldehydes was opposite to those yielded in the reaction of aromatic aldehydes. In addition, the combination of Sc(DS)$_3$ with **L1**, an efficient catalyst for asymmetric hydroxymethylation,[26] could catalyze the reaction of aliphatic aldehydes with highly enantioselectivity as a complementary catalyst. The opposite sense of enantioselection between Sc(OTf)$_3$-catalyzed reaction in aqueous media and Sc(DS)$_3$-catalyzed reaction in water is noteworthy, which was not observed in asymmetric hydroxymethylation of silicon enolates.[23,26] Similar phenomena reported in enantioselective protonation (Chapter 4) implies the involvement of hydrogen bonding in chiral induction.

The ability of silicon atoms to adopt higher coordination states sometimes facilitates the Mukaiyama aldol reaction under basic conditions even in aqueous environments.[78] Hosomi *et al.* disclosed that the uncatalyzed reaction of benzaldehyde with dimethylsilyl (DMS) enolates proceeded under thermal conditions in DMF, while trimethylsilyl enolates hardly reacted.[98] Extensive examination of additives to promote the Mukaiyama aldol reactions led to the discovery of calcium chloride as a catalyst, which effectively suppressed associated side reactions. The rate-accelerating ability of the calcium salt depends on the intrinsic nucleophilicity of the counter anion: $TfO^- < I^- < Br^- < Cl^-$. Tetrabutylammonium chloride also exhibited good catalytic activity for the Mukaiyama aldol reaction of DMS-enolates. Given the diametrically different observations on rate acceleration between TMS- and DMS-enolate and the chloride ion's higher nucleophilicity compared with those of bromide or iodide ions in an aprotic solvent such as DMF, and the low Lewis acidity of $CaCl_2$,[99] chloride ion was determined to function as a Lewis base to activate the DMS enolate. In spite of a much lower tolerance to water, DMS enolate turned out to be a competent nucleophile in the presence of $CaCl_2$ in water or aqueous DMF. Consequently, the $CaCl_2$-promoted system could be utilized for the reaction of aqueous aldehydes such as aqueous formaldehyde, phenylglyoxal and chloral, and this was the first example of Lewis base-catalyzed Mukaiyama aldol reactions in aqueous media (Scheme 31). The combination with alkali metals for aldol reactions[100] would be classified into the same category.
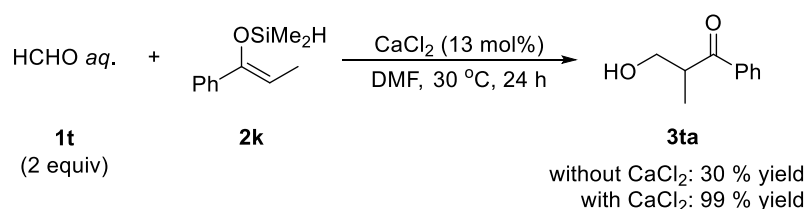
Scheme 31. $CaCl_2$-catalyzed Mukaiyama aldol reaction using aqueous formaldehyde.

A report on the distinctive behavior of ScF_3 which was different from that of either a Lewis acid (Sc^{3+}) or a Lewis base (F^-) in the Mukaiyama aldol reaction in aqueous media[101] suggests the synthetic utility of silicon reagents bearing a less bulky silyl group still remains unexplored. Comparison of the reactivity between TMS and DMS enolates derived from propiophenone for

hydroxymethylation reactions was examined using typical Lewis acids or bases (Table 31).[101] The hydroxymethylation was sluggish without a catalyst (entry 1), whereas both enolates reacted to afford the product in the presence of a Lewis acid catalyst (scandium chloride); the TMS enolate provided a higher yield (entry 2). The products were also obtained from both enolates in the presence of KF and 18-crown-6 with the TMS enolate demonstrating slightly better reactivity (entry 3). The addition of HF resulted in lower yields with both enolates (entry 4). Interestingly, ScF_3 produced the product only from DMS enolate (entry 5). This unique character of ScF_3 denoted that its reactivity toward TMS and DMS enolates was different from that of a conventional Lewis acid or fluoride ion[102] (Lewis base)-catalyzed reactions. Some reports have shown that fluoride ions can activate silicon enolates effectively even in a protic solvent.[103] The detailed mechanism of the preferential activation of DMS enolates by ScF_3 remains unknown.

Table 31. Comparison of the reactivity of TMS or DMS enolates with various catalysts.[101]
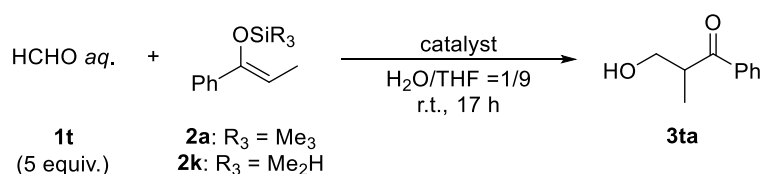
Entry	Catalyst (mol%)	Yield (%)	
		2a	**2k**
1	–	2	29
2	$ScCl_3\ 6H_2O$ (20)	69	41
3	KF (20) + 18-crown-6 (20)	63	51
4	HF (20)	14	13
5	ScF_3 (20)	Trace	81

The first example on the concomitant use of DMS enolate with Lewis acid catalysts (Table 25) implies the promising directions for fine organic synthesis. The use of DMS enolate **2k** instead of TMS enolate **2a** led to the improvement of both reactivity and enantioselectivity (Scheme 32). A less bulkiness on a silicon atom would facilitate the nucleophilic activation with the competitive coordination of water molecule as well as benzoate anion, hampering the contribution of less rigid transition state on the reaction pathway.
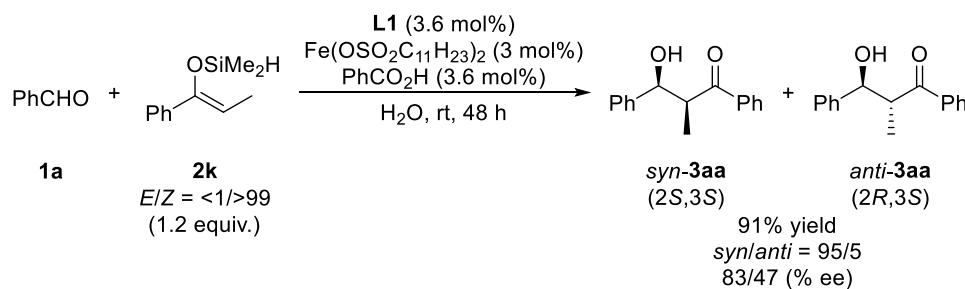
Scheme 32. Rate-enhancement & higher stereoselectivity using DMS enolate.

After re-optimization of reaction conditions, new catalytic system was applied to the Mukaiyama aldol reactions of various aldehydes with DMS enolate **2k** in water (Scheme 33). The lower concentration resulted in higher yield and higher stereoselectivity. As for aromatic aldehydes, both electron-donating and electron-withdrawing substituents did not have any influence on the chemical yield or the stereoselectivity even when the catalyst loading was 3 mol%, which is contrast to the tendency shown in Table 24.   The substitution at *ortho* position resulted in a slight decrease in enantioselectivity, presumably due to the steric repulsion on central iron(II) core.   However, aldehydes bearing the heteroaromatic ring could be reacted stereoselectively under Fe(II) catalysis.   Especially in the reaction of thiophenecarboxyaldehyde **1o** catalyzed by two Fe(II) systems (in water *vs.* in aqueous media), the contrastive reactivity would arise from the micellar influence.   The Fe(II)-based micellar system was also applicable to the reaction of aliphatic aldehydes with sustaining a high level of enantioselectivity.   Even water-soluble acetaldehyde could be reacted with DMS enolate **2k** with high enantioselectivity.
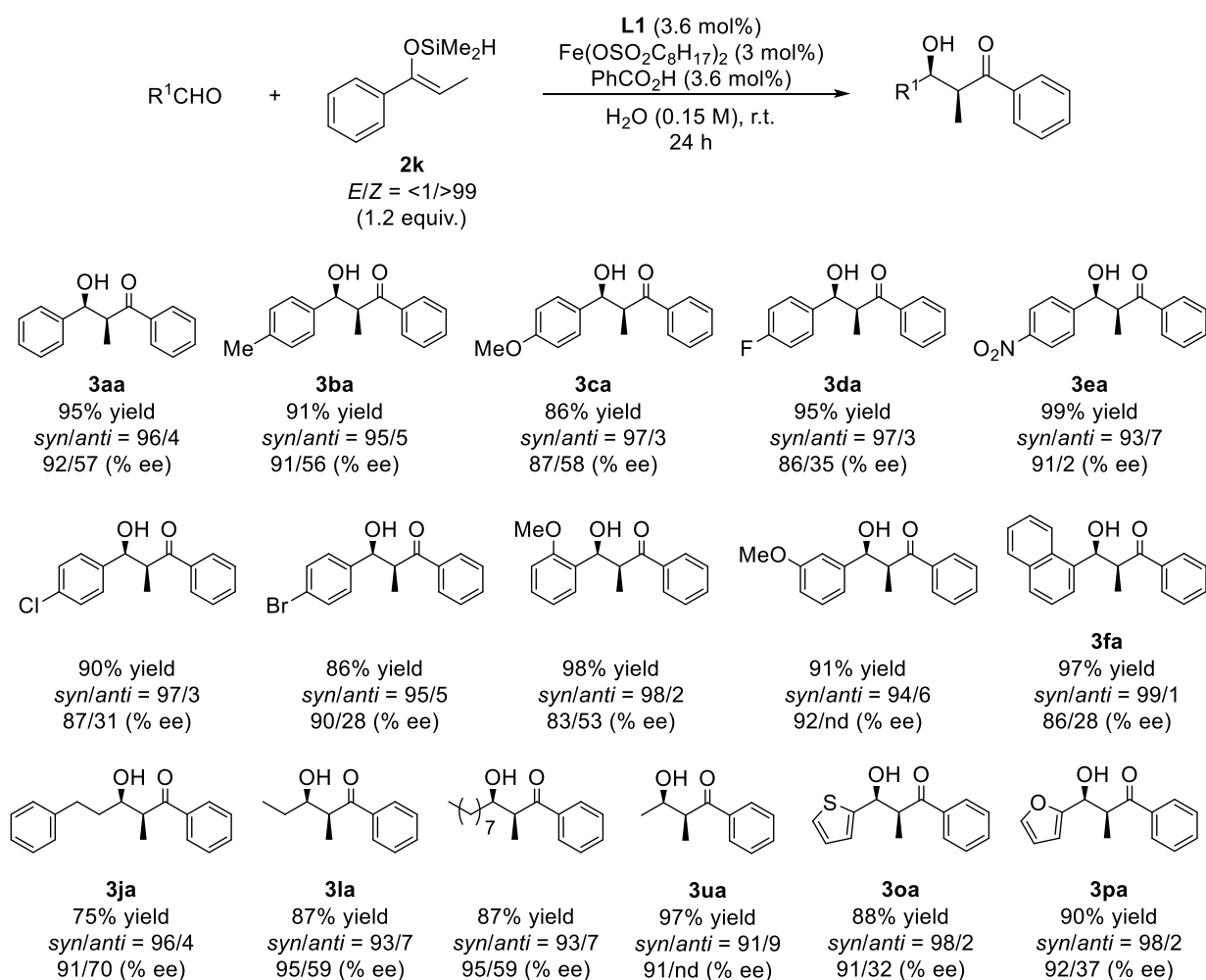
Scheme 33. Substrate scope using DMS enolate in water

With the optimal condition in hand, the reaction of a DMS enolate derived from 3-pentanone **2l** was examined in water (Table 32).   The reaction proceeded sluggishly to afford the desired product **3ae** with comparatively high enantioselectivity (entry 1).   Unfortunately, the

increased concentration, the addition of surfactants, excessive use of **L1** and higher catalyst loading failed to improve the reaction yield (entries 2-10). At higher catalyst loading with 3-fold excess of **L1**, the reaction produced a promising result without addition of any additive (entry 11). The increased amount of **2l** then resulted in the highest yield with the highest enantioselectivity (entry 12). When other LASCs base on Ni(II) or Sc(III) was employed, the reaction suffered from low yield and the stereochemical outcome of the corresponding product **3ae** was quite similar (entries 13, 14).

Table 32. Optimization of reaction conditions for pentanone-derived DMS enolate.
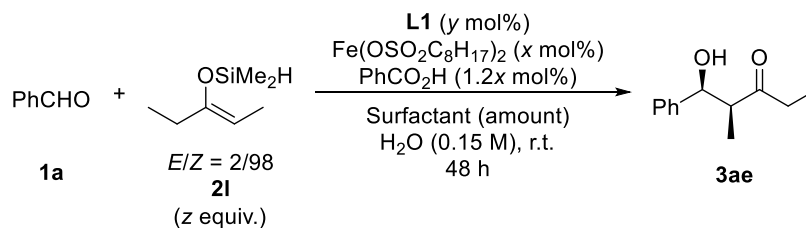
Entry	LASC	x	y	z	Surfactant	Yield (%)[a]	Dr (*syn/anti*)[b]	Ee (%)[c]
1	Fe(II)	3	3.6	1.2	–	14	80/20	70/25
2[d]	Fe(II)	3	3.6	1.2	–	15	71/29	28/33
3	Fe(II)	3	3.6	1.2	NaOSO$_2$C$_8$H$_{17}$ (3.6 mol%)	19	74/26	60/33
4	Fe(II)	3	3.6	1.2	NaOSO$_2$C$_8$H$_{17}$ (9 mol%)	20	76/24	60/28
5	Fe(II)	3	3.6	1.2	Triton X-114 (300 mg)	NR	–	–
6	Fe(II)	3	3.6	1.2	Triton X-114 (100 mg)	11	72/28	69/34
7	Fe(II)	3	9	1.2	–	22	75/25	70/24
8	Fe(II)	5	6	1.2	–	31	76/24	73/26
9	Fe(II)	5	6	1.2	Triton X-114 (100 mg)	12	79/21	65/26
10	Fe(II)	5	6	1.2	Triton X-114 (50 mg)	8	77/23	67/37
11	Fe(II)	5	15	1.2	–	52	90/10	76/33
12	Fe(II)	5	15	1.5	–	80	93/7	80/78
13	Sc(III)	5	15	1.5	–	20	80/20	76/33
14	Ni(II)	5	15	1.5	–	26	80/20	69/45

[a] Isolated yield. [b] Determined by ^{1}H NMR analysis. [c] Determined by HPLC analysis.

[d] The reaction was carried out at 0.5 M concentration.

The asymmetric reaction of (*E*)-enolate proceeded in a *syn*-selective manner under Fe(II)-based micellar system, albeit a significant drop in the reaction yield. The direct comparison on the effect of enolate geometry was undergone by using 3-pentanone-derived

enolate (Scheme 34).   The reaction of (*Z*)-enolate followed the same stereochemistry, which was in accord with water-DME system.
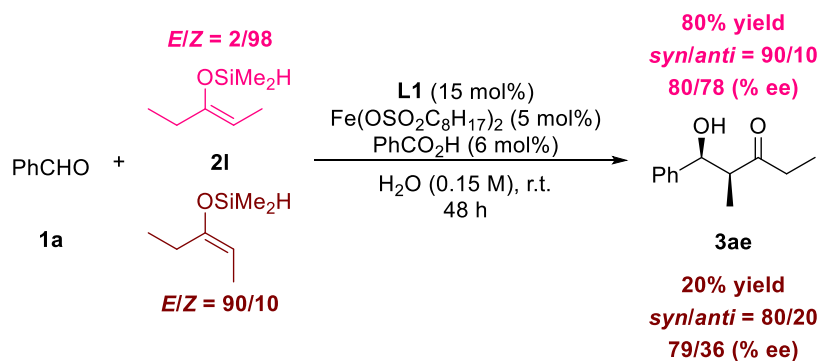
Scheme 34. Correlation between stereochemical outcome and enolate geometry.

1.2-3 *Novel Catalysis for Asymmetric Reactions of (E)-Enolates*

While (*E*)-enolates such as cyclic ketone-derived enolates are less stable to undergo hydrolysis in aqueous environments, enamine-type organocatalyses have been established for highly-selective reactions with cyclic ketones themselves.   In the meanwhile, chemistry has still limited catalytic protocol capable of accessing optically active *anti*-aldols without use of any chiral auxiliary.[104]   Indeed, thorough screening of chiral metal complexes formed with **L1** for the reaction of **1a** with **2a** in aqueous media (Section 1.1) did not dig up any metal exhibiting *anti*-preference, implying that there appears to be little to no interaction between the Lewis acid and the silyl group in the transition-state structures.   Most Lewis acid-catalyzed Mukaiyama aldol reactions was known to exhibit stereochemical convergence to one diastereomers irrespective of enolate geometry, which has been rationalized based on the well-known open-transition-state model.   Throughout the fine-tooth-comb search, we have encountered a profound catalysis exerted by nickel(II) complex in aqueous media (Scheme 35).   (*Z*)-Enolate **2d** furnished *syn*-product predominantly, whereas the formation of *anti*-product was favored in the reaction with (*E*)-enolate.   A much higher level of enantioselection for *anti*-aldol in the reaction with (*E*)-enolate compared with that for *syn*-aldol in the reaction with (*Z*)-enolate is noteworthy.
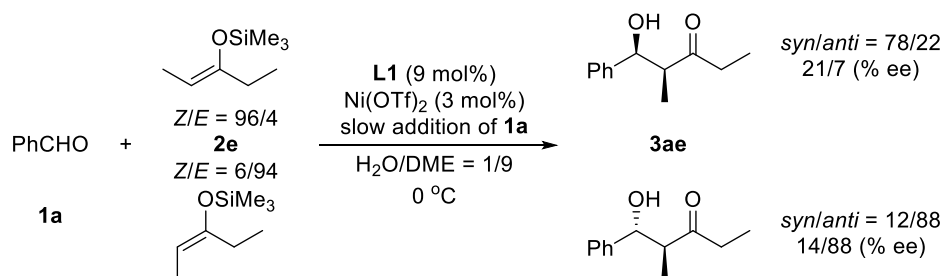
Scheme 35. Dependence of enolate geometry on stereochemical outcome in nickel-catalyzed reaction.

Encouraged by these results, the reaction conditions were applied to the reaction with cyclic enolate.   In order to compensate the inherent weakness of Ni(II) as a Lewis acid especially in aqueous environments,[105] DMS enolate **2e** was used as a nucleophile (Scheme 36).   The 3-fold excess of **L1** was required to allow the reaction progress, although the reaction suffered from low yield.   Nevertheless, the excellent enantioselectivity was achieved for the major *anti*-conformation.
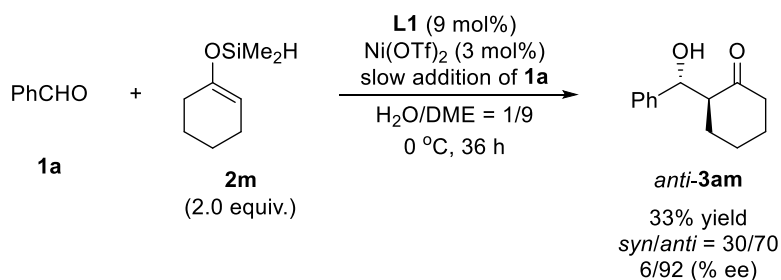
Scheme 36. *Anti*-selective reaction of DMS enolate in aqueous media.

A strong positive non-linear relationship between enantiopurity of the chiral ligand and the resulting product was recorded (Figure 26).   Using a chiral ligand **L1** of even 5% ee led to the formation of a product *anti*-**3am** with >80% ee.   This pronounced deviation from linearity is indicative of the involvement of mixed aggregate catalyst formation, fitting best with Kagan's ML_2 model by K = 10^4, g = 0.[106] This shows the overwhelming predominance of the heterodimeric (meso) complex in an equilibrium and that its activity is ignorable in comparison with that of homochiral one.
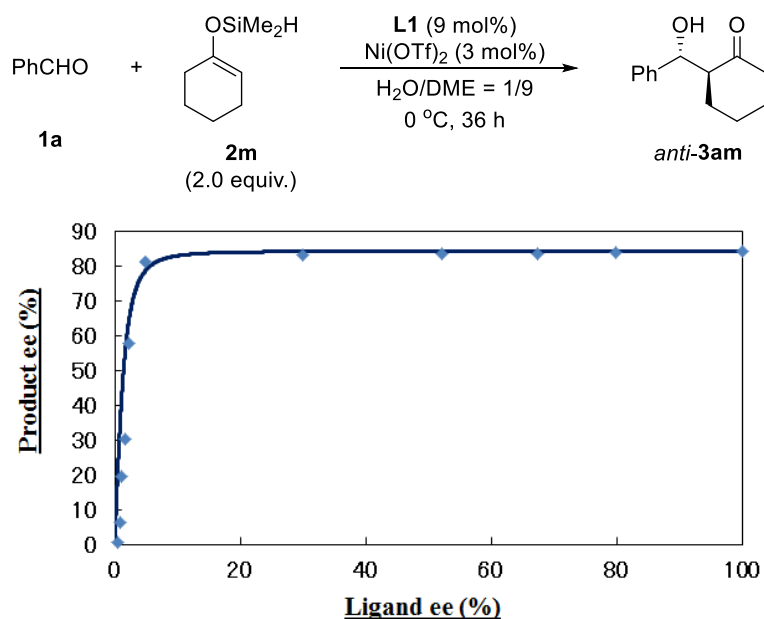
Figure 26. Correlation between the enantiopurity of the product and that of **L1** in nickel-catalyzed reaction.
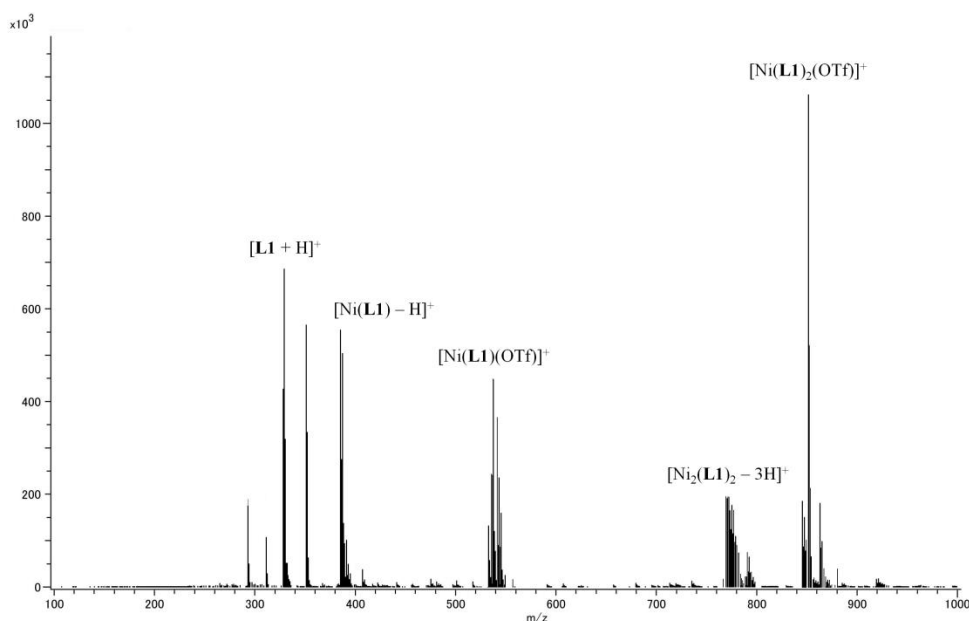
Figure 27. ESI-MS Spectra of chiral nickel(II) complex formed with **L1** in aqueous media.

An aqueous solution of chiral Ni(II) complex formed with **L1** was then amenable to electrospray analysis, probing the predominance of dimeric structure (Figure 27). Judging from molecular weight and isotope pattern, a major peak corresponded to $[Ni^{II}(\mathbf{L1})_2(OTf)]^+$ comprising 2 equivalents of the chiral ligand. It must, however, be added that the actual activation of aldehyde by chiral Ni(II) complex would be more complicated, in consideration of observing the miscellaneous species containing Ni(II).

In order to address the dominance of inactive heterodimer which resulted in low reactivity, we focused on leveraging the micellar catalysis. The expected enhancement of the reaction yield was observed, albeit under unoptimized conditions. The reaction with cyclic enolates **2m** or **2n** exhibited *anti*-preference in a high enantiomeric manner (Scheme 37). Under the assumption that the coordinated Lewis acid adopts a *cis* conformation, open-transition-state models were proposed to account for the unusual stereochemical outcomes induced by Ni(II) (Scheme 38, above). Synclinal conformers were deemed unfavorable due to the destabilizing dipole-dipole interaction between the two carbon-oxygen bonds.[107] In an antiperiplanar model, the steric interaction between R^3 and chiral nickel complex would cause further destabilization of the transition state. It is noted that even the reaction with (*Z*)-enolate preferred *anti*-product with moderate diastereoselectivity, although it did not induce enantioselection. Since reaction with (*Z*)-TMS enolate afforded *syn*-product predominantly, *anti*-selectivity for (*Z*)-DMS enolate is pregnant for the mechanism. The willingness of DMS enolate toward activation by Lewis base would make the unfavorable conformer more reactive (Scheme 38, below). In viewpoints of mechanistic clarification as well as *anti*-selective protocol, unprecedented nickel(II) catalysis exerted in water warrants further investigation.
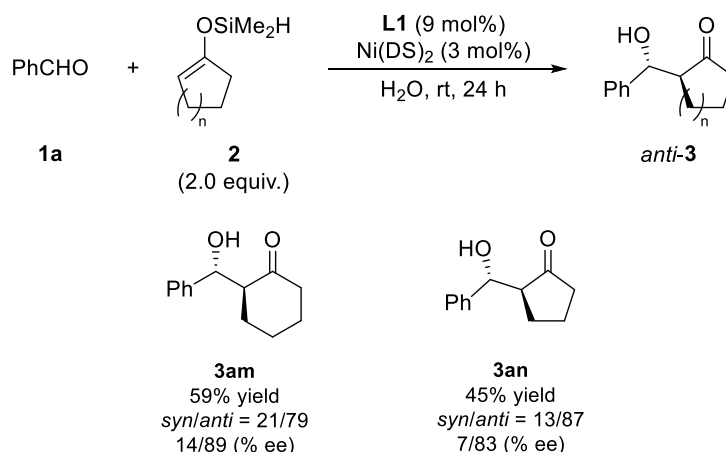
Scheme 37. Ni(DS)$_2$-catalyzed *anti*-selective Mukaiyama aldol reactions in water.
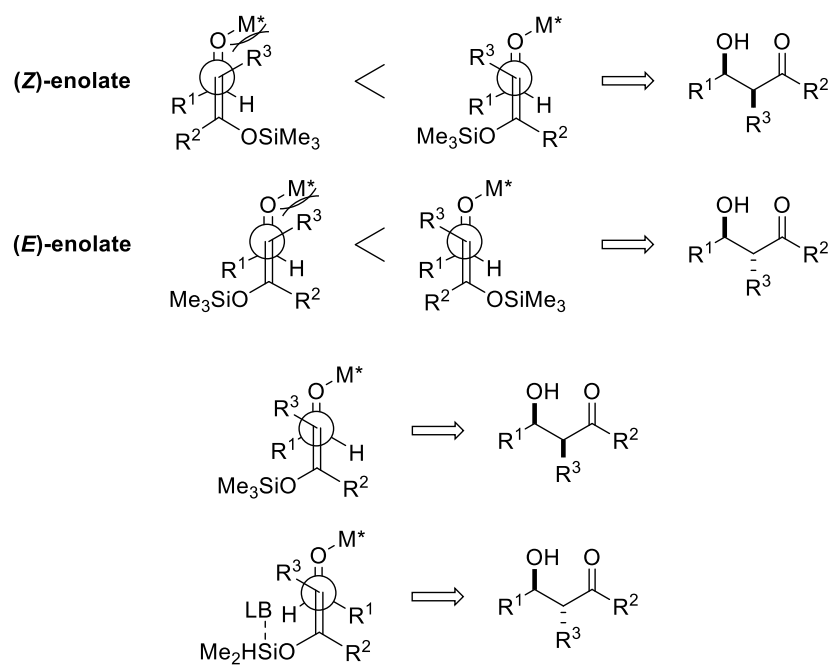
Scheme 38. Rationale of *anti*-selectivity in Ni(II)-catalyzed Mukaiyama aldol reactions in aqueous environments.

1.2-4 LASC Catalysis for Asymmetric Reactions of Thioketene Silyl Acetals

Preliminary studies on the LASC-mediated reaction of **1a** with **2i** in water have revealed the order of catalytic activity of LASCs (*e.g.* Cu(II) > Sc(III), Yb(III)).[90] In the beginning, the optimized conditions developed in aqueous dimethoxyethane were applied to the reaction with thioketene silyl acetal (Table 33). The reaction of **1a** with **2i** proceeded sluggishly with a moderate *syn*-preference in the presence of any metal trilfate. While Sc(III), Cu(II) and Hg(II) gave comparatively high enantioselectivity, Fe(II)-catalyzed reaction was unselective in the presence of either pyridine or benzoic acid used as additive (entries 1-4, 9). In Hg(II)-catalyzed reaction the absolute configuration of a major adduct was opposite enantiomer with that generated in the reaction with propiophenone-derived silyl enol ether **2a** (Table 1). Another catalytic system for asymmetric Mukaiyama aldol reaction with ketene silyl acetals was required for better result. Based upon such background, several metal triflates were examined in the Mukaiyama aldol reaction with thioester-derived ketene silyl acetal, which were turned to be all in vain (entries 5-8). Chiral bismuth complex was revealed to be less effective in the reaction with thioester-derived ketene silyl acetals (entry 10). Generally speaking, the reactions suffered from low yield. As a result, the highest enantioselectivity in the case of Hg(II) is noteworthy albeit quite low yield.

Table 33. Reaction with (*E*)-thioketene silyl acetal.
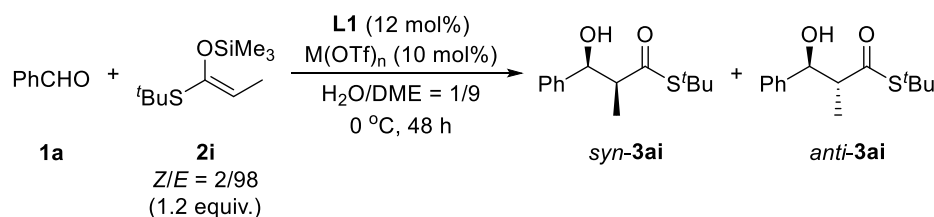
Entry	Metal triflate	x	y	Yield (%)[a]	Dr (*syn/anti*)[b]	Ee (%)[c]
1[d]	Sc(OTf)$_3$	5	6	17	81/19	57/5
2[e]	Fe(OTf)$_2$	3	3.6	30	87/13	5/4
3[f]	Fe(OTf)$_2$	3	3.6	32	88/12	0/23
4	Cu(OTf)$_2$	3	9	5	76/24	–43/10
5	Sn(OTf)$_2$	3	9	10	86/14	24/4
6	Yb(OTf)$_3$	5	6	15	86/14	27/7
7	Lu(OTf)$_3$	5	6	20	85/15	26/3
8	Hf(OTf)$_4$	5	6	4	83/17	7/14
9	Hg(OTf)$_2$	5	6	3	73/27	–66/–5
10[g]	Bi(OTf)$_3$	3	9	46	69/31	–1/73

[a] Isolated yield. [b] Determined by ^{1}H NMR analysis.
[c] Determined by HPLC analysis; minus values indicate opposite enantioselectivity.
[d] 6 mol% of pyridine was added.
[e] 7.2 mol% of pyridine was added. [f] 3.6 mol% of PhCO$_2$H was added.
[g] 12 mol% of pyridine was added.

As the correlation between each chiral metal complex and the enolate geometry had remained unknown, the reactions with (*Z*)-enolate were also examined (Table 34). When Sc(III) was used as a catalyst, the enantioselectivity of the corresponding product decreased significantly (entry 1). The absolute configuration of a major adduct was opposite enantiomer with that generated in the reaction with propiophenone-derived silyl enol ether **2a**, although the steric bulkiness of *tert*-butyl group seems to impede the interaction between sulfur and iron (entries 2, 3). This absolute configuration of a major isomer in iron(II)-mediated reaction was confirmed similarly in the reaction of cinnamaldehyde **1h**. While most metal salts catalyzed the reaction to afford the same stereoisomer as a major product shown in Table 31, Hg(II)-catalyzed reaction afforded the opposite enantiomer along with a significant drop in enantioselectivity (entry 9). Considering previous knowledge on Hg(II) catalysis in aqueous media, Hg(II)-catalyzed mechanism should be different from typical Lewis acid-catalyzed Mukaiyama aldol reaction; the recognition of olefin in thioketenesilyl acetal by Hg(II) is assumed to be a trigger in the reaction. Based upon a report on asymmetric hydroxymethylation of thioester-derived ketene silyl acetal,[23] chiral scandium complex was focused upon as one of the most promising candidate. The stereochemical differences between (*Z*)- and (*E*)-enolate is suggestive of the interference by sulfur at the stereochemical determining step.

Table 34. Reaction with (*Z*)-thioketene silyl acetal.
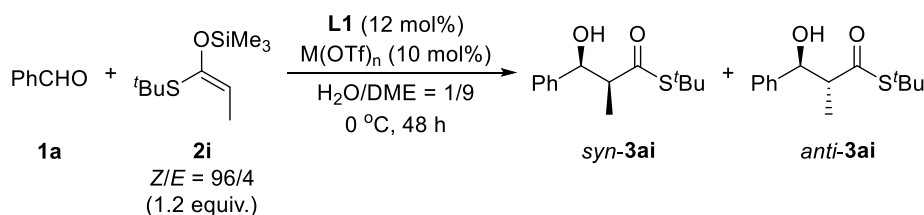
Entry	Metal Triflate	x	y	Yield (%)[a]	Dr (*syn/anti*)[b]	Ee (%)[c]
1	Sc(OTf)$_3$	5	6	12	84/16	23/19
2[d]	Fe(OTf)$_2$	3	3.6	45	73/27	−20/8
3[e]	Fe(OTf)$_2$	3	3.6	30	77/23	−26/19
4	Cu(OTf)$_2$	3	9	5	62/38	−7/20
5	Sn(OTf)$_2$	3	9	5	72/28	−5/3
6	Yb(OTf)$_3$	5	6	22	79/21	23/25
7	Lu(OTf)$_3$	5	6	17	80/20	27/31
8	Hf(OTf)$_4$	5	6	3	69/31	7/−5
9	Hg(OTf)$_2$	5	6	4	61/39	11/<1
10	Bi(OTf)$_3$	3	9	4	72/28	−11/53

[a] Isolated yield. [b] Determined by ^{1}H NMR analysis.

[c] Determined by HPLC analysis; minus values indicate opposite enantioselectivity.

[d] 6 mol% of pyridine was added.

[e] 7.2 mol% of pyridine was added. [f] 3.6 mol% of PhCO$_2$H was added.

[g] 12 mol% of pyridine was added.

In the presence of chiral scandium complex, the correlation between the structure of **2i** and stereochemical outcome was surveyed (Table 35).   Unfortunately all reactions proceeded sluggishly, since the steric bulkiness of silyl group tended to be reluctant to react with aldehyde in aqueous environments (entries 1-3).   After all, TMS enolate afforded the desired product with the highest enantioselectivity when (*E*)-enolate was reacted (entries 4-6).   When the *tert*-butyl group was replaced into other substituents, the stereoselectivity diminished presumably due to their unsteadiness in aqueous environments (entries 7-9).   The rate of hydrolysis was faster than that of catalytic desired pathway, thus leading to a decrease in the reaction yield.

Table 35. Sc(III)-catalyzed reaction with thioketene silyl acetals.
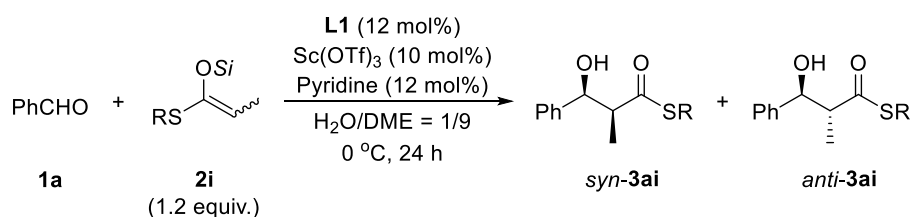
Entry	*Si*	R	*E/Z* ratio	Yield (%)[a]	Dr (*syn/anti*)[b]	Ee (%)[c]
1	SiMe$_2$^{t}Bu	^{t}Bu	98/2	NR	–	–
2	SiEt$_3$	^{t}Bu	98/2	NR	–	–
3	SiMe$_2$Et	^{t}Bu	98/2	8	73/27	44/–11
4[d]	SiMe$_3$	^{t}Bu	98/2	17	87/13	57/5
5	SiMe$_3$	^{t}Bu	98/2	12	86/14	60/–2
6[d]	SiMe$_3$	^{t}Bu	4/96	12	84/16	23/19
7	SiMe$_3$	Et	90/10	3	87/13	–
8	SiMe$_3$	Et	4/96	NR	–	–
9	SiMe$_3$	Ph	24/76	Trace	83/17	–

[a] Isolated yield. [b] Determined by ^{1}H NMR analysis.

[c] Determined by HPLC analysis; minus values indicate opposite enantioselectivity.

[d] 5 mol% catalyst loading.

The DMS enolate-based strategy was then adopted to increase the reactivity (Table 36).   When Fe(II)-based LASC was employed as a catalyst, a drastic influence of DTBP among several additives on the reaction yield was observed (entries 1-5).   It is assumed that the stability of thioester-derived DMS enolate **2o** in micellar system should be responsible for high yield.   The reaction catalyzed by Ni(II)-based LASC was slightly *anti*-selective with no enantioselection (entry 6).   On the other hand, Sc(III)-based LASC gave a comparatively higher yield of the corresponding product with moderate enantioselectivity without any additive (entry 8).   In contrast, the addition of either acidic or basic additives to Sc(III)-based micellar system retarded the reaction significantly (entries 9-11).   It was found that the addition of a suitable amount of non-ionic surfactants contributed to the enhancement of reactivity and selectivity (entries 12-17).   A significant increase in reactivity is assumed to be caused by the increased stability of thioester-derived DMS enolate **2o** in micellar system.

Table 36. Optimization of reaction conditions for thioester-derived DMS enolate.
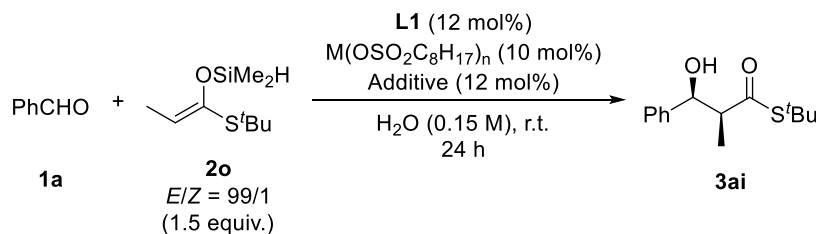
Entry	LASC	Additive	Yield (%)[a]	Dr (*syn/anti*)[b]	Ee (%)[c]
1	Fe(II)	–	Trace	–	–
2	Fe(II)	PhCO$_2$H	33	90/10	31/19
3	Fe(II)	Pyridine	11	76/24	–3/1
4	Fe(II)	DTBP	83	83/17	–4/–8
5	Fe(II)	Triton X-114 (200 mg)	Trace	–	–
6	Ni(II)	–	30	35/65	–6/0
7	Sc(III)	–	35	88/12	55/–10
8[d]	Sc(III)	–	61	81/19	60/–5
9	Sc(III)	PhCO$_2$H	5	–	–
10	Sc(III)	Pyridine	NR	–	–
11	Sc(III)	DTBP	Trace	–	–
12	Sc(III)	Triton X-114 (200 mg)	32	90/10	53/8
13	Sc(III)	Triton X-114 (100 mg)	74	90/10	71/–2
14	Sc(III)	Triton X-114 (50 mg)	86	92/8	74/–4
15	**Sc(III)**	**Triton X-114 (25 mg)**	**94**	**93/7**	**76/–2**
16	Sc(III)	Triton X-100 (100 mg)	66	93/7	67/2
17	Sc(III)	Triton X-100 (25 mg)	69	93/7	72/3

[a] Isolated yield. [b] Determined by ^{1}H NMR analysis.   [c] Determined by HPLC analysis. [d] The reaction was carried out at 0.5 M concentration.

At lower catalyst loading, higher concentration and excessive use of **L1** afforded higher yield and higher enantioselectivity (Table 1, entry 1).   When the 2-fold excess of **L1** was employed, further imporovement of the reaction yield was achieved (entry 2).   The reaction retarded in the presence of other non-ionic surfactant with sustaining a high level of enantioselectivity (entry 3). In contrast, the reaction using a lower amount of chiral ligand resulted in an erosion of enantioselectivity along with the same reaction yield (entry 4).

Table 37. Optimization of reaction conditions for thioester-derived DMS enolate.

PhCHO + [2o structure, OSiMe$_2$H, S^{t}Bu] → [3ai structure, OH O, Ph, S^{t}Bu]

1a

2o
E/Z = 99/1
(1.5 equiv.)

L1 (*y* mol%)
M(OSO$_2$C$_8$H$_{17}$)$_n$ (10 mol%)
Additive
H$_2$O (0.5 M), r.t., 48 h

3ai
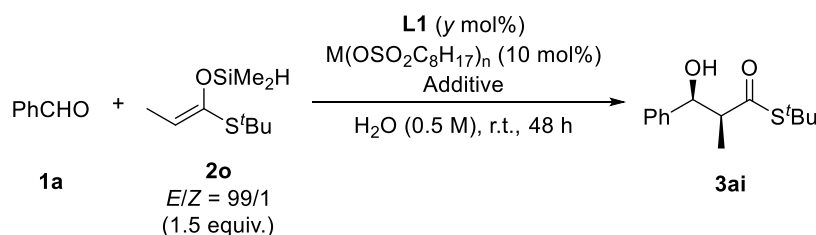
Entry	LASC	Additive	*y*	Yield (%)[a]	Dr (*syn/anti*)[b]	Ee (%)[c]
1	Sc(OSO$_2$C$_8$H$_{17}$)$_3$	Triton X-114 (100 mg)	15	68	95/5	81/8
2	Sc(OSO$_2$C$_8$H$_{17}$)$_3$	Triton X-114 (100 mg)	10	84	96/4	81/7
3[d]	Sc(OSO$_2$C$_8$H$_{17}$)$_3$	Triton X-100 (100 mg)	10	75	95/5	81/9
4[d]	Sc(OSO$_2$C$_8$H$_{17}$)$_3$	Triton X-114 (100 mg)	6	77	92/8	74/9

[a] Isolated yield. [b] Determined by ^{1}H NMR analysis.   [c] Determined by HPLC analysis.
[d] Conducted for 24 h.

Then acetaldehyde was employed as an aliphatic electrophile (Table 38).   As expected, the catalytic activity and enantioselectivity caused by chiral scandium complex was higher than that generated by chiral bismuth complex (entries 1, 4).   In order to stabilize the silicon enolate and then to enhance the reactivity, addition of 2,6-di-*tert*-butylpyridine as a proton-scavenger was often chosen in Lewis acid-catalyzed Mukaiyama aldol reaction such as asymmetric hydroxymethylation catalyzed by praseodymium complex with chiral bis-pyridino-18-crown-6.[16a] Indeed, a stability of ketene silyl acetal became higher by addition of DTBP; however both reactivity and selectivity was not affected (entry 2).   It was also revealed that the reaction with (*Z*)-enolate did not proceed at all, although (*E*)-enolate produced the desired product successfully (entry 3, 5).   The combination of bismuth triflate with Trost-type ligand **L12** was not effective for a stereocontrol, either.

Table 38. Sc(III)-catalyzed reaction with thioketene silyl acetals.

MeCHO + [2i structure, OSiMe$_3$, S^{t}Bu] → [syn-3ui structure, OH O, Me, S^{t}Bu]

1u

2i
(1.2 equiv.)

Ligand (*y* mol%)
M(OTf)$_3$ (*x* mol%)
H$_2$O/DME = 1/9

syn-**3ui**
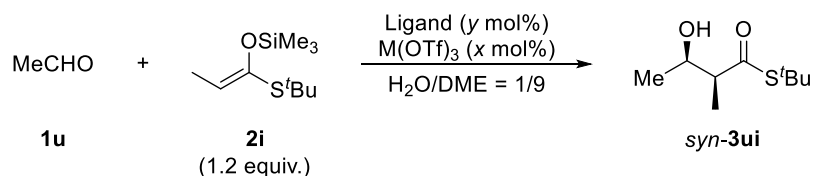
Entry	Ligand	Metal salt (*x*)	*E/Z* ratio	Yield (%)[a]	Dr (*syn/anti*)[b]	Ee (%)[c]
1	**L1** (12)	Sc(OTf)$_3$ (10)	96/4	32	78/22	63/19
2[d]	**L1** (12)	Sc(OTf)$_3$ (10)	96/4	30	76/24	62/5
3	**L1** (12)	Sc(OTf)$_3$ (10)	6/94	NR	–	–
4	**L1** (9)	Bi(OTf)$_3$ (3)	96/4	6	85/15	9/62
5	**L1** (9)	Bi(OTf)$_3$ (3)	6/94	NR	–	–
6	**L12** (12)	Bi(OTf)$_3$ (10)	96/4	5	72/28	0/0

[a] Isolated yield. [b] Determined by ^{1}H NMR analysis.

[c] Determined by HPLC analysis; minus values indicate opposite enantioselectivity.

[d] 30 mol% of DTBP was added.

The low reactivity was successfully overcome when STDS was used as a catalyst in the coexistence of Triton X as additional surfactant (Scheme 39). Since the addition of non-ionic surfactant (Triton X) was an aid for STDS catalysis in asymmetric hydroxymethylation, the formation of stable micelle would be a key for suppressing the decomposition of thioketenesilyl acetal in water. Although still unoptimized, the result is promising enough to warrant further investigations.
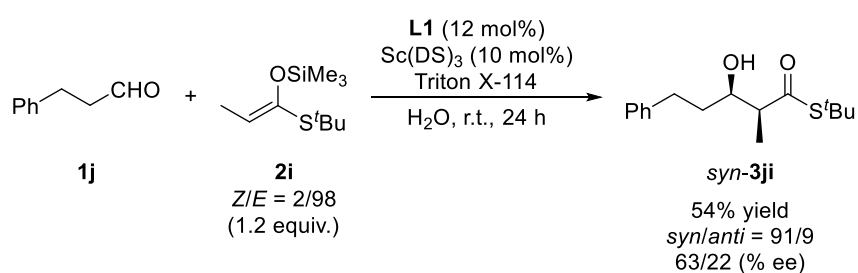
Scheme 39. Sc(DS)$_3$-catalyzed Mukaiyama aldol reactions of thioketenesilyl acetal in water.

1.2-5 Conclusions

The venerable aldol reaction has provided us indispensably with the useful synthetic tactics for the construction of stereochemically complex compounds.   Among innovative discoveries in asymmetric catalysis of the aldol reaction, the asymmetric Mukaiyama aldol reactions are willing to proceed under mild conditions to generate up to two stereocenters under Lewis acid catalysis. Thus, multifarious chiral catalysts that function competently in asymmetric Mukaiyama aldol reactions have been expanded considerably.   Consequently, our complete understanding of the Mukaiyama aldol reaction is just around the corner.   The intimate dependence of the catalyst structure on the substrate in highly selective Mukaiyama aldol reactions, a great problem for chemists, is nearly surmounted.   There was room for improvement in the use of organic solvents, the reaction temperature, and the application to the reaction with challenging substrates.   It was envisioned that realization of further efficiency or mildness, and acquisition of new catalysis as a result of synergistic effect between Lewis acid and micelle.   The Iron(II)-based LASC (Lewis acid–surfactant-combined catalyst) exhibited superior performance with a wide substrate range for asymmetric Mukaiyama aldol reactions in water, whereas the reaction is *anti*-selective with high enantioselectivity in the presence of nickel(II) catalyst.   The micellar catalytic system could be applied to the reaction with water-sensitive thioketenesilylacetals without use of any organic solvent. Leveraging the micellar catalysis in combination with Lewis acid catalysis resulted in considerable promising results, albeit under unoptimized conditions.   Detailed mechanistic studies as well as the versatility of these protocols will be discussed in due course.

[1] March, J. *Advanced Organic Chemistry: Reactions, Mechanisms and Structure*, 4th Edn.; Wiley-Interscience: New York, **1992**.

[2] a) S. Kobayashi, Y. Fujishita, T. Mukaiyama, *Chem. Lett.* **1990**, 1455–1458; b) T. Mukaiyama, S. Kobayashi, H. Uchiro, I. Shiina, *Chem. Lett.* **1990**, 129–132.

[3] a) A. Lubineau, *J. Org. Chem.* **1986**, *51*, 2142–2144; b) A. Lubineau, E. Meyer, *Tetrahedron* **1988**, *44*, 6065–6070.

[4] S. Kobayashi, *Chem. Lett.* **1991**, 2187–2190.

[5] a) D. A. Evans, E. J. Olhava, J. S. Johnson, J. M. Janey, *Angew. Chem. Int. Ed.* **1998**, *37*, 3372-3375; b) D. A. Evans, S. J. Miller, T. Lectka, P. Von Matt, *J. Am. Chem. Soc.* **1999**, *121*, 7559–7573.

[6] As an example of other uses of aqua complexes, hydrated nickel complex: a) S. Kanemasa, Y. Oderaotoshi, H. Yamamoto, J. Tanaka, E. Wada, D. P. Curran, *J. Org. Chem.* **1997**, *62*, 6454–6455; b) S. Kanemasa, Y. Oderaotoshi, S. Sakaguchi, H. Yamamoto, J. Tanaka, E. Wada, D. P. Curran, *J. Am. Chem. Soc.* **1998**, *120*, 3074–3088; c) S. Kanemasa, Y. Oderaotoshi, J. Tanaka, E. Wada, *Tetrahedron Lett.* **1998**, *39*, 7521–7524.

[7] a) S. Kobayashi, S. Nagayama, T. Busujima, *Chem. Lett.* **1999**, 71–72; b) S. Kobayashi, S. Nagayama, T. Busujima, *Tetrahedron* **1999**, *55*, 8739–8746.

[8] S. Kobayashi, Y. Mori, S. Nagayama, K. Manabe, *Green Chem.* **1999**, 175–178.

[9] S. Kobayashi, C. Ogawa, In *Asymmetric Synthesis–The Essentials*, Eds. M. Christmann & S. Bräse, Weinheim: Wiley-VCH, **2007**, pp 110–115.

[10] a) R. D. Shannon, C. T. Prewitt, *Acta Crystallogr.* **1969**, *B25*, 925–946; b) R. D. Shannon, *Acta Crystallogr.* **1976**, *A32*, 751–767.

[11] a) E. P. Kyba, R. C. Helheson, K. Madan, G. W. Gokel, T. L. Tarnowski, S. S. Moore, D. J. Cram, *J. Am. Chem. Soc.* **1977**, *99*, 2564–2571; b) E. P. Kyba, G. W. Gokel, F. de Jong, K. Koga, L. R. Sousa, M. G. Siegel, L. Kaplan, G. D. Y. Sogah, D. J. Cram, *J. Org. Chem.* **1977**, *42*, 4173–4184.

[12] S. Nagayama, S. Kobayashi, *J. Am. Chem. Soc.* **2000**, *122*, 11531–11532.

[13] S. Kobayashi, T. Hamada, S. Nagayama, K. Manabe, *J. Braz. Chem. Soc.* **2001**, *12*, 627–633.

[14] Ionic diameter of Pb^{2+} (CN = 8) is 258 pm (see ref. 10) and the hole size of 18-crown-6 was reported to be 260–320 pm.

[15] O. Muñoz-Muñiz, M. Quintanar-Audelo, E. Juaristi, *J. Org. Chem.* **2003**, *68*, 1622–1625.

[16] a) T. Hamada, K. Manabe, S. Ishikawa, S. Nagayama, M. Shiro, S. Kobayashi, *J. Am. Chem. Soc.* **2003**, *125*, 2989–2996; b) S. Kobayashi, T. Hamada, S. Nagayama, K. Manabe, *Org. Lett.* **2001**, *3*, 165–167; c) C. H. Heathcock, In *Asymmetric Synthesis, Vol. 3, Part B*; J. D. Morrison, Ed.; Academic Press: New York, **1984**, pp 111.

[17] For complexation of rare-earth metals with macrocyclic ligands, see: a) V. Alexander, *Chem. Rev.* **1995**, *95*, 273–342; b) D. E. Fenton, P. A. Vigato, *Chem. Soc. Rev.* **1988**, *17*, 69–90.

[18] P. Caravan, J. J. Ellison, T. J. McMurry, R. B. Lauffer, *Chem. Rev.* **1999**, *99*, 2293–2352.

[19] a) D. J. Averill, M. J. Allen, *Catl. Sci. Technol.* **2014**, *4*, 4129-4137; b) Y. Mei, D. J. Averill, M. J. Allen, *J. Org. Chem.* **2012**, *77*, 5624–5632; c) Y. Mei, P. Dissanayake, M. J. Allen, *J. Am. Chem. Soc.* **2010**, *132*, 12871–12873.

[20] K. Manabe, S. Ishikawa, T. Hamada, S. Kobayashi, *Tetrahedron* **2003**, *59*, 10439–10444.

[21] N. Ozawa, M. Wadamoto, K. Ishihara, H. Yamamoto, *Synlett* **2003**, 2219–2221.

[22] a) C. Bolm, M. Ewald, M. Felder, G. Schlingloff, *Chem. Ber.* **1992**, *125*, 1169–1190; b) C. Bolm, M. Zehnder, D. Bur, *Angew. Chem. Int. Ed. Engl.* **1990**, *29*, 205–207.

[23] S. Ishikawa, T. Hamada, K. Manabe, S. Kobayashi, *J. Am. Chem. Soc.* **2004**, *126*, 12236–12237.

[24] 2,6-Di-*tert*-butylpyridine was added as an additive for Lewis acid-catalyzed Mukaiyama aldol reactions. See: a) S. Murata, M. Suzuki, R. Noyori, *Tetrahedron* **1988**, *44*, 4275–4277.

[25] a) D. Shang, J. Xin, Y. Liu, X. Zhou, X. Liu, X. Feng, *J. Org. Chem.* **2008**, *73*, 630–637; b) M. Nakajima, M. Yamaguchi, S. Hashimoto, *Chem. Commun.* **2001**, 1596–1597.

[26] M. Kokubo, C. Ogawa, S. Kobayashi, *Angew. Chem. Int. Ed.* **2008**, *47*, 6909–6911.

[27] a) S. Kobayashi, T. Ogino, H. Shimizu, S. Ishikawa, T. Hamada, K. Manabe, *Org. Lett.* **2005**, *7*, 4729–4731; b) S. Kobayashi, M. Ueno, T. Kitanosono, *Top. Curr. Chem.* **2012**, *311*, 1–17.

[28] S. Répichet, A. Zwick, L. Vendier, C. L. Roux, J. Dubac, *Tetrahedron Lett.* **2002**, *43*, 993–995.

[29] Trost developed a dinuclear zinc catalyst system with a chiral semi-crown ether, which was applied in catalytic asymmetric direct aldol reactions, Henry reactions, Mannich-type reactions, and diol-desymmetrizations. For example, see: a) B. M. Trost, H. Ito, *J. Am. Chem. Soc.* **2000**, *122*, 12003–12004; b) B. M. Trost, H. Ito, E. R. Silcoff, *J. Am. Chem. Soc.* **2001**, *123*, 3367–3368; c) B. M. Trost, V. S. C. Yeh, *Angew. Chem. Int. Ed.* **2002**, *41*, 861–863; d) B. M. Trost, V. S. C. Yeh, H. Ito, N. Bremeyer, *Org. Lett.* **2002**, *4*, 2621–2623; e) B. M. Trost, V. S. C. Yeh, *Org. Lett.* **2002**, *4*, 3513–3516; f) B. M. Trost, L. R. Terrell, *J. Am. Chem. Soc.* **2003**, *125*, 338–339; g) B. M. Trost, T. Mino, *J. Am. Chem. Soc.* **2003**, *125*, 2410–2411; h) B. M. Trost, A. Fettes, B. T. Shireman, *J. Am. Chem. Soc.* **2004**, *126*, 2660–2661.

[30] H. –J. Li, H. –Y. Tian, Y. –J. Chen, D. Wang, C. –J. Li, *Chem. Commun.* **2002**, 2994–2995.

[31] H. –J. Li, H. –Y. Tian, Y. –C. Wu, Y. –J. Chen, L. Liu, D. Wang, C. –J. Li, *Adv. Synth. Catal.* **2005**, *347*, 1247–1256.

[32] a) J. Mlynarski, J. Jankowska, *Adv. Synth. Catal.* **2005**, *347*, 521–525; b) J. Jankowska, J. Mlynarski, *J. Org. Chem.* **2006**, *71*, 1317–1321.

[33] J. Jankowska, J. Paradowska, J. Mlynarski, *Tetrahedron Lett.* **2006**, *47*, 5281–5284.

[34] a) J. Jankowska, J. Paradowska, B. Rakiel, J. Mlynarski, *J. Org. Chem.* **2007**, *72*, 2228–2231; b) J. Mlynarski, J. Paradowska, *Chem. Soc. Rev.* **2008**, *37*, 1502–1511.

[35] This is substantiated experimentally, see Ref. 27 and 30.

[36] M. V. Nandakumar, A. Tschöp, H. Krautscheid, C. Schneider, *Chem. Commun.* **2007**, 2756-2758.

[37] A. Tschöp, A. Marx, A. R. Sreekanth, C. Schneider, *Eur. J. Org. Chem.* **2007**, 2318-2327.

[38] a) M. Kokubo, T. Naito, S. Kobayashi, *Tetrahedron* **2010**, *66*, 1111-1118; b) C. Ogawa, M. Kokubo, S. Kobayashi, *J. Synth. Org. Chem. Jpn.* **2010**, *68*, 718-728; c) M. Kokubo, T. Naito, S. Kobayashi, *Chem. Lett.* **2009**, *38*, 904-905.

[39] S. Kobayashi, T. Endo, M. Ueno, *Angew. Chem. Int. Ed.* **2011**, *50*, 1-5.

[40] T. Ollevier, B. Plancq, *Chem. Commun.* **2012**, *48*, 2289-2291.

[41] a) M. Kokubo, T. Naito, S. Kobayashi, *Chem. Lett.* **2009**, *38*, 904-905; b) M. Kokubo, T. Naito, S. Kobayashi, *Tetrahedron* **2010**, *66*, 1111-1118.

[42] a) C. Ogawa, N. Wang, M. Boudou, S. Azoulay, K. Manabe, S. Kobayashi, *Heterocycles* **2007**, *72*, 589-598; b) M. Boudou, C. Ogawa, S. Kobayashi, *Adv. Synth. Catal.* **2006**, *348*, 2585-2589; c) S. Azoulay, K. Manabe, S. Kobayashi, *Org. Lett.* **2005**, *7*, 4593-4595.

[43] M. Kokubo, S. Kobayashi, *Chem. Asian. J.* **2009**, *4*, 526-528.

[44] R. D. Shannon, *Acta Cryst.* **1976**, *A32*, 751-767.

[45] a) Y. Mori, K. Manabe, S. Kobayashi, *Angew. Chem. Int. Ed.* **2001**, *40*, 2815-2818; b) Y. Mori, J. Kobayashi, K. Manabe, S. Kobayashi, *Tetrahedron* **2002**, *58*, 8263-8268.

[46] a) K. Manabe, S. Kobayashi, *Tetrahedron Lett.* **1999**, *40*, 3773-3776; b) K. Manabe, Y. Mori, S. Nagayama, K. Odashima, S. Kobayashi, *Inorg. Chim. Acta*, **1999**, *296*, 158-163.

[47] S. Kobayashi, Y. Mori, S. Nagayama, K. Manabe, *Green Chem.* **1999**, 175–178.

[48] S. Kobayashi, K. Manabe, *Pure Appl. Chem.* **2000**, *72*, 1373-1380.

[49] Greeves et al. reported benzoic acid (1 equiv.) acceleration in Yb(OTf)$_3$-catalyzed allylation of aldehydes in acetonitrile and proposed the mechanism whereby it accelerated the catalyst regeneration step, see: H. C. Aspinall, N. Greeves, E. G. McIver, *Tetrahedron Lett.* **1988**, *39*, 9283–9286.

[50] Evans et al. reported that the addition of TMSOTf accelerated the rate-limiting catalyst turnover step in their chiral Lewis acid-catalyzed Mukaiyama aldol reaction under anhydrous conditions, see: D. A. Evans, M. C. Kozlowski, C. S. Burgey, D. W. C. MacMillan, *J. Am. Chem. Soc.* **1997**, *119*, 7893–7894.

[51] Brønsted acids have been used as catalysts for Mukaiyama aldol reactions in organic solvents, see: M. Kawai, M. Onaka, Y. Izumi, *Bull. Chem. Soc. Jpn.* **1988**, *61*, 1237–1245.

[52] For other examples of Brønsted acid-assisted chiral Lewis acid catalyst, see: K. Ishihara, H. Yamamoto, *J. Am. Chem. Soc.* **1994**, *116*, 1561–1562; For acetic acid acceleration in Yb(fod)$_3$-catalyzed ene reaction of aldehydes with alkyl vinyl ethers, see: M. V. Deaton, M. A. Ciufolini, *Tetrahedron Lett.* **1993**, *34*, 2409–2412.

[53] Full recovery of the starting materials.

[54] Lewis acid-Lewis base catalysts can be classified into two groups; independent system and bifunctional catalyst (see Chapter 4). The former example, see: a) S. Kobayashi, M. Arai, I. Hachiya, *J. Org. Chem.* **1994**, *59*, 3758-3759 (chiral scandium catalyst prepared from Sc(OTf)$_3$, (*R*)-BINOL and tertialy amine); b) C. Palomo, M. Oiarbide, A. Laso, *Angew. Chem. Int. Ed.* **2005**, *44*, 3881-3884 (chiral zinc catalyst prepared from Zn(OTf)$_2$, a chiral amino alcohol ligand and Hünig base); c) P. S. Tiseni, R. Peters, *Org. Lett.* **2008**, *10*, 2019-2022 (chiral erbium catalyst prepared from Er(OTf)$_3$, optically active norephedrine ligand and Hünig base).

[55] T. Ollevier, B. Plancq, *Chem. Commun.* **2012**, *48*, 2289-2291.

[56] For the use of Bi compounds in organic synthesis, see a) T. Ollevier, *Org. Biomol. Chem.* **2013**, *11*, 2740–2755; b) *Bismuth-Mediated Organic Reactions*, in *Topics in Current Chemistry*, ed. T. Ollevier, Springer-Verlag, Berlin, Heidelberg, **2012**, Vol. 311.

[57] a) Y. Qiao, Q. Chen, S. Lin, B. Ni, A. D. Headley, *J. Org. Chem.* **2013**, *78*, 2693-2697; b) T. Itoh, H. Ishikawa, Y. Hayashi, *Org. Lett.* **2009**, 11, 3854-3857; c) Y. Hayashi, T. Itoh, M. Ohkubo, H. Ishikawa, *Angew. Chem. Int. Ed.* **2008**, *47*, 4722-4724; d) P. García- García, A. Ladépêche, R. Halder, B. List, *Angew. Chem. Int. Ed.* **2008**, *47*, 4719-4721; e) J. W. Yang, C. Chandler, M. Stadler, D. Kampen, B. List, *Nature* **2008**, *452*, 453-455.

[58] F. Eustache, P. I. Dalko, J. Cossy, *J. Org. Chem.* **2003**, *68*, 9994-10002.

[59] S. Ishikawa, T. Hamada, K. Manabe, S. Kobayash, *Synthesis,* **2005**, 2176-2182.

[60] a) C. H. Heathcock, in *Comrehensive Carbanion Chemistry*, Part B (Eds.: Buncel, E.; Dust, T.), Elsevier, Amsterdam **1984**, Chap. 4; b) C. H. Heathcock, in *Asymmetric Synthesis* Vol. 3, Part B (Ed.: Morrison, J. D.), Academic Press, New York **1984**, Chap. 2. c) C. H. Heathcock, *Science* **1981**, *214*, 395-400; d) D. A. Evans, J. V. Nelson, T. R. Taber, *Top. Stereochem.* **1982**, *13*, 1-115.

[61] a) J. E. Dubois, P. Fellmann, *C. R. Acad. Sci., Sér. C* **1972**, *274*, 1307; b) J. E. Dubois, M. Dubois, *Bull. Soc. Chim. Fr.* **1969**, *3120*, 3553; c) J. E. Dubois, M. Dubois, *Tetrahedron Lett.* **1967**, *8*, 4215-4219.

[62] H. E. Zimmerman, M. D. Traxler, *J. Am. Chem. Soc.* **1957**, *79*, 1920-1923.

[63] D. A. Evans, L. R. McGee, *Tetrahedron Lett.* **1980**, *25*, 3975-3977.

[64] a) C. Gennari, L. Colombo, C. Scolastico, R. Todeschini, *Tetrahedron* **1984**, *40*, 4051-4052; b) R. W. Hoffmann, K. Ditrich, *Tetrahedron Lett.* **1984**, *25*, 1781-1784.

[65] Y. Yamamoto, K. Maruyama, *Tetrahedron Lett.* **1980**, *21*, 4607-4610.

[66] a) T. Chan, M. Brook, *Tetrahedron Lett.* **1985**, *26*, 2943-2946; b) R. Helmer, R. West, *Organometallics* **1982**, *1*, 877-879; b) G. Morris, R. Freeman, *J. Am. Chem. Soc.* **1979**, *101*, 760-762.

[67] I. Kuwajima, E. Nakamura, *Acc. Chem. Res.* **1985**, *18*, 181-187.

[68] C. T. Wong, M. W. Wong, *J. Org. Chem.* **2007**, *72*, 1425-1430.

[69] C. Mukherjee, T. Kitanosono, S. Kobayashi, *Chem. Asian J.* **2011**, *6*, 2308-2311.

[70] D. Rehder, K. Hink, *Inorg. Chim. Acta.* **1989**, *158*, 265-271.

[71] S. P. Petrosvants, A. B. Ilyukhin, *Russ. J. Coord. Chem.*, **2003**, *30*, 194-197.

[72] For example, see: a) A. A. El-Sherif, M. M. Shoukry, W. M. Hosny, M. G. Abd-Elmoghny, *J. Solution Chem.* **2012**, *41*, 813-827; b) T. S. Venkatakrishman, S. Sahoo, N. Bréfuel, C. Duhayon, C. Paulsen, A. –L. Barra, S. Ramasesha, J. –P. Sutter, *J. Am. Chem. Soc.* **2010**, *132*, 6047-6056; c) N. Suprava, D. Anadi, N. Pranaba, D. Dipankar, *Transition Metal Chem.* **2005**, *30*, 917-932.

[73] CCDC 828098, CCDC 850236 and CCDC 864123. These data can be obtained free of charge from Cambridge Crystallographic Data Center.

[74] B. Plancq, T. Ollevier, *Aust. J. Chem.* **2012**, *65*, 1564-1572.

[75] a) B. J. Coe, S. Glenwright, *J. Coord. Chem. Rev.* **2000**, *203*, 5-80; b) T. G. Appleton, H. C. Clark, L. E. Manzer, *Coord. Chem. Rev.* **1973**, *10*, 335-422.

[76] For example, see: I. Iwakura, T. Ikeno, T. Yamada, *Angew. Chem. Int. Ed.* **2005**, *44*, 2524-2527.

[77] Taking low reactivity in the reaction of ketene silyl acetal into consideration, silyl enol ether should be activated through d-π interaction with iron(II) ion.

[78] T. Nakagawa, H. Fujisawa, Y. Nagata, T. Mukaiyama, *Bull. Chem. Soc. Jpn.* **2004**, *77*, 1555-1567.

[79] It was confirmed that the reaction did not proceed at all in the presence of only an additive.

[80] Full recovery of the starting materials.

[81] a) S. Kobayashi, I. Hachiya, *J. Org. Chem.* **1994**, *59*, 3590-3596; b) S. Kobayashi, *Synlett* **1994**, 689-699; c) S. Kobayashi, I. Hachiya, *Tetrahedron Lett.* **1992**, *33*, 1625-1628.

[82] E. J. Corey, D. Barnes-Seeman, T. W. Lee, *Tetrahedron Lett.* **1997**, *38*, 4351-4354.

[83] The speculation is in accord with the calculation studies, see: M. Hatanaka, K. Morokuma, *J. Am. Chem. Soc.* **2013**, *135*, 13972-13979.

[84] S. Kobayashi, C. Ogawa, In Asymmetric Synthesis—The Essentials, Eds. M. Christmann & S. Bräse, Weinheim: Wiley-VCH, 2007, pp. 110–115.

[85] For example, sodium dodecylsulfate (SDS).

[86] For example, Triton X.

[87] S. Kobayashi, T. Wakabayashi, S. Nagayama, H. Oyamada, *Tetrahedron Lett.* **1997**, *38*, 4559–4562.

[88] a) S. Kobayashi, T. Wakabayashi, *Tetrahedron Lett.* **1998**, *39*, 5389–5392; b) S. Kobayashi, K. Manabe, In *Clean Solvents*, ACS Symposium Series, **2002**, *819*, 151–1665; c) M. Shiri, M. Zolfigol, *Tetrahedron* **2009**, *65*, 587–598.

[89] The rate acceleration by copper(II) bis(dodecylsulfate) Cu(DS)$_2$ in Diels–Alder reactions in water was described previously, see: S. Otto, F. Bertoncin, J. B. F. N. Engberts, *J. Am. Chem. Soc.* **1996**, *118*, 7702–7707.

[90] a) K. Manabe, S. Kobayashi, *Synlett* **1999**, 547–548; b) S. Kobayashi, K. Manabe, *Acc. Chem. Res.* **2002**, *35*, 209–217.

[91] For example, Mannich-type reactions: K. Manabe, S. Kobayashi, *Org. Lett.* **1999**, *1*, 1965–1967; Diels–Alder reactions: K. Manabe, Y. Mori, S. Kobayashi, *Tetrahedron* **1999**, *55*, 11203–11208; Michael reactions: Y. Mori, K. Kakumoto, K. Manabe, S. Kobayashi, *Tetrahedron Lett.* **2000**, *41*, 3107–3111.

[92] H. J. Li, H. Y. Tian, Y. J. Chen, D. Wang, C. –J. Li, *J. Chem. Res. (S)* **2003**, 153–156.

[93] a) K. Otsuka, S. Terabbe, *J. Chromatogr. A.* **2000**, *875*, 163–178; b) C. Partric, *Electrophoresis* **1997**, *18*, 2322–2330.

[94] M. Benaglia, M. Cinquini, F. Cozzi, G. Celentano, *Org. Biomol. Chem.* **2004**, *2*, 3401–3407.

[95] M. Kokubo, C. Ogawa, S. Kobayashi, *Angew. Chem. Int. Ed.* **2008**, *47*, 6909–6911.

[96] K. Manabe, Y. Mori, T. Wakabayashi, S. Nagayama, S. Kobayashi, *J. Am. Chem. Soc.* **2000**, *122*, 7202–7207.

[97] T. Nagano, S. Kobayashi, *Chem. Lett.* **2008**, 1042-1043.

[98] a) K. Miura, T. Nakagawa, A. Hosomi, *J. Am. Chem. Soc.* **2002**, *124*, 536-537; b) K. Miura, H. Sato, K. Tamaki, H. Ito, A. Hosomi, *Tetrahedron Lett.* **1998**, *39*, 2585–2588.

[99] CaCl$_2$ has been reported to be ineffective in the reaction with TMS enolate.

[100] a) S. Yamamoto, H. Morita, S. Hayashi, O. Moriya, *J. Polym. Sci. Part A: Polym. Chem.* **2005**, *43*, 2075-2084; b) S. Yamamoto, S. Hayashi, H. Morita, O. Moriya, *J. Polym. Sci. Part A: Polym. Chem.* **2004**, *42*, 5021-5025.

[101] M. Kokubo, S. Kobayashi, *Synlett* **2008**, 1562–1564.

[102] For fluoride ion-catalyzed reactions, see: a) R. Noyori, I. Nishida, J. Sakata, *J. Am. Chem. Soc.* **1983**, *105*, 1598–1608; b) E. Nakamura, M. Shimizu, I. Kuwajima, J. Sakata, K. Yokoyama, R. Noyori, *J. Org. Chem.* **1983**, *48*, 932–945.

[103] a) A. Yanagisawa, Y. Nakatsuka, K. Asakawa, H. Kagayama, H. Yamamoto, *Synlett* **2001**, 69–72; b) A. Yanagisawa, Y. Nakatsuka, K. Asakawa, M. Wadamoto, H. Kageyama, H. Yamamoto, *Bull. Chem. Soc. Jpn.* **2001**, 1477–1484.

[104] Recent examples, see: a) C. Allais, P. Nuhant, W. R. Roush, *Org. Lett.* **2013**, *15*, 3922-3925; b) D. Sureshkumar, Y. Kawato, M. Iwata, N. Kumagai, M. Shibasaki, *Org. Lett.* **2012**, *14*, 3108-3111; c) S. Díaz-Oltra, P. Ruiz, E. Falomir, J. Murga, M. Carda, J. A. Marco, *Org. Biomol. Chem.* **2012**, *10*, 6937-6944; d) S. Li, C. Wu, X. Fu, Q. Miao, *Int. Eng. Chem. Res.* **2011**, *50*, 13711-13716; e) H. Yang, S. Mahapatra, P. H. –Y. Cheong, R. G. Carter, *J. Org. Chem.* **2010**, *75*, 7279-7290; f) M. Raj, G. S. Parashari, V. K. Singh, *Adv. Synth. Catal.* **2009**, *351*, 1284-1288; g) M. E. Jung, T. Zhang, *Org. Lett.* **2008**, *10*, 137-140; h) Z. Tang, Z. –H. Yang, X. –H. Chen, L. –F. Cun, A. –Q. Mi, Y. –Z. Jiang, L. –Z. Gong, *J. Am. Chem. Soc.* **2005**, *127*, 9285-9289; i) R. Thayumanavan, F. Tanaka, C. F. III. Barbas, *Org. Lett.* **2004**, *6*, 3541-3544; j) S. E. Denmark, T. Wynn, G. L. Beutner, *J. Am. Chem. Soc.* **2002**, *124*, 13405-13407; k) A. B. Northrup, D. W. C. MacMillan, *J. Am. Chem. Soc.* **2002**, *124*, 6798-6799; l) Y. Yamashita, H. Ishitani, H. Shimizu, S. Kobayashi, *J. Am. Chem. Soc.* **2002**, *124*, 3292-3302.

[105] Exchange rate constants for substitution of inner-sphere water ligands (water exchange rate constants (WERC)) for Ni^{2+} (2.7×10^4) is much lower than Fe^{2+} (3.2×10^6) or Sc^{3+} (4.8×10^7). See: S. Kobayashi, S. Nagayama, T. Busujima, *J. Am. Chem. Soc.* **1998**, *120*, 8287-8288.

[106] C. Girard, H. Kagan, *Angew. Chem. Int. Ed.* **1998**, *37*, 2922-2959.

[107] J. M. Lee, P. Helquist, O. Wiest, *J. Am. Chem. Soc.* **2012**, *134*, 14973-14981.

Chapter 2 : Design of the Simplest Metalloenzyme-like Catalyst System in Water

Section 2.1   Direct-type Aldol Reaction in Water

2.1-1   Introduction

Since the emergence of life on Earth, Nature has had 3.8 billion years foster her excellent catalysts, enzymes, so as to allow virtually all biological reactions to occur within the homeostasis constraints of a living system. Protracted ruminant evolution and natural selection had long remained their catalysis a kind of "divine wisdom" beyond human comprehension. Thus the enzymatic reactions in existing organisms are completely chemo-, regio- and stereoselective even at low concentrations, although performed without any protection methodology and under remarkably mild conditions; generally in neutral aqueous solution, at atmospheric pressure and temperature.[1]

Today at one level can we already elucidate how they function.   The more we get to know them, the more they make us realize how far conventional artificial catalysts are from highly-evolved natural enzymes, albeit rapid evolution in chemistry.   To date, the variety of them has been extensively increasing for use in industrial applications.[2] There are, however, not without practical drawbacks. As easy to be denatured inconveniently even by many chemicals such as surfactant, enzymes are basically labile and difficult to preserve their catalytic activity constant.[3] Until recently, to obtain new enzymes, we have taken natural enzymes and evolved them by mutation or modification of their active sites (engineering proteins[4]) or catalytic antibodies[5]. However, these methodologies cannot offer a fundamental prescription to completely overcome the disadvantages of enzymes. Hence chemists have still dreamed of outdoing 3.8 billion years of evolution and natural selection by a clean-sheet design that is *not* based upon enzymatic motifs from nature. It is the ultimate goal for chemistry to directly design "privileged" catalysts that outdo enzymes. For instance, such catalysts might perform predefined tasks, natural or unnatural reaction in water; a profound impact would be exerted upon science and the definition of our future.[6] The rational design of catalyst for the mutual coexistence with water and exhibition of predefined catalytic activity in water was reported herein.

Deep yearning for enzymes in chemistry has coined the term "artificial enzyme", which is focused upon a single aspect in enzymes: the ability to bind substrate with catalytic functional groups.[7] Despite such deep yearning for truly "artificial enzymes," there has been no success without the use of excess amounts of surfactants in water or the use of organic solvents as cosolvents.[8,9,10,11,12,13] The staggering difficulties that thwart the realization of the ultimate goal are chiefly attributed to the problems of aqueous conditions: weak, noncovalent interactions among substrates, a chiral ligand and a metal ion under competitive polar conditions. Coordination of water molecules is prone to ruin the active species, especially metal catalyst in the reaction system. Hydrogen bond and flexibility of water molecules often disrupt the molecular orientations or noncovalent interactions to cause the extraordinary difficulties with stereoselective installation of the reactant, besides those with the enhancement of reactivity. In addition, the solubility of a

designed catalyst in water is another problem. The utilization of a host-molecule, such as protein scaffolds,[14] cyclodextrins,[15] crown ethers[16] and calixarenes,[17,18] has enabled us to construct a hydrophobic cavity in water and to accelerate the reaction rate as enzyme do.[19] In the biological or biochemical field, catalytic antibodies[5] or artificial modification of natural enzymes involves exploitation of natural wisdom as catalyst template. Progress made in interdisciplinary area of science is enormous in recent years. There has been, however, little success in most attempts of rational design for genuine "artificial enzymes" based on rational design. And it is noted that in spite of recent advances on computational design, no valuable rationale has been obtained for the resulting catalytic activity.[20] Therefore for the last decades, almost all endeavors have been dedicated to the advances in organocatalysts.[21] Indeed, relatively ease of use, design, synthesis, solubility in water and substrate binding seems to make them suitable candidates for "artificial enzyme" design. Aldolase-type organocatalytic reactions in pure water, however, generally result in very poor yield and selectivity so far without using any organic solvent even in the case of polymer-type organocatalysts.[22] The exploitation of metal is, however, indispensable to exert multifarious functions in natural protein structure and in this context metal-containing enzyme design is of tremendous significance (Figure 1).
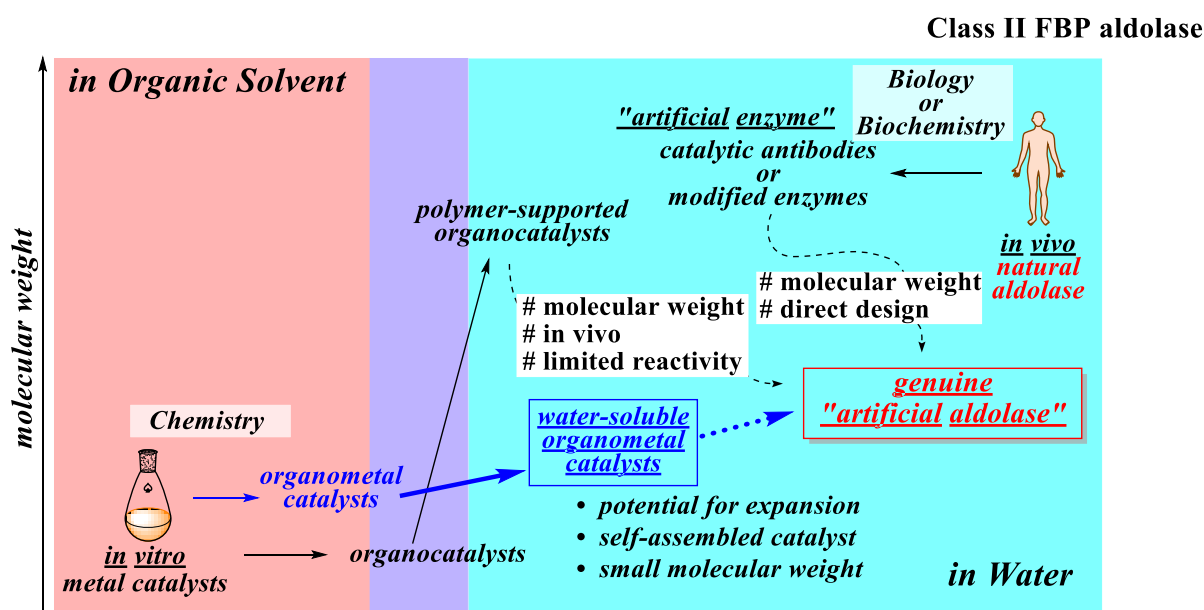
Figure 1. Various approaches for genuine "artificial aldolase"

It was therefore considered that an understanding of the principles of enzyme catalysis *must* surmount those problems and accomplish the formidable task. As one example, the active site of class II Fructose-1,6-Bisphosphate (FBP) aldolase, which is a zinc-dependent catalyst of reversible direct-type asymmetric aldol reaction in organisms, can construct a highly systematized reaction environment that engenders prodigious catalysis.[23] Shibasaki *et al*. compiled pioneering work in this field in organic solvents.[9] While some organocatalysts as class I aldolase mimics work in water, such reactions have generally resulted in poor reactivity and selectivity in the absence of any organic solvent, even in the case of polymer-type organocatalysts.[19,24] Inspired by their three-dimensional elaboration, direct-type asymmetric aldol reaction was focused upon as a model

reaction.   The proposed catalytic mechanism of class II FBP aldolase bears eloquent testimony to the fact that the aldol reaction is one of the most formidable and attractive subjects because of its many requirements.[25] The precise alignment of the substrate assisted by a zinc ion which is surrounded by three histidine residues facilitates it to function as a Lewis acid and to polarize the carbonyl bond of the substrate, while increases the acidity of the hydrogen atoms on α-position in conjugate with the efficiently adjusted pKa value in the reaction system.[26] A glutamic acid residue works as a Brønsted base to abstract the acidic proton, prompting the formation of enolate transition intermediate at the active site.[27] A tyrosine residue acts as a Brønsted acid to activate the aldehyde. And intricate three-dimensional structure irrelevant to the catalytic site provides the hydrophobicity enough to take in hydrophobic substrates.[28] The approach toward the ultimate goal was not mimicking their structure but mimicking their process of evolution.

2.1-2 Conceptual Description for Aldolases

It was envisaged that compaction of the independent factors crucial for catalysis into one structure could be an attractive highway to the realization of the simplest enzyme-like catalysis.[29] The designed molecule is characterized by multiple strategies; 1. being soluble and able to function as catalyst in water, 2. a precise placement of catalytically crucial functional groups, 3. the formation of a hydrophobic pocket to provide the efficient reaction field for hydrophobic substrate, 4. the construction of mildly basic conditions to promote the proton transfer and to regulate acidity of the system. Whereas substrates of aldolases are α-hydroxyketone due to the stabilization of carbanion intermediate, my interest was devoted to the monodentate substrates more difficult to activate. Aggregation of these crucial factors in one catalyst seemed to be an attractive highroad to realization of the impossible.

Focused upon was a catalyst system consisting of a Sc(OTf)$_3$–chiral *N*-oxide ligand complex, an excess amount of surfactant, and a catalytic amount of pyridine for a direct-type enantioselective aldol reaction in water.[13] Based upon this speculation, concreteness was added to the conceptual structure (Figure 3). In order to address the solubility issue, an amphiphilic structure was designed, which was modeled after the architecture of a membrane protein. At the active site, a chiral *N*-oxide ligand was expected to form a chelate complex with a scandium ion to promote intramolecular electron transfer, which would result in a drastic change of the free energy change of electron transfer. It is to be desired the terminal pyridine moieties form pyridinium salts to undertake the regulation of acidity and proton transfer enhances across water in conjunction with amide protons as Brønsted acid. The two polarized bonds and the two ion pairs in the structure were expected to improve the solubility of the catalyst in water as an amphipathic molecule. It is also assumed that noncovalent interactions between the metal center and substrates, which are essential for the reaction, would be more stable within the surrounding shield of hydrophobic "bipods"

Class II FBP aldolases
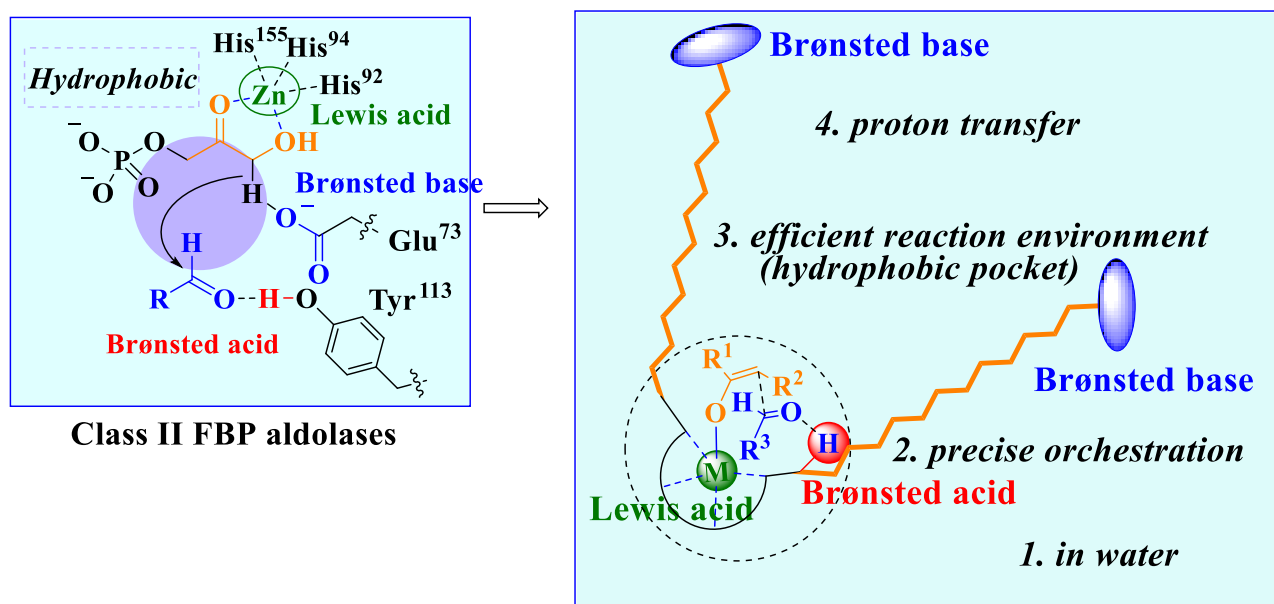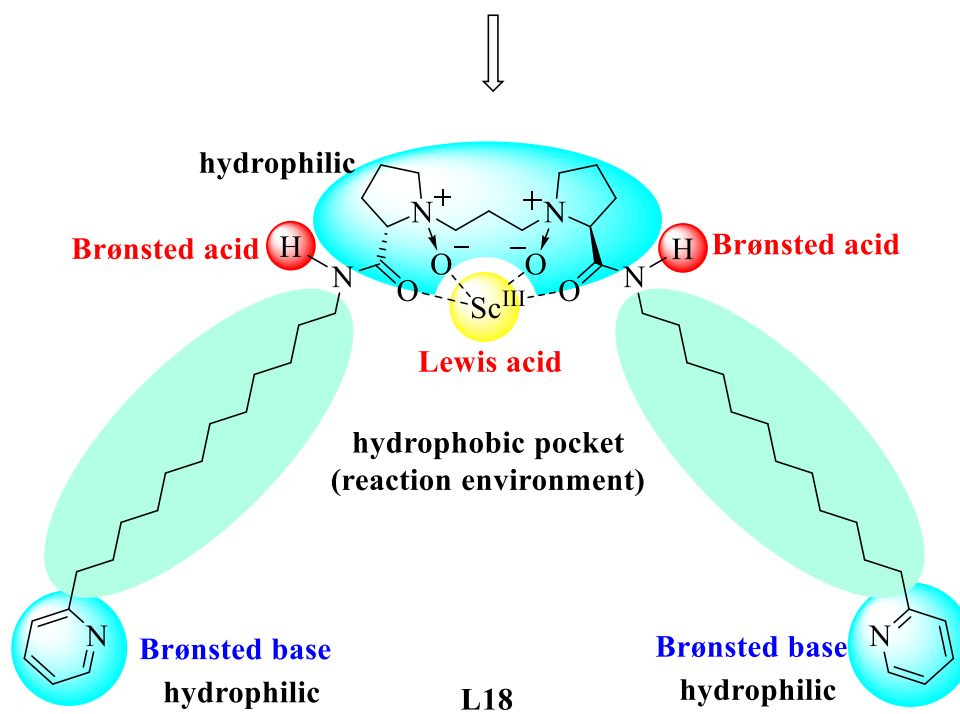
Figure 3. Design of highly systemized catalytic system

2.1-3 Synthesis and Characterization of Designed Catalyst

The designed ligand **L18** was finally synthesized after many twists and turns (Scheme 1). The synthesis commenced with the construction of two segments, **7** and **10**. The synthesis of aminoalkylpyridine **7** involved three steps; lithiation of α-picoline **4** and coupling with 1,10-dibromodecane furnished compound **5**, which underwent cyanidation to elongate the carbon chain. Successful reduction of **6** afforded **7** in 48% overall yield. The synthesis of fragment **10** involved an appropriate cross-linking of *L*-proline benzyl ester **8** with 1,3-dibromopropane and the subsequent debenzylation. Finally, a condensation between fragments **10** and **7** followed by selective *N*-oxidation of primary amine produced **L18** in an enantiopure form.
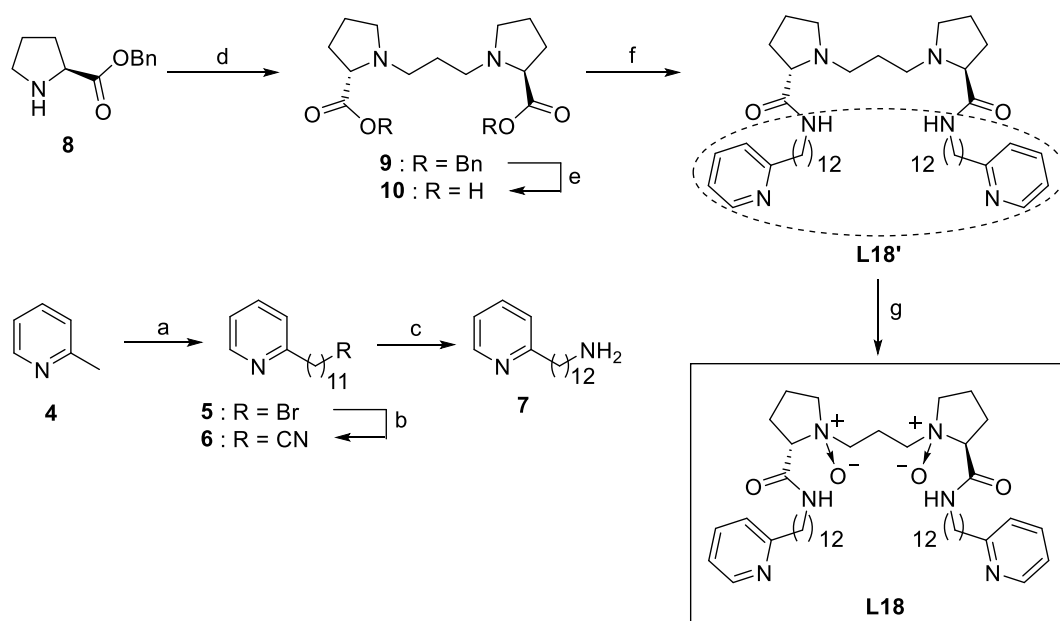
a 1) ^{n}BuLi, THF, −78 °C, 3 h, 2) Br(CH$_2$)$_{10}$Br (1.5 equiv.), THF, −25 °C, 10 h, 61%; b KCN (2.0 equiv.), DMSO, 80 °C, 3 h, 87%; c LiAlH$_4$ (0.75 equiv.), THF, rt, 3 h, 90%; d K$_2$CO$_3$ (2.1 equiv.), Br(CH$_2$)$_3$Br (0.45 equiv.), MeCN, reflux, 8 h, 88%; e Pd/C, H$_2$, EtOH, 3h, Quant.; f 1) ClCO$_2$^{i}Bu (2.2 equiv.), CH$_2$Cl$_2$, 1 h 2) **7** (2.0 equiv.), CH$_2$Cl$_2$, 2 h, 72%; g *m*CPBA (2.0 equiv.), CH$_2$Cl$_2$, 2 h, 99%

Scheme 1. General procedure for preparation of **L18**

In the final *N*-oxidation step, chemoselectivity between a pyridine moiety and a tertiary amine was confirmed by a following control experiment. When NMO (*N*-methylmorpholine) and pyridine were mixed and stirred for 2 h in the presence of *m*CPBA at 0 ˚C, NMO underwent *N*-oxidation predominantly over pyridine (Scheme 2). As a result, *m*CPBA led to the quantitative oxidation of NMO, and pyridine *N*-oxide was not obtained at all. The *N*-oxide moieties were characterized by the deshielding effect on the amide N–H bonds, which arise from intermolecular hydrogen bonds with *N*-oxide moieties, in ^{1}H NMR spectra (Figure 4).[30] The fixation of the amide plane inferred from these intermolecular hydrogen bonds suggests intermolecular and intramolecular aggregation of "bipod" moieties.
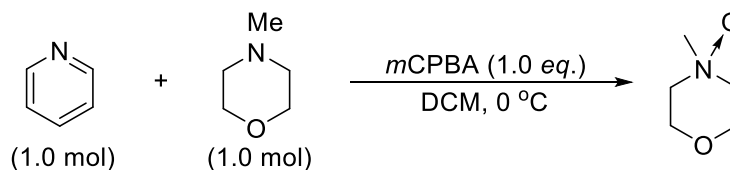
Scheme 2. Control experiment of *N*-oxidation step
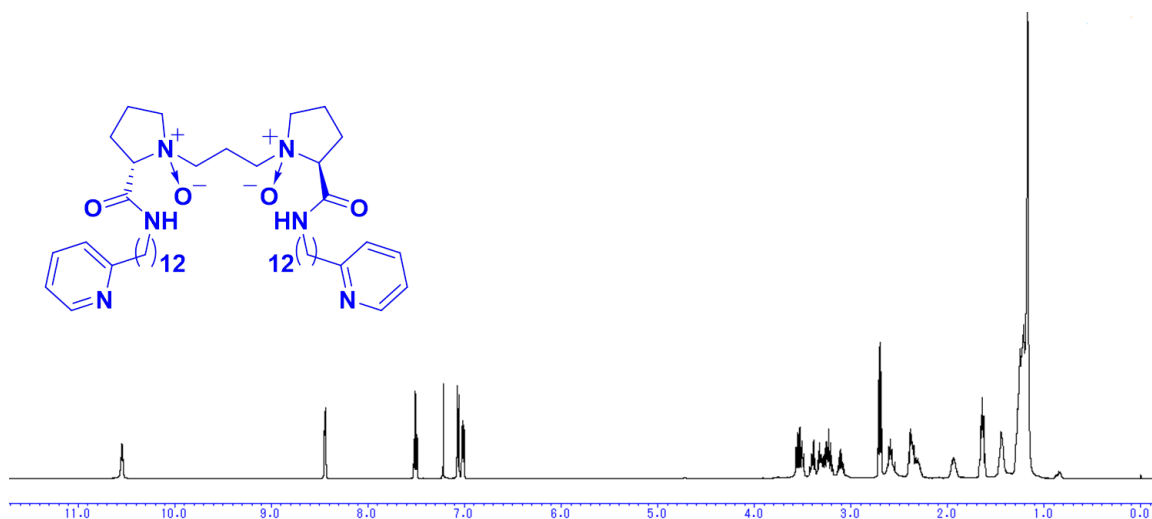
Figure 4. ^{1}H NMR spectrum of **L18**

One of the most intriguing aspects of designed Sc(OTf)$_3$-**L18** complex is its behavior in water. Self-assembly in water is especially desired to enable the functional operation by the addition of an external metal ion as enzymes do. Based upon the initial design, the solubility of **L18** in water might be dramatically improved by chelation with Sc^{3+} ion and the formation of ion pairs at the pyridinyl moieties. As expected, the catalyst solution prepared from just mixing Sc(OTf)$_3$ and **L18** seemed to be a colloidal dispersion. No sooner was an excess amount of Sc(OTf)$_3$ added to the aqueous solution of **L18** than the resultant solution turned transparent; the complex solution turned out to be acidic (Figure 5).[31]

Given the aqueous solution of **L18** itself was clouded, it indicates the solubility of **L18** was dramatically improved by chelation with Sc(OTf)$_3$ as homogeneous solution. Spectroscopic investigation of the catalyst was then performed to gain insight into the catalyst structure and the structure–function relationship. The major concern is, however, the catalyst behavior *in water*. Generally "in water" can be main disadvantages for most spectrometric investigations due to their high flexibility or low affinity with the spectrometric environment. In order to address these issues, in enzymatic investigations CD$_3$OD has been often employed instead of D$_2$O.[32] ^{1}H NMR analysis supports the formation of Sc(OTf)$_3$–**L18** complex (Figure 5). When Sc(OTf)$_3$ and **L18** were combined, all of the signals corresponding to the pyridinyl moieties were shifted downfield . It is assumed that the formation of ion pairs is attributed to the ionic character of Sc–O bonds in Sc(OTf)$_3$, which is suggested by the fact that ^{19}F NMR spectrum shows a constant peak regardless of the complexation with chiral ligand.[33,34]
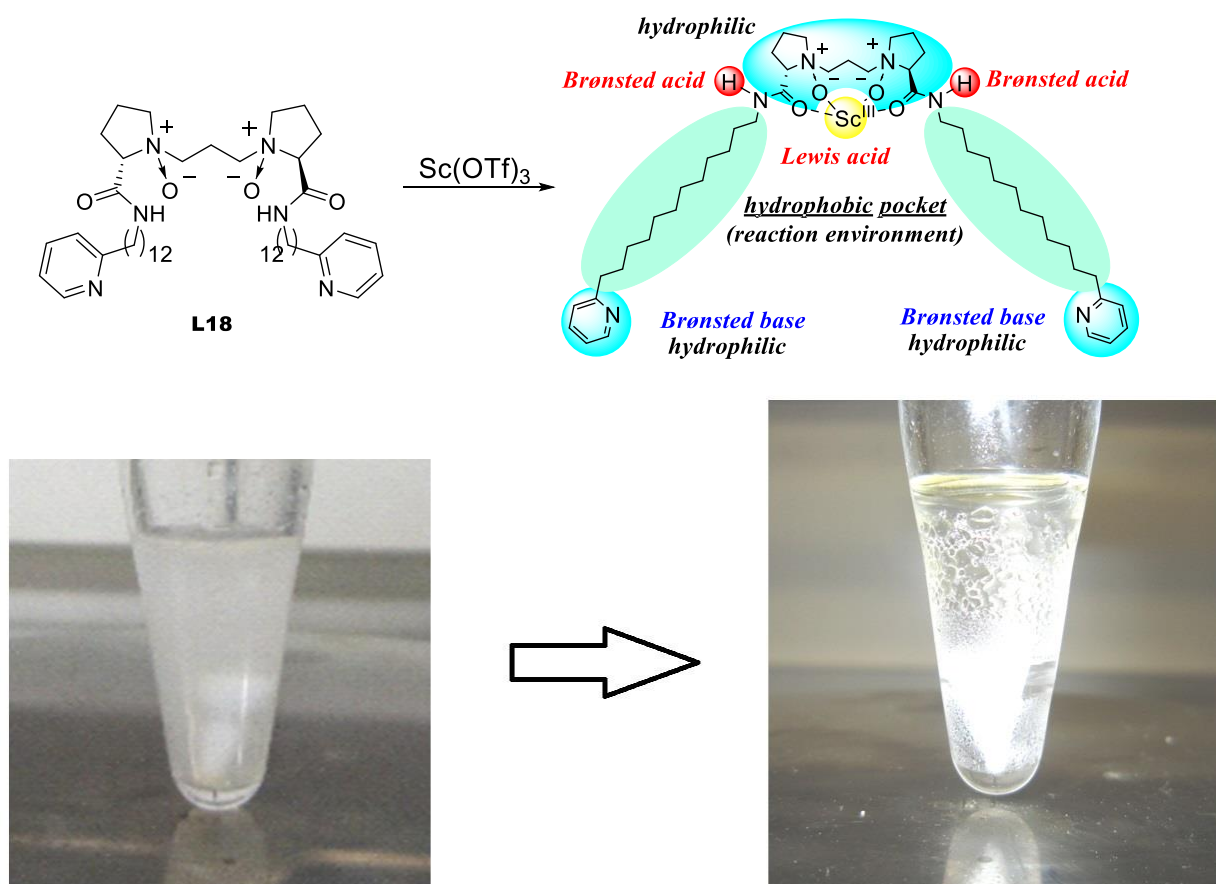
Figure 5. Desired self-assembly (above), appearance of reaction solution before [left] and after [right] addition of substrates (below)

¹H NMR

^{13}C NMR

L18 + Sc(OTf)₃

L18
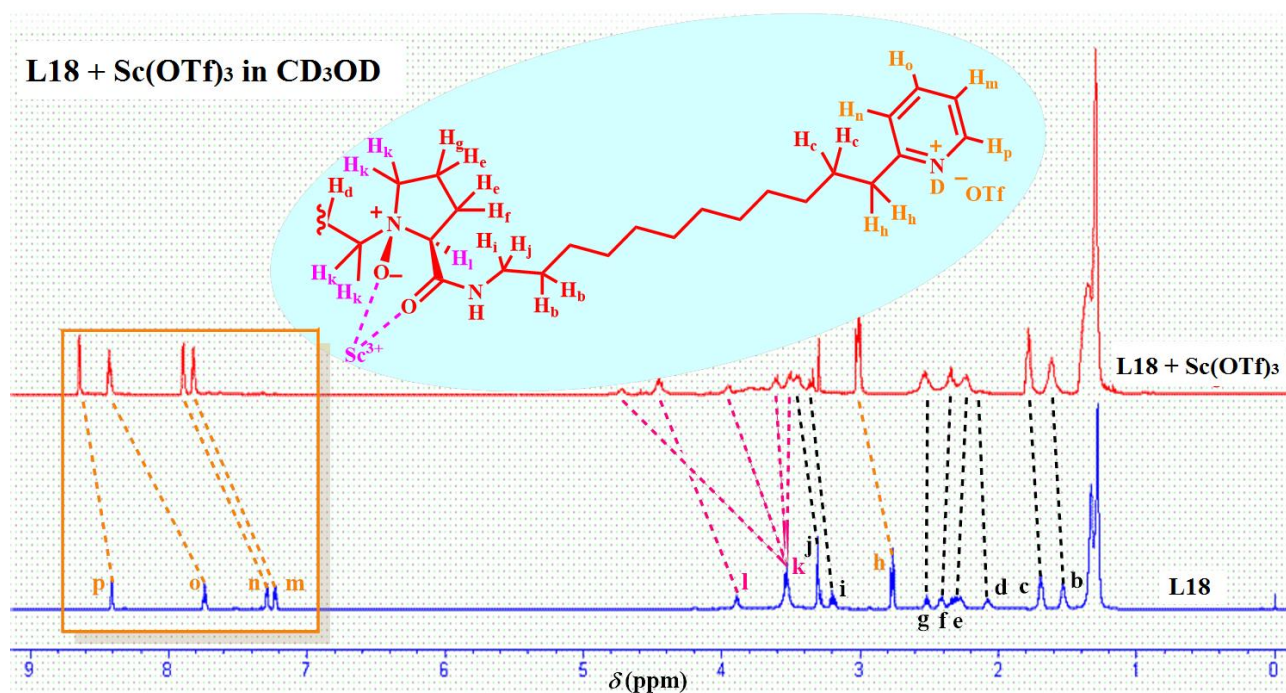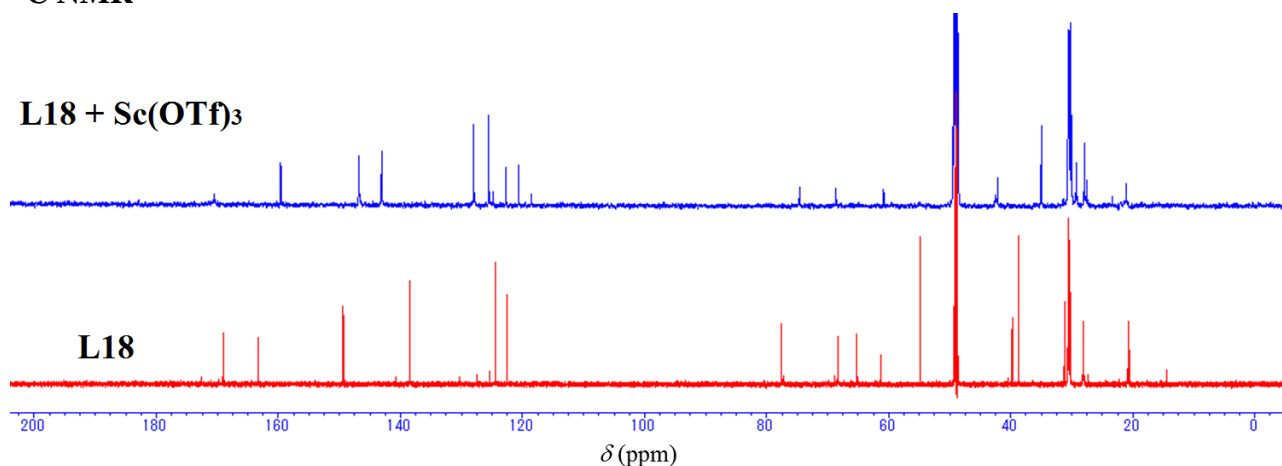
Figure 5. Spectroscopic changes in ^{1}H (above) and ^{13}C (below) NMR spectrum by addition of Sc(OTf)₃ in CD₃OD

When Sc(OTf)₃ and **L18** were combined, all of the signals corresponding to the pyridinyl moieties were shifted downfield. Similar peak shifts were observed when 2-ethylpyridine and Sc(OTf)₃ were mixed in a ratio of 3:1, which indicated the formation of ion pairs rather than Sc–pyridine complexes (Figure 6). It is assumed that the formation of ion pairs can be ascribed to the ionic character of Sc–OTf bonds in Sc(OTf)₃. The constant signal observed in the ^{19}F NMR spectrum regardless of the complexation with chiral ligand indicated the formation of triflic anion in the reaction system, which might contribute to the formation of a pyridinium cation in the catalyst structure. This pyridinium cation seems to play a vital role in the solubility or construction of an efficient reaction environment, resulting in good yield and enantioselectivity. For metal salts with a small hydrolysis constant, the generation of Brønsted acids through cation hydrolysis in an aqueous environment is well documented.[35] In that sense, the coexistence of Lewis acid and Lewis base is of immense interest. Therefore, the behavior of Lewis base (2-ethylpyridine [pK_a = 5.89]) in the presence of Lewis acid (scandium triflate) was monitored by ^{1}H NMR analysis in D₂O.

^{1}H NMR
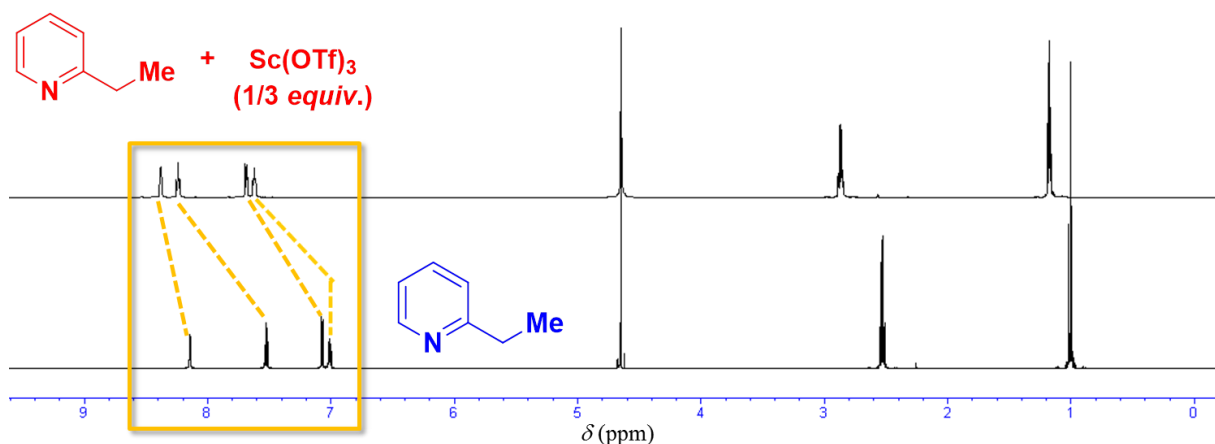
¹³C NMR

¹³C NMR
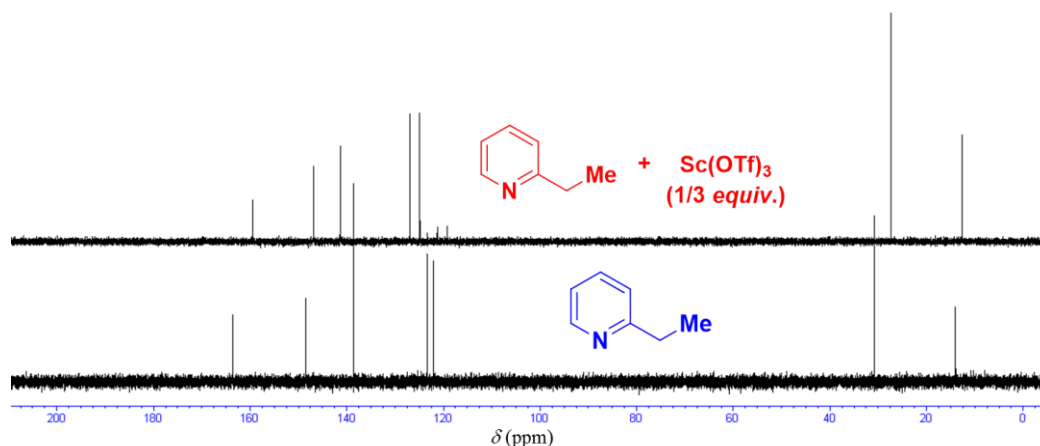
Figure 6. Changes in NMR spectrum by addition of Sc(OTf)$_3$ in D$_2$O

The significant downfield of the signals especially corresponding to the pyridine moiety indicates the formation of pyridinium cation, which is <u>in accord with that corresponding to pyridine moieties in the structure of **L18**</u>. Notably, the identical spectrum was recorded irrespective of the ratio of scandium to pyridine in ^{1}H NMR analysis [exception: more than 3-fold excess of pyridine will lead to the complete hydrolysis of scandium triflate]. The remarkable changes in ^{1}H NMR spectrum observed in the presence of scandium triflate should result from the formation of either H$^+$-pyridine interaction (pyridinium ion) or Sc^{3+}-pyridine interaction. Therefore, clarification of the coordination environment around Sc^{3+} is of great importance. When Sc(OTf)$_3$ and pyridine were combined in the ratio of 3 : 1, any interaction was hardly observed. The dwarf and broad peak was detected at approximately 36 ppm (peak *a*). The 2-fold excess of pyridine eliminated free scandium cation and instead two broad peaks were obtained (peak *a* [δ (^{45}Sc) = 36 ppm] & *b* [δ (^{45}Sc) = 16 ppm]). Aqueous solutions of scandium salts contain, in the pH/D range of *ca*. 2–4, the species Sc(H$_2$O)$_6$$^{3+}$, Sc(OH)(H$_2$O)$_5$$^{2+}$ and Sc$_2$(OH)$_2$(H$_2$O)$_8$$^{4+}$ in fast exchange with each other (See Section 1.1-5-3 in Chapter 1). At pH > 4, a slowly exchanging trinuclear complex, Sc$_3$(OH)$_5$(H$_2$O)$_n$$^{4+}$ [δ (^{45}Sc) = 36 ppm] is also present. Due to its d^0 configuration, the scandium ion was not fastidious whether it coordinates with solvent molecule or pyridine. Therefore, the coordination through weak interaction should be in dynamic equilibrium with non-coordinating scandium ion. On the basis of these considerations, dominant peak *a*, which was detected even in the presence of small amount of pyridine, probably corresponds to Sc(py)(H$_2$O)$_5$$^{3+}$ species (simple hydroxo-complex *must* correspond to a sharp signal). Sc(py)$_2$(H$_2$O)$_4$$^{3+}$ or Sc(py)(OH)(H$_2$O)$_4$$^{3+}$ was the odds-on candidate for the peak *b*. Given the difference spectrometric pattern between ^{1}H and ^{45}Sc, it is suggested that changes in ^{1}H NMR correspond to the formation of pyridinium ion (counterion is either $^-$OTf or $^-$OH). Moreover, the pyridinium trifluoromethanesulfonate exhibits the similar spectra in ^{1}H NMR analysis. The downfield phenomenon was observed irrespective of the amount of Sc(OTf)$_3$ (1/3, 1/2, 1.0 equiv.), presumably through the release of a proton due to partial hydrolysis.

Figure 7. ESI-MS spectrum of Sc(OTf)$_3$-**L18** complex

The positive-mode ESI-HRMS spectrum showed that the major signal at $m/z = 492.27$ corresponded to $[\textbf{L18}+\text{Sc(OTf)}]^{2+}$, which robustly suggested the formation of a 1:1 complex of chiral *N*-oxide **L18** and Sc(OTf)$_3$ (Figure 7). Because of its highly oxophilic character, scandium ion might be coordinated by the four oxygen atoms of the carbonyl and *N*-oxide groups.[36] The equal intervals of signals from $m/z = 983.54$ to 1433.42 correspond to TfOH, arising from the formation of trifluoromethanesulfonic salts at the pyridinyl moieties. The observation of H–D exchange between the Sc-**L18** complex and CD$_3$OD corroborated the high acidity of the amide protons as Brønsted acids and the assumed coordination environment.

2.1-4 Complex-Catalyzed Asymmetric Direct Hydroxymethylation

As a model reaction to evaluate the catalytic activity of the Sc–**L18** complex, the enantioselective direct-type aldol reaction of 2-methyl-1-indanone using aqueous formaldehyde in water was carried out.   A catalyst solution was afforded by stirring a mixture of chiral ligand and Sc(OTf)$_3$ with the optimized ratio (see Table 3) at room temperature for 1 h (see Figure 5).   It was confirmed that the reaction hardly proceeded in the presence of (*S*)-proline, the simplest organocatalyst, presumably due to the solubility of ketone (entry 1 in Table 1).   Generally speaking, less acidic ketones show a reluctance to generate active enolates under aqueous and catalytic conditions.[37] To my delight, the reaction proceeded smoothly to afford the desired product along with the construction of a chiral quaternary carbon in 75% yield with 60% ee (entry 3).   While direct-type aldol reactions of monodentate ketones that have no activated functional groups generally have very low catalytic turnover,[38,39] the catalytic efficiency of this catalyst system is anomalous.   Furthermore, the yield improved to 91% (catalytic turnover number, CTN = 18.2), amazingly without damaging the enantioselectivity at 40 °C (entry 4).[40] The enantiopurity of the product was maintained even at 100 °C (See Section 2-6).   Especially the example of metal-dependent catalyst for direct-type aldol reaction performed in pure water is limited only to the previous report with the aid of stoichiometric amount of surfactant.[13,41] In addition, it is quite intriguing that the functional integration also produced significant rate acceleration as well as enhancing the enantioselectivity compared with an independently functioned system composed of 10 mol% Sc(OTf)$_3$, 12 mol% **L17**, 20 mol% pyridine, and 20 mol% SDS; the reaction rate was increased by *ca* 16 times (entry 2).

In order to identify the suitable structure, several modified chiral ligands (**L19-L28**) complexed with Sc(OTf)$_3$ were initially investigated in the hydroxymethylation reaction in water. Whereas use of **L19,** which is linked at *m*-position of pyridine, instead of **L18** gave almost the same result as **L18** (entry 5), in the case of **L20**, which is linked at *p*-position of pyridine, both reactivity and enantioselectivity were decreased significantly (entry 6), which is referable to the basicity and solubility as a pyridinyl salt.   Changing the chain length of surfactant moiety was effective neither for reactivity nor for selectivity (entries 7-9).   A pyridine substituent proximal to the amide moiety (**L24**) exhibited no catalytic activity because of the coordination to scandium center (entry 10). Without pyridine moiety, the chiral induction was not suppressed irrespective of its lower reactivity (entry 11).   In the meanwhile, when half ligand **L26** or a precursor of *N*-oxide ligand **L18'** were employed as a ligand, a chiral induction was hardly observed (entry 12 & 13). Prolineamide-derived **L27** which is basic backbone of **L18** afforded the corresponding product in 14% ee (entry 14).   Attachment of surfactant moiety on upper fragment did not have better effect for reactivity or selectivity (entry 15).   That is to say, it was found that both surfactant and pyridine moieties at precise positions perform the coorperative role in defining the reactivity and enantioselectivity of this reaction.

Table 1. Effect of ligand structure.

HCHO *aq.* + [structure **11**] → [structure **12t**]

Sc(OTf)$_3$ (8 mol%)
Ligand (5 mol%)
H$_2$O (0.3 M), 25 °C
24 h

1t   **11**   **12t**

Entry	Ligand	Yield (%)	CTN[a]	Ee (%)[b]
1	–[c]	3	0.6	0
2	**L17**[d]	12	2.4	1 (*S*)
3	**L18**	75	15.0	60 (*S*)
4	**L18**	91	18.2	60 (*S*)
5	**L19**	74	14.8	60 (*S*)
6	**L20**	28	5.6	34 (*S*)
7	**L21**	67	13.4	51 (*S*)
8	**L22**	68	13.6	52 (*S*)
9	**L23**	55	11	52 (*S*)
10	**L24**	Trace	–	–
11	**L25**	2	0.4	58 (*S*)
12	**L26**	3	0.6	3 (*S*)
13	**L18'**	6	1.2	2 (*S*)
14	**L27**	1	0.2	14 (*S*)
15	**L28**	34	6.8	39 (*S*)

[a] Catalytic Turnover Number (= yield/equivalents of catalyst).

[b] Determined by HPLC analysis.

[c] 20 mol% of proline was employed.

[d] Sc(OTf)$_3$ (10 mol%), **L17** (12 mol%), pyridine (20 mol%), SDS (20 mol%)

L17 : 12% y, 1% ee (*S*)[a]
[a] Sc(OTf)$_3$ (10 mol%), L0 (12 mol%) pyridine (20 mol%), SDS (20 mol%)

L18 : 75% y, 60% ee (*S*)
91% y, 60% ee (*S*)[b]
[b] at 40 °C

L19 : 74% y, 60% ee (*S*)

L20 : 28% y, 34% ee (*S*)

L21 (n = 14) : 67% y, 51% ee (*S*)
L22 (n = 10) : 68% y, 52% ee (*S*)
L23 (n = 8) : 55% y, 52% ee (*S*)

L24 : trace

L25 : 2% y, 58% ee (*S*)   **L26** : 3% y, 3% ee (*S*)   **L18'** : 6% y, 2% ee (*S*)

L27 : 1% y, 14% ee (*S*)   **L28** : 34% y, 39% ee (*S*)

As mentioned above, the formation of pyridinium cation would play a crucial role in this reaction.   In order to evaluate the effect of counterion, several scandium salts were examined by using **L18** as a chiral ligand (Table 2).

Table 2. Effect of scandium salt.

Entry	Scandium Salt	Yield (%)	Ee (%)[a]
1	Sc(NO$_3$)$_3$·4H$_2$O	73	47 (*S*)
2	ScCl$_3$·6H$_2$O	39	48 (*S*)
3	ScF$_3$·4H$_2$O	5	1 (*S*)
4	Sc(CO$_3$)$_3$	26	40 (*S*)
5	Sc$_2$O$_3$	10	6 (*S*)
6	Sc(OAc)$_3$	33	16 (*S*)
7	Sc(OTf)$_3$	88	60 (*S*)
8	Sc(SO$_3$C$_2$F$_5$)$_3$	79	61 (*S*)
9	Sc(SO$_3$C$_6$F$_{13}$)$_3$	31	9 (*S*)
10	Sc(SO$_3$C$_{12}$H$_{25}$)$_3$	18	16 (*S*)
11	Sc(OSO$_3$C$_{12}$H$_{25}$)$_3$	44	18 (*S*)
12	Sc(SO$_3$C$_6$F$_5$)$_3$	74	47 (*S*)

[a] Determined by HPLC analysis.

To my astonishment, counterions were proved to produce dramatic differences in defining reactivity or enantioselectivity in this reaction system.   This intriguing aspect of counterion emphasizes the significance of *in situ* formed pyridinium triflate.   The amount of scandium triflate

compared with **L18** has been examined at the initial stage (Table 3). As a result of multiple attempts, an excess amount of Sc(OTf)$_3$ ensured the formation of pyridinium salt, which was turned out to be suitable conditions in terms of reproducibility.

Table 3. Correlation between ratio of Sc(OTf)$_3$ to **L1** and catalytic activity or enantioselectivity.

Entry	Sc(OTf)$_3$ (x mol%)	Yield (%)	Ee (%)[a]
1	0	4	8 (S)
2	2.5	40	58 (S)
3	4	60	57 (S)
4	4.25	62	59 (S)
5	4.5	63	60 (S)
6	4.75	77	59 (S)
7	5	80	59 (S)
8	6	80	59 (S)
9	7	81	60 (S)
10	8	81	60 (S)
11	9	77	59 (S)
12	10	73	59 (S)
13	20	79	59 (S)

[a] Determined by HPLC analysis.

In order to exclude that trace other metals in scandium salts might affect yield and enantioselectivity of the product, other metal triflates were examined under the same conditions (Table 4). Among tested metals scandium exhibited the most excellent and distinguished catalysis.

Since lanthanides such as La^{III}, Yb^{III} and Lu^{III} have large WERC values, these metals are unsuitable for this reaction conditions (entries 13-15) in spite of characters homologous to scandium.   Thus it was confirmed that Sc-**L18** complex catalyzed asymmetric hydroxymethylation most efficiently in water.

Table 4. Metal screening.

Entry	Metal triflate	Yield (%)	Ee (%)[a]
1	NaOTf	10	5 (*S*)
2	Mg(OTf)$_2$	8	0
3	Ca(OTf)$_2$	10	4 (*S*)
4	Sc(OTf)$_3$	88	60 (*S*)
5	Fe(OTf)$_2$	5	24 (*S*)
6	Co(OTf)$_2$	5	9 (*S*)
7	Cu(OTf)$_2$	6	21 (*S*)
8	Zn(OTf)$_2$	11	10 (*S*)
9	Y(OTf)$_3$	12	12 (*S*)
10	AgOTf	10	6 (*S*)
11	In(OTf)$_3$	2	16 (*S*)
12	Ba(OTf)$_2$	8	2 (*S*)
13	La(OTf)$_3$	6	14 (*S*)
14	Yb(OTf)$_3$	16	21 (*S*)
15	Lu(OTf)$_3$	15	23 (*S*)
16	Bi(OTf)$_3$	4	9 (*S*)

[a] Determined by HPLC analysis.

The interaction between scandium and formaldehyde was verified by kinetic and NMR studies. The amount of formaldehyde had almost no effect in the definition of enantioselectivity. And the difference in the reaction rate was not so remarkable even when the amount of formaldehyde was doubled or more. This result indicates that the interaction between scandium and formaldehyde is predominant and forms rapidly in water.

Table 5. Correlation between amount of formaldehyde and catalytic activity or enantioselectivity.

Entry	HCHO *aq*. (*x* equiv.)	Yield (%)	Ee (%)[a]
1	1.5	55	57 (*S*)
2	2.0	62	58 (*S*)
3	3.0	69	60 (*S*)
4	4.0	72	59 (*S*)
5	5.0	75	60 (*S*)
6	10.0	75	60 (*S*)

[a] Determined by HPLC analysis.

2.1-5 Substrate Scope

The designed catalyst system was applicable to other substrates. Representative unoptimized examples were shown below (Scheme 2).

Scheme 2. Unoptimized examples for Sc-**L18** complex catalyzed reaction

Indanone derivatives behaved as an efficient pronucleophile to afford the satisfactory level of enantioselectivity. Although ketones or thioesters with high pK_a values considerably retarded the catalytic turnover, the reaction took place under well-stereocontrolled conditions. The initial step in such kind of direct-type reaction is deprotonation of the pronucleophile by the catalyst to generate an active feudo-carbanion nucleophile. Consequently the direct-type reaction has been constantly haunted with the pK_a problem, which severely limits the scope of applicable pronucleophiles. In order to conquer such difficulties, an ingenious contrivance should be required. The use of a strong Brønsted base should be generally avoided because it can trigger some undesired side reactions. Indeed, a significant drop in enantioselectivity was observed when 10 mol% of sodium hydroxide solution was added. On the other hand, a further addition of a weaker base such as pyridine improved the reactivity without the loss of enantioselectivity. That is to say, efficient asymmetric environment was constructed and a critical issue was the formation of active nucleophile.

Contrary to ketones, other aldehydes affected the chiral environment constructed by Sc-**L8** complex (Scheme 3).

Scheme 3. Substrate Scope of Aldehyde

The reaction proceeded *anti*-selectively and enantioselectivity of the product is lower than that obtained in hydroxymethylation.   When glycolaldehyde was employed, 27% *ee* was obtained as a major *anti*-aldol adduct.   In order to rationalize the differences between formaldehyde and other aldehydes, two kinds of aldehyde were stirred simultaneously under the same conditions (Scheme 4).

[a] Determined by HPLC analysis.   [b] Determined by ^{1}H NMR analysis.

Scheme 4. Competitive experiment between formaldehyde and benzaldehyde.

As a result benzaldehyde turned out to be more reactive than formaldehyde.   While benzaldehyde reacted with 2-methyl-1-indanone without any chiral induction, hydroxymethylation reaction proceeded stereoselectively.   It was confirmed that cross aldol reaction between benzaldehyde and formaldehyde did not proceed at all.   It is indicated that the hydrophobicity of substrate might affect the definition of enantioselectivity.

2.1-6   *Thermo-stability of L18-Sc Complex*

The enantiopurity of the product was maintained even at 100 °C (Table 6).   This property is in complete contrast to that of an enzyme, as an enzyme generally has an optimum temperature at which it works best.   Although the tertiary amine *N*-oxide moiety is generally easy to undergo thermal rearrangement, the Sc(OTf)$_3$–**L18** catalyst has high stability and identical catalytic activity even at high temperatures.   It is assumed that the strong Lewis acidity of the scandium ion reinforces and stabilizes complexation with **L18**.   In particular, we could prove that an efficient asymmetric environment was maintained constantly in water by the catalyst system, which is chemically much simpler than natural enzymes.   The designed catalyst system has no relationship between temperature and enantioselectivity.

This property is a complete contrast to an enzyme's: generally an enzyme has an optimum temperature at which it works best.   Even the aldolase from *B. cereus*, known to be very resistant to heat, retained only half of its activity after 10 minutes of incubation at 90 °C.[42] Generally speaking enantioselectivity should be determined by a balance of the enthalpy and entropy terms as described in Eyring equation.   It is assumed that strong Lewis acidity of scandium ion reinforces and stabilizes the complexation with **L18**.   This attractive thermo-stability of an asymmetric environment has still not been accomplished in the case of modified-enzymes and conventional artificial catalysts.

Table 6. Temperature-dependence of enantioselectivity.

Entry	Temperature	Yield (%)	Ee (%)[a]
1	0 ˚C	12	59 (*S*)
2	18 ˚C	75	60 (*S*)

3	40 ˚C	91	60 (*S*)
4	60 ˚C	93	59 (*S*)
5	80 ˚C	92	58 (*S*)
6	100 ˚C	92	58 (*S*)

[a] Determined by HPLC analysis.

2.1-7 Mechanistic Elucidation

Two distinct substrates displayed a linear correlation, which obviously suggests that only a set of diastereomeric transition state are operating in the reaction.

Figure 8. Eyling plot for chiral induction catalyzed by Sc-*N,N'*-dioxide complex

There are two reaction pathways, which are concerted pathway and stepwise pathway. For the concerted pathway a boat-shaped six-membered-ring transition state is located. This concerted transition state involves a simultaneous C-C bond formation. There is a favorable in-phase orbital overlap between the HOMO of ketone and the LUMO of formaldehyde.

Figure 9. Proposed transition state

A reasonable saturated fit of the reaction profile can be achieved as Figure 39.   Although amine oxide is generally easy to undergo thermal rearrangements, Sc(OTf)$_3$-**L8** catalyst has strong stability and identical catalytic activity even at high temperature at least during 24 hours.

Figure 10. Reaction profile on hydroxymethylation of 2-methyl-1-indanone.

In contrast to organocatalytic aldol reactions, metal-dependent direct-type aldol reactions are assumed to proceed via the formation of enolate intermediates.   When the scandium catalyst was released into deuterium oxide in coexistence with a ketone, the formation of a reactive enolate

was confirmed by the observation of an α-deuterated ketone.[43] The assumed mechanism based upon this information was thus attributed to the existence of a stable substrate-binding intermediate (Scheme 5). To deepen the insight into the reaction mechanism of this metalloenzyme-like reaction in water, we then attempted to characterize it through kinetic analysis. The elaborately designed catalyst system possesses no cavity to completely capture a hydrophobic substrate, which makes microscopic heterogeneity inevitable, especially in the initial stage before the dispersion of an added substrate comes to equilibrium. To reiterate, the microscopically heterogeneous system in which hydrophobic and hydrophilic substrates were reacted with each other in water thwarts direct spectrometric measurements. Therefore, a simple quenching at regular intervals should be implemented without relying on general enzymological and chemical methodologies in kinetic investigations. The analytical method for obtaining reliable kinetic profiles using high-performance liquid chromatography (HPLC) measurements was established through a continuous process of trial and error.

Scheme 5. Schematic representation of Sc–**L1** catalyzed direct-type aldol reaction.

In order to determine the concentration of each species from the chromatograms, calibration curves were established that describe relationship between the concentration of species to be analyzed and the area of each peak. Judging from ^{1}H NMR monitoring of the crude sample, it was verified that the catalyst system did not provide any byproducts in the least. The integrated areas of peaks representing 2-methyl-1-indanone and the corresponding hydroxymethylated product are found to possess excellent linear correlation with their concentrations, where the correlation coefficient was always above 0.997. The hydrophobic internal standards such as anisole could not be used, whereas the hydrophilic compounds such as acetaminophen were available. However, the use of acetaminophen as an internal standard was not suitable for rapid kinetic experiments, because retention time for the hydrophilic chemicals is much far from those of species to be analyzed.

The plotted progress curve consists of a brief initial transient and an ensuing period during which the reaction is proceeding at the maximum velocity. Eventually, the reaction approached the final equilibrium asymptotically. Because the reaction is viewed as being in a kind of quasiequilibrium that follows a quasisteady-state approximation during the second phase, the slope in this phase corresponds to the initial reaction rate (Figure 11). It indicates the rigid interaction between a catalyst complex and a substrate, implying the formation of an enolate intermediate.

Thus the reaction can be represented with the reaction scheme below (**S** stands for 2-methyl-1-indanone).

Figure 11. Determination of rate constants

The reaction follows first-order kinetics in the catalyst, whereas saturation kinetics was recorded on the concentration of 2-methyl-1-indanone (Figure 13). The saturated correlation observed in this reaction system indicates the existence of a substrate-binding step in the catalytic cycle, implying a rigid interaction between the catalyst and the substrate. Displaying these experimental data on a Hanes–Woolf plot[44] demonstrated a first-order dependence (Figure 14).

Figure 12. Plots of yield vs time (top) and rate vs concentration (bottom) for the kinetics experiments.

Figure 13. Hanes–Woolf plot.

According to steady-state assumption, the concentration of a substrate can be described as:

$$\frac{d[\boldsymbol{S}]}{dt} = -k_1([\boldsymbol{E}]_0 - [\boldsymbol{ES}])[\boldsymbol{S}] + k_{-1}[\boldsymbol{ES}]$$

$$= -\frac{k_2[\boldsymbol{E}]_0[\boldsymbol{S}]}{\frac{k_{-1}+k_2}{k_1} + [\boldsymbol{S}]} \equiv -\frac{k_2[\boldsymbol{E}]_0[\boldsymbol{S}]}{K_m + [\boldsymbol{S}]}$$

Integrating both sides of the equation with respect to $[\boldsymbol{S}]$, we have

$$[\boldsymbol{S}]_t = K_m W\left(-\frac{exp\big((tk_2[\boldsymbol{E}]_0 + C)/K_m\big)}{K_m}\right)$$

W stands for Lambert's W function. We also admit simple Taylor series expansions at 0 by using the Lagrange inversion formula when the reaction follows the assumption below.

$$0 < \frac{k_2[\boldsymbol{E}]_0}{K_m} < 1$$

$$[\boldsymbol{S}]_t = exp\left(-\frac{tk_2[\boldsymbol{E}]_0 + C}{K_m}\right) - \frac{\left[exp\left(\frac{(tk_2[\boldsymbol{E}]_0 + C)}{K_m}\right)\right]^2}{K_m} + \cdots$$

$$= [\boldsymbol{S}]_0 exp\left(-\frac{k_1 k_2[\boldsymbol{E}]_0}{k_{-1} + k_2}t\right)$$

Therefore the raw data for the concentration of a substrate were fit to an exponential function using the least-squares method. Because of the sophisticated kinetic profile of the reaction, other kinetic models using different mathematical treatments were applied. Based upon the concept that the reaction between a substrate and a catalyst was regarded as a probabilistic event, time-dependent characterization was carried out. The concrete derivation was the same as the reported approach.[45]

$$\frac{t}{[\boldsymbol{S}]_0 - [\boldsymbol{S}]_t} = \frac{exp([\boldsymbol{S}]_0/K_m)}{V_{max}\{[exp([\boldsymbol{S}]_0/K_m)] - 1\}} + \frac{t}{K_m\{[exp([\boldsymbol{S}]_0/K_m)] - 1\}}$$
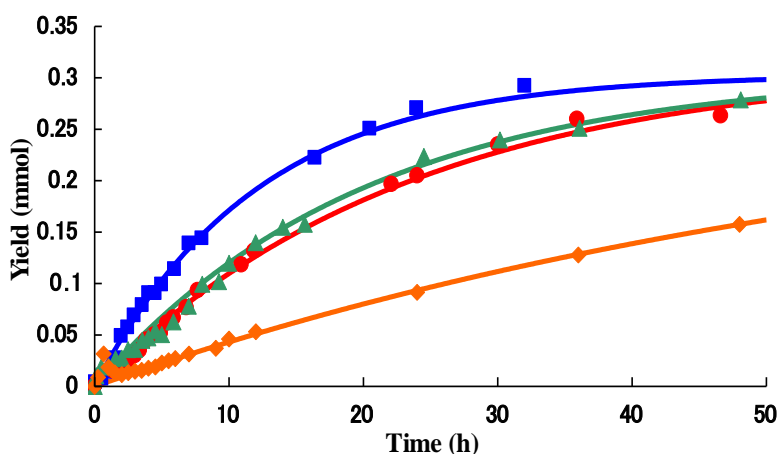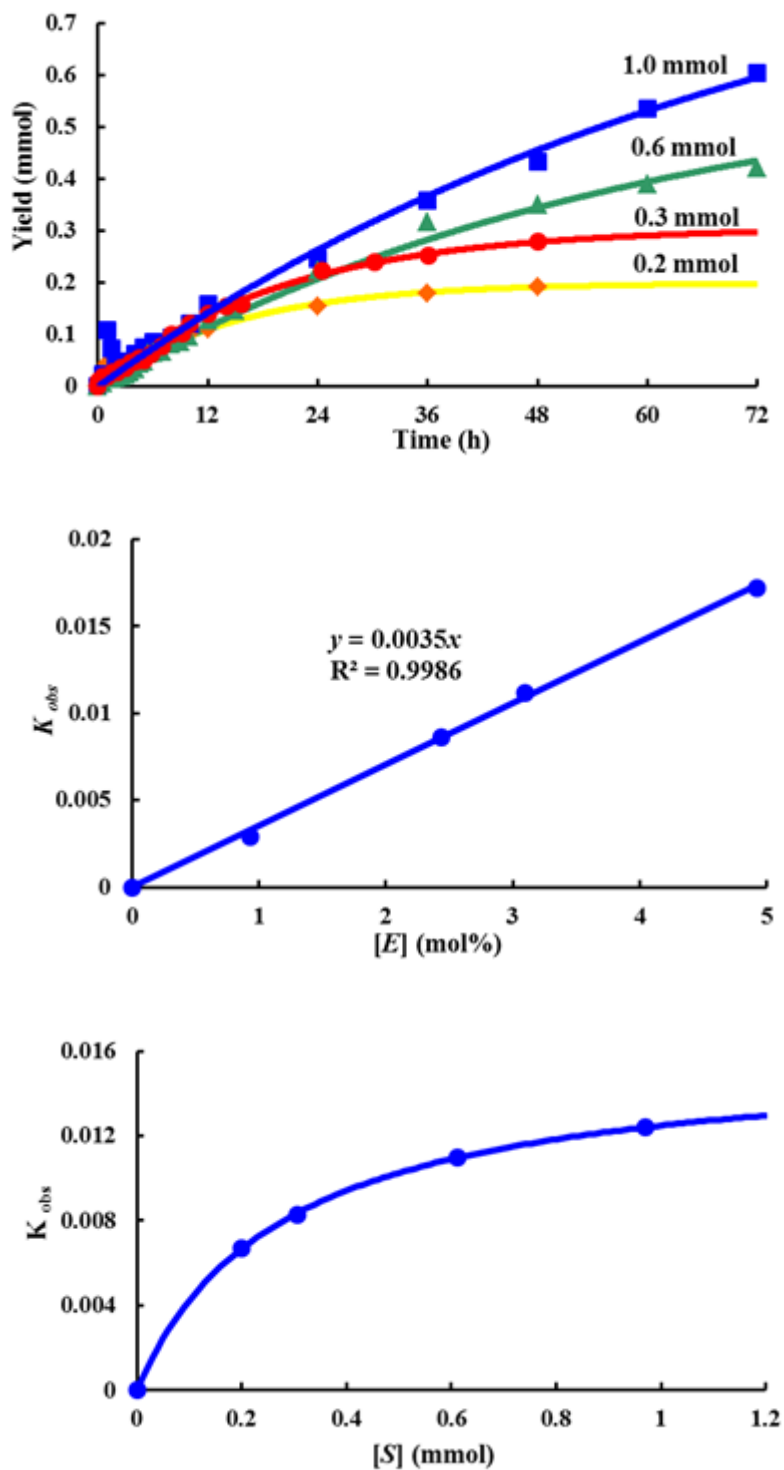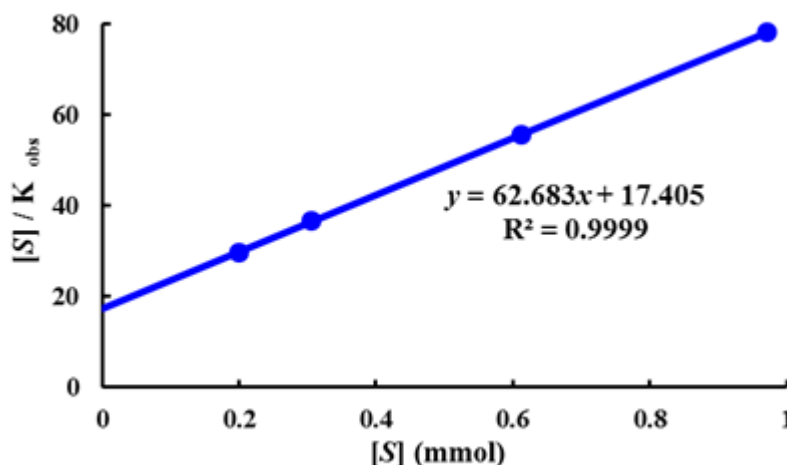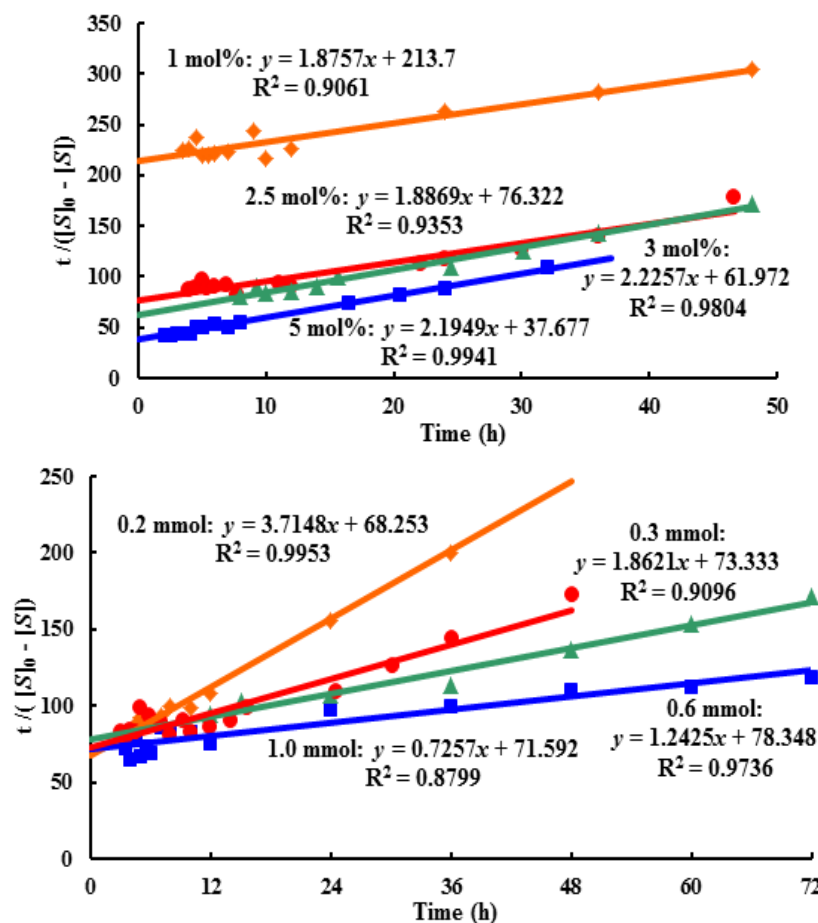
Figure 14. Logistic kinetics; substrate (above) and catalyst (below).

We used a logistic approach based on the probability of the reaction that enabled us to approximate the reaction profile as a linear expression against time.   This analysis indicates that the heterogeneity in the initial stage of the reaction did not affect the reaction rate.   Thus, it has been shown that asymmetric hydroxymethylation catalyzed by the Sc–**L1** complex follows Michaelis–Menten kinetics, as enzymatic reactions do.   In addition, the observation of burst kinetics in the initial period, which did not converge to zero, could be interpreted as resulting from a steady- state rate-determining step following product release.   Hanes-Woolf (half-reciprocal) plot of $[S]/K_{obs}$ against $[S]$ gave intercepts at K_m/V_{max} and K_m.   The specificity constant of the catalyst system is 3.41 M^{-1} s^{-1}.   The kinetic parameters obtained were computed using the least-squares method: maximum velocity $V_{max} = k_2[\text{catalyst}]_0 = 0.0160$ mmol h^{-1}, $k_2 = 2.18$ h^{-1}. The values obtained through three approaches shown above are consistent with one another, insisting that the reaction catalyzed by the designed catalyst system follows Michaelis-Menten kinetics.   In addition, the observation of burst kinetics in the initial period, which did not converge to zero, can be interpreted to the result from a steady-state rate-determining step following product release.   The catalyst system turns over a product as soon as a catalyst-substrate complex is formed.

Toward an in-depth understanding of the mode of action in aldol reactions catalyzed by a chiral Lewis acid complex, the kinetic behavior of this reaction was compared with that of a chiral scandium-catalyzed aldol reaction using a silicon enolate (Scheme 6).   The formation of the same

product over time exhibited a linear correlation in the concentration of both catalyst and substrate, indicating that the overall rate is equal to k[silicon enolate][catalyst].[46] The rate constant k was calculated to be 0.0192 h^{-1} mmol^{-2} using the least-squares method.[47] It was therefore assumed that the reaction of a silicon enolate proceeded through a Lewis acid activation involving a weak interaction. Consequently, active species in the reaction of the silicon enolate are based upon only a weak interaction, such as coordinating or ionic bonds and generated through equilibrium with the starting substrate.
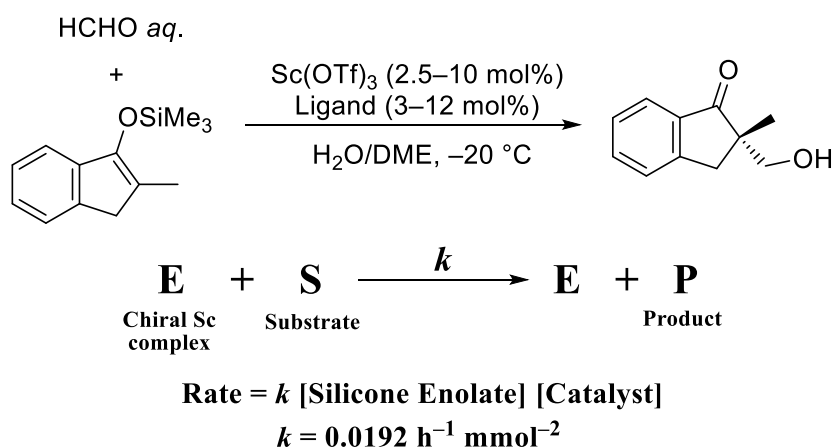
Scheme 6. Asymmetric hydroxymethylation of silicon enolate in aqueous media.

2.1-8　Summary

　　　　Enzymes exhibit overwhelmingly superior catalysis compared with artificial catalysts. Current strategies to rival the enzymatic catalysis are known as "protein engineering", "catalytic antibodies" and "chemozymes" based on host-molecules. However, they require unmodified or minimally-modified structure of active sites, gigantic molecular weight, and sometimes the use of harsh conditions such as extremely low temperature in organic solvents. In addition, quantitative functionalization is indispensable to modify the structure. On the other hand, valuable rationale has never been obtained for the enzymatic catalytic activity, in spite of recent advances on computational design. It was envisioned the compaction of the independent functions crucial for catalysis in one structure. As a result, the simplest metalloenzyme-like catalyst system was designed without employing the enzyme structure. The synthesized ligand formed a self-assembly system in the presence of scandium ion in water. This artificial system efficiently catalyzed enantioselective direct-type aldol reactions using aqueous formaldehyde, although a sterically hindered product was generated. The significant rate acceleration and stereoselective control were achieved by the compaction and self-assembling. Not only did it follow the Michaelis-Menten kinetics, but also it could construct the unusual heat-resistant asymmetric environments in water. The simplest design including the precise replacement of minimal functions was successfully achieved. These achievements should be valued as the first example of *exactly* rational design *not* based upon the enzymatic basement. It is highly expected that this results will indicate guidelines for an artificial design of enzyme-like catalysis in water.

---

[1] '*Enzyme Catalysis in Organic Synthesis*' ed. by K. Drauz, H. Waldmann, Wiley-VCH, Weinheim, **2002**.

[2] '*Enzymes in Industry*' 3 edn., Wiley-VCH, Weinheim, **2007**.

[3] A. M. Klibanov, *Science* **1983**, *219*, 722-727.

[4] a) M. T. Reetz, *Angew. Chem. Int. Ed.* **2001**, *40*, 284–310; b) G. Winter, A. R. Fersht, A. J. Wilkinson, M. Zoller, M. Smith, *Nature* **1982**, *299*, 756–758.

[5] a) A. Tramontano, K. D. Janda, R. A. Lerner, *Science* **1986**, *234*, 1566–1569; b) S. J. Pollack, J. W. Jacobs, P. G. Schultz, *Science* **1986**, *234*, 1570–1573.

[6] M. D. Toscano, K. J. Woycechowsky, D. Hilvert, *Angew. Chem. Int. Ed.*, **2008**, *46*, 4468-4470.

[7] First example of the use of the term, "artificial enzyme", see: R. Breslow, L. E. Overman, *J. Am. Chem. Soc.* **1970**, *92*, 1075.

[8] Racemic reaction, see: T. Darbre, C. Dubs, E. Rusanov, H. Stoeckli-Evans, *Eur. J. Inorg. Chem.* 2002, 3284-3291

[9] a) A. Matsuzawa, C. R. Opie, N. Kumagai, M. Shibasaki, *Chem. Eur. J.* **2014**, *20*, 68–71; b) N. Yoshikawa, Y. M. A. Yamada, J. Das, H. Sasai, M. Shibasaki, *J. Am. Chem. Soc.* **1999**, *121*, 4168–4178; c) Y. M. A. Yamada, N. Yoshikawa, H. Sasai, M. Shibasaki, *Angew. Chem. Int. Ed.* **1997**, *36*, 1871–1873.

[10] a) B. M. Trost, H. Ito, E. R. Silcoff, *J. Am. Chem. Soc.* **2001**, *123*, 3367–3368; b) B. M. Trost, E. R. Silcoff, H. Ito, *Org. Lett.* **2001**, *3*, 2497–2500; c) B. M. Trost, H. Ito, *J. Am. Chem. Soc.* **2000**, *122*, 12003–12004.

[11] a) S. Itoh, T. Tokunaga, M. Kurihara, S. Aoki, *Tetrahedron: Asymmetry* **2013**, *24*, 1583–1590; b) S. Itoh, T. Tokunaga, S. Sonoike, M. Kitamura, A. Yamano, S. Aoki, *Chem. Asian J.* **2013**, *8*, 2125–2135; c) S. Itoh, M. Kitamura, Y. Yamada, S. Aoki, *Chem. Eur. J.* **2009**, *15*, 10570–10584.

[12] J. Kofoed, T. Darbre, J. –L.l Reymond, *Org. Biomol. Chem.* **2006**, *4*, 3268–3281.

[13] S. Kobayashi, M. Kokubo, K. Kawasumi, T. Nagano, *Chem. Asian J.* **2010**, *5*, 490–492.

[14] J. Collot, J. Gradinaru, N. Humbert, M. Skander, A. Zocchi, T. R. Ward, *J. Am. Chem. Soc.* **2003**, *125*, 9030–9031.

[15] For instance, see: a) W. B. Motherwell, M. J. Bingham, Y. Six, *Tetrahedron* **2001**, *57*, 4663–4686; b) P. Tastan, E. U. Akkaya, *J. Mol. Catal. A: Chem.* **2000**, *157*, 261–263; c) R. Breslow, N. Nesnas, *Tetrahedron Lett.* **1999**, *40*, 3335–3338; d) R. Breslow, S. D. Dong, *Chem. Rev.* **1998**, *98*, 1997–2012.

[16] S. Sasaki, K. Koga, *Chem. Pharm. Bull.* **1989**, *37*, 912–919.

[17] Y. K. Agrawal, H. Bhatt, *Bioinorg. Chem. Appl.* **2004**, *2*, 237–274.

[18] Examples of enzyme mimics based on polymers, see: J. Matsui, I. A. Nicholls, I. Karube, K. Mosbach, *J. Org. Chem.* **1996**, *61*, 5414–5417.

[19] J. Bjerre, C. Rousseau, L. Marinescu, M. Bols, *Appl. Microbiol. Biotechnol.* **2008**, *81*, 1–11.

[20] O. Khersonsky et al, *J. Mol. Bio.*, 396, 1025-1042.

[21] Recent reports on asymmetric aldol reaction using organocatalysts, see: a) S. Bertelsen, K. A. Jørgensen, *Chem. Soc. Rev.* **2009**, *38*, 2178-2189; b) L. M. Geary, P. G. Hultin, *Tetrahedron: Asymmetry* **2009**, *20*, 131-173; c) S. G. Zlotin, A. S. Kucherenko, I. P. Beletskaya, *Russ. Chem. Rev.* **2009**, *78*, 737-784; d) J. N. Moorthy, S. Saha, *Eur. J. Org. Chem.* **2009**, 739-748; e) D. Almasi, D. A. Alonso, A. N. Balaguer, C. Nájera, *Adv. Synth. Catal.* **2009**, *351*, 1123-1131; f) B. Wang, G. Chen, L. Liu, W. Chang, J. Li, *Adv. Synth. Catal.* **2009**, *351*, 2441-2448; g) B. Wang, X. Liu, L. Liu, W. Chang, J. Li, *Eur. J. Org. Chem.* **2010**, 5951-5954; h) A. L. Fuentes de Arriba, L. Simón, C. Raposo, V. Alcázar, F. Sanz, F. M. Muñiz, J. R. Morán, *Org. Biomol. Chem.* **2010**, *8*, 2979-2985; i) N. Mase, C. F. Baras, III, *Org. Biomol. Chem.*, **2010**, *8*, 4043-4050.

[22] a) J. -L. Reymond, Y. Chen, *J. Org. Chem.* **1995**, *60*, 6970; b) J. Kofoed, T. Darbre, J. –L. Reymond, *Org. Biomol. Chem.* **2006**, *4*, 3268; c) D. Font, S. Sayalero, A. Bastero, C. Jimeno, M. A. Pericàs, *Org. Lett.* **2008**, *10*, 337-340.

[23] a) D. Veot, J. G. Veot, Biochemistry, John Wiley & Sons, Inc., Weinheim, **1990**; b) H. J. M. Gijsen, L. Qiao, W. Fitz, C. -H. Wong, *Chem. Rev.* **1996**, *96*, 443-473.

[24] a) A. H. Henseler, C. Ayats, M. A. Pericàs, *Adv. Synth. Catal.* **2014**, *356*, 1795–1802; b) N. Mase, C. F. Barbas III, *Org. Biomol. Chem.* **2010**, *8*, 4043–4050; c) S. Bertelsen, K. A. Jørgensen, *Chem. Soc. Rev.* **2009**, *38*, 2178–2189; d) D. Font, S. Sayalero, A. Bastero, C. Jimeno, M. A. Pericàs, *Org. Lett.* **2008**, *10*, 337–340; e) S. S. Chimni, D. Mahajan, *Tetrahedron: Asymmetry* **2006**, *17*, 2108–2119; f) J. –L. Reymond, Y. Chen, *J. Org. Chem.* **1995**, *60*, 6970–6979.

[25] a) J. Schmidt, C. Ehasz, M. Epperson, K. Klas, J. Wyatt, M. Hennig, M. Forconi, *Org. Biomol. Chem.* **2013**, *11*, 8419–8425; b) B. M. Trost, C. S. Brindle, *Chem. Soc. Rev.* **2010**, *39*, 1600-1632.

[26] For a review on a role of zinc ion, see; E. Kimura, E. Kikuta, *J. Biol. Inorg. Chem.* **2000**, *5*, 139-155.

[27] a) G. Schulz, M. Dreyer, *J. Mol. Biol.* **1996**, *259*, 458-466; b) B. S. Szwergold, K. Ugurbil, T. R. Brown, *Arch. Biochem. Biophys.* **1995**, *317*, 244-252; c) N. S. Bolm, S. Tetreault, R. Coulombe, J. Sygusch, *Nat. Struct. Biol.* **1996**, *3*, 856-862.

[28] D. Sinou, *Adv. Synth. Catal.* **2002**, *344*, 221-237.

[29] Class II aldolases have molecular weights of approximately 70 000; see: W. J. Rutter, T. Rajkumar, E. Penhoet, M. Kochman, *Ann. N. Y. Acad. Sci.* **1968**, *151*, 102–117.

[30] I. A. O'Neil, N. D. Miller, J. V. Barkley, C. M. R. Low, S. B. Kalindjian, *Synlett* **1995**, 617–618.

[31] The pH value is 3.55 (average of 10 measurements).

[32] The spectrum of Sc(OTf)$_3$-**L2** complex was invisible in D$_2$O.

[33] Reported ^{19}F NMR shift of Bi(OTf)$_3$: approximately 78 ppm, see: K. Komeyama, M. Miyagi, K. Takaki, *Heteroatom Chem.* **2008**, *19*, 644-648.

[34] Trifluoromethanesulfonic acid: δ (^{19}F) = −77.3.

[35] Representative examples, see: a) S. Kobayashi, T. Ogino, H. Shimizu, S. Ishikawa, T. Hamada, K. Manabe, *Org. Lett.* **2005**, *7*, 4729–4731; b) S. Kobayashi, S. Nagayama, T. Busujima, *J. Am. Chem. Soc.* **1998**, *120*, 8287–8288.

[36] Recently X-ray crystallography on chiral Sc complex with N-oxide backbone derived from L-proline was reported, see: Y. Liu, D. Shang, X. Zhou, X. Liu, X. Feng, *Chem. Eur. J.* **2009**, *15*, 2055-2058.

[37] Several trials of organocatalysts in pure water have been reported, see: a) J. Paradowska, M. Stodulski, J. Mlynarski, *Angew. Chem. Int. Ed.* **2009**, *48*, 2–18; b) N. Mase, Y. Nakai, N. Ohara, *J. Am. Chem. Soc.* **2006**, *128*, 734–735; c) Y. Hayashi, T. Sumiya, J. Takahashi, *Angew. Chem. Int. Ed.* **2006**, *45*, 958–961; d) H. Torii, M. Nakadai, K. Ishihara, *Angew. Chem. Int. Ed.* **2004**, *43*, 1983–1986.

[38] For reported catalytic turnover number (CTN = yield/equivalent of catalyst) values for direct-type aldol reactions without any directing group, see: 4.8 (chiral organocatalyst in water/DMF = 8/92, ref. 24a), 9.9 (chiral organocatalytic resin, ref. 24d), 11.1 (chiral metal catalyst with 16 mol% of water, ref. 9b and 9c), 16.8 (chiral dimetallic catalyst under anhydrous conditions, ref. 10b and 10c), 19.2 (chiral metal catalyst with solvent amount of a substrate in NMP–MeOH cosolvent, ref. 11a-c).

[39] B. List, R. A. Lerner, C. F. Barbas III, *J. Am. Chem. Soc.* **2000**, *122*, 2395–2396.

[40] The CTN value reached more than 50 even at 25 °C in the presence of 1 mol% of catalyst, although this is an unoptimized result. For comparison with reported values, see ref. 32.

[41] Asymmetric hydroxymethylation of ketones were reported only in organic solvent: (a) in DMSO: J. Casas, H. Sundén, A. Córdova, *Tetrahedron Lett.* **2004**, *45*, 6117-6119; (b) in DCM: N. Mase, A. Inoue, M. Nishio, K. Takabe, *Bioorg. Med. Chem. Lett.* **2009**, *19*, 3955-3958.

[42] Geneviève, L. (2009), Dynamics and Inhibition of Class II Fructose 1,6-bisphosphate Aldolase, doctoral dissertation, the University of Waterloo, Ontario, Canada.

[43] T. Imamoto, *Lanthanides in Organic Synthesis*, Academic Press, London, **1994**.

[44] Among the several linear plots of the Michaelis–Menten equation, this method is preferable on statistical grounds because of smaller and more consistent errors across the plot.

[45] M. V. Putz, A. M. Lacrămă, V. Ostafe, *J. Optoelectron. Adv. Mater.* **2007**, *9*, 2910–2916.

[46] a) T. Kitanosono, S. Kobayashi, *Chem. Rec.* **2014**, *14*, 130–143; b) C. Mukherjee, T. Kitanosono, S. Kobayashi, *Chem. Asian J.* **2011**, *6*, 2308–2311.

[47] Calculated standard deviation is 0.00180.

Chapter 3 : Asymmetric Boron Conjugate Additions in Water

Section 3.1   Regioselectivity Switch Induced by Water in Asymmetric β-Borylation

3.1-1   Introduction

Enantioenriched α-chiral boron derivatives are an important class of compounds due to their versatile applicability.   Their C–B linkage can be transferred into C–O, C–N, as well as C–C bonds through 1,2-migration of intermediary ate complexes with appropriate nucleophiles, retaining stereogenic centers.[1] For instance, chiral boronates undergo 1,2-homologations with carbon nucleophiles to give chiral C-C bonds through asymmetric lithiation and borylation (Scheme 1).[2] The combination with Pd(II)-mediated 1,3-borotropic rearrangement enabled a three-carbon homologation of pinacol boronic esters to afford di- or trisubstituted allylic boronic esters with high *E* selectivity (Scheme 2).[3]

Scheme 1. Reaction of boronic ester with enantioenriched lithiated carbamates

Scheme 2. One-pot Matteson homologation/alkylation/1,3-rearrangement of boronic esters.

The Suzuki-Miyaura cross coupling reaction has recently been demonstrated with retention of stereochemistry by several groups. Among them, Molanders' group reported that the enantioenriched potassium b-trifluoroboratoamides were successfully cross-coupled with an array of aryl and heteroaryl chlorides or bromides with complete stereochemical fidelity as the transmetalation proceeds through an S_E2 mechanism *via* an open transition state (Scheme 3).[4] The major limitation of these reactions was unwanted side reactions that compete with the much slower transmetallation and reductive elimination steps associated with the more-hindered organometallic intermediates.[5] The addition of an electron-rich aryl lithium reagent to the stereodefined secondary boronic esters gave aryl-coupled product stereospecifically through a 1,2-migration and the subsequent elimination (Scheme 4).[6]
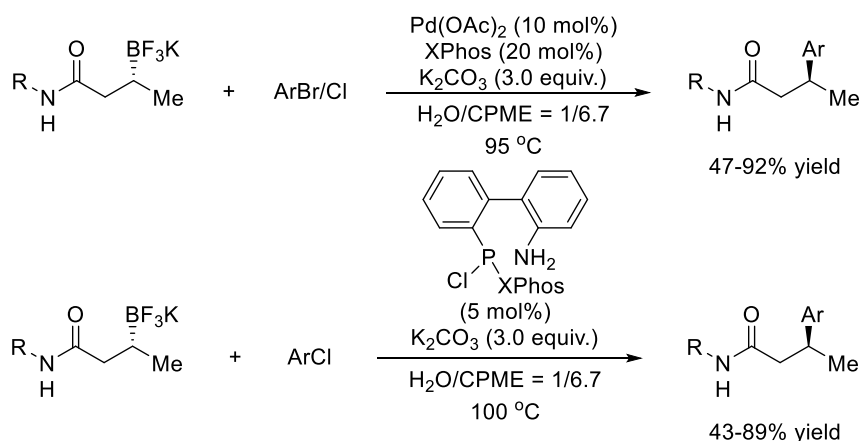
Shceme 3. Cross-coupling reactions using configurationally stable, optically active secondary alkyl nucleophiles.
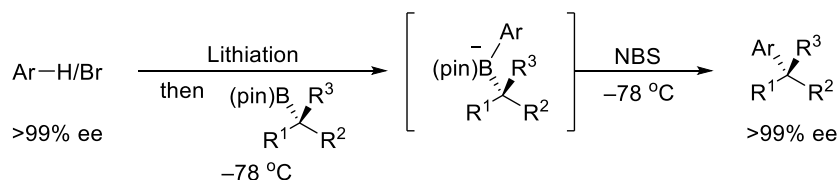
Scheme 4. Stereospecific cross-coupling of boronic esters.

In addition to their chemical importance as versatile intermediates to make complex molecules, optically active organoboranes have been directly targeted for pharmaceutical applications. Boronic acids represent an exciting class of enzyme inhibitors such as serine

proteases.[7] Boronic acids are not only strong Lewis acids, but they are also capable of generating reversible covalent complexes with sugars,[8] amino acids and hydroxamic acids. These interactions are recently applied to a molecular recognition of saccharides for the fluorescent detection or selective transport of saccharides across membranes. The appropriate substitution on empty *p* orbital of boron would lead to swift conversion from a neutral and triagonal planar sp^2 boron to an anionic tetrahedral sp^3 boron under physiologic conditions. The first successful proteasome inhibitor and the first boron-containing pharmaceutical approved for the treatment of newly diagnosed, relapsed/refractory multiple myeloma and mantle cell lymphoma, is bortezomib (Velcade[TM]).[9] Bortezomib, which reversibly inhibits the chymotrypsin-like activity at the β5-subunit of proteasome (PSMB5), has marked efficacy against multiple myeloma and several non-Hodgkin's lymphoma subtypes and has a potential therapeutic role against other malignancy diseases through the formation of tetrahedral adduct (Scheme 5).[10]
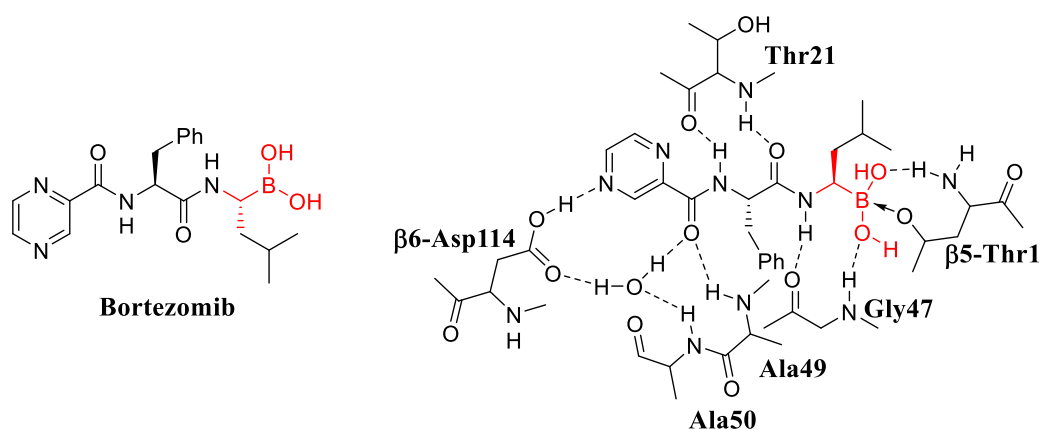
Scheme 5. Interaction model of bortezomib with active site of β5 subunit of proteasome.

In order to overcome the drawbacks of bortezomib, including limited activity in solid tumors, side effects such as the emergence of reversible peripheral neuropathy and the invasive intravenous route of administration, extensive researches have oriented to the development of second-generation proteasome inhibitors such as delanzomib and ixazomib (Scheme 6). Delanzomib is a P2 threonine boronic acid and adanced into Phase I clinical trials as advanced solid tumors or non-Hodgkin's lymphoma.[11] Ixazomib is a reversible inhibitor of primarily the chymotrypsin-like activity of the 20S proteasome and orally available.[12] In contrast to bortezomib, it has a shorter dissociation half-time and it demonstrated greater tissue penetration in the preclinical studies.[13]
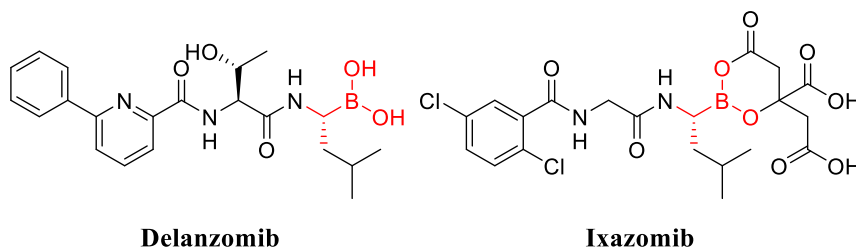
Scheme 6. Bortezomib derivatives.

The progressive exploration toward therapeutic applications is now producing several boronic acid-containing therapeutic agents (Scheme 7). Since B–O bonds have higher dissociation energy than C–O bonds, the boronic acid-enzyme adduct may more closely mimic the transition state of the natural substrate than the corresponding adduct of aldehyde inhibitor. The extensive structure-activity relationship has identified the boroproline derivatives as orally bioavailable selective dipeptidyl peptidase IV (DPP4) inhibitor.[14] Talabostat, the first clinical in hibitor of FAP-a enzymatic activity in Phase II study, stimulates the T-cell-independent antitumor activity of macrophages, neutrophils and natural killer cells, and it also enhances the tumor-specific T-cell immunity by increasing the production of cytokines and chemokines.[15] Dutogliptin is expected as a new antidiabetic agent that has a high solubility in water (currently in Phase III).[7d, 16] The boron-based compound TRI50c, in Phase III clinical trials as anticoagulants,[7c] proved to be a highly potent (K_i = 22 nM) and selective competitive inhibitor of thrombin with high efficacy in animal models of venous and arterial thrombosis and minimal effect on bleeding.[17] Similarly, an exploration of the boceprevir (Victrelis) template resulted in the discovery of boronic acid, which demonstrated improved activity in the picomolar range (K_i = 200 pM).[18]

TRI50c

Talabostat

Dutogliptin

Boceprevir analog
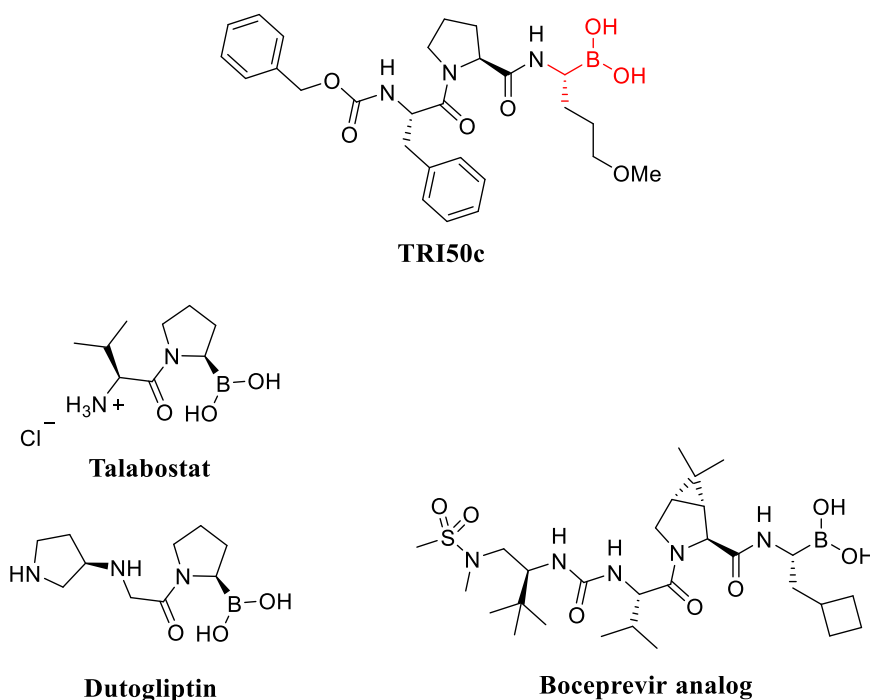
Scheme 7. Boronic acid-containing therapeutic agents.

The chemistry of boron flourished in the 20th century through the advent of an array of reactions, which was characterized by the 1997 and 2010 Nobel Prize for Chemistry to Herbert C. Brown[19] and Akira Suzuki,[20] respectively. Since then, a plethora of approaches have evolved toward a high level of stereocontrol and a wide range of substrate scope. Matter *et al.* have first demonstrated addition reactions of diboron reagents to electron-deficient olefins catalyzed by rhodium catalyst.[21,22] Hydroboration with HB(cat) or 9-borabicyclononane delivered the boron enolates, whereas the borylation did the 1,4-borylated product. The scope of metal catalysts for

β-borylation using the diboron reagents extended to Pt,[23] Ag,[24] Ni,[25] Zn,[26] Pd,[25a,27] Fe[28] and non-metal catalysts[29,30].   Hoveyda *et al.* developed the first non-metallic *N*-heterocyclic carbenes (NHC) catalyst for the β-borylation of cyclic and acyclic enones (Scheme 8).[29] They postulated an acid-base interaction between the NHC and the Lewis acidic diboron reagent could facilitate the reaction.   Besides NHC catalysts combined with a strong base NaO*t*Bu (45-98%), the catalytic activity of phosphine oxide is also noteworthy (50%).[31]
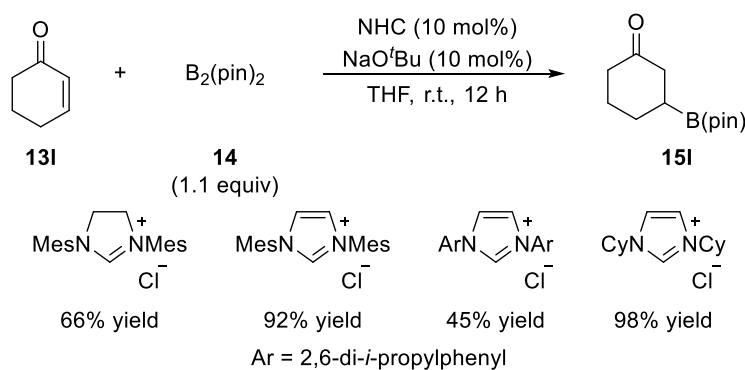
Scheme 8. Non-metal-catalyzed β-borylations.

A borylation of alkenes is often based upon *in situ* formation of an isolatable borylcopper(I) species via σ-bond metathesis between the diboron reagents and Cu(I) salts. Concomitantly, Hosomi *et al.* (Scheme 9)[32] and Miyaura *et al.* (Scheme 10)[33] reported a Cu(I)-mediated conjugate borylation using the diboron reagent in 2000, which has led to a stunning progress toward the creaction of stereogenic centers containing C–B bond.   Hosomi *et al.* showed that the addition of tri-*n*-butylphosphine was essential in Cu(I)-catalyzed system.   It is to be noted that phosphine alone had the ability to facilitate the reaction progress, albeit in low yield (7%). Miyaura *et al.* presented the applicability of Cu(I) protocol for a wide range of substrates in the presence of stoichiometric amounts of Cu(I) salt and demonstrated the isolation of a borylcopper(I) species acting as a nucleophilic boron source.   The insufficience of the catalytic activity in their systems was improved by Yun *et al.* through the use of alcohol additives and xanthene-type biphosphine ligands.[34]
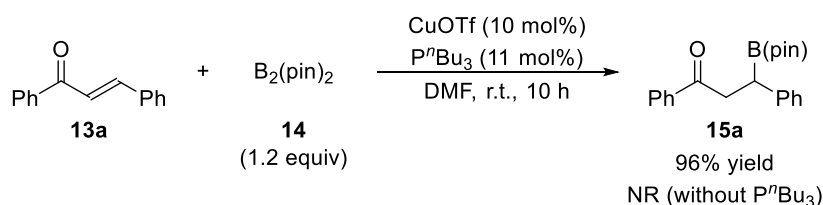
Scheme 9. The first example of Cu(I)-catalyzed boron conjugate additions
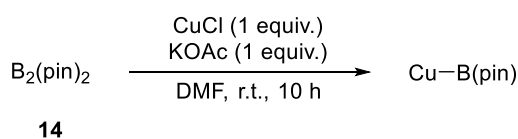
Scheme 10. Evidence for a nucleophilic borylcopper(I) species

Enantioselective boron conjugate addition to α,β-unsaturated carbonyl and related compounds provides one of the most efficient routes to chiral organoboron compounds and an incremental attraction toward enantioriched organoboron compounds led to emergence of a facile and straightforward methodology.[35] Yun *et al.* applied their optimized Cu(I)-based system to a chiral induction for asymmetric boron conjugate addition to α,β-unsaturated nitrile using Josiphos ligand (Scheme 11).[34b]
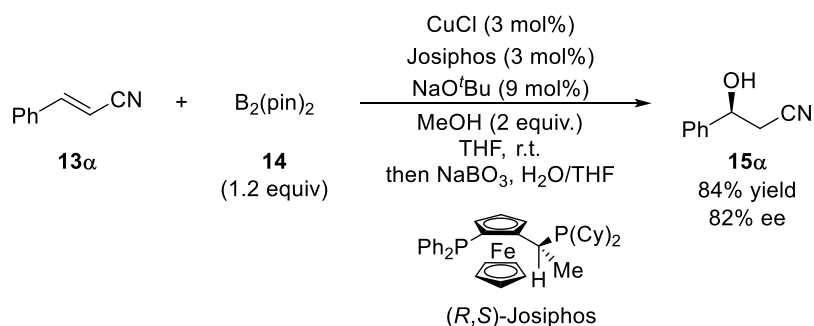
Scheme 11. Enantioselective β-borylation of cinnamonitrile **13α**.

The scope of enantioselective Cu(I) protocol with the addition of strong bases, alcohol additives and biphosphine ligands (**L29** or Mandyphos) was then expanded to a series of α,β-unsaturated esters and nitriles with high enantioselectivity.[36] The β-substituents mostly did not have a dominant effect on the enantioselection, but the introduction of electron-withdrawing groups resulted in a little drop in enantioselectivity. The catalyst composed of Cu(I) salt with biphosphine ligands was applicable to asymmetric boron conjugate additions with acyclic α,β-unsaturated amides[37] and acyclic α,β-unsaturated ketones[38], albeit a limited substrate scope (Scheme 12).
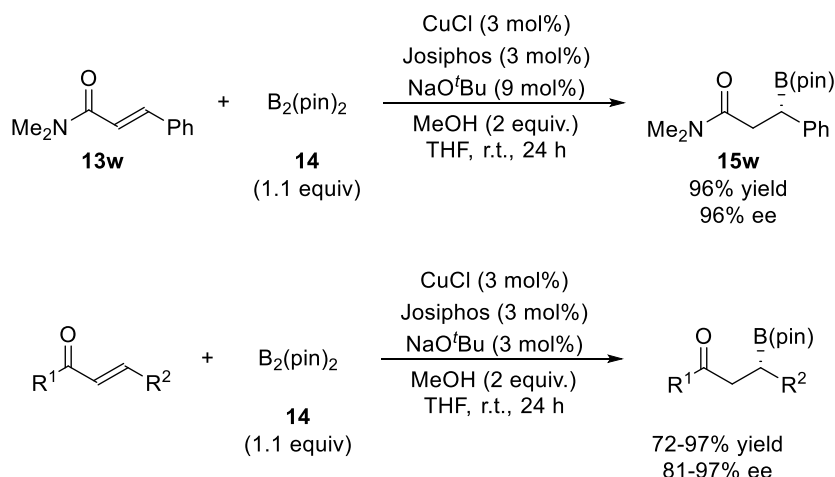
Scheme 12. Enantioselective β-borylation of N,N-dimethylcinnamylamine **13w** (above) and α,β-unsaturated ketones (below)

Yun *et al.* also developed a catalyst system for enantioselective conjugate addition with acyclic β,β-disubstituted α,β-unsaturated esters to construct chiral tertiary organoboronic esters (Scheme 13).[39]
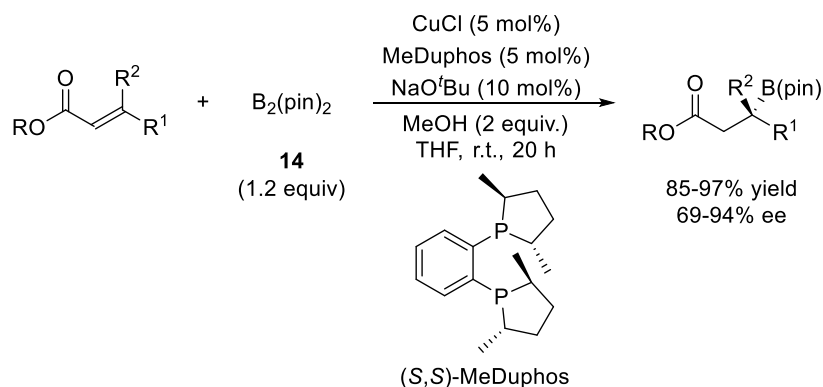
Scheme 13. Enantioselective β-borylation of β,β-disubstituted α,β-unsaturated esters.

The asymmetric reactions of various β-substituted cyclic α,β-unsaturated ketones were developed by Shibasaki *et al* (Scheme 14).[40] Their optimized conditions did not require alcohol additives. A modifided catalyst system using ligands bearing 1,2-diphenylethylenediamine skeleton could catalyze asymmetric boron conjugate addition with acyclic α,β-unsaturated ketones.[41] The boron enolate as an intermediate could be reacted with electrophiles (Scheme 15).[40] The N,P-type ligand quinap was also examined in the reaction of crotonates by Fernández's group (50-79% ee).[42]
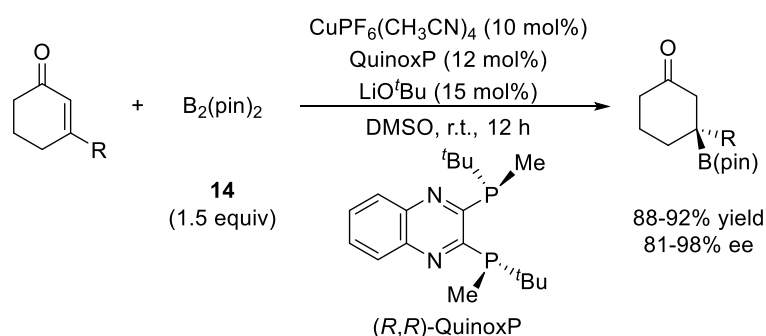
Scheme 14. Cu(I)-catalyzed asymmetric β-borylation to generate β-tetrasubstituted carbon
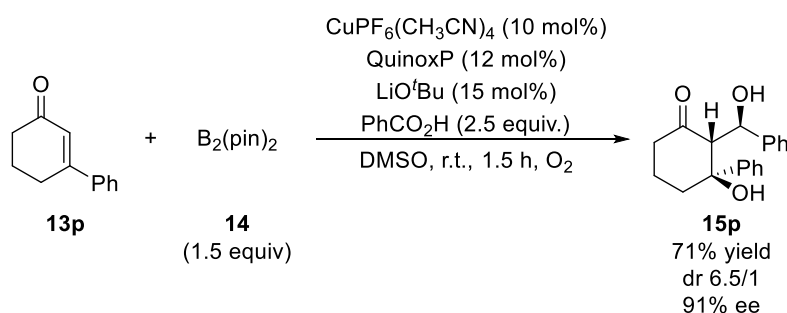
Scheme 15. Tandem conjugated addition/aldol reaction with benzaldehyde.

In the meanwhile, the chemistry of organocopper(I) complexes supported by NHC ligands was merged with a borylcopper(I) complex in 2005, leading to the formation of β-boroalkyl complexes *via* alkene insertion.[43] Chiral Cu(I)-based NHC complexes were then examined in enantioselective β-borylation, albeit with low enantioselectivity.[44] The C_1-symmetric NHCs generally outperformed their C_2-symmetric analogues in terms of a chiral induction.   The potential of Cu(I)-based NHC complexes was successfully demonstrated by Hoveyda *et al.* to generate quaternary stereogenic centers in boron conjugate additions (Scheme 16).[45] In the absence of a protic additive, the corresponding boron enolate was obtained as an intermediate.
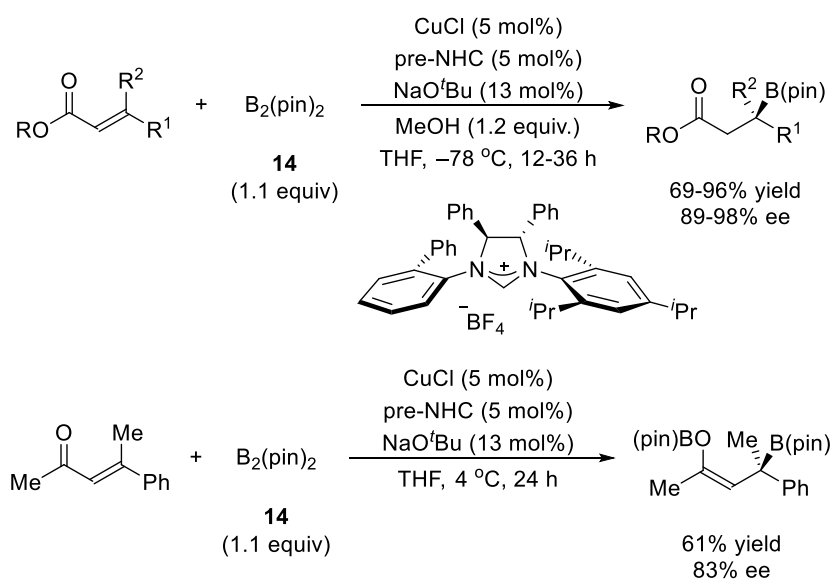
Scheme 16. NHC-Cu(I)-catalyzed enantioselective β-borylation of β,β-disubstituted α,β-unsaturated esters.

Hong *et al.* reported the structural modification of NHC precursor for asymmetric α,β-unsaturated *N,N*-dialkylated amides (Scheme 17).[46] Strange to say, the conversions and enantioselectivities decreased when *Z* isomer of α,β-unsaturated amide was used or when the sterically less congested diboron reagent was used.
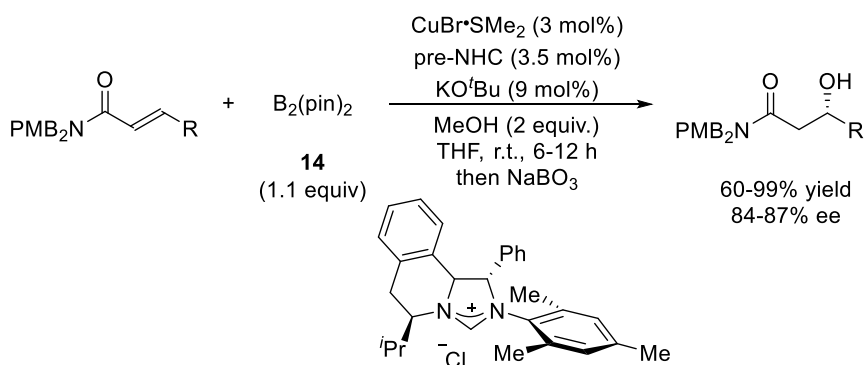
Scheme 17. NHC-Cu(I)-catalyzed enantioselective β-borylation of α,β-unsaturated amides.

In contrast to aforementioned 5-membered NHC rings, the advamtages of a 6-membered NHC ring stem from the change in both steric and electronic properties along with the increase in ring size.   The increase in the N–C–N bond angle would have a steric influence on the carbine-metal bond, providing a more restrictive chiral pocket constructed with a blocking group on one side.   Electron-donating ability directly correlates to a nucleophilicity of NHC, which is corresponding to its IR strectching.[47] The successful application of 6-membered NHC-Cu(I) catalyst was demonstrated by McQuade *et al.* (Scheme 18).[48] The superb activity of their catalyst was noteworthy, showing 10,000 catalytic turnover numbers (TONs) at 0.01 mol% of catalyst, the highest value at that time.   Subsequently, a 6-membered NHC catalyst bearing chiral 3,4-dihydroquinazolinium core was examined in asymmetric boron conjugate addition to α,β-unsaturated esters at 1 mol% catalyst loading.[49]
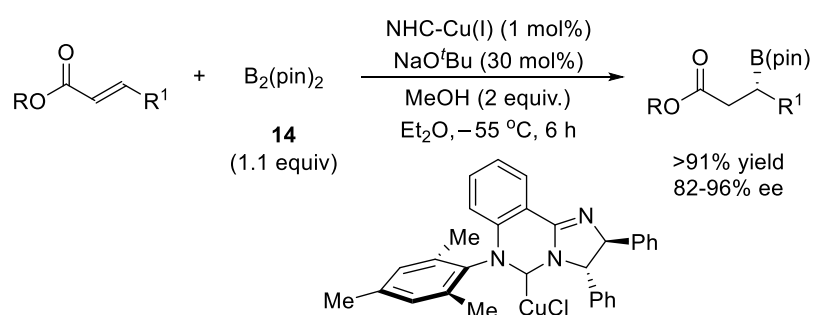
Scheme 18. NHC-Cu(I)-catalyzed enantioselective β-borylation of α,β-unsaturated esters.

Sawamura *et al.* designed a novel chiral imidazolinium zwitterion bearing a *m*-terphenyl-based phosphate moiety as an anionic coordination site (Scheme 19).[50] The ^{31}P NMR spectrum of a rhodium complex indicated that phosphiate moiety coordinated to metal center through a negatively charged O atom to form a *C,O*-chelate complex.
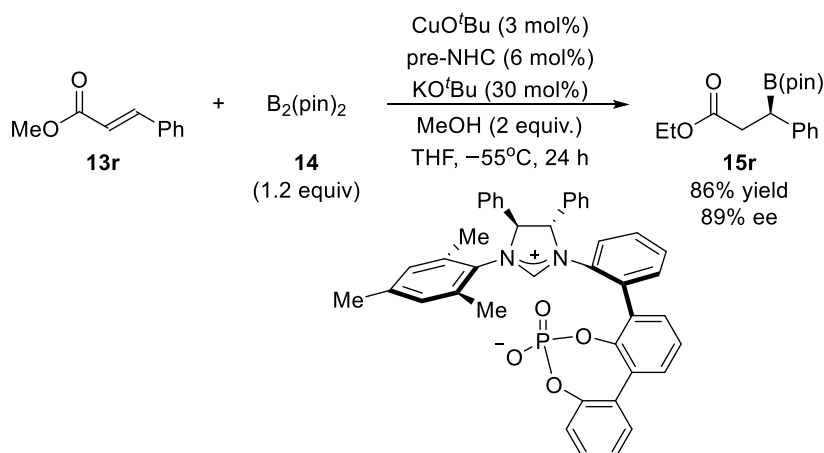
Scheme 19. Design of zwitterionic NHC ligand.

Since the first synthesis and application of *pseudo-ortho*-disubstituted [2,2]paracyclophane bidentate oxazoline-carbene ligands,[51] they have been applied to several asymmetric reactions.   Among them, the combination with Cu_2O solid was successfully applied to asymmetric

β-borylation of α,β-unsaturated aromatic ketones,[52] *N*-acyloxazolidinones[53] and α,β-unsaturated esters[54] (Scheme 20). The catalytic reactions are characterized by excellent enantioselectivity and reactivity.
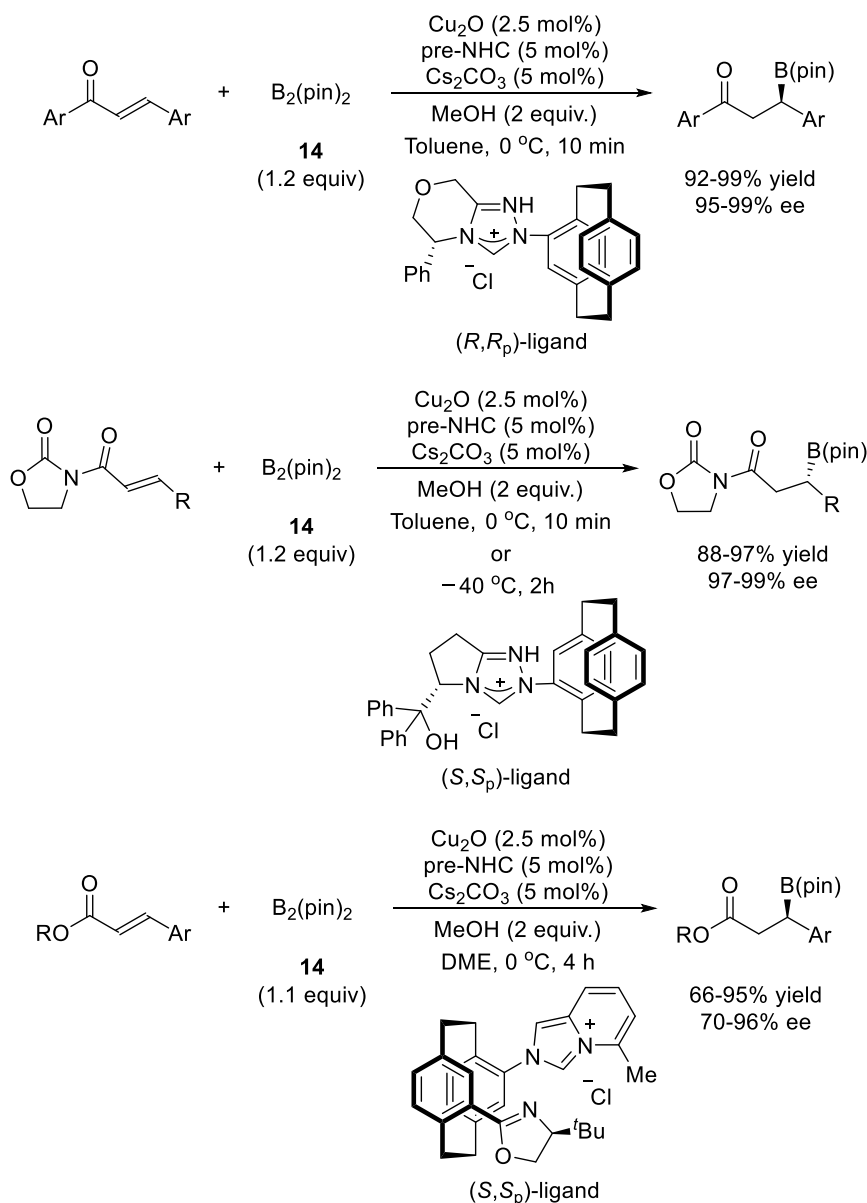
Scheme 20. NHC-Cu(I)-catalyzed asymmetric β-borylation of α,β-unsaturated aromatic ketones (above),[52] *N*-acyloxazolidinones (middle)[53] and α,β-unsaturated esters (below)[54].

It was also revealed that chiral free NHCs (Scheme 21)[55] or tertiary phosphorous organocatalysts[56] provided effective alternatives to the Cu(I)-based complexes as Lewis base catalysts to promote enantioselective β-borylations. The NHC would interact with a boron atom to make the resultant elongated B–B bond polarize, which are supported by quantum simulation and ^{1}H or ^{11}B NMR studies.[57]
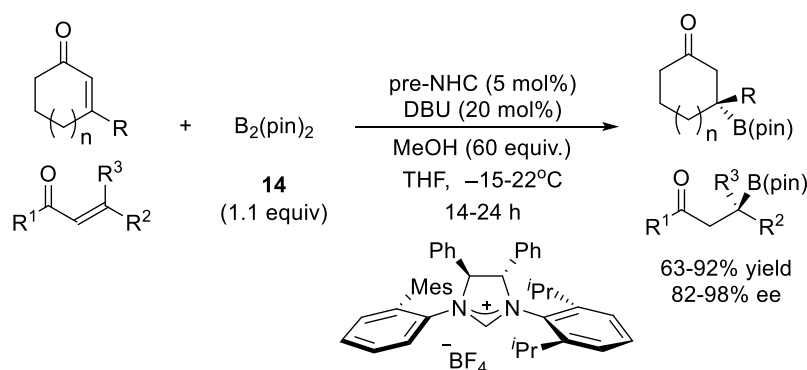
Scheme 21. NHC-catalyzed asymmetric β-borylation of α,β-unsaturated ketones.

The use of nickel (0) or palladium (0) combined with Taniaphos or Josiphos ligands and cesium carbonate resulted in a comparable enantioselection (Scheme 22).[58] The catalytic cycle was assumed to commence with η^2-coordination of the olefin to Ni(0) or with Lewis pair formation of the carbonyl moiety and a boron atom, followed by the oxidative addition and thereby generating an η^2-coordinated Ni(II) complex. The complex would undergo the cleavage of B–B bond to form Ni(II)-borate complex and reductive elimination with concomitant C–B bond would close the cycle.
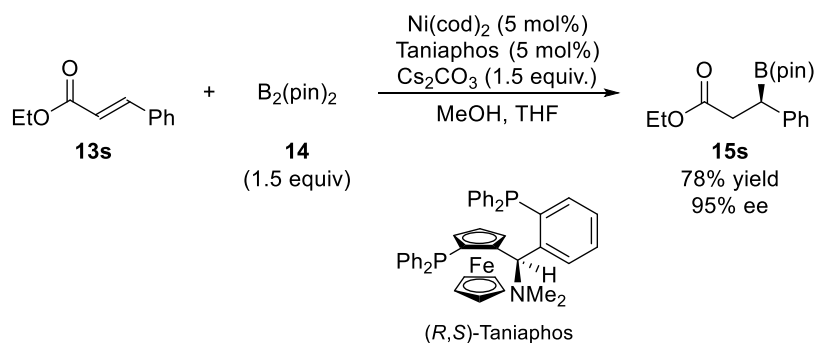
Scheme 22. Nickel(0)-catalyzed asymmetric β-borylation of α,β-unsaturated esters.

The β-borylation in the presence of chiral rhodium[bis(oxazolinyl)phenyl] catalysts underwent a direct production of rhodium enolate species and the subsequent hydrolysis, exhibiting high catalytic activity and enantioselectivtity (Scheme 23).[59]
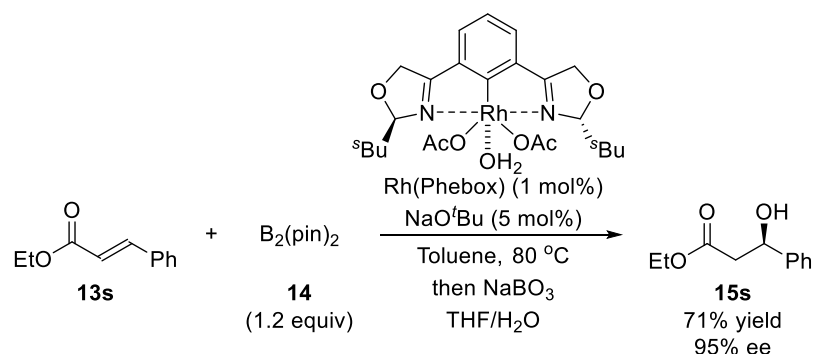
Scheme 23. Rhodium-catalyzed asymmetric β-borylation of α,β-unsaturated esters.

Thus, enantioselective boron conjugate additions to α,β-unsaturated carbonyl and related compounds have also been reported.[60] Recently, alternatives to sp^2-hybridized organoboron compounds such as *N*-methyliminodiacetic acid (MIDA) boronate,[61] cyclic triollborate[62] and potassium trifluoroboronate[63] were extensively studied as well. Contrary to many other boron surrogates, MIDA boronates adapt a distorted tetrahedral structure, leading to their air-stable nature. In addition to lengthened B–C bond, the B–O bond is elongated significantly and is destabilized. Santos *et al.* developed a sp^2-sp^3 hybridized diboron reagent on the basis of a preactivated form of borylcopper species (Scheme 24).[64] Its superb reactivity toward boron conjugate addition was successfully demonstrated without addition of phosphine or inorganic bases and sp^2-boron was selectively transferred to the corresponding β-borylated product in the presence of 5 mol% of CuCl (up to 96% yield). The pyramidal coordinated boron atom was identified by X-ray crystallography of the enantiopure (*R*,*R*)-pinacolato diisopropanolaminato diboron (PDIPA diboron).[65] The scope of the reaction was expanded even to α,β-unsaturated aldehydes and substrates bearing other functional groups.
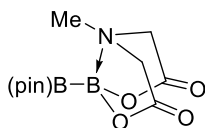
Scheme 24. Structure of pinacolato diisopropanolaminato diboron.

On the other hand, the replacement of diboron reagent with tetrahydroxydiboron $B_2(OH)_4$ allows the direct installation of boronic acids, simplifying purification and providing access to a variety of boronate derivatives through a single intermediate. Molander *et al.* revealed that $B_2(OH)_4$ could undergo conjugate additions to acyclic or cyclic α,β-unsaturated ketones, esters and amides in a racemic manner (71-98% yield, Scheme 25).[66] Adding 30 mol% of NaO^{t}Bu enabled a reduction in the amount of CuCl and CyJohnPhos to 2 mol% while retaining efficient conversions. High throughput experimentation (HTE) disclosed the optimal reaction conditions toward asymmetric protocol.[4a]

(2R,5R)-1-{[(2R,5R)-2,5-diphenylpyrrolidin-1-yl]methylene}-2,5-diphenylpyrrolidinium tetrafluoroborate
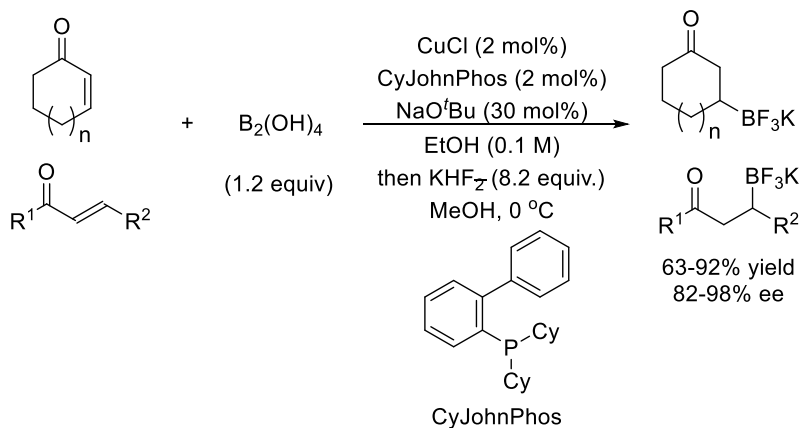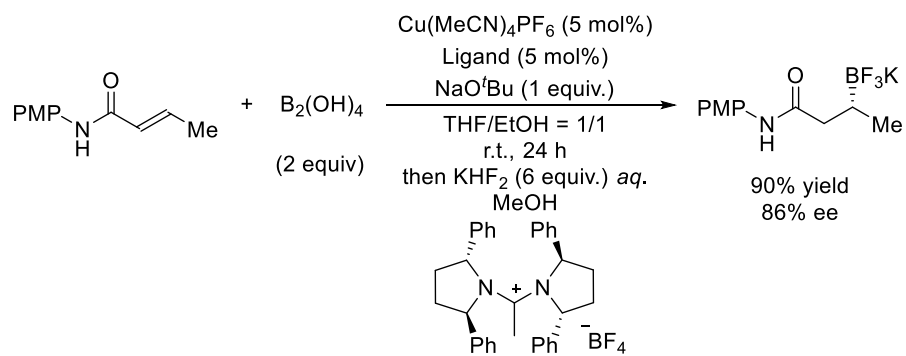
Scheme 25. Cu(I)-catalyzed conjugate addition of tetrahydroxydiboron.

3.1-2 Preliminary Findings

The foregoing subsection described the catalytic synthetic protocols for enantioenriched organoboron compounds. Notably, Cu(I) catalysis appears to be the most widely explored, because of its alluring cost advantage and its reliability as a soft Lewis acid. Nevertheless, well-established Cu(I) protocol entailed the use of a strong base to accelerate the reactions.[67] Copper has a wide range of oxidation state (0, I, II, III and IV) as a transition element. Oxidation states III and IV exist only in a specific environment, whereas I and II readily form stable complexes yielding a variety of coordination compounds.[68] That is why Cu(I) and Cu(II) have been incorporated into multifarious organic reactions as catalysts.[69] Since Cu(I) is much softer than Cu(II), Cu(I) catalysis is highly liable for couplings with sp^2 carbons represented by conjugate additions through d-π interaction between them. Despite a number of Cu(I)-based protocols of asymmetric β-borylations, high yields are only ensured by the addition of strong base such as *tert*-butoxides. In addition, the reaction often entails low temperature and the use of expensive phosphine ligands which match with each substrate for more precise stereocontrol. Due to the nature of Cu(I) toward disproportionation and the use of air-sensitive phosphine ligands, this chemistry has been cultivated in anhydrous organic solvent and under inert atmosphere. The assumed catalytic cycle commences with insertion of *in situ* generated Cu-B bond into C-C double bond, which is activated by the coordination of a base to boron.[33b] Although the formed intermediate is in equilibrium between *O*-enolate and *C*-enolate tautomers, a preference for *C*-enolate over *O*-enolate is generally accepted.[70] The cleavage of *O*-enolate is almost barrierless, whereas that of *C*-enolate is energetically unfavorable. In Cu(I) chemistry, it is believed that methanol facilitates the subsequent liberation of the borylated product through alcoholysis along with the formation of a reactive Cu-OMe complex (Scheme 26).[71] A protonation step where Cu(I)-enolate intermediate is quenched by methanol is generally considered to be a rate-determining step.
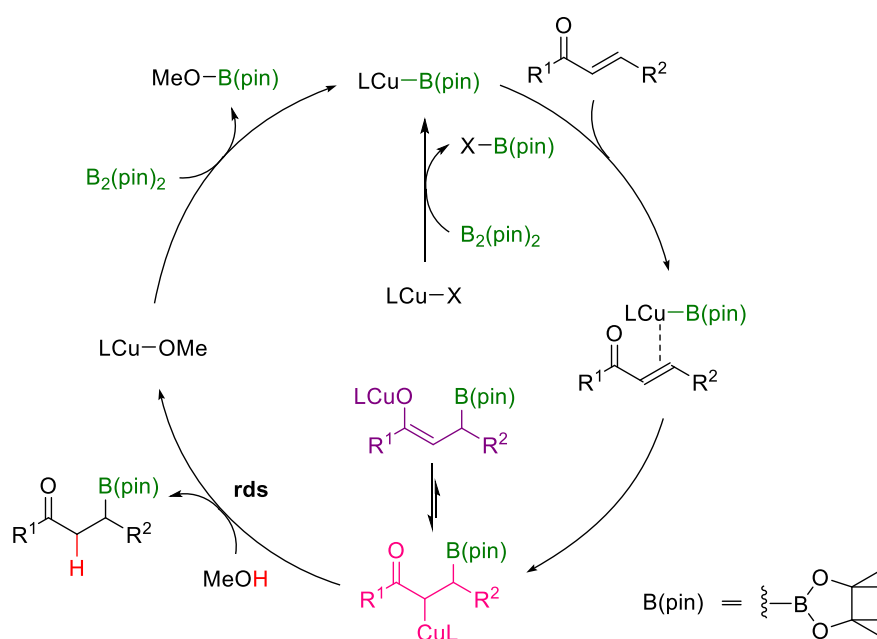
Scheme 26. Accepted mechanism of Cu(I) catalysis for β-borylation.

On the other hand, metal-mediated transformation of C-B bond into C-C bond has been cultivated well in aqueous environments. The preliminary report on zinc fluoride-chiral diamine complex that catalyzes allylation of hydrazonoesters in aqueous media[72] was expanded to the asymmetric α-selective allylation of aldehydes catalyzed by chiral $Zn(OH)_2$ complex.[73] The proposed mechanism involves the generation of organozincate through the exchange processes from B to Zn which is a key step to promote the reactions. In the reaction of allenylboronate with hydrazonoester in aqueous media, divergent reactivity was displayed through a formal α-addition under either $Cu(OH)_2$- or $Bi(OH)_3$-based conditions that resulted in the predominant formation of propargylated and allenylated product, respectively.[74] Allenylboronate would undergo a B to Bi transmetalation, whereas $Cu(OH)_2$ would function as a Lewis acid to activate both the boronate and hydrazonoester. It is noteworthy that $Cu(OH)_2$-catalyzed reaction completed within 5 min. In order to support transmetalation hypothesis between B and Bi, $Bi(OH)_3$-catalyzed homocoupling reaction was demonstrated in aqueous media (Scheme 27).

$$PhB(OH)_2 \xrightarrow[\substack{H_2O/CH_3CN = 1/4 \\ 80\ ^\circ C,\ 48\ h}]{\substack{Bi(OH)_3\ (10\ mol\%) \\ 2,9\text{-}Me_2\text{-}1,10\text{-}Phen\ (12\ mol\%)}} Ph-Ph$$

30% yield
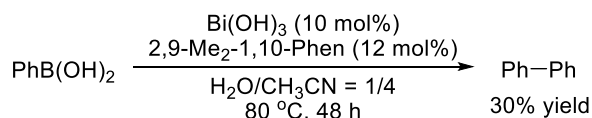
Scheme 27. $Bi(OH)_3$-catalyzed homocoupling reaction of phenylboronic acid in aqueous media (unreported result).

As shown in Chapter 1, ytterbium salts with more-nucleophilic counteranions such as Cl^-, AcO^-, NO_3^- and SO_4^{2-} have lower catalytic activity than corresponding salts with less-nucleophilic counteranions such as ^-OTf and $^-ClO_4$ in Mukaiyama aldol reactions in aqueous media.[75] In contrast, addition reactions of allylboronates and allenylboronates with aldehydes and acylhydrazones performed in an aqueous environment was disclosed to prefer much more nucleophilic counteranions such as F^- and OH^- (*vide infra*). It was also revealed that water was highly responsible for the catalytic activity of metal hydroxides toward C–B bond cleavage. These successful transformations of boron reagents by metal hydroxides in aqueous environments invoked the application to the appropriate activation of diboron reagent toward C-B bond forming process with higher catalytic turnover than ever before. With the motivation in mind, the reaction between chalcone **13a** and $B_2(pin)_2$ **14a** was carried out in water (Table 1). Metal hydroxides themselves did not have any catalytic activity toward β-borylation presumably due to their insolubility in water. Nevertheless, the reaction proceeded smoothly in the coexistence of dibenzylamine (entries 1-3). The exertion of catalytic performance by metal hydroxides were confirmed by inactivity of dibenzylamine as a catalyst (entry 4). In marked contrast to dibenzylamine, pyridine did not assist the catalytic activity of metal hydroxides (entry 5). The reaction was then extended to preparation of optically active β-borylated product with bidentate-type chiral *N,N*- ligands (entries 6-8). It was disclosed that $Cu(OH)_2$-**L1** complex showed superior performance, resulting in the formation of desired β-borylated product **15a** in high yield with high enantioselectivity. The enantiopure β-borylated product **15a** was probed to be converted into β-hydroxy ketone **16a** quantitatively or β-amino ketone **17a** *via* subsequent oxidation or a substitution reaction (Scheme 28).

Table 1. Initial screening for boron conjugate addition in water.

Entry	M(OH)$_n$	Additive	Yield (%)	Ee (%)[b]
1	Cu(OH)$_2$	DBA[b]	88	–
2	Zn(OH)$_2$	DBA[b]	64	–
3	Bi(OH)$_3$	DBA[b]	92	–
4	–	DBA[b]	NR	–
5	Cu(OH)$_2$ or Zn(OH)$_2$ or Bi(OH)$_3$	Pyridine	NR	–
6	Cu(OH)$_2$	**L30**	79	36
7	Cu(OH)$_2$	**L31**	80	37
8	Cu(OH)$_2$	**L1**	83	81

[a] Determined by HPLC analysis.   [b] Dibenzylamine.

L30   **L31**
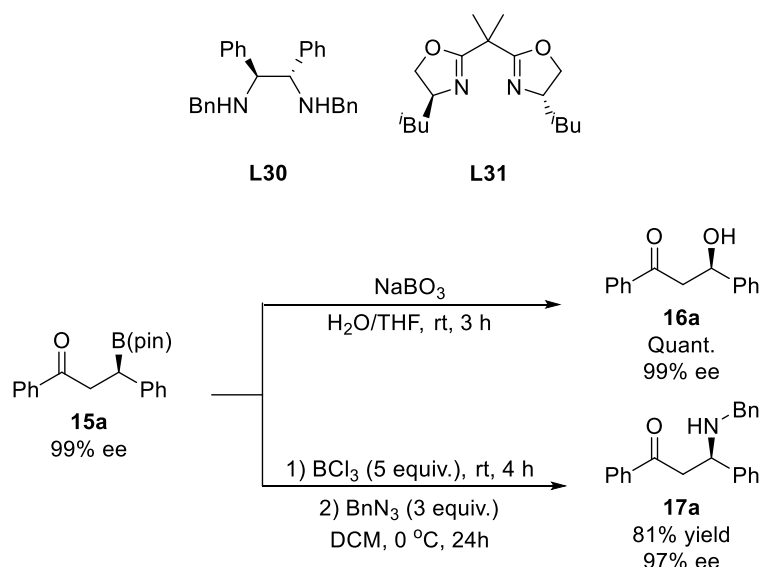
Scheme 28. Quantitative transformation of β-borylated product **15a**.

Various metal hydroxides, oxides and oxyhydroxides were thus screened in the reaction between chalcone **13a** and B$_2$(pin)$_2$ **14a** together with 1.2 equivalent of **L1** in water (Table 2).   It should be noted that both substrates, a given metal, chiral ligand **L1** are all insoluble in water and **14a** can undergo the attack by water to decompose into (pin)B–B(OH)$_2$, and successively into boronic acid.   Despite the immiscibility of all components including catalyst and incompatibility of **14a** with water, Cu(OH)$_2$ exhibited the outstanding catalytic activity in water among the screened metal species (entry 8).   In the presence of some lanthanide hydroxides, trace amount of chalcone dimerized.   When bismuth hydroxide was used a catalyst, excessive use of chiral ligand was required for the reaction progress with high enantioselectivity albeit poor reproducibility (entry 28). As the reaction proceeds, Bi(OH)$_3$ itself turned viscous gradually presumably due to self-polymerization (Scheme 29), leading to a loss of its catalytic activity.

Table 2. Effect of metal hydroxides-**L1** complex for asymmetric β-borylation in aqueous media.

$$\text{13a} \xrightarrow[\substack{\text{H}_2\text{O, r.t., 24 h}}]{\substack{\text{MX}_n \text{ (5 mol\%)} \\ \text{L1 (5 mol\%)}}} \text{15a} \xrightarrow[\text{H}_2\text{O/THF}]{\text{NaBO}_3} \text{16a}$$

13a (Ph–CH=CH–CO–Ph) + B$_2$(pin)$_2$ 14a (1.2 equiv.) → 15a (Ph–CO–CH$_2$–CH(B(pin))–Ph) → 16a (Ph–CO–CH$_2$–CH(OH)–Ph)

Entry	MX$_n$	Yield (%)	Ee (%)[a]	Entry	MX$_n$	Yield (%)	Ee (%)[a]
1	Mg(OH)$_2$	NR	–	15	Ag$_2$O	NR	–
2	Al(OH)$_3$	13	32	16	Cd(OH)$_3$	7	25
3	Fe(OH)$_3$	2	18	17	In(OH)$_3$	NR	–
4	α-FeOOH	NR	–	18	La(OH)$_3$	NR	–
5	β-FeOOH	4	51	19	Ce(OH)$_4$	NR	–
6	Co(OH)$_2$	4	16	20	Pr(OH)$_3$	NR (2)[c]	–
7	Ni(OH)$_2$	5	57	21	Nd(OH)$_3$	NR (1)[c]	–
8	Cu(OH)$_2$	84	78	22	Sm(OH)$_3$	NR (3)[c]	–
9	CuO	NR	–	23	Gd(OH)$_3$	NR	–
10	Cu$_2$O	NR	–	24	Dy(OH)$_3$	2	3
11	Zn(OH)$_2$	17	26	25	Yb(OH)$_3$	3	23
12	Ga(OH)$_3$	3	29	26	Au(OH)$_3$	NR	–
13	Zr(OH)$_4$	NR	–	27	Bi(OH)$_3$	NR	–
14	Pd(OH)$_2$	Trace	8	28[b]	Bi(OH)$_3$	5-22	5-88

[a] Determined by HPLC analysis.   [b] Bi(OH)$_3$ (3 mol%), **L1** (9 mol%).
[c] Isolated yield of chalcone dimer.
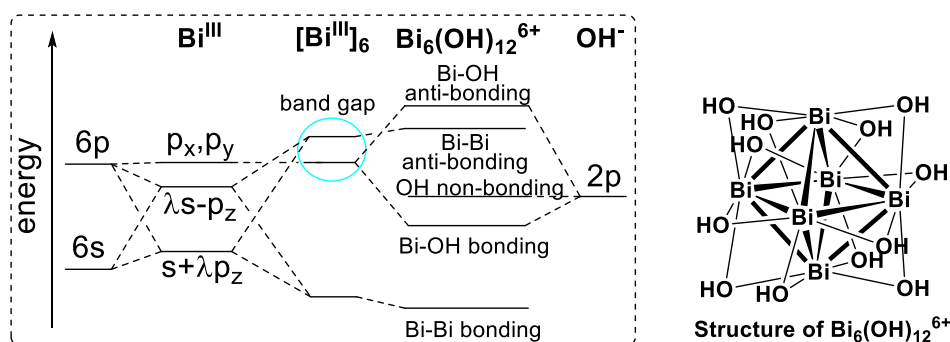
Scheme 29. Theoretical consideration on polymeric structure of bismuth hydroxide.

The marked pivotality of water in the reaction was well presented in Table 3.   The reactions did not proceed at all in typical organic solvents such as toluene, CH$_2$Cl$_2$, DMF, DMSO and THF (entries 1–5).   Although **13a** underwent a self-dimerization in some solvents, the desired β-borylated product was not obtained at all.   The reaction proceeded sluggishly in alcohols with quite low enantioselectivity (entries 6, 7).   In marked contrast to organic solvents and even co-solvent system containing miscible solvents, the outstanding catalytic activity was exerted only in water both in terms of reactivity and enantioselectivity (entries 8-10).   Despite the fact that all involved species are practically insoluble in water, the reaction failed to give the adduct completely under neat (solvent-free) conditions (entry 11).

Table 3. Solvent screening.

$$\text{13a} \quad + \quad \text{B}_2\text{(pin)}_2 \quad \xrightarrow[\substack{\text{H}_2\text{O, r.t., 12 h} \\ \text{then NaBO}_3, \text{H}_2\text{O/THF}}]{\substack{\text{M(OH)}_n \ (10 \text{ mol\%}) \\ \text{Ligand } (12 \text{ mol\%})}} \quad \text{16a}$$
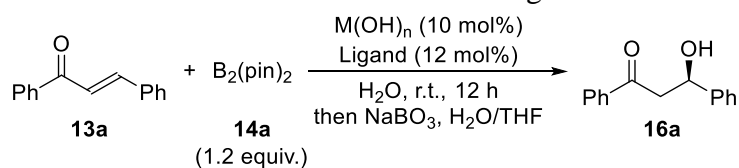
Entry	Solvent	Yield (%)	Ee (%)[a]
1	Toluene	NR (32)[b]	–
2	CH$_2$Cl$_2$	NR (12)[b]	–
3	DMF	NR (trace)[b]	–
4	DMSO	NR	–
5	THF	NR	–
6	EtOH	1	–
7	MeOH	17	29
8	H$_2$O/THF = 1/4	77	79
9	H$_2$O/MeOH = 1/1	82	49
10	**H$_2$O**	**83**	**81**
11	neat	NR	–

[a] Determined by HPLC analysis.   [b] Isolated yield of chalcone dimer.

In contrast to conventional Cu(I) protocol in organic solvents, Cu(II) protocol in water is quite impressive in terms of no necessity of adding strong base, alcohol additive, air-sensitive Cu(I) salt or phosphine ligand and low temperature.   Since Cu(I) disproportionates to Cu(0) and Cu(II) in water (Scheme 29), the current catalysis in water is most efficient with Cu(II) (*vide infra*). Regardless of solvent, there are a limited number of Cu(II) catalysis for boron conjugate additions. Yun *et al*. reported the use of a ligandless systeml based on the combination between CuCl and NaO^{t}Bu reaction in aqueous THF solution (THF/H$_2$O = 2/1) at room temperature for preparation of racemic oraganoboron compounds.[76] Taking a rapid disproportionation of Cu(I) ion in water (Scheme 30) into consideration, the actual catalyst is likely to be Cu(II) species, albeit not described in the original paper.   Although using Cu(I) salt in principal investigation, they demonstrated few experiments in the presence of CuO instead of Cu(I) salt.   They reported that CuO/NaO^{t}Bu catalyst afforded higher conversion than Cu$_2$O/NaO^{t}Bu catalyst.   Presumably this is the first example of Cu(II) catalyst to catalyze boron conjugate addition.
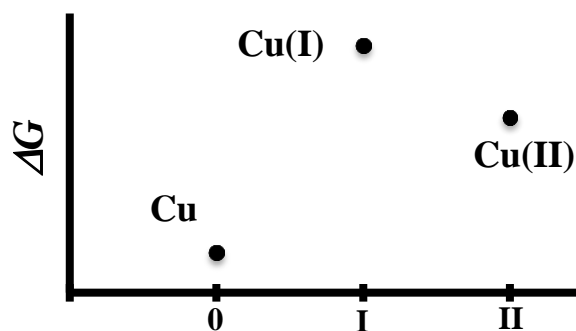
Scheme 30. Latimer diagram of copper.

      It appears that a solid-solid reaction is successfully catalyzed by a solid chiral catalyst in water.   In contrast, the use of Cu(II) salts has hardly reported for boron conjugate additions thus far. The detailed study on the use of Cu(II) salt for asymmetric boron conjugate addition was reported by Córdova *et al* (Scheme 31).[77] Their strategy is characterized by an iminium activation to lower the LUMO of the enal combined with copper-catalyzed β-borylation, and the subsequent Wittig reaction delivered the enantioenriched homoallylicboronates. Although they did not clarify the actual valence of copper, the reaction did not proceed at all when Cu(I) salt was used instead of Cu(OTf)$_2$.
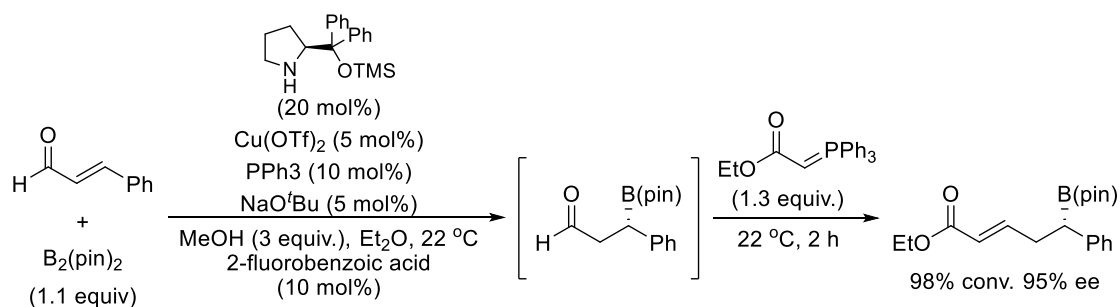
Scheme 31. Córdova's example using Cu(II) salt.[77]

      The recyclable impregnated copper hydroxide on magnetite Cu(OH)$_x$/Fe$_3$O$_4$ prepared through Prof. Mizuno's method[78] was examined in boron conjugate addition by Spanish group.[79] Although they did not mention anything about the valence of copper, Cu(II) should involve in a catalytic cycle. Recently, Santos *et al.* carried out racemic boron conjugate additions in the presence of Cu(II) salt combined with 4-picoline as a base in water without any organic solvent (Scheme 32).[80] Their catalyst composed of 1:5 stoichiometry of CuSO$_4$ to amine is responsible for the β-borylation of acyclic α,β-unsaturated ketones. In the reaction of cyclic α,β-unsaturated ketones or α,β-unsaturated esters, its catalytic performance toward β-borylation dropped. It should be noted that the catalyst was not applicable to the reaction of α,β-unsaturated amides.
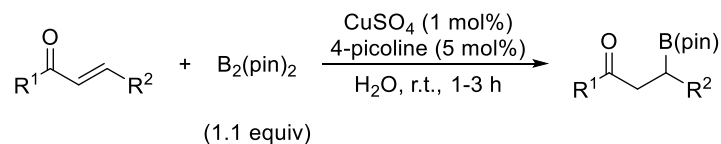
Scheme 32. Santos's example on Cu(II) catalysis in water[80]

      In the same year, the first methodologies for asymmetric boron conjugate addition to α,β-unsaturated carbonyl compounds and nitrile in water emerged.[81] The optimal conditions were composed of Cu(OH)$_2$, acetic acid, and a chiral 2,2′-bipyridine ligand **L1** (Table 4). Compared with basic additives (entries 2, 3), acetic acids were turned out to be efficacious against both reactivity and enantioselectivity (entry 4, 5). Although other acids were less effective (entries 6-9), boronic acid was also effective as an additive (entry 10). Acidic proton seems to be of importance

(entry 11).　When performed at 5 °C with an exquisite set of catalyst system, the reaction afforded the desired product in 95% yield with 99% ee (entry 12).

Table 4. Additive screening.

Cu(OH)$_2$ (5 mol%)
L1 (6 mol%)
Additive (6 mol%)

Ph—(13a) + B$_2$(pin)$_2$ (14a, 1.2 equiv.) $\xrightarrow[\text{then NaBO}_3,\ \text{H}_2\text{O/THF}]{\text{H}_2\text{O, r.t., 12 h}}$ Ph—(16a)
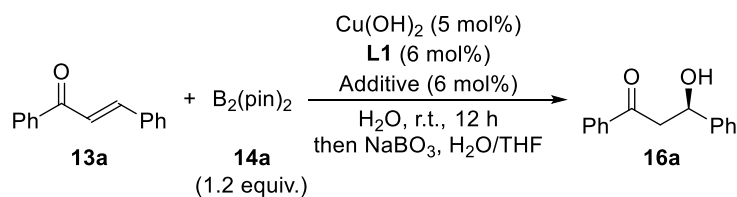
Entry	Additive	Yield (%)	Ee (%)[a]
1	–	84	78
2	pyridine	72	70
3	Et$_3$N	95	81
4	AcOH	93	89
5	TFA	93	86
6	HCO$_2$H	82	77
7	lactic acid	86	79
8	PhCO$_2$H	86	81
9	PhB(OH)$_2$	91	77
10	H$_3$BO$_3$	94	87
11	AcOK	90	81
12[b]	AcOH	95	99

[a] Determined by HPLC analysis.　[b] The reaction was conducted at 5 °C.

The steric influence of diboron reagent was then examined (Scheme 32).　Given the comprehensive inspections to elucidate the relationship between boronate geometry and reactivity in an aqueous environment compared with in organic solvents,[73a] borate formation of **14a** by coordination of water molecule on boron is slower than that of **14b**, which means that **14a** has higher resistance toward hydrolysis.　Since the reaction with **14d** proceeded in unselective manner, the steric hindrance caused by five-membered ring is assumed to be of importance.

Cu(OH)$_2$ (5 mol%)
L1 (6 mol%)
Additive (6 mol%)

Ph—(13a) + **B–B** (14, 1.2 equiv.) $\xrightarrow[\text{then NaBO}_3,\ \text{H}_2\text{O/THF}]{\text{H}_2\text{O, r.t., 12 h}}$ Ph—(16a)

14a
93%y, 89% ee

14b
67%y, 54% ee

14c
92%y, 48% ee

14d
B$_2$(OH)$_4$
<10%y, 0% ee
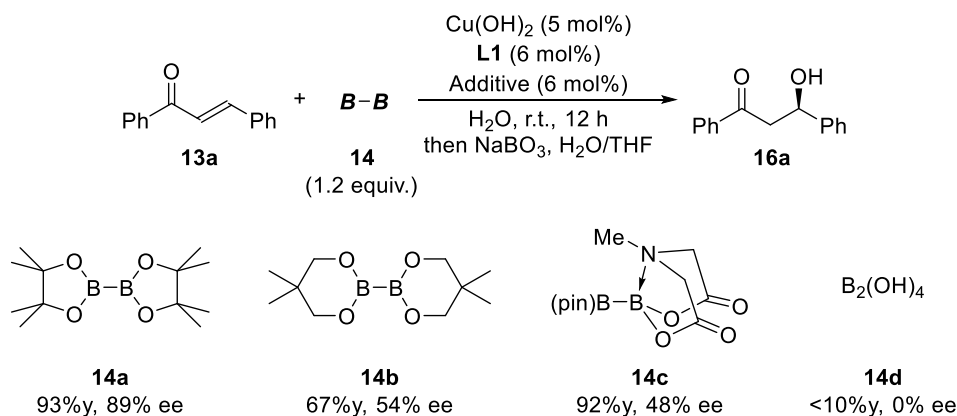
Scheme 32. Screening of diboron reagent.

Although acetate anion was expected to function as an activator for diboron reagent,[27a, 33b] its influence on the catalyst function of Cu(OH)$_2$-**L1** complex remained unclear. The effect of counteranion was thus examined (Table 5). As mentioned above, both the reaction yield and the enantioselectivity improved when 6 mol% of acetic acid was added in this system (entry 2). The *in situ* formation of Cu(OH)(OAc) was assumed to understand the homogeneity of the reaction solution. The use of Cu(OAc)$_2$ resulted in a slight decrease in enantioselection, albeit with still a high level (entry 3). The reaction result of CuF$_2$ can be interpreted by its decomposition in water (CuF$_2$ + H$_2$O → CuFOH + HF) and its insufficient coordination ability with **L1** (entries 4-6). When more Lewis acidic Cu(II) salts were used, the yields and the enantioselectivities became lower (entries 7-11). A chiral catalyst consisting of Cu(OSO$_2$C$_{11}$H$_{23}$)$_2$, one of Lewis acid–surfactant-combined catalysts (LASCs), and **L1** was reported to catalyze enantioselective ring-opening reactions of *meso*-epoxides with aniline and indole derivatives in water;[82] however, it did not exhibit superior performance over Cu(OH)$_2$ (entry 12). While Cu(acac)$_2$ gave the product in 96% yield with 81% ee (entry 13), the reaction did not proceed at all using CuO (entry 16). Participation of covalent bond in copper(II) salts led to higher selectivity (entries 1, 14 and 15). Quite recently the use of basic copper carbonate Cu$_2$(OH)$_2$CO$_3$-based catalyst combined with PPh$_3$ for boron conjugate addition was developed mainly in racemic β-borylation of olefins.[83]

Table 5. Effect of copper salts.
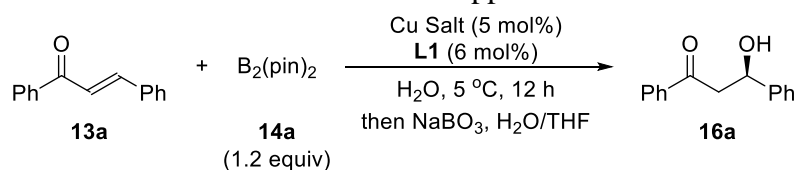
Entry	Cu(II) Salt	Yield (%)	Ee (%)[a]
1	Cu(OH)$_2$	83	81
2[b]	Cu(OH)$_2$	95	99
3	Cu(OAc)$_2$	94	91
4	CuF$_2$	67	65
5[b]	CuF$_2$	59	64
6[c]	CuF$_2$	12	23
7	CuCl$_2$	71	61
8	CuBr$_2$	82	54
9	Cu(NO$_3$)$_2$	54	66
10	CuSO$_4$	62	65
11	Cu(OTf)$_2$	89	70
12	Cu(OSO$_2$C$_{11}$H$_{23}$)$_2$	62	54
13	Cu(acac)$_2$	96	81
14	Cu$_2$(OH)$_2$CO$_3$	89	87
15[b]	Cu$_2$(OH)$_2$CO$_3$	90	94
16	CuO	NR[b]	–

[a] Determined by HPLC analysis. [b] 6 mol% AcOH was added as an additive.

[c] The reaction was quenched within 15 min.

The appearances of the reactions using Cu(OH)$_2$ (entry 1) and Cu(OAc)$_2$ (entry 3) at several stages were shown in Figure 1. In Cu(OH)$_2$-catalized reaction, a heterogeneous system colored with light blue [above (a), (b)] changed an appearance into blown immediately after addition of **14a** [above (c)], and gradually into dark within 15 min [above (d)]. The color remained unchanged even after 30 min and 60 min [above (e) and (f)]. In marked contrast, the reaction solution in the presence of Cu(OAc)$_2$ with **L1** was homogeneous [below (a)]. After addition of **13a** and **14a**, the color gradually became brown [below (d), (e), and (f)].

(a)　　**(b)**　　**(c)**　　**(d)**　　**(e)**　　**(f)**
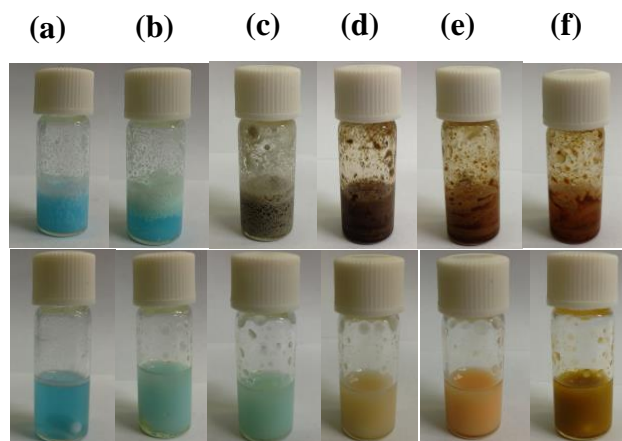
Figure 1. Comparison of the appearance of the reaction systems comprising Cu(OH)$_2$ (above) and Cu(OAc)$_2$ (below)
(a) Prepared catalyst solution with **L1**; (b) Just after addition of **13a**; (c) 2 min after addition of 2; (d) 15 min; (e) 30 min; (f) 60 min.

Through the investigation, it was found that *the use of Cu(OH)$_2$ alone* (**Cat 1**), *the combined use of equimolar amounts of Cu(OH)$_2$ and acetic acid* (**Cat 2**) and *the use of Cu(OAc)$_2$ alone* (**Cat 3**) displayed different properties including the catalytic activity in enantioselective boron conjugate additions in water. The substrate scope was then explored under the optimal three conditions. It is noteworthy that the investigated catalyst systems are extremely versatile and are applicable to various array of α,β-unsaturated carbonyl compounds and nitrile including acyclic and cyclic α,β-unsaturated ketones, acyclic and cyclic β,β-disubstitued enones, acyclic and cyclic α,β-unsaturated esters including β,β-disubstitued ones, acyclic α,β-unsaturated amides including β,β-disubstitued one, and α,β-unsaturated nitrile in high yield with excellent enantioselectivity. The catalysts that cover all these substrates with high yields and high enantioselectivities have never been precedent in boron conjugate addition reactions. Some common properties of three catalytic systems could be noted. The heterogeneous catalyst system (**Cat 1**) showed relatively poor results both in reactivity and enantioselection and did some limitations in tolerance toward certain classes, among which the reaction of cyclcic substrates was most evident. In contrast, superior catalytic performance was generally observed in the reaction of acyclic α,β-unsaturated esters when homogeneous system (**Cat 2**) was adopted. Nevertheless, another homogeneous system (**Cat 3**) was slightly less efficient. From a synthetic point of view, the formation of enantioenriched tertiary alcohols readily prepared from β,β-disubstitued α,β-unsaturated carbonyl compounds is valuable.

Scheme 33. Enantioselective boron conjugate addition with three catalytic systems

16a

Cat 1 : 83% y, 81% ee
Cat 2 : 95% y, 99% ee
Cat 3 : 94% y, 91% ee

16b

Cat 1 : 81% y, 72% ee
Cat 2 : 91% y, 90% ee
Cat 3 : 84% y, 82% ee

16c

Cat 1 : 80% y, 85% ee
Cat 2 : 90% y, 96% ee
Cat 3 : 93% y, 94% ee

16d

Cat 1 : 81% y, 75% ee
Cat 2 : 90% y, 92% ee
Cat 3 : 91% y, 89% ee

16e

Cat 1 : 79% y, 79% ee
Cat 2 : 90% y, 88% ee
Cat 3 : 93% y, 86% ee

16f

Cat 1 : 81% y, 84% ee
Cat 2 : 95% y, 89% ee
Cat 3 : 90% y, 82% ee

16g

Cat 1 : 56% y, 72% ee
Cat 2 : 98% y, 82% ee
Cat 3 : 99% y, 81% ee

16h

Cat 1 : 59% y, 76% ee
Cat 2 : 92% y, 92% ee
Cat 3 : 90% y, 88% ee

16i

Cat 1 : 49% y, 70% ee
Cat 2 : 91% y, 88% ee
Cat 3 : 79% y, 82% ee

16j

Cat 1 : 45% y, 67% ee
Cat 2 : 87% y, 91% ee
Cat 3 : 79% y, 85% ee

16k

Cat 1 : 84% y, 65% ee
Cat 2 : 88% y, 80% ee
Cat 3 : 86% y, 80% ee

16l

Cat 1 : 37% y, 42% ee
Cat 2 : Quant, 82% ee
Cat 3 : 97% y, 80% ee

16m[b]

Cat 1 : 71% y, 84% ee
Cat 2 : 87% y, 97% ee
Cat 3 : 90% y, 97% ee

16n[b]

Cat 1 : 68% y, 78% ee
Cat 2 : 91% y, 93% ee
Cat 3 : 91% y, 92% ee

16o

Cat 1 : 43% y, 47% ee
Cat 2 : 91% y, 86% ee
Cat 3 : 90% y, 82% ee

16p[b]

Cat 1 : 21% y, 63% ee
Cat 2 : 83% y, 89% ee
Cat 3 : 84% y, 87% ee

16q[b]

Cat 1 : 57% y, 24% ee
Cat 2 : 89% y, 85% ee
Cat 3 : 80% y, 84% ee

16r

Cat 1 : 85% y, 82% ee
Cat 2 : 58% y, 40% ee
Cat 3 : 55% y, 35% ee

16s

Cat 1 : 73% y, 82% ee
Cat 2 : 49% y, 53% ee
Cat 3 : 32% y, 41% ee

16t

Cat 1 : 80% y, 84% ee
Cat 2 : 80% y, 86% ee
Cat 3 : 75% y, 81% ee

16u

Cat 1 : 42% y, 59% ee
Cat 2 : 81% y, 87% ee
Cat 3 : 80% y, 84% ee

16v[b]

Cat 1 : 70% y, 81% ee
Cat 2 : 77% y, 87% ee
Cat 3 : 78% y, 83% ee

16w

Cat 1 : 15% y, 55% ee
Cat 2 : 76% y, 91% ee
Cat 3 : 83% y, 89% ee

16x

Cat 1 : 12% y, 49% ee
Cat 2 : 80% y, 89% ee
Cat 3 : 79% y, 86% ee

16y

Cat 1 : 5% y, 66% ee
Cat 2 : 83% y, 91% ee
Cat 3 : 65% y, 78% ee

16z

Cat 1 : 32% y, 59% ee
Cat 2 : 61% y, 72% ee
Cat 2[a] : 83% y, 81% ee
Cat 3 : 75% y, 81% ee

16α

Cat 1 : 55% y, 72% ee
Cat 2 : 85% y, 81% ee
Cat 3 : 86% y, 82% ee

[a] 20 mol% AcOH was added as additive.   [b] 1.6 equivalent of **2** was employed.

In the reaction of **13l** with **14a**, 0.005 mol% of Cu(OAc)$_2$ could be used efficiently in a gram-scale experiment without any loss of enantioselectivity (Scheme 33, 1.08 g, 96% yield, 81% ee).   α,β-Unsaturated esters, amides and cinnamyl nitrile were amenable to the optimal conditions, leading to high yields and high enantioselectivities.   In contrast to extensively-examined Cu(I) catalysis, Cu(II) protocol performed in water had a solid performance over wide range of substrates. Furthermore, it is more expedient and environmentally benign methodology.

13l

14a
(1.2 equiv)

Cu(OAc)$_2$ (0.005 mol%)
L1 (0.006 mol%)
H$_2$O, 5 °C, 12 h
then NaBO$_3$, H$_2$O/THF

16l
96% yield [1.08 g]
90.5:9.5 e.r.
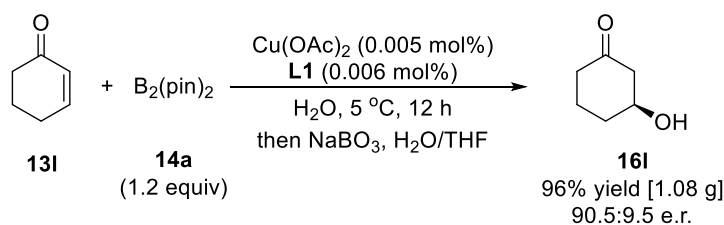
Scheme 34. Gram-scale synthesis.

3.1-3 *Heterogeneous vs. Homogeneous*

Among all tested Cu(II) salts, Cu(OH)$_2$-based system (**Cat 1**) appeared to operate under heterogeneous conditions, whereas other systems seemed to function under nearly homogeneous conditions. The heterogeneity of Cu(OH)$_2$-based system (**Cat 1**) and the homogeneity of Cu(OAc)$_2$-based system (**Cat 3**) were confirmed by filteration test and inductively-coupledplsdms (ICP) analysis of the filterates obtained after the filteration test (Scheme 35). The filterate resulting from **Cat 1**-catalyzed reaction of **13a** with **14a** displayed no activity with freshly-added substrates (**13a** and **14a**), whereas that obtained from **Cat 3**-catalyzed reaction could catalyze β-borylation in 89% yield with 91% ee. It was confirmed that Cu content in the former filtrate was below the detection limit of the ICP equipment (5 ppb).
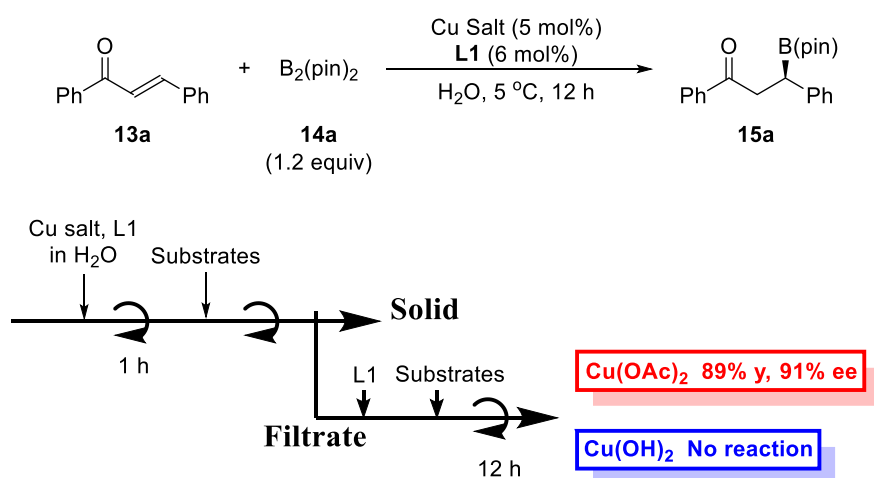
Scheme 35. Filteration test experiments.

Preliminary kinetic profiles of the reaction between **13a** and **14a** revealed the rate accerelation under heterogeneous conditions (Figure 2).
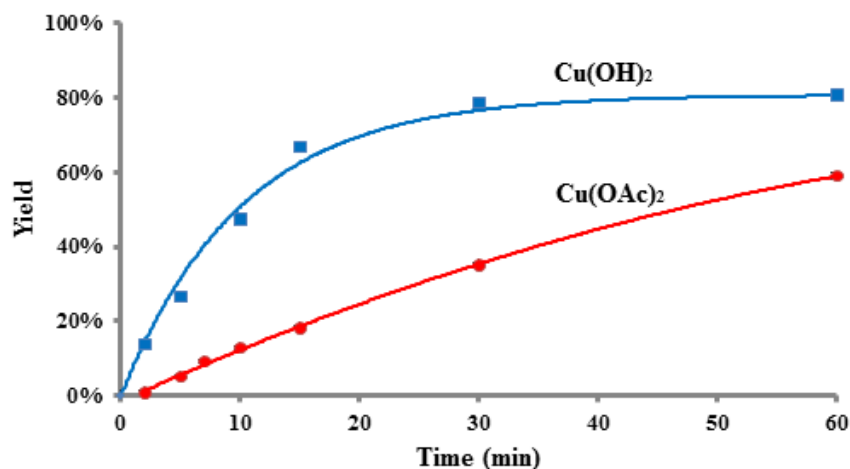
Figure 2. Profiles of reactions catalyzed by Cu(OH)$_2$ and Cu(OAc)$_2$ in water.

Strikingly, overwhelmingly high turnover frequency (TOF) of 12,800-43,200 h^{-1} was recorded in the demonstration in the presence of 0.005 mol% of $Cu(OH)_2$ or $Cu(OAc)_2$ (**Cat 1-3**), representing the highest values ever observed for boron conjugate additions (see McQuade's example in 3.1-1).
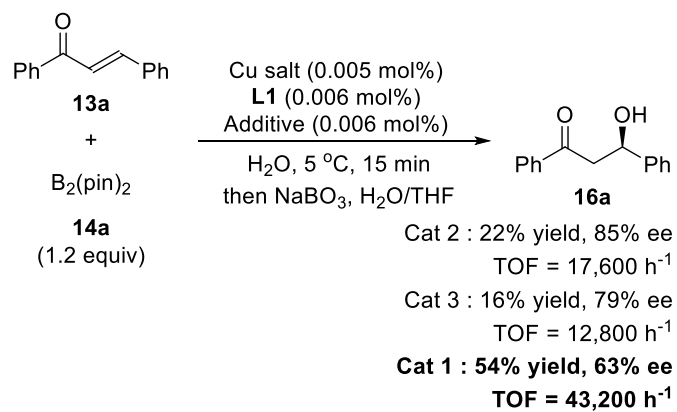
Scheme 36. Turnover frequency test.

Cu salt (0.005 mol%)
L1 (0.006 mol%)
Additive (0.006 mol%)

H_2O, 5 °C, 15 min
then $NaBO_3$, H_2O/THF

Cat 2 : 22% yield, 85% ee
TOF = 17,600 h^{-1}
Cat 3 : 16% yield, 79% ee
TOF = 12,800 h^{-1}
Cat 1 : 54% yield, 63% ee
TOF = 43,200 h^{-1}

3.1-4   *Reaction of Conjugated Dienones and Their Derivatives*

Site- and enantioselective boron conjugate addition to $\alpha,\beta,\gamma,\delta$-unsaturated dienones provides a direct approach to accessing enantiomerically enriched functionalized allylboranes.   In contrast to well-established protocols for β-borylation of α,β-unsaturated system, the reaction of $\alpha,\beta,\gamma,\delta$-unsaturated dienones or their derivatives is rarely studied at that time.   Chiral Cu(II) catalysis in water was then extended to enantioselective boron conjugate addition with $\alpha,\beta,\gamma,\delta$-unsaturated dienones in water.
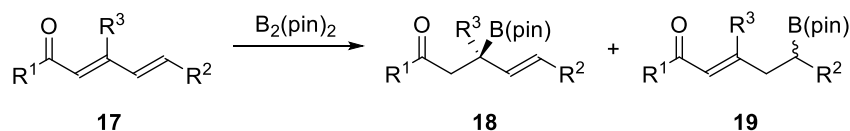
Scheme 37. Boron conjugate addition to $\alpha,\beta,\gamma,\delta$-unsaturated dienones.

The reaction of $\alpha,\beta,\gamma,\delta$-unsaturated acyclic dienone **17a** with **14a** in the presence of Cu(OH)$_2$, **L1** and AcOH (**Cat 1**) was demonstrated at 5 $^{\circ}$C, resulting that a 1,4-mode of addition was exclusively favored to produce **18a** with high enantioselectivity (Table 6, entry 2).   No 1,6-addition product **19a** was produced.   In preliminary report, the reaction performed at room temperature output a predominant formation of 1,4-adduct **18a** together with 2% of 1,6-adduct **19a**.[81] Although the use of nucleophilic counteranion led to a significant drop in enantioselectivity, selective 1,4-addition proceeded irrespective of counteranion, either hetero- or homogeneous catalysis (entries 1-6).   The reaction proceeded, however, sluggishly in the presence of CuCl$_2$ or CuSO$_4$ and showed deteriorated enantioselection (entries 4, 5).   The Cu(OTf)$_2$-based system showed high reactivity with low enantioselectivity (entry 6).   The same tendency on counteranions was observed in the case of another dienone **17b**-**17d** (entries 7-15).   It is assumed that the strong preference of 1,4-addition is ascribed to the difference of electronic density between β-position and δ-position and their resultant susceptibility to nucleophilic attack of borylcopper species.   Quite recently enantioselective 1,6-borylation of $\alpha,\beta,\gamma,\delta$-unsaturated acyclic dienone was reported with Cu(I) catalysis in organic solvent.[84] Among all tested substrates, the 1,6-selective borylation of **17c** is noteworthy since their result is antipodal to outcomes in entries 10-12 (Scheme 38, below). Although based upon Yun's condition (Cu(I) salt, Josiphos ligand, strong base and alcohol additive in THF [see Scheme 11 or 12]), their optimal conditions does not require the addition of strong base. In their condition optimization process using benzyl sorbate as a substrate, they found that the presence of a strong base produced a 1:1 mixture of 1,4- and 1,6-borylated products.   Considering Yun's example on β-borylation of dienone substrate (Scheme 38, above),[38] a fundamental understanding on 1,4- and 1,6-addition of dienone substrates remains difficult at this stage. Dienoester **17e** was also amenable to 1,4-addition predominantly with high enantioselectivity (entries 16-18).   Acyclic dienone bearing a methyl substituent at the β-position was known to be amenable to 1,6-addition presumably because of a reluctance to react at the β-position.[85] However the reaction of sterically congested dienone **17f** or dienoester **17g** furnished exclusively the corresponding 1,4-adducts with high enantioselectivity (entries 19-24).

Table 6. β-Borylation to acyclic dienones.
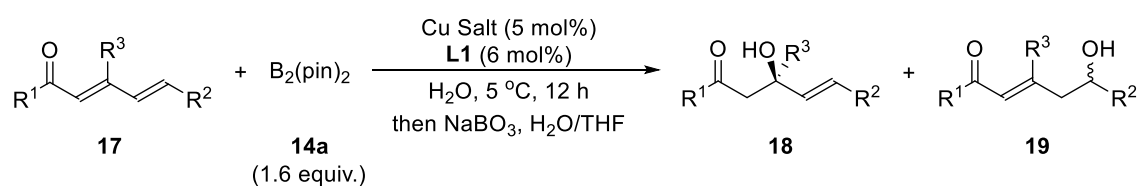
Entry	Substrate	Cu Salt	Yield (%)	Ee (%)[a]
1		**Cat 1**	81 (**18a**)	77
2		**Cat 2**	93	89
3	**17a**	**Cat 3**	91	89
4		CuCl$_2$	42	59
5		CuSO$_4$	37	34
6		Cu(OTf)$_2$	92	41
7		**Cat 1**	87 (**18b**)	84
8	**17b**	**Cat 2**	87	91
9		**Cat 3**	91	91
10		**Cat 1**	73 (**18c**)	75
11	**17c**	**Cat 2**	86	89
12		**Cat 3**	84	83
13		**Cat 1**	67 (**18d**)	72
14	**17d**	**Cat 2**	83	84
15		**Cat 3**	81	82
16		**Cat 1**	83 (**18e**)	85
17	**17e**	**Cat 2**	87	92
18		**Cat 3**	91	90
19		**Cat 1**	75 (**18f**)	83
20	**17f**	**Cat 2**	85	91
21		**Cat 3**	81	92
22		**Cat 1**	86 (**18g**)	90
23	**17g**	**Cat 2**	91	98
24		**Cat 3**	90	94

[a] Ee value of major adduct. Determined by HPLC analysis.

Yun *et al.*

Yun et al. scheme:
Ph-C(=O)-CH=CH-CH=C(Me)₂ + B₂(pin)₂ (1.1 equiv.) →
CuCl (3 mol%)
(*R*,*S*)-Josiphos (3 mol%)
NaO*t*Bu (3 mol%)
MeOH (1.0 equiv.)
THF, r.t.
→ product
93% yield, 96% ee
*i*PrOH: 70% conv. (>50 h), 95% ee

Lam *et al.*

Lam et al. scheme:
Ph-C(=O)-CH=CH-CH=CH-Me + B₂(pin)₂ (1.2 equiv.) →
CuF(PPh₃)₃•2MeOH (0.2 mol%)
(*R*,*S*)-Josiphos (0.24 mol%)
*i*PrOH (2.0 equiv.)
THF, r.t.
then NaBO₃, H₂O/THF
→ product
68% yield, 95% ee
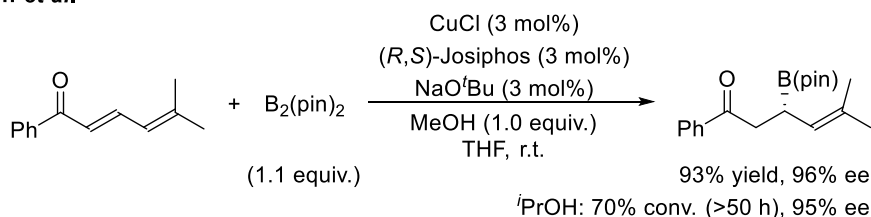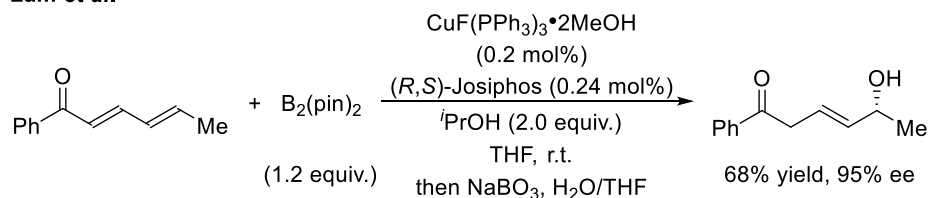
Scheme 38. 1,4-addition vs. 1,6-addition described in two papers.[38, 84]

In order to investigate how conformations of the conjugated system affect the reactivity and stereocontrol, three dienoester **17e** isomers were prepared. Having these isomers in hands, their boron conjugate addition was then performed (Table 7). As mentioned above, all chiral copper(II) catalysts resulted in the exclusive formation of 1,4-adduct. After the reaction reached the completion, 1,4-adduct **18e** was obtained with the same levels of reactivity and enantioselectivity irrespective of the substrate geometry (entries 2, 4, 6). Forming 1,6-borylated adduct **19e** was not obtained in all entries. The initial reaction rate was also turned out to be constant in entry 1 and 3. On the other hand, (*E*, *Z*)-dienoester suffered from a drop in the initial reaction rate (entry 5). These results suggest that Lewis acid-assisted isomerization of the conjugated system is facile to some extent under the reaction conditions.

Table 7. Effect of *E/Z* isomerization.

Table scheme: EtO₂C-CH=CH-CH=CH-Ph (17e, A site / B site) + B₂(pin)₂ (14a, 1.6 equiv) →
Cu Salt (5 mol%)
L1 (6 mol%)
H₂O, 5 °C, 12 h
then NaBO₃, H₂O/THF
→ 18e + 19e
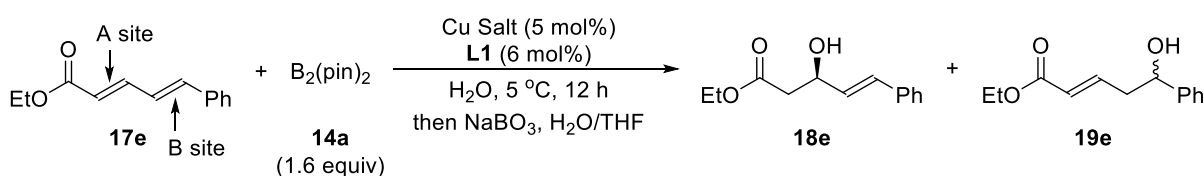
Entry	A site	B site	Reaction Time	Yield (%)	Ee (%)[a]
1	*E*	*E*	15 min	17 (**18e** only)	91
2	*E*	*E*	12 h	91	90
3	*Z*	*E*	15 min	17	90
4	*Z*	*E*	12 h	88	90
5	*E*	*Z*	15 min	7	89
6	*E*	*Z*	12 h	90	91

[a] Ee value of major adduct. Determined by HPLC analysis.

Cyclic dienones have also been served as acceptors congenial to 1,6-addition. Several reports[86] have appeared on copper-catalyzed 1,6-conjugate addition of organometallic reagents to cyclic dienones, although 1,6-boron conjugate addition remained unexplored. For instance, Alexakis *et al.* disclosed a regiodivergent copper catalyst for asymmetric conjugate addition to

α,β,γ,δ-cyclic Michael acceptors (Scheme 39).[86d] The regioselectivity of asymmetric conjugate additions to cyclic dienones depends upon the nature of the nucleophile, chiral ligand and solvent.[86a-d,f] Organozinc or organoaluminium reagents afforded the corresponding 1,6-adducts, whereas Grignard reagents tended to produce more substituted 1,4-adducts. Eventually, regioselective governing between 1,4- and 1,6-addition of a given organometallic reagent is appeared to be difficult. Additionally, few catalytic methods are available for direct and enantioselective functionalization at the remote δ-position.[87,88]
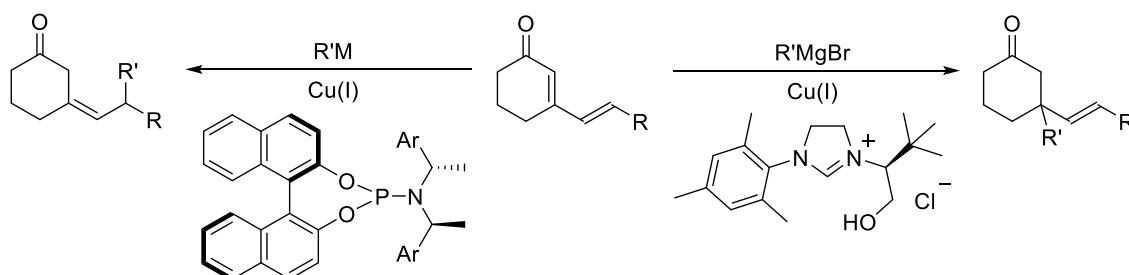
Scheme 39. Alexakis's representative example on regiodivergent 1,4- vs. 1,6-conjugate addition.

Several copper(II) salts were therefore examined closely in the reaction of six-membered cyclic dienone **20a** performed in water (Table 8). To our astonishment, a simple swap of counteranion was disclosed to switch the regioselectivity between 1,4- and 1,6-addition. The 1,6-adduct **22a** was formed exclusively in the presence of the heterogeneous catalyst composed of Cu(OH)$_2$ and **L1** (**Cat 1**) with good enantioselectivity (entry 1). The 1,4-addition pathway took precedence to afford **21a** in a highly stereomeric manner under the homogeneous conditions (**Cat 2, 3**) (entries 2, 3). While the heterogeneous system gave slightly inferior results in enantioselectivity, both 1,4- and 1,6-pathways competed with each other in the presence of other copper(II) salts (entries 4-6). In addition, both 1,4- and 1,6-mode showed a quite low level of enantioselection. The *E/Z* ratio of γ,δ-olefin did not have any influence in this reaction. These results suggested that a 1,4-addition pathway seemed to be somewhat predominant in spite of the construction of quaternary asymmetric carbon. To the best of our knowledge, the dependence of regioselectivity not on nucleophile or chiral ligand but on a simple inorganic counteranion has never been observed in asymmetric Michael-type additions. Sterically congested electrophilic site at δ-position in the reaction of **20b** did not shift the preference of Cu(OH)$_2$ toward 1,6-addition (entry 7). Both 5-membered and 7-membered cyclic dienones **20c** or **20d** could serve as efficient substrates to exert the same regioselectivity switch as 6-membered one (entries 8, 9, 13, 14). The effect of counteranion showed the same tendency on regioselectivity, irrespective of ring size of given cyclic dienones. Another type of cyclic dienones **20e** and **20g** did not react with diboron **14a** at δ-position even in the presence of Cu(OH)$_2$, presumably due to the steric issue on nucleophilic addition.[89] Although dienone **20f** exhibited the reactivity at δ-position, the reaction suffered from appreciable amount of many byproducts which could not be separated.[90]

Table 8. Additions to β-substituted cyclic dienones.
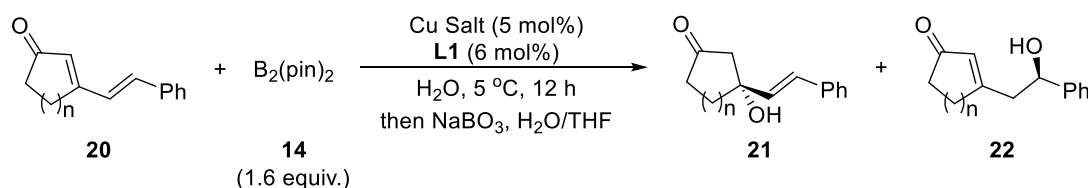
Entry	Substrate	Cu Salt	Yield (%)	21[a]/22	Ee (%)[b]
1		Cu(OH)$_2$ (**Cat 1**)	81 (**21a + 22a**)	**<1/>99**	–/78
2[c]		Cu(OH)$_2$ (**Cat 2**)	92	**>99/<1**	87/–
3		Cu(OAc)$_2$ (**Cat 3**)	94	**>99/<1**	91/–
4		CuCl$_2$	49	69/31	32/3
5	**20a**	CuSO$_4$	37	56/44	14/1
6		Cu(OTf)$_2$	81	91/9	45/1
7		Cu(OH)$_2$ (**Cat 1**)	69 (**21b + 22b**)	**<1/>99**	–/85
8[c]		Cu(OH)$_2$ (**Cat 2**)	87	**>99/<1**	88/–
9		Cu(OAc)$_2$ (**Cat 3**)	92	**>99/<1**	89/–
10	**20b**	CuCl$_2$	43	65/35	29/6
11		Cu(OH)$_2$ (**Cat 1**)	77 (**21c + 22c**)	**<1/>99**	–/81
12[c]		Cu(OH)$_2$ (**Cat 2**)	84	**>99/<1**	93/–
13		Cu(OAc)$_2$ (**Cat 3**)	84	**>99/<1**	92/–
14		CuCl$_2$	21	73/27	32/0
15	**20c**	CuSO$_4$	32	69/31	18/1
16		Cu(OTf)$_2$	22	82/18	53/1
17		Cu(OH)$_2$ (**Cat 1**)	39 (**21d + 22d**)	**<1/>99**	–/29
18[c]		Cu(OH)$_2$ (**Cat 2**)	77	**>99/<1**	82/–
19		Cu(OAc)$_2$ (**Cat 3**)	81	**>99/<1**	61/–
20	**20d**	CuCl$_2$	18	53/47	7/1

[a] The *E/Z* ratio of **21** was constantly ca. 5/5 irrespective of dienone geometry.
[b] Determined by HPLC analysis.   [c] 6 mol% AcOH was added.
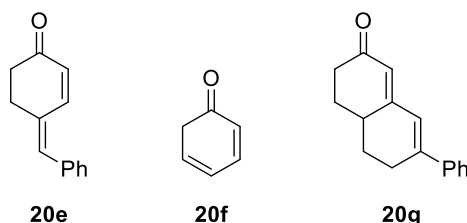
It should be noted that most chiral copper catalysts generally furnish β,γ-unsaturated 1,6-adducts via kinetic protonation of dienolate intermediates in the reactions of organometallic reagents or silylboron reagent to cyclic dienones (Scheme 39, 40).[85,86a] The isomerization of these deconjugated adducts was known to lead easily to totally reconjugated adducts especially under basic conditions.[86f] Nevertheless, it was verified that our protocol performed in water furnished

thermodynamically favorable conjugated product through the reaction conducted in D_2O (Scheme 41).   Deuteration of the dienolate took place exclusively at γ-position.
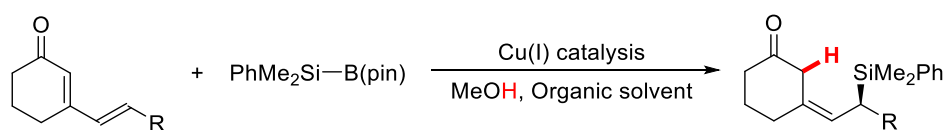
Scheme 40. Hoveyda's example on forming deconjugated product through 1,6-addition to cyclic dienone.
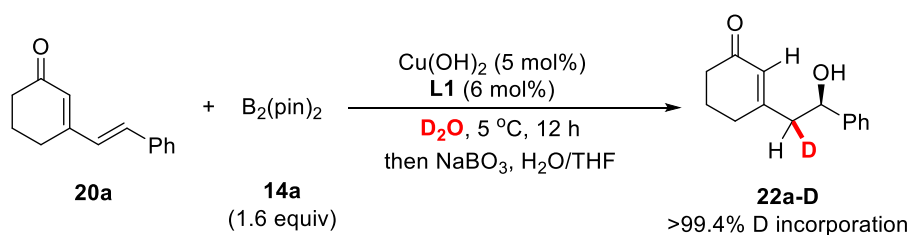
Scheme 41. Deuteration of enolate intermediate through δ-borylation of cyclic dienone **20a** in D_2O.

These results encouraged us to investigate the addition of **14a** to trienone **23a** bearing the additional electrophilic site at ζ position (Table 9).   The use of $CuCl_2$ resulted in the formation of messy reaction mixture which could not be separated, the desired products were obtained in the presence of $Cu(OH)_2$ or $Cu(OAc)_2$.   The 1,6- and 1,8-adduct were obtained in the reaction catalyzed by $Cu(OH)_2$, albeit moderate selectivity (entry 1).   It is noteworthy that functionalization at the remotest ζ position could be achieved.   On the other hand, homogeneous catalysis rendered 1,4-adduct **24a** exclusively (entries 2, 3).

Table 9. Additions to cyclic trienones.
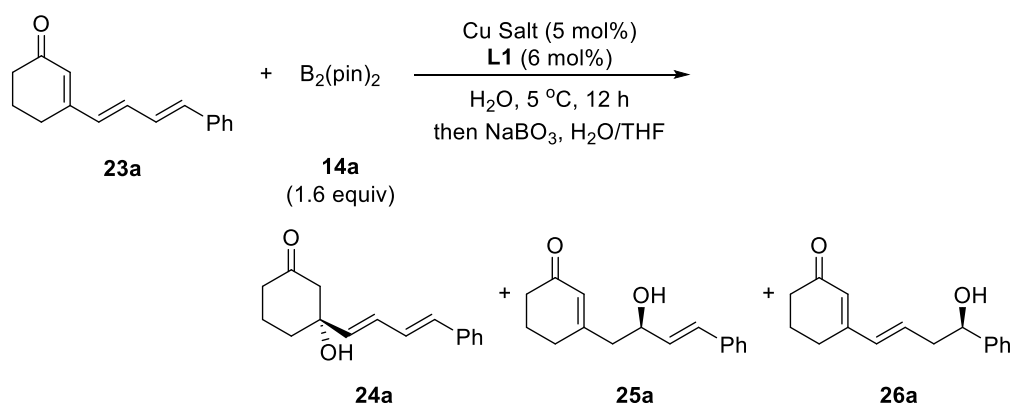
Entry	Cu Salt	Yield (%)	24a/25a/26a	Ee (%)[a]
1	$Cu(OH)_2$ (**Cat 1**)	71	< 1/74/26	72 (**25a**), 46 (**26a**)
2[b]	$Cu(OH)_2$ (**Cat 2**)	86	> 99/< 1/< 1	92 (**24a**)
3	$Cu(OAc)_2$ (**Cat 3**)	87	> 99/< 1/< 1	91 (**24a**)

[a] Determined by HPLC analysis.   [b] 6 mol% AcOH was added.

3.1-5   Reaction Mechanisms

3.1-5-1   Insights into Active Species

The pH changes were recorded during the reaction (Figure 3).   Efficient catalytic systems (**Cat 1-3**) was identified with the fast pace of pH changes after addition of both substrates, whereas inefficient system such as $CuSO_4$ appeared to be slower to respond.   It is assumed that low responsiveness of $CuSO_4$–system toward pH changes would be ascribed to the diffusion of substrates in water or low reactivity of diboron reagent toward hydrolysis due to the acidity. Although the heterogeneous reaction solution involving $Cu(OH)_2$ (**Cat 1**) exhibited almost neutrality, the character of other homogeneous reaction solutions turned out to be basic.   In particular, $CuSO_4$-catalyzed reaction appeared to proceed under strongly basic conditions.
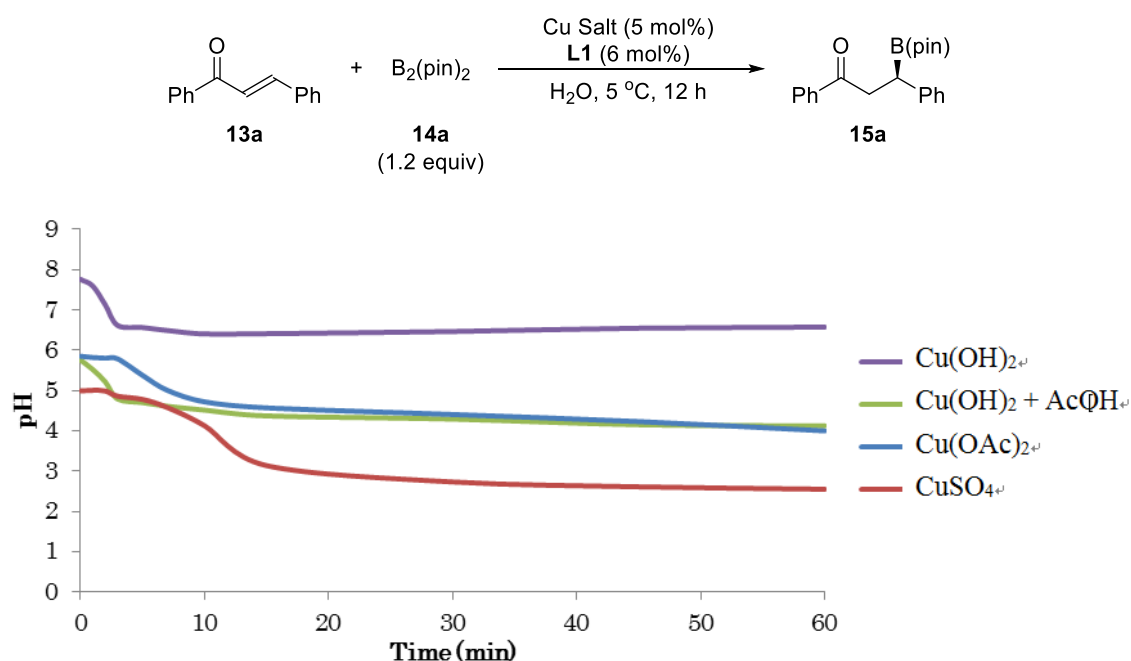
Figure 3. The pH changes during the reaction.

The calculated diagram between the relationship between the concentration of possible species derived from $Cu(OH)_2$ and pH value in water is shown in Figure 4.   It indicates that solid $Cu(OH)_2$ or $Cu(OH)^+$ is an active catalyst in the reaction system.
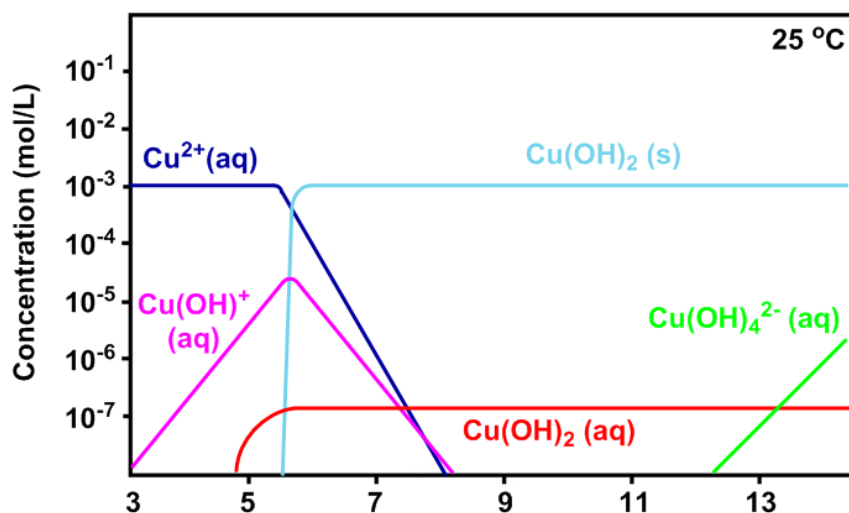
Figure 4. Concentration vs. pH value.

Dynamic light scattering (DLS) analysis is a useful tool to know the aggregation and polydispersity of materials in the system trhough translational diffusion. Considering the pH changes during the reaction shown in Figure 3, the efficient catalysis is related with the diffusion of involved materials in the reaction system.
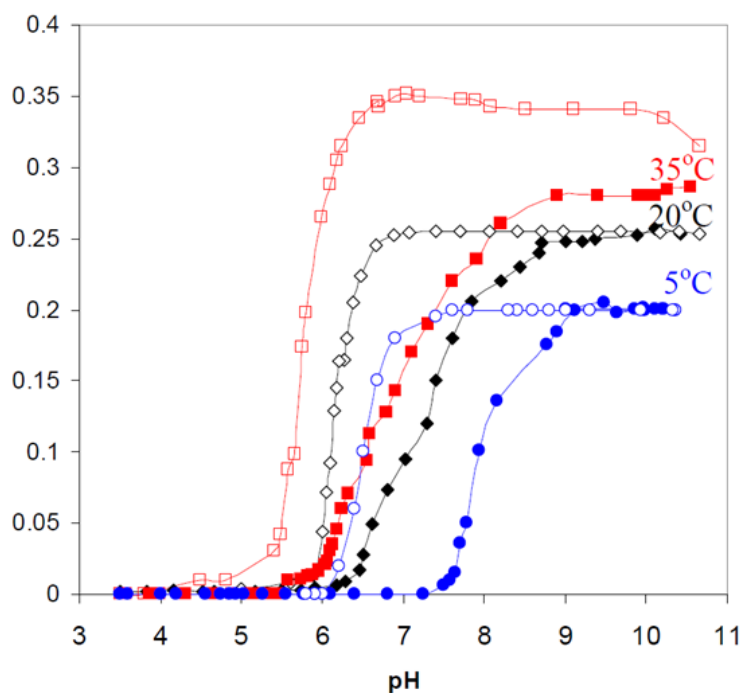
Figure 5. The changes in light scattering.

3.1-5-2   Insights into Cu(II) Complexes with L1

Crystallographic investigations of $CuBr_2$-**L1** complex in 2010 has revealed the complex core to be a monopositive species with the chelation in a tridentate manner.[82a] Actually both hydroxyl groups were not required for this reaction; a chiral catalyst composed of $Cu(OH)_2$ and **L2**, where one hydroxyl group was protected with a methyl group, afforded much the same result (82% yield, 77% ee).   Historically, much attention has been paid to Cu(II)-2,2'-bipyridine(bpy) complexes and extensive studies both in the solid state and in solution were described in many reports.[91] Electron paramagnetic resonance (EPR) spectra has indicated that the dimeric bis-μ-hydroxide cation $[Cu(bpy)(\mu\text{-}OH)]_2^{2+}$ was favored in aqueous solution at pH 8-12.[91a] The dimeric structure can make us understood the heterogeneous catalysis exerted by $Cu(OH)_2$ and **L1**. In our catalytic system, the predominant formation of the dimeric cation was also validated through an ESI-MS analysis. $Cu(OAc)_2$ was mixed with 1.2 equivalent of **L1** in aqueous THF (H_2O/THF = 1/1)[92] and the resultant homogeneous solution was directly submitted to ESI-MS analysis.   The obtained single peak m/z 863.3484 is corresponding to dimeric Cu(II) complex $[(\mathbf{L1})_2Cu_2(OAc)(OH_2) - 2H]^+$.   To the homogeneous solution of $Cu(OAc)_2$ and **L1** in aqueous tetrahydrofuran was added both substrates **13a** and **14a**, and then the reaction solution was submitted to ESI-MS analysis, which provided a strong peak m/z 726.3265 corresponding to $[\mathbf{L1} + CuB(pin) + \mathbf{13a} - H]^+$ in the light of isotope pattern.
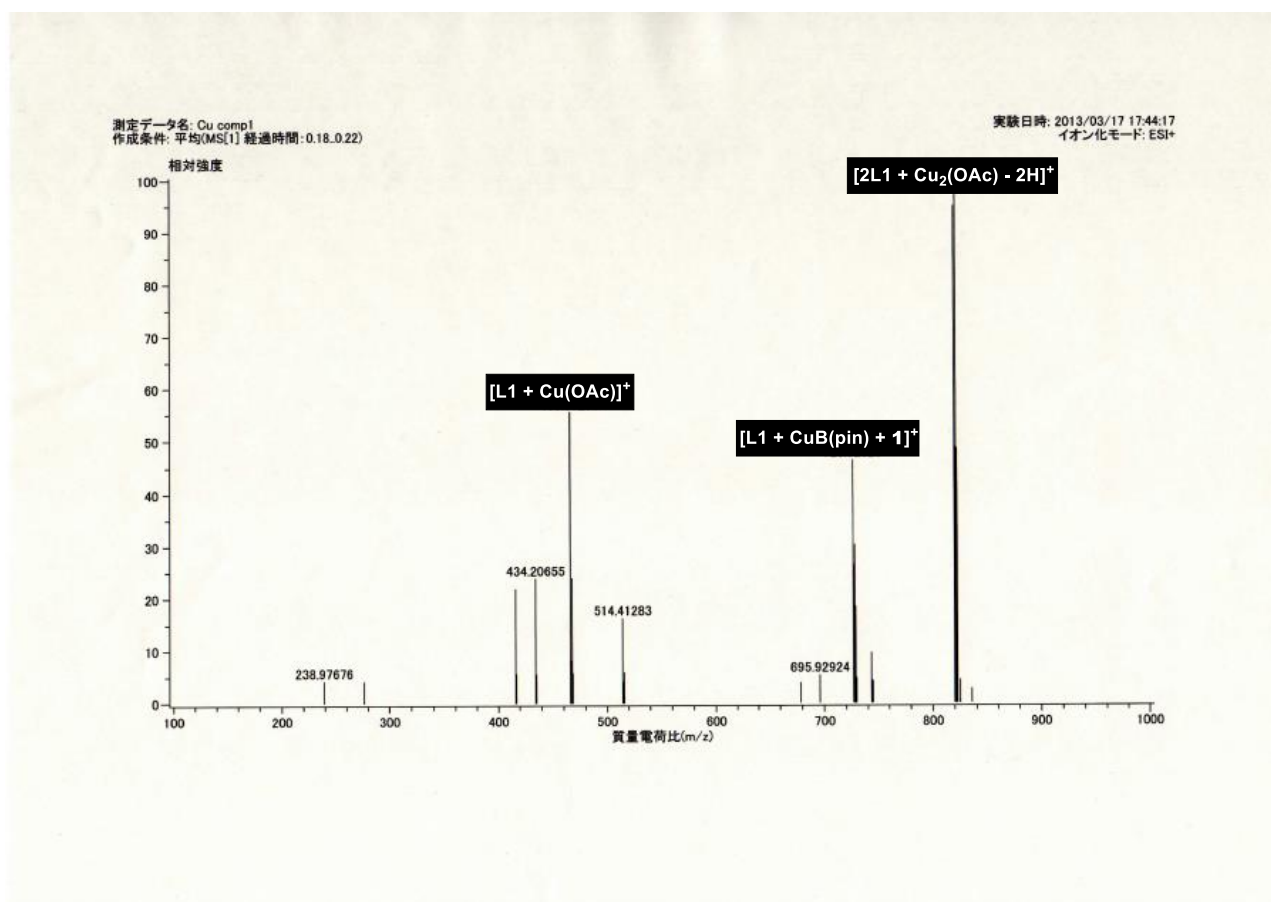
Figure 6. ESI-MS spectrum of borylcopper(II) species.

When **17b** was employed instead of **13a**, the corresponding peak of [**L1** + CuB(pin) + **17b** – H]$^+$ was detected successfully. It indicates that the postulated reaction pathway based upon Cu(II) catalysis entails the key complex consisting of enones and Cu–B species. Assumed here were the structural changes of the intermediate depending upon counteranions. As observed in ESI-MS analysis, the monomeric complex [**L1** + CuB(pin) + **13a**]$^+$ should form in the case of Cu(OAc)$_2$. Indeed, noninvolvement of oligomeric copper complex in the nucleophilic addition step is assumed through non-observation of non-linear effect in homogeneous system (**Cat 1 & 2**).
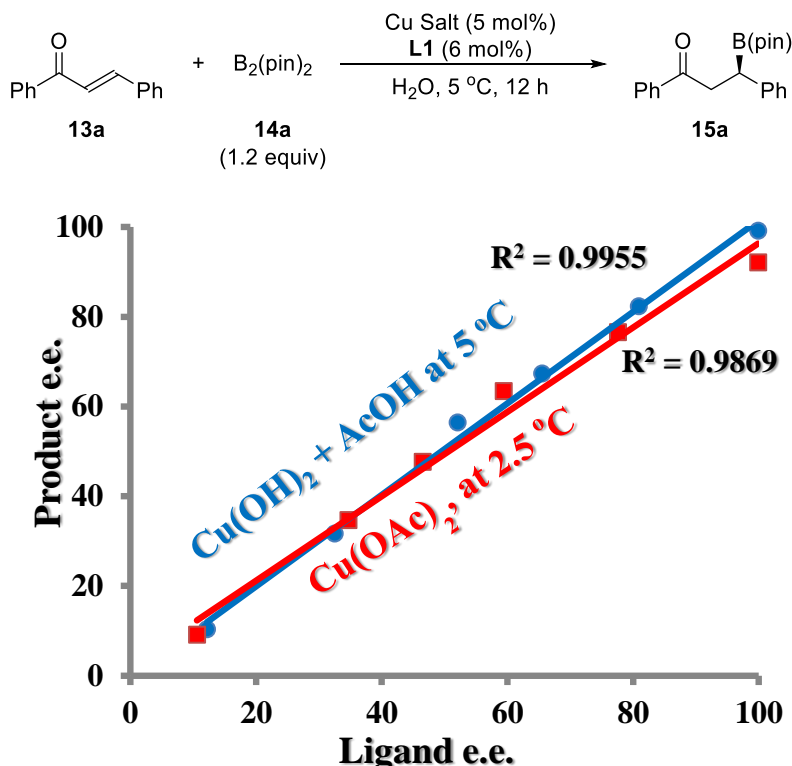
Figure 7. Non-linear experiments in homogeneous system.

It was indicated that the postulated reaction pathway based upon Cu(II) catalysis entailed the key complex consisting of enones and borylcopper(II) species generated *via* σ-metathesis. The stereochemical model of borylcopper(II)-**L1** complex is shown in Figure 8. One hydroxyl group of **L1** is in use for the coordination to Cu(II) center and the other is free, juding from X-ray crystallographic structure of Cu(II)-**L1** complex. The free OH group is highly suggested to involve in the activation of borylcopper(II) species toward the subsequent nucleophilic addition. The catalytic cycle would commence with the interaction between Cu(II) and carbonyl groups (presumably π electrons of C=O), since Cu(II) is harder Lewis acid than Cu(I) which prefers the insertion into C=C double bond. The polarization of the Cu–B bond towards the boron could facilitate the interaction. The direction of the carbonyl interaction may be determined by the steric bulkiness of chiral ligand and α,β-unsaturated carbonyl compounds. Steric bulkiness of two *tert*-butyl groups in chiral borylcopper(II) complex may give rise to enantiofacial preference towards accessible *Si* face, which is consistent with the observed sense of chiral induction. The

Cu(II) enolate formed after the nucleophilic addition is amenable to the equilibrium between *C*-enolate and *O*-enolate. The well-established Cu(I) pathway prefers *C*-enolate that can interact with the vacant p_z orbital of boron, whereas Cu(II) is presumed to be favorable to *O*-enolate due to its unsatisfied d orbital.
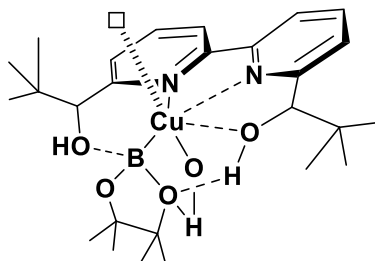
Figure 8. Structural model of the chiral borylcopper(II) complex formed with **L1**.

Unlike Cu(OAc)$_2$, the oligomeric structure of Cu(OH)$_2$ might remain stabilized by the participation of covalent property in bridged bis-μ-hydroxide. Since certain chiral induction was demonstrated, **L1** should coordinated to the polymeric copper(II) center in a tridentate manner. As depicted in Figure 9, one Cu would activate the carbonyl moiety and dimeric structure would be responsible for mounting boron on an adjacent another Cu toward the subsequent nucleophilic addition. The suitable distance between carbonyl moiety and the position expected to undergo the nucleophilic addition should be significantly longer in the reaction catalyzed by a polymeric borylcopper(II) complex than that in the reaction catalyzed by monomeric one. Thus, polymeric borylcopper(II) complex would permit a 1,6-Addition which is sterically impossible in the reaction catalyzed by a monomeric complex, which is in accord with the distance assumed as a result of calculation.
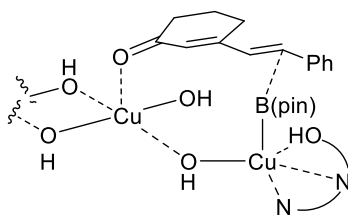
Figure 9. Polymeric borylcopper(II) complex derived from Cu(OH)$_2$ with cyclic dienone **20a**.

In order to gain experimental support for polymeric structure of borylcopper(II) complex derived from Cu(OH)$_2$, the conjugate addition to bis(dibenzylideneacetone) **27** yielded bisadduct **29** after 12 h in the presence of both Cu(OH)$_2$ and Cu(OAc)$_2$ (Table 6). However, in the initial 15 min Cu(OAc)$_2$ rendered monoadduct **28** exclusively, whereas bis-adduct **29** was observed preferentially in the presence of Cu(OH)$_2$. In a word, Cu(OAc)$_2$ provided bis-adduct **29** through a stepwise addition through a monomeric borylcopper(II) complex. A monomeric borylcopper(II) species was detected by ESI-MS spectrum ([**L1** + CuB(pin) + **27** – H]$^+$ *m/z* 902.1672). In contrat, Cu(OH)$_2$ allowed a simultaneous addition, strongly indicating a multinucleated constitution in the catalyst structure.

Table 10. Monoaddition vs. bisaddition.
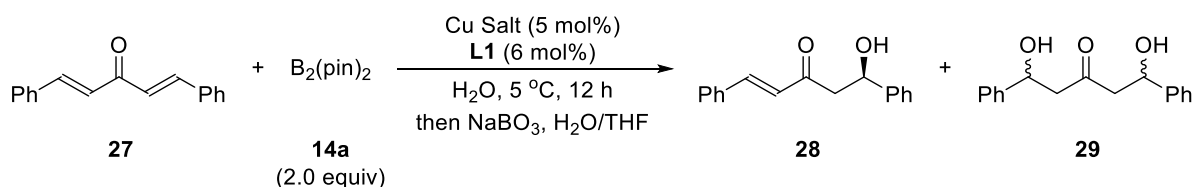
Entry	Cu Salt	Reaction Time	Yield (%)	28/29	Ee (%)[a]
1	Cu(OH)$_2$ (**Cat 1**)	15 min	16 (**28** + **29**)	12/88[b]	67/23
2	Cu(OAc)$_2$ (**Cat 3**)	12 h	56	9/91[b]	67/24
3	Cu(OH)$_2$ (**Cat 1**)	15 min	9	>99/<1	83/–
4	Cu(OAc)$_2$ (**Cat 3**)	12 h	73	37/63[c]	84/81

[a] Determined by HPLC analysis. [b] A mixture with ca. 70% of *meso*-isomers.

[c] A mixture with ca. 30% of *meso*-isomers.

Since the rapid protonation subsequent to the nucleophilic addition is expected to be responsible for liberation of the product in water, a close inspection of a protonation event will help us understand the reaction "in water" better. In order to examine each contribution of many candidates as a proton source, deuterium was introduced in copper hydroxide [Cu(OD)$_2$] or OH group in chiral ligand **L1**, resulting in exclusive protonation in the same level of enantioselective manner. Kinetic isotope effects were also explored with D$_2$O followed by the same procedure. The small isotope effect proves that the rate-determining step does not involve the protonation/deuteration of enolate intermediate (in the reaction of **13a** with **14a**; 1.01 for Cu(OH)$_2$ system (**Cat 1**) and 1.16 for Cu(OAc)$_2$ system (**Cat 3**)).[93]

Section 3.2   Asymmetric Boron Conjugate Addition of Imines in Water

3.2-1   Introduction

Enantiopure β-hydroxy imines are useful precursors of optically active γ-amino alcohols, and compounds with backbones composed of the latter are often observed in natural products including antibiotics[94] as well as in chiral auxiliaries[95] and chiral ligands[96] for asymmetric synthesis.   Asymmetric synthesis of γ-amino alcohols has received much attention in recent years because of the versatility of such compounds in chemical transformations and because of their anticipated pharmacology in areas such as "second-generation" serotonin-norepinephrine reuptake inhibitor (SNRI) antidepressants[97] and μ-opioid receptor agonist analgesics.[98] Intensivee work over the past decade on developing efficient protocols to furnish enantioenriched γ-amino alcohols has led to the emergence of asymmetric catalysts for the construction of suitable precursors.   A widely implemented technique is based upon asymmetric synthesis of precursors such as β-hydroxy imines,[99,100] β-amino carbonyl compounds,[101] and isoxazolidines,[102] or other cyclic compounds,[103] followed by appropriate selective reduction.   A limited number of reports on β-hydroxy imines have been published[100,104] whereby chiral Cu(I) catalysts were used for asymmetric β-borylation of electron-deficient alkenes as mentioned above.   These protocols entailed the use of air-sensitive phosphine ligands as well as the addition of strong bases such as sodium *tert*-butoxide to activate bis(pinacolato)diboron.[105]

3.2-2 *Optimization of Reaction Conditions and Unique Reactivities*

In order to examine the applicability of newly-developed chiral Cu(II) catalysis, the use of imines in water was focused upon. While imines (Schiff bases) are versatile intermediates in organic transformations, their use in water is very limited because they readily decompose in the presence of even a small amount of water.

At the outset, $Cu(OH)_2$ with chiral 2,2'-bipyridine (**Cat 1**) was applied to the reaction of benzalacetone-derived imines with bis(pinacolato)diboron in water (Table 11). As described above, despite the insolubility of all materials (both substrates, $Cu(OH)_2$ and chiral ligand) in water, the reaction of benzalacetone proceeded smoothly to afford the desired product in high yield with moderate enantioselectivity after subsequent oxidation (entry 1). Whereas the reactions of α,β-unsaturated imines derived from isopropylamine or aniline gave low yields with low enantioselectivities (entries 2 and 3), the use of the α,β-unsaturated imines derived from benzylamine resulted in high reactivity and excellent enantioselectivity (entry 4). Besides steric hindrance, the exocyclic C=N double bonds as well as C=C bonds tend to undergo the isomerization,[106] exerting the influence on the stereochemical outcomes. The reactions of α,β-unsaturated oxime or hydrazone produced poor results, presumably because of the strong coordination between copper and the substrates (entries 5 and 6).

Table 11. Comparative reaction of benzalacetone and the corresponding imines.
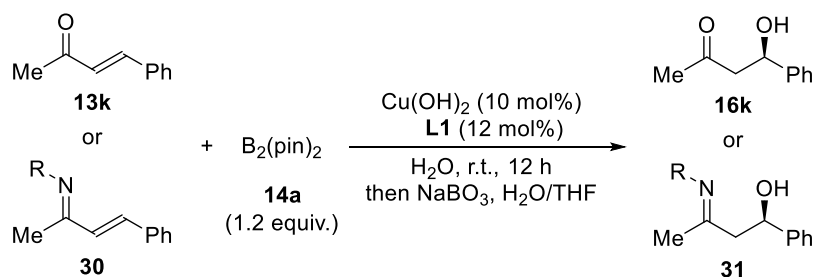
Entry	R	Yield (%)[a]	Ee (%)[b]
1[c]	–	84	65
2	^{i}Pr	20	32
3	Ph	19	35
4	**Bn**	**65**	**99**
5	OH	43	17
6	NHPh	Trace	–

[a] Isolated yield. [b] Determined by HPLC analysis.
[c] Performed with 5 mol% catalyst loading at 5 °C.

Based on the fact that β-borylation reactions of multifarious unsaturated compounds were efficiently catalyzed in water by chiral Cu(II) complexes formed from $Cu(OH)_2$ or $Cu(OAc)_2$, irrespective of whether the catalyst was homogeneous or heterogeneous, the effect of Cu(II) salts on the outcome of the reaction was then examined (Table 12). The addition of one equivalent of AcOH to $Cu(OH)_2$ increased the reactivity slightly while retaining excellent enantioselectivity (entry 2). The catalytic system became homogeneous under these conditions, which implied an

exchange of one hydroxide with an acetate group. Catalytic use of Cu(II) acetate resulted in higher yield of the desired product, which was formed with >99% *ee* (entry 3). Whereas a similar result was obtained by decreasing the catalyst loading from 10 to 5 mol%, the yield and the enantioselectivity decreased slightly when 1 mol% catalyst was used (entries 4 and 5). Copper salts with more nucleophilic counteranions such as Cl^- and SO_4^{2-} exhibited lower enantioselectivity compared with Cu(OTf)$_2$, and the use of Cu(OTf)$_2$ gave a poor yield (entries 6–8). Performing the reaction with Cu(II) acetylacetonate afforded similar results to those obtained with Cu(II) acetate (entry 9).

Table 12. Effect of copper salts.
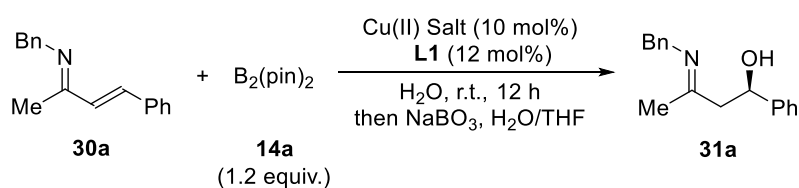
Entry	Cu Salt	Yield (%)[a]	Ee (%)[b]
1	Cu(OH)$_2$	65	99
2[c]	Cu(OH)$_2$	69	99
3	Cu(OAc)$_2$	83	99
4[d]	Cu(OAc)$_2$	86	99
5[e]	Cu(OAc)$_2$	67	94
6	CuCl$_2$	10	45
7	CuSO$_4$	43	85
8	Cu(OTf)$_2$	5	99
9	Cu(acac)$_2$	80	99

[a] Isolated yield. [b] Determined by HPLC analysis.

[c] 10 mol% of AcOH was added as an additive.

[d] 5 mol% of catalyst loading. [e] 1 mol% of catalyst loading.

A range of α,β-unsaturated imines underwent Cu(II)-catalyzed enantioselective β-borylation to afford the desired enantioenriched β-hydroxy imines in high yields with excellent enantioselectivities (Scheme 42). It is noteworthy that imines bearing chalcone and benzalacetone backbones gave β-hydroxy imines with outstanding enantioselectivities (>99% *ee*). The use of a substrate with an electron-withdrawing substituent at the β-position resulted in lower enantioselectivity.
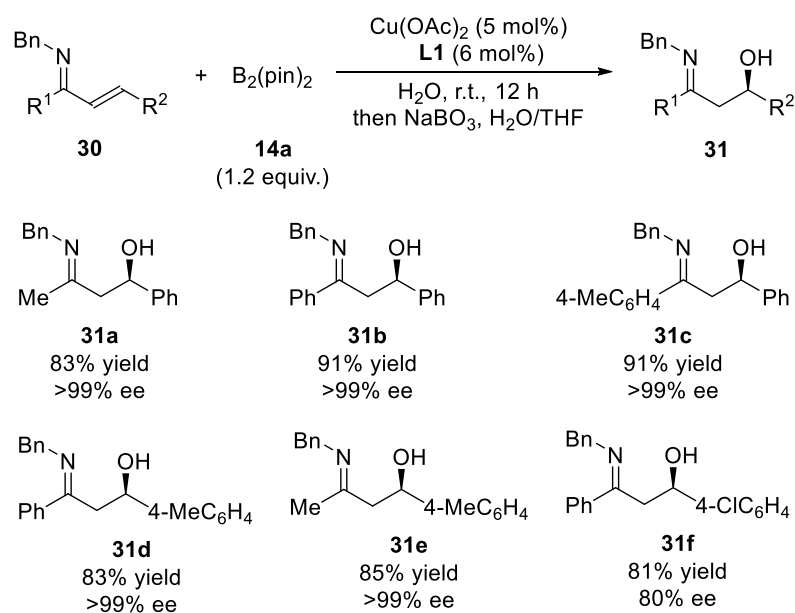
Scheme 42. Enantioselective β-borylation of α,β-unsaturated imines.

The decomposition rate of imine was measured (Table 13). It was revealed that the appropriate value of pH allowed α,β-unsaturated imine tolerant against the decomposition and that Cu(II) species may stabilize α,β-unsaturated imine in water.

Table 13. Decomposition study of α,β-unsaturated imine in water.
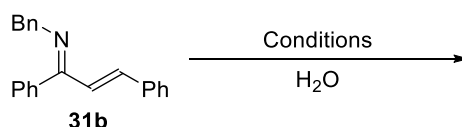
Condition \ Time	Recovery yield				
	15 min	**30 min**	**60 min**	**3 h**	**2 h**
Cu(OAc)$_2$ (aq)	93%	90%	84%	7%	9%
Cu(OAc)$_2$+L1 (aq)	97%	95%	92%	9%	3%
H$_2$O only	Quant.	97%	95%	4%	0%
Pyridine (aq)	Quant.	Quant.	Quant.	5%	5%

The reaction profile of Cu(OAc)$_2$-catalyzed β-borylation reactions of an α,β-unsaturated imine was compared with that of the reaction of the corresponding ketone (Figure 10). Although the β-borylation of the α,β-unsaturated imine was slightly slower than that of the corresponding ketone, the relatively rapid completion of the reaction implied sufficient and efficient activation of the α,β-unsaturated imine by Cu(OAc)$_2$.
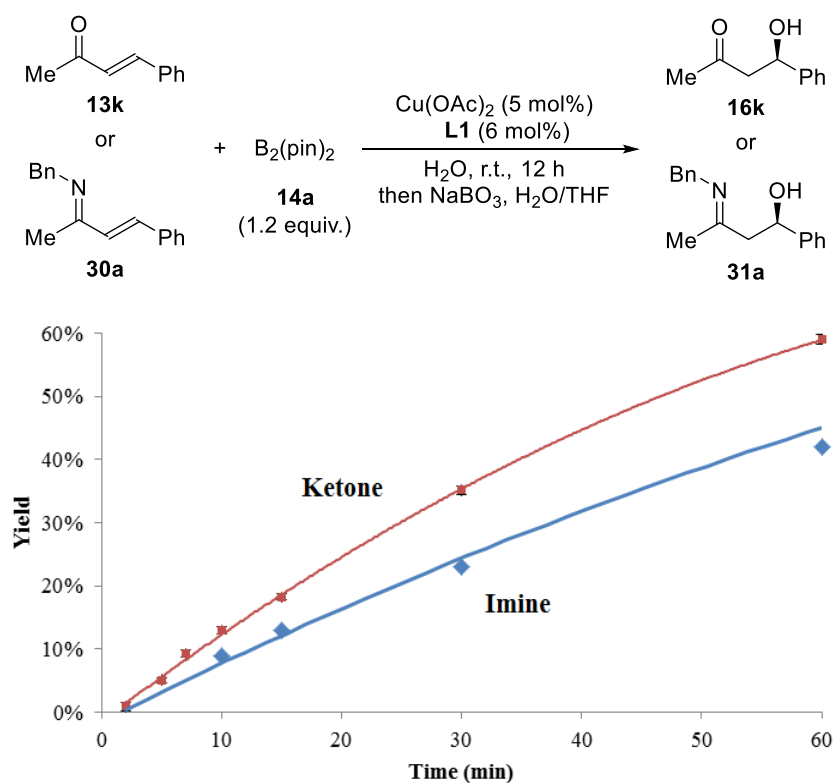
Figure 10. Competitive reactivity against α,β-unsaturated ketone and the corresponding imine as an independent system.

On the other hand, when a 1:1 mixture of benzalacetone **13k** and the corresponding imine **30a** was added to the catalyst solution, ketone **13k** was consumed almost quantitatively and the competitive β-borylation of the imine **30a** was clearly hampered (Scheme 43). Considering decomposition of the imine in water, the amounts of recovered imine and the ketone are reasonable. The preferential consumption of the α,β-unsaturated ketone over the corresponding imine under Cu(II) catalysis is interesting, considering the preferential activation of an aldimine over an aldehyde by a Cu(II) salt.[107]
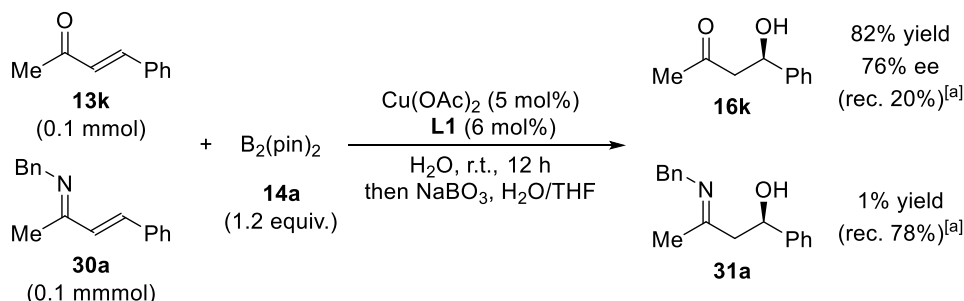
Scheme 43. Competitive reactivity against α,β-unsaturated ketone and the corresponding imine as a mixed system.

Based upon aforementioned mechanism for β-borylation of α,β-unsaturated carbonyl compounds in water, the asymmetric boron conjugate addition to α,β-unsaturated imines in water is assumed to follow the catalytic cycle shown in Scheme 44.   *In situ* formation of a borylcopper(II) species was confirmed by ESI-MS analysis, and this intermediate was assumed to be a key component in the Cu(II) catalysis.   In contrast to Cu(I) catalysis, which demands a strong base to activate diboron, counteranions of Cu(II) salts or noncoordinating hydroxy groups of the chiral ligand (**1**) were expected to function as an activator in water, resulting in potentially base-free conditions.   Given the instability of the d^9-π interaction due to its unpaired electron, a nucleophilic addition would take place to produce an *N*-enolate intermediate **3**.   The polarization of the Cu–B bond toward the boron could facilitate the interaction.   Steric bulk of the two *tert*-butyl groups in the ligand may give rise to enantiofacial preference toward the more accessible *Si* face, which is consistent with the observed sense of chiral induction.   Because the proton-transfer rate in water is known to be in the order of picoseconds, rapid protonation subsequent to the nucleophilic addition would afford the product in water, lowering the activation energy and facilitating the catalytic turnover.
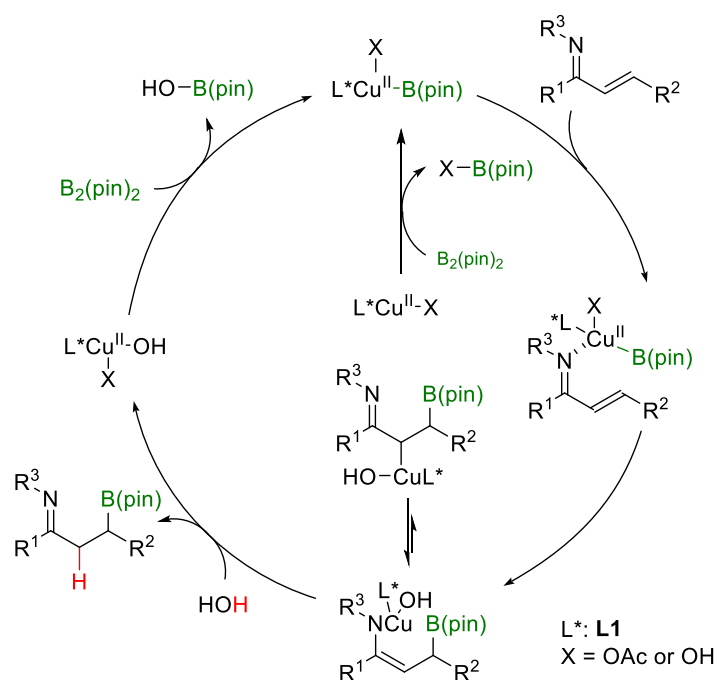
Scheme 44. Proposed mechanism of Cu(II) catalysis.

It was found that a chiral Cu(II) complex formed with chiral 2,2′-bipyridine was suitable for use in the β-borylation of to α,β-unsaturated imines in water.   The use of Cu(OAc)$_2$ as the Cu(II) source gave superior performance, affording enantioenriched β-hydroxy imines after oxidation, which are known to be useful precursors of γ-amino alcohols.   Excellent stereocontrol was achieved with a range of substrates.   In contrast to the known Cu(I) catalyses in organic solvents, this Cu(II) protocol in water is expedient and free from the use of air-sensitive phosphine ligands and strong bases.   The use of unstable imines in water is also remarkable.

Section 3.3   Catalytic Use of Copper(0) for Asymmetric Boron Conjugate Addition in Water

3.3-1   Initial Discovery

An extensive effort dedicated to deepen our understanding of copper catalysis in water led to the discovery of novel Cu(0) catalysis.   To my astonishment, a simple combination of Cu(0) powder[108] and 2,2'-bipyridine **L1** could catalyze asymmetric β-borylation of chalcone **13a** with **14a** in water without any additive.   It is noteworthy that despite insolubility of all materials (both substrates **13a** and **14a**, Cu(0) and chiral ligand **L1**) in water, the desired product was obtained in 92% yield with 83% ee (Table 14, entry 1; pictures below table shows the change in appearance of the reaction system during the reaction).[109] As a control experiment, the reaction did not proceed at all in the absence of Cu(0).   The heterogeneity of the catalysis was verified by filtration experiments. After the reaction completed, glutinous precipitates were observed on a wall of a reaction flask. Thermal exposure is essential to some extent for the catalysis because the reaction did not take place at all below 20 $^{\circ}$C.   A deficiency in reactivity without any solvent emphasizes the pivotal role of water in this reaction (entry 2).   Although aprotic solvents were ineffective for the Cu(0) catalysis (entries 3-6), acetonitrile afforded the desired product in moderate yield with low selectivity (entry 7).   Alcohols as solvents also showed the same levels of the reactivity as acetonitrile with moderate enantioselectivities (entries 8, 9).

Table 14. Effect of solvent in Cu(0) catalysis.
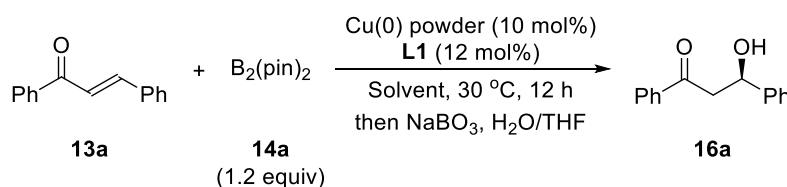
Entry	Solvent	Yield (%)[a]	Ee (%)[b]
1	H$_2$O	92	83
2	neat	NR	–
3	Toluene	NR	–
4	DCM	NR	–
5	DMF	NR	–
6	THF	NR	–
7	MeCN	52	30
8	MeOH	45	57
9	EtOH	60	60

[a] Isolated yield.   [b] Determined by HPLC analysis.

Heterogeneous!

12 h

Aggregation

It was revealed that other metal(0) also displayed the catalytic activity in boron conjugate additions (Table 15).   The catalytic activity of Cu(0) is, however, outstanding in terms of both reactivity and enantioselection.

Table 15. Effect of metal(0).
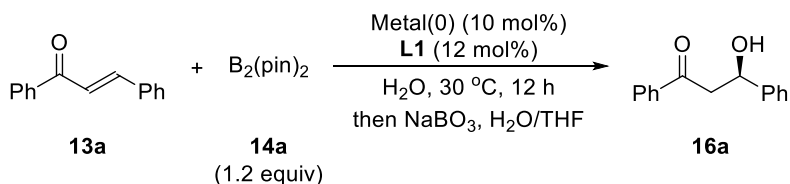
Entry	Cu salts	Yield (%)[a]	Ee (%)[b]
1	Ni(0)	NR	-
2	Zn(0)	3	8
3	In(0)	5	6
4	Bi(0)	2	18

[a] Isolated yield.   [b] Determined by HPLC analysis.

Assuming the precise exertion of Cu(0) catalysis, electron transfer between Cu(0) and chiral ligand should play a prominent role in determining catalytic activity as well as stereocontrol. Chiral 2,2'-bipyridine **L1** rendered the best result among the screened chiral ligands (Scheme 45). The box-type ligands **L31-33** or diamine ligand **L30**, which are known to be an efficient catalyst in the presence of Cu(I) or Cu(II) salts in a number of reactions, did not give good results.   In addition, bis(oxazolinyl)pyridine derivatives **L13** & **L34** afforded the product in good yield with moderate enantioselectivity.   Generally speaking, chiral ligands containing nitrogen and hydroxyl group in the structure exhibited comparatively higher reactivity.   For example, (*S*)-quinidine **L36** and (*R,R*)-bisprolinol **L13** gave the product in high yield, albeit in almost no selective manner. Although the structure of *N,N,O,O*-cavity (**L35**, **37**, **38**) was also evaluated based on the structure of **L1**, the reaction suffered from low yield and low enantioselectivity.   The use of Josiphos ligand **L40** led to high level of enantioselectivity but reactivity is lower.   Introduction of larger bulkiness in the side chain in 2,2'-bipyridine led to the significant decrease in both reactivity and

enantioselectivity (**L7**).   Less bulkiness had the same tendency for reactivity and enantioselectivity (**L4**).

Scheme 45. Evaluation of chiral complexes formed with Cu(0) in water.

3.3-2   Difference between Cu(0), Cu(I) and Cu(II)

It was so far demonstrated that either Cu(I) or Cu(II) can catalyze the reaction of **13a** with **14a** in the coexistence of **L1**.   The difficulty of distinguishing three oxidation states would place obstacles on the road to clarification of the reaction mechanism.[110]   In that sense, their behaviors on the asymmetric β-borylation were examined in water (Table 16).   *In situ* prepared Cu(0) fine particles, generally fabricated utilizing a Cu(II) salt, ascorbic acid and sometimes SDS in aqueous media,[111]   provided the similar result as that in entry 1 (entry 2).   A combination of Cu(II) with **L1** exhibited inferior performance (entry 4), whereas the use of Cu(I) in the reaction performed in water led to an intermediate result between those of Cu(0) and Cu(II) (entry 3).   We have a suspicion of competitive reaction pathways involving Cu(0) and Cu(II) *via* a disproportionation from Cu(I), since immediate precipitation of Cu(0) was observed.   Although Cu(I)-**L1** complex (similar Cu(I)-**L3** complex was shown in Figure 11) exhibited catalytic activity in THF when 1 equivalent of MeOH was added, the obtained borylated product **15a** was completely racemic (Scheme 47).   Judging from this result, we confirmed that catalysis exerted in the presence of Cu(0) was quite different from that exerted by Cu(I).   The superior performance in the presence of Cu(0) implies chiral induction exerted by Cu(0) catalysis.

Table 16. Effect of copper salts with various oxidation states.

Entry	Cu salts	Yield (%)[a]	Ee (%)[b]
1	Cu(0)[c]	92	83
2	Cu(0)[d]	82	81
3	CuCl	79	71
4	CuCl₂	71	61

[a] Isolated yield.   [b] Determined by HPLC analysis.

[c] Prepared from CuSO₄ by preferential oxidation of the zinc(0) atom.

[d] Prepared *in situ* from CuCl₂ in the presence of *L*-ascorbic acid (vitamin C) as a reductant.

Scheme 47. β-borylation catalyzed by Cu(I)-**L1** complex in organic solvent with an alcohol additive.

Figure 11. X-ray crystal structure of [CuBr$_2$·**L1**·H$_2$O] (left) and [CuCl·**L3**] (right).

Unselective deuteration experiments displayed by Yun *et al.* resulted from a rapid quenching of a *C*-enolate intermediate (Scheme 48a).[38] Meanwhile, Cu(II) catalysis furnished the α-deuterated borane with *syn*-selectivity in D$_2$O (Scheme 48b). The intrinsic *syn*-preference of the deuteration at the α-position was contrastive to almost unselective result reported by Yun *et al*. Given instability of the d^9-π interaction due to its unpaired electron, this impressive phenomenon can be elucidated by enantiofacial differentiation of an *O*-enoalte intermediate toward deuteron. When Cu(0) was employed instead of Cu(II), the identical preference toward the *syn*-conformation was observed (Scheme 48c). In contrast to non-materialization of a deuterium kinetic isotope effect in Cu(II) catalysis, deuterium oxide retarded the reaction rate in the presence of Cu(0) and a slight decrease in the enantioselectivity of the α-deuterated borane was observed.
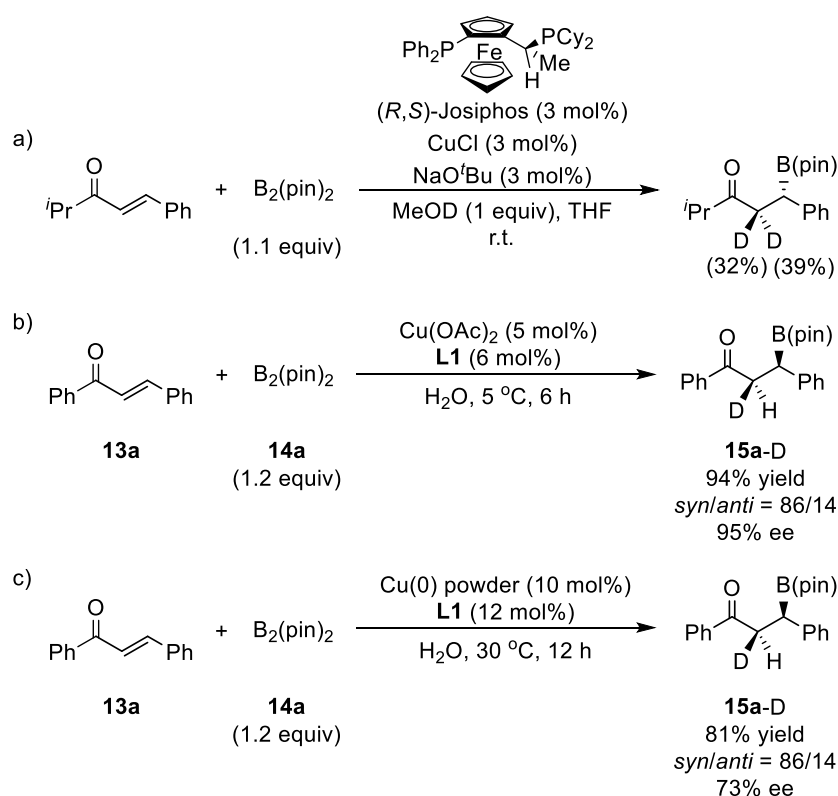
Scheme 48. Deuteration experiments for a) Cu(I),[38] b) Cu(II) and c) Cu(0) catalyses.

Assuming the precise exertion of the Cu(0) catalysis, electron transfer between Cu(0) and a chiral ligand should play a prominent role in determining catalytic activity as well as stereocontrol. In order to gain insights into catalyst structures, the role of hydorxy groups in **L1** was investigated (Table 17).   The reaction catalyzed by the Cu(II)-**L1** complex did not require both hydroxyl groups; a chiral catalyst composed of Cu(OH)$_2$ and **L2**, in which one hydroxyl group was protected with a methyl group, afforded almost the same result (Condition B).   Indeed, the crystallographic structure of the CuBr$_2$-**L1** complex adopts a square pyramidal structure as mentioned above (Figure 11).   In contrast, the use of **L2** led to a significant drop in both reactivity and enantioselectivity in the presence of Cu(0) (Condition A)

Table 17. Effect of OH group in chiral ligands.
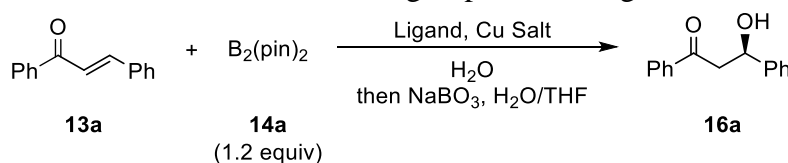
Entry	Ligand	Condition A[a]		Condition B[b]	
		Yield (%)[c]	Ee (%)[d]	Yield (%)[c]	Ee (%)[d]
1	**L1**	92	83	83	81
2	**L2**	31	30	82	77

[a] Condition A: Cu(0) powder (10 mol%), Ligand (12 mol%), 30 ^{o}C, 12 h.

[b] Condition B: Cu(OH)$_2$ (5 mol%), Ligand (6 mol%), 5 ^{o}C, 12 h.

[c] Isolated yield.   [d] Determined by HPLC analysis.

When methyl-substituted chiral 2,2'-bipyridine **L4** was mixed with Cu(0) powder in water, homogeneous red solution was unexpectedly obtained.   The homogeneity of the catalyst solution was confirmed by a filteration test.   It is noted that this red solution (Figure 12, left) turned green (Figure 12, right) after exposed to oxidant such as H$_2$O$_2$ or air (5 days or longer is necessary for aerobic oxidation).   A reduction of the green solution could regenerate the red solution.
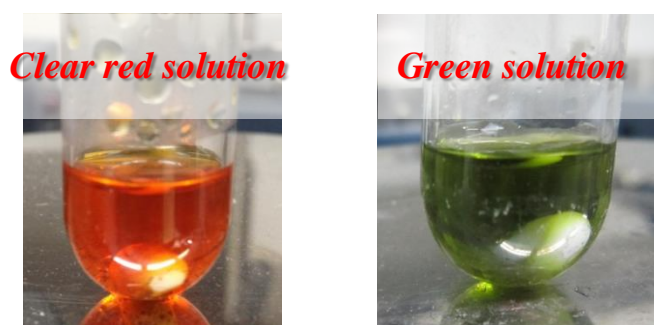
Figure 12. Catalyst Solution composed of Cu(0) and **L4** (left) and Oxidized Catalyst Solution (right) in Water.
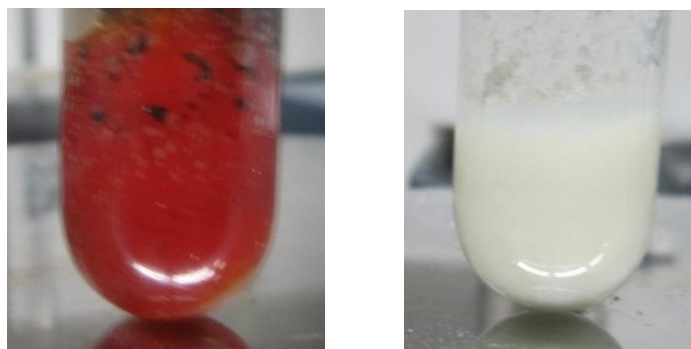
Figure 13. Catalyst solution [**after 12 h**] composed of Cu(0) and **L4** (left) and Oxidized Catalyst Solution (right) in Water.

When amenable to ESI-MS analysis, the former red solution showed a single strong signal (Figure 14, above).   Judging from molecular weight and isotope pattern, this peak corresponded to $[Cu^I(\mathbf{L4})_2]^+$ formed with Cu(I) and 2 equivalents of the chiral ligand.   Contrariwise, spectrum of the green solution attributed to multifarious peaks, which corresponded to multi-nuclear Cu(II) species such as $[Cu^{II}(\mathbf{L4})_2–H]^+$, $[Cu^{II}_2(\mathbf{L4})_2–3H]^+$, $[Cu^{II}_2(\mathbf{L4})_3–3H]^+$, $[Cu^{II}_3(\mathbf{L4})_3–5H]^+$ and so on (Figure 14, below).   Notwithstanding the detection of Cu(I) species in the red solution, observing considerable multi-nuclear species in the oxidized condition may imply the existence of Cu(0) in the red solution.[112] Indeed, reduction or oxidation of metal center under electrospray conditions is known.[113] According to Cole *et al.*, the electrospray instrument produces higher abundance intact molecular cations from compounds with relatively low half-wave potentials for oxidation [$E_{1/2}$(ox)] and ionization energies (IE) values.[113b] Copper meets the criteria, which they showed [$E_{1/2}$(ox) < 1.0 V *vs* SCE, and IE < 8.0 eV].[114]
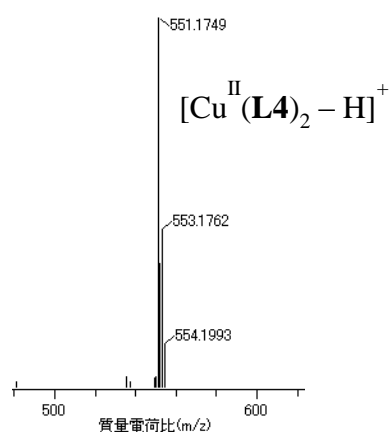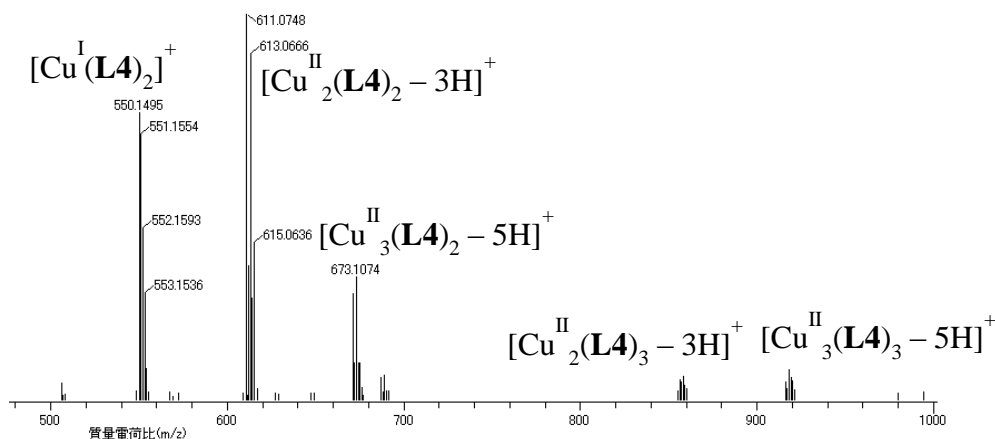
Figure 14. ESI-MS Spectra of aqueous solution prepared by mixing Cu(0) and **L4** before (above) and after (below) oxidation.

Figure 14 shows the UV-vis absorption profiles of the Cu(0)-**L4** complex before and after oxidation. Adsorption bands at less than 400 nm in the UV region was attributed to π-π^* transitions of **L4**.[115] In the former red solution, well-defined two peaks were detected at 432 and 970 nm (Figure 15, above). The peak at 432 nm may be ascribed to the interband electronic transitions due to the discrete energy levels.[116] The absorption at 970 nm indicates a peudo-tetrahedral geometry. The latter green solution showed broad and weak peak at 650 nm and strong peak at 975 nm (Figure 15, below). The absorption at 650 nm is believed to originate from LMCT (Ligand to Metal Charge Transfer), which is characteristic of Cu(II).[115] The latter absorption may be assigned to the transition of d_{xz} or $d_{yz} \rightarrow d_{x^2-y^2}$, indicating a trigonal bipyramidal geometry.[116] Although we can distinguish neither catalysis of Cu(0) nor Cu(I) through ESI-MS and UV-vis analysis, the possibility that the red solution was identified as Cu(II) was absolutely denied. Although able to prove the formation of a complex between Cu and **L4**, NMR spectra of both red and green solutions were identical to each other (Figure 16).
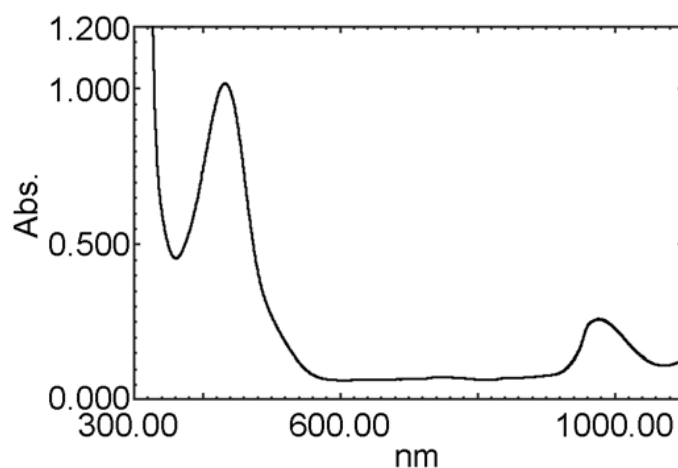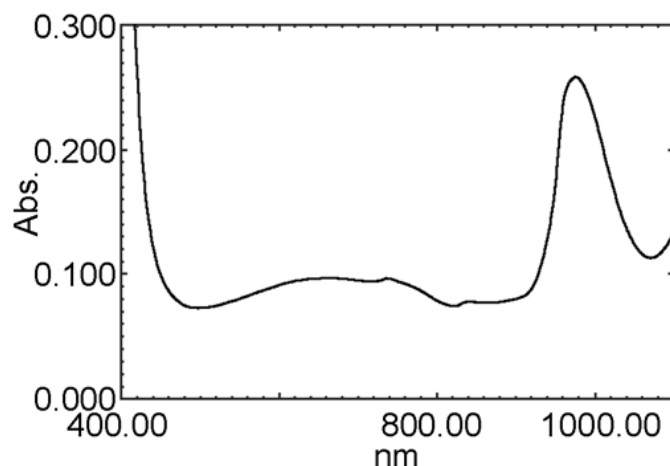
Figure 15. UV-vis spectra of aqueous solution prepared by mixing Cu(0) and **L4** before (above) and after (below) oxidation.
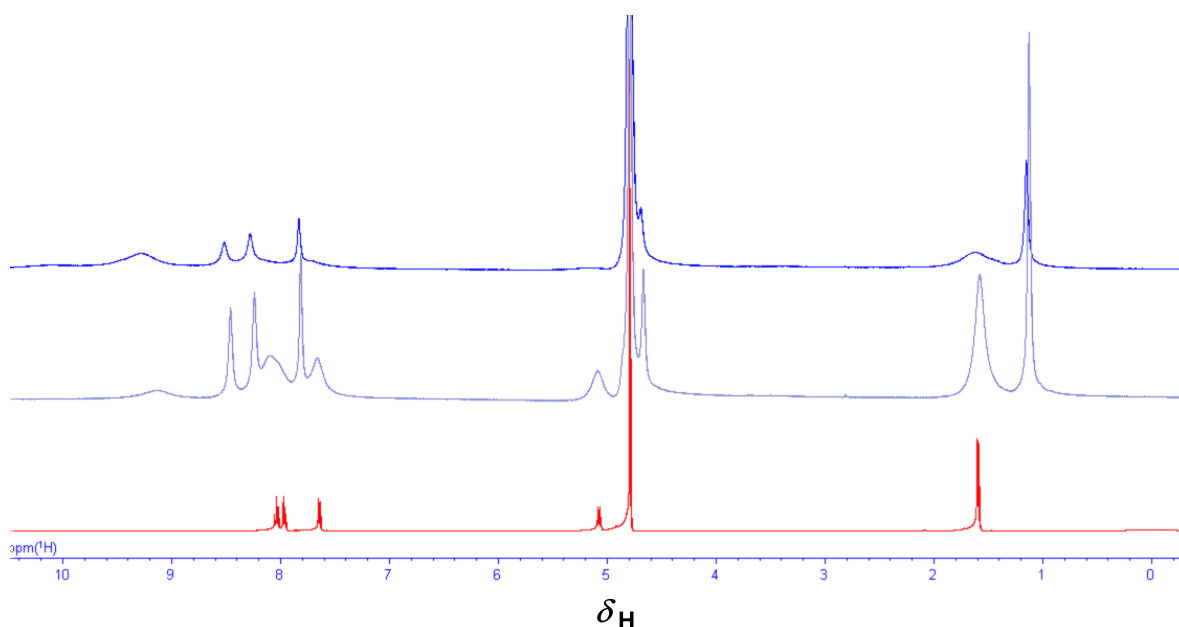
Figure 16. NMR spectra of aqueous solution prepared by mixing Cu(0) and **L4** before (middle), after (above) oxidation and that of **L4** itself (below).

In contrast to classical Cu(I) protocols, where the range of applicable substrates is known to be highly dependent upon the chiral ligand, the Cu(II) protocol established recently is a versatile system, which covers a wide range of substrates, including α,β-unsaturated ketones, esters, amides, nitrile and β,β-unsaturated compounds whether cyclic or acyclic. In opposition to them, Cu(0) catalysis exhibited definite substrate specificity (Scheme 49). While phenylpropenylketone (**13g**) and benzalacetone (**13k**) reacted with diboron successfully to afford the desired products **16g** and **16k**, respectively in high yields with good enantioselectivities, the reaction of 4,4-dimethyl-1-phenylpent-2-en-1-one (**13j**) suffered from a significant decrease in reactivity. In addition, the reactions of cyclic enones **13l**, α,β-unsaturated ester **13r**, and amide **13x** hardly proceeded. Extended conjugation **17b** did not react under Cu(0) catalysis, neither. These results

indicate that electron density of the π-orbital on the olefin moiety and the coordination ability of the carbonyl moiety are vital for comprehending the catalysis of Cu(0).
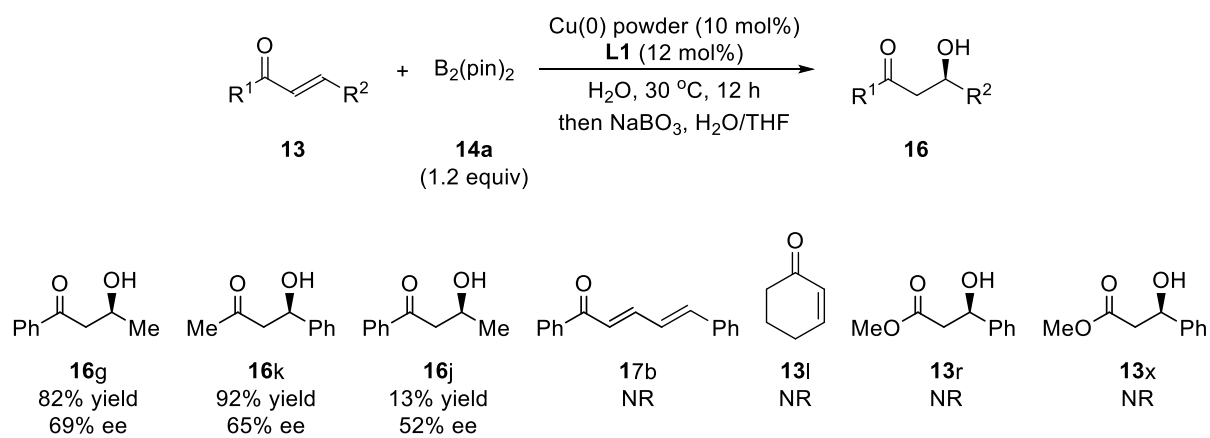
Scheme 49. Substrate specificity for Cu(0) catalysis.

3.3-3 Mechanistic Considerations

Three different alternatives to elucidate the reaction mechanism in the presence of Cu(0) are conceivable.   (1) Simple Cu(I)-catalyzed pathway.   (2) Cu(II)-catalyzed pathway.   (3) A radical intermediate *via* single electron transfer.   (4) Oxidative addition of an enone on Cu(0) resulting in an intermediate Cu(II) species.   Alternative (1) can be excluded by the inconsistency in catalytic activities between Cu(0) and Cu(I) (Scheme 47, Table 15).   Alternative (2) is an irrelevant argument, denied by many facts including spectrometric investigations.   Radical trap experiments using TEMPOL were suggestive of the existence of undominated and competitive radical pathway (3).

In order to examine the involvement of SET pathway in the reaction mechanism, addition of a radical trap in the reaction solution was carried out (Scheme 50).   Since it was confirmed that TEMPO itself did not react directly with bis(pinacolato)diboron,[117] TEMPO was chosen as a suitable radical trap.   Contrary to my expectation, the significant suppression was observed in the case of both Cu(0) and Cu(OH)$_2$.   In both cases almost same level of reactivity was obtained.   It was also turned out that TEMPOL itself could catalyze the reaction sluggishly.   Hence we could not deny the existence of the competitive pathway involving radical intermediate as a minor pathway.   A SET on the Cu(0) surface is, however, still an alternative mechanistic possibility and cannot be excluded.
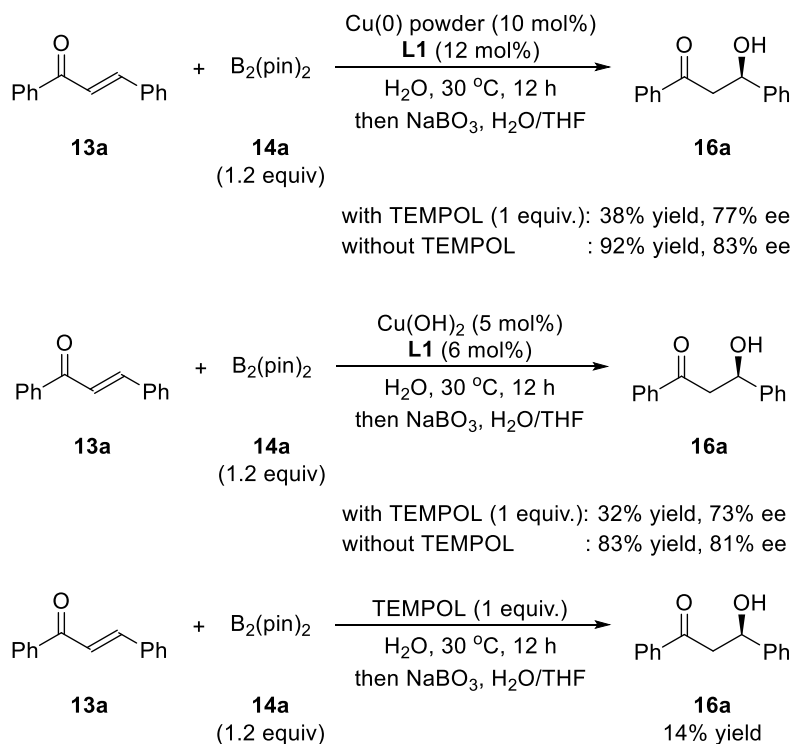
Scheme 50. Radical trap experiments.

It should be noted again that elevated temperature is indispensable for the regular reaction pathway and that an active species tends to aggregate after the completion of the reaction.   The strict substrate specificity suggests a vital interaction between Cu(0) and an enone.   An exiguous

isotope effect is indicative of an instantaneous protonation. Taking the empirical information into consideration, it is likely that the reaction pathway would involve oxidative cyclometalation as a rate-determining step, in accord with some reported examples (Scheme 51).[118] The subsequent transmetalation with bis(pinacolato)diboron would furnish a boron enolate intermediate. Reductive elimination would release the 1,4-diborated product. The B-O bond of the 1,4-diborated product is known to be hydrolyzed rapidly to afford a β-borylated ketone.[23] In that sense, we tentatively consider preferential hydrolysis of a boron enolate and the subsequent reductive elimination in water. In an aprotic solvent such as MeCN, the generated 1,4-diborylated product would be converted into the corresponding β-borylated ketone by aqueous treatment. The hydroxy groups in the chiral ligand would regulate redox of copper. The detailed mechanism is still under debate.[119]
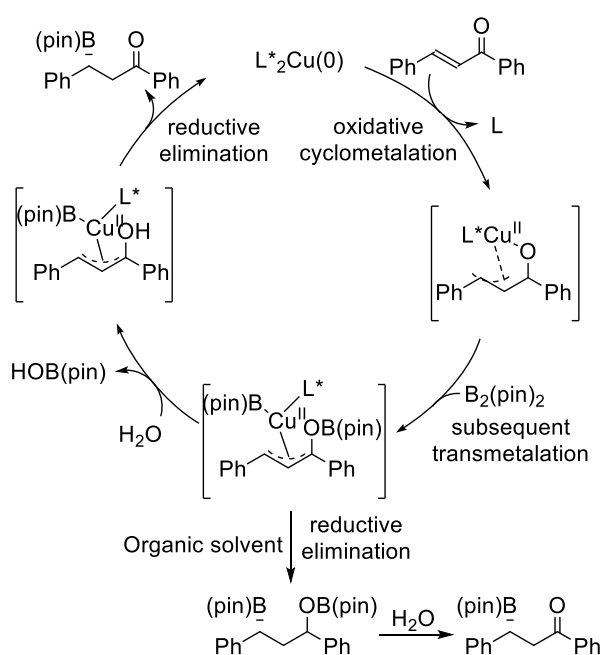
Scheme 51. Tentative Reaction Mechanism involving Cu(0).

Section 3.4   New Insight into Cu(II) Catalysis for Asymmetric Boron Conjugate Addition

3.4-1   Consideration on mechanistic disparity between Cu(I) and Cu(II) catalyses

First of all, the scattered discussions on the mechanism of Cu(I) and Cu(II) catalysis. It is assumed that the observable disparities between Cu(I) and Cu(II) catalyses should arise from their mechanistic difference. The assumed catalytic cycle commences with insertion of *in situ* generated Cu-B bond into C-C double bond, which is activated by the coordination of a base to boron.[33b] Although the formed intermediate is in equilibrium between *O*-enolate and *C*-enolate tautomers, a preference for *C*-enolate over *O*-enolate is generally accepted.[38] The cleavage of *O*-enolate is almost barrierless, whereas that of *C*-enolate is energetically unfavorable. In Cu(I) chemistry, it is believed that methanol facilitates the subsequent liberation of the borylated product through alcoholysis along with the formation of a reactive Cu-OMe complex (Scheme 26).[71] A protonation step where Cu(I)-enolate intermediate is quenched by methanol is generally considered to be a rate-determining step. In contrast, Cu(II) seems to prefer a lone pair electron on the carbonyl oxygen to a π-electron of double bond because of an intrinsic instability of the d^9-π interaction caused by its unpaired electron, implying an alternative mechanism involving an *O*-enolate intermediate. The expected lowering the energy barrier at the protonation step in water would force an another step to be a rate-determining step, which is supported by a small solvent kinetic isotope effect. From an experimental approach, a homogeneous solution of Cu(OAc)$_2$ with chiral 2,2'-bipyridine **L1** in aqueous tetrahydrofuran was successfully amenable to ESI-MS instrument together with chalcone **13a** and bis(pinacolato)diboron **14a**, resulting in a strong peak corresponding to $[\mathbf{L1} + \mathrm{CuB(pin)} + \mathbf{13a}]^+$ in the light of isotope pattern. The working hypothesis on homogeneous catalysis of Cu(OAc)$_2$ in water is mainly classified into two possible catalytic cycles to rationalize these results (Scheme 52). Both mechanisms follows the same road starting from a borylcopper(II) species and leading to a C–B bond formation. A key borylcopper(II) intermediate would undergo an electronic stabilization through an orbital overlap between a vacant *p* orbital of boron and an occupied *p* orbital of OH oxygen of **L1**. The stereochemical trajectory of **1a** toward Cu(II) center would be regulated toward accessible *Si* face through a donation of C=O π electrons toward Cu(II) center and the steric bulkiness of *tert*-butyl groups of **L1**, which is consistent with the observed sense of chiral induction. The polarization of Cu-B bond toward the boron would trigger the subsequent bond rearrangement *via* a six-membered transition state. The resultant Cu(II) enolate is in the equilibrium between *C*-enolate and *O*-enolate intermediate with a predominant presence of the latter one. In the ***route (A)***, the interaction between *O*-enolate intermediate and diboron reagent furnishes 1,4-diborated enolate along with regeneration of a key borylcopper(II) species. The B–O bond of the 1,4-diborated product is hydrolyzed rapidly to afford a desired β-borylated ketone.[23] The ***route (B)*** involves a rapid quenching of Cu(II) *O*-enolate intermediate by water or *in situ*-formed AcOH. The pH measurement of the reaction solution revealed that the pH value ranged from 4 to 5 in the course of Cu(OAc)$_2$-catalyzed reaction of **13a** with **14a** (see Section 3.1-5-1), indicating the thermodynamic dominance of a copper(II) free cation under an equilibrium and the making the ***route (B)*** to be more plausible.
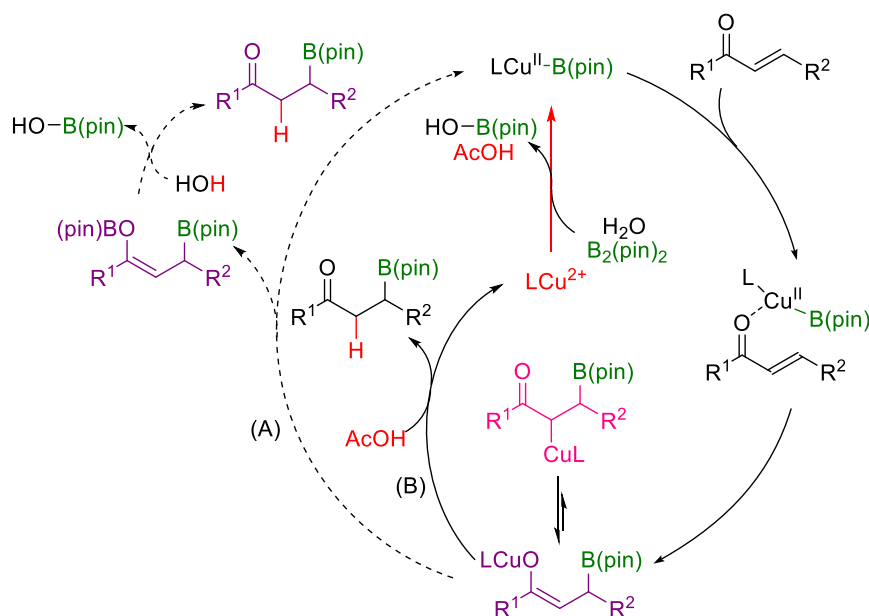
Scheme 52. Postulated mechanism for Cu(II) catalysis for β-borylation in water.

In order to comprehend our envisioned mechanistic model based on the difference between Cu(I) and Cu(II), the reaction coordinates for Cu(I)- and Cu(II)-catalyzed boron conjugate addition of **13a** with **14a** and for their catalytic cycles have been inspected using a density functional theory (DFT) method. Realistic modeling of Cu(II) complexes including the consideration on the description of the Jahn-Teller distortion around the aqueous Cu^{2+} ion was demonstrated by combining DFT with a COSMO continuum solvent model.[120] The initial borylcupration would commence with the activation of **14a** to form adduct (Scheme 53). The sp^2 boron atom of the activated diboron reagent would then interact with copper center. In contrast to the concerted bond exchange between Cu(I)-O and B-B *via* σ-bond metathesis, unsatisfied electron of Cu(II) shows the preference toward both boron atoms due to its unsatisfied electron. The exothermicity forces this step to be irreversible.
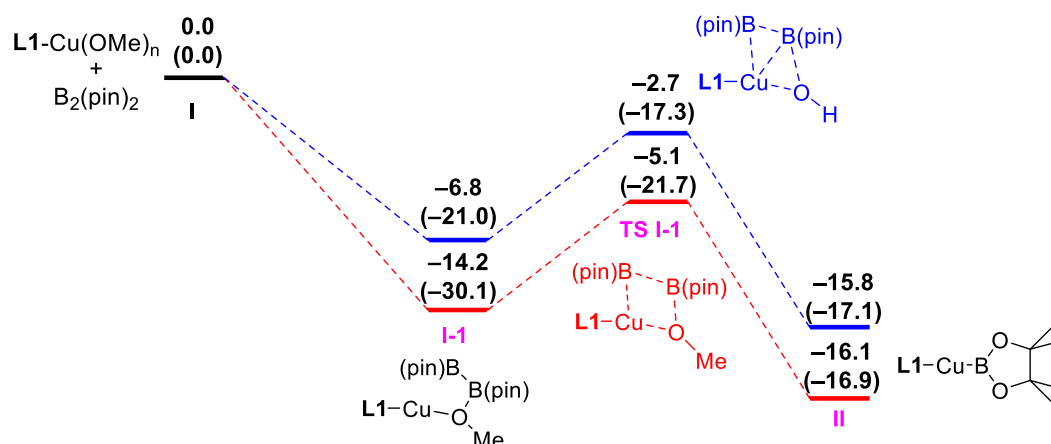
Scheme 53. Reaction coordinate diagram for the formation of borylcopper species. Cu(I) (red) and Cu(II) (blue). Relative Gibbs free energies and electronic energies (in parentheses) are given in kcal/mol.

The structures were subjected to geometry optimization using the MPW1B95/6-311+G (2df, 2pd) basis set for boron, carbon, nitrogen and oxygen atoms and B3LYP/LanL2DZ was employed for copper atoms.

In the nucleophilic addition of borylcopper species to **13a**, DFT calculations revealed the difference between Cu(I) and Cu(II) on the reaction coordinates (Scheme 54). The polarized Cu-B bond would overlap as a HOMO with the antibonding π^* orbital of C=C double bond, thus facilitating the transition state leading to a *C*-enolate intermediate. In contrast, Cu(II) prefers a six-membered transition state to a sterically-congested four-membered transition state. As expected, stabilization of a vacant *p* orbital of boron through an overlap with an occupied *p* orbital of OH oxygen of **L1** may preclude the interaction with π orbital of C=C double bond.
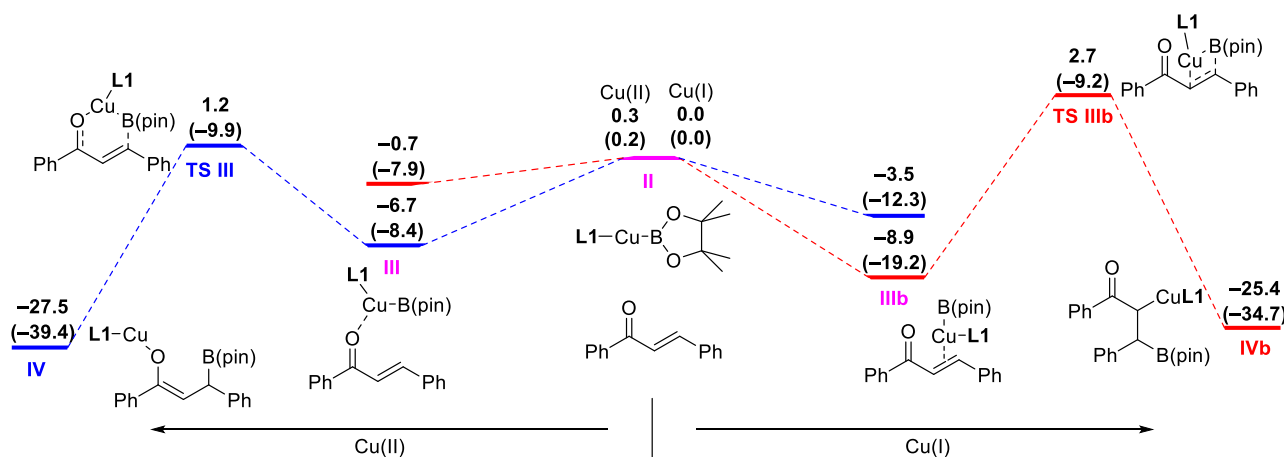
Scheme 54. Reaction coordinate diagram for the formation of copper enolates. *O*-enolate (blue) vs. *C*-enolate (red).

As much discussed,[71] alcoholysis of Cu(I)-*C*-enolate intermediate is highly preferred along with the formation of a reactive Cu-OMe complex. It is noted that the existence of alcohol lowers the energy barrier toward the reaction completion significantly. In the case of Cu(II), three viable reaction pathways were inspected. Among them, a [2+2] hydrolysis involving external protic solvent *via* the transition state **TS IV$_H$** has the highest barrier that is unlikely to overcome (Cu(I)-type mechanism). The transition state **IVp** resulting from the σ-bond metathesis of *O*-enolate intermediate gives the boron enolate, undergoing a rapid hydrolysis in the presence of alcohol (**Route (A)** in Scheme 52). On the other hand, the internal [4+2] hydrolysis *via* the six-membered transition state **TS IVc** would take place without any energy barrier to afford the final product directly (**Route (B)** in Scheme 52). The protons proximal to the coordination sphere of Cu(II) enabled an implementation of a rapid hydrolysis as the most favorable pathway. The *in silico* results revealed that a rate-determining step in water was not a protonation step but a nucleophilic addition of borylcopper species, which is in accordance with our assumption on the **route (B)**. Although the rate of a protonation event seems to be much slower in organic solvent than that in water due to its absolute exiguousness of a proton source and its apparent dilatoriness of a proton-transfer, the Cu(II)-based mechanism can be applied to the organic synthesis in organic solvent and it should possess some unique characters different from that obtained through the conventional Cu(I)-based mechanism.
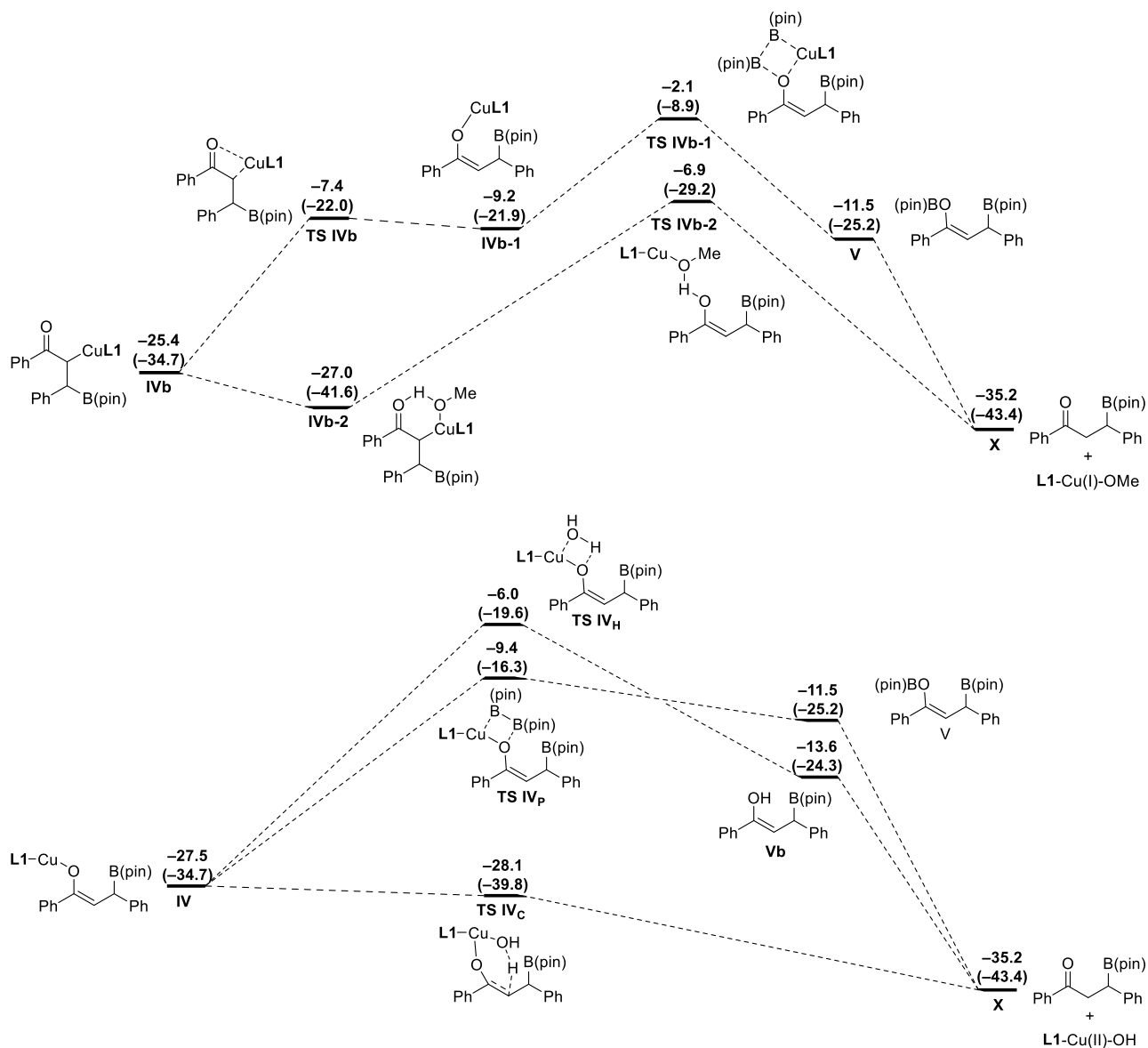
Scheme 55. Computed profiles for protonation based on Cu(I) catalysis (above) and Cu(II) catalysis (below).

3.4-2 *Cu(II) catalysis that works in organic solvent*

In order to probe our hypothesis, the comparative Cu(II) catalytic system was envisaged that works even in organic solvent on the basis of conventional Cu(I) protocol. When Cu(OAc)$_2$ and **L1** was mixed in tetrahydrofuran with an equivalent of methanol as an additive, the reaction proceeded smoothly to afford the desired product with high enantioselectivity after the subsequent treatment with NaBO$_3$ (Table 18, entry 1). Acetate anion was expected to function as an activator of **14a**.[33,121] A significant drop in enantioselectivity is noteworthy in the presence of Josiphos ligand **L41**, one of the most efficient ligand in conventional Cu(I) source in Yun's protocol (entry 2). Although a number of reports on copper(II) complex notice the effective combination of Cu(II) salt with bis(oxazolinyl)pyridine (pybox, *e.g.* **L13**), bis(oxazolidine) ligands (box, *e.g.* **L42-L44**) and dibenzylamine (*e.g.* **L45**), the reaction generally suffered from low yield and low enantioselectivity (entries 3-7).

Table 18. Ligand effect on Cu(II) catalysis for β-borylation.
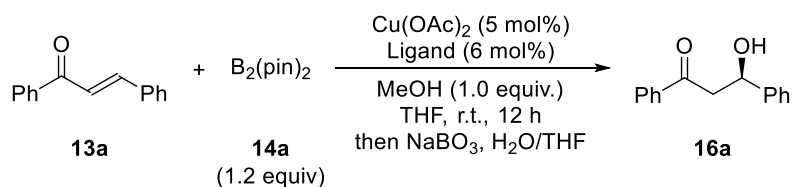
Entry	Ligand	Yield (%)[a]	Ee (%)[b]
1	**L1**	61	81
2	**L41**	57	4
3	**L13**	55	37
4	**L42**	50	56
5	**L43**	56	10
6	**L44**	94	–4
7	**L45**	36	–6

[a] Isolated yield of oxidized product. [b] Determined by HPLC analysis.
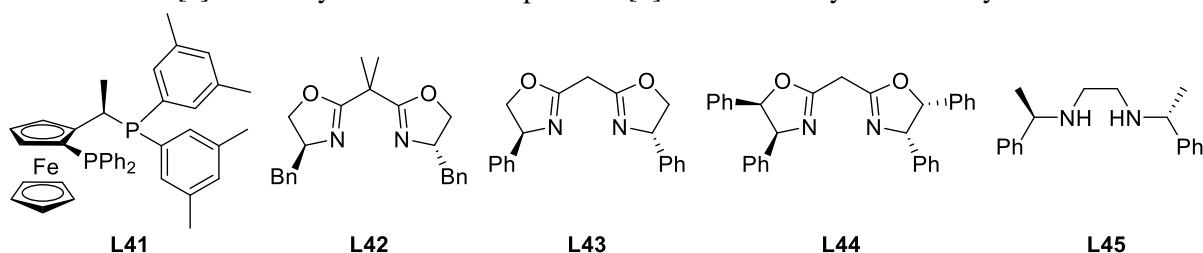
Replacement of methanol with water resulted in no change in the reaction rate and an increase in enantioselectivity of the desired product (Table 19, entry 2). Given the instantaneous proton transfer in water and the resultant lowering of the energy barrier, the use of water as an additive is assumed to lead to the rate retardation at the nucleophilic addition. A significant erosion of enantioselection in the presence of catalytic amount of water suggests the important role of hydrogen bonding at the nucleophilic addition (entry 3). In spite of the known Cu(I)-**L1** complex in a bidentate fasion,[122] the reaction catalyzed by Cu(I) salt suffered from a significant

drop in enantioselectivity (entries 4, 5). In contrast to a tridentate Cu(II)-**L1** complex, the irrelevance of two OH groups in a complexation of Cu(I) with **L1** may cause the chiral induction to be violated.

Table 19. Fundamental elucidation of Cu(II) catalysis for β-borylation.
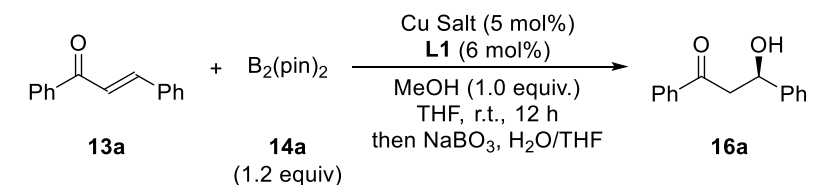
Entry	Cu source	Additive	Yield (%)[a]	Ee (%)[b]
1	Cu(OAc)$_2$	MeOH	61	81
2	Cu(OAc)$_2$	H$_2$O	59	89
3	Cu(OAc)$_2$·H$_2$O	–	56	13
4	CuCl	MeOH	56	10
5[c]	CuCl	MeOH	37	36

[a] Isolated yield of oxidized product. [b] Determined by HPLC analysis.

[c] 5 mol% of NaO^{t}Bu was added.

The chiral Cu(II) complex formed with **L1** was then applied to various solvent (Table 20). Toluene and ethers were effective for the reaction, whereas the coordinating solvent such as DMF and MeCN hampered the chiral induction.

Table 20. Solvent effect on Cu(II) catalysis for β-borylation.
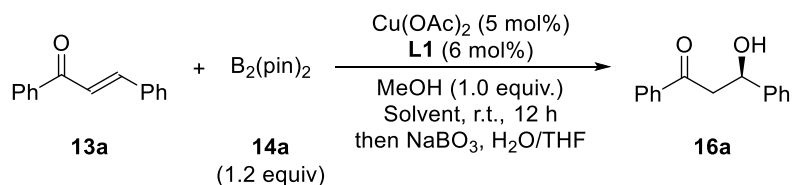
Entry	Solvent	Yield (%)[a]	Ee (%)[b]
1	THF	61	81
2	Et$_2$O	95	94
3	CPME	49	91
4	TBME	68	87
5	DME	70	87
6	Toluene	34	93
7	DCM	90	82
8	CHCl$_3$	76	17
9	DMF	79	21
10	MeCN	71	13
11	MeOH	82	46

[a] Isolated yield of oxidized product. [b] Determined by HPLC analysis.

A crystallographic structure of $CuBr_2$-**L1** complex, which adopts a square pyramidal structure where two nitrogens and only one of the oxygens of **L1** are attached to Cu(II) in a tridentate manner.[82] An involvement of hydroxyl group of **L1** in the reaction was verified by a catalytic activity of chiral catalyst composed of $Cu(OH)_2$ and **L2**, where one hydroxyl group was protected with a methyl group. As observed in water, the almost same reactivity and enantioselectivity were achieved (Table 21, entry 2). In contrast, the use of **L3** resulted in a significant suppression of catalytic cycle and serious enantiomeric loss (entry 3). It was turned out that the reaction yield decreased significantly under acidic conditions presumably due to the rapid decomposition of **2** (entry 4). High acidity would also affect the complex formation, leading to lowering a stereoinduction. When methanol was replaced with other alcohols, the reaction was less selective along with a decrease in reactivity (entries 5-7). The proportional relationship between the solvent polarity and the catalytic acitivty or the stereochemical outcome implies the interplay of hydrogen bondings both at the nucleophilic addition and at the protonation.

Table 21. Solvent effect on Cu(II) catalysis for β-borylation.
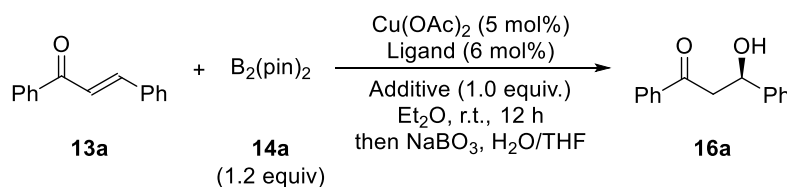
Entry	Ligand	Additive	Yield (%)[a]	Ee (%)[b]
1	**L1**	MeOH	95	94
2	**L2**	MeOH	92	92
3	**L3**	MeOH	31	4
4	**L1**	AcOH	23	32
5	**L1**	EtOH	90	90
6	**L1**	^{i}PrOH	73	88
7	**L1**	^{t}BuOH	53	62

[a] Isolated yield of oxidized product. [b] Determined by HPLC analysis.

As mentioned above, acetate anion is expected to activate **14a** toward a smooth reaction progress. In contrast, the covalent nature of Cu-X (X = Br, Cl) bond impeded the reaction progress completely (Table 22, entries 2, 3). Although the reaction proceeded in the presence of $Cu(OH)_2$, it did not exhibit superior performance over $Cu(OAc)_2$ (entry 4). The use of $Cu(acac)_2$ gave a moderate result, whereas the reaction hardly proceeded when $Cu(OTf)_2$ was used as a catalyst (entries 5, 6). The remarkable catalytic activity of CuO was impressive and suggestive of the heterogeneity of reaction progress (entry 7).

Table 22. Counteranion effect on Cu(II) catalysis for β-borylation.
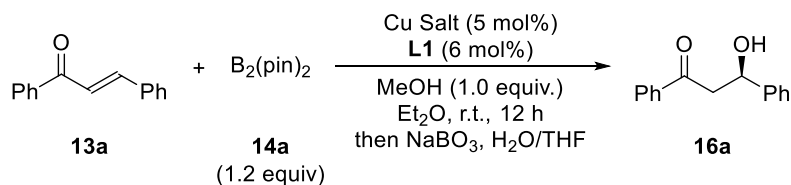
Entry	Cu(II) salt	Yield (%)[a]	Ee (%)[b]
1	Cu(OAc)$_2$	95	94
2	CuCl$_2$	NR	–
3	CuBr$_2$	Trace	–
4	Cu(OH)$_2$	44	81
5	Cu(OTf)$_2$	Trace	–
6	Cu(acac)$_2$	68	84
7	CuO	96	93

[a] Isolated yield of oxidized product. [b] Determined by HPLC analysis.

It is noteworthy that these catalyst systems are applicable to various types of α,β-unsaturated carbonyl compounds and nitrile including acyclic and cyclic α,β-unsaturated ketones including α,β,γ,δ-unsaturated dienones, α,β-unsaturated esters including β,β-disubstitued one, α,β-unsaturated amide, and α,β-unsaturated nitrile (Scheme 56). It should be pointed out that in well-established Cu(I) catalytic system, a series of highly specific modified phosphine ligands should be designed to satisfy the substrate generality and also a strong base should be usually added.

16x
81% yield
93% ee[a]

16α
86% yield
81% ee[a]

17c
82% yield
90% ee[a]

17d
85% yield
88% ee[a]
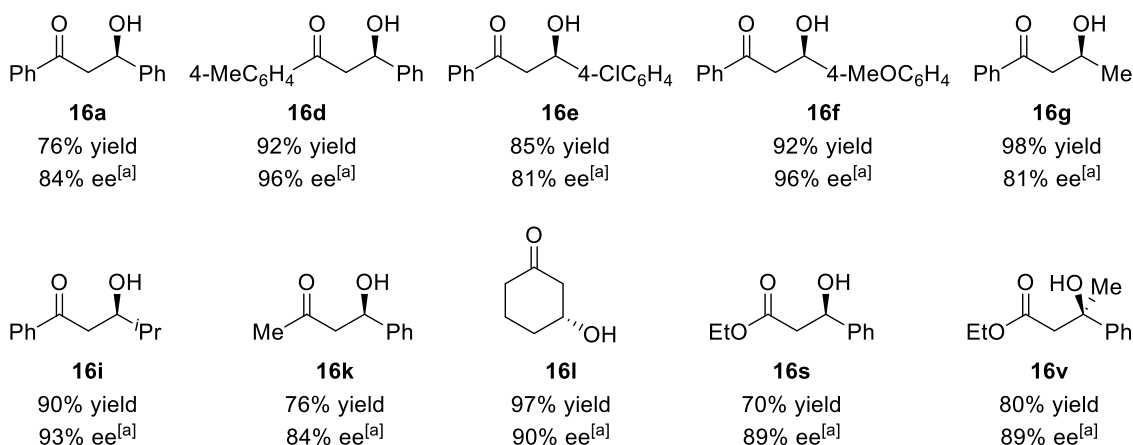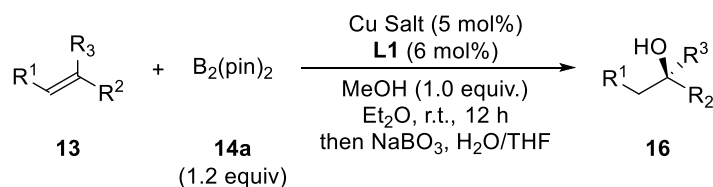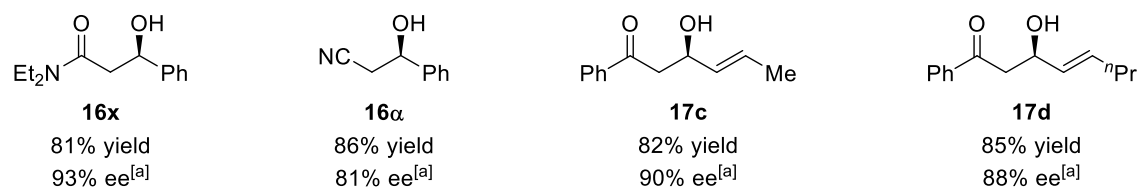
Scheme 56. Substrate scope in Cu(II)-catalyzed asymmetric boron conjugate addition.

3.4-3 *Comprehension of Cu(II) catalysis between In Water and In Organic Solvent*

The reaction took place in Et$_2$O with black precipitates remaining on the bottom of flask, which indicates the heterogeneity of the reaction condition. A significant decrease in stereoinduction was noteworthy when the reaction was performed in CHCl$_3$, despite the homogeneity of the reaction solution. A preliminary kinetic study on Cu(OAc)$_2$-catalyzed boron conjugate addition of **13a** with **14a** was carried out in Et$_2$O with the combined use of an equimolar of methanol and compared with that recorded in water (Figure 17). It was revealed that the Cu(OAc)$_2$-catalyzed reaction in Et$_2$O was accelerated over Cu(OAc)$_2$-catalyzed reaction in water but slower than Cu(OH)$_2$-catalyzed reaction in water.
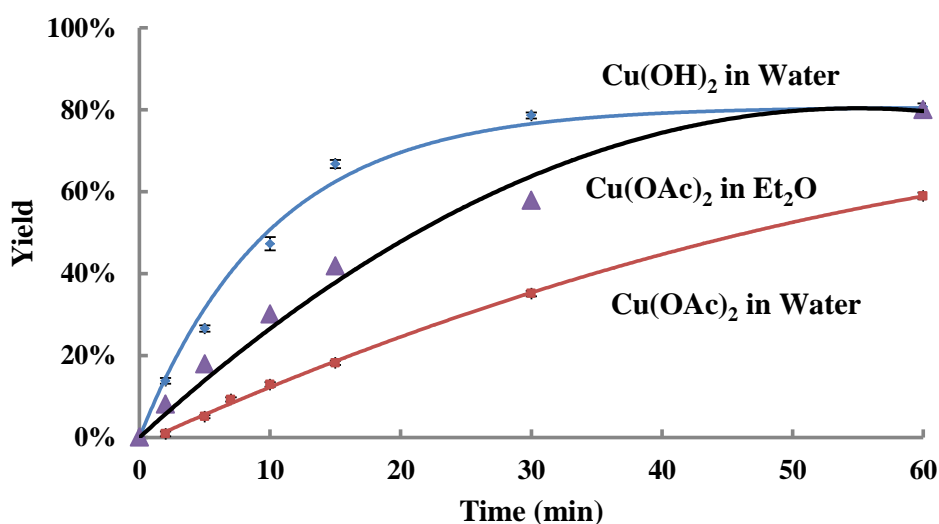
Figure 17. Profiles of reactions catalyzed by Cu(OAc)$_2$ in Et$_2$O and water.

In Cu(II)-catalyzed asymmetric reaction of **13a** with **14a** in the coexistence of methanol, the reaction solution was filtered after stirring for 2 hour. ICP analysis of the filtrate revealed that Cu content was below the detection limit of the ICP equipment (0.005 ppm). After additional substrates **13a** and **14a** were thrown into the filtrate with methanol, further stirring for 12 hours delivered the desired product with a little bit poor result (76% yield, 88% ee *vs*. 95% yield, 94% ee [entry 1 in Table 21]). Even though different substrate (benzalacetone **13k** instead of **13a**) was added to the filtrate with **14a**, the resultant solution afforded the desired product (70% yield, 86% ee *vs*. 76% yield, 84% ee [Scheme 56]). It should be emphasized that considerably high catalytic turnover was achieved even in organic solvent. However, a highly sensitive catalytic performance by a minute quantity of copper(II) ion cannot deny the possibility of heterogeneous catalysis. The inherently low solubility of both materials forces the reaction to take place on solid-state. In contrast to the homogeneous catalyst solution obtained when Cu(OAc)$_2$ and **L1** are mixed in water, the insoluble copper salt occupies the vast majority of a given amount during the reaction performed in Et$_2$O. Compared with our previous paper concluding the complete heterogeneity of

Cu(OH)$_2$-catalyzed reaction in water, Cu(OAc)$_2$-catalyzed reaction in Et$_2$O seems to take on the combined nature between homogeneous- and heterogeneousness.

3.4-4   Conclusions

In summary, *de novo* Cu(II)-based catalysis was successfully establibed which is applicable even in organic solvent, on the basis of up-to-date Cu(II) catalysis cultivated in water. A scrutiny through empirical and speculative approaches led to a reinforcement of organic chemistry by supplementing a new Cu(II)-based mechanism that has never been observed in conventional Cu(I)-based chemistry.   In asymmetric boron conjugate addition, a conventional Cu(I)-based pathway has been considered to pass through a nucleophilic addition of borylcopper(I) species to form a *C*-enolate intermediate and the subsequent alcoholysis as a rate-determining step. In contrast, a new Cu(II)-based pathway would pass through the nucleophilic addition of borylcopper(II) species to form a *O*-enolate intermediate which seems to be a rate-determining step and the instantaneous protonation.   Chiral 2,2'-bipyridine **L1** would play a prominent role in both electronic and stereochemical stabilization of borylcopper(II) species through the donation of electrons on a free OH group toward a vacant *p* orbital on boron atom.   Since the thermodynamically unfavorable Cu(I)-*C*-enolate relies on the orbital overlap between C=C double bond and Cu-B bond depicted in **TS IIIb**, the electronic nature of transient Cu-C bond as well as the stereochemistry of *C*-enolate should be dominated by the nature of carbonyl moiety such as ketone, ester, amide and so on, thus restricting the substrate range that a single catalyst can cover without changing the ligand structure.   Contrariwise, the cleavage of Cu(II)-*O*-enolate is almost barrierless and its stereochemistry is almost irrelevant to the electronic nature of carbonyl moiety due to the six-membered transition state.   In addition, its catalytic performance in water should be outstanding due to the instantaneous hydrolysis.   The accumulated new insights led to a conceptual expansion that is applicable even in organic solvent.   In the early stage, the discoveries on some reactions performed in water were provoked by traditional chemistry explored in organic solvent. To date, a number of reactions, techniques and methodologies have been cultivated in water independently.   I believe that one of these insights cultivated in water can be fed back to organic chemistry explored in organic solvent.

[1] a) J. C. H. Lee, R. McDonald, D. G. Hall, *Nature Chem.* **2011**, *3*, 894-899; b) C. Solé, A. Tatla, J. A. Mata, A. Whiting, H. Gulyás, E. Fernández, *Chem. Eur. J.* **2011**, *17*, 14248-14257; c) H. K. Scott, V. K. Aggarwal, *Chem. Eur. J.* **2011**, *17*, 13124-13132; d) T. Ohmura, T. Awano, M. Suginome, *J. Am. Chem. Soc.* **2010**, *132*, 13191-13193; e) D. Imao, B. W. Glasspoole, V. S. Laberge, C. M. Crudden, C. M. *J. Am. Chem. Soc.* **2009**, *131*, 5024-5025; f) J. L. Stymiest, V. Bagutski, R. M. French, V. K. Aggarwal, *Nature*, **2008**, *456*, 778-782.

[2] a) R. Rasappan, V. K. Aggarwal, *Nature Chem.* **2014**, *6*, 810-814; b) S. P. Thomas, R. M. French, V. Jheengut, V. K. Aggarwal, *Chem. Rec.* **2009**, *9*, 24-49.

[3] a) P. J. Unsworth, D. Leonori, V. K. Aggarwal, *Angew. Chem. Int. Ed.* **2014**, *53*, 9846-9850; b) D. S. Matteson, *J. Org. Chem.* **2013**, *78*, 10009-10023.

[4] a) G. A. Molander, S. R. Wisniewski, M. H. –Sarvari, *Adv. Synth. Catal.* **2013**, *355*, 3037-3057; b) G. A. Molander, S. R. Wisniewski, *J. Am. Chem. Soc.* **2012**, *134*, 16856-16868; c) D. L. Sandrock, L. J. –Gerald, C. –Y. Chen, S. D. Dreher, G. A. Molander, *J. Am. Chem. Soc.* **2010**, *132*, 17108-17110.

[5] S. D. Dreher, P. G. Dormer, D. L. Sandrock, G. A. Molander, *J. Am. Chem. Soc.* **2008**, *130*, 9257-9259.

[6] A. Bonet, M. Odachowski, D. Leonori, S. Essafi, V. K. Aggarwal, *Nature Chem.* **2014**, *6*, 584-589.

[7] a) C. D. Bhaskar, P. Thapa, R. Karki, C. Schinke, S. Das, S. Kambhampati, S. K. Banerjee, P. V. Veldhuizen, A. Verma, L. M. Weiss, T. Evans, *Future Med. Chem.* **2013**, *5*, 653-676; b) P. V. Ramachandran, *Future Med. Chem.* **2013**, *5*, 611-612; c) R. Smoum, A. Rubinstein, V. M. Dembitsky, M. Srebnik, *Chem. Rev.* **2012**, *112*, 4156-4220; d) S. J. Baker, C. Z. Ding, T. Akama, Y. –K. Zhang, V. Hernandez, Y. Xia, *Future Med. Chem.* **2009**, *1*, 1275-1288; e) D. S. Matteson, *Med. Res. Rev.* **2008**, *28*, 233-246.

[8] a) B. B. Pappin, M. Kiefel, T. A. Houston, In "*Carbohydrates – Comprehensive Studies on Glycobiology and Glycotechnology*", C. –F. Chang Ed., **2012**, 37-54; b) M. Dowlut, D. G. Hall, *J. Am. Chem. Soc.* **2006**, *128*, 4226-4227; L. Polgar, *Cell. Mol. Life Sci.* **2005**, *62*, 2161-2172.

[9] J. Adams, *Oncologist* **2002**, *7*, 9-16.

[10] a) S. Lü, J. Wang, *Biomarker Res.* **2013**, *1*, 13-22; b) M. Groll, C. R. Berkers, H. L. Ploegh, H. Ovaa, G. Bourenkov, *Structure* **2006**, *14*, 451-456.

[11] a) A. Allegra, A. Alonci, D. Gerace, S. Russo, V. Innao, L. Calabrò, C. Musolino, *Leukemia Res.* **2014**, *38*, 1-9; b) R. Piva, B. Ruggeri, M. Williams, G. Costa, I. tamagno, D. Ferrero, V. Giai, M. Coscia, S. Peola, M. Massaia, G. Pezzoni, C. Allievi, N. Pescalli, M. Cassin, S. di Giovine, P. Nicoli, P. de Feudis, I. Strepponi, I. Roato, R. Ferracini, B. Bussolati, G. Camussi, S. Jones–Bolin, K. Hunter, H. Zhao, A. Neri, A. Palumbo, C. Berkers, H. Ovaa, A. Bernareggi, G. Inghirami, *Blood* **2008**, *111*, 2765-2775.

[12] a) P. Moreau, *Blood* **2014**, *124*, 986-987; b) B. Cvek, *Drug Future* **2012**, *37*, 561-565.

[13] E. Kupperman, E. C. Lee, Y. Cao, B. Bannerman, M. Fitzgerald, A. Berger, J. Y. Yang, P. Hales, F. Bruzzese, J. Liu, J. Blank, K. Garcia, C. Tsu, L. Dick, P. Fleming, L. Yu, M. Manfredi, M. Rolfe, J. Bolen, *Cancer Res.* **2010**, *70*, 1970-1980.

[14] S. J. Coutts, T. A. Kelly, R. J. Snow, C. A. Kennedy, R. W. Barton, D. A. Drolikowski, D. M. Freeman, S. J. Campbell, J. F. Ksiazek, W. W. Bachovchin, *J. Med. Chem.* **1996**, *39*, 2087-2094.

[15] a) J. Jia, T. A. Martin, L. Ye, W. G. Jiang, *BMC Cell Biology* **2014**, *15*, 16-29; b) C. C. Cunningham, *Expert Opin. Investig. Drug* **2007**, *16*, 1459-1465.

[16] a) K. M. S. Johnson, *Curr. Opin. Invest. Drug* **2010**, *11*, 455-463; b) G. Garcia–Soria, G. Gonzalez–Galvez, G. M. Argoud, M. Gerstman, T. W. Littlejohn III, S. L. Schwartz, A. –M. O'Farrell, X. Li, J. M. Cherrington, C. Bennett, H. –P. Guler, *Diabetes Obes. Metab.* **2008**, *10*, 293-300.

[17] G. Abbenante, D. P. Fairlie, *Med. Chem.* **2005**, *1*, 71-104.

[18] S. Venkatraman, W. Wu, A. Prongay, V. Girijavallabhan, N. F. George, *Bioorg. Chem. Lett.* **2009**, *19*, 180-183.

[19] H. C. Brown, B. C. Subba Rao, *J. Am. Chem. Soc.* **1956**, *78*, 5694-5695.

[20] a) N. Miyaura, A. Suzuki, *J. Chem. Soc., Chem. Commun.* **1979**, 866-867; b) N. Miyaura, K. Yamada, A. Suzuki, *Tetrahedron Lett.* **1979**, *20*, 3437-3440.

[21] a) N. J. Bell, A. J. Cox, N. R. Cameron, J. S. O. Evans, T. B. Marder, M. A. Duin, C. J. Elservier, X. Baucherel, A. A. D. Tilloch, R. P. Tooze, *Chem. Commun.* **2004**, 1854-1855; b) Y. G. Lawson, M. J. G. Lesley, T. B. Marder, N. C. Norman, C. R. Rice, *Chem. Commun.* **1997**, 2051-2052; c) J. D. Hewes, C. W. Kreimendahl, T. B. Marder, M. F. Hawthorne, *J. Am. Chem. Soc.* **1984**, *106*, 5757-5759.

[22] a) T. Shiomi, T. Adachi, K. Toribatake, L. Zhou, H. Nishiyama, *Chem. Commun.* **2009**, 5987-5989; b) G. W. Kabalka, Z. Wu, M. Yao, *Appl. Organomet. Chem.* **2008**, *22*, 516-552; c) G. W. Kabalka, B. C. Das, S. Das, *Tetrahedron Lett.* **2002**, *43*, 2323-2325.

[23] a) B. Liu, M. Gao, L. Dang, H. Zhao, T. B. Marder, Z. Lin, *Organometallics* **2012**, *31*, 3410-3425; b) N. J. Bell, A. J. Cox, N. R. Cameron, J. S. O. Evans, T. B. Marder, M. A. Duin, C. J. Elsevier, X. Baucherel, A. A. D. Tulloch, R. P. Tooze, *Chem. Commun.* **2004**, 1854-1855; c) H.

A. Ali, I. Goldberg, M. Srebnik, *Organometallics* **2001**, *20*, 3962-3965; d) Y. G. Lawson, M. J. G. Lesley, T. B. Marder, N. C. Norman, C. R. Rice, *Chem. Commun.* **1997**, 2051-2052.

24 J. Ramírez, R. Corberán, M. Sanaú, E. Peris, E. Fernández, *Chem. Commun.* **2005**, 3056-3058.

25 a) V. Lillo, M. J. Geier, S. A. Westcott, E. Fernández, *Org. Biomol. Chem.* **2009**, *7*, 4674-4676; b) K. Hirano, H. Yorimitsu, K. Oshima, *Org. Lett.* **2007**, *9*, 5031-5033.

26 T. Kajiwara, T. Terabayashi, M. Yamashita, K. Nozaki, *Angew. Chem. Int. Ed.* **2008**, *47*, 6606-6610.

27 a) C. Pubill-Ulldemolins, A. Bonet, C. Bo, H. Gulyás, E. Fernández, *Org. Biomol. Chem.* **2011**, *8*, 2667-2682; b) A. Bonet, H. Gulyás, I. O. Koshevoy, F. Estevan, M. Sanaú, M. A. Úbeda, E. Fernandéz, *Chem. Eur. J.* **2010**, *16*, 6382-6390.

28 A. Bonet, C. Solé, H. Gulyás, E. Fernández, *Chem. Asian J.* **2011**, *6*, 1011-1014.

29 A. H. Hoveyda, K. S. Lee, A. R. Zhugralin, *J. Am. Chem. Soc.* **2009**, *131*, 7253-7255.

30 K. Wen, J. Chen, F. Gao, P. S. Bhadury, E. Fan, Z. Sun, *Org. Biomol. Chem.* **2013**, *11*, 6350-6356.

31 When triphenylphosphine was used instead of triphenylphosphine oxide, the reaction yield decreased significantly (less than 2%).

32 H. Ito, H. Yamanaka, J. Tateiwa, A. Hosomi, *Tetrahedron Lett.* **2000**, *41*, 6821-6825.

33 a) K. Takahashi, J. Takagi, T. Ishiyama, N. Miyaura, *Chem. Lett.* **2000**, *29*, 126-127; b) K. Takahashi, T. Ishiyama, N. Miyaura, *J. Organomet. Chem.* **2001**, *625*, 47-53.

34 a) D. Kim, B. –M. Park, J. Yun, *Chem. Commun.* **2005**, 1755-1757; b) S. Mun, J. –E. Lee, J. Yun, *Org. Lett.* **2006**, *8*, 4887-4889.

35 The initial discovery of utilizing transition metals with diboron reagent: P. Nguyen, G. Lesley, N. J. Taylor, T. B. Marder, N. L. Pickett, W. Clegg, M. R. J. Elsegood, N. C. Norman, *Inorg. Chem.* **1994**, *33*, 4623-4624.

36 J. –E. Lee, J. Yun, *Angew. Chem., Int. Ed.* **2008**, *47*, 145-147.

37 H. Chea, H. –S. Sim, J. Yun, *Adv. Synth. Catal.* **2009**, *351*, 855-858.

38 H. Sim, X. Feng, J. Yun, *Chem. Eur. J.* **2009**, *15*, 1939-1943.

39 X. Feng, J. Yun, *Chem. Eur. J.* **2010**, *16*, 13609-13612.

40 I. –H. Chen, L. Yin, W. Itano, M. Kanai, M. Shibasaki, *J. Am. Chem. Soc.* **2009**, *131*, 11664-11665.

41 I. –H. Chen, M. Kanai, M. Shibasaki, *Org. Lett.* **2010**, *12*, 4098-4101.

42 W. J. Fleming, H. Müller-Bunz, V. Lillo, E. Fernández, P. J. Guiry, *Org. Biomol. Chem.* **2009**, *7*, 2520-2524.

43 D. S. Laitar, P. Müller, J. P. Sadighi, *J. Am. Chem. Soc.* **2005**, *127*, 17196-17197.

44 A. Bonet, M. M. Díaz-Requejo, E. Fernández, V. Lillo, P. J. Pérez, A. Prieto, J. Ramírez, *Organometallics* **2009**, *28*, 659-662.

45 J. M. O'Brien, K. –S. Lee, A. H. Hoveyda, *J. Am. Chem. Soc.* **2010**, *132*, 10630-10633.

46 D. Hirsch-Weil, K. A. Abboud, S. Hong, *Chem. Commun.* **2010**, *46*, 7525-7527.

47 M. Iglesias, D. J. Beetstra, A. Stasch, P. N. Horton, M. B. Hursthouse, S. J. Coles, K. J. Cavell, A. Dervisi, I. A. Fallis, *Organometallics* **2007**, *26*, 4800-4809.

48 J. K. Park, H. H. Lackey, M. D. Rexford, K. Kovnir, M. Shatruk, D. T. McQuade, *Org. Lett.* **2010**, *12*, 5008-5011.

49 L. Huang, Y. Cao, M. Zhao, Z. Tang, Z. Sun, *Org. Biomol. Chem.* **2014**, *12*, 6554-6556.

50 T. Iwai, Y. Akiyama, M. Sawamura, *Tetrahedron: Asymmetry* **2013**, *24*, 729-735.

51 C. Bolm, T. Focken, G. Raabe, *Tetrahedron: Asymmetry* **2003**, *14*, 1733-1746.

52 a) L. Zhao, Y. Ma, F. He, W. Duan, J. Chen, C. Song, *J. Org. Chem.* **2013**, *78*, 1677-1681; b) B. Hong, Y. Ma, L. Zhao, W. Duan, F. He, C. Song, *Tetrahedron: Asymmetry* **2011**, *22*, 1055-1062.

53 L. Zhao, Y. Ma, W. Duan, F. He, J. Chen, C. Song, *Org. Lett.* **2012**, *14*, 5780-5783.

54 Z. Niu, J. Chen, Z. Chen, M. Ma, C. Song, Y. Ma, *J. Org. Chem.* **2015**, *80*, 602-608.

[55] a) S. Radomkit, A. H. Hoveyda, *Angew. Chem. Int. Ed.* **2014**, *53*, 3387-3391; b) K. S. Lee, A. R. Zhugralin, A. H. Hoveyda, A. *J. Am. Chem. Soc.* **2009**, *131*, 7253-7255 (Correction: *J. Am. Chem. Soc.* **2010**, *132*, 12766).

[56] A. Bonet, H. Gulyás, E. Fernandéz, *Angew. Chem. Int. Ed.* **2010**, *49*, 5130-5134.

[57] C. Kleeberg, A. G. Crawford, A. S. Batsanov, P. Hodgkinson, D. C. Apperley, M. S. Cheung, Z. Lin, T. B. Marder, *J. Org. Chem.* **2012**, *77*, 785-789.

[58] V. Lillo, M. J. Geier, S. A. Westcott, E. Fernández, *Org. Biomol. Chem.* **2009**, *7*, 4674-4676.

[59] a) K. Toribatake, L. Zhou, A. Tsuruta, H. Nishiyama, *Tetrahedron* **2013**, *69*, 3551-3560; b) T. Shiomi, T. Adachi, K. Toribatake, L. Zhou, H. Nishiyama, *Chem. Commun.* **2009**, 5987-599.

[60] The authoritative reviews on boron conjugate additions, see: a) A. D. J. Calow, A. Whiting, *Org. Biomol. Chem.* **2012**, *10*, 5485-5497; b) E. Hartmann, D. J. Vyas, M. Oestreich, *Chem. Commun.* **2011**, *47*, 7917-7932; c) J. A. Schiffner, K. Müther, M. Oestreich, *Angew. Chem. Int. Ed.* **2010**, *49*, 1194-1196.

[61] D. M. Knapp, E. P. Gillis, M. D. Burke, *J. Am. Chem. Soc.* **2009**, *131*, 6961-6963.

[62] Y. Yamamoto, T. Takizawa, X. –Q. Yu, N. Miyaura, *Angew. Chem. Int. Ed.* **2008**, *47*, 928-931.

[63] a) S. Darses, J. –P. Genet, *Chem. Rev.* **2008**, *108*, 288-325; b) G. A. Molander, N. Ellis, *Acc. Chem. Res.* **2007**, *40*, 275-286.

[64] M. Gao, S. B. Thorpe, W. L. Santos, *Org. Lett.* **2009**, *11*, 3478-3481.

[65] M. Gao, S. B. Thorpe, C. Kleeberg, C. Slebodnick, T. B. Marder, W. L. Santos, *J. Org. Chem.* **2011**, *76*, 3997-4007.

[66] G. A. Molander, S. A. McKee, *Org. Lett.* **2011**, *13*, 4684-4687.

[67] Quite recently, alkaline-free protocol was released, see: J. –B. Xie, S. Lin, J. Luo, J. Wu, T. R. Winn, G. Li, *Org. Chem. Front.* **2015**, *2*, 42-46.

[68] a) T. V. Popova, N. V. Aksenova, *Russ. J. Coord. Chem.* **2003**, *29*, 743-765; b) F. A. Cotton, G. Wilkinson, C. A. Murillo, M. Bochmann, in *Advanced Inorganic Chemistry*, John Wiley&Sons, **1999**, pp 854-876; c) B. J. Hataway, *Coord. Chem. Rev.* **1981**, *35*, 211-252; d) B. J. Hataway, D. E. Billing, *Coord. Chem. Rev.* **1970**, *5*, 143-207.

[69] H. Yamamoto, M. P. Sibi, G. R. Cook, in *"Lewis Acids in Organic Synthesis"*, **2001**, John Wiley & Sons, pp1014.

[70] X. Feng, J. Yun, *Chem. Commun.* **2009**, 6577-6579.

[71] This mechanism is supported by quantum-chemical calculations; L. Dang, Z. Lin, T. B. Marder *Organometallics* **2008**, *27*, 4443-4454.

[72] M. Fujita, T. Nagano, U. Schneider, T. Hamada, C. Ogawa, S. Kobayashi, *J. Am. Chem. Soc.* **2008**, *130*, 2914-2915.

[73] a) S. Kobayashi, T. Endo, T. Yoshino, U. Schneider, M. Ueno, *Chem. Asian J.* **2013**, *8*, 2033-2045; b) S. Kobayashi, T. Endo, M. Ueno, *Angew. Chem. Int. Ed.* **2011**, *50*, 12262-12265; c) S. Kobayashi, T. Endo, U. Schneider, M. Ueno, *Chem. Commun.* **2010**, *46*, 1260-1262.

[74] a) S. Kobayashi, M. Ueno, T. Kitanosono, *Top. Curr. Chem.* **2012**, *311*, 1-18; b) S. Kobayashi, T. Kitanosono, M. Ueno, *Synlett* **2010**, 2033-2036.

[75] a) S. Kobayashi, I. Hachiya, *J. Org. Chem.* **1994**, *59*, 3590-3596; b) S. Kobayashi, *Synlett* **1994**, 689-699; c) S. Kobayashi, I. Hachiya, *Tetrahedron Lett.* **1992**, *33*, 1625-1628.

[76] H. Chea, H. –S. Sim, J. Yun, *Bull. Korean Chem. Soc.* **2010**, *31*, 551-552.

[77] I. Ibrahem, P. Breistein, A. Córdova, *Angew. Chem. Int. Ed.* **2011**, *50*, 12036-12041.

[78] M. Kotani, T. Koike, K. Yamaguchi, N. Mizuno, *Green Chem.* **2006**, *8*, 735-741.

[79] R. Cano, D. J. Ramón, M. Yus, *J. Org. Chem.* **2010**, *75*, 3458-3460.

[80] S. B. Thorpe, J. A. Calderone, W. L. Santos, *Org. Lett.* **2012**, *14*, 1918–1921.

[81] S. Kobayashi, P. Xu, T. Endo, M. Ueno, T. Kitanosono, *Angew. Chem. Int. Ed.* **2012**, *51*, 12763–12766.

[82] a) M. Kokubo, T. Naito, S. Kobayashi, *Tetrahedron* **2010**, *66*, 1111–1118; b) C. Ogawa, M. Kokubo, S. Kobayashi, *J. Synth. Org. Chem. Jpn.* **2010**, *68*, 718–728; c) M. Kokubo, T. Naito, S. Kobayashi, *Chem. Lett.* **2009**, *38*, 904–905.

[83] G. Stavber, Z. Časar, *Appl. Organomet. Chem.* **2013**, *27*, 159-165. One example of asymmetric version was demonstrated using Walphos-type phosphine ligand toward formal synthesis of sitagliptin.

[84] Y. Luo, I. D. Roy, A. G. E. Madec, H. W. Lam, *Angew. Chem. Int. Ed.* **2014**, *53*, 4186-4190.

[85] K. S. Lee, H. Wu, F. Haeffner, A. H. Hoveyda, *Organometallics* **2012**, *31*, 7823-7826.

[86] a) M. Magrez, J. Wencel–Delord, A. Alexakis, C. Crévisy, M. Mauduit, *Org. Lett.* **2012**, *14*, 3576-3579; b) M. Tissot, D. Poggiali, H. Hénon, D. Müller, L. Guénée, M. Mauduit, A. Alexakis, *Chem. Eur. J.* **2012**, *18*, 8731–8747; c) J. Wencel-Delord, A. Alexakis, C. Crévisy, M. Mauduit, *Org. Lett.* **2010**, *12*, 4335–4337; d) H. Hénon, M. Mauduit, A. Alexakis, *Angew. Chem. Int. Ed.* **2008**, *47*, 9122–9124; e) T. den Hartog, S. R. Harutyunyan, D. Font, A. J. Minnaard, B. L. Feringa, *Angew. Chem. Int. Ed.* **2008**, *47*, 398–401; f) T. Hayashi, S. Yamamoto, N. Tokunaga, *Angew. Chem. Int. Ed.* **2005**, *44*, 4224–4227; g) R. R. Cesati, J. de Armas, A. H. Hoveyda, *J. Am. Chem. Soc.* **2004**, *126*, 96–101.

[87] X. Tian, Y. Liu, P. Melchiorre, *Angew. Chem. Int. Ed.* **2012**, *51*, 6439–6442; and references cited therein.

[88] Y. –C. Hong, P. Gandeepan, S. Mannathan, W. –T. Lee, C. –H. Cheng, *Org. Lett.* **2014**, *16*, 2806-2809.

[89] Although the cyclic dienone **20e** react with **14a** at β-position, the reaction of **20g** hardly took place.

[90] The major product was phenol.

[91] a) S. M. Barnett, K. I. Goldberg, J. M. Mayer, *Nature Chem.* **2012**, *4*, 498-502; b) E. Garribba, G. Micera, D. Sanna, L. S. –Erre, *Inorg. Chim. Acta* **2000**, *299*, 253-261; and references cited therein.

[92] Only aqueous tetrahydrofuran co-solvent system could provide the product with a minimum loss of reactivity and enantioselectivity. Namely, water is indispensable to obtain the product in this reaction.

[93] The solvent KIE value for $Cu(OH)_2$-catalyzed β-borylation of **13t** with **14a** is 1.47.

[94] a) F. Benedetti, S. Norbedo, *Chem. Commun.* **2001**, 203–204; b) S. Knapp, *Chem. Rev.* **1995**, *95*, 1859–1876.

[95] a) S. M. Lait, D. A. Rankic, B. A. Keay, *Chem. Rev.* **2007**, *107*, 767–796; b) R. Pedrosa, C. Andrés, J. Nieto, S. Del Pozo, *J. Org. Chem.* **2003**, *68*, 4923–4931; c) D. W. L. Sung, P. Hodge, P. W. Stratford, *J. Chem. Soc., Perkin Trans. 1* **1999**, 1463–1472; d) C. Andrés, J. Nieto, R. Pedrosa, M. Vicente, *J. Org. Chem.* **1998**, *63*, 8570–8573.

[96] For recent examples, see: a) L. Zhan, S. Ma, *Angew. Chem. Int. Ed.* **2008**, *47*, 258–297; b) Z. Szakonyi, Á. Balázs, T. A. Martinek, F. Fülöp, *Tetrahedron: Asymmetry* **2006**, *17*, 199–204; c) M. Panda, P.-W. Phuan, M. C. Kozlowski, *J. Org. Chem.* **2003**, *68*, 564–571; d) M. J. Vilaplana, P. Molina, A. Arques, C. Andrés, R. Pedrosa, *Tetrahedron: Asymmetry* **2002**, *13*, 5–8; e) T. Mino, S. Hata, K. Ohtaka, M. Sakamoto, T. Fujita, *Tetrahedron Lett.* **2001**, *42*, 4837–4839; f) G. Palmieri, *Tetrahedron: Asymmetry* **2000**, *11*, 3361–3373; g) S. R. Davies, M. C. Mitchell, C. P. Cain, P. G. Devitt, R. J. Taylor, T. P. Kee, *J. Organomet. Chem.* **1998**, *550*, 29–57.

[97] J. Wang, D. Liu, Y. Liu, W. Zhang, *Org. Biomol. Chem.* **2013**, *11*, 3855–3861.

[98] A. Pohland, H. R. Sullivan, *J. Am. Chem. Soc.* **1953**, *75*, 4458–4459.

[99] T. Kashiwagi, S. Kotani, M. Sugiura, M. Nakajima, *Tetrahedron* **2011**, *67*, 531–539.

[100] a) A. D. J. Calow, A. S. Batsanov, A. Pujol, C. Solé, E. Fernández, A. Whiting, *Org. Lett.* **2013**, *15*, 4810–4813; b) A. D. J. Calow, C. Solé, A. Whiting, E. Fernández, *ChemCatChem* **2013**, *5*, 2233–2239; c) A. D. J. Calow, A. S. Batsanov, E. Fernández, C. Solé, A. Whiting, *Chem. Commun.* **2012**, 11401–11403; d) C. Solé, A. Bonet, A. H. M. de Vries, J. G. de Vries, L. Lefort, H. Gulyás, E.

Fernández, *Organometallics* **2012**, *31*, 7855–7861; e) C. Solé, A. Whiting, H. Gulyás, E. Fernández, *Adv. Synth. Catal.* **2011**, *353*, 376–384; f) C. Solé, A. Tatla, J. A. Mata, A. Whiting, H. Gulyás, E. Fernández, *Chem. Eur. J.* **2011**, *17*, 14248–14257.

[101] a) R. Abonia, D. Arteaga, J. Castillo, B. Insuasty, J. Quiroga, A. Ortíz, *J. Braz. Chem. Soc.* **2013**, *24*, 1396–1402; b) C. Appayee, A. J. Fraboni, S. E. Brenner-Moyer, *J. Org. Chem.* **2012**, *77*, 8828–8834; c) F. A. Davis, P. M. Gaspari, B. M. Nolt, P. Xu, *J. Org. Chem.* **2008**, *73*, 9619–9626.

[102] Y. Xie, K. Yu, Z. Gu, *J. Org. Chem.* **2014**, *79*, 1289–1302; b) J. Cornil, A. Guérinot, S. Reymond, J. Cossy, *J. Org. Chem.* **2013**, *78*, 10273–10287; c) K. V. Gothelf, K. A. Jørgensen, *Chem. Rev.* **1998**, *98*, 863–909; d) V. Jäger, V. Buß, W. Schwab, *Tetrahedron Lett.* **1978**, *19*, 3133–3136.

[103] a) G. T. Rice, M. C. White, *J. Am. Chem. Soc.* **2009**, *131*, 11707–11711; b) J. –L. Liang, S. –X. Yuan, J. –S. Huang, W.-Y. Yu, C. –M. Che, *Angew. Chem. Int. Ed.* **2002**, *41*, 3465–3468.

[104] For racemic examples, see: a) A. Bonet, C. Solé, H. Gulyás, E. Fernández, *Chem. Asian J.* **2011**, *6*, 1011–1014; b) C. Solé, E. Fernández, *Chem. Asian J.* **2009**, *4*, 1790–1793.

[105] A base-free catalytic system comprising Cu_2O was reported recently. See Ref. 100b.

[106] H. Görner, E. Fischer, *J. Photochem. Photobiol. A: Chem.* **1991**, *57*, 235–246.

[107] S. Kobayashi, T. Busujima, S. Nagayama, *Chem. Eur. J.* **2000**, *6*, 3491–3494.

[108] Prepared from $CuSO_4$ by preferential oxidation of the zinc(0) atom.

[109] It was confirmed that the subsequent oxidation of the β-borylated product into the β-hydroxy ketone proceeded quantitatively retaining the stereogenic centers.

[110] The recent insights toward the Cu-catalyzed coupling reaction, see: C. He, G. Zhang, J. Ke, H. Zhang, J. T. Miller, A. J. Kropf, A. Lei, *J. Am. Chem. Soc.* **2013**, *135*, 488-493.

[111] K. S. Gayen, T. Sengupta, Y. Saima, A. Das, D. K. Maiti, A. Mitra, *Green Chem.* **2012**, *14*, 1589-1592.

[112] For instance, copper nanoclusters stabilized by 2-mercapto-5-*n*-propylpyrimidine were characterized as many multi-nuclear species, see: W. Wei, Y. Lu, W. Chen, S. Chen, *J. Am. Chem. Soc.* **2011**, *133*, 2060-2063.

[113] Representative papers: a) R. Arakawa, *J. Mass Spectrom. Soc. Jpn.* **2008**, *56*, 247-262; b) X. Xu, S. P. Nolan, R. B. Cole, *Anal. Chem.* **1994**, *66*, 119-125.

[114] $E_{1/2}(ox) = 0.76$ V *vs* SCE, IE = 7.726 eV: ref. J. Sugar, A. Musgrove, *J. Phys. Chem. Ref. Data* **1990**, *19*, 527-616.

[115] M. Ghosh, P. Biswas, U. Flörke, K. Nag, *Inorg. Chem.* **2008**, *47*, 281-296.

[116] A. B. P. Lever, *Inorganic Electronic Spectroscopy, 2nd Ed.*, Elsevier, Amsterdam, **1984**.

[117] F. Mo, Y. Jiang, D. Qiu, Y. Zhang, J. Wang, *Angew. Chem. Int. Ed.* **2010**, *49*, 1846-1849.

[118] a) H. Y. Cho, J. P. Morken, *J. Am. Chem. Soc.* **2010**, *132*, 7576-7577; b) S. Ogoshi, K. Tonomori, M. Oka, H. Kurosawa, *J. Am. Chem. Soc.* **2006**, *128*, 7077-7086; c) K. K. D. Amarasinghe, S. K. Chowdhury, M. J. Heeg, J. Montgomery, *Organometallics* **2001**, *20*, 3370-372.

[119] A remarkable analogy is known in the case of In(0), which eventually leads to a little enantiopurity of the product. For instance, water is remarkably effective for reactivity, redox-disproportionation readily takes place in an aqueous environment, the catalyst tends to aggregate to form metal ingot after the reaction, and so on. U. Schneider, M. Ueno, S. Kobayashi, *J. Am. Chem. Soc.* **2008**, *130*, 13824-13825.

[120] V. S. Bryantsev, M. S. Diallo, A. C. T. van Duin, W. A. Goddard III, *J. Phys. Chem. A* **2008**, *112*, 9104-9112.

[121] a) J. Cid, H. Gulyás, J. J. Carbó, E. Fernández, *Chem. Soc. Rev.* **2012**, *41*, 3558–3570; b) C. P. Ulldemolins, A. Bonet, C. Bo, H. Gulyás, E. Fernández, *Chem. Eur. J.* **2012**, *18*, 1121–1126.

[122] W. –S. Lee, C. –T. Yeung, K. –C. Sham, W. –T. Wang, H. –L. Kwong, *Polyhedron* **2011**, *30*, 178-186.

Chapter 4 : Manipulation of Proton in Aqueous Environments

Section 4.1 Intoduction: Enantioselective Protonation Events in Water

When learning organic reactions, undergraduates always start with how the electron moves. It is no mistake. For instance, when asked to draw a mechanism for hydrolysis of acyl chloride, they will submit an answer sheet involving tetrahedral intermediate. One might think that an intramolecular proton transfer can neutralize the zwitterion followed by regeneration of carbonyl through a 1,2-elimination (Scheme 1, above). However, the other might answer that oxygen lone pair comes down to the carbon to trigger the liberation of Cl$^-$ and then deprotonation takes place (Scheme 1, below). Both are generally approved of without any point deducing, which perplexed me a lot when an undergraduate. It made me feel a sense of incongruity at that time. Considering the fundamental difference between proton transfer and electron transfer from tetrahedral intermediate, it seemed unlikely that the probabilities are identical. The difference between the basicity of neighboring O$^-$ and the acidity of $^+$OH$_2$ would determine the rate of intramolecular proton transfer. When electron transfer triggers 1,2-elimination, we have to consider the principle of least motion concerned with the geometrical change of C atom from sp^3 to sp^2.
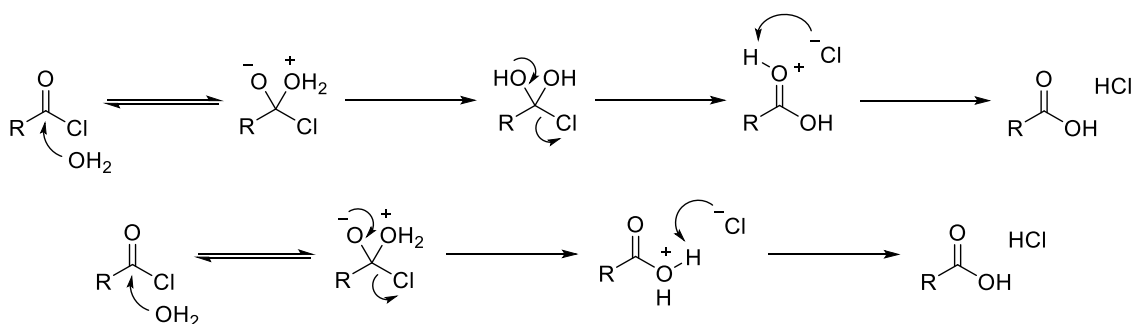
Scheme 1. General mechanism on hydrolysis of acid chloride.

Although the nature of R group should have an influence on the mechanism, many textbook tend to evade the careful inspection of these processes. It should be added that the third mechanism involving a concerted S$_N$2 reaction on the sp^2-hybridized carbon without formation of tetrahedral intermediate was proposed by DFT calculations.[1] Anyway, all chemical reactions rely on the processes of proton and electron transfer, although they are the lightest of the particles with opposite electric charges. In particular, proton and electron transfer in water is closely associated with biological functions as the most fundamental factor. Proton-transfer in water plays an essential role in processes in life such as muscle contraction and electron transport chain (ETC) in mitochondrial matrix. A proton-coupled electron transfer is thought to be a common mechanism of redox reactions. Numerous investigations, both experimental and theoretical, have been explored toward understanding the relationships between kinetics and thermodynamics of these processes.

A prochiral enolate, produced through deprotonation of the parent carbonyl compounds or through nucleophilic addition to ketenes or enones, can undergo the enantioselective protonation with chiral proton donor either from the top or bottom face, thus forming chiral compounds under a kinetic control (Scheme 2).[2] The vertical approach of proton against the planar π-system defines the preferred trajectory with a preferential ccolinear arrangement between donor atom, proton and acceptor atom.
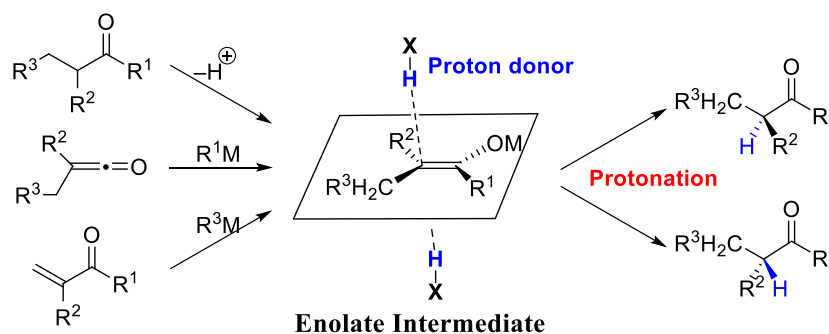
Scheme 2. Enantioselective protonation based upon enolate intermediate.

Enantioselective control of proton transfer event, in other words manipulating the smallest atom while suppressing product racemization at a particularly labile stereocenter, represents arduous challenges.   First of all, since a rapid proton exchange often disables the kinetic control of protonation, the proton source is restricted to be weakly acidic.   Second, the competitive *O*-protonation of enolate intermediates delivers enols which are in equilibrium with the desired product in a racemic manner (Scheme 3).   In order to hamper this racemic pathway, the successful stereoselection can often be achieved by an excessive use of a chiral proton donor.
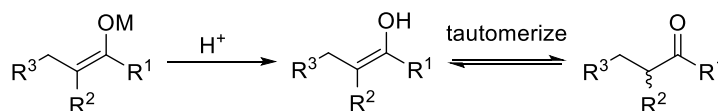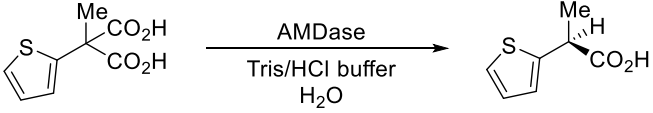
Scheme 3. Competition with *O*-protonation of enolate intermediate.

Because the reaction should be strictly under kinetic control to prevent concomitant racemization, the reaction temperature and reaction time should be adjusted appropriately.   In addition, *E/Z* isomerization of starting materials or the corresponding enolate intermediates, their solvation and their aggregation were also burdensoeme, considering the key enantiofacial differenciation.   That is why the substrate scope for a number of protocols is specifically restricted to a certain substrate class.

Nature has cleverly been operating the catalytic enantioselective protonation.   For instance, esterases are known to release latent enolate from prochiral substrates.[3] The catalytic activity of arylmalonate decarboxylase (AMDase) isolated from the Gram-negative bacterium *Alcaligenes bronchisepticus* was disclosed in the decarboxylative protonation of α-aryl-α-methyl-malonates.[4] Based on the estimated reaction mechanism where Cys 188 is working as a proton donor (Table 1, below), the introduction of mutations was performed.[5] Introduction of the new proton-donating amino acid residue at position 74 replacing Gly resulted in

the formation of the product in a racemic manner (entry 2).   The decreased proton-donating ability at the essential Cys188 led to the inversion of enantioselectivity (entries 3, 4).

Table 1. Enzymatic decarboxylative protonation with wild-type and mutant decarboxylases.

Entry	Enzyme	Relative acitivity	Ee (%)
1	Wild-type	100	99 (*S*)
2	G74C	0.79	0
3	C188S	0.77	50 (*R*)
4	G74C/C188S	0.52	94 (*R*)
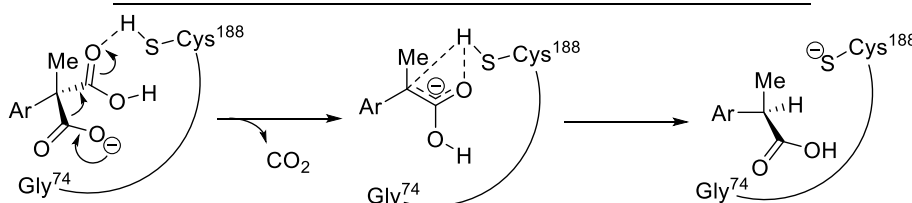
Since the pioneer report by Duhamel and Plaquevent regarding the first catalytic enantioselective pronation of lithium enolates,[6] several strategic approaches have been investigated especially in the last three decades.[7] One of the most popular methods is quenching the stoichiometric formation of enolates or surrogates such as silicon enolates with a catalytic amount of chiral proton donor such as Brønsted acid.   This concept was demonstrated using a chiral Lewis acid-assisted Brønsted acid (LBA)[8] in 1996 for the first time (Scheme 4).[9] The catalysts responsible for the protonation of lithium enolates were then extended to other LBA systems,[10] tetraamine ligand with solvent amount of achiral proton source (Scheme 5),[11] dipeptide catalyst with phenol,[12] BINOL *N*-triflyl thiophosphoramide with phenol,[13] chiral gadolinium complex with phenol,[14] chiral sulfinamide/achiral sulfonic acid system,[15] cinchona-type organocatalysts[16] and so on.   The cooperative catalysts with fluoride source to convert silyl enol ethers into the corresponding optically active ketones were also reported.[17] Enantioselective protonation of enamine[18] or enol ether derivatives[19] is also noteworthy.
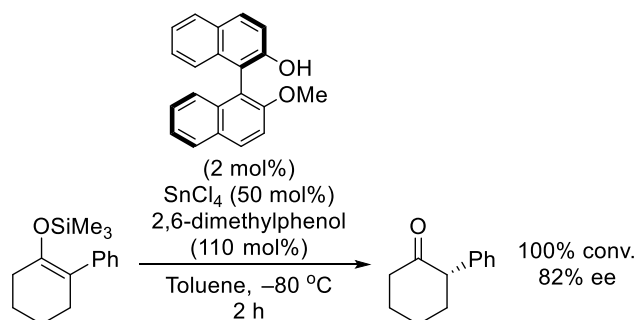
Scheme 4. Chiral LBA-catalyzed enantioselective protonation of silicon enolate.
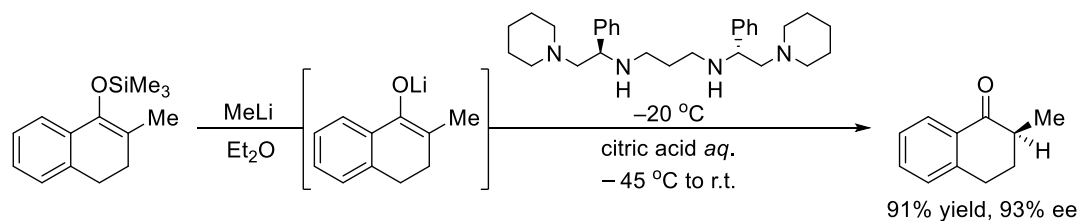
Scheme 5. Enantioselective protonation of achiral lithium enolates catalyzed by tetraamine catalyst.

An attractive alternative is catalytic formation of chiral enolates after addition to ketenes or their equivalents [20] or tandem conjugate addition/enantioselective protonation protocols. Shibasaki *et al.* revealed the enantioselective protonation of *in situ* formed enolate intermediates *via* Michael addition of thiols to α,β-unsaturated thioesters using LaNa₃tris(binaphthoxide) (LSB) at low temperature (Scheme 6).[21] Thiols protonate one of the binol ligands and the acidic OH moiety protonates the samarium enolate efficiently. The importance of acidic OH moiety was strongly indicated from the decreased enantioselection in the presence of sodium thiolate.
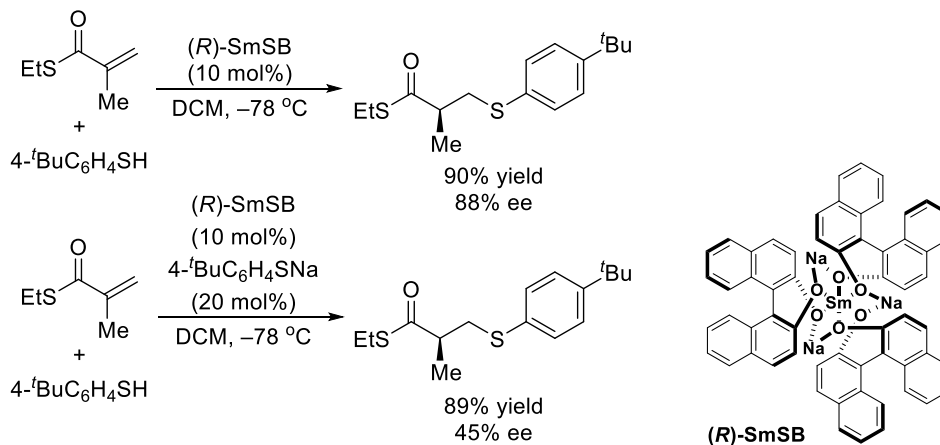
Scheme 6. Catalytic enantioselective protonation in Michael addition to α,β-unsaturated thioesters.

In addition to organometal catalysts, a number of organocatalysts have been developed. Among them, quinines and thiourea derivatives are often used to activate both nucleophiles and electrophiles through hydrogen bonding network. For instance, they possess a basic tertiary amine moiety to recognize nucleophiles and a hydrogen-bond donating moiety to activate electrophiles, operating bifunctionally in conjugate addition to nitroalkenes, α,β-unsaturated sulfones and enones. On the basis of the assumed transition state in enantioselective conjugate addition catalyzed by bifunctional cincona alkaloid-derivatives, their catalytic activity was examined in the subsequent protonation step. The reaction proceeded enantioselectively to afford the desired product bearing 1,3-tertiary–quarternary stereocenters in the presence of quinine derivatives (Scheme 7).[22] The authors assumed that C6'-OH played an important role in the setereoselective generation of stereocenters at both nucleophilic addition and protonation steps through a network of hydrogen bonds. The thiourea-based catalysts were also developed in the enantioselective protonation after addition of α-substituted Meldrum's acids to α-substituted nitroalkenes.[23]
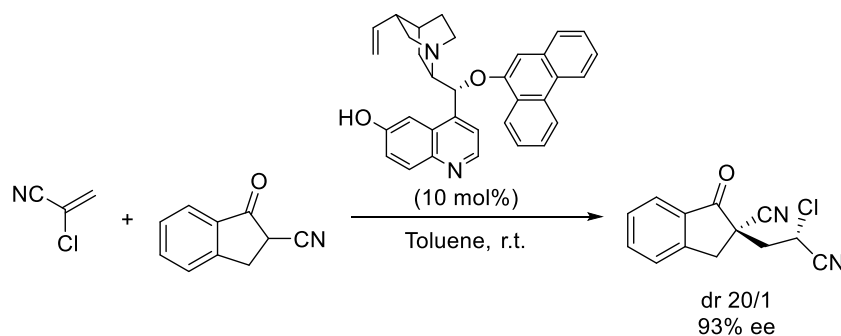
Scheme 7. Catalytic enantioselective protonation in Michael addition to α-chloroacrylonitrile.

Chiral calcium alkoxide complexes catalyzed Michael addition/enantioselective sequences using dibenzyl malonate in the presence of an achiral phenol additive (Scheme 8).[24] The transient enolate geometry would be controlled by chelation of the auxiliary with calcium complex at protonation step. The significant decrease in enantioselectivity was observed in the reaction of α-aryl-substituted derivative (Ph-substituted substrate: 48% ee).
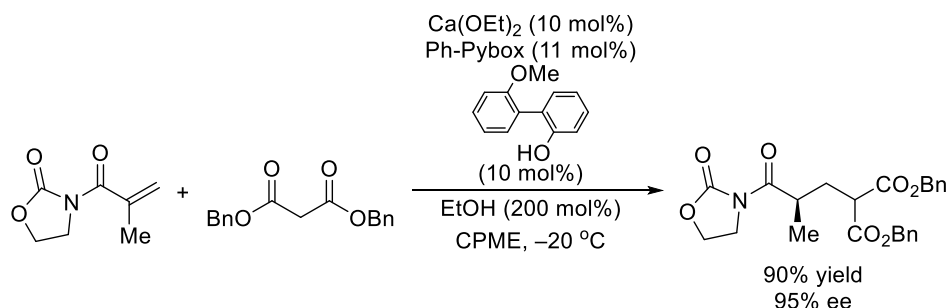
Scheme 8. Chiral calcium-catalyzed protonation in Michael addition of malonates.

Enantioselective protonation of *N*-acyl pyrroles was successfully catalyzed by chiral gadolinium complex after conjugative cyanation using TMSCN and HCN (Scheme 9).[14] Not only α-alkyl but also α-aryl analogues were transformed with high enantioselectivity.
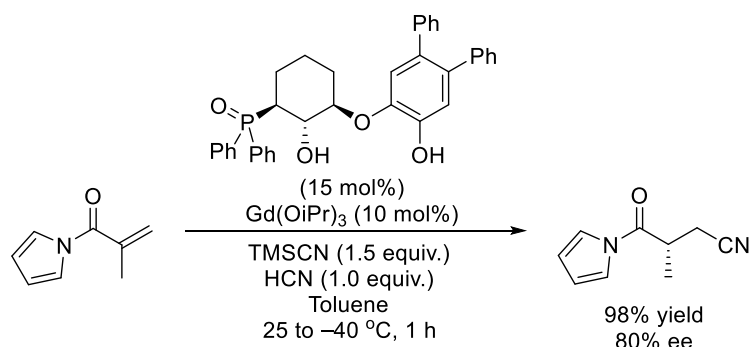
Scheme 9. Catalytic conjugative cyanation/enenatioselective protonation of *N*-acyl pyrroles.

Rhodium-catalyzed tandem carbometalation/enantioselective protonation was also released as a method for accessing β-amino acid derivatives (Scheme 10).[25] The 2-methoxyphenol added as

a proton source was crucial for achieving satisfactory levels of stereoselection and for the reproducibility.   The DFT calculations support the divergent mechanism involving a β-hydride elimination, the subsequent hydride transfer overall from nitrogen to the adjacent carbon and a final protonation.
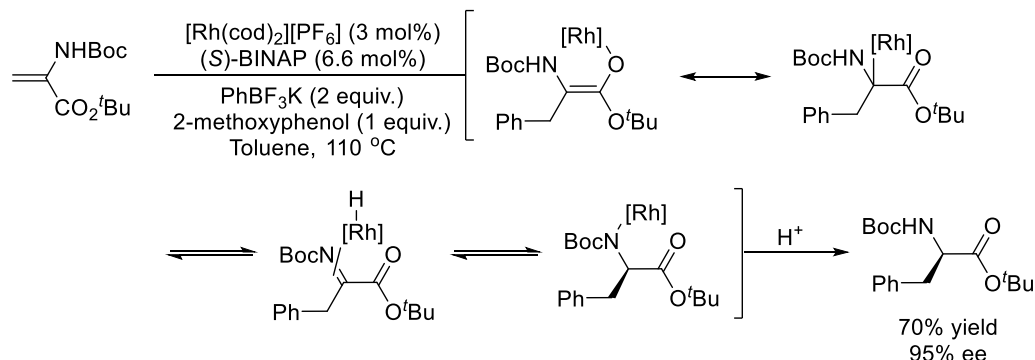
Scheme 10. Rhodium-catalyzed conjugate addition/enantioselective protonation.

Several researchers have explored rhodium-catalyzed conjugate addition/enantioselective protonation sequences with various activated electrophiles and carbon-based nucleophiles.[26] It was also revealed that chiral rhodium complex formed with (S)-DifluorPhos delivered the 1,4-addition-type enantioselective protonation of 2-phthalimidoacrylate with phenylboronic acid (Scheme 11).[27]   The phthalimide, with a reasonably acidic N–H, was added as the proton source to quench the oxa-π-allylrhodium intermediate with high enantioselectivity.
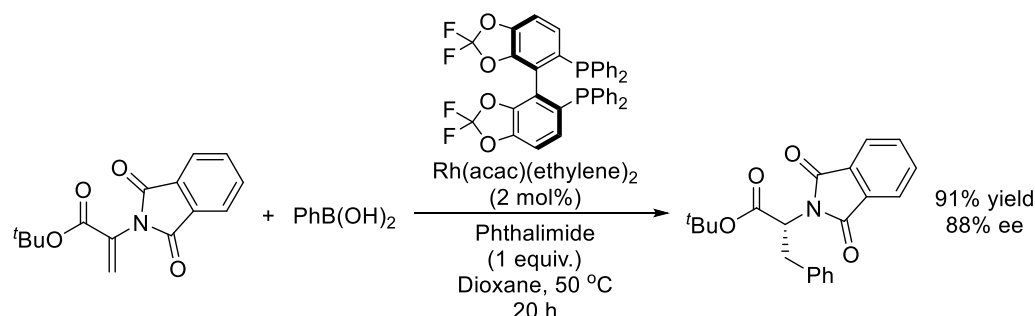
Scheme 11. Rhodium-catalyzed conjugate addition/enantioselective protonation.

The tandem enantioselective protonation strategy consisting of a Friedel-Crafts-type addition of pyrroles was achieved by chiral zinc complex formed with Ph-DBFOX (Scheme 12).[28] The Z-enolate intermediate binding with chiral zinc complex would be protonated by a proton from the pyrrole fragment.
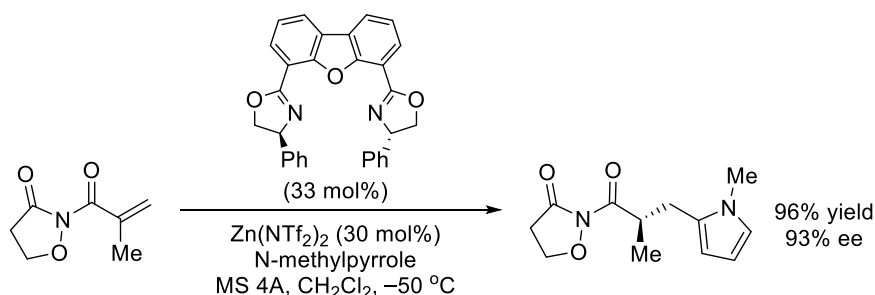
Scheme 12. Chiral zinc-catalyzed Friedel-Crafts-type reaction/enantioselective protonation.

Chiral primary-tertiary diamine catalyst was found to catalyze the Friedel-Crafts-type conjugate addition of indoles/enantioselective protonation to α-substituted vinyl ketones with high enantioselectivity (Scheme 13).[29] The reaction to vinyl ketones bearing bulky group at α-position led to a slight decrease in enantioselecitivity. C2-unsubstituted indoles were also applicable, albeit with lower enantioselectivity ranging from 72 to 74% ee. It should be noted that α-functionalized acrolein derivatives can be used as a substrate instead of vinyl ketones. They reacted with diamine ligand to form activated iminium salts, followed by nucleophilic addition furnishing an enamine intermediate. The protonated tertiary amine moiety would work as a proton source to quench the generated enamine intermediate. The authors highlighted the pronounced role of water in stereoselection, based upon the observation of primary kinetic isotope effects with the aid of DFT calculations. The postulated mechanism involves the protonation of *E*-enamine intermediate impaled by the O–H/π interaction with the indole backbone, where water molecule act both as a proton source and as a scafford of the indole backbone.
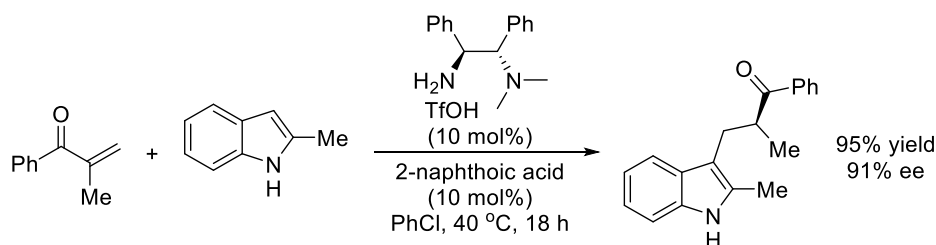
Scheme 13. Organocatalyzed Friedel-Crafts-type conjugate addition/enantioselective protonation.

The catalytic activity of chiral NHC catalyst bearing triazole ring was disclosed even in Stetter reaction-type enantioselective protonation (Scheme 14).[30] Assumed Breslow intermediates after the reaction between aldehydes and NHC catalyst underwent 1,4-addition to *N*-acylamido acrylates as nucleophiles, furnishing the transient chiral alcohol enolate intermediates. The stereoselective intramolecular protonation from alcohol moiety to α-positon would transfer the chiral information. DFT calculations explained that the Gibbs free energies were significantly lower for transition states with explicit bound *t*BuOK as compared with the conventional pathways without the counterions.[31] The stereocontrol would be executed in an intermolecular proton transfer from HO*t*Bu to the prochiral carbon atom.
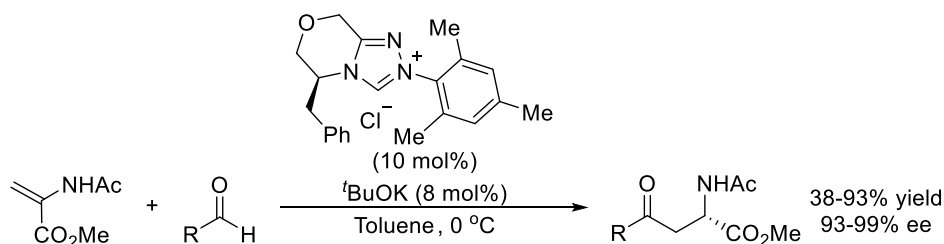
Scheme 14. NHC catalysis for enantioselective protonation.

In the first key catalytic transformations toward total synthesis of R207910, a promising anti-tuberculosis agent, Shibasaki *et al.* implemented an elaborate approach through chiral yttrium-catalyzed enantioselective proton migration (Scheme 15).[32] The marked increase in stereoinduction was attained by the addition of *p*-methoxyprydine *N*-oxide.   Added Bu$_4$NCl was responsible for the rate acceleration without impinging on the level of enantioselection.
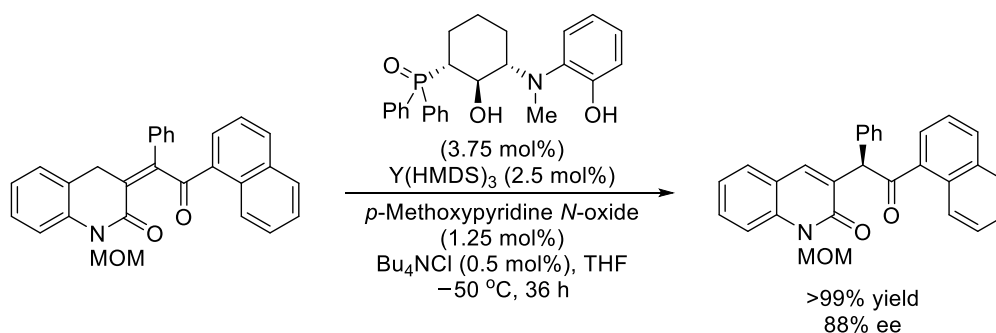
Scheme 15. Catalytic enantioselective proton transfer catalyzed by chiral yttrium complex.

Section 4.2   Thia-Michael Addition/Enantioselective Protonation in Water

4.2-1   Introduction

Asymmetric Michael addition of thiols to α,β-unsaturated ketones is mainstay in biosynthesis as well as in the synthesis of biologically active organosulfur compounds such as diltiazem, calcium antagonists (Scheme 16).[33]
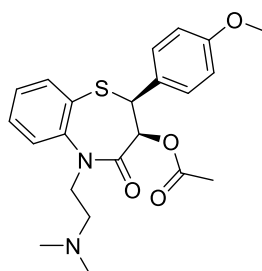
Scheme 16. Structure of diltiazem.

The thiols are ideal nucleophiles from the standpoint of their lower pKa value[34] than the enolisable products, their ease of deprotonation by catalytic amounts of soft bases, and high nucleophilicity of their conjugate bases.   In addition, Michael addition of thiols is, in principle, an ideal reaction which proceeds in ultimate atom economy under proton-transfer conditions to afford enantiomerically enriched building blocks without the employment of any auxiliary groups.   This concept invoked the strategy for the construction of asymmetric carbogenic center *via* enantioselective proton-transfer.

Following the seminal report in 1977,[35] not only organocatalysts including C_2-symmetric bicyclic guanidines,[36] cinchona alkaloid[37] and cinchonidine-thiourea[38] but also metal catalysts[21] emerged.   Another type of organocatalyst, C_2-symmetric bicyclic guanidines was found to catalyze the enantioselective protonation of 2-phthalimidoacrylate (Scheme 17, above) at low temperature.[39] Since the addition of water did not adversely affect the stereochemical outcomes, the reaction could be performed in biphasic system ($Et_2O/D_2O = 5/1$) at the same temperature to afford the deuterated product (97% D incorporation).   The reaction with deuterium-labeled aryl thiols suffered from the moderate level of deuterium incorporation in the product.   The catalyst was applicable for the reaction of sterically hindered *N*-aryl itaconimides (Scheme 17, below).   Cyclic 1,4-dicarbonyl architectures allow the exclusive formation of *Z*-enolate intermediates.   When *tert*-butyl substituent was located at the *ortho* position of the *N*-aryl group, the reaction furnished a 1:1 mixture of atropisomers among which *anti*-diastereomer was obtained in a high enantiomeric manner.
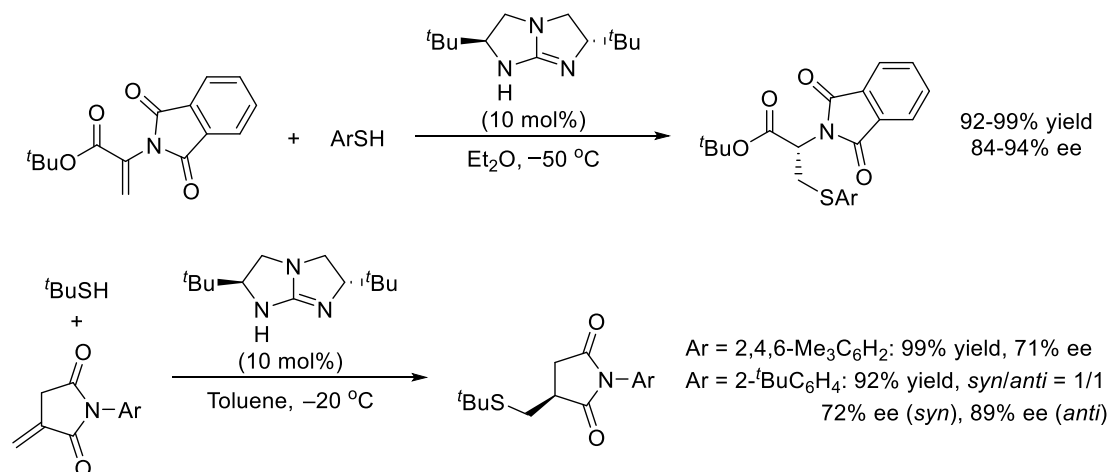
Scheme 17. Enantioselective protonation of tert-butyl-2-phthalimidoacrylate (above) and itaconimides (below) catalyzed by guanidine catalyst.

The conventional bifunctional organocatalysts were also evolved toward highly enantioselective protonation. The *epi*-aminoquinine squaramide was responsible for recognition of *N*-acylic imide skeleton (Scheme 18).[40] The parasitic racemic pathway was successfully suppressed under strictly anhydrous conditions.
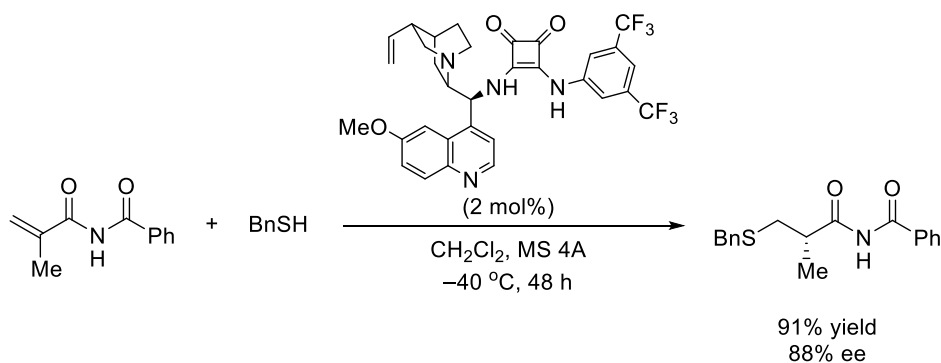
Scheme 18. Enantioselective protonation of acrylic imides catalyzed by chiral squaramides.

In *epi*-aminocinchonidine thiourea was effective for the transformation of *N*-acyloyloxazolidinones[41] and was characterized by a low catalyst loading (Scheme 19). As is often the case, thiourea moiety would activate the oxazolidinone moiety even at the subsequent protonation step. The formed *Z*-enolate was thus quenched stereoselectively with a protonated quinuclidinium salt.
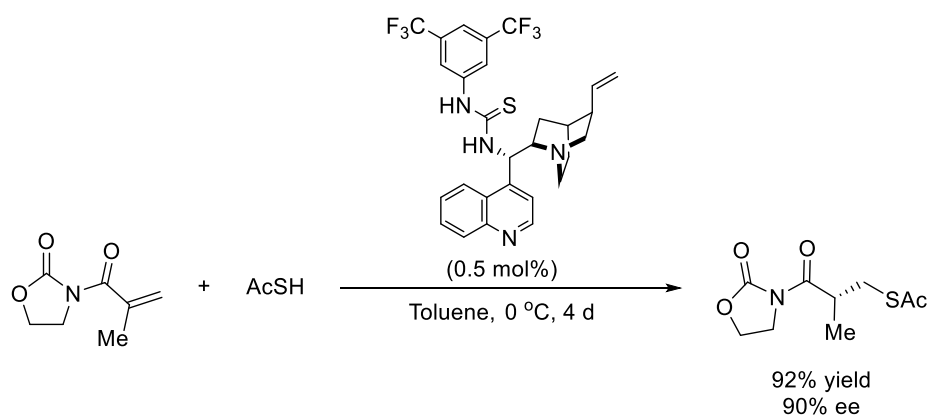
Scheme 19. Enantioselective protonation of N-acyloyloxazolidinones with thioacetic acid.

Simpler chiral primary-tertiary diamine catalyst derived from *L*-phenylalanine was developed quite recently for the transformation of simle α-substituted vinyl ketones (Scheme 20).[42] The reaction with thiol bearing 2-aminoethylene skeleton could be catalyzed by the optimized diamine combined with TfOH.
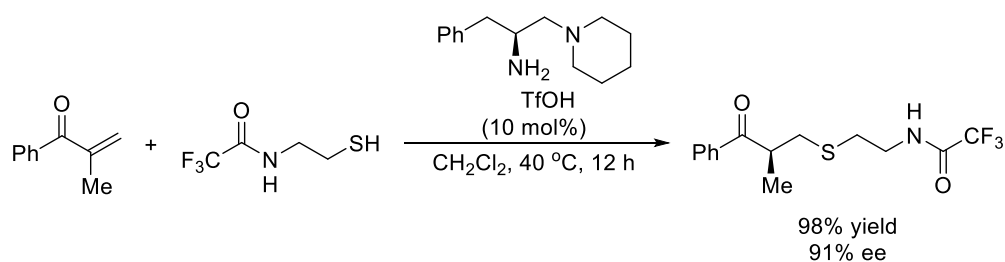
Scheme 20. Enantioselective protonation to α-substituted vinyl ketones.

However, most of them require strictly anhydrous and basic conditions, and extremely high or low temperatures, to obtain high selectivity, and the substrate scope is relatively narrow. Herein described is the new methodology on chiral Sc-catalyzed asymmetric Michael addition of thiols with enones in water.

4.2-2 Thia-Michael Addtion-type

As an extension of a preliminary report[43] on the chiral Sc-catalyzed Michael addition of thiols to α,β-unsaturated enones in water, substituents at the α-position of enones might provide us with a new strategy for the construction of two successive stereogenic centers.   When fixed s-*cis* compound, 2-(*E*)-butylidene-3,4-dihydro-2*H*-naphthalen-1-one **32a** was served as a Michael acceptor, it was disclosed that chiral scandium complex formed with **L1** exhibited unexpected preference for *syn*-isomer (Table 1).

Table 1. Michael addition of thiol to α,β-disubstituted ketone in water.
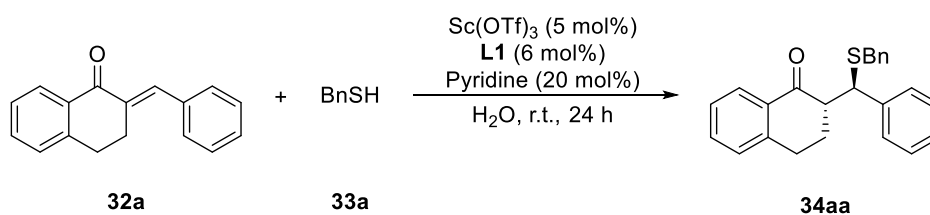
Entry	Solvent	Ligand	Yield (%)	Dr (*syn/anti*)[a]	Ee (%)[b]
1	H$_2$O	+	90	90/10	96/38
2	CH$_2$Cl$_2$	+	63	77/23	54/72
3	H$_2$O	–	58	48/52	–
4	CH$_2$Cl$_2$	–	44	28/72	–

[a] Determined by ^{1}H NMR analysis.   [b] Determined by HPLC analysis.

The substrate tolerance was then examined with ternary catalytic system consisting of Sc(OTf)$_3$, **L1** and pyridine (Scheme 21).   It is curious that the corresponding product was obtained in high yield with high diastereo- and enantioselectivities.   Both electron-withdrawing and electron-donating substituents afforded high selectivities, although they affected electrophilicity at the β-position of enones.   In contrast, when indanone-derived enone **32e** or cyclohexanone-derived enone **32f** was employed as a substrate, the diastereoselectivity decreased with retaining the high level of enantioselectivity.

34aa

90% yield
syn/anti = 90/10
96/38 (% ee)

34ba

83% yield
syn/anti = 97/3
98/6 (% ee)

34ca

56% yield
syn/anti = 94/6
97/88 (% ee)

34da

75% yield
syn/anti = 95/5
97/86 (% ee)

34ea

85% yield
syn/anti = 68/32
97/80 (% ee)

34fa

76% yield
syn/anti = 62/38
96/81 (% ee)
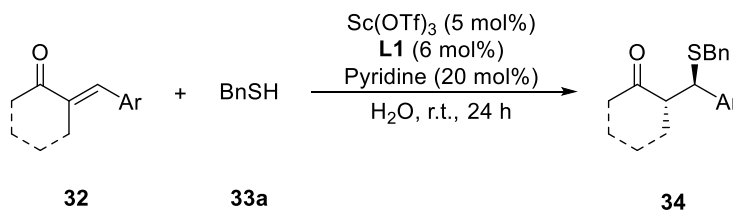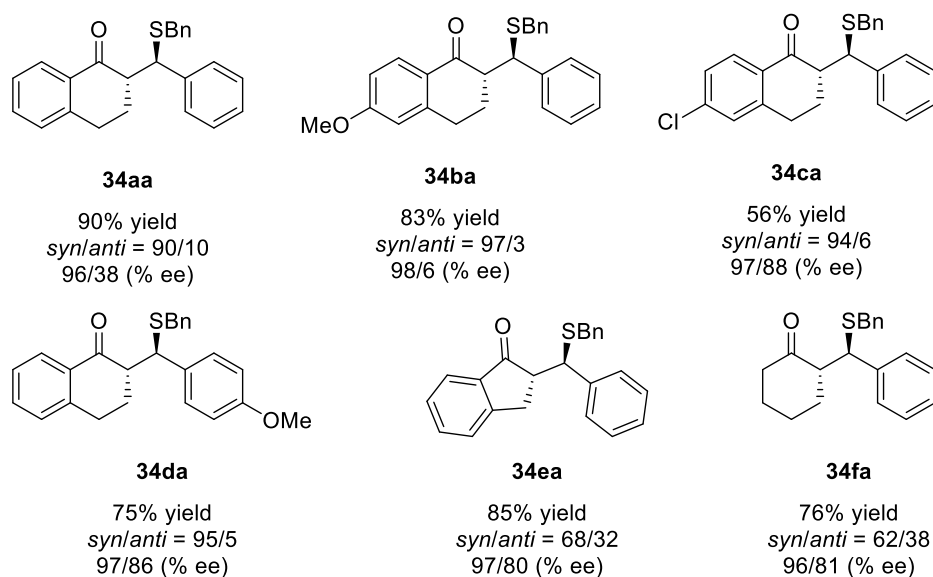
Scheme 21. Scope of s-*cis* α,β-unsaturated compounds.

The transformation of α-branched α,β-unsaturated acyclic ketone **32g** has a potential to generate two adjacent stereocenters through a tandem sequence. Although steric hindrance caused lower conversion, the reaction proceeded in a high enantiomeric manner (Scheme 22). The observed diastereoselectivity is, however, moderate presumably because of a possible isomerization of **32g** in water.

32g   **33a**   **34ga**

26% yield
syn/anti = 44/56
85/94 (% ee)
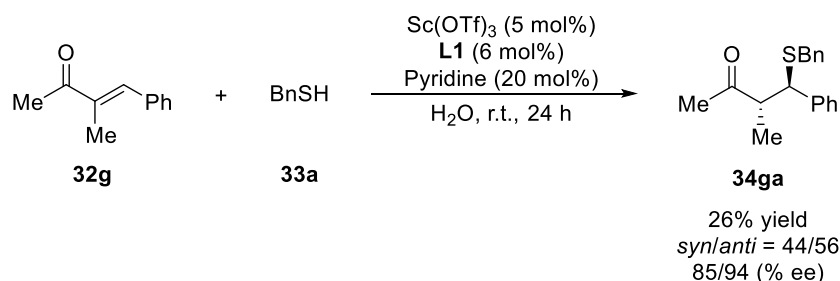
Scheme 22. Sc-catalyzed Michael addition to α,β-disubstituted enone in water.

The interest was then directed toward α-substituted enones bearing unsubstituted terminal sp^2 carbon to generate a prostereogenic enolate intermediate which can undergo stereoconvergent enantioselective protonation. Initially, 2-methyl-1-phenyl-2-propen-1-one **35a** was treated with benzylmercaptan **33a** using previously-optimized ternary catalytic system in water (Table 2). The reaction proceeded smoothly to afford the desired protonated adduct **36aa** in 77% yield with 51% ee, in the presence of 1 mol% of chiral scandium catalyst (entry 1). When the loading of catalyst was increased to 5 mol%, the enantiomeric excess of **36aa** improved successfully to 67% ee with the same level of reaction progress (entry 2). Although the conversion of **35a** was incomplete, the reaction seemed to complete within 24 hours, whether desired catalytic pathway or undesired unselective pathway without impinging on the enantioselection (entry 3). Further increase of the catalyst amount could improve neither reaction yield nor enantioselectivity of **36aa** likely because of rise in acidity of the reaction solution caused by the solubility difference between **L1** and

Sc(OTf)$_3$ (entry 4).   Meanwhile, chiral information of **L1** did not transfer to the product **36aa** in the least without adding pyridine (entry 5).   The reaction progressed in the presence of pyridine alone to deliver 46% yield of **36aa** in a racemic manner (entry 6).   It is noteworthy that chiral induction could be executed at protonation event in water, despite the significant competition of unselective reaction pathway as well as the high mobility of protons in water.   A simple recrystallization of **36aa** obtained through this reaction provided the enantiopure compound with >99% ee (Figure 1).

Table 2. Initial trials for enantioselective protonation in water.

Entry	x (mol%)	y (mol%)	Yield (%)	Ee (%)[a]
1	1	10	77	51
2	5	20	78	67
3[b]	5	20	76	67
4	10	20	78	54
5	5	–	36	0
6	–	20	43	–

[a] Determined by HPLC analysis.   [b] Performed for 48 h.
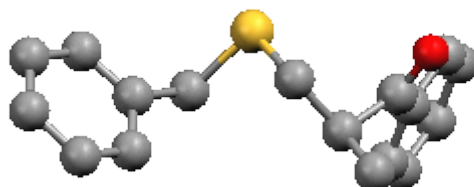
Figure 1. X-ray crystal structure of **36aa**.

As mentioned above, although the nortorious unselective pathway cannot be ignored especially in the presence of pyridine, addition of pyridine seemed to assist the catalysis exerted by chiral scandium complex.   The influence of base was thus examined minutely (Table 3).   The comparison of the results obtained in the reaction of **13k** is quite insightful.   The nucleophilic addition of **33a** takes place with stereoselection followed by nonselective protonation in the reaction of **13k**, whereas the stereo-determining step in the reaction of **35a** comes after nonselective nucleophilic addition.   When any base was not added to the system, a significant decrease in enantioselectivity was observed in nucleophilic addition.   By contrast, the reaction of **35a** was completely racemic in the absence of pyridine (entry 1).   The amount of pyridine ranging from 5 mol% to 20 mol% did not have any influence on the reaction, both in the reaction of **13k** and **35a** (entries 2-5).   In contrast to the reaction of **13k**, even more addition of pyridine deteriorated the enantioselectivity due to the promotion of unselective pathway (entries 6, 7).   When other organic bases were used, the degree of adverse influence was different between two reactions.   The

remarkable difference in range of enantioselecitivity drop appeared in enantioselective protonation of **35a** (entries 8, 9). Not only organic base but also inorganic base was effective for the enantioselective 1,4-addition. Likewise, protonation event was controlled sterically even in the presence of inorganic base. The reaction of **35a** was, however, more sensitive to the amount of inorganic base than the reaction of **13k** (entries 10-12). In particular, even 20 mol% of KOH hampered the desired catalytic pathway remarkably (entry 12). Compared with alkali metal hydroxides, alkali earth metal hydroxides was not so effective although they are both strongly basic (entries 13-18). The addition of 10 mol% of NaOH or KOH allowed the reaction to be most stereoselective (entries 11, 15). Added base can shift the equilibrium between Sc(OTf)$_3$ and **L1** toward a fixed and tetradentate complexation as discussed in Chapter 1. Although the reaction performed in buffer solution was turned out to be unselective, *ca.* 6 times higher yield of the reaction was recorded in pH 5.0 buffer solution. The use of Brønsted acid such as benzoic acid, hydrogen chloride and trifluoroacetic acid as an additive (5 mol%) resulted in the formation of messy byproducts.

Table 3. Effect of base on enantioselective protonation.
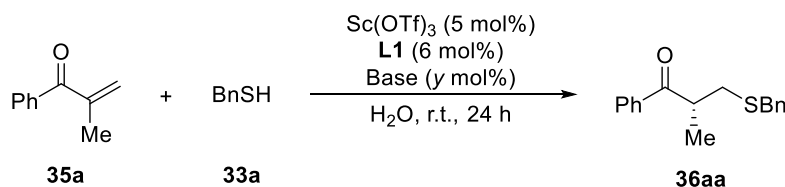
Entry	Base	y (mol%)	36aa		37ka[c]	
			Yield (%)	Ee (%)[a]	Yield (%)	Ee (%)[a]
1	–	–	36	0	34	57
2	Pyridine	5	71	61	84	91
3	Pyridine	10	70	64	83	92
4	Pyridine	15	73	62	85	91
5	Pyridine	20	76	67	85	91
6	Pyridine	30	75	58	91	91
7	Pyridine	40	65	57	89	91
8	DBU[b]	20	71	3	86	80
9	2,6-Lutidine	20	83	40	91	89
10	KOH	5	60	59		
11	KOH	10	69	70	90	89
12	KOH	20	75	−10	93	90
13	NaHCO$_3$	10	73	65		
14	LiOH	10	71	60		
15	NaOH	10	67	71	83	87
16	CsOH	10	79	58		
17	Ca(OH)$_2$	5	68	34		
18	Ba(OH)$_2$	5	67	54		

[a] Determined by HPLC analysis.   [b] DBU = 1,8-diazabicyclo[5,4,0]undec-7-ene.

[c] Examined in the presence of 10 mol% of Sc(OTf)$_3$, 12 mol% of **L1**.

Sc(OTf)$_3$ (10 mol%)
L1 (12 mol%)
Pyridine (*y* mol%)
H$_2$O, r.t., 24 h

13k   **33a**   **37ka**
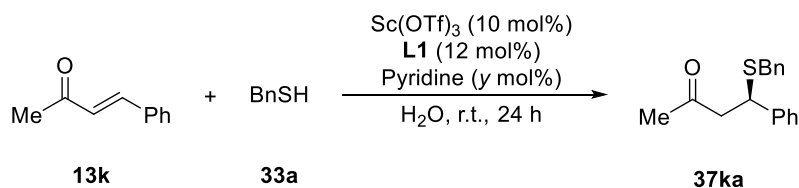
A conspicuous effect of water was seen in enantioselective protonation of **35a** (Table 4, entry 1).   When carried out in organic solvents including protic solvents or mixture of water and water-miscible solvents, the reaction exhibited impressively lower level of enantioselectivity than that in water (entries 2–7).   I have to annotate that major configuration constructed in the reaction performed in organic solvents was opposite stereoisomer to that obtained in water, albeit with weak preference.

Table 4. Effect of solvent on enantioselective protonation.

Sc(OTf)$_3$ (5 mol%)
L1 (6 mol%)
Pyridine (20 mol%)
Solvent, r.t., 24 h

35a   **33a**   **36aa**
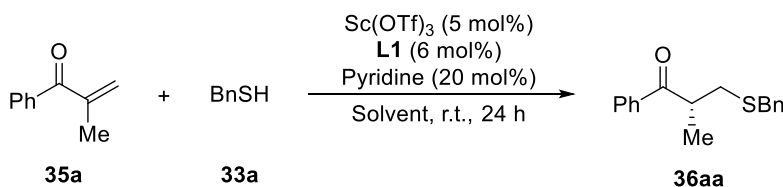
Entry	Solvent	36aa		37ka[b]	
		Yield (%)	Ee (%)[a]	Yield (%)	Ee (%)[a]
1	H$_2$O	76	67	84	91
2	CH$_2$Cl$_2$	54	–5	93	28
3	THF	43	–15	91	31
4	EtOH	54	–19	88	63
5	Toluene	39	–17	82	75
6	H$_2$O/THF = 1/9	45	–16	54	64
7	H$_2$O/EtOH = 1/9	51	–21	90	59

[a] Determined by HPLC analysis.   [b] Examined in the presence of 10 mol% of Sc(OTf)$_3$, 12 mol% of **L1**.

Sc(OTf)$_3$ (10 mol%)
L1 (12 mol%)
Pyridine (20 mol%)
Solvent, r.t., 24 h

13k   **33a**   **37ka**
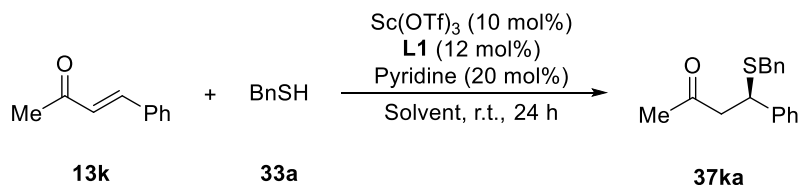
It is evident that chiral scandium complex is responsible for the stereoinduction not only at nucleophilic addition but also at protonation.   The metal effect on the stereoselection in enantioselective protonation of **35a** was then surveyed (Table 5).   When Sc(OTf)$_3$ was replaced into other scandium species, the reaction suffered from a retarding reaction rate and a plunge of enantioselectivity (entries 2–4).   A close resemblance between the reaction outcomes induced by other scandium salts in water and those obtained in organic solvents (Table 4) is implicative.   Poor enantioselectivity was obtained in the presence of other metal cations such as Zn(II) and Fe(II) (entries 5, 6).   Although scandium and lutetium are congener as rare-earth metals, almost

unselective manner in Lu(OTf)$_3$-catalyzed reaction was antithetical to the stereoselective performance of chiral Lu(III) catalyst exerted at the nucleophilic addition to **13k** (entry 7). This disparity implies the outstanding potential of Sc(III) for enantioselective protonation in water.

Table 5. Effect of metal salt on enantioselective protonation.

Entry	Metal salt	36aa		37ka[b]	
		Yield (%)	Ee (%)[a]	Yield (%)	Ee (%)[a]
1	Sc(OTf)$_3$	76	67	84	91
2	Sc(DS)$_3$	54	–21	94	72
3	ScCl$_3$	43	–3		
4	Sc(OAc)$_3$	54	–10		
5	Fe(OTf)$_2$	45	–13	46	7
6	Zn(OTf)$_2$	58	–4	45	0
7	Lu(OTf)$_3$	72	–8	73	66
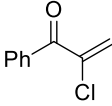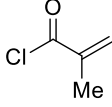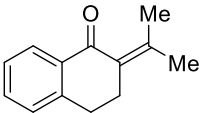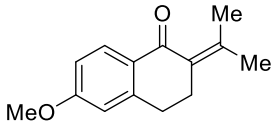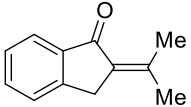
[a] Determined by HPLC analysis. [b] Examined in the presence of 10 mol% of Sc(OTf)$_3$, 12 mol% of **L1**.
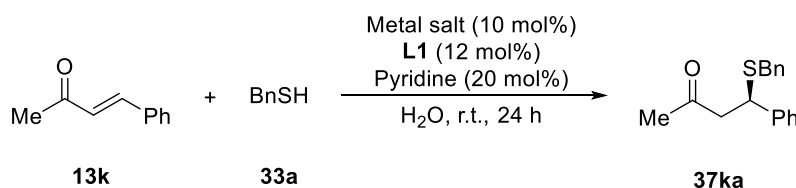
With the optimal conditions in hands, substrate tolerance of enantioselective protonation in water was evaluated (Table 6). The catalyst system was applicable to various types of α-substituted enones bearing unsubstituted terminal sp^2 carbon, delivering the corresponding protonated products in good to high yields with moderate to good enantioselectivities ranging from 53 to 74% (entries 1-12). When oxazolidinone-derived acrylamide **35i** was served as a Michael acceptor, the reaction also proceeded smoothly in water to afford the corresponding adduct with good enantioselectivity (entry 13). Given the oxazolidinone moiety can be readily transformed into various functional groups, the successful applicability to oxazolidinone-derived acrylamide is noteworthy. The reaction of α,β-unsaturated ester **35j**, which is known to be less reactive than ketone, afforded the poor result (entry 14). The imidazole-derived ketone **35k** reacted with **33a** efficiently in almost racemic manner (entry 15). α,β-Unsaturated amides did not react under the conditions (entries 16, 17). The α-chloro enone **35n** and acyl chloride **35o** were found to be imapplicable (entries 18, 19). Tetralones flanked by dimethyl-substituted terminal olefin systems also furnished the corresponding adducts with excellent enantioselecitivity, albeit in low yield (entries 20, 21). This is because undesired racemic pathway was successfully suppressed due to the reluctance of sterically crowded β-position to the nucleophilic addition. In contrast, the reaction of indanone-derivative analogue **35r** resulted in poor enantioselectivity (entry 22).

Table 6. Scope of α-substituted α,β-unsaturated carbonyl compounds.
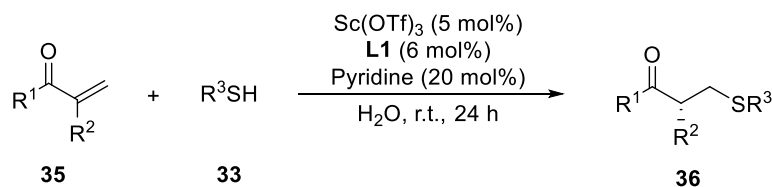
Entry	Electrophiles 35			Nucleophiles 33		Yield (%)	Ee (%)[a]
	R^1	R^2		R^3			
1	Ph	Me	**35a**	BnSH	**33a**	78	67
2	Ph	^{n}Bu	**35b**	BnSH	**33a**	60	69
3	Ph	Ph	**35c**	BnSH	**33a**	75	74
4	4-MeOC$_6$H$_4$	Me	**35d**	BnSH	**33a**	85	54
5	4-BrC$_6$H$_4$	Me	**35e**	BnSH	**33a**	74	70
6	Ph	Bn	**35f**	BnSH	**33a**	70	60
7	3-CF$_3$C$_6$H$_4$	Bn	**35g**	BnSH	**33a**	51	63
8	4-MeOC$_6$H$_4$	Bn	**35h**	BnSH	**33a**	74	60
9	Ph	Me	**35a**	4-ClC$_6$H$_4$CH$_2$SH	**33b**	78	53
10	Ph	Me	**35a**	4-MeOC$_6$H$_4$CH$_2$SH	**33c**	82	60
11	Ph	Me	**35a**	4-^{t}BuC$_6$H$_4$CH$_2$SH	**33d**	74	58
12	Ph	Me	**35a**	2-FurylCH$_2$SH	**33e**	92	60
13			**35i**	BnSH	**33a**	29	68
14			**35j**	BnSH	**33a**	7	21
15			**35k**	BnSH	**33a**	83	3
16			**35l**	BnSH	**33a**	NR	–
17			**35m**	BnSH	**33a**	NR	–

18	Ph—C(=O)—C(Cl)=CH₂	**35n**	BnSH	**33a**	messy	–
19	Cl—C(=O)—C(Me)=CH₂	**35o**	BnSH	**33a**	NR	–
20[b]	**35p**	**35p**	BnSH	**33a**	37	92
21[b]	**35q**	**35q**	BnSH	**33a**	26	94
22[b]	**35r**	**35r**	BnSH	**33a**	56	45

[a] Determined by HPLC analysis.   [b] Performed for 96 hours.

Finally, the synthetic potential of the protonated adducts was demonstrated as one example. The product **36pa** was converted to optically active α-branched ketone through desulfurization with Raney Nickel W-2 without compromising the optical purity and the subsequent recrystallization (Scheme 23).

36pa
92% ee

Raney Ni W-2
NaPH₂O₂
acetate buffer/EtOH
r.t., 1 h

92% ee
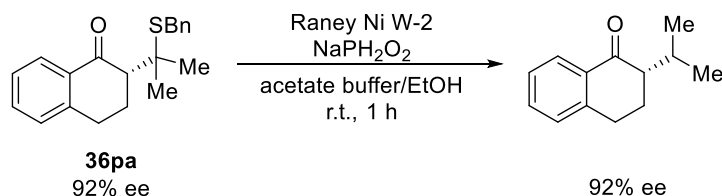
Scheme 23. Desulfurization with Raney nickel W-2.

4.2-3 *Mechanism*

It is evident that Sc(OTf)$_3$–**L1** complex and pyridine used as an additive are crucial for the reaction progress and the enantioselection. As discussed in Chapter 1, ^{45}Sc NMR spectroscopy revealed that the catalytic system prepared by simply mixing Sc(OTf)$_3$ and 1.2 equivalent of **L1** in water was in dynamic equilibrium between two environmentally distinct scandium species. The one spectrum (δ = 0.0 ppm) is assigned to the Sc(III) ion, and the other (δ = 47.3 ppm) is considered to be a 1:1 Sc–**L1** complex. Crystallographic analysis of the chiral scandium complex formed with **L1** has been characterized to be pentagonal bipyramidal geometry. The role of two hydroxyl groups of **L1** was investigated (Table 7). Since both monoprotected ligand **L2** and bisprotected **L3** forced the reaction to be sluggish and much less stereoselective, it appears that **L1** coordinates to a scandium ion in a tetradentate fashion in water. The inferior performance due to the increased bulkiness of chiral ligand side chain is assumed to arise from the increased insolubility of **L6** in water. Meanwhile, the extinction of a peak corresponding to free Sc(III) ion (δ = 0.0 ppm) and the significantly downfield chemical shift (δ = 79.7 ppm) on ^{45}Sc NMR spectroscopy induced by addition of pyridine are quite insightful. Since having a d0 configuration, scandium ion should be irrelevant to the nature of its coordinating ligands. The drastic change in the coordination environment around scandium ion triggered by addition of pyridine would be rationalized by the formation of chiral scandium monohydroxide complex.

Table 7. Effect of chiral 2,2'-bipyridine ligands on stereoselection.

Entry	Ligand	36aa		37aa[b]	
		Yield (%)	Ee (%)[a]	Yield (%)	Ee (%)[a]
1	**L1**	76	67	84	91
2	**L2**			22	18
3	**L3**			2	19
4	**L6**	43	0	28	14

[a] Determined by HPLC analysis.

[b] Examined in the presence of 10 mol% of Sc(OTf)$_3$, 12 mol% of **L1**.

The observation of positive non-linear effect (NLE) in asymmetric Michael addition of **33a** with benzalacetone **13k** implies the existence of heterodimeric chiral complex in water (Figure 2). Taking metal hydroxide can generally form μ-hydroxide dimeric structure into consideration, this experimental result is reasonable.
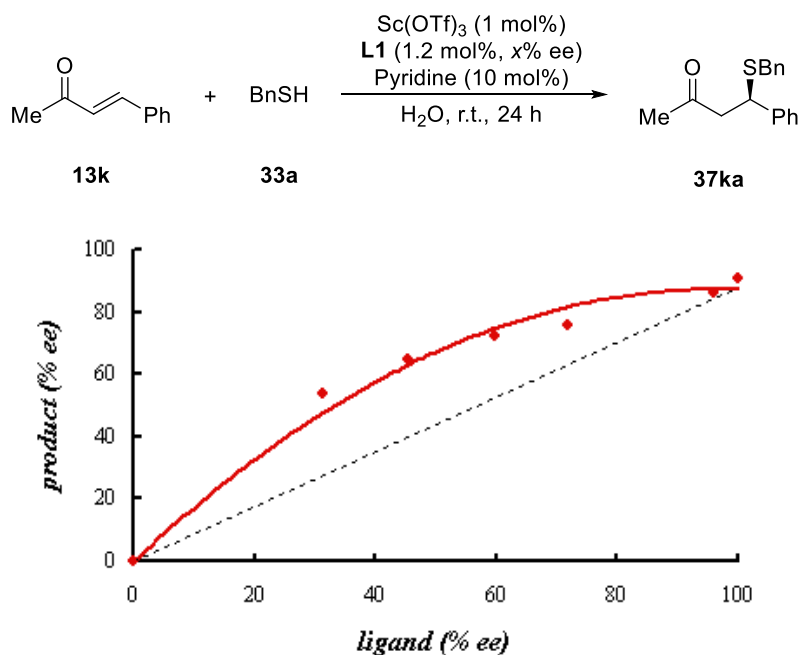
Figure 2. Non-linear effect observed in chiral Sc-catalyzed reaction of **13k** with **33a**.

The ternary catalytic system comprising the Lewis acid and the base exhibits two distinct reaction pathways. One is a desired cooperative pathway depicted by precise orchestration of Lewis acid-base. The other is a base-catalyzed undesired pathway with no chiral induction. In this base-catalyzed pathway, the rate-determining step is an attack of thiolates to enones to generate enolates.[44] On the other hand, the desired catalytic pathway may have multiple steps (Scheme 24). The initial trigger of the reaction is catalytic generation of an activated enone, which is known to be confirmed by significant changes in ^{13}C chemical shift.[45] The activated enone is then amenable to nucleophilic addition of either thiol or thiolate, which is under acid-base equilibrium.[46] Cronin *et al*. suggested that the nucleophilic addition of thiols in water phase proceeded *via* concerted mechanism.[47] On the other hand, the addition of thiolates entails the stepwise mechanism via the formation of enolate intermediates.
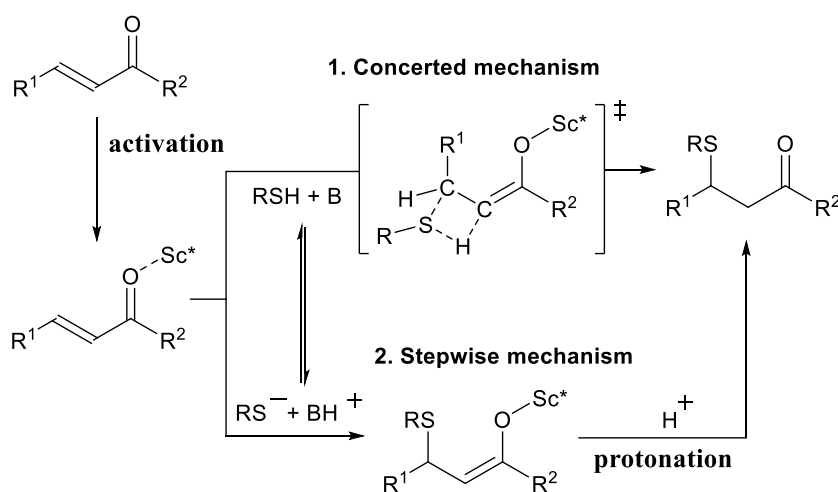
Scheme 24. Possible reaction mechanism for catalytic pathway

The observation of significant rate acceleration by addition of pyridine strongly proves that major nucleophilic species are not *thiols* but *thiolate anions*. The nucleophilic attack of thiolate anions led to products via stepwise process. In the absence of pyridine, the nucleophilic attack of thiols is possible. However, the β-substituted enone led to an enantioselective adduct, while the α-substituted enone led to a racemic product (Scheme 25). The concerted process is influential with stereochemistry on the carbon both at the α-position and at the β-position. Therefore, this difference indicates that the major reaction pathway is a stepwise process even for the attack of thiols.
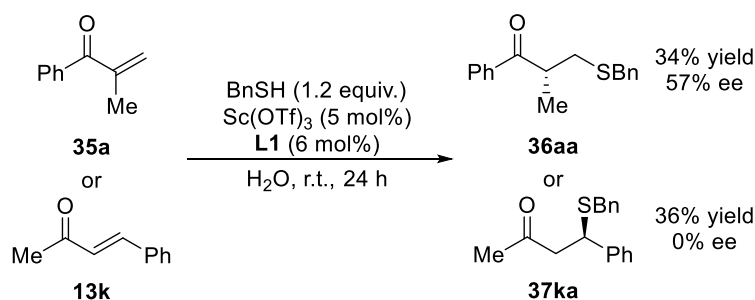
Scheme 25. Reaction in the absence of pyridine.

The stepwise process involves two enantiofacial differentiations; nucleophilic attack and protonation step. In the light of the X-ray structure of the Sc-**L1** complex, a nucleophile prefers to attack the *Si* face in order to rationalize the observed sense of chiral induction (Scheme 26). This tendency of the nucleophilic attack should be the same even in organic solvents.
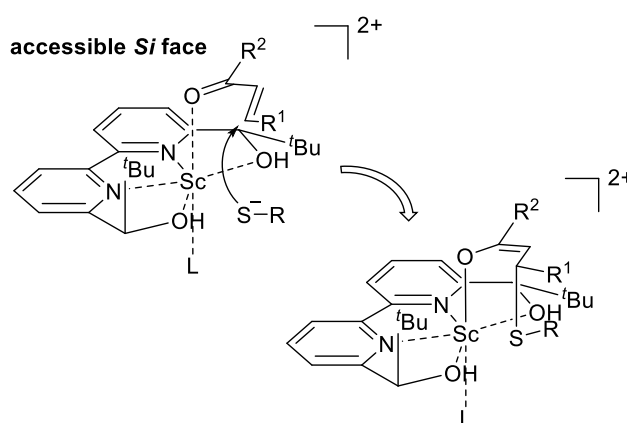
Scheme 26. Plausible reaction mechanism *via* stepwise process.

In contrast, H_2O and other organic solvents differ in enantiofacial differentiation at the protonation step. For instance, the results obtained in H_2O and in EtOH were compared and summarized in Scheme 27.

Scheme 27. Comparison of reaction medium.
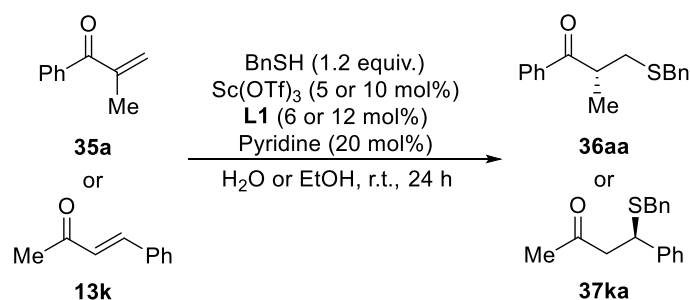
	Stereo-determining step	in H_2O	in EtOH
35a → 36aa	Michael addition	84% yield 91% ee	88% yield 63% ee
13k → 37ka	Protonation	76% yield 67% ee	54% yield −19% ee

Given significant competition of the racemic pathway against the desired catalytic pathway, minimization of structural fluctuation through the interaction between scandium and sulfur may play an important role in governing the enantioselectivity. According to the stereochemistry observed in the enantioselective protonation, proton should be introduced preferentially as shown in Scheme 28.
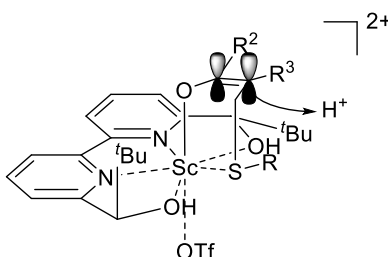
Scheme 28. Enantiofacial differentiation of proton.

In ethanol or other organic solvents, only pyridinium cation generated through the equilibrium with thiols can behave as proton source and enantiofacial differentiation must be based upon steric hindrance. However this explanation is also possible in water. It is considered that the key factor for chiral induction is abnormally high mobility of proton in water, which has more than 10^3 times as a large value as in organic solvents.[48]

In order to examine solvent kinetic isotope effect, the reaction of **33a** with **13k** was carried out in D_2O. Theoretically deuteration should be slower than protonation, which was verified by simple comparison of the reaction rate (Figure 3, **B**).
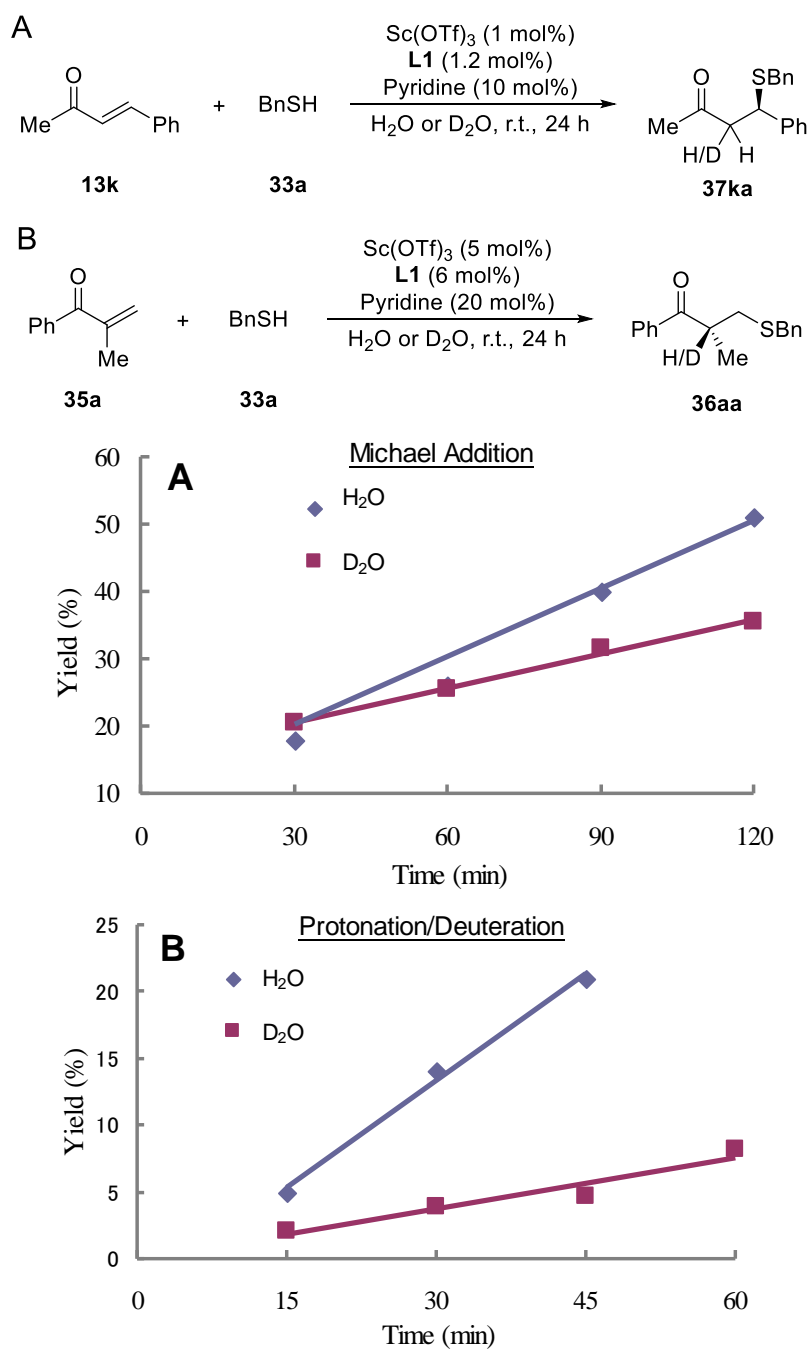
Figure 3. Solvent kinetic isotope effect in the reaction rate of Michael addition and protonation/deuteration

As expected, a prominent isotope effect was exhibited in the reaction of **33a** with **13k** (B) compared with Michael addition (**A**), which seems to originate from the activation energies in protonation/deuteration step. It is obvious that in the latter reaction protonation/deuteration step should be both rate-determining and stereo-determining step. In addition, proton was introduced dominantly in an initial stage of the reaction with excellent reproducibility, in spite of significant competition of the undesired unselective pathway catalyzed by pyridine (Table 8).

Table 8. Comparison between protonation and deuteration.

Entry	Time (h)	Conditions	Total yield (%)	H/D ratio[a]	Ee (%)[b]
1	1	–	14 (6)[c]	43/57	67
2	24	–	71 (7)[c]	10/90	67
3	24	BnSH (3 equiv.)	72 (7)[c]	10/90	67

[a] Determined by ^{1}H NMR analysis.   [b] Determined by HPLC analysis.

[c] Yield of the protonated product

A definitive H/D ratio of the product was finally 10/90, although a total H/D ratio in this system is <1/>99 including an exchangeable proton in thiol (entry 2).   It was confirmed that H/D exchange of generated product does not proceed any more.   It is also noteworthy that proton was barely introduced after an initial stage; the protonated product **36aa-H** was obtained in 6% yield in an initial 1 hour and 7% yield in 24 hours.   Employment of twice amount of thiol **33a** did not affect a definitive H/D ratio, which denied the involvement of free proton in total reaction system. In that sense, hydroxyl groups of **L1** seem to function as proton sources in this catalytic system. Although quantitative argument using ^{1}H NMR was impossible because of the involvement of hydrogen bond, it was verified that protons in the structure of **L1** were not so easy to exchange. Fortunately, this significantly high H/D ratio corresponds to the amount of hydroxy groups in chiral scandium catalyst formed with Sc(OTf)$_3$ and **L1**.   In addition, enantiofacial differentiation illustrated in Scheme 28 implies the proactive involvement in enantioselective protonation of such hydroxy groups.   In Scheme 28, this hydrogen can be affected by the reactive π-orbital of enolate. To my regret, this simplest phenomenon poses limitations to the demonstration of immediate evidence because of proton-rich environment.   Based upon such insight into the sense of chiral induction, possible reaction mechanism is postulated in Scheme 29.   Due to the ionic character between scandium cation and triflate anion, ligand exchange with solvent molecule seems to be very fast on scandium atom.   As proton-transfer rate is picosecond-order, rate-determining step must be Michael addition step of thiolate anion with enone.
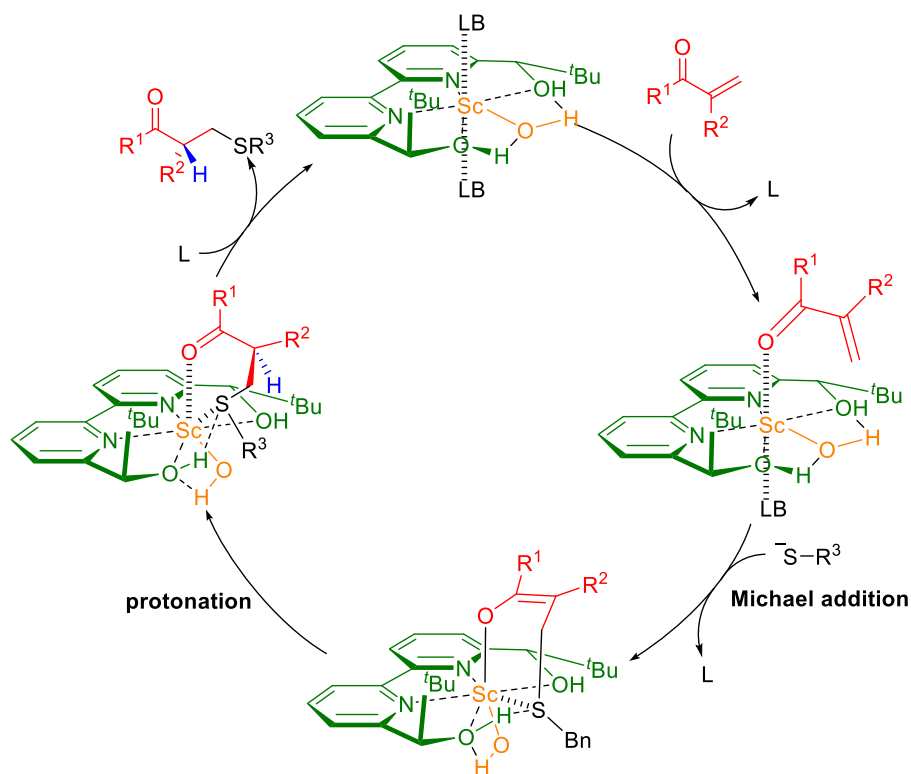
Scheme 29. Possible catalytic cycle for enantioselective protonation

Due to a labile ligand exchange, catalyst structure should be $[(\text{Ligand})\text{Sc}^{\text{III}}(\text{H}_2\text{O})_m(\text{pyr})_n(\text{OTf})_{3-m-n}]^{(m+n)+}$

$(m+n)\ \text{OTf}^-$

Section 4.3 Aza-Micael Addition/Enantioselective Protonation in Water

4.3-1 Introduction

Compounds with α,β-unsaturated carbonyl fragment are of great importance as industrial substances, for example in the manufacture of polymers, textiles or potential medicinal agents. Aza-Michael addition is also important class of chemical transformations to construct synthetically useful building blocks that are optically active including β-amino acid precursors.[49] Although tremendous efforts have been dedicated to develop asymmetric protocols using various amine nucleophiles, catalytic asymmetric protocols with satisfactory level of selectivity, versatility, applicability and practical easiness are limited.

Therefore, there are only a few reports on tandem aza-Michael/enantioselective protonation until now. Sodeoka *et al*. reported BINAP-based palladium-μ-hydroxo complex in aza-Michael addition/protonation sequence using *N*-benzyloxycarbonyl acrylamide.[50] Both nucleophilic addition and protonation were turned out to be highly stereoselective in the presence of their developed catalyst (Scheme 30). The subtle ligand exchange from dimeric μ-hydroxo complex into bidentate acrylamide forms a monomeric palladium complex where the acrylamides are activated toward nucleophilic addition.
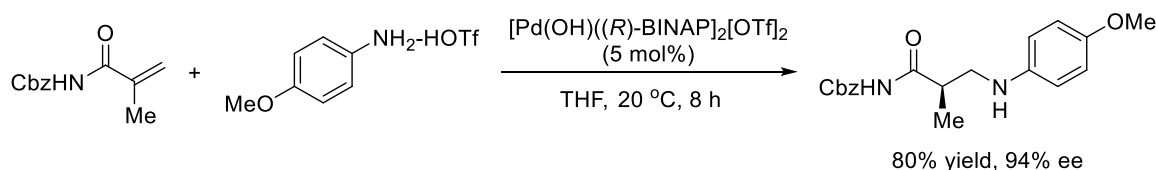
Scheme 30. Palladium-catalyzed tandem aza-Michael addition/enantioselective protonation.

European group reported on the use of amino acid derivatives in base-mediated tandem conjugate addition/protonation protocol (Scheme 31).[51] In the presence of stoichiometric amount of 1,4-diazabicyclo[2,2,2]octane (DABCO), amino acid ester hydrochloride can be reacted efficiently with α-trifluoromethyl Michael acceptor, delivering the trifluoromethyl-containing peptide mimics with high diastereoselectivity.
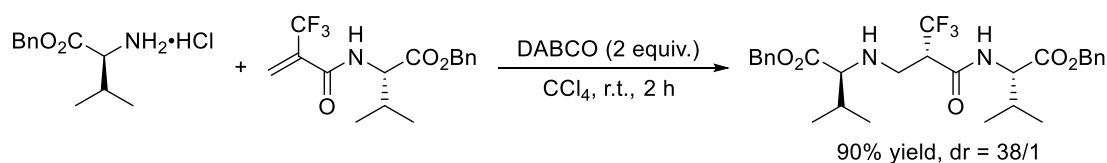
Scheme 31. Tandem aza-Michael addition/protonation using amino acids HCl salts.

Feng *et al*. demonstrated that a tandem aza-Michael/enantioselective protonation of pyrazoles to α-aromatic substituted vinyl ketones was catalyzed efficiently by chiral *N,N'*-dioxide scandium complex (Scheme 32).[52] The addition of aqueous HCl could greatly enhance the

reactivity compared with ther reaction without HCl. It was suggested that HCl and water might serve as the dominate proton donor that mediated the enantioselective proton transfer.

Scheme 32. Tandem aza-Michael addition/protonation using pyrazoles.

4.3-2　Aza-Michael Addition/Enantioselective Protonation in Water

At the outset, α-branched enone **35a** was treated with aniline **38a** in water at room temperature based upon a tandem conjugate addition/enantioselective protonation strategy (Table 9). It was disclosed that scandium dodecylsulfate Sc(DS)$_3$ had a catalytic activity in the desired achiral transformation (entry 1). A simple mixing with chiral 2,2'-bipyridine **L1** as a chiral ligand accelerated the reaction significantly to afford the desired aza-adduct **39aa** with moderate enantioselectivity (entry 2). When another-type of surfactant, dodecylsulfonate Sc(OSO$_2$C$_{12}$H$_{25}$)$_3$ was used instead of Sc(DS)$_3$, the reaction suffered from 64% decline in the reaction yield in compensation for a slightly increased enantioselection (entry 3). As the length of the alkyl chain in surfactant moiety was shortened, the reactivity tended to rise with retaining the level of enantioselection (entries 3-5). In contrast, Sc(OTf)$_3$-catalyzed reaction was much less stereoselective albeit in a high conversion (entry 6).

Table 9. Sc-catalyzed tandem aza-Michael/protonation reaction in water.

Entry	ScX$_3$	Yield (%)	Ee (%)[a]
1[b]	Sc(DS)$_3$[c]	56	–
2	Sc(DS)$_3$[c]	83	42
3	Sc(OSO$_2$C$_{12}$H$_{25}$)$_3$	30	44
4	Sc(OSO$_2$C$_{11}$H$_{23}$)$_3$	53	44
5	Sc(OSO$_2$C$_{10}$H$_{21}$)$_3$	74	45
6	Sc(OTf)$_3$	79	11

[a] Determined by HPLC analysis.　[b] Performed without pyridine.
[c] DS = OSO$_3$C$_{12}$H$_{25}$.

The catalytic activity of LASCs combined with **L1** was evaluated in enantioselective protonation (Table 10). Almost all first-row transition metal complexes formed with **L1** did not convey the chiral information to the desired aza-adduct generated in low to moderate yield (entries1-10). Among them, outstanding stereoselective performance of copper(II)-based LASC was excavated (entry 9). Although aerobic polymerization of aniline was promoted in the presence of copper(II) ion,[53] aniline **38a** was successfully coupled with **35a** steresoselectively in water. The reaction catalyzed by second- and third-row metals was almost racemic, too (entries 11-17). Although the greater performance of zirconium(IV)-based LASC has been displayed in racemic 1,4-addition reactions of aromatic amines and indoles in water,[54] the combination with **L1** seemed to have an adverse influence (entry 11). Unlike scandium(III) catalysis, the reaction proceeded sluggishly in quite low enantiomeric manner in the presence of Yb(III)-based LASC. It is to be noted that the Cu(II)-catalyzed reaction exhibited the inverted stereochemistry of product **39aa** compared with scandium catalysis.

Table 10. Screening of LASC.

$$Ph\text{—}C(=O)\text{—}C(=CH_2)\text{—}Me \quad (35a) \quad + \quad PhNH_2 \quad (38a) \xrightarrow[\text{H}_2\text{O, r.t., 24 h}]{\substack{\text{LASC (5 mol\%)} \\ \textbf{L1} \text{ (6 mol\%)}}} Ph\text{—}C(=O)\text{—}\overset{\underset{Me}{}}{CH}\text{—}CH_2\text{—}NHPh \quad (39aa)$$

Entry	LASC	Yield (%)	Ee (%)[a]
1	$Sc(OSO_2C_{11}H_{23})_3$	53	–44
2	$V(OSO_2C_{11}H_{23})_3$	10	1
3	$Cr(OSO_2C_{11}H_{23})_3$	15	1
4	$Mn(OSO_2C_{11}H_{23})_2$	14	–2
5	$Fe(OSO_2C_{11}H_{23})_2$	31	1
6	$Fe_2O(DS)_4$[b]	32	0
7	$Co(OSO_2C_{11}H_{23})_2$	16	1
8	$Ni(OSO_2C_{11}H_{23})_2$	15	2
9	$Cu(OSO_2C_{11}H_{23})_2$	46	70
10	$Zn(OSO_2C_{11}H_{23})_2$	14	–3
11	$Zr(DS)_4$[b]	55	0
12	$AgOSO_2C_{11}H_{23}$	14	2
13	$Cd(OSO_2C_{11}H_{23})_2$	7	0
14	$In(OSO_2C_{11}H_{23})_3$	11	0
15	$Sn(OSO_2C_{11}H_{23})_2$	28	0
16	$Yb(OSO_2C_{11}H_{23})_3$	18	–14
17	$Hg(OSO_2C_{11}H_{23})_2$	8	1
18	$Ru(DS)_3$[b]	18	0
19	$Rh(DS)_3$[b]	16	0
20	$Pd(DS)_2$[b,c]	5	–88
21	$Ir(DS)_4$[b]	13	0

[a] Determined by HPLC analysis.　　[b] DS = $OSO_3C_{12}H_{25}$.
[c] Prepared in situ by mixing $Pd(TFA)_2$ and SDS.

With the metal screening in hands, the catalytic activity of copper(II) cation combined with **L1** toward stereoselective execution was examined in detail (Table 11).　Compared with alkylsulfonate-based structure, alkylsulfate-based LASC exhibited a bit inferior performance of both the reaction progress and enantioselection (entry 1).　Although a chain length of alkylsulfonate-based LASC did not have powerful influence in both aspects, copper(II) bis(nonasulfonate) produced somewhat higher enantioselectivity than others (entries 2-6).　The copper(II) salts which were distinctly effective for asymmetric β-borylation performances, afforded poor results regardless of the heterogeneity of copper(II) salts (entries 7-9).　Similarly, other homogeneous copper(II) salts catalyzed the reaction in a moderate enantioselective manner (entries 10-13).

Table 11. Effect of copper salt on enantioselective protonation.
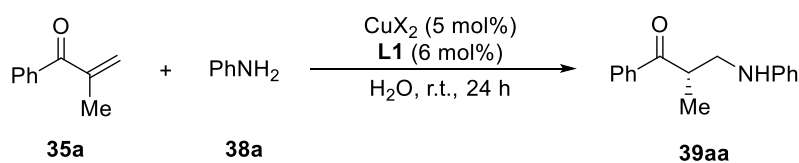
Entry	CuX$_2$	Yield (%)	Ee (%)[a]
1	Cu(DS)$_2$[c]	40	64
2	Cu(OSO$_2$C$_{11}$H$_{23}$)$_2$	46	70
3	Cu(OSO$_2$C$_{10}$H$_{21}$)$_2$	42	74
4	Cu(OSO$_2$C$_9$H$_{19}$)$_2$	34	76
5	Cu(OSO$_2$C$_8$H$_{17}$)$_2$	39	69
6	Cu(OSO$_2$C$_7$H$_{15}$)$_2$	44	69
7	Cu(0)	3	19
8	Cu(OH)$_2$	8	20
9	Cu(OAc)$_2$	35	42
10	CuCl$_2$	36	51
11	Cu(OTf)$_2$	44	47
12	Cu(SO$_4$)$_2$	28	52
13	Cu(NO$_3$)$_2$	49	48

[a] Determined by HPLC analysis.   [b] DS = OSO$_3$C$_{12}$H$_{25}$.

The reaction conditions required the chiral ligand **L1** not only to construct the asymmetric environment around the core but to prevent the plural coordinating aniline molecules from killing the catalytic activity of copper(II) core toward tandem conjugate addition/enantioselective protonation process.   A series of control experiments verify its necessity (Table 12).   Although **L1** alone does not have any catalytic activity, improved reactivity of the Cu(II)-based LASC was observed along with a high level of enantioselection (entries 1-4).   An excess amount of the ligand didn't affect the reaction outcome (entry 5).   In contrast, excessive use of Cu(II)-based LASC resulted in the formation the product in higher yield with lower enantioselectivity, indicating the Cu(II)-**L1** complex to be a 1:1 complex under the reaction conditions (entry 6).   At higher catalyst loading, improved catalytic activity of Cu(II)-based LASC and increased enantioselectivity of **39aa** were observed (entry 7).

Table 12. Control experiments.
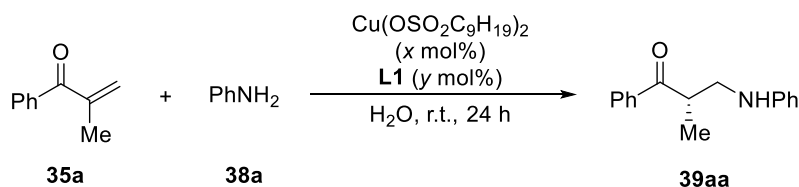
Entry	x (mol%)	y (mol%)	Yield (%)	Ee (%)[a]
1	–	–	0	–
2	5	–	27	–
3	–	6	0	–
4	5	6	34	76

5	5	15	35	77
6	7.5	5	43	68
7	10	12	60	82

[a] Determined by HPLC analysis.

In addition, the importance of geometry around Cu(II) core was investigated (Table 13). The square bipyramidal structure formed with pybox ligand **L13** resulted in much lower sense of chiral induction (entry 1). Assumed tetradentate fashion coordinated with *N,N'*-dioxide **L35** generally shows a strong tendency toward square-planar geometry,[55] allowing the reaction to be completely racemic (entry 2). Although a few patterns of a strong square-planar structure through a few box-type ligands were also investigated, the enantioselectivity of the product **39aa** remained low (entries 3-5).

Table 13. Effect of ligand.
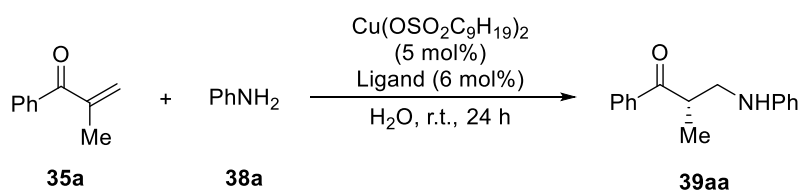
Entry	Ligand	Yield (%)	Ee (%)[a]
1	**L13**	36	15
2	**L35**	13	0
3	**L38**	31	4
4	**L44**	27	1
5	**L46**	25	22

[a] Determined by HPLC analysis.

L46
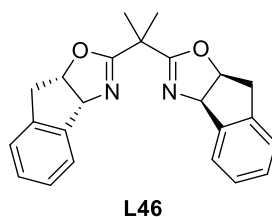
A number of additives have been explored to improve the catalytic performance of Cu(II)-based LASC coordinating with **L1** (Table 14). The effective rate acceleration by the combination between LASC and Brønsted acid that is discussed in Chapter 1 motivated me to screen Brønsted acid additives strenuously (entries 1-18). Unlike the previous observations in Mukaiyama aldol reactions in water,[56] addition of a strong Brønsted acid was turned out to be not effective so drastically (entries 2-5). More effective acceleration effect was observed when benzoic acid was added as an additive (entry 6). To a greater or less extent, the reaction was accelerated significantly in the presence of 4-substituted benzoic acid derivatives (entries 7, 8). For all that, an imperceptible electronic effect indicated that electron-withdrawing substituent on benzoic acid was more effective (entry 8). The resonance effect by electron density at *ortho-* or

para-positions suggests the electronic contribution of substituents (entries 9-11). In contrast, aliphatic carboxylic acids were less effective (entries 12-15). Effect of weak acids such as phenol was also small (entries 16, 17). Solid acid resin, Amberlyst-15 depressed both reaction yield and enantioselectivity (entry 18). When base was added as an additive, the reaction became less stereoselective because of strong basicity of the reaction solution (entries 19, 20).[57] Unexpected assistance of sodium benzoate on Cu(II) catalysis was noticeable (entry 21). It was strongly suggested that benzoate anion played a crucial role for superior performance of Cu(II) catalysis. Other anions such as chloride and iodide were ineffective (entries 22, 23). Addition of tetrabutylammonium bromide (TBAB) had a positive but weak influence on the reaction outcome (entry 24). Sodium sulfonate impeded the desired catalytic pathway (entry 25).

Table 14. Effect of additive on enantioselective protonation.
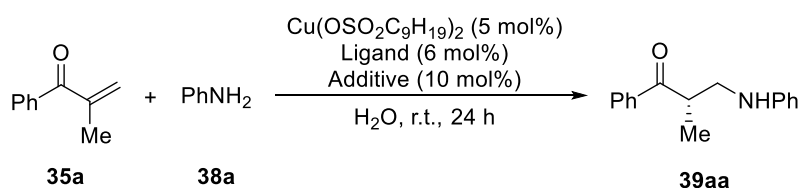
Entry	Additive	Yield (%)	Ee (%)[a]
1	–	34	76
2	TfOH	48	74
3	H_2SO_4	39	79
4	*p*TsOH	36	74
5	HCl	46	77
6	$PhCO_2H$	56	73
7	$4\text{-}MeOC_6H_4CO_2H$	52	72
8	$4\text{-}NO_2C_6H_4CO_2H$	61	75
9	$3\text{-}NO_2C_6H_4CO_2H$	47	71
10	$2\text{-}NO_2C_6H_4CO_2H$	54	76
11	$3,5\text{-}(NO_2)_2C_6H_3CO_2H$	31	20
12	AcOH	42	73
13	TFA	44	79
14	(+)-Tartaric acid	8	20
15	$C_{11}H_{23}CO_2H$	36	51
16	PhOH	35	42
17	$(CF_3)_2CHOH$	44	47
18	Amberlyst 15	28	52
19	Pyridine	40	69
20	KOH	35	45
21	$PhCO_2Na$	60	68
22	NaCl	46	71
23	NaI	19	53
24	TBAB	43	70
25	$C_9H_{19}SO_3Na$	28	57

[a] Determined by HPLC analysis.   [b] DS = $OSO_3C_{12}H_{25}$.

Curiously, the reaction could be catalyzed by Brønsted acid alone, albeit low catalytic turnover (Scheme 33).   When 4-nitrobenzoic acid was added as an additive, reactivity enhanced without impairing the stereoselective performance of Cu(II)-**L1** complex.   It is indicated that 4-nitrobenzoic acid does not work independently but assist the chiral Cu(II) complex to improve its catalytic activity toward high turnover without affecting its stereoselective performance.
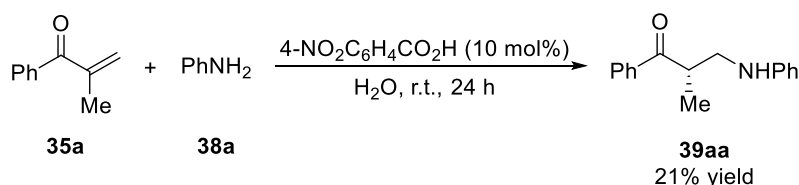
Scheme 33. Acid-catalyzed aza-Michael addition/protonation in water.

The amount of an additive was examined (Table 15).   When added 4-nitrobenzoic acid was less than 10 mol%, the enantioselectivity of **39aa** was held to a high level, 76% ee (entries 1-3). A larger amount of the additive was, however, directed the raction toward inferior enantioselection (entries 4, 5).   The threshold of enantioselectivity drop was observed in the presence of more than one equivalent of 4-nitrobenzoic acid, implying that the counteranion was exchanged from alkylsulfonate to benzoate.

Table 15. Effect of additive amount.
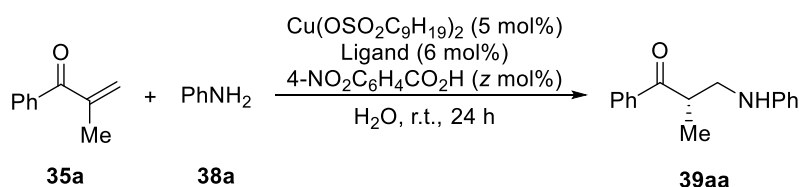
Entry	z (mol%)	Yield (%)	Ee (%)[a]
1	0	36	76
2	5	53	77
3	10	62	76
4	20	62	67
5	40	65	58

[a] Determined by HPLC analysis.

Since Brønsted acid assisted efficiently Cu(II) catalysis for enantioselective protonation, the stoichiometric amount of Brønsted acid was used as a form of anilinium salt (Scheme 34). Obviously, the reaction suffered from the sluggish progress and almost no chiral induction, which denies that acid-base interaction between aniline substrate and Brønsted acid additives was crucial for the reaction.
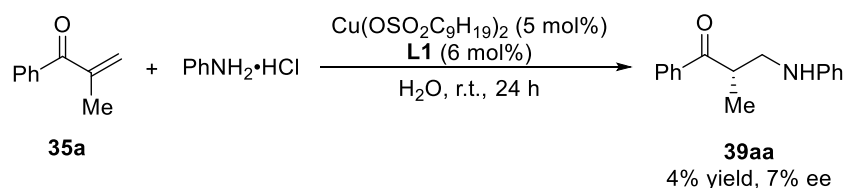
Scheme 34. Tandem aza-Michael addition/protonation using anilinium salt.

The effect of reaction temperature was tabulated in Table 16.   The reaction retarded and enantioselectivity decreased a little bit at low temperature (entry 1).   Increased yielding of 39aa was observed without loss of stereoselection at 40 °C (entry 3).   Further addition of 4-nitrobenzoic acid doubled the reaction yield compared with that recorded at room temperature, albeit with slight decrease in enantioselectivity (entry 4).   When the reaction temperature was raised to 60 °C, the enantioselectivity decreased significantly (entry 5).

Table 16. Effect of reaction temperature.
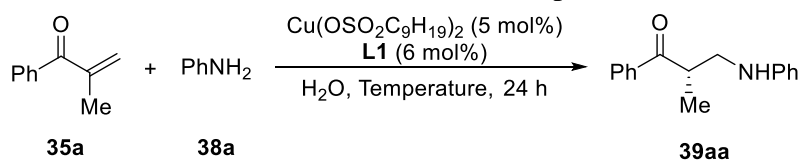
Entry	Temperature	Yield (%)	Ee (%)[a]
1	0	25	69
2	r.t. (20 °C)	36	76
3	40 °C	61	75
4[b]	40 °C	78	68
5	60 °C	65	60

[a] Determined by HPLC analysis.   [b] $4\text{-}NO_2C_6H_4CO_2H$ (10 mol%).

The amount of water as a solvent is assumed to be crucial for the micelle formation (Table 17).   Less amount of water led to the improved reactivity and slight decrease in enantioselectivity (entry 1).   By contrast, the reaction under the diluted condition resulted in a drop in the rate retardation with retaining the level of enantioselection (entry 3).

Table 17. Effect of concentration.
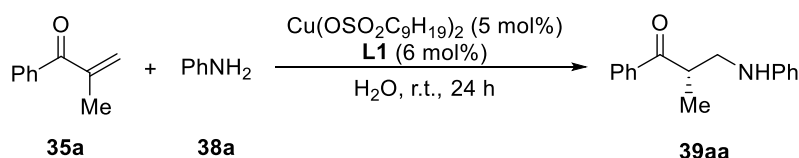
Entry	Concentration	Yield (%)	Ee (%)[a]
1	1.0	54	73
2	0.33	36	76
3	0.1	30	76

[a] Determined by HPLC analysis.

The reaction profile was compared between in the presence and in the absence of 4-nitrobenzoic acid (Table 18).   Without any additive, the reaction yield increased gently but it seems saturated after 48 hours along with a decrease in enantioselectivity (entries 1-3).   I'd like to annotate that the starting material was recovered even after 72 h and any byproduct was not formed. The same tendency toward loss of catalytic activity after 48 hours was also seen in the presence of additive (entries 4-6).   The slow addition of aniline into the reaction system was not effective (entries 7, 8).

Table 18. Optimization of reaction conditions.

Entry	Acid additive	Time (h)	Yield (%)	Ee (%)[a]
1	–	24	36	76
2	–	48	51	75
3	–	72	55	71
4	+	24	61	75
5	+	48	73	74
6	+	72	76	71
7[b]	–	24	46	71
8[b]	+	24	30	76

[a] Determined by HPLC analysis.   [b] Aniline was added slowly over 3 hours.

The story of kinetic resolution or an erosion of enantioselectivity resulting from retro-Michael reaction was denied completely (Scheme 35).   The mixture of two enantiomers **39aa** with a ratio biased toward one enantiomer was stirred for 24 hours under the optimal conditions. The resultant solution gave neither α-branched enone **35a** nor aniline **38a** (Scheme 35, above). The enantiopurity of recovered **39aa** remained unchanged.   A racemic 1:1 mixture of two enantiomers traced the same way (Scheme 35, below).   It was confirmed that tandem conjugate addition/enantioselective protonation was irreversible under the reaction conditions.

Scheme 35. Checking possibility of retro-Michael addition.

In order to know the superiority and the role of water, the catalytic behavior of Cu(OTf)$_2$ was evaluated for tandem conjugate addition/enantioselective protonation conducted in organic solvents or a co-solvent system or a biphasic system (Table 19). Although the reaction was less selective than that catalyzed by Cu(OSO$_2$C$_9$H$_{19}$)$_2$, enantiofacial differentiation of prochiral enolate intermediate took place to some extent in water (entry 1). In contrast, the reactivity fell down seriously in all organic solvents, in aqueous ethanol and in biphasic system (entries 2-7). The protonated product **39aa** was obtained with high enantioselectivity in dichloromethane or toluene (entries 2, 5). The reaction hardly proceeded in protic solvent (entry 4). The proton should be transferred directly from aniline **38a** to a prochiral enolate intermediate either *via* concerted mechanism between C=C double bond and aniline or *via* antecedent nucleophilic addition and the subsequent intramolecular 1,3-proton transfer.

Table 19. Effect of solvent on enantioselective protonation.

Entry	Solvent	Yield (%)	Ee (%)[a]
1	H$_2$O	44	47
2	CH$_2$Cl$_2$	6	61
3	THF	4	6
4	EtOH	Trace	–
5	Toluene	4	76
6	MeCN	2	49
7	H$_2$O/EtOH = 1/9	8	21
8	H$_2$O/Toluene = 1/9	2	–

[a] Determined by HPLC analysis.

With the optimized reaction conditions in hands, a series of α-branched α,β-unsaturated carbonyl compounds and nitrile bearing unsubstituted terminal *sp*^{2} carbon was then tested as electrophiles (Table 20). The reaction yield of corresponding products enhanced at higher catalyst loading and at an elevated temperature (entries 2, 4). A bidentate-type α-methyl *N*-benzoyl acrylamide **35t** reacted with **38a** sluggishly to afford the desired product **39ta** in almost unselective manner (entry 5). Directing group-free α-methyl α,β-unsaturated ester **35j**, amide **35l**, thioester **35u** and nitrile **35v** were not converted into any product (entries 6-8, 10). Although increased

catalyst loading and elevated temperature allowed the thioester analogue **35u** to give the desired product **35ua**, the reaction still remained sluggish and less stereoselective (entry 9).   When β,β-dimethyl α,β-unsaturated ketone **35p** derived from tetralone was used, the reaction did not proceed at all (entry 11).   In the identical strategy using benzylmercaptan **33a**, the analogue **35p** furnished the corresponding thia-Michael adduct with excellent enantioselectivity because of the complete suppression of the undesired unselective pathway (Chapter 4.2-3, entry 20 in Table 6). The sterically crowded β-postion would inherently disabled aniline **38a** from attacking as a nucleophile.

Table 20. Scope of electrophiles.

Entry	R^1	R^2		Yield (%)	Ee (%)[a]
1	Ph	Me	**35a**	61	75
2[b]				71	78
3	4-ClC$_6$H$_4$	Me	**35s**	55	75
4[b],[c]				78	67
5			**35t**	18	–9
6			**35j**	NR	–
7			**35l**	NR	–
8			**35u**	NR	–
9[b],[c]				8	33
10			**35v**	NR	–
11			**35p**	NR	–

[a] Determined by HPLC analysis.

[b] Cu(OSO$_2$C$_9$H$_{19}$)$_2$ (10 mol%), **L1** (12 mol%), 4-NO$_2$C$_6$H$_4$CO$_2$H (20 mol%).

[c] Performed at 40 $^\circ$C.

Subsequently, substrate tolerance of nucleophile was examined (Table 21). The reaction with 4-bromoaniline **38b** delivered the product **39ab** with decreased enantioselectivity (entry 3), whereas the reaction with 4-methoxyaniline **38c** suffered from decreased reactivity and almost no stereoinduction (entry 4). In contrast to the reaction with **38c**, the reaction with 2-methoxyaniline **38d** was much more stereoselective albeit in low reactivity (entry 5). Increased catalyst loading and elevated temperature facilitated higher catalyst turnover with the same level of enantioselectivity (entry 6). The use of secondary *N*-methylaniline **38e** resulted in a drastic plunge of reactivity due to its steric hindrance (entry 7). Although less bulky secondary amines such as *N*-methylbenzylamine **38f** and dimethylamine **38g** could react successfully, the reaction proceeded in a racemic manner (entries 8, 9).[57,58] Unfortunately, the catalyst system was turned out to be inapplicable for more valuable amine nucleophiles including CbzNH$_2$ **38h**, TsNH$_2$ **38i**, and BzNHOH **38j** (entries 10-12). It was suggested that both reactivity and selectivity were quite sensitive to the electronic nature of nucleophiles.

Table 21. Scope of nucleophiles.
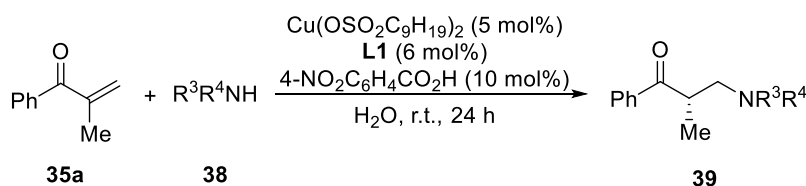
Entry	R^3	R^4		Yield (%)	Ee (%)[a]
1	Ph	H	**38a**	61	75
2[b]				71	78
3	4-BrC$_6$H$_4$	H	**38b**	64	55
4[b]	4-MeOC$_6$H$_4$	H	**38c**	40	6
5	2-MeOC$_6$H$_4$	H	**38d**	24	64
6[c],[d]				75	66
7	Ph	Me	**38e**	2	–
8	Bn	Me	**38f**	55	1
9	Me	Me	**38g**[e]	49	1
10[b]	Cbz	H	**38h**	NR	–
11[b]	Ts	H	**38i**	NR	–
12	Bz	OH	**38j**	NR	–

[a] Determined by HPLC analysis. [b] Without 4-NO$_2$C$_6$H$_4$CO$_2$H.
[c] Cu(OSO$_2$C$_9$H$_{19}$)$_2$ (10 mol%), **L1** (12 mol%), 4-NO$_2$C$_6$H$_4$CO$_2$H (20 mol%).
[d] Performed at 40 $^\circ$C. [e] Added as aqueous solution.

The experimental results suggested a strong electronic effect of nucelophiles and benzoic acid additives on both reactivity and chiral induction. It is likely that the exquisite combination of nucleophile and benzoic acid derivative might be a key to improve the catalytic performance. That

is why the correlation between additive and nucleophile was investigated (Table 22). The electronic effect of *para*-substituents on benzoic acid additives was hardly observed in the reaction of simple aniline **38a**, considering the outcome of the reaction performed without any additive. The substituents at *meta*-position resulted in a significant drop in selectivity. In contrast, the reaction with 2-methoxyaniline **38d** was affected by electronic nature of benzoic acid additives. Simple benzoic acid or 4-methoxybenzoic acid made the enantioselective performance of the reaction decrease significantly. When $3,5\text{-}(NO_2)_2C_6H_3CO_2H$ was used as an additive, the remarkable drop in enantioselectivity was not observed.

Table 22. Correlation between additive and nucleophile.
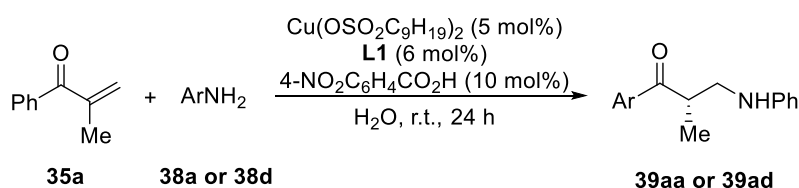
Entry	Additive	39aa		39ad[b]	
		Yield (%)	Ee (%)[a]	Yield (%)	Ee (%)[a]
1	–	34	76	63	72
2	$3,5\text{-}(NO_2)_2C_6H_3CO_2H$	31	20	77	57
3	$4\text{-}NO_2C_6H_4CO_2H$	61	75	75	66
4	$PhCO_2H$	56	73	84	59
5	$4\text{-}MeOC_6H_4CO_2H$	57	72	78	57

[a] Determined by HPLC analysis.

[b] $Cu(OSO_2C_9H_{19})_2$ (10 mol%), **L1** (12 mol%), $4\text{-}NO_2C_6H_4CO_2H$ (20 mol%) at 40 $^{\circ}$C.

When optically active amine **38k** was served as a nucleophile, the reaction furnished a diastereomeric mixture (Scheme 36). Due to the strong basicity of the reaction solution,[57,58] high level of diastereofacial differentiation was not executed.
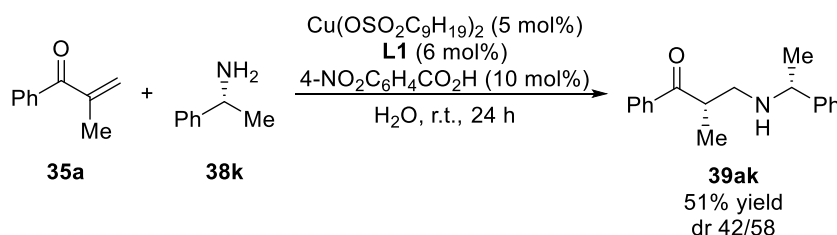
Scheme 36. Enantioselective protonation using chiral amine as nucleophile.

In order to determine the absolute configurateion of the product, the analogue **39ad** was transformed into literature-known compound after cerium ammonium nitrate (CAN)-mediated cleavage of C–N bond and the subsequent protection by Boc group (Scheme 37).[59]

1) CAN, MeCN/H_2O
2) Boc_2O, Toluene/H_2O

39ad

46% yield
$[\alpha]_D^{20}$ = +45.8
(c = 0.56 in $CHCl_3$)

Lit.

$[\alpha]_D^{20}$ = −45.4
(c = 0.56 in $CHCl_3$)
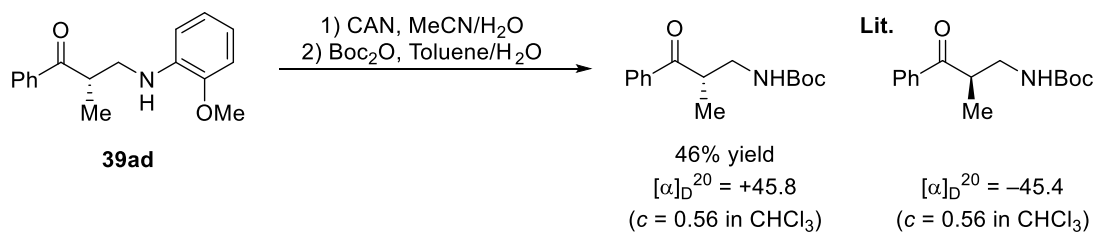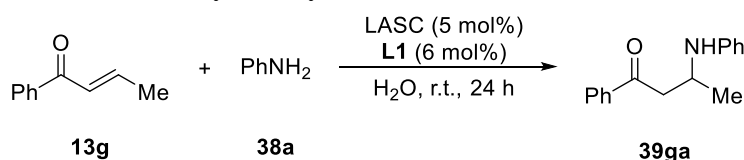
Scheme 37. Determination of absolute configuration.

4.3-3 Mechanistic Insights

In order to examine the behavior of developed catalysts in the reaction where stereo-determining step is not protonation but nucleophilic addition step, 1-phenyl-2-buten-1-one **13g** was treated with aniline **38a** in water in the presence of LASC and **L1** (Table 23). However, the presented chiral copper(II) complex consisting of Cu(II)-based LASC and **L1** catalyzed the reaction to produce the product with low enantioselectivity, albeit in high yield (entry 1). In contrast, the reaction proceeded sluggishly in a completely racemic manner in the presence of scandium catalysts (entries 2, 3). Although chiral catalysts were responsible for stereoinductions both at nucleophilic addition and at protonation in tandem thia-Michael addition/protonation reactions in water, tandem aza-Michael addition/protonation reactions underwent a meaningful chiral induction only at protonation step in water.

Table 23. LASC-catalyzed asymmetric aza-Michael addition in water.

Entry	LASC	Yield (%)	Ee (%)[a]
1	$Cu(OSO_2C_9H_{19})_2$	83	16
2	$Sc(OSO_2C_{11}H_{23})_3$	7	0
3	$Sc(DS)_3$[c]	20	0

[a] Determined by HPLC analysis.　[b] $4\text{-}NO_2C_6H_4CO_2H$ (10 mol%).
[c] $DS = OSO_3C_{12}H_{25}$.

In addition to such difference, the opposite sense of chiral induction between Cu(II)-**L1** and Sc(III)-**L1** complex for enantioselective protonation of **35a** with **38a** in water is curious (Table 10). The mutual opposition in the sense of chiral induction between them is, however, not the first example. In asymmetric ring-opening reaction of *meso*-epoxide with aniline **38a** and indole in water, Sc(III)-**L1** complex gave one enantiomer of the product and Zn(II)-**L1** or Cu(II)-**L1** complex produced the opposite enantiomer.[60] As mentioned above, Sc(III)-**L1** complex adopts a pentagonal bipyramidal structure where the tetradentate ligand occupies four of the equatorial planar sites. In contrast, Cu(II)-**L1** or Zn(II)-**L1** complex adopts square pyramidal structure in a *N,N,O*-tridentate manner and one hydroxyl group does not involve in the coordination to centered core (Figure 4). The scenario postulated in enantioselective protonation of **35a** with **38a** in water is remarkably similar to that done in asymmetric ring-opening reaction using **38a** in water. Since both enone **35a** and aniline **38a** can interact with metals, A definitive gap in the structural geometry between Sc(III)-**L1** complex and Cu(II)-**L1** complex should be closely related with the sense of chiral induction.
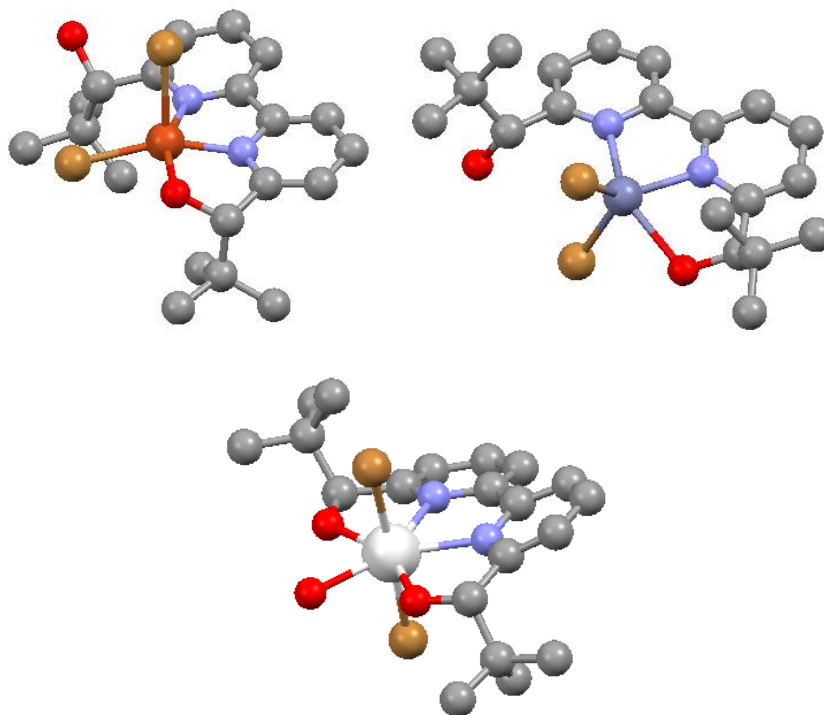
Figure 4. Comparison of metal-**L1** complexes based on molecular geometry.
[CuBr$_2$·**L1**·H$_2$O] (above, left), [ZnBr$_2$·**L1**] (above, right) and [ScBr$_2$·**L1**·H$_2$O]$^+$ (below)

In order to gain more insights into the structural geometry of Cu(II)-**L1** complex, several chiral 2,2'-bipyridine derivatives were tested in enantioselective protonation with **38a** in water (Table 24). Compared with enantiofacial differentiation induced by Cu(II)-**L1** complex (entries 2, 3), monomethylated nonsymmetrical Cu(II)-**L2** complex showed poor selective performance (entries 4, 5). Although one hydroxyl group of **L1** is not bound to copper(II) core, a tridentate ligand **L2** was much less effective. The use of bisprotected ligands **L3** and **L47** allowed the reaction to be racemic as expected (entries 6, 7).

Table 24. Effect of coordination between copper core and ligand.
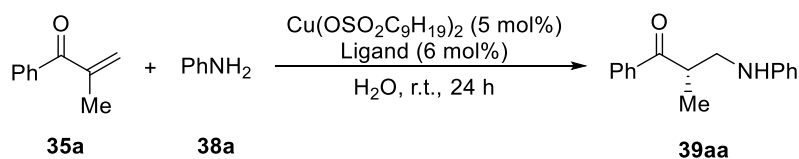
Entry	Ligand	Yield (%)	Ee (%)[a]
1	–	27	–
2	**L1**	34	76
3[b]	**L1**	61	75
4	**L2**	30	10
5[b]	**L2**	37	17
6	**L3**	21	1
7	**L47**	27	0

[a] Determined by HPLC analysis.   [b] 4-NO$_2$C$_6$H$_4$CO$_2$H (10 mol%).

L47
R = SiMe$_3$
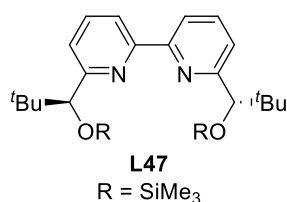
Overlooking two types of tandem conjugate addition/enantioselective protonation reactions catalyzed by scandium(III) or copper(II) complex, we will become aware of a fact that not only metal cation but also surfactant moiety plays a vital role in determining the sense of stereoinduction (Table 25). In aza-Michael addition/enantioselective protonation in water, both surfactant-combined catalysts and non-surfactant catalysts (Sc(OTf)$_3$ and Cu(OTf)$_2$) tend to output the same stereochemistry during enantiofacial differentiation of a prochiral enolate intermediate. In contrast, a swap of counteranion from triflate to surfactant-based anion tends to switch the sense of chiral induction in thia-Michael addition/enantioselective protonation in water. It must, however, be added that there is no chiral induction in the presence of Cu(II)-based LASC.

Table 25. Correlation between LASC and stereochemical outcome.
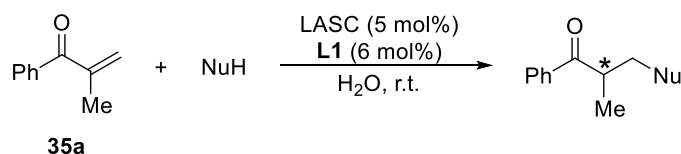
Entry	LASC	39aa (thiol)		39ad (aniline)	
			Ee (%)[a]		Ee (%)[a]
1	Sc(OTf)$_3$		67		11
2	Sc(DS)$_3$		21		42
3	Cu(OTf)$_2$		24		47
4	Cu(OSO$_2$C$_9$H$_{19}$)$_2$		0		76

[a] Determined by HPLC analysis.

The solvent kinetic isotope effect was examined (Table 26). The reaction of **35a** with **38a** in D$_2$O could produce deuterated product **39aa-D** concomitant with the formation of protonated product **39aa**. Comparison of the reaction profile revealed that the reaction in water was twice as fast as that in deuterium oxide. As observed in thia-Michael addition/enantioselective protonation (deuteration), proton was incorporated preferentially at the initial stage. After stirring for 4 hours, the rate of competitive protonation became almost constant.

Table 26. Comparison between protonation and deuteration.

Entry	Time (h)	Conditions	Total yield (%)	H/D ratio[a]	Ee (%)[b]
1	4	in H_2O	$(13)^{[c]}$	–	75
2	14	in H_2O	$(32)^{[c]}$	–	75
3	24	in H_2O	$(61)^{[c]}$	–	75
4	1	–	$2\ (0.6)^{[c]}$	24/76	75
5	4	–	$7\ (0.7)^{[c]}$	10/90	75
6	14	–	$16\ (1.2)^{[c]}$	8/92	75
7	24	–	$32\ (1.6)^{[c]}$	5/95	75
8	24	Without acid additive	$11\ (1.1)^{[c]}$	10/90	75

[a] Determined by ^1H NMR analysis.   [b] Determined by HPLC analysis.

[c] Yield of the protonated product

The added 4-nitrobenzoic acid could accelerate the reaction efficiently without impairing a stereoselective performance of chiral copper(II) complex.   Moreover, sodium benzoate also works as an effective additive, albeit with a bit inferior performance (Table 14).   Since the contribution of acid-base interaction with aniline **38a** was denied (Scheme 31), *in situ* formed benzoate anion is assumed to electronically modify the activity of Cu(II)-**L1** complex.   It is likely that the exchange of counteranion on copper(II) from alkylsulfonate to benzoate is of great importance.   Not only NMR study but ESI-MS analysis could not provide any insights to support the hypothesis on active species.   Both two aqueous catalyst solutions with and without 4-nitrobenzoic acid were submitted to ESI-MS analysis, resuling in almost the same output which contains the strongest peak corresponding to $[Cu(\mathbf{L1}) - H]^+$ and other miscellaneous peaks including $[Cu(OSO_2C_9H_{19})(\mathbf{L1})]^+$ or $[Cu(OH)(H_2O)(\mathbf{L1})]^+$ (uncertain at this stage).   Although the catalytic activity of prepared copper(II) benzoate was not high (Scheme 38), *in situ* formed $Cu^{II}(OSO_2C_9H_{19})(O_2CPh)(\mathbf{L1})$ species would be responsible for higher catalytic turnover as well as high level of stereoselection in water.
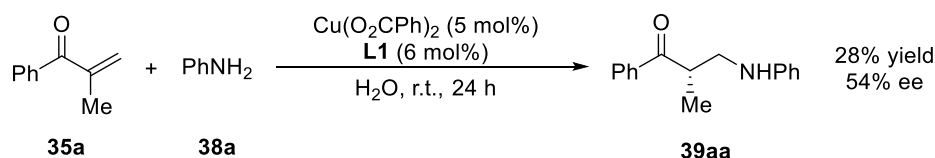
Scheme 38. Enantioselective protonation catalyzed by copper(II) benzoate.

It seems that the hydrogen bonding network of inner sphere surrounding copper(II) core is important for the recognition, fixation of substrate or controlling a trajectory of proton.   On the

basis of such assumption, aromatic group was introduced near the centered copper(II) core in the surfactant structure.　　The configuration of the obtained product **39aa** was inversed when copper(II) dodecylbenzenesulfonate was used instead of copper(II) alkylsulfonate (Figure 5).　　Sterically more bulkiness introduced in Cu(II)-based LASC resulted in excellent enatntioselection (90% ee).
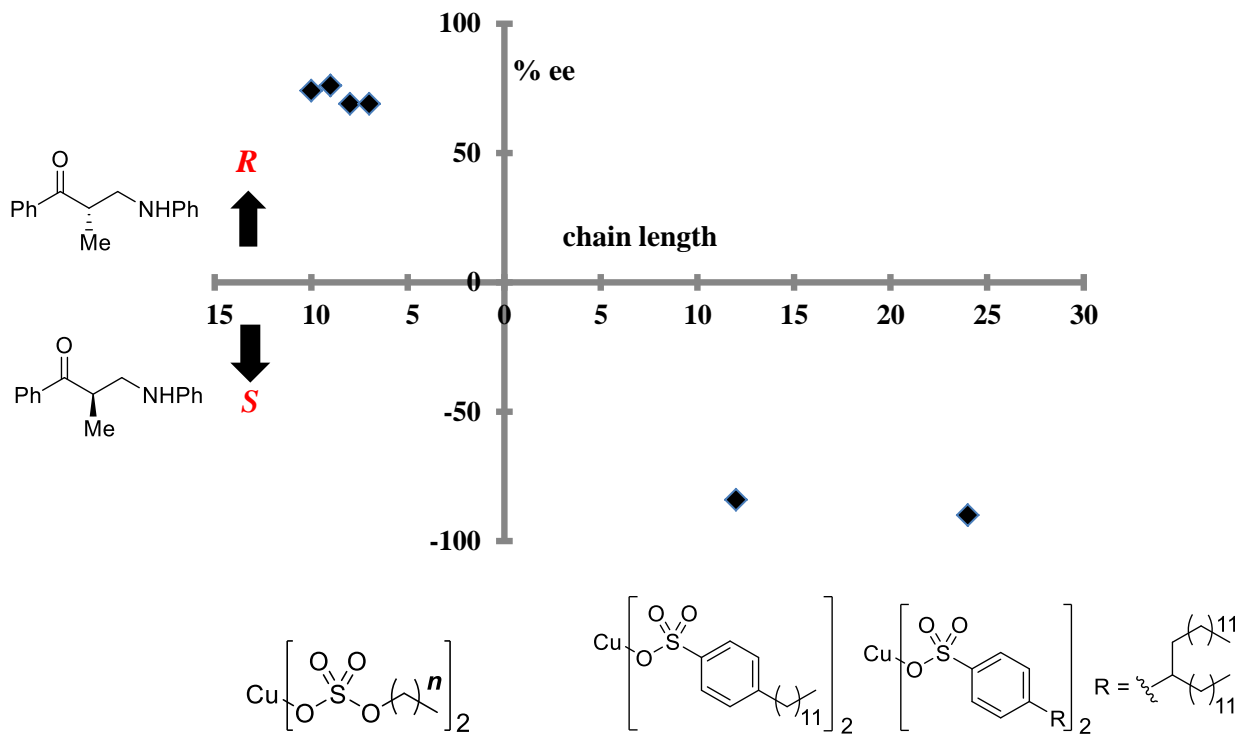
Figure 5. Hydrogen bonding network and enantioselective protonation.

Section 4.4 Conclusions and Overlooks for Other Michael-type Reactions in Aqueous Environment

A new catalytic system for asymmetric Michael addition of thiols with enones was unearthed in water and established the new aspect of water about methodology for enantioselective protonation. An exquisite set of catalyst and additive was effective for two enantiofacial differentiations of both Michael addition and protonation step in the course of the reaction. The astonishing governing the enantioselectivity for simple introduction of proton in spite of abnormally high mobility in water may provide us not only new synthetic opportunities but also epoch-making chemical advances. Further investigations to develop new catalytic systems or reactions in water that allow for enantioselective proton transfer are overlooked as follow.

Indole nucleophiles are, in particular, one of the most attractive Michael-donor to accomplish asymmetric carbon-carbon bond formation. Optically active indole derivatives are valuable as building blocks for the construction of chiral indole architecture. In addition, this process is involved in the total synthesis of a class of bioactive indole alkaloids known as hapalindoles and other 3-substituted indoles. Immense attraction on carbon-carbon bond formation to furnish enantioriched indole derivatives have led to the emergence of catalytic systems over the past decade. These strategies can be categorized as Lewis acid catalyst such as chiral zirconium complex,[61] chiral Brønsted base catalyst formed from barium salt and [H]$_8$ BINOL,[62] and chiral Brønsted acid containing phosphoric acid.[63] Recently elaborate optimization made by Feng *et al*. established highly-enantioselective Friedel-Crafts-type reaction of indoles with chalcones catalyzed by chiral *N,N'*-dioxide scandium complexes.[64] Despite these impressive contributions, the highly efficient chiral catalyst for this type of reaction is still limited. For instance, non-chelating character of chalcone makes enantiofacial differentiation using a simple asymmetric catalytic system one of the most challenging tasks. In addition, solvent often plays an important role in governing the reaction rate and enantioselectivity. Broad substrate generality has not been attained in the presence of any chiral catalyst. Thus highly enantioselective Friedel-Crafts-type reactions of indoles with enones call for chiral catalysts possessing extremely specific structure and specific solvent. Therefore the development of easily accessible and highly efficient chiral ligands which can function under mildest conditions is still one great challenge in asymmetric catalysis.

When indole is employed as a nucleophile, the desired reaction pathway should involve C–H activation step (depicted in Figure 6) and enantioselective protonation step. In addition, the reaction should be C–C bond forming reaction. Thus this reaction seemed to be one of the most challenging tasks. The results obtained about two years ago suggested that racemic reaction proceeded in the presence of scandium triflate, whereas stereoselectively to some extent in the presence of scandium dodecylate. Another interest was palladium catalysis in water. The use of palladium acetate led to trace amount of the desired product. In order to achieve higher reactivity 10 mol% of palladium trifluoroacetate was then employed, producing the desired product to some extent. Chiral induction induced by chiral 2,2'-bipyridine was also accomplished. Michael-type reaction with chalcone **13a** afforded lower enantioselectivity in the presence of the same catalytic system.
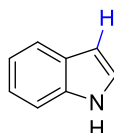
40a

Figure 6. Indole **40a**.

The reaction catalyzed by palladium(II) salts suffered from quite low reactivity. After the reaction we can see the brown line on the wall of flask, implying deactivation of palladium(II) salts in the course of the reaction. As for the actual function of palladium(II) in this reaction, there are two possibilities. First, interaction between palladium(II) and π-bond can provide *O*-enolate and *C*-enolate through the resonance. Second, insertion to C-H bond of indole can form palladium(II)-indole complex after release of trifluoroacetic acid. Of course both activations might be possible. In order to stabilize such kind of intermediate in water, several additives were explored. Addition of oxidant to regenerate Pd(II) from Pd(0) formed *in situ* had no effect on the result. On the other hand, the use of some surfactants led to the improvement of the reaction yield. When the reaction was conducted in the presence of SDS or Triton X-100, the reactivity enhanced. However, almost racemic product was obtained in the presence of Triton X-100. Other surfactants suffered from lower yield and lower enantioselectivity. It can regenerate palladium trifluoroacetate even after the release of trifluoroacetate through C–H insertion process in the presence of surfactant.

Introduction of aromatic ring by using phenylboronic acid was tried in protonation. The reaction did not proceed at all at room temperature. At higher temperature the desired product was obtained with inseparable byproducts which might correspond to polymerization of enone. And the competitive formation of Heck-type adduct was also observed as a serious problem. This fact indicates that β-elimination takes place somewhere in catalytic cycle. In order to regenerate palladium trifluoroacetate and suppress the undesired β-elimination pathway, trifluoroacetic acid was added as an additive. However the yield of the undesired Heck-type adduct increased and the desired pathway suppressed slightly. The use of phenyltrifluoroborate instead of boronic acid did not improve these problems. Although homo-coupling product was obtained competitively, when bismuth hydroxide was used as a catalyst the desired product was slightly formed with good enantioselectivity (52% ee). On the other hand, copper hydroxide was postulated to function as a Lewis acid to assist C–C bond formation. Therefore these hydroxides were applied to this reaction at higher temperature.

---

[1] F. Ruff, Ö. Farkas, *J. Phys. Org. Chem.* **2011**, *24*, 480-491.

[2] C. Fehr, *Angew. Chem. Int. Ed.* **1996**, *35*, 2566-2587.

[3] a) K. Matsumoto, S. Tsutsumi, T. Ihori, H. Ohta, *J. Am. Chem. Soc.* **1990**, *112*, 9614-9619; b) H. Ohta, *Bull. Chem. Soc. Jpn.* **1997**, *70*, 2895-2911.

[4] a) K. Matoishi, M. Ueda, K. Miyamoto, H. Ohta, *J. Mol. Catal. B* **2004**, *27*, 161-168; b) K. Miyamoto, H. Ohta, *Eur. J. Biochem.* **1992**, *210*, 475-481; c) K. Miyamoto, H. Ohta, *J. Am. Chem. Soc.* **1990**, *112*, 4077-4078.

[5] a) Y. Terao, Y. Ijima, K. Miyamoto, H. Ohta, *J. Mol. Catal. B: Enzymatic* **2007**, *45*, 15-20; b) Y. Ijima, K. Matoishi, Y. Terao, N. Doi, H. Yanagawa, H. Ohta, *Chem. Commun.* **2005**, 877-879.

6 a) L. Duhamel, J. –C. Plaquevent, *J. Am. Chem. Soc.* **1978**, *100*, 7415-7416; b) L. Duhamel, J. –C. Plaquevent, *Tetrahedron Lett.* **1977**, *18*, 2285-2288.

7 a) S. Oudeyer, J. –F. Brière, V. Levacher, *Eur. J. Org. Chem.* **2014**, 6103-6119; b) J. T. Mohr, A. Y. Hong, B. M. Stoltz, *Nature Chem.* **2009**, *1*, 359-369.

8 H. Yamamoto, K. Futatsugi, *Angew. Chem. Int. Ed.* **2005**, *44*, 1924-1942.

9 a) S. Nakamura, M. Kaneeda, K. Ishihara, H. Yamamoto, *J. Am. Chem. Soc.* **2000**, *122*, 8120-8130; b) K. Ishihara, S. Nakamura, M. Kaneeda, H. Yamamoto, *J. Am. Chem. Soc.* **1996**, *118*, 12854-12855.

10 a) C. H. Cheon, O. Kanno, F. D. Toste, *J. Am. Chem. Soc.* **2011**, *133*, 13248-13251; b) C. H. Cheon, T. Imahori, H. Yamamoto, *Chem. Commun.* **2010**, 6980-6982.

11 Y. Yamashita, Y. Emura, K. Odashima, K. Koga, *Tetrahedron Lett.* **2000**, *41*, 209-213.

12 K. Mitsuhashi, R. Ito, T. Arai, A. Yanagisawa, *Org. Lett.* **2006**, *8*, 1721-1724.

13 C. H. Cheon, H. Yamamoto, *J. Am. Chem. Soc.* **2008**, *130*, 9246-9247.

14 M. Morita, L. Drouin, R. Motoki, Y. Kimura, I. Fujimori, M. Kanai, M. Shibasaki, *J. Am. Chem. Soc.* **2009**, *131*, 3858-3859.

15 E. M. Beck, A. M. Hyde, E. N. Jacobsen, *Org. Lett.* **2011**, *13*, 4260-4263.

16 A. Claraz, G. Landelle, S. Oudeyer, V. Levacher, *Eur. J. Org. Chem.* **2013**, 7693-7696.

17 a) D. Uraguchi, N. Kinoshita, T. Ooi, *J. Am. Chem. Soc.* **2010**, *132*, 12240-12242; b) T. Poisson, S. Oudeyer, V. Dalla, F. Marsais, V. Levacher, *Synlett* **2008**, 2447-2450; c) T. Poisson, V. Dalla, F. Marsais, G. Dupas, S. Oudeyer, V. Levacher, *Angew. Chem. Int. Ed.* **2007**, *46*, 7090-7093; d) A. Yanagisawa, T. Touge, T. Arai, *Pure Appl.Chem.* **2006**, *78*, 519-523; e) A. Yanagisawa, T. Touge, T. Arai, *Angew. Chem. Int. Ed.* **2005**, *44*, 1546-1548.

18 a) N. Fu, L. Zhang, S. Luo, J. –P. Cheng, *Chem. Eur. J.* **2013**, *19*, 15669-15681; b) M. Rueping, T. Theissmann, S. Raja, J. W. Bats, *Adv. Synth. Catal.* **2008**, *350*, 1001-1006.

19 a) A. Yanagisawa, T. Sugita, K. Yoshida, *Chem. Eur. J.* **2013**, *19*, 16200-16203; b)

20 a) J. Guin, G. Varseev, B. List, *J. Am. Chem. Soc.* **2013**, *135*, 2100-2103; b) X. Dai, T. Nakai, J. A. C. Romero, G. C. Fu, *Angew. Chem. Int. Ed.* **2007**, *46*, 4367-4369; c) B. L. Hodous, J. C. Ruble, G. C. Fu, *J. Am. Chem. Soc.* **1999**, *121*, 2637-2638; d) C. Fehr, I. Stempf, J. Galindo, *Angew. Chem. Int. Ed.* **1993**, *32*, 1044-1046.

21 E. Emori, T. Arai, H. Sasai, M. Shibasaki, *J. Am. Chem. Soc.* **1998**, *120*, 4043-4044.

22 a) B. Wang, F. Wu, Y. Wang, X. Liu, L. Deng, *J. Am. Chem. Soc.* **2007**, *129*, 768-769; b) Y. Wang, X. Liu, L. Deng, *J. Am. Chem. Soc.* **2006**, *128*, 3928-3930.

23 K. L. Kimmel, J. D. Weaver, M. Lee, J. A. Ellman, *J. Am. Chem. Soc.* **2012**, *134*, 9058-9061.

24 T. Poisson, Y. Yamashita, S. Kobayashi, *J. Am. Chem. Soc.* **2010**, *132*, 7890-7892.

25 a) L. Navarre, R. Martinez, J. –P. Genet, S. Darses, *J. Am. Chem. Soc.* **2008**, *130*, 6159-6169; b) L. Navarre, S. Darses, J. –P. Genet, *Angew. Chem. Int. Ed.* **2004**, *43*, 719-723.

26 a) C. G. Frost, S. D. Penrose, K. Lambshead, P. R. Raithby, J. E. Warren, R. Gleave, *Org. Lett.* **2007**, *9*, 2119-2122; b) T. Nishimura, S. Hirabayashi, Y. Yasuhara, T. Hayashi, *J. Am. Chem. Soc.* **2006**, *128*, 2556-2557; c) J. D. Hargrave, J. Herbert, G. Bish, C. G. Frost, *Org. Biomol. Chem.* **2006**, *4*, 3235-3241; d)R. J. Moss, K. J. Wadsworth, C. J. Chapman, C. G. Frost, *Chem. Commun.* **2004**, 1984-1985.

27 M. P. Shibi, H. Tatamidani, K. Patil, *Org. Lett.* **2005**, *7*, 2571-2573.

28 M. P. Shibi, J. Coulomb, L. M. Stanley, *Angew. Chem. Int. Ed.* **2008**, *47*, 9913-9915.

29 a) N. Fu, L. Zhang, S. Luo, J. –P. Cheng, *Chem. Eur. J.* **2013**, *19*, 15669-15681; b) N. Fu, L. Zhang, S. Luo, J. –P. Cheng, *Angew. Chem. Int. Ed.* **2011**, *50*, 11451-11455.

30 T. Jousseaume, N. E. Wurz, F. Glorius, *Angew. Chem. Int. Ed.* **2011**, *50*, 1410-1414.

31 R. Kuniyil, R. V. Sunoj, *Org. Lett.* **2013**, *15*, 5040-5043.

32 Y. Saga, R. Motoki, S. Makino, Y. Shimizu, M. Kanai, M. Shibasaki, *J. Am. Chem. Soc.* **2010**, *132*, 7905-7907.

[33] a) J. H. Clark, *Chem. Rev.* **1980**, *80*, 429-452; b) B. M. Trost, D. E. Keely, *J. Org. Chem.* **1975**, *40*, 2013-2013; c) K. Nishimura, M. Ono, Y. Nagaoka, K. Tomioka, *J. Am. Chem. Soc.* **1997**, *119*, 12974-12975.

[34] H. –Z. Yu, Y. –M. Yang, L. Zhang, Z. –M. Dang, G. –H. Hu, *J. Phys. Chem. A* **2014**, *118*, 606-622.

[35] H. Pracejus, F. –W. Wilcke, K. Hanemann, *J. Prakt. Chem.* **1977**, *319*, 219-229.

[36] a) S. Lin, D. Leow, K. –W. Huang, C. –H. Tan, *Chem. Asian J.* **2009**, *4*, 1741-1744; b) D. Leow, S. Lin, S. K. Chittimalla, X. Fu, C. –H. Tan, *Angew. Chem. Int. Ed.* **2008**, *47*, 5641-5645.

[37] A. Kumar, R. V. Salunkhe, R. A. Rane, S. Y. Dike, *J. Chem. Soc., Chem. Commun.* **1991**, 485-486.

[38] B. –J. Li, L. Jiang, M. Liu, Y. –C. Chen, L. –S. Ding, Y. Wu, *Synlett* **2005**, *4*, 603-606.

[39] a) B. Cho, C. –H. Tan, M. W. Wong, *J. Org. Chem.* **2012**, *77*, 6553-6362; b) S. Lin, D. Leow, K. –W. Huang, C. –H. Tan, *Chem. Asian J.* **2009**, *4*, 1741-1744; c) D. Leow, S. Lin, S. K. Chittimalla, X. Fu, C. –H. Tan, *Angew. Chem. Int. Ed.* **2008**, *47*, 5641-5645.

[40] L. Dai, H. Yang, J. Niu, F. –E. Chen, *Synlett* **2012**, *23*, 314-316.

[41] a) N. R. Rana, V. K. Singh, *Org. Lett.* **2011**, *13*, 6520-6523; b) R. A. Unhale, N. K. Rana, V. K. Singh, *Tetrahedron Lett.* **2013**, *54*, 1911-1915.

[42] N. Fu, L. Zhang, S. Luo, J. –P. Cheng, *Org. Lett.* **2014**, *16*, 4626-4629.

[43] M. Ueno, T. Kitanosono, M. Sakai, S. Kobayashi, *Org. Biomol. Chem.*, **2011**, *9*, 3619-3621.

[44] B. Dmuchovsky, B. D. Vineyard, F. B. Zienty, *J. Am. Chem. Soc.* **1964**, *86*, 2874-2877.

[45] T. C. Wabnitz, J.-Q. Yu, J. B. Spencer, *Chem. Eur. J.* **2004**, *10*, 484-493.

[46] Proton exchange between thiols and base was suggested from ^{1}H NMR spectroscopy in D_2O.

[47] J. A. H. Schwöbel, J. C. Madden, M. T. D. Cronin, *SAR QSAR Environ. Res.* **2010**, *21*, 693-710.

[48] As one example proton-transfer studies in water-alcohol solutions, see; D. Huppert, E. Kolodney, *Chem. Phys.* **1981**, *63*, 401-410.

[49] Selected reviews, see: a) M. S. Roselló, J. L. Aceña, A. S. –Fuentes, C. del Pozo, Chem. Soc. Rev. **2014**, *43*, 7430-74533; b) J. Wang, P. Li, P. Y. Choy, A. S. C. Chan, F. Y. Kwong, *Chem. Cat. Chem.* **2012**, *4*, 917-925; c) P. R. Krishna, A. Sreeshailam, R. Srinivas, *Tetrahedron* **2009**, *65*, 9657-9672; d) D. Enders, C. Wang, J. X. Liebich, *Chem. Eur. J.* **2009**, *15*, 11058-11076; e) L. W. Xu, C. G. Xia, *Eur. J. Org. Chem.* **2005**, 633-639.

[50] a) Y. Hamashima, S. Suzuki, T. Tamura, H. Somei, M. Sodeoka, *Chem. Asian J. 2011*, *6*, 658-668; b) Y. Hamashima, T. Tamura, S. Suzuki, M. Sodeoka, *Synlett 2009*, 1631-1634; c) P. H. Phua, S. P. Mathew, A. J. P. White, J. G. Vries, D. G. Blackmond, K. K. M. Hii, *Chem. Eur. J.* **2007**, *13*, 4602-4613; d) Y. Hamashima, H. Somei, Y. Shimamura, T. Tamura, M. Sodeoka, *Org. Lett.* **2004**, *6*, 1861-1864.

[51] M. Sani, L. Bruche, G. Chiva, S. Fustero, J. Piera, A. Volonterio, M. Zanda, *Angew. Chem. Int. Ed.* **2003**, *42*, 2060-2063.

[52] J. Zhang, Y. Zhang, X. Liu, J. Guo, W. Cao, W. Cao, L. Lin, X. Feng, *Adv. Synth. Catal.* **2014**, *356*, 3545-3550.

[53] a) A. Le Cocq, M. R. Gizdavic-Nikolaidis, A. J. Easteal, G. A. Bowmaker, *Aust. J. Chem.* **2011**, *65*, 723-729; b) N. Bicak, B. Karagoz, *J. Poly. Sci. Part A: Poly. Chem.* **2006**, *44*, 6025-6031.

[54] a) H. R. Safaei, M. Shekouhy, S. Khademi, V. Rahmanian, M. Safaei, *J. Indus. Eng. Chem.* **2014**, *20*, 3019-3024; b) M. Jafarpour, A. Razaeifard, M. Aliabadi, *Helv. Chim. Acta* **2010**, *93*, 405-413; c) M. Jafarpour, A. Rezaeifard, M. Aliabadi, *Lett. Org. Chem.* **2009**, *6*, 94-99; b) A. Hasaninejad, A. Zare, M. A. Zolfigol, M. Shekouhy, *Synth. Commun.* **2009**, *39*, 569-579.

[55] B. J. Hathaway, In "*Comprehensive Coordination Chemistry*", Pergamon Press: New York, **1987**, Vol. 5, Chapter 53.

[56] a) K. Manabe, S. Kobayashi, *Tetrahedron Lett.* **1999**, *40*, 3773-3776; b) K. Manabe, Y. Mori, S. Nagayama, K. Odashima, S. Kobayashi, *Inorg. Chim. Acta*, **1999**, *296*, 158-163.

---

[57] Under the optimal conditions, the catalyst solution was acidic enough (*ca*. pH 3.8). After waiting for sequentially-added aniline to be dispersed enough, pH value turned mild (*ca*. pH 5.6). After stirring for 24 hours, the reaction solution became a little bit acidic again (*ca*. pH 5.0).

[58] The loss of chiral induction is assumed to be arisen from the basicity of the reaction solution. After addition of *N*-methylbenzylamine, the pH value of the resultant solution became basic (*ca*. pH 10.5).

[59] R. M. Figueiredo, R. Frohlich, M. Christmann, *J. Org. Chem.* **2006**, *71*, 4147-4154.

[60] a) M. Kokubo, T. Naito, S. Kobayashi, *Tetrahedron* **2010**, *66*, 1111-1118; b) C. Ogawa, M. Kokubo, S. Kobayashi, *J. Synth. Org. Chem. Jpn.* **2010**, *68*, 718-728; c) M. Kokubo, T. Naito, S. Kobayashi, *Chem. Lett.* **2009**, *38*, 904-905.

[61] G. Blay, I. Fernandez, J. R. Pedro, C. Vila, *Org. Lett.* **2007**, *13*, 2601-2604.

[62] T. Tsubogo, Y. Kano, Y. Yamashita, S. Kobayashi, *Chem. Asian J.* **2010**, *5*, 1974-1977.

[63] a) T. Sakamoto, J. Itoh, K. Mori, T. Akiyama, *Org. Biomol. Chem.* **2010**, *23*, 5448-5454; b) E. G. Gutierrez, E. J. Moorhead, E. H. Smith, V. Lin, L. K. G. Ackerman, C. E. Knezevic, V. Sun, S. Grant, A. G. Wenzel, *Eur. J. Org. Chem.* **2010**, 3027-3031.

[64] a) Y. Liu, D. Shang, X. Zhou, X. Liu, X. Feng, *Chem. Eur. J.* **2009**, *15*, 2055-2058; b) W. Wang, X. Liu, W. Cao, J. Wang, L. Lin, X. Feng, *Chem. Eur. J.* **2010**, *16*, 1664-1669.

Chapter 5: *Catalytic Construction of Hydrogen Isotope Chirality in Deuterium Oxide*

5-1   Introduction

Along with the growth of organic chemistry, the ever-evolving catalysis impacts heavily on our daily lives. Further advances in organic synthesis rely on the invention of unprecedented catalytic performance toward novel mode of stereoinduction as well as bond activation, ultimately leading to fortuitous applicability or usefulness and fundamentally new methodology. Despite tremendous efforts dedicated by researchers of all ages and countries, enzymes still exhibit overwhelmingly superior catalysis to artificial catalysts in many aspects.   Enzymes can even discern between the two identical groups bound to a prochiral center in accordance with their three-dimensional information. For example in the β-oxidation of fatty acids, enoyl-CoA hydratases catalyze the reversible abstraction/addition of proton alpha to a carbonyl group with *syn* stereochemistry in spite of the unfavorable eclipsed geometry, albeit with high substrate specificity.[1] When incubated in deuterium oxide, this enzymatic reaction resulted in a stereospecific incorporation of deuterium into α-position, rendering the compound which owes its chirality to an isotopic substitution.[2] In contrast, artificial catalysis for discernment of such nice distinction represents one of the greatest challenges so far, due to its limited discriminability.
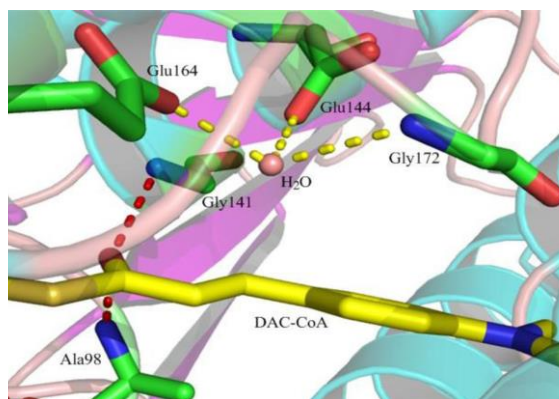
Figure 1. X-ray crystallographic structure of the active site of enoyl-CoA hydratase (obtained from Protein Data Bank)
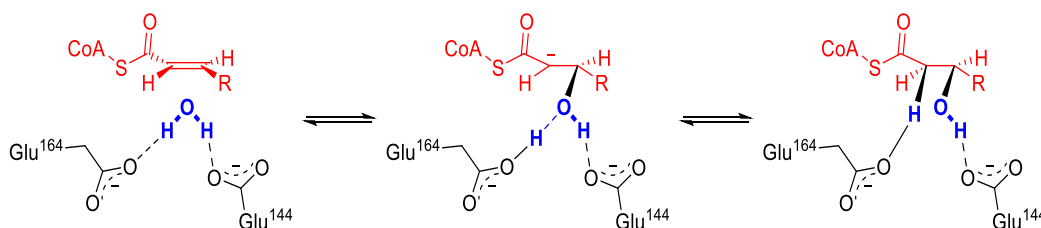
Scheme 1. The most favorable mechanistic scenario for *syn*-hydration by enoyl-CoA hydratase.[3]

Isotopically chiral compounds have been valued in the fields of stereochemistry and biochemistry[4] to comprehend the protein dynamics[5] or the reaction mechanisms.[6] A minute disparity between isotopes of the same element, especially hydrogen, has been spotlighted in the past decade, not only since related to the extraterrestrial origin of biological homochirality[7] but since it sometimes carries macroscopic properties such as optical activity,[8] lower lipophilicity,[9] parity energy difference,[10] helicity of aggregates (Scheme 2),[11] catalytic chiral amplification[12] and so on. Moreover, encouraged by the promisingness through clinical trials, pharmaceutical companies are snapping up the idea of selective deuterium-labeling at specific place in a currently approved drug.[13] The "heavy drugs" can modify the metabolic fate to substantially alter their overall therapeutic profile, retaining the biochemical potency.
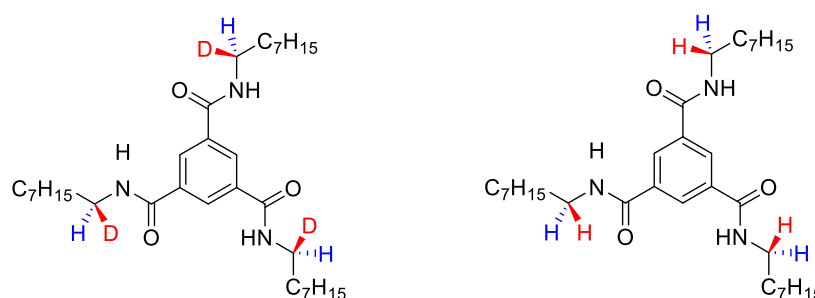
Scheme 2. Isotopic chirality can induce the change in a preferred helical sense in the supramolecular aggregate. Left-handed (left) and right-handed (right) helical superstructures are preferably formed, respectively.

Although chiral isotopic labeling seems to have infinite potentialities multidisciplinarily, conventional methodologies are deficient in applicability, versatility and unmanageablility. A fundamental and catalytic strategy relies on asymmetric reduction of aldehydes to construct the hydrogen isotope chirality alpha to alcohols, entailing the preparation of deuterated reducing agents or aldehydes (Scheme 3).[14] The absolute configuration of the α-deuterated alcohols can be determined after the conversion into the corresponding Mosher esters.
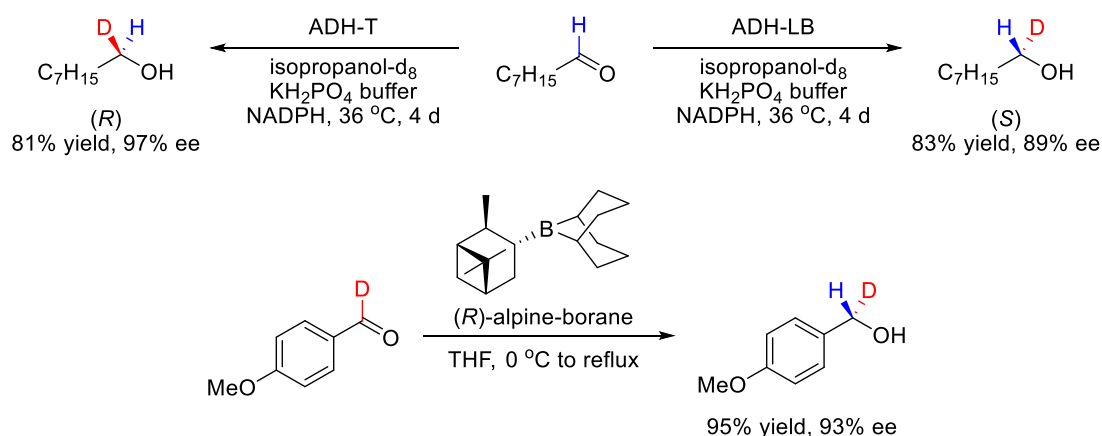
Scheme 3. Construction of hydrogen isotope chirality at α-position of alcohols through reduction. Enzymatic method (above)[14b] and asymmetric reduction using chiral borane (below).[14a]

The biotinated iridium complex incorporated into streptavidin was exploited in the diastereoselective reduction of NAD$^+$ using DCOO$_2$Na as a hydride source.[15] The complex itself showed poor selectivity, whereas the complexes incorporated with streptavidin mutant S112A and S112K are responsible for (*R*)-conformation. A selective one-dimentional TOCSY NMR experiment using irradiation on H6 enabled reliable integration of two resonances attributed to both diastereomers.
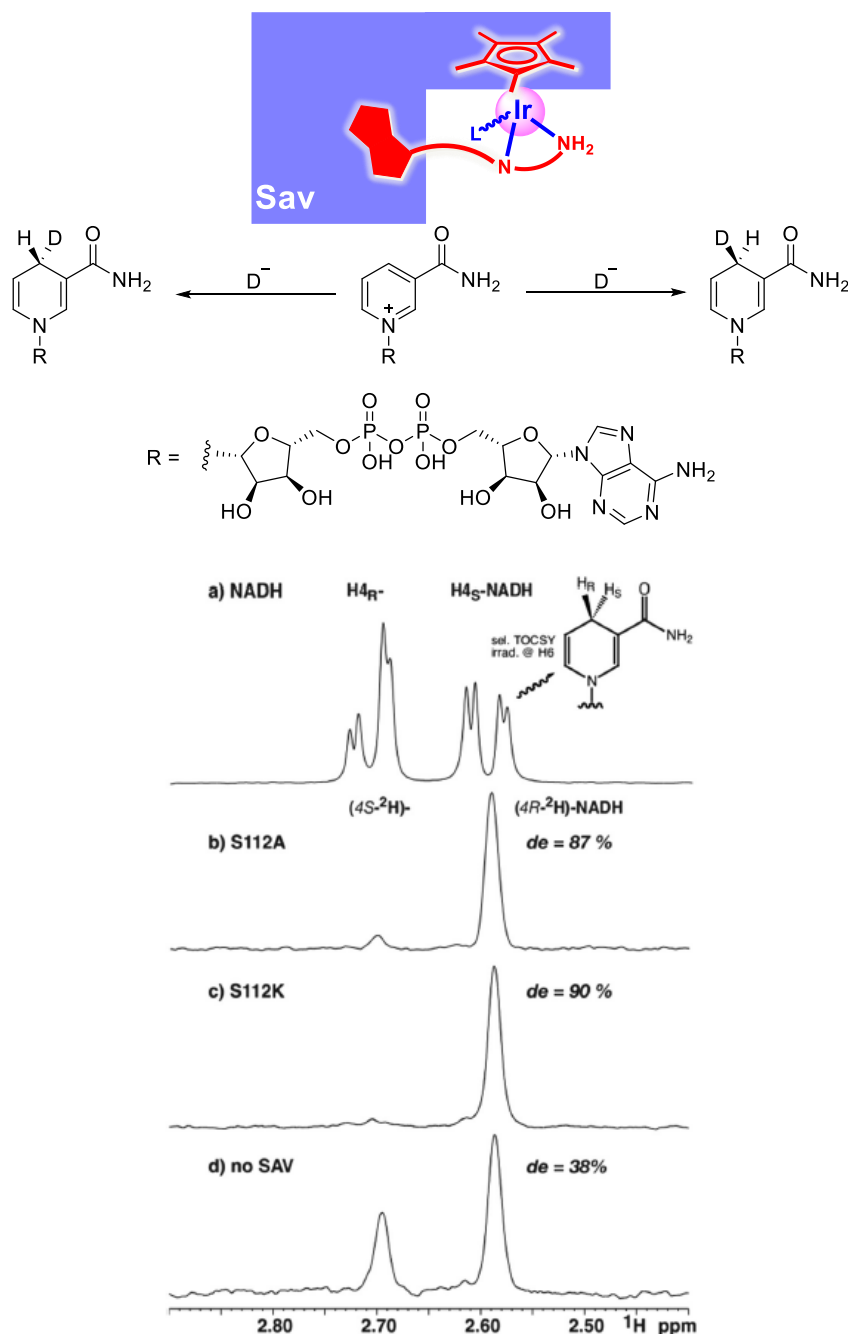
Scheme 4. Diastereoselective reduction of NAD$^+$ to NAD^{2}H

(spectra were reprinted from original paper without any modification)[15]

Another architectural target is an α-position of carbonyl bearing some substituents at β-position to determine the absolute configuration,[16] as enoyl-CoA hydratases do. A few strategies can be undertaken: 1) H/D exchange under basic conditions, 2) reaction of aldehyde with dialkylzinc reagent, 3) 1,4-addition and subsequent protonation/deuteration (Scheme 5).

\<H/D exchange protocol\>

\<Dialkylzinc protocol\>
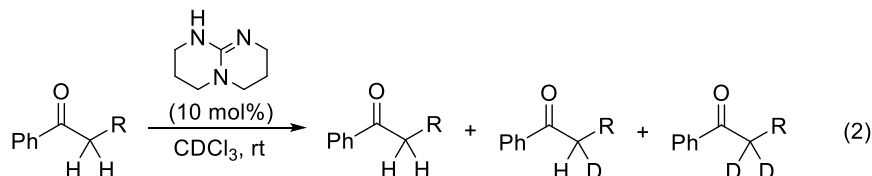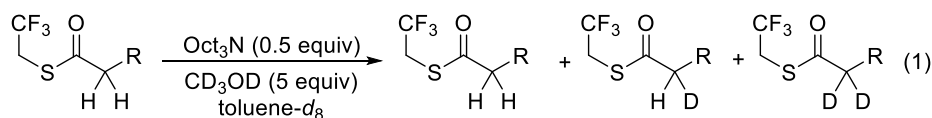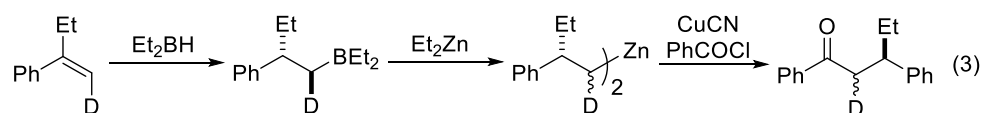
\<1,4-Addition protocol\>
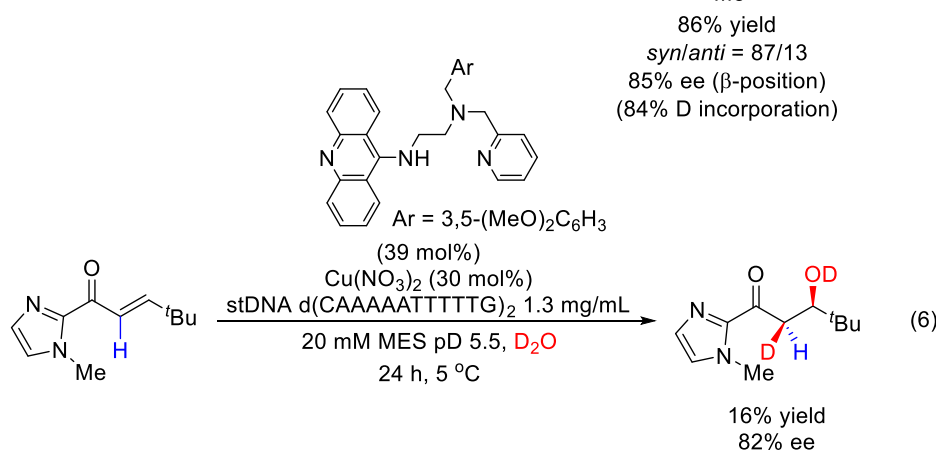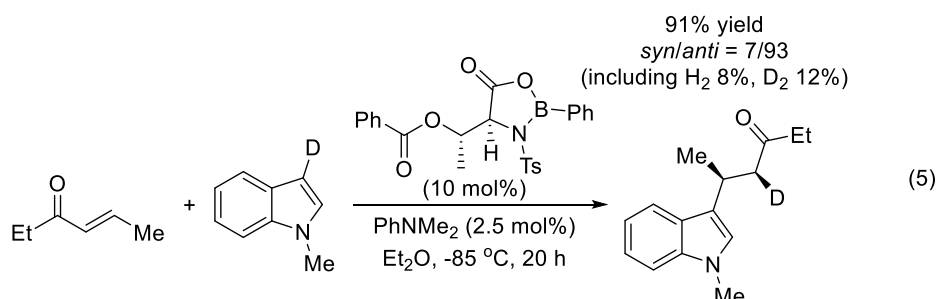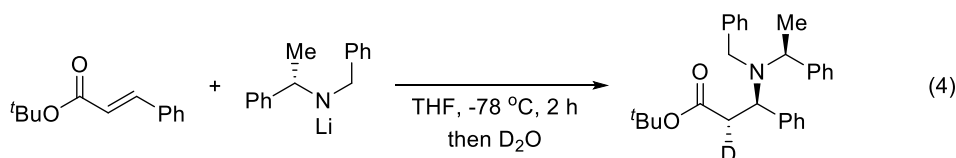
Scheme 5. Conventional strategies to introduce deuterium at α-position of carbonyl groups.

The base-mediated H/D exchange reactions of ketones or thioesters generally proceed along with the competitive protonation and over-deuteration, relating a fundamental control inability resulting from the infinitesimal difference in acidity between a starting material and a corresponding product (typical example: Scheme 5 (1), (2)).[17] Since these three analogues ([H$_2$]- (= starting material), [H,D]- and [D$_2$]-analogues) are chemically identical, it is impossible to know the exact ratio of them for us. Setting aside the analytical development of vibrational optical activity,[18] a convenient determination of the absolute configuration is another matter of concern. The geminal proton alpha to a ketone becomes diastereotopic and anisochronous when the ketone bears chirality at β-position. The use of alkylzinc reagents prepared by the diatereoselective hydroboration of the deuterated styrene produced a diastereo-mixture due to the intrinsic characteristic of the boron-zinc exchange, albeit with tedious procedures and with low atom-economy (Scheme 5 (3)).[19]

Although selective deuteration of an enolate or protonation of a deuterated enolate represent the most promising protocol using chiral auxiliary (Scheme 5 (4))[20] and chiral oxazaborolidinone cataslyst (Scheme 5 (5)),[21] the detrimental side-reactions such as competitive protonation and over-deuteration impairs remarkably their practical value. Chiral auxiliary method provides access to anti-configured α-deuterio-β-amino esters after deprotection using Pearlman's catalyst (Scheme 6).   It is to be noted that the byproduct obtained competitively has optical activity. We can calculate the exact distribution of deuterium in byproduct from the reported ^{1}H NMR and mass spectrum.
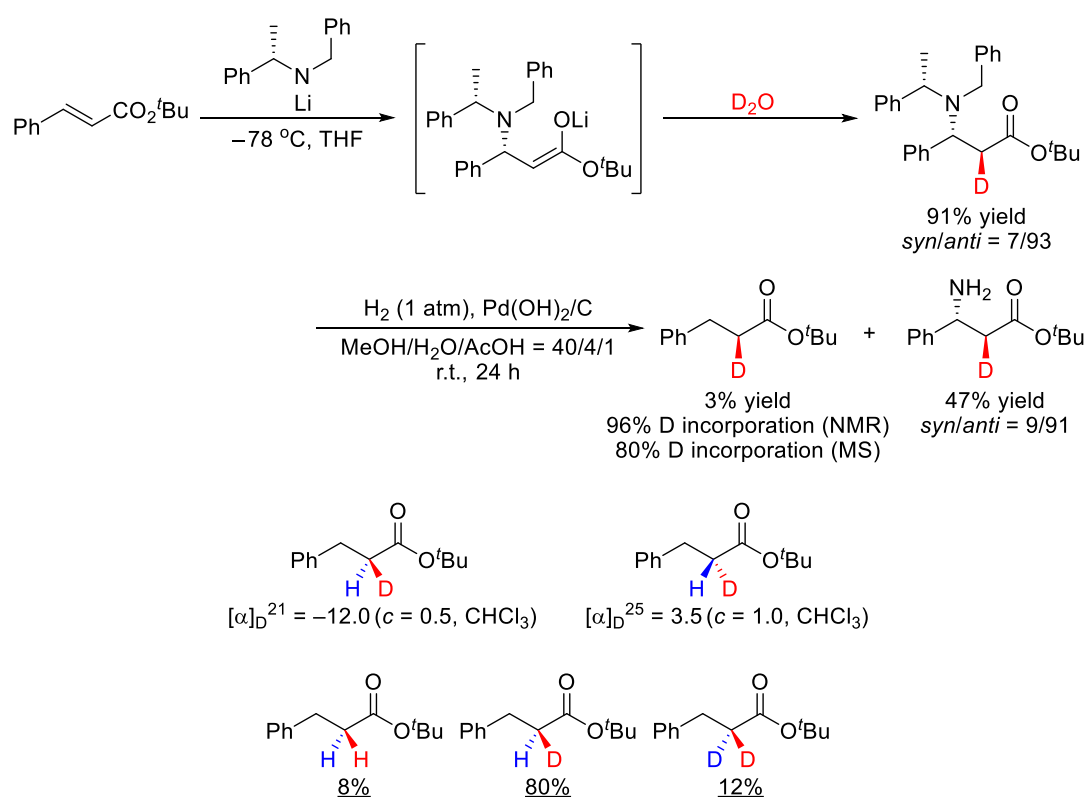
Scheme 6. Tandem conjugate addition/deuteration using chiral auxiliary and deprotection (above). The optical rotation of formed 2-deuterio-3-phenylpropanoate (middle). Calculated ratio of three possible isomers (below).

Feringa *et al*. reported that their Cu^{2+}-based catalyst composed of 2-(aminomethyl)pyridine-based ligand and st-DNA was responsible for *syn*-selective hydration of α,β-unsatruted *N*-acylimidazole in deuterium oxide (Scheme 5 (6)).[22] Although the reaction suffered from quite low yield, they stated that a single diastereomer was produced through the reaction, due to the suppression of dehydration process. The exclusive *syn*-selection is questionable since ^{1}H NMR spectrum of deuterated product (Figure 5, II) seems to have some irregularities such as overlapping shoulder. The result of catalytic hydration of deuterium-labeled substrate with water (Figure 5, III) indicates a suspicion on H/D scrambling in the product during the reaction.
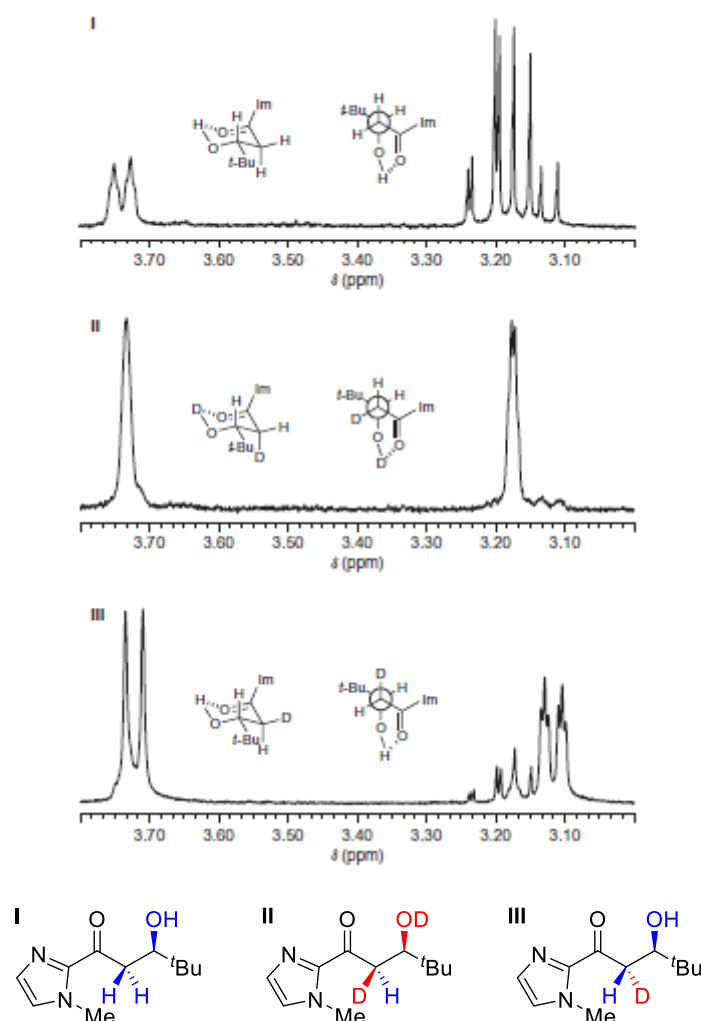
Figure 5. Feringa's evidence on selectivity in catalytic hydration.
(spectra were reprinted from original paper without any modification)[22]

Herein is described the findings for an expedient and catalytic construction of hydrogen isotope chirality. Not only its synthetic challenge but a multidisciplinary anticipation of hydrogen isotope chirality serves as driving forces behind this work.

5-2   *Preliminary Insights*

The remarkable governance of the enantioselective execution at the protonation was preliminarily disclosed in water, despite their abnormally high mobility in water as described in Chapter 4.   The reaction underwent a dramatic drop in enantioselectivity when performed in organic solvents including ethanol, dichloromethane and so on, along with a bit to significant lowering of reactivity.   To sum up, the catalytic cycle commences with a catalytic generation of an activated enone, which is then amenable to a nucleophilic addition of either *thiol* or *thiolate*.   The nucleophilic addition of *thiols* in aqueous media proceeds via a concerted mechanism, whereas the addition of *thiolates* involves a stepwise mechanism, accompanied by the subsequent protonation. Multiple experimental results revealed an overall responsibility of a catalytic amount of base for the precise control of enantioselection.   Since hydrogen is the smallest element, enantioselective protonation event claims manipulation of a tiny atom at protonation step and avoidance of product racemization at a labile stereocenter.   There are two kinds of steering for the enantioselection at protonation step; (A) confining the trajectory of a proton toward a chiral enolate intermediate and (B) leveraging the size difference between an intramolecular C–CH$_3$ bond and a newly-forming C–H bond.   With this deliberation in mind, a catalytic construction of hydrogen isotope chirality was envisaged through the reaction performed in deuterium oxide (Scheme 7).
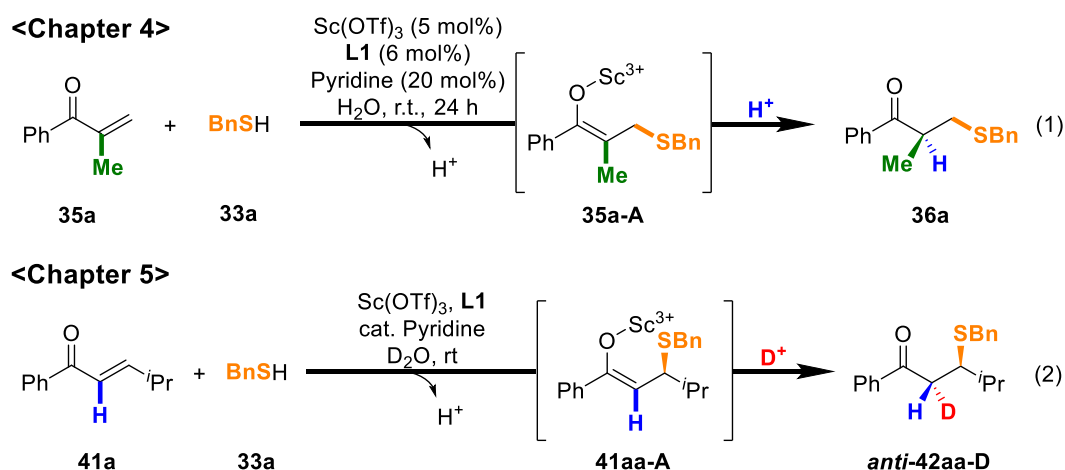
Scheme 7. Strategy toward catalytic construction of hydrogen isotope chirality.

As anticipated, the reaction of β-substituted enone **41a** with thiol **33a** furnished α-deuterated thia-Michael adduct **42a** in the presence of 1 mol% of scandium catalyst under basic conditions, via chiral enolate **41aa-A** (Scheme 8).   β-Chirality plays a pivotal role not only in determination of H/D chirality but also in suppression of undesired protonation process.   The geminal proton alpha to a ketone becomes diastereotopic and anisochronous, *syn*-, *anti*- and protonated isomers show a little bit different chemical shift in NMR spectrum (Scheme 8, below). Moreover, the reaction exhibited an exclusive preference for *anti*-conformation with the effective inhibition of the competitive protonation.   There are six possible isomers as the reaction product including two protonated enantiomers **42aa** and **43aa**.   Since these six isomers are chemically equivalent and small molecules, physical separation is impossible.   The initial nucleophilic

addition of *thiolate* constructs a chirality at β-position, providing two possible chiral enolate intermediates **41aa-A** and **41aa-B** as an enantiotropic pair. Deuteration of the intermediate **41aa-A** and **41aa-B** delivers two diastereomers, ***syn/anti*-42aa** and ***syn/anti*-43aa**, respectively (Scheme 9). Protonated product **42aa** and **43aa** have no diastereomer. That is, three isomers derived from **41aa-A** and the other three isomers derived from **41aa-B** can be separated by HPLC as enantiomeric pairs.
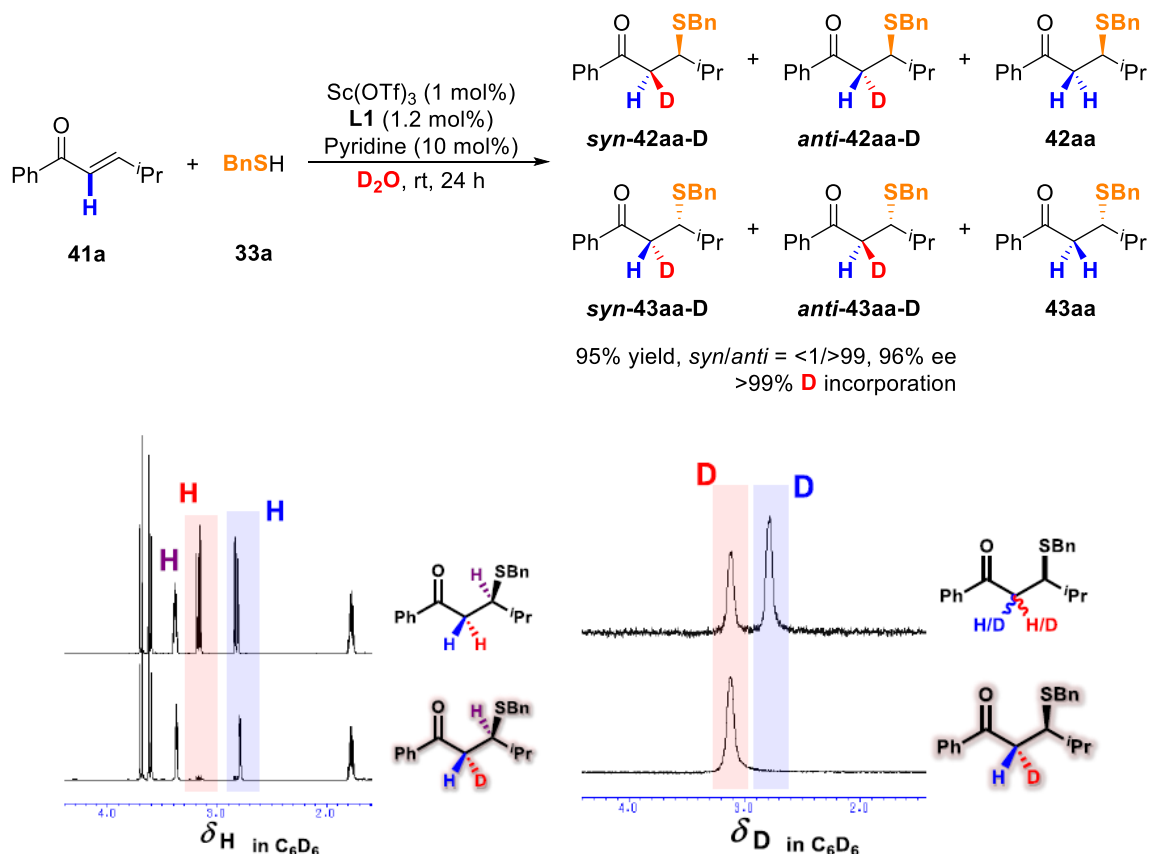
Scheme 8. Initial trial for construction of hydrogen isotope chirality using deuterium oxide (above) and ^{1}H & ^{2}H NMR spectra of obtained isomers (below).
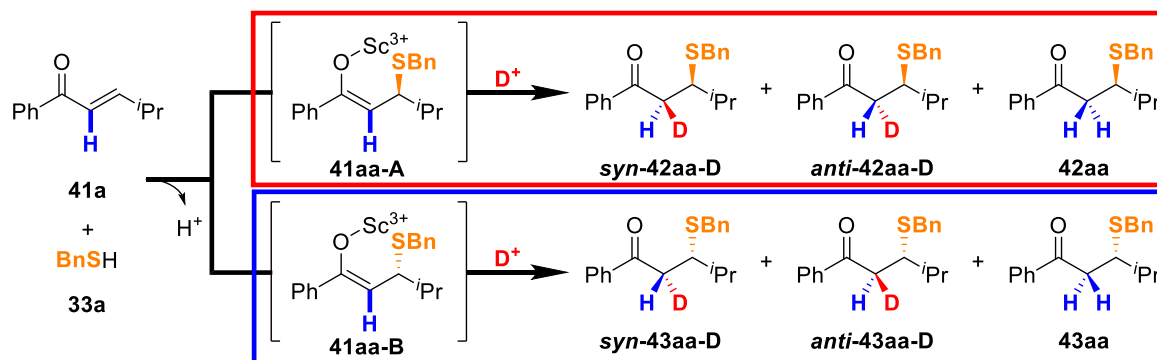
Scheme 9. Reaction pathways to produce possible six isomers.

The quenching of *in situ*-generated lithium enolate prepared from **42aa** with deuterium oxide delivered a racemic 1:1 mixture of two diasteroisomers, proving that a selective deuteration was not a substrate-specific but a catalyst-controlled event (Scheme 10).
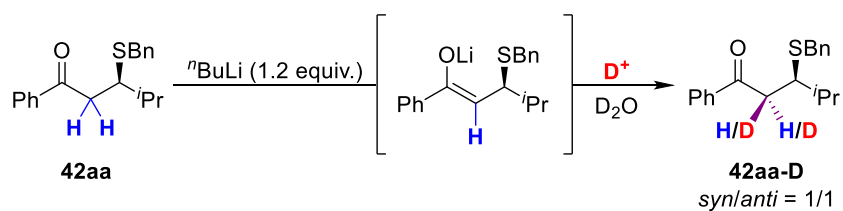
Scheme 10. Quenching of a lithium enolate with deuterium oxide.

5-3　*What is Responsible for the Stereochemical Outcome?*

Based upon the speculation that the structural information of **41aa-A** or **41aa-B** dictated the stereochemistry of **42aa** or **43aa**, the influence of a base and a deuterium-source on the reaction outcome was examined (Table 1).　The reaction in the presence of α-substituted pyridines became a bit less reactive and selective (entries 2, 3).　When 1 mol% of deuterium-labeled inorganic base was added, the reaction underwent an exclusive selection identical to the reaction using pyridine (entries 4, 6).　In contrast, 4 mol% of NaOD led to a significant drop in selectivity to afford a completely racemic product (entry 5).　When the reaction conducted in deuterium-labeled alcohols, the deuteration event was much less selective along with a high level of chiral induction at nucleophilic addition step (entries 7-9).　The proportional relationship between the solvent polarity and the diastereomeric ratio implies the interplay of hydrogen bondings at the deuteration of a chiral enolate intermediate.　The importance of hydrogen bondings on selective deuteration was indicated by the reaction outcome based upon a scandium complex formed with 2,2'-bipyridyl (entry 10).　The resemblance in the stereochemical outcome between entries 7-10 underscores a pivotality of hydroxy group of **L1**.

Table 1. Effect of base and deuterium-source in selective deuteration.

Entry	Base (mol%)	Solvent	Yield (%)[a]	*syn/anti*[b]	**42aa/43aa**[c]
1	Pyridine (10)	D_2O	95	<1/>99	98/2
2	α-Picoline (10)	D_2O	84	4/96	94.5/5.5
3	2,6-Lutidine (10)	D_2O	89	5/95	92/8
4	NaOD (1)	D_2O	82	<1/>99	98/2
5	NaOD (4)	D_2O	Quant.	50/50	50/50
6	KOD (1)	D_2O	87	<1/>99	97.5/2.5
7	Pyridine (10)	CD_3OD	94	35/65	96/4
8	Pyridine (10)	C_2D_5OD	97	37/63	95.5/4.5
9	Pyridine (10)	Isopropanol-d_8	98	45/55	92/8
10[d]	Pyridine (10)	D_2O	61	37/63	(50/50)

[a] Isolated yield.　[b] Determined by ^{2}H NMR analysis.　[c] Determined by HPLC analysis.
[d] 2,2'-Bipyridyl was used instead of **L1**.

Scandium catalyst preferred *anti*-diastereomer irrespective of the enantiopurity of chiral 2,2'-bipyridine **L1** (Table 2, entries 1, 2).　Based upon the hypothesis that the enantiofacial differentiation of deuteron is independent from the previous nucleophilic addition, racemic **L1** was

then tested.   As expected, exclusive diastereoselectivity appeared (entry 3).   This result clearly shows that the deuteration event was independent from the nucleophilic addition, except for a steric influence at β-position.   When *tert*-butyl group was changed into methyl in the structure of **L1**, high diastereoselectivity was still obtained although nucleophilic addition was not selective at all (entry 4).   When phenyl-substituted ligand **L5** was employed, the reaction was slightly *syn*-selective (entry 5).   Encouraged by the fact that chirality of ligand can control the hydrogen isotope chirality, I changed the substrate from **41a** to 1-phenylbut-2-en-1-one **41b**.   Under the optimal conditions, the stereoselective performance was not exclusive but still high (entry 6).   The opposite enantiomer (*R*, *R*)-**L1** gave the product with the same preference as (*S*,*S*)-**L1**, whereas *meso*-isomer influenced the selectivity in the presence of racemic **L1** (entries 7, 8).   It is noteworthy that the reaction proceeded *syn*-selectively in the absence of pyridine (entry 9). Nevertheless, the reaction exhibited a *syn*-preference, albeit low level of enantioselection. Aromatic group also furnished *syn*-product as a major conformation with the same level of enantioselectivity.   Of interest is the fact that the reaction result is the same as the reaction performed in CD$_3$OD with pyridine (entries 9 & 10).   Pyridine itself catalyzed the reaction quantitatively with almost no stereoselection (entry 11).   It means that chiral scandium complex is responsible for the selective deuteration event.   Contrary to the case of **41a**, the reaction of **41b** was *syn*-selective in the presence of **L4**-**L6** with pyridine (entries 12-14).

Table 2. Effect of chiral ligand in selective deuteration.

Entry	Ligand	Substrate	Yield (%)[a]	*syn/anti*[b]	42aa/43aa[c]
1	(*S*, *S*)-**L1**		94	<1/>99	98/2
2[d]	(*S*, *S*)-**L1**		91	<1/>99	98/2
3	rac-**L1**[e]	**41a**	88	<1/>99	(50/50)
4	(*S*, *S*)-**L4**		98	17/83	50/50
5	(*S*, *S*)-**L5**		61	65/35	60.5/39.5
6	(*S*, *S*)-**L1**		87	11/89	98/2
7	rac-**L1**[e]		89	23/77	(50/50)
8	(*R*, *R*)-**L1**		89	10/90	95.5/4.5
9[f]	(*S*, *S*)-**L1**		77	68/32	91/9
10[g]	(*S*, *S*)-**L1**	**41b**	77	67/33	96.5/3.5
11[h]	–		Quant.	41/59	(50/50)
12	(*S*, *S*)-**L4**		81	71/29	60/40
13	(*S*, *S*)-**L5**		84	75/25	98/2
14	(*S*, *S*)-**L6**		64	76/24	96.5/3.5

[a] Isolated yield. [b] Determined by ^{2}H NMR analysis. [c] Determined by HPLC analysis.
[d] At low catalyst loading: 0.6 mol% **L1**, 0.5 mol% Sc(OTf)$_3$, 1.5 mol% pyridine.
[e] Containing *meso*-isomer (1 : 1). [f] Without pyridine. [g] Performed in CD$_3$OD.
[h] Without scandium and ligand.

As shown in Table 1, the influence of added bases on selectivity is quite curious. The amount of base was examined in detail (Table 3). In contrast to almost invariable reactivity across the amount of base, the change in diastereoselectivity is drastic. The highest selectivity was recorded in the presence of 3 mol% of pyridine (entry 4). As the reaction of **41a** did, the reaction of **41b** showed high level of diastereoselection when 1 mol% of deuterium-labeled inorganic base was added.

Table 3. Effect of base amount in selective deuteration.

Entry	Base (mol%)	Solvent	Yield (%)[a]	syn/anti[b]	42aa/43aa[c]
1	None	D$_2$O	77	68/32	91/9
2	Pyridine (1.2)	D$_2$O	89	17/83	96/4
3	Pyridine (2)	D$_2$O	87	12/88	97/3
4	Pyridine (3)	D$_2$O	87	11/89	98/2
5	Pyridine (4)	D$_2$O	86	14/86	97.5/2.5
6	Pyridine (5)	D$_2$O	82	18/82	97/3
7	Pyridine (10)	D$_2$O	82	17/83	95.5/4.5
8	Pyridine (15)	D$_2$O	88	25/75	96/4
9	Pyridine (20)	D$_2$O	86	25/75	96/4
10	Pyridine (10)	CD$_3$OD	77	67/33	96/4
11	NaOD (1)	D$_2$O	82	15/85	96/4

[a] Isolated yield. [b] Determined by ^{2}H NMR analysis. [c] Determined by HPLC analysis.
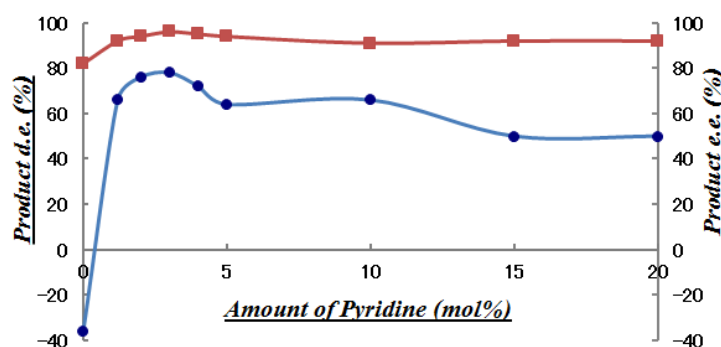
Since bases do not involve directly in high level of diastereoselection, base should have an influence on chiral scandium complex.   First of all, it shifts the equilibrium toward a fixed and tetradentate complexation as discussed in Chapter 1.   Second, formation of hydroxide is assumed through a hydrolysis of scandium core, as described in Chapter 4.   Acid-base titration of aqueous scandium triflate solution with base is impressive (Figure 6).   At the beginning of titration curve, the pH started off low and increase gradually as the amount of NaOH increased up to 1 equivalent. The curve then got less steep and almost stable until 2 equivalent of NaOH was added.   There was a major steep soar of pH value near the equivalence point where 3 equivalent of NaOH was required.   When titrated with pyridine, the pH kept almost unchanged ungil near the equivalence point (more than 3 equivalents) and beyond that point the pH increased gradually toward an asymptote around pH 6.   The solution of $Sc(OTf)_3$ with excess pyridine resists any large increase in pH as a buffer solution, which suggested the incomplete hydrolysis of $Sc(OTf)_3$ producing monohydroxide or bishydroxide.   In contrast, more than 3 equivalents of NaOH seem to hydrolyze $Sc(OTf)_3$ completely to form $Sc(OH)_3$ or its aggregates, which is clearly supported by the formation of precipitates.   The formation of bishydroxide $Sc(OH)_2^+$ seems to take place when the curve gets past the half-way point around 2 equivalents.   The pH value obtained when 3 equivalents of pyridine or 1 mol% of NaOH was added ranged from 5 to 5.5, which suggests the formation of monohydroxide $Sc(OH)^{2+}$.
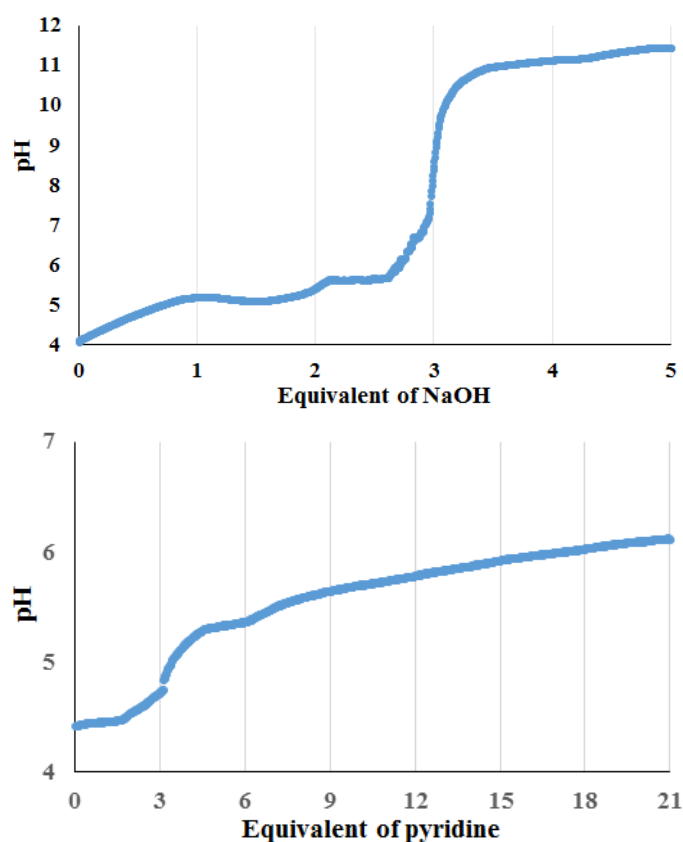
Figure 6. Acid-base titration using $Sc(OTf)_3$ with NaOH (above) and pyridine (below) in water.

In order to prove that selection at α-position was determined by metal-**L1** complex, several metal cations were screened under the optimal conditions. The detailed values (yield or stereoselectivity) were omitted and results are summarized in Figure 7. The screened metals can be categolized mainly into three groups. Moderate *anti*-selectivity (*syn/anti* = 32/68) was observed without any metal in the presence of **L1** and pyridine. Compared with this selection, most Lewis acids and a few lanthanides (La^{3+} and Ce^{4+}) catalyzed the reaction in almost same selective manner, which appears to have no direct influence on dictating the selectivity at deuteration step. It is noteworthy that $Sc(OTf)_3$ alone exhibited *anti*-preference, whereas rare earth metals except for Sc^{3+}, La^{3+} and Ce^{4+} afforded *syn*-isomer as a major product. Based upon these results, effective metals on diastereoselectivity were limited to lanthanide series.
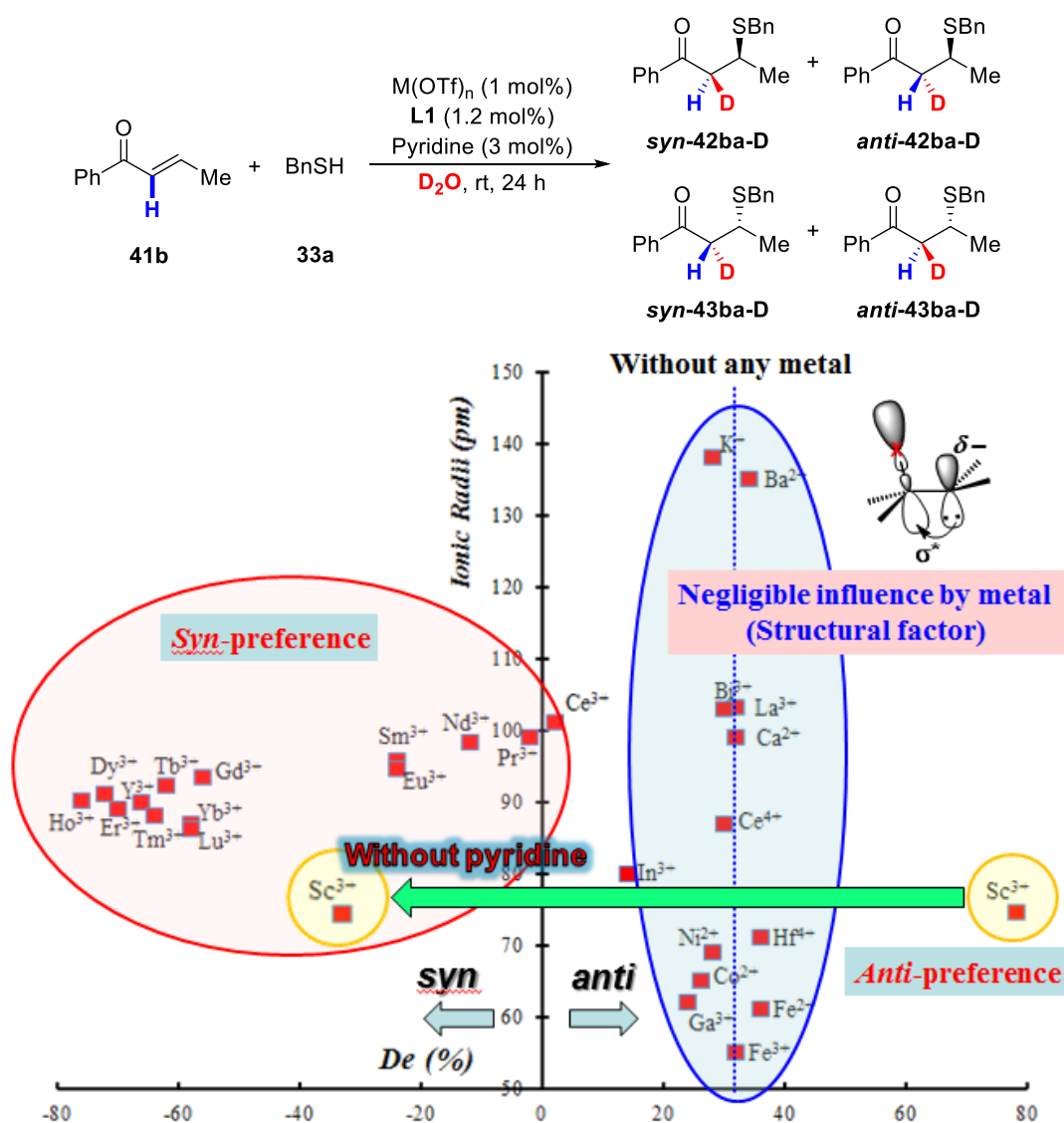
Figure 7. Summary of metal screening and correlation between metals and diastereoselectivity.

Correlation between diastereoselectivity and ionic radii (Scheme 8, left) or f electron number (Scheme 8, right) was shown. Both factors seem to be suitable for elucidation of diastereoselectivity. The difference between Ce^{3+} and Ce^{4+}, the similarity between La^{3+} and Ce^{4+}

were well reflected in diastereoselectivity-f electron number correlation. It is also noteworthy that *syn*-preference was observed in the absence of pyridine even when scandium catalyst was employed. The same level of diastereoselection was recorded when the reaction was performed in deuterium-substituted methanol in the combination of scandium catalyst with pyridine. Given the result of acid-base titration, in deuterium oxide scandium monohydroxide seemed to form. The formation of monohydroxide did not take place in the absence of pyridine or in methanol. The detailed discussion will be described later.
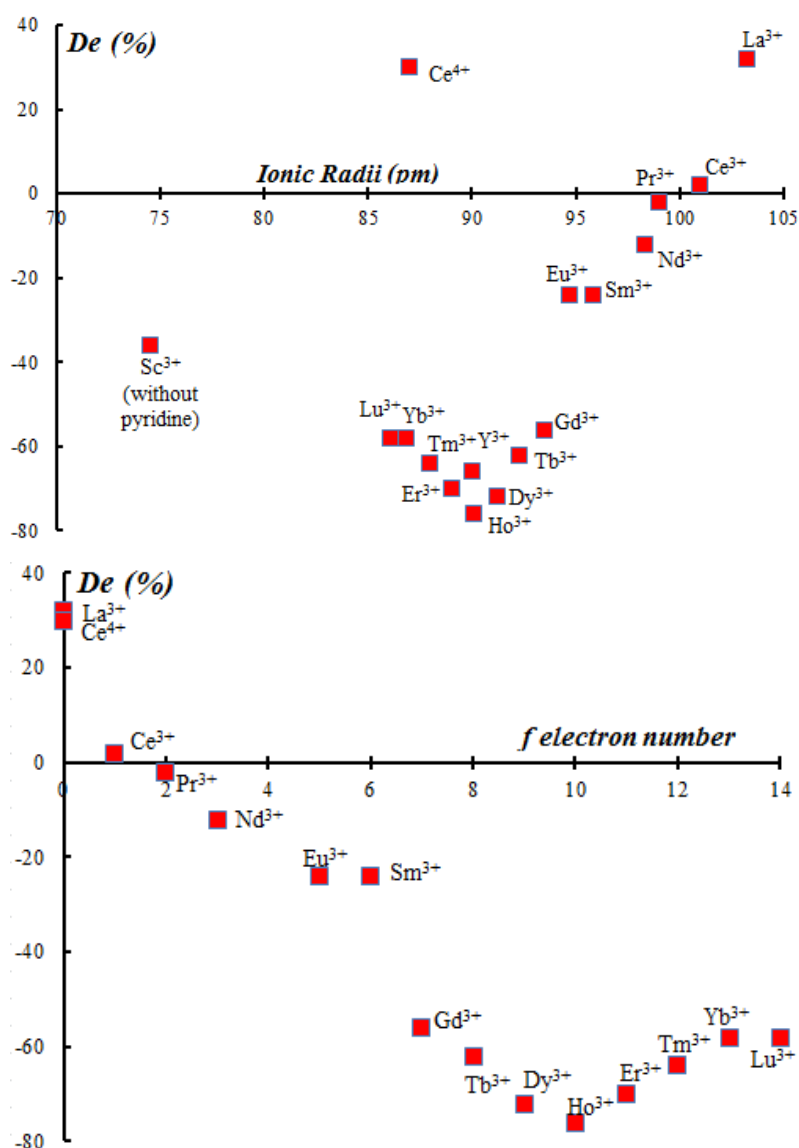
Figure 8. Effect of lanthanide triflates in selctive deuteration.

In order to gain insights into the steric effect of β-substituent, several α,β-unsaturated ketones were subjected to the optimal conditions (Scheme 11). When secondary or tertiary group was substituted at β-position, the reaction underwent an exclusive *anti*-selection (**41d**, **41e** and **41f**). The reaction of 1,5-diphenylpenta-2,4-dien-1-one **41c** afforded α-deuterated 1,4-adduct **42ca-D** in a high selective manner. Chalcone derivatives delivered α-deuterated adducts with high selectivity, too (**41g-j**). Although the electronic nature of β-substituent had generally almost negligible effect

on the diastereoselection, electron-donating group on aromatic ring adjacent to carbonyl group made diastereoselectivity increase (**41i**).   The catalytic system was, however, inapplicable for the reaction of α,β-unsaturated esters, nitriles, amides and *N*-acyl pyrroles.   When cyclohexenone was used as a substrate, the reaction furnished the desired product almost quantitatively with low diastereo- and enantioselectivity.   Since ca. 5% of α-methylene protons were replaced with deuterium, deprotonation by only 3 mol% of pyridine might lead to a slight drop in the diastereoselectivity.   Although the nitroolefin was reacted with thiol, deuterium incorporation at α-position was more than 130%, suggesting the over-deuteration.
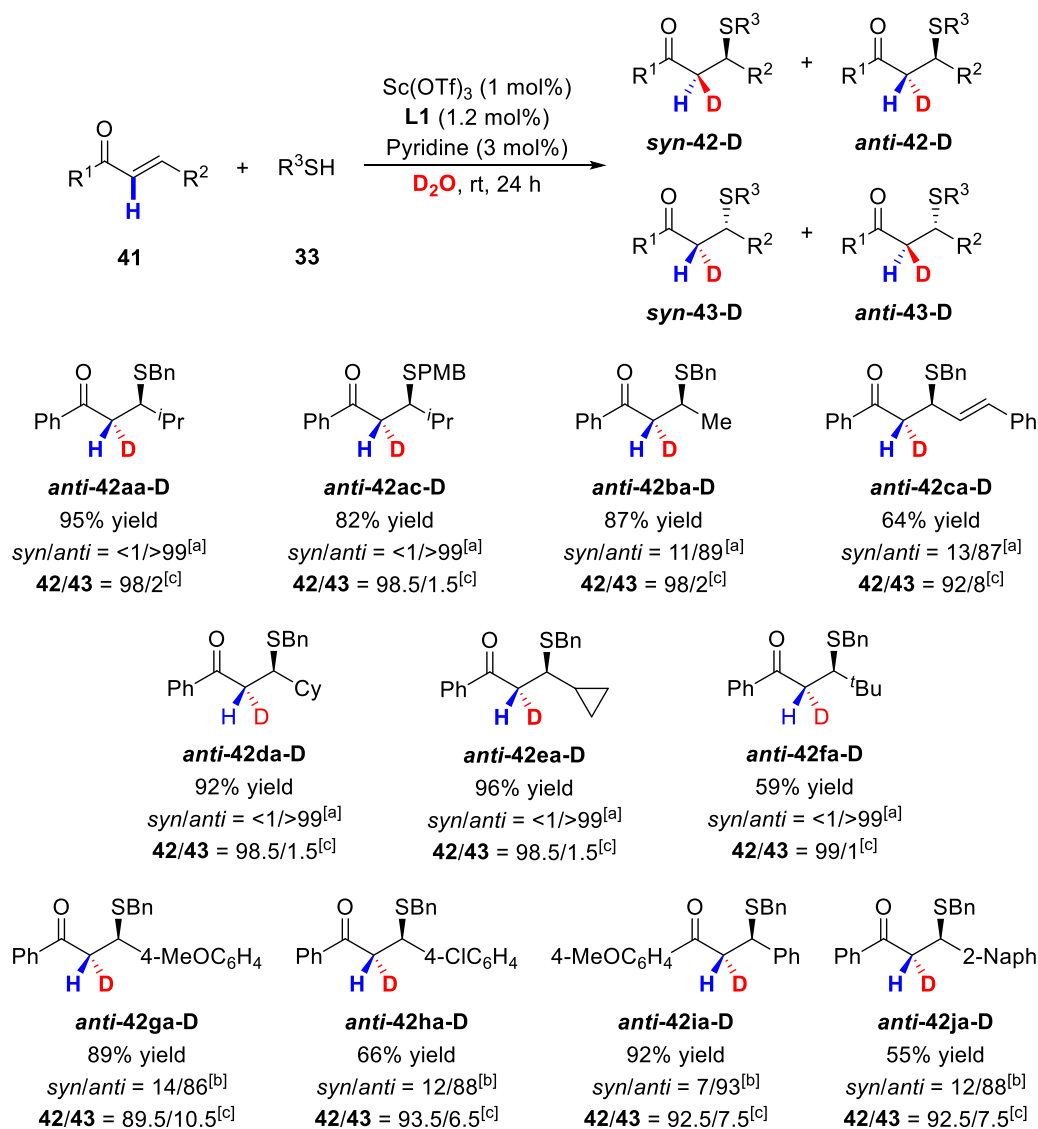
Scheme 11. Effect of β-substituent of Michael acceptor in selective deuteration.

In order to enlarge the structural constructability through selective deuteration, the α,β-unsaturated *N*-acylated oxazolidin-2-one **41k** was subjected to the optimal condition (Table 4). Its enormous utility such as transformability to ester, Weinreb amide and so on was amply demonstrated by many reports.   The reaction proceeded smoothly to afford the α-deuterated product **42ka** in high yield with high diastereo- and enantioselectivity (entry 1).   Reducing the

amount of pyridine led to a significant drop in diastereoselectivity with retaining chiral induction in the nucleophilic addition step (entry 2). The reaction of **41k** did not take place at all without pyridine (entry 3). Although Koskinen's group reported a Sc-pybox catalyst for this reaction in dichloromethane at 0 ℃,[23] the use of pybox **L13** instead of **L1** in deuterium oxide was in vain (entry 4).[24] As observed in the reaction of **41b**, ytterbium complex formed with **L1** was responsible for preference of the reaction toward *syn*-conformation.

Table 4. Selective deuteration using α,β-unsaturated *N*-acylated oxazolidin-2-one.
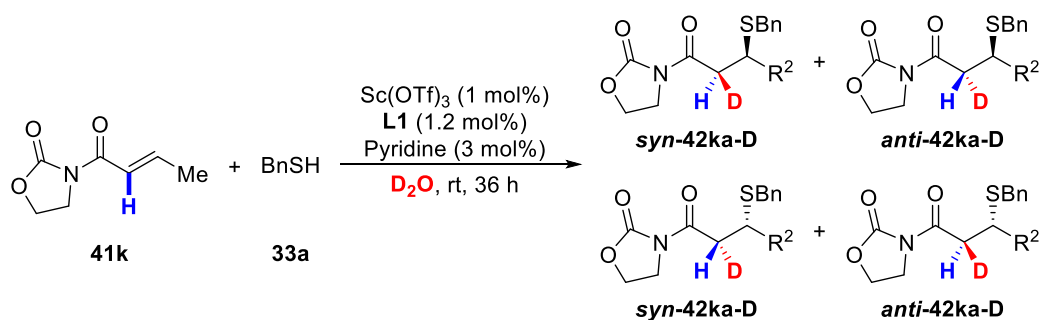
Entry	Lewis acid	Pyridine	Yield (%)[a]	*syn/anti*[b]	42ka/43ka[c]
1	Sc(OTf)$_3$	–	NR	–	–
2	Sc(OTf)$_3$	+	88	21/79	95/5
3	Sc(OTf)$_3$	+[d]	65	32/68	94.5/5.5
4[e]	Sc(OTf)$_3$	+	NR	–	–
5	Yb(OTf)$_3$	+	38	87/13	59.5/40.5

[a] Isolated yield.　　[b] Determined by ^{2}H NMR analysis.　　[c] Determined by HPLC analysis.
[d] 1 mol% of pyridine was added instead of 3 mol%.　　[e] Pybox **L13** was used instead of **L1**.

5-4 Toward Comprehension of Fundamental Mechanism

With the empirical knowledge in hands, the stereoelectronic and steric contributions at deuteration step were speculated as rationales of governing the stereoselectivity. The congenital nature of an enolate anion, as demonstrated without any metal, can be understood using a model to avoid destabilizing allylic 1,3-interactions. The hyperconjugative interaction between C–S σ^* orbital and π orbital will make the trajectory of an electrophile antiperiplanar to a C–S bond (Figure 9).
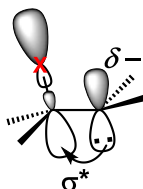
Figure 9. Assumed interaction in enolate intermediate anion.

In the meanwhile, the electronic tuning of the substrate substituents had much less influence on stereochemical consequence than their steric factor. Extensive research revealed that metal cation and its coordinating fashion were deeply responsible for high level of stereoselection, implying a sterically key role of inner-sphere water molecules or OH group in **L1**. The stereochemical independence of deuteration from preceding nucleophilic addition suggests that the electrochemical property of metal enolate intermediates appears to be irrelevant to selective deuteration event. Attention was then paid to two inscrutable points lying on a curve of diastereoselectivity across lanthanide series. A discontinuity between Eu^{3+} and Gd^{3+} can be regarded as a kind of so-called "gadolinium break", changes in a number of physicochemical properties around gadolinium.[25] Comprehension of a trough at Ho^{3+} seems to be a highroad to the origin of stereoselection at deuteration step.
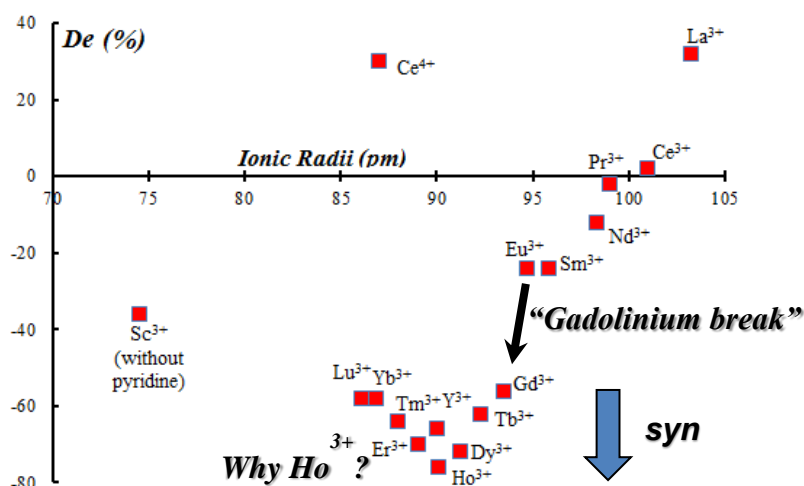
Figure 10. Points to be considered in the diastereoselectivity change across lanthanides.

On the assumption that a metal enolate intermediate is deuterated, proton transfer at primary coordination sphere should play a prominent role. Generally speaking, the hydrated

tervalent lanthanide(III) ions were known to adopt tricapped trigonal prismatic structure in aqueous environments (Figure 11, left). Given the contribution of f-orbital on sp^3d^5 hybridization, electronic repulsion between inner-sphere water molecules should increase along with a diminution of ionic radii proportional to atomic number, leading to a change in coordination number. Since 4f orbital
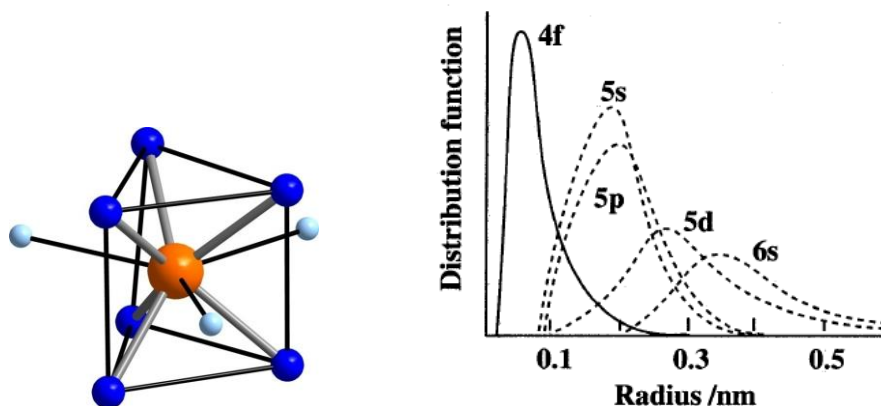
Figure 11. General conformation of tricapped trigonal prism (left) and general illustration of orbital radius (right).

Indeed, a phenomenon that full occupancy of nine-coordination become unable to be maintained around Ho^{3+} was revealed by EXAFS analysis (Figure 13).[26] An implicative curve of diastereoselectivity can be interpreted as a multiplex result of equilibrium of the catalyst complex formation, an ionic radius and an exchange rate for the substitution of inner-sphere water ligands. Beyond holomium across the lanthanide series, full occupancy of hydration around the core cannot be maintained due to its ionic radii, leading to a water deficit and a resultant decrease in its coordination number. At gadolinium, changes in symmetry of capped water molecule or hydrogen bonding is assumed.
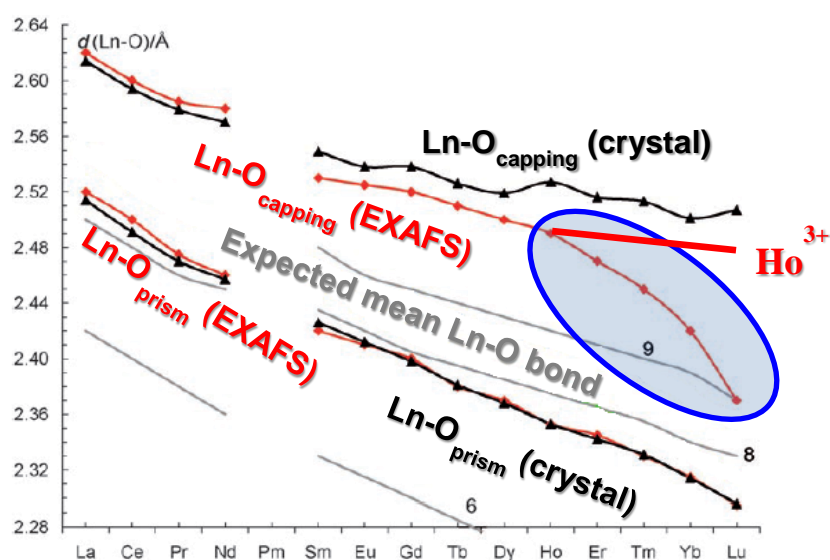
Figure 13. Reported EXAFS results for the hydrated lanthanoid(III) ions in the solid trifluoromethanesulfonates salts. (graph was excerpted from original paper with slight modification)

Among rare-earth metals, X-ray crystallographic studies of scandium[27] and yttrium[28] complex formed with **L1** were carried out previously (Figure 12). The structure of scandium complex is in a heptacoordination fashion with distorted pentagonal bipyramidal. Due to its smallest ionic radii among all metal cations, **L1** would coordinate strongly with the core. Althoug the water molecule surrounding scandium core should be fluxional theoretically, water molecule on equatorial plane should be more fixed through hydrogen bonding with OH group of **L1**. In contrast, the yttrium center adopts a dodecahedral octacoordination. Two water molecules occupy two sites. Compared with scandium complex, coordination with **L1** should be weaker and the flexibility of water molecules is quite obvious. Therefore yttrium complex would have more stubborn resistance toward hydrolysis and higher fluxionality in inner-sphere of the core than scandium complex.

Sc–O (ligand) bond 2.17 Å

Sc–OH$_2$ bond 2.23 Å

$[\text{ScBr}_2(\text{L1})(\text{H}_2\text{O})]^+ \text{Br}^- \cdot \text{H}_2\text{O}$

Y–O (ligand) bond 2.31 Å

Y–OH$_2$ bond 2.34 Å

$[\text{Y(OTf)}_2(\text{L1})(\text{H}_2\text{O})_2]^+ \text{OTf}^- \cdot 0.5\text{CH}_2\text{Cl}_2$
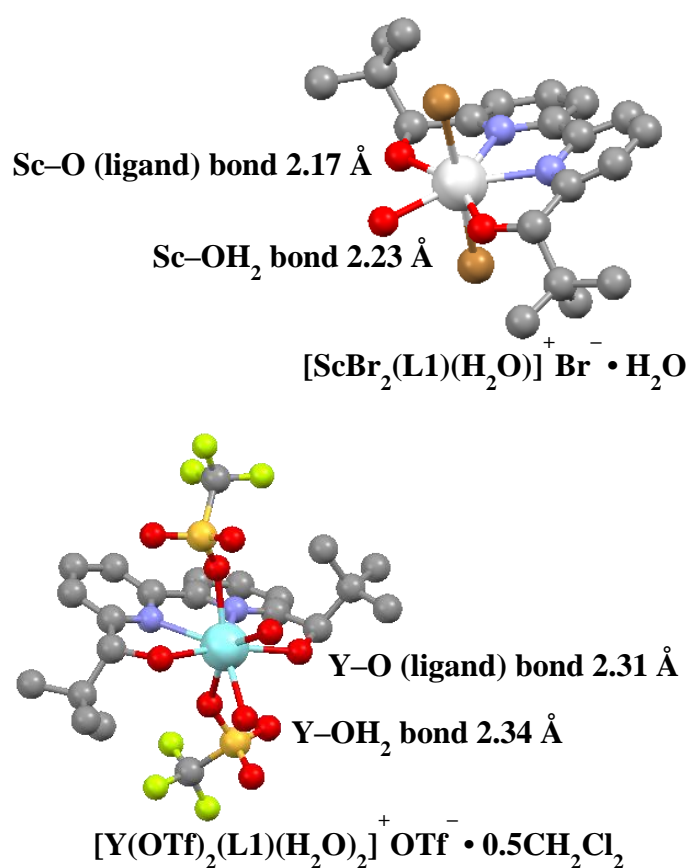
Figure 12. X-ray crystallographic structure of scandium (above) and yttrium (below) complex formed with **L1**.

With these considerations in mind, the lanthanide-**L1** complexes would show a dodecahedral octacoordination or an antiprismatic nonacoordination. Both coordination number of the core and the distance between coordinating water molecules and the core are of great imporatance for the stereocontrol at deuteration step. One water molecule would replace with Michael acceptor and other water molecules or OD group of **L1** would act as a deuterium source. It should be asserted that the stereoselective deuteration event after the nucleophilic addition in

deuterium oxide is dominated by the stereochemistry around the inner-sphere of hydrated metal-**L1** complex.

The selective protonation of an enolate intermediate **41aa-A** bearing a C–D bond alpha to carbonyl group delivered the identical conformation ***anti*-42aa** (Scheme 1 (3)), suggesting that a chiral metal-enolate complex would not stipulate the trajectory of proton/deuteron but spot the tiny difference between a C–H bond and a C–D bond. In principle, since a vibrational behavior define a shape and size of the bond,[29] the anharmonicity of the vibrational potential energy and the zero-potential energy between them make the average C–D bond length typically shorter than an equivalent C–H bond, which is in accordance with the stereochemical outcome.

5-5　*Application of Stereoselective Deuteration in Deuterium Oxide*

The strategy of hydrogen isotope chirality at α-position of carbonyl compounds by chiral catalyst invoked further application.　Preliminary investigations shown here were carried out basically using racemic **L1**.
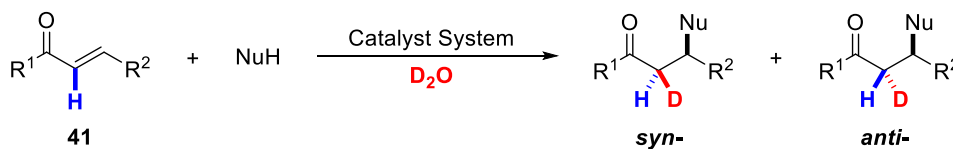
Scheme 12. Application of stereoselective deuteration strategy.

The oxa-Michael addition was catalyzed by copper(II) catalysis composed of $Cu(OH)_2$ and **L1** when alcohol was used as a solvent (Table 5).　In non-deuterated solvent, the use of chiral ligand did not provide any chirality (entries 1-3).　The use of deuterated methanol led to a slight level of enantioselectivity (entries 4, 5).　Besides, the diastereoselectivity of deuterated product was slightly *syn*-selective with 2:1 ratio.　Based upon aforementioned insights, low *syn/anti* ratio is attributed to the use of methanol.

Table 5. Oxa-Michael addition of methanol or deuterium-labeled methanol.
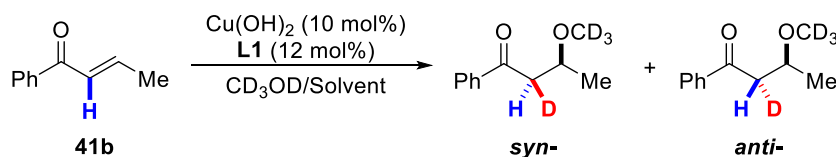
Entry	Solvent	Yield (%)	*syn/anti*[a]	% ee[b]
1	$H_2O/MeOH = 1/4$	63	–	0
2[c]	$H_2O/MeOH = 1/4$	79	–	0
3[d]	$H_2O/MeOH = 1/4$	58	–	0
4	CD_3OD	16	65/35	26
5	$D_2O/CD_3OD = 1/4$	22	68/32	29

[a] Determined by ^{1}H NMR analysis.　[b] Determined by HPLC analysis.
[c] **L30** was used instead of **L1**.　[d] **L8** was used instead of **L1**.

The aza-Michael reaction with aniline proceeded smoothly even without any catalyst (Table 6, entry 1).　The product is regarded as a precursor of β-amino acids.　However, more than half amount of the obtained product was protonated adduct.　Under the optimal conditions described in Chapter 4 using $Cu(OSO_2C_9H_{21})_2$ as a LASC and $4\text{-}NO_2C_6H_4CO_2H$ as an additive, the reaction was almost unselective albeit with a significant suppression of the competititve protonation pathway (entry 2).　In deuterium-labeled methanol, almost same tendency was observed but the competititve protonation was not suppressed so much compared with the reaction in deuterium oxide (entry 3).　In contrast, it was revealed that $Cu(OSO_2C_9H_{21})_2$ alone allowed the reaction to be *syn*-selective (entry 4).　Further addition of **L1** increased the selectivity up to 91/9 (entry 5).[30]

Brønsted acid-catalyzed reaction exhibited a slightly higher *syn*-selectivity than the reaction without any catalyst (entry 6).

Table 6. Aza-Micael addition in deuterium oxide.

Entry	Catalyst	Ligand	Additive	Solvent	Yield (%)	*syn/anti*[a]
1	–	–	–	D_2O	57 (53)[b]	–
2	+	+	+	D_2O	82 (2)[b]	53/47
3	+	+	+	CD_3OD	Quant. (20)[b]	46/54
4	+	–	–	D_2O	83 (2)[b]	77/23
5	+	+	–	D_2O	88 (2)[b]	91/9
6	–	–	+	D_2O	89 (2)[b]	68/32

[a] Determined by ^{1}H NMR analysis.
[b] The abundance of protonated product **44ba** in the obtained mixture.

It was turned out that metal cation could switch the selectivity at the deuteration step between *syn*- and *anti*-preference (Table 7). Intriguigly, in contrast to *syn*-preference in Sc^{3+}- or Cu^{2+}-catalyzed reaction, Ni^{2+}-catalyzed reaction was anti-favorable (entries 1-3). The reaction performed in deuterium-labeled methanol exhibited the opposite selectivity to that in deuterium oxide as thia-Michael addition did (entry 4). The coincidence between the selectivity in Ni^{2+}-catalyzed reaction in deuterium oxide and that in Cu^{2+}-catalyzed reaction in deuterated methanol is suggestive. Considering the hydrolysis constants of metal cation, nickel has a strong resistance to hydrolysis. It was strongly suggested that the formation of metal monohydroxide species was responsible for the selectivity switch, *syn*-preference in this reaction.

Table 7. Metal-induced preference of deuteration in aza-Michael addition.

Entry	Metal	Hydrolysis constant	Solvent	Yield (%)	*syn/anti*[a]
1	Sc^{3+}	4.3	D_2O	83 (<1)[b]	82/18
2	Ni^{2+}	9.86	D_2O	83 (8)[b]	36/64
3	Cu^{2+}	7.53	D_2O	88 (2)[b]	91/9
4	Cu^{2+}		CD_3OD	Quant. (9)[b]	37/63

[a] Determined by ^{1}H NMR analysis.

[b] The abundance of protonated product **44ba** in the obtained mixture.

It was also interesting that catalytic amount of Brønsted acid increased the selectivity slightly (Table 6, entry 6). The effect of Brønsted acid was then investigated (Table 8). The reaction became almost unselective in the presence of binol phosphoric acid (entry 2). However mandelic acid or camphanic acid switch the selectivity to strong *anti*-preference (entries 3, 4). In the presence of CSA, the highest selectivity was observed for *anti*-conformation (entry 5).

Table 8. Brønsted acid-induced preference of deuteration in aza-Michael addition.
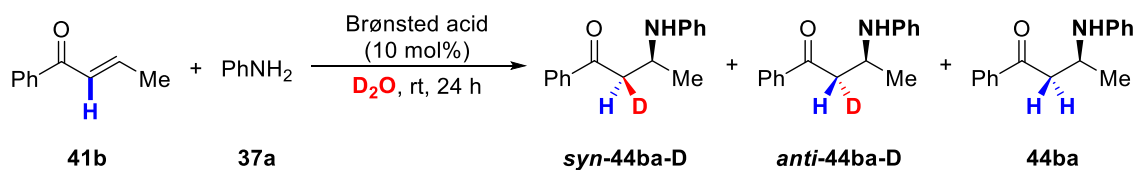
Entry	Brønsted acid	pKa	Yield (%)	*syn/anti*[a]
1	4-NO$_2$C$_6$H$_4$CO$_2$H	3.4[c]	89 (2)[b]	68/32
2	Binol phosphoric acid (BPA)	3.4	73 (4)[b]	54/46
3	OAc-mandelic acid	3.4	88 (7)[b]	18/82
4	Camphanic acid	3.0	87 (9)[b]	25/75
5	CSA	1.2	88 (1)[b]	8/92

[a] Determined by ^{1}H NMR analysis.

[b] The abundance of protonated product **44ba** in the obtained mixture.

[c] *c.f.* The reported value of benzoic acid: 4.2.
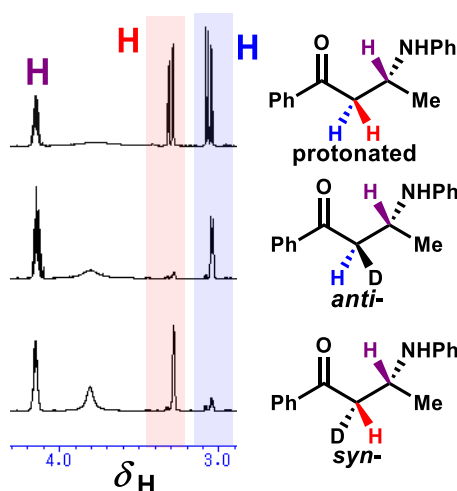
The combination of C–H activation and diastereoselective protonation was also feasible in Friedel-Crafts-type reaction using indole **40a** catalyzed by palladium catalyst (Table 9). The reaction proceeded quantitatively along with a small amount of protonated product **45ba**, suggesting that hydrogen-deuterium exchange on palladium took place before reductive elimination or that Pd-*O*-enolate anion was deuterated after tautomerization of Pd-*C*-enolate forming through oxidative addition. Intriguingly, much amount of protonated product **45ba** was obtained and the reaction proceeded less *anti*-selectively in deuterated methanol.

Table 9. Friedel-Crafts-type reaction in deuterium oxide.
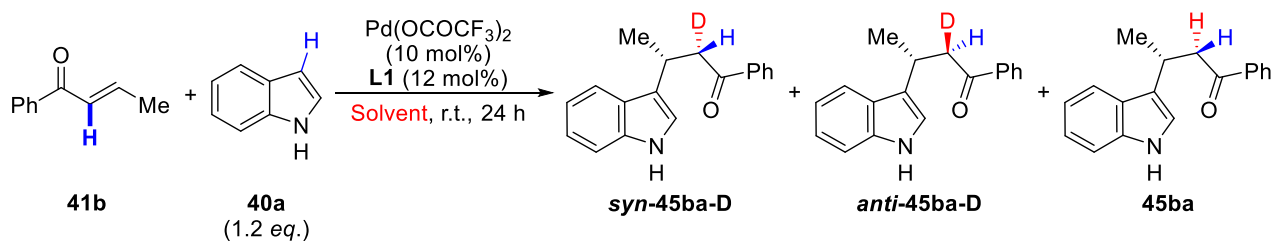
Entry	Solvent	Yield (%)	syn/anti[a]
1	D$_2$O	Quant. (3)[b]	26/74
2	CD$_3$OD	67 (10)[b]	38/62

[a] Determined by ^{1}H NMR analysis.

[b] The abundance of protonated product **45ba** in the obtained mixture.

The application to boron conjugate addition catalyzed by Cu(II) catalysts was described in Chapter 3.

5-6   Conclusions

In conclusion, an exquisite set of catalytic system enabled construction of a hydrogen isotope chirality alpha to a carbonyl group through the deuteration of the corresponding chiral enolate intermediate with deuterium oxide. The accordance of stereochemistry between the deuteration of chiral enolate intermediate and the protonation of corresponding isotopologue indicates a catalytic discernment of the size between C–H bond and C–D bond. The Sc-catalyzed reaction is *anti*-selective when a catalytic amount of base was co-existed, whereas *syn*-conformation was generated in the absence of base. The reactions catalyzed by the other rare earth metals are *syn*-selective even when 3 mol% of base was added. Given lower hydrolysis constant of Sc^{3+}, *anti*-preference would attribute to the formation of scandium monohydroxide. Not only solvent but a ligand coordinating to scandium core played a significant role in the stereoselection at deuteration step, implying the interplay of hydrogen bondings. Both the steric hindrance tuned by ligand and substrate and the stereoelectronic properties of enolate intermediates are sufficiently pronounced to induce appreciable facial differentiation. The process offered an inexpensive, efficient and expedient route to access isotopically chiral compounds as candidates of undeveloped medication. Successful stereoinduction in some Michael-type reactions, albeit unrefined, underscores the prospective applicability and versatility. A multidisciplinary anticipation of hydrogen isotope chirality warrants further investigations. The reaction system takes on a heterogeneous aspect and kinetic investigation is a formidable task.

[1] a) G. Agnihotri, H. Liu, *Bioorg. Med. Chem.* **2003**, *11*, 9-20; b) H. Xiang, L. Luo, K. L. Taylor, D. Dunaway–Mariano, *Biochemistry* **1999**, *38*, 7638-7652; c) J. R. Mohrig, K. A. Moerke, D. L. Cloutier, B. D. Lane, E. C. Person, T. B. Onasch, *Science*, **1995**, *269*, 527-529; d) P. Willadsen, H. Eggerer, *Eur. J. Biochem.* **1975**, *54*, 247-252; e) O. Gawron, T. P. Fondy, *J. Am. Chem. Soc.* **1959**, *81*, 6333-6334.

[2] W. –J. Wu, Y. Feng, X. He, H. A. Hofstein, D. P. Raleigh, P. J. Tonge, *J. Am. Chem. Soc.* **2000**, *122*, 3987-3994.

[3] X. Cui, R. He, Q. Yang, W. Shen, M. Li, *J. Mol. Model* **2014**, *20*, 2411-2422.

[4] a) B. Barabás, L. Caglioti, K. Micskei, C. Zucchi, G. Pályi, *Origins Life Evol. Biosphere* **2008**, *38*, 317-327; b) K. Mislow, In *Topics in Compounds* Ed. by S. E. Denmark, John Wiley & Sons, Inc., **1999**, *22*, pp 1; c) D. Arigoni, E. L. Eliel, In *Topics in Stereochemistry*, Ed. by S. E. Denmark, John Wiley & Sons, Inc., **1999**, *4*, pp 127.

[5] a) R. Caputo, L. Longobardo, *Amino Acids* **2007**, *32*, 401-404; b) F.–X. Felpin, E. Doris, A. Wagner, A. Valleix, B. Rousseau, C. Mioskowski, *J. Org. Chem.* **2001**, *66*, 305-308; c)

[6] K. R. Hanson, *J. Biol. Chem.* **1975**, *250*, 8309-8314.

[7] a) D. G. Blackmond, *Phil. Trans. R. Soc. B* **2011**, *366*, 2878-2884; b) D. G. Blackmond, *Cold Spring Harb Perspect. Biol.* **2010**, *2*, 1-17.

[8] M. M. Green, C. Andreola, B. Muñoz, M. P. Reidy, K. Zero, *J. Am. Chem. Soc.* **1988**, *110*, 4063-4065

[9] K. Kimata, K. Hosoya, T. Araki, N. Tanaka, *Anal. Chem.* **1997**, *69*, 2610-2612.

[10] R. Berger, G. Laubender, M. Quack, A. Sieben, J. Stohner, M. Willeke, *Angew. Chem. Int. Ed.* **2005**, *44*, 3623-3626.

[11] a) T. Kawasaki, M. Shimizu, D. Nishiyama, M. Ito, H. Ozawa, K. Soai, *Chem. Commun.* **2009**, 4396-4398; b) K. Soai, T. Kawasaki, A. Matsumoto, *Chem. Rec.* **2014**, *14*, 70-83; c) Y. Nakano, A.

J. Markvoort, S. Cantekin, I. A. W. Filot, H. M. M. ten Eikelder, E. W. Meijer, A. R. A. Palmans, *J. Am. Chem. Soc.* **2013**, *135*, 16497-16506; d) S. Cantekin, D. W. R. Balkenende, M. M. J. Smulders, A. R. A. Palmans, E. W. Meijer, *Nature Chem.* **2011**, *3*, 42-46.

[12] a) T. Kawasaki, M. Shimizu, D. Nishiyama, M. Ito, H. Ozawa, K. Soai, *Chem. Commun.* **2009**, 4396-4398; b) T. Kawasaki, K. Soai, *Bull. Chem. Soc. Jpn.* **2011**, *84*, 879-892

[13] a) T. G. Gant, *J. Med. Chem.* **2014**, *57*, 3595-3611; b) A. Katsnelson, *Nature Med.* **2013**, *19*, 656; c) N. A. Meanwell, *J. Med. Chem.* **2011**, *54*, 2529-2591; d) K. Sanderson, *Nature* **2009**, *458*, 269.

[14] a) J. R. Walker, W. Curley Jr., *Tetrahedron* **2001**, *57*, 6695-6701; b) C. W. Bradshaw, J. J. Lalonde, C. Wong, *Appl. Biochem. Biotechnol.* **1992**, *33*, 15-24.

[15] T. Quinto, D. Häussinger, V. Köhler, T. R. Ward, *Org. Biomol. Chem.* **2015**, *13*, 357-360.

[16] J. R. Mohrig, R. E. Rosenberg, J. W. Apostol, M. Bastienaansen, J. W. Evans, S. J. Franklin, C. D. Frisbie, S. S. Fu, M. L. Hamm, C. B. Hirose, D. A. Hunstad, T. L. James, R. W. King, C. J. Larson, H. A. Latham, D. A. Owen, K. A. Stein, R. Warnet, *J. Am. Chem. Soc.* **1997**, *119*, 479-486.

[17] a) D. A. Alonso, S. Kitagaki, N. Utsumi, C. F. Barbas III, *Angew. Chem. Int. Ed.* **2008**, *47*, 4588-4591; b) C. Sabot, K. A. Kumar, C. Antheaume, C. Mioskowski, *J. Org. Chem.* **2007**, *72*, 5001-5004.

[18] a) J. Haesler, I. Schindelholz, E. Riguet, C. G. Bochet, W. Hug, *Nature* **2007**, *446*, 526-529; b) G. Holzwarth, E. C. Hsu, H. S. Mosher, T. R. Faulkaner, A. Moscowitz, *J. Am. Chem. Soc.* **1974**, *96*, 251-252.

[19] F. Langer, L. Schwink, A. Devasagayaraj, P.–Y. Chavant, P. Knochel, *J. Org. Chem.* **1996**, *61*, 8229-8243.

[20] S. G. Davies, E. M. Foster, C. R. McIntosh, P. M. Roberts, T. E. Rosser, A. D. Smith, J. E. Thomson, *Tetrahedron Asymmetry* **2011**, *22*, 1035-1050.

[21] S. Adachi, F. Tanaka, K. Watanabe, A. Watada, T. Harada, *Synthesis* **2010**, 2652-2669.

[22] A. J. Boersma, D. Coquière, D. Geerdink, F. Rosati, B. L. Feringa, G. Roelfes, *Nature Chem.* **2010**, *2*, 991-99995.

[23] A. M. M. Abe, S. J. K. Sauerland, A. M. P. Koskinen, *J. Org. Chem.* **2007**, *72*, 5411-5413.

[24] After the reaction, **41j** was fully recovered.

[25] a) F. H. Spedding, K. C. Jones, *J. Phys. Chem.* **1966**, *70*, 2450-2455; b) F. H. Spedding, M. J. Pikal, B. O. Ayers, *J. Phys. Chem.* **1966**, *70*, 2440-2449; c) F. H. Spedding, M. J. Pikal, *J. Phys. Chem.* **1966**, *70*, 2430-2440.

[26] a) P. D'Angelo, A. Zitolo, V. Migliorati, G. Chillemi, M. Duvail, P. Vitorge, S. Abadie, R. Spezia, *Inorg. Chem.* **2011**, *50*, 4572-4579; b) P. D'Angelo, A. Zitolo, V. Migliorati, I. Persson, *Chem. Eur. J.* **2010**, *16*, 684-692; c) I. Persson, P. D'Angelo, S. De Panfilis, M. Sandström, *Chem. Eur. J.* **2008**, *14*, 3056-3066.

[27] S. Ishikawa, T. Hamada, K. Manabe, S. Kobayashi, *J. Am. Chem. Soc.* **2004**, *126*, 12236–12237.

[28] A. Tschöp, A. Marx, A. R. Sreekanth, C. Schneider, *Eur. J. Org. Chem.* **2007**, 2318-2327.

[29] a) H. J. Bernstein, *Spectrochimica Acta* **1962**, *18*, 161-170; b) D. C. McKean, J. L. Duncan, L. Batt, *Spectrochimica Acta Part A: Mol. Spectro.* **1973**, *29*, 1037-1049.

[30] Asymmetric variant: 44% ee in deuterium oxide, 16% ee in water and 23% in CD_3OD. Compare to Table 7.

Chapter 6 : Electrochemical Manipulation of Metal for Catalysis in Aqueous Environments

6-1   Introduction

Catalysis occupies a pivotal place in implementation of novel modes for chemical transformations as well as streamlining an existing organic synthesis.[1] Further advances in organic synthesis rely on the discovery of innovative catalysis toward unprecedented reactivity and high level of selectivity, ultimately leading to fundamentally new concepts and the outlook for next-generation organic synthesis.   Despite the ceaseless endeavor in academia, establishing general and convenient methodology to invent the unexplored or unrecognized catalysis has still proven a formidable task.   The previously unrecognized reaction possesses the inherent proclivity toward undesired pathway, which constitutes serious drawbacks that have to be overcome.   For instance, inherently inert metals or aggregation/deactivation of even active metals would lead to the decreased catalytic activity or competition with undesired side-reactions.[2] In addition, for asymmetric catalysis, the release and leaching of ligand-free metal is often the other detrimental factor leading to unselective reaction pathways.   In addition, the absolute stereochemistry is dictated through three-dimensional architecture with a precise orchestration of substrates and catalysts.[3] Based upon the electronic modification of metals, the outstanding reactive performances are sometimes exerted by nanoparticle,[4] bimetal catalysis[5] and photocatalysis[6] or even their combinations,[7] albeit their limited tunability, durability and versatility and their unmanageablility in stereoinduction.   Harnessing micellar system is regarded as another prescription to suppress the aggregation of organic materials and to acquire unique rate acceleration,[8] although the compatibility and immiscibility between water molecules and many reagents or reactive species such as Lewis acid catalysts sometimes remain as a huge problem.   Incorporation of these benefits was herein envisioned to create an innovative catalysis.   The underlying strategies are: **1) high reactivity gained through electrochemical property superior to that of an existing catalyst**; **2) a highly dispersed system that can inhibit self-aggregation of organic materials and other superfluous interactions**; and **3) an exquisite assemblage of all the components into the reaction centers**.

Lewis acid catalysis was merged with micellar catalysis in the late 1990s.[9] The subsequent emergence of Lewis acid–surfactant-combined catalyst (LASC) enabled entrapping hydrophobic small-molecules and the construction of stable and dispersed lipophilic environment surrounding a Lewis acidic cation.[10] The construction of an appropriate reaction environment in water is anticipated to impose stricter stereochemical regulation than in organic solvents through the hydrogen bond network, specific solvation, and hydrophobic interactions.   However the LASC-mediated reaction sometimes has an inclination toward self-agglomeration of metals or substrates incurring undesired pathway, due to the difficulty in controlling micellar behavior.   The limited application toward versatile reactions is another unsolved challenge, because the consequent potentiality of LASC cannot exceed the inherent reactivity of metal cation itself.   We then became interested in leveraging unique physical properties of π-materials such as large specific surface

areas or excellent electron conductivity that would aid LASC catalysis.

Fullerene   **Graphene**   **Carbon nanotube**
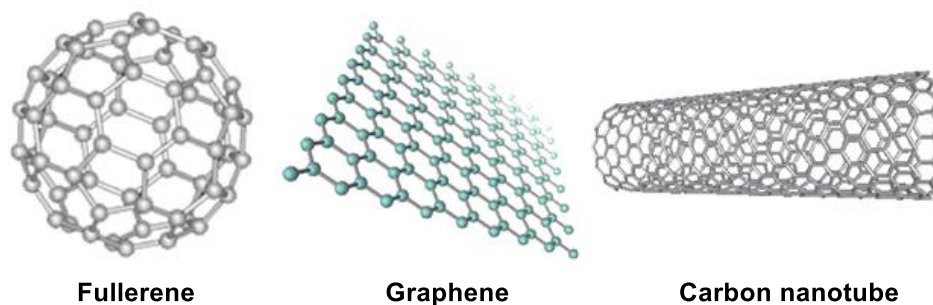
Figure 1. π-electron materials.

Single-walled carbon nanotube (SWNT) has gathered a wide attraction in many interesting characteristics[11] including electronic and physical properties since its first advent[12] in 1991.   It was also used as a support for clustering metals, metal nanoparticles and metal oxides *via* physical absorption, adhesion and chemical modification.[13]

The application of CNTs to enantioselective reactions were achieved by anchoring of homogeneous chiral catalysts,[14] metal nanoparticles supported on CNTs in the co-existence of chiral catalysts[15] and chiral metal catalysts incarcerated in CNTs[16] toward recyclable catalyst and further applications such as flow synthesis.   Any significant synergic effects by merging chiral metal catalysts with CNTs have not been achieved so far.

Recently, it was reported that purely-made MWNTs modified by chemically drilling their walls, namely holes and topological defects on MWNTs exhibited high activity without any additives, neither noble metals nor also nitrogen.[17] The possibility of the formed radicals and dangling bonds is denied by the result of electron spin resonance (ESR) analysis.

Although CNTs-supported metal catalysts underscore their stability, durability and reusability, in addition to its chemical inertness and its relatively high resistance to oxidation, their preparation process to decollate CNTs with metal particles entails tedious pre-functionalization and the catalyst loading, size and distribution were difficult to control.   Moreover, SWNT has not been applied to stereoselective reactions.   Herein, the strong Van der Waals force including C–H---π interaction between SWNT and carbon chains of surfactants in water to attach LASCs is focused upon.   Recently many groups reported the optical resolution of SWNT by utilizing the strong interactions with surfactants.[18] An interesting electric field interaction between SDS and SWNT was suggested and it was found that SDS was the most efficient and effective mediate to disperse SWNT in water.[19]

6-2　*Preparation of Designed Catalyst and Characterizations*

Newly-designed catalyst is characterized by three feasible interactions without any chemical modification (Figure 2). The interaction between surfactants and π-electron material would be controlled by tuning both amounts and conditions of homogenization, playing a crucial role in dispersing all the involved organic components uniformly. Binding the metals into the dispersed catalytic center is also of great importance which is provided by an ionic interaction between metal and anionic surfactant. The resultant rigid reaction environment would be effective for inhibition of undesired reaction pathways. The strength of ionic interaction insures the fixation of metal near SWNT, which would trigger the third interaction between metal and SWNT.

2. Ionic interaction between metal center and DS⁻

3. d-π interaction between Metal center and SWNT

1. "Hydrophobic" interaction between DS⁻ and SWNT
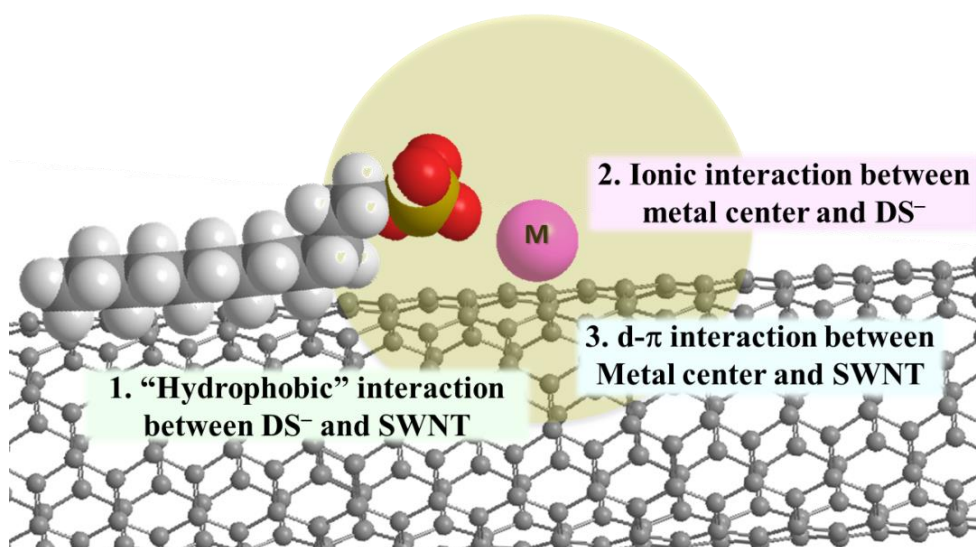
Figure 2. Schematic picture of newly-designed catalyst.

The interaction between π orbital of carbon atoms and the d-orbital of metals dominant near the Fermi energy would completely modify the electronic nature of the metal center. Although SWNT is known to interact strongly with metal,[20] the principle of this interaction is not fundamentally considered in chemical society. This interaction is, however, quite curious to create innovative catalysis with superior electric natures in organic chemistry as well as in physical chemistry including applications such as electron transistors. There are two expected advantages of d-π orbital integration especially in asymmetric reactions. First, SWNT can occupy one dimension of metal through the expected strong orbital overlap to **sever the weaker and superfluous interactions between metal and other components leading to undesired reaction pathways**. Second, **electronic property of metals would be capable of a tremendous modification** toward high catalytic performance both in reactivity and in stereoselection.

The virtue of the electrochemical modification is exemplified in Figure 3. The effective catalytic performance of pentagonal bipyramidal iron(II) core assisted by additives was stated in Chapter 1. The additive (LB) occupying at apical position of metal would stimulate the hybrid orbital spreading in the z-axis direction, variegating the coordination at apical position symmetrical to the site occupied by LB. The catalytic activity of iron(II) would ascend through the spin transition caused by electronic manipulation along the z-axis direction (Figure 3, above). When

additive (LB) is replaced into electron-rich materials such as SWNT, approaching of massive electron clouds at apical position would have an enormous impact on the energy level of the half-occupied $d_{x^2-y^2}$ along with the energetic gain through a spin transition.   The distorted electronic delocalization was rectified by coordination of electrophile at symmetrical apical position, thus leading to a stupendous influence on both HOMO and LUMO of centered metal (Figure 3, below).
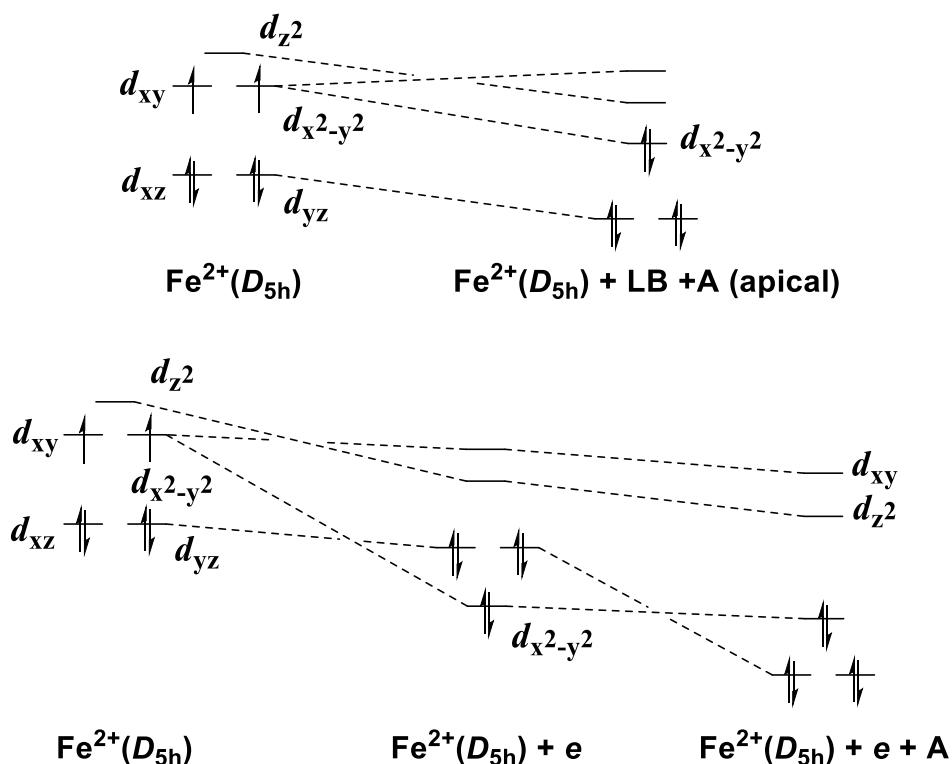
Figure 3. Illustrated scheme of metal d-orbital modification without SWNT (above) and with SWNT (below).
LB = Lewis base (additive), A = aldehyde, *e* = electron-rich materials such as SWNT.

As mentioned above, the strategy can be applied to modify the electronic property of even inherently inert metal cation.   Generally speaking, the rate of substitution reaction on metal cations is related with their catalytic activity (Figure 4).   When we run our eyes through water exchange rate constants (Table 5 in Chapter 0), we will find out metal cations such as V(III), Cr(III), Ni(II), Ga(III) and so on to be reluctant to exchange their coordinating ligand into an external ligand.   Taking Ni(II) as an example, its substitution rate is much slower ($2.7*10^4$) with its hydrolysis constant (9.86) within the criteria ranging from 4.3 to 10.1 than that of efficient water-compatible Lewis acids defined by the original report.[21]
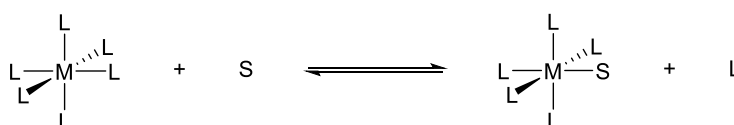
Figure 4. Ligand exchange mechanism.

Ni(II) d8 square planar complexes generally undergo a ligand exchange *via* associative mechanism because vacant non-bonding p_z orbital can accept the electron density of the incoming substrate. When an apical solvent molecule is substituted with an aldehyde molecule on square bipyramidal Ni(II) complex, incoming electron density would make empty $d_{x^2-y^2}$ orbital approximate to d_{z^2} orbital. The "high-spin" complex is thus formed and activation of aldehyde is unable to be expected. In contrast, incoming massive electron clouds would stabilize trigonal bipyramidal structure through Berry feudo-rotation (Figure 5). Modified electronic nature of centered metal cations can not only increase their catalytic activity but a stronger interaction with aldehyde molecule can also increase both chemo- and stereoselectivity through the shortened distance and resulting suppression of superfluous interactions leading to undesired reaction pathways in a given chemical reaction.
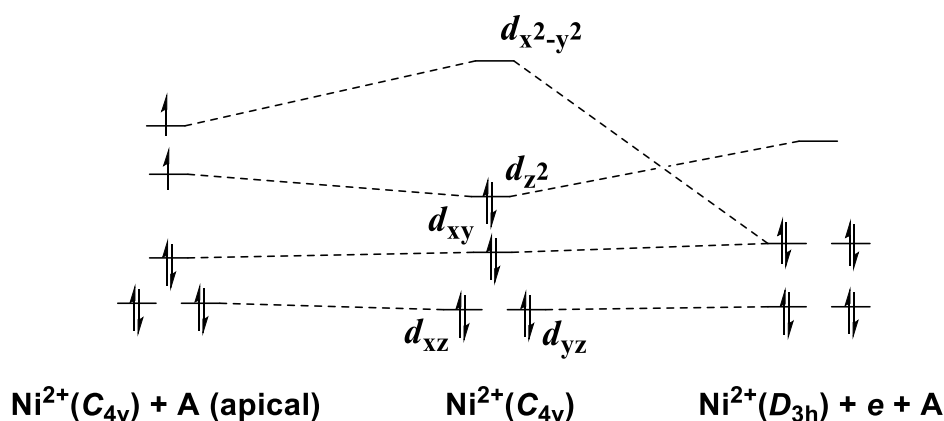
Figure 5. Illustrated scheme of Ni(II) d-orbital modification with SWNT.
A = aldehyde, *e* = electron-rich materials such as SWNT.

Based upon the assumption, drastic effect cannot be expected for SWNTs twined by LASCs containing metals with empty or filled d orbital (*e.g.* Sc^{3+} and Zn^{2+}). Although the electronic contribution of the unpaired 4f electrons doping on SWNTs can be considered, the hybridization of embedded 4f electrons should be lower than that of d electrons.[22]

The three main synthetic methods producing SWNTs are 1) arc-discharge, 2) laser ablation, and 3) chemical vapor deposition (CVD).[23] The first two methods involve carbon vaporization at high temperature (thousands of degrees centigrade) based on solid-state carbon precursors for nanotube growth. A CVD approach involves a growth at relatively lower temperature (less than 1000 °C) based on hydrocarbon gases with a catalytic use of metal particles. At present, CVD approaches including the high-pressure CO (HiPco) method[24], alcohol catalytic CVD (ACCVD) method[25] and super growth CVD method[26] became dominant for their mass production in terms of the improved efficiency or productivity of the bulk synthesis of SWNTs. Among them, SWNT produced through ACCVD method developed by Prof. Maruyama has a high quality with narrow chirality distributions (Figure 6), where the formation of amorphous or MWNT was prohibited at the early stage of synthesis. Influence of nanotube chirality on the dispersibility and resultant catalytic activity is quite intriguing but still remains unknown at present due to the current scientific and

technical limitations. In this work, SWNTs produced by three CVD techniques were applicable to the demonstration of chemical reactions. Preparation and characterization of the designed solution is explained only based on super growth CVD technique.
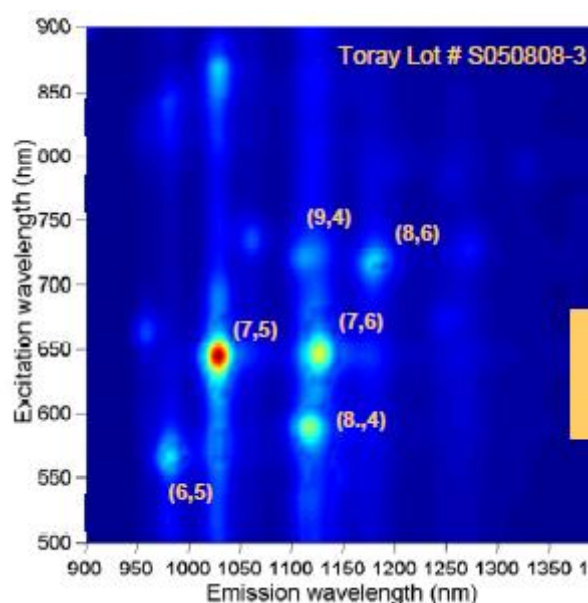
Figure 6. Chirality distribution of SWNTs prepared through ACCVD technique (The dispersed and centrifugated SWNTs in SDBS/D_2O were examined by the fluorescence spectroscopy with scanning excitation energy)[27]

At the first onset, the dispersion of SWNT in aqueous solution of Ni(DS)$_2$ was focused upon to unravel a tangled SWNT toward a genuine embodiment of the design. Dynamic light scattering (DLS) measurement is instrumental in estimating the degree of dispersibility. Thermal homogenization provided various aggregates with a size ranging from 117 to 4496 nm (Figure 7, above). The sonication using homogenizer under appropriate control of heat generation successfully contributed to a significant decrease (150.8 nm) in the micellar size (Figure 7, middle). The minimum size of micelles (34.1 nm) was obtained by shortened homogenization (Figure 7, bottom). It was noteworthy that not only the inherent property of metal cations but also their valences were relevant to micelle sizes.
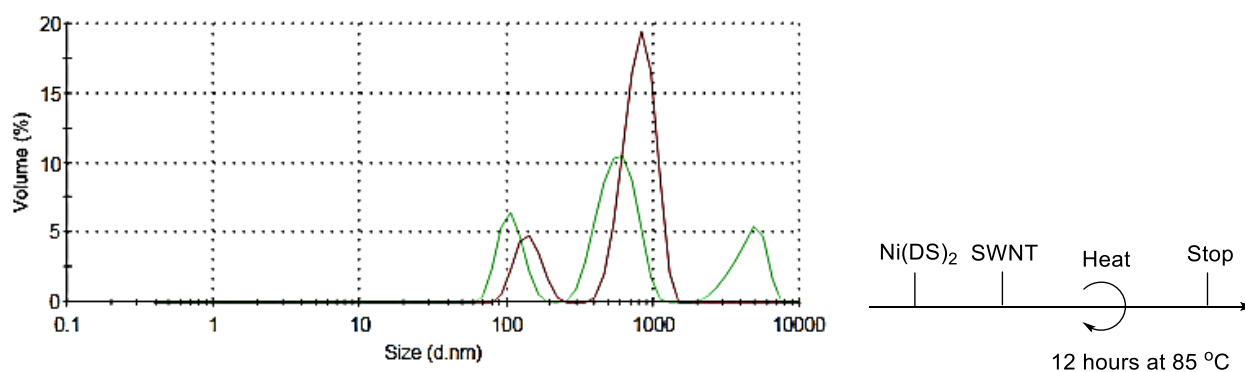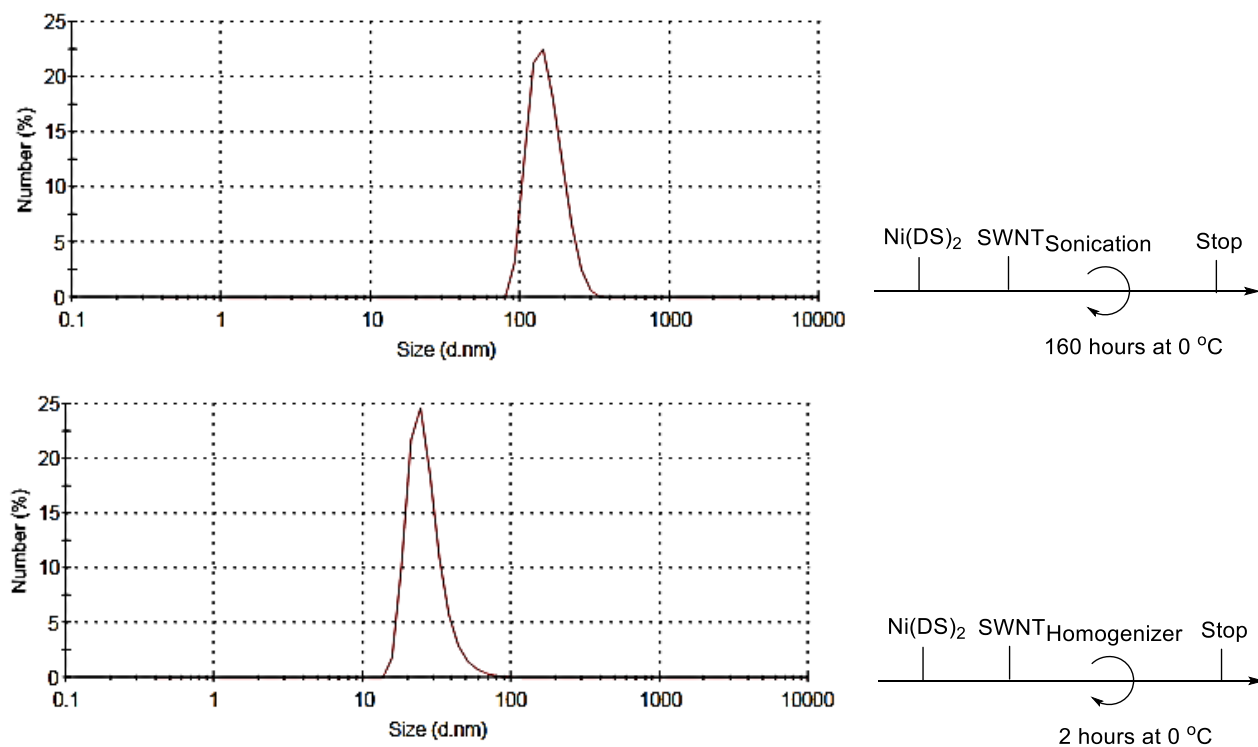
Figure 7. DLS analysis of the designed solution.

In addition, ^{1}H NMR study of prepared solutions also suggests the importance of dispersibility. The ununiformed mixture prepared at high temperature produced almost same spectra as that of Ni(DS)$_2$ alone (Figure 8, bottom). The solution sonicated at low temperature showed the pronounced upfielded chemical shifts of proton resonances corresponding to the surfactant moiety and a significant degradation of the peak intensity of these protons (Figure 8, middle). Furthermore, when the solution sonicated at low temperature for shorter time was submitted to NMR analysis, all peaks disappeared except for solvent peak (Figure 8, above). It suggests that surfactant moiety was strongly bound with SWNT.
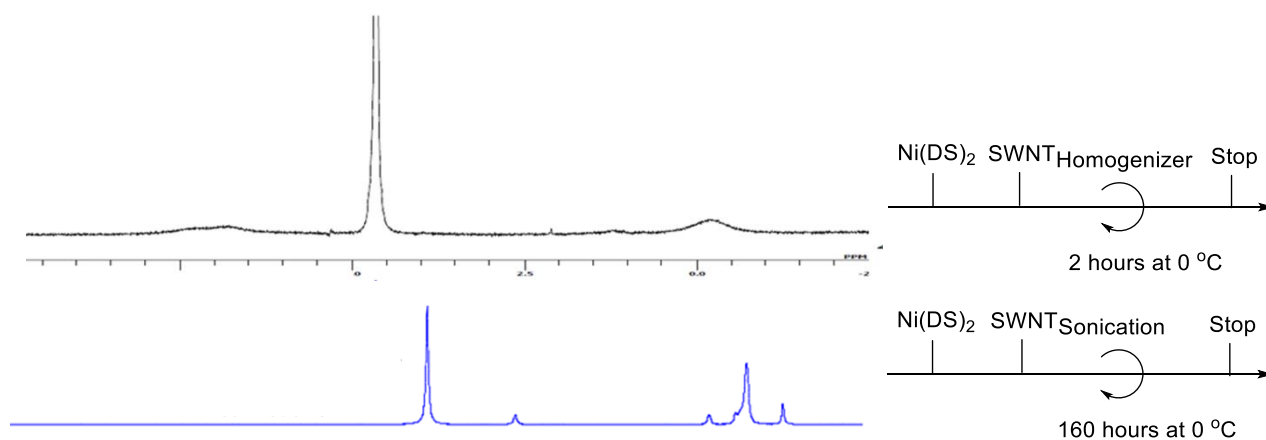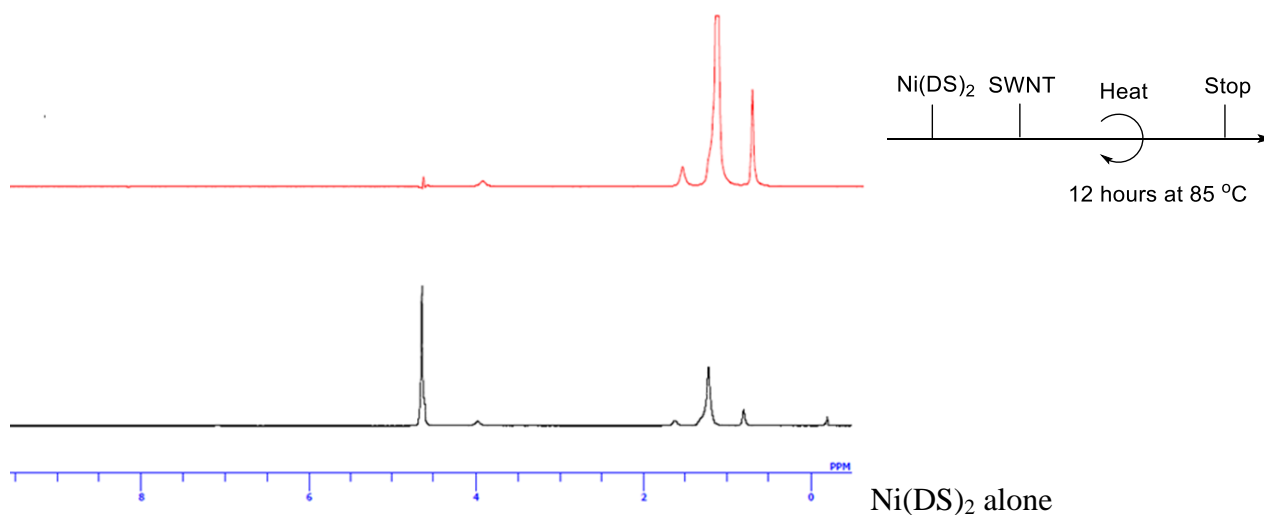
Figure 8. ^{1}H NMR study.

Therefore the sonication using homogenizer takes responsibility for the generation of the nanosize micelles in water.   Thermal treatment should be avoided and shorter sonication time is better for the dispersibility.   The established protocol is as follow:

Method

The designed solution LASC-SWNT catalysts were prepared as follows.   SWNT 28 mg and LASC 0.14 mmol were combined together in 20 mL water and the resultant solution was sonicated (Hielscher, 400W maximum power, 24 kHz, in pulsed mode with 125 ms pulses) for 6 hours at 0 ^{o}C.   Centrifugation was then performed for 1.5 hour and the solution was carefully decanted from the pellet.   The centrifugated LASC-SWNT mixture (Figure 9) was directly subjected to spectrometric investigations and was also used as the starting suspension before the catalyst preparations.
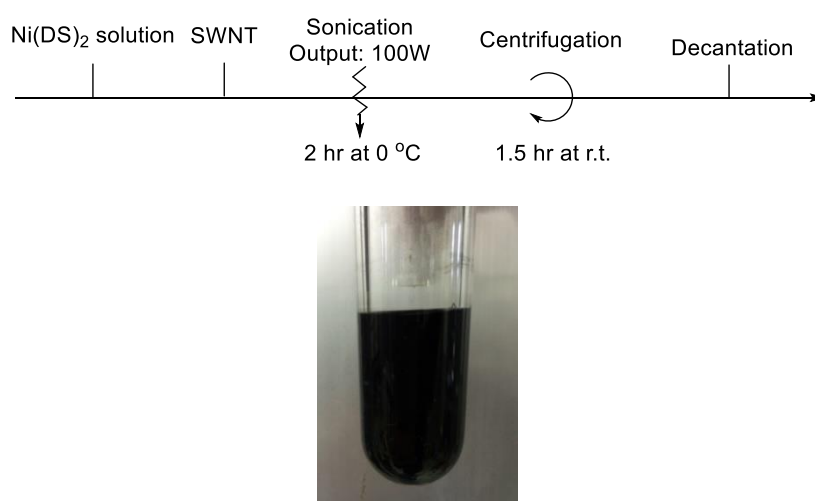
Figure 9. Homogenized solution of Ni(DS-SWNT)$_2$.

Scanning transmission electron microscopy (STEM) imaging provided us with a direct and visualized method to examine the behavior of the designed solution.
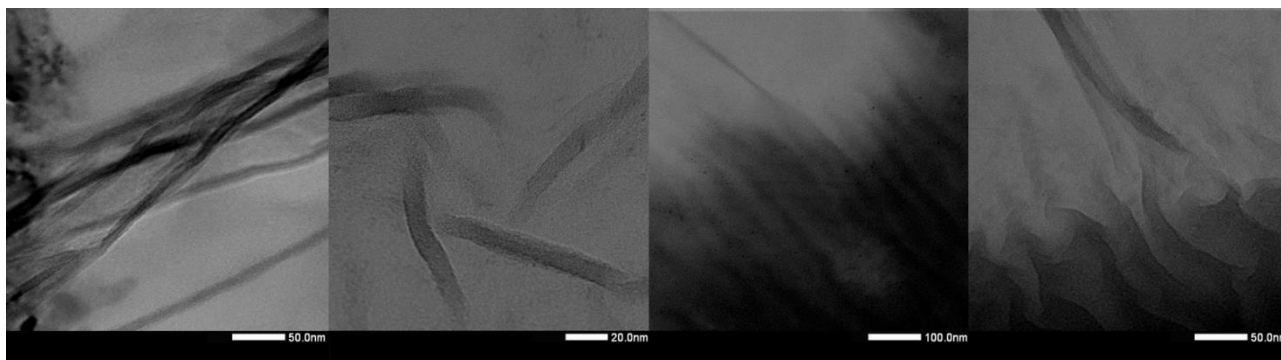
Figure 10. Complete disentangling and dispersing of SWNT.

The obtained energy dispersive spectroscopy (EDS) mapping image was well consistent with the hypothesis underlying the design (Figure 11). Both Ni and S atoms were aligned on a single line of SWNT, proving the successful decoration of SWNT with Ni(DS)$_2$. The solution that was prepared not based on the established protocol provided a lump of SNWT and LASC mixture. As with the metal nanoparticles immobilized on SWNT, the obtained Ni(DS-SWNT)$_2$ solution is suggested to possess a huge surface area.
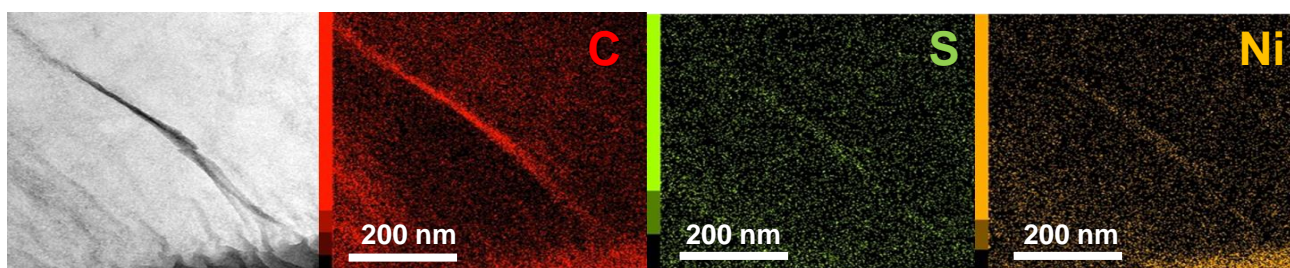
Figure 11. EDS mapping.

Next, Raman spectroscopy was measured to gain another insight into the electronic and photonic changes on carbon nanotube after decorated with LASCs. There are three important features in Raman spectrum of SWNT.[28] First, low frequency peak ranging from 150 to 300 cm^{-1} are assigned to the radical breathing mode (RBM) area which corresponds to the coherent vibration of C atoms in the radical direction and is useful for estimating diameter.[29] Second, a large feature around 1350 cm^{-1} is named as D band, with the information on defects originating from edge configurations of a graphene or the open end of a nanotube where the sheet configuration is disrupted. Third, G band corresponds to 1593 cm^{-1}, the tangential mode vibration of sp^2-bonded C atoms. In addition, the 2D-band, an overtone mode of the D-band is sometimes measured since it can be more or less sensitive than the D-band to specific changes in the sample. Currently, numerous reports discuss monitored impurity, defect and functionalization of SWNTs measuring the ratio of G-band/D-band intensity.[30] The increase of G/D ratio suggests the attachment of substance

to the defect sites and the increase of impurity.   The measured G/D ratio of SWNT itself (*ca.* 30/1) denotes the sufficient purity to be used as the source in this work.

Meanwhile, Raman scattering provides the powerful tool to characterize organic materials even in a solution phase as well as carbon-based skeletons.   Since the energy of the scattered photon is smaller than that of the incident photon, accurate information on the phonon frequencies corresponding to the slight changes on the molecular behaviors can be obtained by measuring the scattered light.   Extensive investigations on SDS aqueous solutions reported that the peaks around 1120 cm^{-1} and 1175 cm^{-1} from the normal area and 2950 cm^{-1} from the 2-D area were indicative area for the variations of surfactant moiety.   After the minute adjustment to get much higher resolutions, the suitable images of Ni(DS-SWNT)$_2$ solution was obtained in Raman scattering. Although the S/N ratio still leaves something to be desired, most of the peaks can be identified (Figure 12).   It is noted that even though SWNT was dispersed uniformly in aqueous solution of LASC, the peaks attributed to G-band and D-band remained unshifted at 1587 cm^{-1} and 1357 cm^{-1}, respectively.   Among many other peaks, the peaks at 1081 cm^{-1}, 1124 cm^{-1} and 1167 cm^{-1} seem to be shifted from 1066 cm^{-1}, 1104 cm^{-1} and 1160 cm^{-1}, respectively, observed in the spectrum of aqueous solution of Ni(DS)$_2$.   The former peak may contain the S–O stretching modes, whereas the latter may contain the C–H bending and C–C stretching modes.[31]   The dependence of peak shift on both metal cations and their valences is of great interest (e.g. divalent metals: 1079-1089 cm^{-1}; trivalent metals: 1064-1089 cm^{-1}; tetravalent: 1065-1091 cm^{-1}; pentavalent: 1123 cm^{-1}).   The vibrational changes on C–H bonds and C–C bonds inherent in surfactant moiety are incontrovertible evidence of the interaction between surfactants and SWNTs.
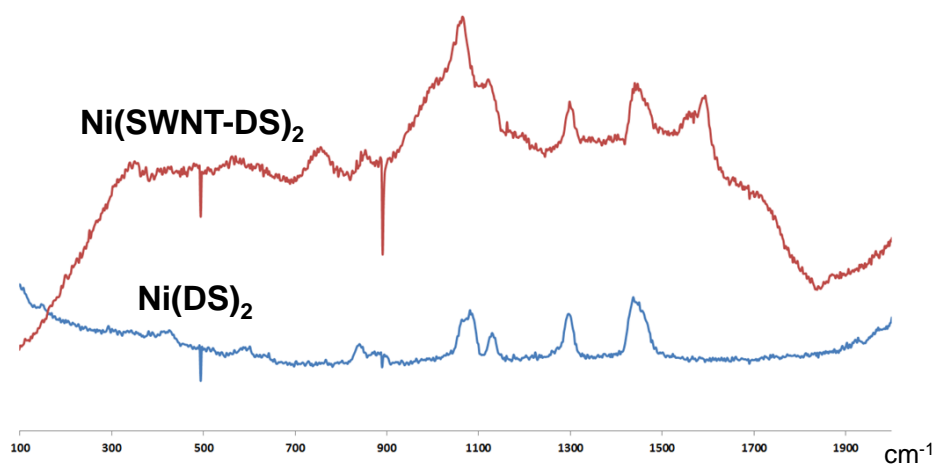
Figure 12. Raman spectrum of Ni(DS-SWNT)$_2$ (red) and Ni(DS)$_2$ aqueous solution (blue).

In the 2D area, the peaks at 2950 cm^{-1} shifted distinctly to 2680 cm^{-1} compared between aqueous solution of Ni(DS)$_2$ and that of Ni(SWNT-DS)$_2$ (Figure 13).   The peak may be associated to the C–H bending modes.   The significant shifts of these peaks strongly suggested that the electronic environments of surfactants varied through their chemical adsorption on SWNTs. Although cyclic voltammetry is a direct method to confirm the d-π integration between Ni^{2+} and SWNT, a fine observation of the redox potential of Ni(II) finds to be formidable due to the bubbling

during measurement or overlapping with water oxidation region.   It means, however, that centered metal undergoes the exiguous shift of the anodic potentials and more critical and significant shift toward positive potentials, implying a d-π integration with SWNT.   Other suitable metals provided further verification of the strong interaction between metal center and SWNT.[32]
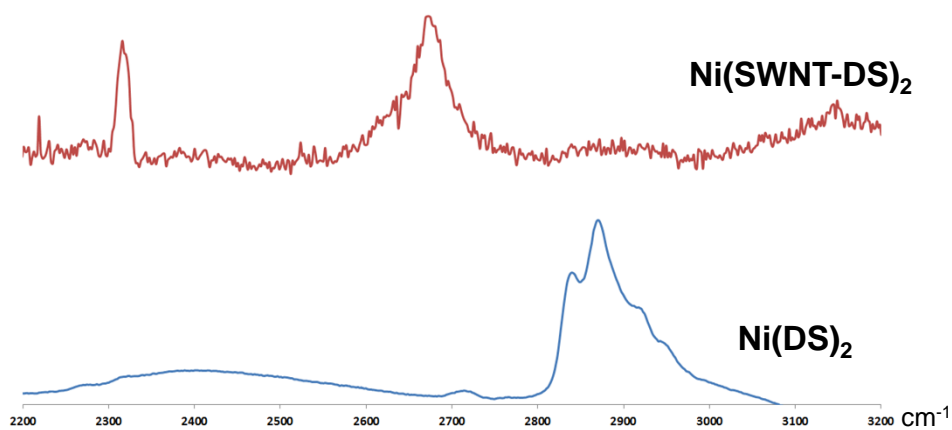
Figure 13. 2D-area of Raman spectrum.

6-3 *Evaluation of Increased Catalytic Activity*

With aqueous solutions of the novel LASC-SWNT catalysts in hands, our focus was then turned toward the evaluation of its activity in chemical reactions. The interaction between carbonyl and Lewis acid is known to be weak under neutral conditions. Indeed, a simple mixing of $Cu(DS)_2$ with propiophenone in deuterium oxide did not provide any H/D exchange at α-position. To examine the coordination activity at apical position through d-π integration, propiophenone was thrown into deuterated solution of $Cu(DS\text{-}SWNT)_2$. It was revealed that deuterium was significantly incorporated at α-position, in contrast to the result in the case of $Cu(DS)_2$ alone (Scheme 1, above). In aza-Michael addition in deuterium oxide, over-deuteration was not observed at all (88% for 24 h, see Table 6, entry 5 in Chapter 5). In contrast, SWNT decorated with Cu-based LASC catalyzed the reaction quantitatively even within 12 hours and one-third amount of over-deuterated product **44ba-2D** was obtained competitively (Scheme 1, below).[33] It is suggested that the inherent activity of LASCs as Lewis acid catalysts was successfully reinforced by SWNT.
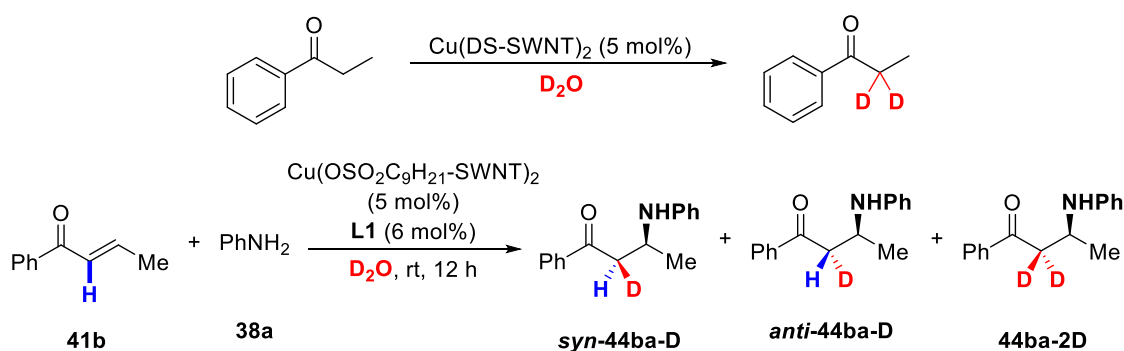
Scheme 1. Evaluation of catalytic activity of LASC-SWNT catalyst.

The remarkable synergic effect of LASC-SWNT integrated catalysts was then examined in several chemical reactions such as aldol reactions, Michael-type reactions, oxidations, esterifications and so on. I have to emphasize that too strong recognition and too strong binding of metal with substrate can lead to strong stabilization and insensitivity toward the subsequent reaction. As a result, the improved catalytic activity often appears by using new catalyst when the weaker and superfluous interactions between metal and other components are assumed in the absence of SWNT. The following is one example (Scheme 2).
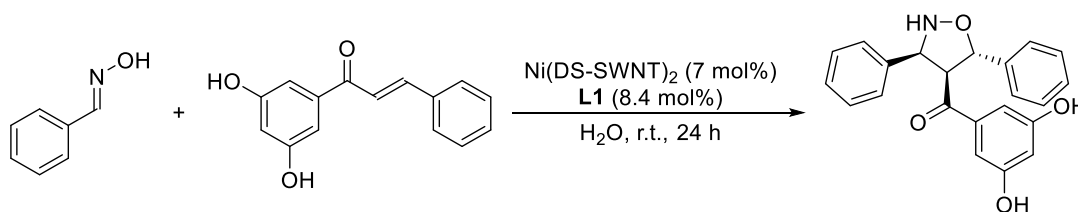
Scheme 2. Successful example toward increased reactivity and stereoselection.

The usefulness of this method was demonstrated in unrecognized reaction between aldoxime and α,β-unsaturated ketone delivering optically active 1,3-dipolar cyclized compound. When Ni(DS)$_2$ was used as a catalyst, quite poor result was recorded because two phenolic OH groups were assumed to intercept nickel catalyst more strongly and kill the interaction necessary for reaction progress and precise stereocontrol.   It is noteworthy that 2.5 times of rate acceleration and 4.5 times higher chiral induction was observed by using LASC-SWNT integrated catalyst.   As mentioned above, SWNT should play a capital role in an electrochemical tuning of centered metal cation and the expulsion of notorious interactions that can kill the interactions essential for catalytic asymmetric reactions.

The 1,3-dipolar cyclization reaction demonstrated above is one of the most efficient methods to afford heterocyclic compounds which are an important class of intermediates for pharmaceutical industries.[34] Especially, isoxazolidines, five-membered heterocyclic compounds containing N-O linkage, are considered as a significant moiety in many anti-cancer drugs.[35] In most reports, nitrones are employed to generate isoxazolidines *via* [3+2] cycloaddition process.[36] Although the use of aldoxime instead of nitrones for racemic 1,3-dipolar cyclization has been reported, in all reports the product contained C=N double bond *via* the reaction of nitrile oxides produced through an oxidative dehydrogenation of aromatic aldoximes.[37] In addition, the products most probably exist as equilibrium of two tautomeric forms (Scheme 3).[37a] Therefore the construction of three adjacent stereogenic centers through asymmetric reactions toward optically active novel heterocyclic isoxazolines has been considered to be difficult.
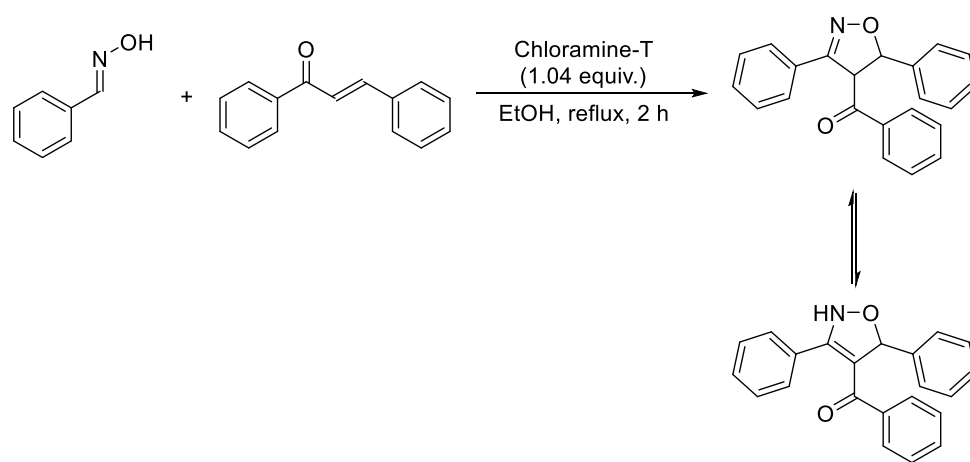
Scheme 3. Example on 1,3-dipolar cycloaddition of aromatic aldoxime with chalcone.

The effect of metal cation is examined in Table 1.   The use of cobalt (entry 2) or copper (entry 3) was not effective at all in this reaction compared with nickel (entry 1).   It was confirmed that the resultant enantioselection was attributing to the environment surrounding nickel cation in the reaction system.

Table 1. Influence of centered metal.
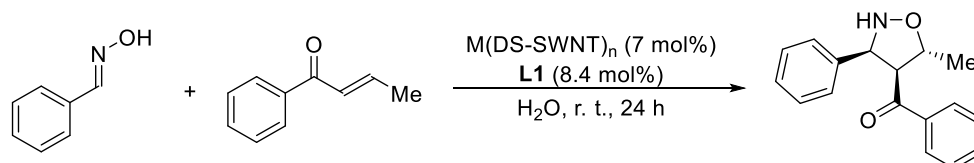
Entry	Metal	π-Materials	Diameter	Length	Yield (%)	% ee[a]
1	Ni^{2+}	SWNT	1-5 nm	1-5 μm	81	91
2	Co^{2+}	SWNT	1-5 nm	1-5 μm	29	8
3	Cu^{2+}	SWNT	1-5 nm	1-5 μm	54	59

[a] Determined by HPLC analysis.

Next, the importance of π-materials was well displayed in Table 2. Compared with a standard condition in entry 1, the use of SWNT with longer length resulted in a significant drop in enantioselectivity (entry 3). MWNT with the minimized diameter and length also produced the desired product in a low enantiomeric manner (entry 4). MWNT with more than 20 nm of diameter did not involve in the formation of micelle at all and enantioselective performance was lost significantly (entries 5, 6). The structure of CNTs also had a great influence on catalytic behavior and appropriate chiral induction did not take place (entries 7-9). Although LASC-fullerene catalyst made homogeneous solution (Figure 14), the drastic effect was not observed (entry 10). The mass spectrometric analysis of the reaction solution (without SWNT) detected the two characteristic peaks responsible for the reaction progress with precise stereocontrol. The observation of a peak m/z = 714.28 corresponding to a complex comprising Ni(II), a chiral ligand **L1**, an aldoxime and a α,β-unsaturated ketone indicated that the formation of a concerted complex comprising all involved materials was one of the likeliest candidate of the rate-determining step in this reaction and the proper interaction between nickel cation and both substrates played a prominent role in high enantioselective performance.

Table 2. Influence of π-materials.
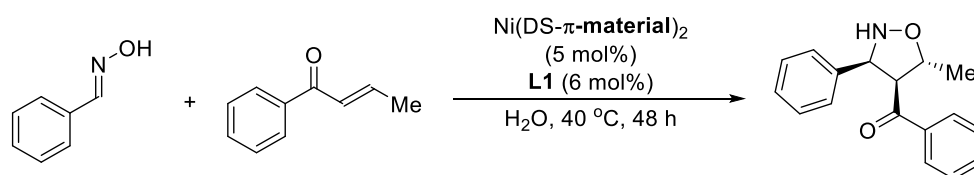
Entry	Metal	π-Material	Diameter	Length	Yield (%)	% ee[a]
1	Ni^{2+}	SWNT	1-5 nm	1-5 μm	61	88
2[b]	Ni^{2+}	SWNT	1-5 nm	1-5 μm	88	91
3	Ni^{2+}	SWNT	<2 nm	5-15 μm	81	78
4	Ni^{2+}	MWNT	<10 nm	1-2 μm	64	79
5[c]	Ni^{2+}	MWNT	20-40 nm	1-2 μm	67	58
6[c]	Ni^{2+}	MWNT	40-60 nm	1-2 μm	54	–2
7	Ni^{2+}	Aligned-MWNT	10-20 nm	5-15 μm	27	47
8	Ni^{2+}	Bundled-MWNT	<10 nm	5-15 μm	31	12

| 9 | Ni^{2+} | Herringbone-MWNT | 10-20 nm | 5-15 μm | 47 | 63 |
| 10 | Ni^{2+} | Fullerene | | >99.5% purity | 54 | 73 |

[a] Determined by HPLC analysis.

[b] 7 mol% of Ni(DS-SWNT)$_2$ and 8.4 mol% of **L1** was used at room temperature for 24 h.

[c] Micelle was not formed.

Figure 14. Fullerene-Ni(DS)$_2$ solution.

6-4 Conclusions

A highly reactive and stereoselective catalytic performance is responsible not only for rationalizing existing synthetic methods but for inventing epoch-making chemical reactions, ultimately leading to fundamentally new concepts and the outlook for next-generation organic synthesis. The previously unrecognized reaction possesses the inherent proclivity toward undesired pathway, which constitutes serious drawbacks that have to be overcome. Despite the substantial interest in creating innovative catalysis, general and convenient tactics to improve catalytic performance is not established yet. The outstanding reactive performance is sometimes exerted by nanoparticle, bimetal catalysis and photocatalysis or even their combinations, albeit their limited tunability, durability and versatility and their unmanageablility in stereoinduction. Herein we report a homogenized encounter of LASCs (Lewis acid–surfactant-combined catalysts) with SWNT (single-walled carbon nanotube) which exhibited the prominent catalytic performance without any chemical modification. The underlying strategies are: 1) high reactivity gained through electrochemical property superior to that of an existing catalyst; 2) a highly dispersed system that can inhibit self-aggregation of organic materials and the subsequent superfluous interactions; and 3) an exquisite assemblage of all the components into the reaction centers. As we had expected, an electrochemical behavior of centered metals was successfully modified through the hybridization between the d-orbital of metal and the p-orbital of carbon atoms near the Fermi level, addressing the inherently low Lewis acidity of metal cation. An interesting electric field interaction between surfactant moiety and SWNT could assist that hybridization. In addition to their enhanced reactivity, their heterodox stereoselective performance was highlighted in asymmetric 1,3-dipolar cyclization reaction. Practical and straightforward applicability of the designed catalysts would have an immense impact on various fields, providing an expedient, environmentally benign, and highly efficient pathway to accessing optically active compounds and opening up new opportunities in organic chemistry.

[1] a) M. Beller, A. Renken, R. van Santen (Ed.) *Catalysis: From Principles to Applications* **2012**, 3-19. Wiley-VCH Verlag GmbH, Weinheim; b) A. Zecchina, S. Bordiga, E. Groppo (Ed.) *Selective Nanocatalysts and Nanoscience* **2011**, 1-27. Wiley-VCH Verlag GmbH, Weinheim; c) A. T. Bell, *Science*, **2003**, *299*, 1688-1691; d) R. Coontz, J. Fahrenkamp-Uppenbrink, P. Szuromi, *Science*, **2003**, *299*, 1683.

[2] For example, see: a) G. A. Somorjai, A. M. Contreras, M. Montano, R. M. Rioux, *Proc. Natl. Acad. Sci. U.S.A.* **2006**, *103*, 10577-10583.

[3] a) T. Kitanosono, S. Kobayashi, *Chem. Asian J.* **2014**, DOI: 10.1002/asia.201403004; b) K. C. Harper, M. S. Sigman *Proc. Natl. Acad. Sci. U. S. A.*, **2011**, *108*, 2179-2183.

[4] Q- L. Zhu, J. Li, Q. Xu, *J. Am. Chem. Soc.* **2013**, *135*, 10210-10213.

[5] a) S. Matsunaga, M. Shibasaki, *Chem. Commun.*, **2014**, *50*, 1044-1057; b) T. Yasukawa, H. Miyamura, S. Kobayashi, *J. Am. Chem. Soc.* **2012**, *134*, 16963-16966; c) R. Ferrando, J. Jellinek, R. L. Johnston, *Chem. Rev.* **2008**, *108*, 845-910.

[6] a) N. Zhang, Y. –J. Xu, *Chem. Mater.* **2014**, DOI: 10.1021/cm400750c; b) J. Schneider, M. Matsuoka, M. Takeuchi, J. Zhang, Y. Horiuchi, M. Anpo, D. W. Bahnemann, *Chem. Rev.* **2014**, *114*, 9919-9986; c) C. K. Prier, D. A. Rankic, D. W. C. MacMillan, *Chem. Rev.* **2013**, *113*, 5322-5363; d) J. M. R. Narayanam, C. R. J. Stephenson *Chem. Soc. Rev.*, **2011**, *40*, 102-113.

[7] S. Sarina, H. Zhu, E. Jaatinen, Q. Xiao, H. Liu, J. Jia, C. Chen, J. Zhao, *J. Am. Chem. Soc.* **2013**, *135*, 5793-5801.

[8] T. Dwars, E. Paetzold, G. Oehme, *Angew. Chem. Int. Ed.* **2005**, *44*, 7174-7199.

[9] S. Kobayashi, T. Wakabayashi, S. Nagayama, H. Oyamada, *Tetrahedron Lett.* **1997**, *38*, 4559-4562.

[10] S. Kobayashi, T. Wakabayashi, *Tetrahedron Lett.* **1998**, *39*, 5389-5392.

[11] R. Saito, G. Dresselhaus, M. S. "*Dresselhaus, Physical Properties of Carbon Nanotubes*", **1998**, London: Imperial College Press.

[12] S. Iijima, *Nature* **1991**,*354*, 56-58.

[13] S. A. Hodge, M. K. Bayazit, K. S. Coleman, M. S. P. Shaffer, *Chem. Soc. Rev.* **2012**, *41*, 4409-4429.

[14] a) C. C. Gheorghiu, B. F. Machado, C. S. –M. de Lecea, M. Gouygou, M. C. R. –Martínez, P. Seerp, *Dalton Trans.* **2014**, *43*, 7455-7463; b) A. Moussaif, R. Martin, Y. Ramli, R. Zniber, R. Achour, M. El Ghoul, M. Alvaro, H. Garcia, *Rev. Roum. Chim.* **2011**, *56*, 675-679.

[15] L. Xing, F. Du, J. –J. Liang, Y. –S. Chen, Q. –L. Zhou, *J. Mol. Catal. A: Chemical* **2007**, *276*, 191-196.

[16] a) K. Hashimoto, N. Kumagai, M. Shibasaki, *Org. Lett.* **2014**, *16*, 3496-3499; b) D. Sureshkumar, K. Hashimoto, N. Kumagai, M. Shibasaki, *J. Org. Chem.* **2013**, *78*, 11494-11500.

[17] K. Waki, R. A. Wong, H. S. Oktaviano, T. Fujio, T. Nagai, K. Kimoto, K. Yamada, *Energy Environ. Sci.* **2014**, *7*, 1950-1958.

[18] a) H. Liu, D. D. Nishide, T. Tanaka, H. Kataura, *Nat. Commun.* **2011**, *2*, 1-8; b) K. Moshammer, F. Hennrich, M. M. Kappes, *Nano Res.* **2009**, *2*, 599-606.

[19] a) P. Angelikopoulos, H. Bock, *Phys. Chem. Chem. Phys.* **2012**, *14*, 9546-9557; b) W –H. Duan, Q. Wang, F. Collins, *Chem. Sci.* **2011**, *2*, 1407-1413; c) L. Vaisman, H. D. Wagner, G. Marom, *Adv. Colloid Interface Sci.* **2006**, 37-46.

[20] W. H. Duan, Q. Wang, F. Collins, *Chem. Sci.* **2011**, *2*, 1407-1413.

[21] S. Kobayashi, S. Nagayama, T. Busujima, *J. Am. Chem. Soc*. **1998**, *120*, 8287–8288.

[22] a) H. –W. Lei, H. Zhang, W. –D. Wu, *Mod. Num. Sim. Mat. Sci.* **2013**, *3*, 9-12; b) R. Kitaura, H. Okimoto, H. Shinohara, T. Nakamura, H. Osawa, *Phys. Rev.* **2007**, *B 76*, 172409-1-172409-4.

[23] H. Dai, "*Nanotube Growth and Characterization*", In *Carbon Nanotubes*; **2001**, Springer, Berlin, pp 29-53.

[24] a) M. J. Bronikowski, P. A. Willis, D. T. Colbert, K. A. Smith, R. E. Smalley, *J. Vac. Sci. Technol.* **2001**, *A 19*, 1800-1805; b) P. Nikolaev, M. J. Bronikowski, R. K. Bradley, F. Rohmund, D. T. Colbert, K. A. Smith, R. E. Smalley, *Chem. Phys. Lett.* **1999**, *313*, 91-97.

[25] S. Maruyama, R. Kojima, Y. Miyauchi, S. Chiashi, M. Kohno, *Chem. Pys. Lett.* **2002**, *360*, 229-234.

[26] K. Hata, D. N. Futaba, K. Mizuno, T. Namai, M. Yumura, S. Iijima, *Science* **2004**, *306*, 1362-1364.

[27] S. Maruyama, Y. Miyauchi, T. Shimada, Y. Murakami, K. Sato, Y. Ozeki, M. Yoshikawa, "Bulk ACCVD Generation of SWNTs with Narrow Chirality Distribution" In the 30th Fullerene-Nanotubes Symposium, **2006**.

[28] A. M. Rao, E. Richter, S. Bandow, B. Chase, P. C. Eklund, K. A. Williams, S. Fang, K. R. Subbaswamy, M. Menon, A. Thess, R. E. Smalley, G. Dresselhaus, M. S. Dresselhaus, *Science* **1997**, *275*, 187-191.

[29] A. Jorio, R. Saito, J. H. Hafner, C. M. Lieber, M. Hunter, T. McClure, G. Dresselhaus, M. S. Dresselhaus, *Phys. Rev. Lett.* **2001**, *86*, 1118-1121.

[30] A. Jorio, M. A. Pimenta, A. G. S. Filho, R. Saito, G. Dresselhaus, M. S. Dresselhaus, *New J. Phys.* **2003**, *5*, 139.1-139.17.

[31] a) G. Cazzolli, S. Caponi, A. Defant, C. M. C. Gambi, S. Marchetti, M. Mattarelli, M. Montagna, B. Rossi, F. Rossi, G. Viliani, *J. Raman Spectrosc.* **2012**, *43*, 1877-1883; b) M. Picquart, *J. Phys. Chem.* **1986**, *90*, 243-250; c) M. Picquart, M. Laborde, *"Raman scattering in Aqueous Solutions of Sodium Dodecyl Sulfate"* In *Surfactants in Solution*, **1986**, Springer, Berlin, pp189-201.

[32] For instance, Fe(II) and Co(II) were successful.

[33] The stereochemical outcome (*syn/anti* ratio) was not changed.

[34] a) R. Narayan, M. Potowski, Z- J. Jia, A. P. Antonchick, H. Waldmann, *Acc. Chem. Res.* **2014**, *47*, 1296-1310; b) Y. Xie, K. Yu, Z. Gu, *J. Org. Chem.* **2014**, *79*, 1289–1302; c) J. Cornil, A. Guérinot, S. Reymond, J. Cossy, *J. Org. Chem.* **2013**, *78*, 10273–10287; d) K. V. Gothelf, K. A. Jørgensen, *Chem. Rev.* **1998**, *98*, 863-909; e) V. Jäger, V. Buß, W. Schwab, *Tetrahedron Lett.* **1978**, *19*, 3133–3136.

[35] a) G. A. Molander, L. N. Cavalcanti, *Org. Lett.* **2013**, *15*, 3166-3169; b) P. P. Shao, F. Ye, A. E. Weber, X. Li, K. A. Lyons, W. H. Parsons, M. L. Garcia, B. T. Priest, M. M. Smith, J. P. Felix, B. S. Williams, G. J. Kaczorowski, E. McGowan, C. Abbadie, W. J. Martin, D. R. McMasters, Y. –D. Gao, *Bioorg. Med. Chem. Lett.* **2009**, *19*, 5329-5333.

[36] D. Chen, Z. Wang, J. Li, Z. Yang, L. Lin, X. Liu, X. Feng, *Chem. Eur. J.* **2011**, *17*, 5226-5229.

[37] a) M. Govindaraju, G. V. Kumar, K. A. Kumar, *Int. J. Chem. Tec. Res.* **2014**, *6*, 886-890; b) R. K. Yhya, K. M. L. Rai, E. A. Musad, *J. Chem. Sci.* **2013**, *125*, 799-806; c) A. V. Velikorodov, O. Y. Poddubnyi, A. K. Kuanchalieva, O. O. Krivosheev, *Russ. J. Org. Chem.* **2010**, *46*, 1826-1829; d) V. N. Pathak, M. Jain, A. Tiwari, *Org. Prep. Proc. Int.* **2008**, *40*, 493-498; e) S. Madapa, D. Sridhar, G. P. Yadav, P. R. Maulik, S. Batra, *Eur. J. Org. Chem.* **2007**, 4343-4351; f) J. –H. Chu, W. –S. Li, I. Chao, G. –H. Lee, W. –S. Chung, *Tetrahedron* **2006**, *62*, 73807389; g) V. Padmavathi, B. J. M. Reddy, B. C. O. Reddy, A. Padmaja, *Teterahedron* **2005**, *61*, 2407-2411; h) W. B. Martin, L. J. Kateley, D. C. Wiser, C. A. Brummond, *J. Chem. Edu.* **2002**, *79*, 225-227.

Recapitulation

The primary objective of the present dissertation was to demonstrate and validate the idea that a simple protocol for exploring asymmetric reactions in an aqueous environment in an attempt to cross Divine Field as an ultimate aim. The elaborate ways to exploit water in catalytic asymmetric chemical transformations were exemplified in multifarious organic reactions. I believe that water occupies a pivotal place in the development of novel modes of chemical transformations oriented to the unprecedented reactivity and stereoselectivity and it ultimately leads to fundamentally new concepts and the outlook for next-generation organic synthesis.

In Chapter 1, an exquisite set of three catalytic systems, comprising metal, chiral ligand **L1** and an additive, for the asymmetric Mukaiyama aldol reaction in aqueous media, were developed to cover a wide range of substrates with excellent stereocontrol. Since the emergence of $TiCl_4$-mediated aldol reactions of silicon enolates with aldehydes in 1973, the renowned Mukaiyama aldol reaction, tremendous efforts have been made to develop a definitive catalyst for asymmetric protocols under mild conditions and broad substrate tolerance. While previous reactions often required relatively harsh conditions, such as strictly anhydrous conditions and quite low temperatures (–78 °C), the present systems work well in aqueous environments at 0 °C. A wide variety of silicon enolates and aldehydes reacted under these conditions to afford the desired aldol products in high yields with high diastereo- and enantioselectivities. Mechanistic studies elucidated the coordination environments around Fe(II) and Bi(III) and the effect of additives in the chiral catalysts. The assumed catalytic cycle and transition states have clarified the important roles of water, a) producing the active metal complexes with high water-exchange rate constant (3.2×10^6) to activate substrates effectively and to catalyze the reaction via acyclic transition states; b) facilitating the catalytic turnover with simultaneous desilylation to directly access the aldol adducts and regenerate the active metal/ligand complex; and c) stabilizing the rigid transition states composed of the metal/ligand complex and the reactants through an entropy-driven aggregation derived from its highest cohesive energy density. The high catalytic activity, simplicity of experimental procedures and a wide substrate range, that includes aqueous aldehydes that are susceptible to poor stereoselectivities in organic solvents, proves the superiority of this methodology over conventional reactions. Forty years after the discovery of the Mukaiyama aldol reaction, a definitive catalytic asymmetric variant was established in aqueous media. There was, however, room for improvement in the use of organic solvents, the reaction temperature, and the application to the reaction with challenging substrates. It was envisioned that realization of further efficiency or mildness, and acquisition of new catalysis as a result of synergistic effect between Lewis acid and micelle. The iron(II)-based LASC (Lewis acid–surfactant-combined catalyst) exhibited superior performance with a wide substrate range for asymmetric Mukaiyama aldol reactions in water, whereas the reaction is *anti*-selective with high enantioselectivity in the presence of nickel(II) catalyst. The micellar catalytic system could be applied to the reaction with water-sensitive thioketene silyl acetals without use of any organic solvent. Leveraging the micellar catalysis in combination with Lewis acid catalysis resulted in considerable promising results, albeit under unoptimized conditions.

R¹CHO + (OSiMe₃ alkene, 1.2 equiv.) $\xrightarrow[\text{H}_2\text{O/DME, 0 °C}]{\text{Fe}^{II}\text{ or Bi}^{III}\text{ (3 mol%)}, \textbf{L1}, \text{Additive}}$ product, *syn/anti* up to >99/<1, up to 98% ee, **L1**

In Chapter 2, based upon the hypothesis that the compaction of the independent functions into a single structure is crucial for catalysis, the simplest possible metalloenzyme-like catalyst system was designed without employing the protein structure. In contrast to enzymes that exhibit overwhelmingly superior catalysis compared with artificial catalysts, current strategies to rival the enzymatic catalysis are known as "protein engineering," "catalytic antibodies" and "chemozymes" based on host-molecules. However, they require unmodified or minimally-modified structure of active sites, gigantic molecular weight, and sometimes the use of harsh conditions such as extremely low temperature in organic solvents. In addition, quantitative functionalization is indispensable to modify the structure. The synthesized ligand self-assembled, in the presence of scandium ions in water to generate an artificial system that efficiently catalyzed enantioselective direct-type aldol reactions using aqueous formaldehyde. With this simplest metalloenzyme-like catalyst, significant rate acceleration and stereoselective control were achieved. In addition, not only did this self-assembled system follow the Michaelis-Menten kinetics, but it also could construct unusual heat-resistant asymmetric environments in water. The simplest design of an artificial enzyme, including the precise replacement of minimal functions, was successfully achieved. These achievements should be valued as the first example of *exactly* rational design *not* based upon the enzymatic basement. It is expected that these results will provide valuable guidelines for artificial design of enzyme-like catalysts in water.
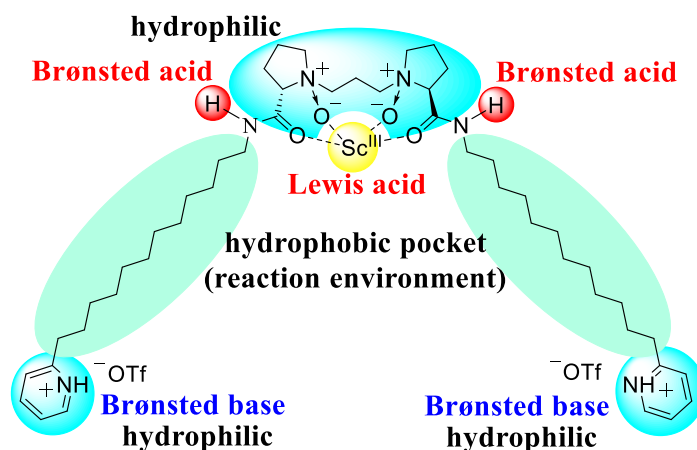
In Chapter 3, a quite expedient, environmentally benign, and broadly applicable protocol was developed for an enantioselective boron conjugate addition to various α,β-unsaturated carbonyl compounds, nitrile and imine derivatives, catalyzed by chiral copper(II) complexes formed with **L1** in water. Historically borylation of alkenes is often based upon *in situ* formation of an isolatable borylcopper(I) species via σ-bond metathesis between diboron and Cu(I) salts in organic solvents under strong basic conditions. Numerous Cu(I)-catalyzed protocols for the enantioselective

construction of α-chiral boranes has been explored by many groups. The use of $Cu(OH)_2$ generates heterogeneous systems, whereas $Cu(OAc)_2$ is homogeneous, and a remarkable switch of regioselectivity between 1,4- and 1,6-modes of the addition through the use of these catalyses for the reaction of cyclic dienones. It should be noted that such control of regioselectivity has yet been discovered in Cu(I) catalysis in organic solvents. Besides, several disparities lie between conventional Cu(I) catalysis and Cu(II) catalysis: 1) necessity of a strong base, 2) coverage for the substrate scope under single chiral catalyst, 3) chemical inclination in a protonation event, 4) deuterium effect. In contrast to Cu(I) catalysis, the Cu(II) protocol performed in water encompassed a wider range of substrates, not only without an addition of a strong base, but without varying the chiral ligand structure or other conditions such as solvents. Although most Cu(I)-catalyzed asymmetric reactions of organometallic reagents or silylboron reagents underwent a kinetic protonation, the Cu(II) protocol performed in water was under thermodynamic control. In contrast to unselective deuteration experiments observed in the Cu(I)-based catalysis, the Cu(II)-based protocol furnished α-deuterated boranes with *syn*-selectivity in D_2O. An extensive effort dedicated to deepen our understanding of copper catalysis in water led to the discovery of novel Cu(0) catalysis. The combination of Cu(0) and **L1** could catalyze the reaction of chalcone with bis(pinacolato)diboron efficiently. The reaction did not proceed at all in the absence of Cu(0). Although Cu(0), Cu(I) and Cu(II) complexes can exhibit the catalytic activity in enantioselective boron conjugate addition, these catalyses seem to a bit differ from one another.
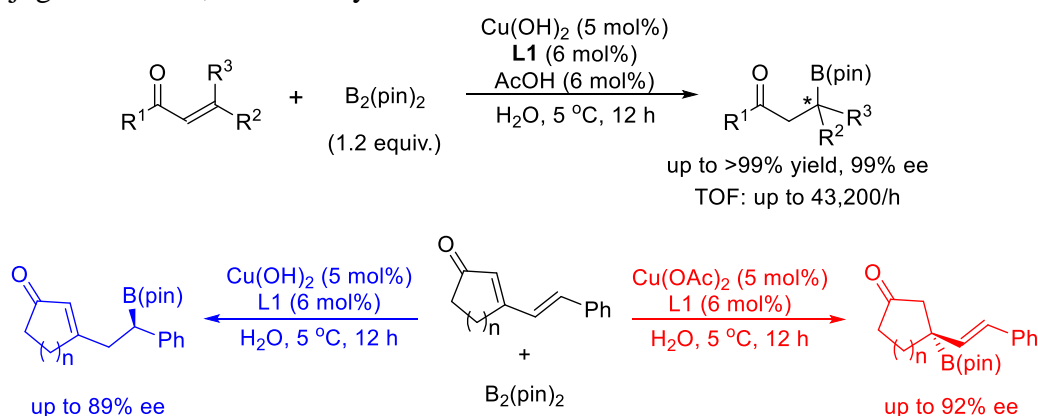
In Chapter 4, a multiple sets of catalytic systems, comprising a Lewis acid, **L1**, and an additive, were developed which gave rise to enantioenriched α-protonated compounds through a tandem nucleophilic addition/protonation sequence of α-branched enones or their equivalents. The remarkable governing of the enantioselectivity for the simple introduction of protons despite their remarkably high mobility in water, was noteworthy. The development of efficient catalytic processes involving enantioselective protonation has hitherto been regarded as a challenging task for synthetic chemists, since the high mobility of protons in water makes enantioselective protonation in water nearly impossible. As the proton-transfer rate is in the order of picoseconds in water, the rate-determining step would be not the protonation step but the conjugate addition step. Experimental results of the scandium-based and copper-based catalytic systems provided profound insights into the nature of the enantioselective protonation step. It suggested that the positive involvement of chiral ligand **L1** and hydrogen bonding surrounding the metal is of importance. In addition to the opposite inclination for additives between scandium and copper, the opposite sense

of chiral induction between them for the asymmetric aza-Michael addition/protonation processes in water was insightful.
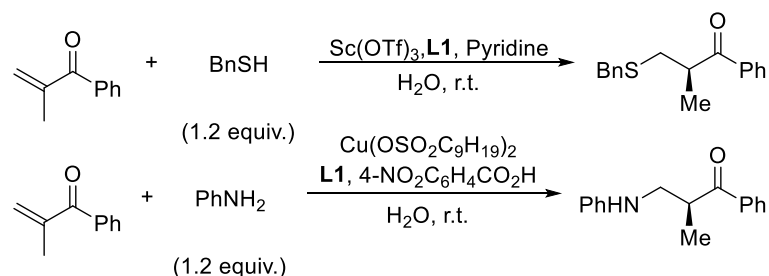
Inspired by the catalytic enantioselective protonation described in the previous section, Chapter 5 describes a Lewis acid-catalyzed Michael addition reaction of thiols in deuterium oxide to render a hydrogen isotope chirality alpha to a carbonyl group through the deuteration of the corresponding chiral enolate intermediate.   The reaction, catalyzed by a scandium complex formed with **L1**, had an inclination for *anti*-conformation when a catalytic amount of a base was used.   In the absence of the base, the conformation to *syn*-structure was favored.   The metal cation, and the coordination of the solvent and **L1** to the scandium core were believed to be responsible for stereoselection of the deuteration, presumably through hydrogen bonding.   Among various metal cations, only rare earth metals governed the stereoinduction to a greater or less extent, forcing the reaction to be *syn*-selective.   Unlike conventional reports, these findings are marked by the catalytic discernment between C–H bonds and C–D bonds through the incorporation of one deuterium atom from deuterium oxide.   This process offers an inexpensive, efficient and expedient route to prepare isotopically chiral compounds that can be expected to be candidates of undeveloped medication.   The successful stereoinduction in some relevant reactions underscores the prospective applicability and versatility.   A multidisciplinary aspect on latent properties of hydrogen isotope chirality, especially in medicinal chemistry and biochemistry, warrants further investigations.
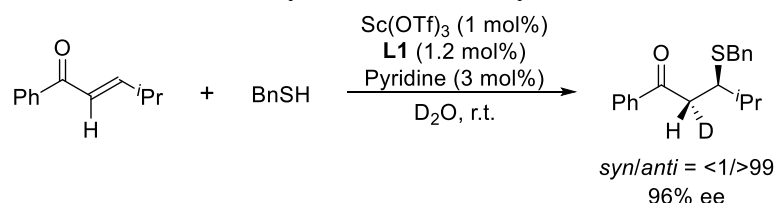
In Chapter 6, dispersing LASCs (Lewis acid–surfactant-combined catalysts) and SWNT (single-walled carbon nanotube) in water was envisioned toward an improved catalytic performance without any chemical modifications to complement the conventional strategies.   Despite a substantial interest in creating innovative catalysis to address the inherent proclivity of the existing catalysis toward undesired pathways, general and convenient tactics to improve catalytic performance has not been established thus far.   Although the outstanding reactive performance is sometimes exerted by nanoparticle, bimetal catalysis and photocatalysis or even their combinations, their limited tunability, durability and versatility and their unmanageablility in stereoinduction still remain as a huge problem.   The underlying strategies are: a) the high reactivity gained through the modification of electronic characteristics of the LASC by the SWNT; b) the formation of a highly dispersed system that can inhibit self-aggregation of organic materials and the subsequent superfluous interactions leading to the formation of undesired byproducts; and 3) the exquisite assemblage of all the components into the reaction center.   Indeed, an electrochemical behavior of

centered metals was successfully modified through the hybridization between the d-orbital of metals and the π-orbital of carbon atoms near the Fermi level, addressing the inherently low Lewis acidity of some metal cations. Their enhanced reactivities were demonstrated in a few reactions such as cycloaddition, 1,4-addition and aldol reactions. Among them, their improved enantioselective performance as well as their improved reactivity was highlighted in Ni(II)-catalyzed asymmetric 1,3-dipolar cyclization reactions of aldoximes with α,β-unsaturated carbonyl compounds. This new catalytic system delivered optically active isoxazolidines, an important class of intermediates both in pharmaceutical industries and in biochemistry, in high yields and enantiopurities. It should be emphasized that the designed catalytic system could offer the novel modes of asymmetric chemical transformations that have hitherto been unrecognized. This demonstration suggests that the inferior performance of the existing metal catalysis be overwritten by a LASC-SWNT-integrated methodology. Practical and straightforward applicability of the designed catalysts would have an immense impact on various fields, providing an expedient, environmentally benign, and highly efficient pathway to accessing optically active compounds and opening up new opportunities in organic chemistry.
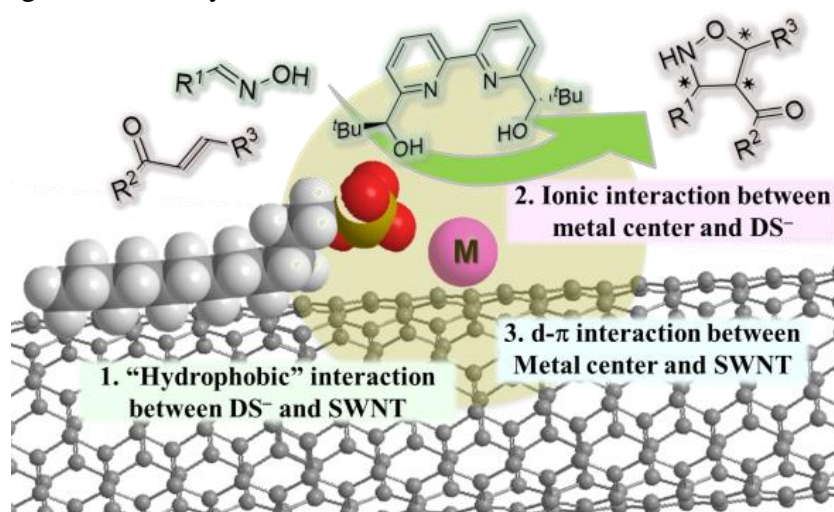
Publications

【**Publications related to the thesis**】

1. T. Kitanosono, M. Sakai, M. Ueno, S. Kobayashi, *Org. Biomol. Chem.*, **2012**, *10*, 7134-7147.
2. T. Kitanosono, P. Xu, S. Kobayashi, *Chem. Commun.*, **2013**, *49*, 8184-8186.
3. T. Kitanosono, S. Kobayashi, *Asian J. Org. Chem.*, **2013**, *2*, 961-966.
4. T. Kitanosono, T. Ollevier, S. Kobayashi, *Chem. Asian J.*, **2013**, *8*, 3051-3062. (Selected as Cover Picture)
5. T. Kitanosono, P. Xu, S. Kobayashi, *Chem. Asian J.*, **2014**, *9*, 179-188.
6. T. Kitanosono, S. Kobayashi, *Chem. Rec.*, **2014**, *14*, 130-143.
7. T. Kitanosono, P. Xu, S. Isshiki, L. Zhu, S. Kobayashi, *Chem. Commun.* **2014**, *50*, 9336-9339.
8. T. Kitanosono, S. Kobayashi, *Chem. Asian J.*, **2015**, *10*, 133-138.

【**Publications not related to the thesis**】

1. S. Kobayashi, T. Kitanosono, M. Ueno, *Synlett*, **2010**, 2033-2036.
2. C. Mukherjee, T. Kitanosono, S. Kobayashi, *Chem. Asian J.*, **2011**, *6*, 2308-2311.
3. M. Ueno, T. Kitanosono, M. Sakai, S. Kobayashi, *Org. Biomol. Chem.*, **2011**, *9*, 3619-3621.
4. S. Kobayashi, M. Ueno, T. Kitanosono, *Top. Curr. Chem.*, **2012**, *311*, 1-17.
5. S. Kobayashi, P. Xu, T. Endo, M. Ueno, T. Kitanosono, *Angew. Chem. Int. Ed.*, **2012**, *51*, 12763-12766. (Highlighted in SYNFACTS, **2013**, *9*, 301)
6. T. Kitanosono, S. Kobayashi, *Adv. Synth. Catal.*, **2013**, *355*, 3095-3118.
7. S. Kobayashi, Y. Yamashita, W. –J. Yoo, T. Kitanosono, J. –F. Soulé, in *Comprehensive Organic Synthesis (2nd Edition)*, London, **2014**, 396-450.

Experimental Section

General

Nuclear magnetic resonance (NMR) spectra were recorded on a JEOL ECX-600 or ECX-500 spectrometer, operating at 600 MHz or 500 MHz for ^{1}H and 150 MHz or 125 MHz for ^{13}C NMR in CDCl$_3$ unless otherwise noted. Tetramethylsilane (TMS) served as the internal standard ($\delta = 0$) for ^{1}H NMR and CDCl$_3$ was used as the internal standard ($\delta = 77.0$) for ^{13}C NMR. The aqueous solution of ScCl$_3$ [Sc(H$_2$O)$_6$$^{3+}$] served as the external standard ($\delta = 0$) for ^{45}Sc NMR analysis. Infrared (IR) spectra were obtained using a JASCO FT/IR-4200 spectrometer. Data are represented as frequency of absorption (cm^{-1}). All melting points were determined on a YAZAWA micro melting point BY-1 apparatus and are uncorrected. High-performance liquid chromatography was carried out using following apparatuses; SHIMADZU LC-10ATvp (liquid chromatograph), SHIMADZU SPD-10A (UV detector) and SHIMADZU C-R8A (Chromatopac) using Daicel chiralpak$^{®}$ or chiralcel$^{®}$ columns. Preparative thin-layer chromatography (PTLC) was carried out using Wakogel B-5F from Wako Pure Chemical Industries, Ltd. High Resolution Mass Spectra (HRMS) were recorded using a JEOL JMS-T100TD (DART) spectrometer or Brucker Daltonics BioTOF II (ESI) spectrometer. Optical Rotations were measured on a JASCO P1010 polarimeter using a 2 mL cell with 1 dm path length. Data are reported as follows: $[\alpha]_D^T$ (c in g/100 mL, solvent). Deionized water from a MILLIPORE MilliQ machine (Gradient A 10) was used as solvent without further treatment. Deuterium oxide purchased from ACROS (99.8 atom % D incorporated) was used without further treatment. All organic solvents used were commercially available dry solvents, which were distilled appropriately under an argon atmosphere or were stored over molecular sieves prior to use.

Chapter 1: Development of Catalytic Asymmetric Mukaiyama Aldol Reactions in Aqueous Environments

<Metal Salts>

$Fe(OTf)_2$ and $Fe(ClO_4)_2 \cdot 6H_2O$ were purchased from Wako (reagent grade purity).

$Sc(OTf)_3$[1] and $Bi(OTf)_3$[2] was prepared from the corresponding metal oxides and triflic acid by the reported method.

Other metal salts such as triflates, perchlorates and so on were basically commercially available.

$Fe[OSO_3C_{12}H_{25}]_2 \cdot 2H_2O$ was synthesized by modified procedure referred to reported examples.[3]

Synthesis of iron(II) dodecylsulfate dihydrate

An aqueous solution of 0.1 M sodium dodecyl sulfate was stirred at 0 ˚C. To the solution was added 4 times excess of 0.1 M $FeCl_2$ solution. A yellow precipitate appeared and it was washed several times with a 0.1 M $FeCl_2$ solution, and then dried over 48 hours to obtain light yellow powder.

Anal. calcd for $C_{24}H_{54}S_2O_{10}Fe$; C: 46.40, H: 8.74, S: 10.32; found C: 46.43, H: 8.94, S: 10.23.

<Chiral 2,2'-Bipyridine Ligand>

All chiral 2,2'-bipyridine derivatives were synthesized following a protocol described in the literature.[4,5,6]

(*S,S*)-6,6'-bis(1-hydroxy-2,2-dimethylpropyl)-2,2'-bipyridine (**L1**)[4]
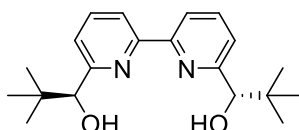
White solid

^{1}H NMR (400 MHz); δ = 0.98 (s, 18H), 4.43 (m, 2H), 7.22 (d, *J* = 7.6 Hz, 2H), 7.79 (dd, *J* = 7.6, 8.0 Hz, 2H), 8.30 (d, *J* = 8.0 Hz, 1H).

^{13}C NMR (100 MHz); δ = 25.9, 36.3, 80.2, 119.6, 123.1, 136.6, 153.8, 159.3.

HPLC (Dialcel Chiralcel OD, ^{n}hexane/ ^{i}PrOH = 19/1, flow rate 1.0 mL/min); t_R = 40.2 min (*R,R*), t_R = 48.7 min (*S,S*), t_R = 19.9 min (*meso* isomer). >99.5% *ee*

(*S*)-1-(6'-((*S*)-1-methoxy-2,2-dimethylpropyl)-[2,2'-bipyridin]-6-yl)-2,2-dimethylpropan-1-ol (**L2**)[5]
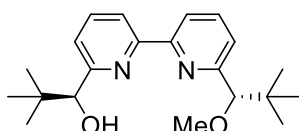
White solid; mp: 116-119 ˚C.

^{1}H NMR (400 MHz, CDCl$_3$): δ = 1.00 (s, 18H), 3.32 (s, 3H), 4.42 (s, 1H), 4.45 (d, *J* = 7.3 Hz, 1H), 4.53 (d, *J* = 7.3 Hz, 1H), 7.23 (d, *J* = 7.3 Hz, 1H), 7.43 (d, *J* = 7.8 Hz, 1H), 7.77-7.86 (m, 2H), 8.29

(d, *J* = 7.8 Hz, 1H), 8.37 (d, *J* = 7.8 Hz, 1H).

^{13}C NMR (100 MHz, CDCl$_3$): δ = 25.9, 26.2, 35.5, 36.2, 57.8, 80.1, 92.8, 119.1, 119.8, 121.9, 122.6, 136.5, 136.6, 154.2, 154.6, 158.9, 159.9.

IR (KBr): ν = 3447, 2958, 2380, 2077, 1638, 1439, 1102, 767, 367 cm^{-1}.

HRMS: calcd for C$_{21}$H$_{31}$N$_2$O$_2$ ([M+H]$^+$): 343.2386, found: 343.2370.

(*S*,*S*)-6,6'-bis(1-methoxy-2-ethyl-2-methylbutyl)-2,2'-bipyridine (**L3**)[5]
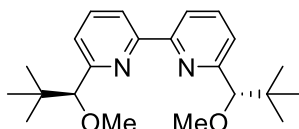
^{1}H NMR (500 MHz, CDCl$_3$): δ = 0.98 (s, 18H), 3.27 (s, 6H), 4.07 (s, 2H), 7.37 (d, *J* = 7.5 Hz, 2H), 7.79 (t, *J* = 7.5 Hz, 2H), 8.25 (d, *J* = 7.5 Hz, 2H)

^{13}C NMR (125 MHz, CDCl$_3$): δ = 26.3, 35.6, 57.8, 92.9, 121.6, 136.6, 155.1, 159.9

IR (KBr): ν = 3448, 2969, 2863, 1571, 1436, 1392, 1101, 814, 777, 673, 631 cm^{-1}.

(*S*,*S*)-6,6'-bis(1-hydroxyethyl)-2,2'-bipyridine (**L4**)[6]
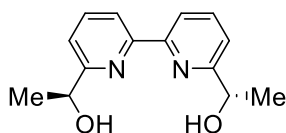
White solid

^{1}H NMR (400 MHz); δ = 1.56 (d, *J* = 6.6 Hz, 6H), 4.66 (brs, 2H), 4.96 (q, *J* = 6.6 Hz, 2H), 7.30 (d, *J* = 7.8 Hz, 2H), 7.81 (dd, *J* = 7.8, 7.8 Hz, 2H).

^{13}C NMR (100 MHz); δ = 24.2, 68.6, 119.4, 119.9, 137.7, 153.8, 162.3.

HPLC (Dialcel Chiralcel OB-H, ^{n}hexane/ ^{i}PrOH = 100/1, flow rate 1.0 mL/min); t$_R$ = 28.2 min (*S*,*S*), t$_R$ = 36.2 min (*R*,*R*), t$_R$ = 54.4 min (*meso* isomer). >99.5% *ee*

(*S*,*S*)-6,6'-bis(1-hydroxy-1-phenylmethyl)-2,2'-bipyridine (**L5**)[6]
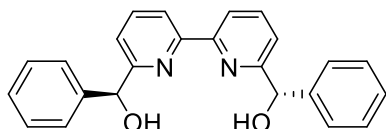
Pale yellow solid

^{1}H NMR (400 MHz); δ = 5.50 (brs, 2H), 5.82 (s, 2H), 7.16 (d, *J* = 7.8 Hz, 2H), 7.26-7.30 (m, 2H), 7.33-7.36 (m, 4H), 7.40-7.42 (m, 4H), 7.78 (dd, *J* = 7.8, 7.8 Hz, 2H), 8.39 (d, *J* = 7.8 Hz, 2H).

^{13}C NMR (100 MHz); δ = 74.8, 119.8, 121.8, 127.2, 127.9, 128.6, 138.0, 143.0, 153.3, 160.3.

HPLC (Dialcel Chiralpak AD, ^{n}hexane/ ^{i}PrOH = 19/1, flow rate 1.0 mL/min); t$_R$ = 39.8 min (*R*, *R*), t$_R$ = 54.1 min (*S*, *S*), t$_R$ = 72.8 min (*meso* isomer). >99.5% *ee*

(*R*, *R*)- 6,6'-bis(1-hydroxy-1-naphthylmethyl)-2,2'-bipyridine (**L6**)
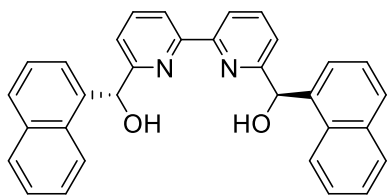
White solid; mp 103-106 $^{\circ}$C

IR (neat) ν = 3409, 1572, 1439, 1392, 1165, 1076, 1052, 800, 780, 635 cm^{-1}.

^{1}H NMR (600 MHz); δ = 5.39 (s, 2H), 6.43 (s, 2H), 7.04 (d, J = 6.9 Hz, 2H), 7.67 (t, J = 7.9 Hz, 2H), 7.77 (d, J = 8.2 Hz, 2H), 7.80-7.82 (m, 2H), 8.10-8.12 (m, 2H), 8.40 (d, J = 7.6 Hz, 2H).

^{13}C NMR (150 MHz); δ = 73.5, 119.8, 121.6, 124.3, 125.3, 125.6, 126.2, 126.3, 128.7, 128.9, 131.3, 134.2, 137.9, 138.0, 153.6, 160.5.

HRMS (DART, Pos.) calcd for C$_{32}$H$_{25}$N$_2$O$_2$ ([M+H]$^{+}$): 469.1916, found: 469.1999.

$[\alpha]_D^{20}$ = $-$16.03 (c = 1.0, EtOH).

(*S*, *S*)-6,6'-bis(1-hydroxy-2-ethyl-2-methylbutyl)-2,2'-bipyridine (**L7**)[5]
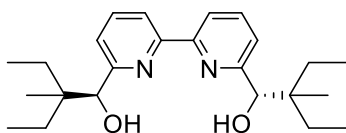
White solid

^{1}H NMR (400 MHz); δ = 0.80-0.91 (m, 18H), 1.26-1.37 (m, 6H), 1.57-1.65 (m, 4H), 4.34 (brs, 2H), 4.66 (m, 2H), 7.22 (d, J = 8.0 Hz, 2H), 7.78 (t, J = 8.0 Hz, 2H), 8.29 (d, J = 8.0 Hz, 2H).

^{13}C NMR (100 MHz); δ = 7.98, 8.00, 19.5, 27.1, 27.5, 41.1, 41.6, 119.5, 123.1, 136.7, 159.0, 159.6.

HPLC (Dialcel Chiralpak AD, ^{n}hexane/ ^{i}PrOH = 19/1, flow rate 1.0 mL/min); t_R = 20.0 min (*R*, *R*), t_R = 26.8 min (*S*, *S*), t_R = 68.1 min (*meso* isomer).   >99.5% *ee*

<Aldehydes>

All aldehydes were purified prior to use based on standard procedures unless otherwise noted.

<Silicon Enolates>

All silicon enolates were known in literatures.

Typical Experimental Procedure for Mukaiyama Aldol Reaction of Silyl Enol Ethers with Various Aldehydes:

Condition A (Scheme 20):

A mixture of Fe(OTf)$_2$ (3.2 mg, 0.009 mmol), chiral 2,2'-bipyridine ligand (3.5 mg, 0.0108 mmol) and pyridine (1.6 mg, 0.0216 mmol) in 650 μL of degassed DME was stirred at room temperature for 30 min.   The catalyst solution was then cooled at 0 $^{\circ}$C for 30 min and 70 μL of water was added.   To the mixture were aldehyde and silyl enol ether added successfully.   After stirred for 24 h at room temperature, the reaction mixture was quenched with satd. aqueous NaHCO$_3$ and brine. The aqueous layer was extracted with dichloromethane (three times), and the combined organic layers were washed with brine, and dried over anhydrous Na$_2$SO$_4$.   After removal of the solvent

under reduced pressure, the residue was purified by preparative TLC to afford the corresponding aldol.

Condition B (Scheme 21):

A mixture of $Fe(ClO_4)_2$ (3.3 mg, 0.009 mmol), chiral 2,2'-bipyridine ligand (3.5 mg, 0.0108 mmol) and benzoic acid (1.3 mg, 0.0216 mmol) in 500 μL of degassed DME was stirred at room temperature for 30 min.   The catalyst solution was then cooled at 0 °C for 30 min and 220 μL of water was added.   To the mixture were aldehyde and silyl enol ether added successfully.   After stirred for 24 h at room temperature, the reaction mixture was quenched with satd. aqueous $NaHCO_3$ and brine.   The aqueous layer was extracted with dichloromethane (three times), and the combined organic layers were washed with brine, and dried over anhydrous Na_2SO_4.   After removal of the solvent under reduced pressure, the residue was purified by preparative TLC to afford the corresponding aldol.

Condition C (Scheme 22):

A mixture of $Bi(OTf)_3$ (6.0 mg, 0.009 mmol), chiral 2,2'-bipyridine ligand (8.9 mg, 0.027 mmol) and pyridine (2.8 mg, 0.036 mmol) in 650 μL of degassed DME was stirred at room temperature for 30 min.   The catalyst solution was then cooled at 0 °C for 30 min and 70 μL of water was added. To the mixture were aldehyde and silyl enol ether added successfully.   After stirred for 24 h at room temperature, the reaction mixture was quenched with satd. aqueous $NaHCO_3$ and brine.   The aqueous layer was extracted with dichloromethane (three times), and the combined organic layers were washed with brine, and dried over anhydrous Na_2SO_4.   After removal of the solvent under reduced pressure, the residue was purified by preparative TLC to afford the corresponding aldol.

Analytical Data for Oxidized or Substituted Compounds

Most aldol adducts are literature-known; obtained analytical data for these compounds is in full agreement with reported data.   The products were isolated as a diastereomeric mixture unless otherwise noted.

3-Hydroxy-2-methyl-1,3-diphenylpropan-1-one (**3aa**)[7]
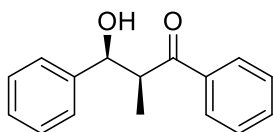
Colorless oil

^{1}H NMR (600 MHz, *syn/anti* = 97/3); δ = 1.05 (d, *J* = 3.5 Hz, 0.09H), 1.19 (d, *J* = 3.5 Hz, 2.91H), 3.68-3.71 (brs+m, 1+0.97H), 3.83 (t, *J* = 7.5 Hz, 0.03H), 4.98 (d, *J* = 4.0 Hz, 0.03H), 5.22 (d, *J* = 2.8 Hz, 0.97H), 7.25 (t, *J* = 7.5 Hz, 1H), 7.34 (t, *J* = 7.5 Hz, 2H), 7.40 (d, *J* = 7.6 Hz, 2H), 7.46 (dd, *J* = 7.6, 7.8 Hz, 2H), 7.57 (t, *J* = 7.8 Hz, 1H), 7.92 (d, *J* = 7.8 Hz, 2H).

^{13}C NMR (*syn*, 150 MHz); δ = 11.2, 47.0, 73.1, 126.0, 127.2, 127.2, 128.2, 128.2, 128.4, 128.4, 128.7, 128.7, 133.5, 135.6, 141.8, 205.6.

HPLC (Dialcel Chiralpak AD, [n]hexane/ [i]PrOH = 30/1, flow rate 1.0 mL/min); t_R = 19.9 min (*syn*, minor), t_R = 25.8 min (*syn*, major), t_R = 37.1 min (*anti*, major), t_R = 42.7 min (*anti*, minor).

3-Hydroxy-1-(4'-methoxyphenyl)-2-methyl-3-phenylpropan-1-one (**3ab**)[8]
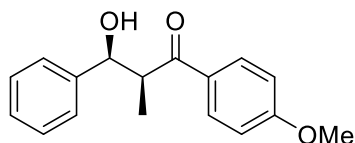
Colorless oil

^{1}H NMR (600 MHz, *syn/anti* = 97/3); δ = 1.08 (d, *J* = 7.1 Hz, 0.09H), 1.17 (d, *J* = 7.5 Hz, 2.91H), 3.61-3.67 (m, 1H), 3.87 (s, 3H), 4.95-4.98 (m, 0.03H), 5.22 (m, 0.97H), 6.92-6.97 (m, 2H), 7.23-7.29 (m, 1H), 7.33-7.37 (m, 2H), 7.38-7.41 (m, 2H), 7.91-7.96 (m, 2H).

^{13}C NMR (*syn*, 125 MHz); δ = 11.2, 46.4, 55.5, 73.1, 113.9, 113.9, 126.0, 127.2, 127.2, 128.2, 128.2, 128.5, 128.5, 130.8, 141.9, 163.9, 204.4.

HRMS (ESI-TOF, Pos.) calcd for $C_{17}H_{18}O_3$ ([M+H]$^+$): 271.1334, found: 271.1325.

HPLC (Dialcel Chiralpak AD-H, ^{n}hexane/ ^{i}PrOH = 9/1, flow rate 1.0 mL/min); t_R = 16.4 min (*syn*, minor), t_R = 22.6 min (*syn*, major), t_R = 35.5 min (*anti*, major), t_R = 48.0 min (*anti*, minor).

3-Hydroxy-1-(4'-chlorophenyl)-2-methyl-3-phenylpropan-1-one (**3ac**)[8]
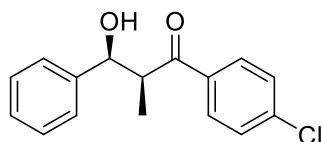
Colorless oil

^{1}H NMR (600 MHz, *syn/anti* = 94/6); δ = 0.95 (d, *J* = 7.6 Hz, 0.18H), 1.12 (d, *J* = 7.6 Hz, 2.82H), 3.42 (s, 3H), 3.55-3.61 (m, 1H), 3.68-3.73 (m, 0.06H), 4.91 (d, *J* = 7.6 Hz, 0.06H), 5.14 (d, *J* = 7.6 Hz, 0.94H), 7.17-7.22 (m, 1H), 7.26-7.34 (m, 3H), 7.37 (d, *J* = 8.3 Hz, 2H), 7.79 (d, *J* = 8.3 Hz, 1.88H), 7.85 (d, *J* = 8.3 Hz, 0.12H).

^{13}C NMR (*syn*, 150 MHz); δ = 11.4, 47.2, 73.2, 126.0, 126.7, 127.4, 127.4, 128.3, 128.5, 129.1, 129.8, 129.8, 134.0, 140.0, 141.7, 204.3.

HRMS (ESI-TOF, Pos.) calcd for $C_{16}H_{16}O_2Cl$ ([M+H]$^+$): 275.0838, found: 275.0805.

HPLC (Dialcel Chiralcel OD-H (double), ^{n}hexane/ ^{i}PrOH = 98/2, flow rate 0.5 mL/min); t_R = 89.3 min (*syn*, minor), t_R = 95.5 min (*syn*, major), t_R = 124.4 min (*anti*, major), t_R = 129.2 min (*anti*, minor).

3-Hydroxy-2-methyl-1-phenyl-3-(*p*-tolyl)propan-1-one (**3ba**)[8]
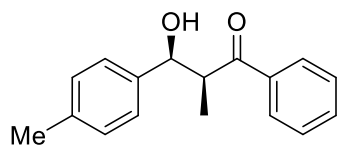
Colorless oil

^{1}H NMR (600 MHz, *syn/anti* = 96/4); δ = 1.03 (d, *J* = 7.6 Hz, 0.12H), 1.19 (d, *J* = 6.9 Hz, 2.88H), 2.32 (s, 3H), 3.60 (brs, 1H), 3.68 (qd, *J* = 3.4, 6.9 Hz, 0.96H), 3.78-3.85 (m, 0.04H), 4.95 (d, *J* = 8.2 Hz, 0.04H), 5.19 (d, *J* = 2.8 Hz, 0.96H), 7.14 (d, *J* = 7.6 Hz, 2H), 7.28 (d, *J* = 7.6 Hz, 2H), 7.45 (dd, *J* = 7.6, 7.6 Hz, 2H), 7.56 (t, *J* = 7.6 Hz, 1H), 7.92 (d, *J* = 7.6 Hz, 1.92H), 7.98 (d, *J* = 7.6 Hz,

0.08H).

^{13}C NMR (*syn*, 150 MHz); δ = 11.3, 21.0, 47.1, 73.0, 125.9, 126.6, 128.4, 128.6, 128.7, 128.9, 129.1, 133.2, 133.4, 135.7, 136.8, 138.8, 205.6.

HPLC (Dialcel Chiralpak AD-H (double), ^{n}hexane/ ^{i}PrOH = 9/1, flow rate 0.5 mL/min); t_R = 74.9 min (*syn*, minor), t_R = 90.5 min (*syn*, major), t_R = 159.6 min (*anti*, minor), t_R = 183.1 min (*anti*, major).

3-Hydroxy-3-(4'-methoxyphenyl)-2-methyl-1-phenylpropan-1-one (**3ca**)[7]
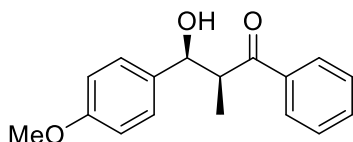
Colorless oil

^{1}H NMR (600 MHz, *syn/anti* = 98/2); δ = 1.19 (d, *J* = 7.4 Hz, 3H), 3.54 (d, *J* = 1.6 Hz, 1H), 3.66 (qd, *J* = 3.5, 7.0 Hz, 1H), 3.77 (s, 2.94H), 3.78 (s, 0.06H), 5.13 (d, *J* = 6.7 Hz, 0.02H), 5.14-5.17 (m, 0.98H), 6.85 (d, *J* = 8.5 Hz, 1.96H), 6.87 (d, *J* = 8.9 Hz, 0.04H), 7.29 (d, *J* = 8.5 Hz, 2H), 7.43-7.46 (m, 2H), 7.54-7.57 (m, 1H), 7.90 (dd, *J* = 1.3, 8.2 Hz, 1.96H), 7.94 (dd, *J* = 1.3, 8.2 Hz, 0.04H).

^{13}C NMR (*syn*, 150 MHz); δ = 11.5, 47.2, 55.2, 72.9, 113.6, 127.2, 128.4, 128.6, 128.7, 133.4, 134.0, 135.7, 158.7, 205.6.

HPLC (Dialcel Chiralpak AS-H, ^{n}hexane/ ^{i}PrOH = 19/1, flow rate 1.0 mL/min); t_R = 18.5 min (*syn*, minor), t_R = 24.1 min (*syn*, major), t_R = 34.2 min (*anti*, minor), t_R = 38.6 min (*anti*, major).

3-Hydroxy-3-(4'-fluoro)-2-methyl-1-phenylpropan-1-one (**3da**)[9]
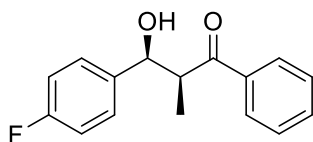
White solid; mp 61-63 °C.

^{1}H NMR (600 MHz, *syn/anti* = 96/4); δ = 1.05 (d, *J* = 7.1 Hz, 0.12H), 1.18 (d, *J* = 7.4 Hz, 2.88H), 3.66 (ddd, *J* = 3.3, 7.4, 14.4 Hz, 0.96H), 3.73-3.82 (brs+m, 1.04H), 4.96-4.99 (m, 0.04H), 5.20 (d, *J* = 2.8 Hz, 0.96H), 7.02 (t, *J* = 8.8 Hz, 2H), 7.36 (dd, *J* = 5.5, 8.5 Hz, 2H), 7.47 (dd, *J* = 7.4, 7.6 Hz, 2H), 7.59 (dd, *J* = 7.4, 7.4 Hz, 1H), 7.92 (d, *J* = 7.4 Hz, 1.92H), 7.96 (d, *J* = 7.3 Hz, 0.08H).

^{13}C NMR (*syn*, 150 MHz); δ = 11.2, 47.0, 72.6, 115.0 (d, *J* = 21.1 Hz), 127.6, 127.7, 128.4, 128.8, 133.6, 135.5, 137.5, 162.0 (d, *J* = 244.2 Hz), 205.6.

HPLC (Dialcel Chiralpak AD-H, ^{n}hexane/ ^{i}PrOH = 30/1, flow rate 0.8 mL/min); t_R = 34.0 min (*syn*, minor), t_R = 35.8 min (*syn*, major), t_R = 55.2 min (*anti*, major), t_R = 64.6 min (*anti*, minor).

3-Hydroxy-3-(4'-nitro)-2-methyl-1-phenylpropan-1-one (**3ea**)[8]
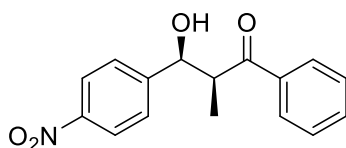
White solid; mp 117-120 °C.

^{1}H NMR (600 MHz, *syn/anti* = 91/9); δ = 1.17 (d, *J* = 7.6 Hz, 3H), 3.67 (ddd, *J* = 2.8, 7.1, 14.6 Hz, 1.82H), 3.80-3.86 (m, 0.18H), 4.05 (brs, 1H), 5.08-5.12 (m, 0.09H), 5.32-5.38 (m, 0.91H), 7.47 (t, *J* = 7.7 Hz, 0.18H), 7.50 (t, *J* = 7.6 Hz, 1.82H), 7.56-7.65 (m, 3H), 7.94 (d, *J* = 8.7 Hz, 2H), 8.21 (d, *J* = 8.7 Hz, 1.82H), 8.29 (d, *J* = 7.7 Hz, 0.18H).

^{13}C NMR (*syn*, 150 MHz); δ = 11.0, 46.5, 72.3, 123.5, 126.9, 128.5, 128.9, 133.9, 135.1, 147.2, 149.2, 205.2.

HPLC (Dialcel Chiralpak AD-H, [n]hexane/ [i]PrOH = 9/1, flow rate 1.0 mL/min); t_R = 19.3 min (*syn*, major), t_R = 22.0 min (*syn*, minor), t_R = 23.8 min (*anti*, major), t_R = 48.6 min (*anti*, minor).

3-Hydroxy-1-(4'-methoxyphenyl)-2-methyl-3-(4''-nitrophenyl)propan-1-one (**3eb**)[10]
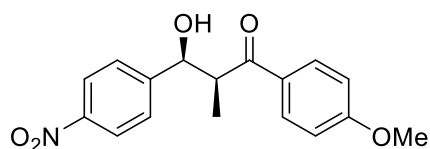
Yellow solid; mp 131-133 °C.

^{1}H NMR (600 MHz, *syn/anti* = 97/3); δ = 1.14 (d, *J* = 7.6 Hz, 3H), 3.65 (qd, *J* = 2.8, 7.6 Hz, 0.97H), 3.78 (q, *J* = 6.9Hz, 0.03H), 3.89 (s, 3H), 4.11 (q, *J* = 7.6 Hz, 0.03H), 4.30 (brs, 1H), 5.06-5.09 (m, 0.03H), 5.31-5.36 (m, 0.97H), 6.92 (d, *J* = 8.9 Hz, 0.06H), 6.96 (d, *J* = 13.7 Hz, 1.94H), 7.59 (d, *J* = 8.9 Hz, 2H), 7.93 (d, *J* = 8.9 Hz, 2H), 8.17 (d, *J* = 8.9 Hz, 0.06H), 8.20 (d, *J* = 8.3 Hz, 1.94H).

^{13}C NMR (*syn*, 150 MHz); δ = 11.1, 45.8, 55.4, 72.4, 114.0, 123.3, 126.8, 127.9, 130.8, 146.9, 149.4, 164.1, 203.6.

HPLC (Dialcel Chiralpak AS-H, [n]hexane/ [i]PrOH = 9/1, flow rate 1.0 mL/min); t_R = 22.9 min (*anti*, major), t_R = 28.8 min (*anti*, minor), t_R = 47.5 min (*syn*, minor), t_R = 69.5 min (*syn*, major).

3-Hydroxy-1-(4'-chlorophenyl)-2-methyl-3-(4''-nitrophenyl)propan-1-one (**3ec**)[10]
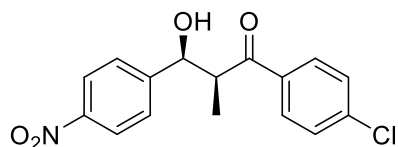
White solid; mp 112-115 °C.

^{1}H NMR (600 MHz, *syn/anti* = 88/12); δ = 1.11 (d, *J* = 6.7 Hz, 0.36H), 1.17 (d, *J* = 7.4 Hz, 2.64H), 3.65 (qd, *J* = 3.1, 7.3 Hz, 0.88H), 3.76 (q, *J* = 7.0Hz, 0.12H), 3.99 (brs, 1H), 5.34 (s, 1H), 7.46 (d, *J* = 8.3 Hz, 2H), 7.59 (d, *J* = 8.6 Hz, 2H), 7.88 (d, *J* = 8.3 Hz, 2H), 8.20 (d, *J* = 8.9 Hz, 1.76H), 8.29 (d, *J* = 8.1 Hz, 0.24H).

^{13}C NMR (*syn*, 150 MHz); δ = 11.1, 46.7, 69.3, 72.3, 123.5, 127.0, 129.3, 129.8, 129.9, 130.0, 133.5, 203.9.

HPLC (Dialcel Chiralpak AS-H, [n]hexane/ [i]PrOH = 9/1, flow rate 1.0 mL/min); t_R = 7.9 min (*anti*, minor), t_R = 17.1 min (*anti*, major), t_R = 22.8 min (*syn*, major), t_R = 34.8 min (*syn*, minor).

3-Hydroxy-2-methyl-3-(naphthalen-1-yl)-1-phenylpropan-1-one (**3fa**)[7]
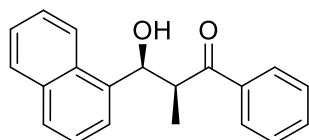
Colorless oil

^{1}H NMR (600 MHz, *syn/anti* = 96/4); δ = 1.09 (d, *J* = 7.1 Hz, 0.12H), 1.16 (d, *J* = 7.6 Hz, 2.88H), 3.91 (qd, *J* = 2.1, 7.2 Hz, 1H), 4.07 (d, *J* = 2.1 Hz, 1H), 7.44-7.50 (m, 4H), 7.52 (dd, *J* = 7.6, 8.2 Hz, 1H), 7.59 (t, *J* = 7.6 Hz, 1H), 7.79 (d, *J* = 7.6 Hz, 1H), 7.82 (d, *J* = 7.6 Hz, 1H), 7.86-7.90 (m, 2H), 7.93 (d, *J* = 7.6 Hz, 2H).

^{13}C NMR (*syn*, 150 MHz); δ = 11.3, 44.9, 53.0, 69.2, 122.3, 124.4, 125.2, 125.4, 126.1, 127.7, 128.5, 128.8, 129.2, 129.7, 133.6, 133.7, 135.5, 136.5, 206.3.

HPLC (Dialcel Chiralpak AS-H, ^{n}hexane/ ^{i}PrOH = 30/1, flow rate 0.5 mL/min); t_R = 21.2 min (*syn*, minor), t_R = 29.0 min (*syn*, major), t_R = 42.6 min (*anti*, minor), t_R = 48.3 min (*anti*, major).

3-Hydroxy-2-methyl-1-phenyl-4-penten-1-one (**3ga**)[11]
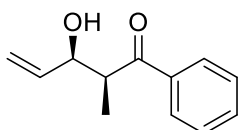
Colorless oil

^{1}H NMR (600 MHz, *syn/anti* = 97/3); δ = 1.27 (d, *J* = 7.6 Hz, 2.91H), 1.45 (d, *J* = 6.9 Hz, 0.09H), 3.20 (brs, 1H), 3.52-3.58 (m, 1H), 4.61 (brs, 1H), 5.21 (d, *J* = 11.0 Hz, 1H), 5.38 (d, *J* = 17.2 Hz, 1H), 5.88 (ddd, J = 5.5, 11.0, 17.2 Hz, 1H), 7.49 (t, *J* = 7.6 Hz, 2H), 7.59 (t, *J* = 7.6 Hz, 1H), 7.95 (d, *J* = 7.6 Hz, 2H).

^{13}C NMR (*syn*, 150 MHz); δ = 11.6, 45.0, 72.3, 115.9, 128.5, 128.5, 128.7, 128.7, 133.5, 135.8, 137.8, 205.2.

HPLC (Dialcel Chiralcel OD-H (double), ^{n}hexane/ ^{i}PrOH = 30/1, flow rate 0.5 mL/min); t_R = 39.8 min (*syn*, minor), t_R = 47.4 min (*syn*, major), t_R = 55.7 min (*anti*, minor), t_R = 57.5 min (*anti*, major).

(*E*)-3-Hydroxy-2-methyl-1,5-diphenylpent-4-en-1one (**3ha**)[7]
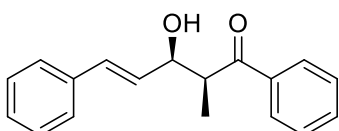
Colorless oil

^{1}H NMR (600 MHz, *syn/anti* = 92/8); δ = 1.25 (d, *J* = 6.9 Hz, 0.24H), 1.31 (d, *J* = 7.6 Hz, 2.76H), 3.40 (brs, 1H), 3.64 (ddd, J = 3.4, 7.1, 14.4 Hz, 0.92H), 3.66-3.72 (m, 0.08H), 4.57-4.62 (m, 0.08H), 4.76-4.82 (m, 0.92H), 6.24 (dd, *J* = 5.7, 15.9 Hz, 0.92H), 6.29 (d, *J* = 7.1 Hz, 0.08H), 6.66 (d, *J* = 15.9 Hz, 0.08H), 6.71 (d, *J* = 15.9 Hz, 0.92H),   7.23 (t, *J* = 7.2 Hz, 1H), 7.30 (t, *J* = 7.6 Hz, 2H), 7.37 (d, *J* = 7.4 Hz, 2H), 7.48 (t, *J* = 7.6 Hz, 2H), 7.59 (t, *J* = 7.6 Hz, 1H), 7.96 (d, *J* = 7.2 Hz, 2H).

^{13}C NMR (*syn*, 150 MHz); δ = 11.8, 12.3, 21.2, 23.4, 52.7, 73.0, 74.0, 126.5, 127.7, 128.4, 128.5, 128.7, 129.5, 130.3, 131.1, 131.7, 133.3, 133.4, 136.5, 136.6, 137.7, 137.9, 204.7, 205.4.

HPLC (Dialcel Chiralpak AS-H, ^{n}hexane/ ^{i}PrOH = 30/1, flow rate 1.0 mL/min); t_R = 28.5 min (*syn*, minor), t_R = 55.0 min (*syn*, major), t_R = 77.7 min (*anti*, minor), t_R = 104.9 min (*anti*, major).

(*E*)-3-Hydroxy-1-(4'-methoxyphenyl)-2-methyl-5-phenylpent-4-en-1-one (**3hb**)[10]
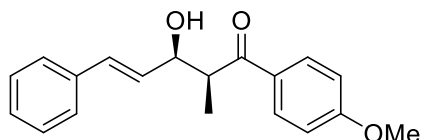
Colorless oil

^{1}H NMR (600 MHz, *syn/anti* = 95/5); δ = 1.27 (d, *J* = 7.4 Hz, 0.15H), 1.30 (d, *J* = 7.6 Hz, 2.85H), 3.54-3.60 (m+brs, 2H), 3.88 (s, 3H), 4.54-4.59 (m, 0.05H), 4.75-4.81 (m, 0.95H), 6.24 (dd, *J* = 5.5, 15.8 Hz, 0.95H), 6.29 (d, *J* = 7.4 Hz, 0.05H), 6.66 (d, *J* = 15.8 Hz, 0.05H), 6.71 (d, *J* = 16.5 Hz, 0.95H), 6.96 (d, *J* = 8.9 Hz, 2H), 7.23 (t, *J* = 8.9 Hz, 1H), 7.31 (dd, *J* = 7.6, 7.6 Hz, 2H), 7.38 (d, *J* = 8.3 Hz, 2H), 7.96 (d, *J* = 8.9 Hz, 2H).

^{13}C NMR (*syn*, 150 MHz); δ = 11.9, 44.8, 55.4, 72.2, 113.9, 126.4, 127.5, 128.5, 128.6, 129.3, 130.8, 130.8, 136.7, 163.8, 203.9.

HRMS (ESI-TOF, Pos.) calcd for $C_{19}H_{20}O_3$ ([M+Na]$^+$): 319.1305, found: 319.1309.

HPLC (Dialcel Chiralpak AD-H (double), ^{n}hexane/ ^{i}PrOH = 9/1, flow rate 1.0 mL/min); t_R = 67.9 min (*syn*, major), t_R = 76.9 min (*syn*, minor), t_R = 79.9 min (*anti*, major), t_R = 148.5 min (*anti*, minor).

(*E*)-3-Hydroxy-1-(4'-chloro)-2-methyl-5-phenylpent-4-en-1-one (**3hc**)
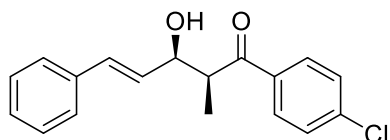
Colorless crystal; mp 116-119 ^{o}C.

IR (neat) ν = 3443, 2941, 2838, 1672, 1490, 1451, 1400, 1367, 1217, 1092, 1014, 969, 844, 749, 695 cm^{-1}.

^{1}H NMR (600 MHz, *syn/anti* = 85/15); δ = 1.22 (d, *J* = 6.9 Hz, 0.45H), 1.29 (d, *J* = 6.9 Hz, 2.55H), 2.88 (brs, 0.15H), 3.24 (brs, 0.85H), 3.58 (qd, *J* = 3.4, 7.6 Hz, 0.85H), 3.60-3.66 (m, 0.15H), 4.55-4.60 (m, 0.15H), 4.73-4.77 (m, 0.85H), 6.22 (dd, *J* = 5.5, 15.8 Hz, 0.85H), 6.25 (dd, *J* = 7.6, 15.8 Hz, 0.15H), 6.51 (d, *J* = 15.8 Hz, 0.15H), 6.69 (d, *J* = 15.8 Hz, 0.85H), 7.21-7.26 (m, 1H), 7.28-7.32 (m, 2H), 7.34-7.38 (m, 2H), 7.43 (d, *J* = 8.3 Hz, 0.30H), 7.44 (d, *J* = 8.3 Hz, 1.70H), 7.89 (d, *J* = 8.9 Hz, 1.70H), 7.91 (d, *J* = 8.9 Hz, 0.30H).

^{13}C NMR (*syn*, 150 MHz); δ = 11.9, 45.6, 72.4, 126.4, 126.5, 127.7, 128.5, 128.9, 129.0, 129.5, 129.9, 131.2, 132.3, 134.2, 136.5, 139.9, 203.7.

HRMS (ESI-TOF, Pos.) calcd for $C_{18}H_{17}O_2Cl$ ([M+Na]$^+$): 323.0809, found: 323.0790.

HPLC (Dialcel Chiralpak AD-H (double), ^{n}hexane/ ^{i}PrOH = 9/1, flow rate 1.0 mL/min); t_R = 46.1 min (*anti*, major), t_R = 52.4 min (*syn*, major), t_R = 60.9 min (*syn*, minor), t_R = 173.3 min (*anti*, minor).

(*E*)-2-Ethyl-3-hydroxy-1,5-diphenylpent-4-en-1-one (**3hd**)
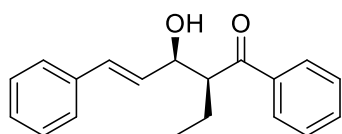
Colorless oil

IR (neat) ν = 3465, 2967, 1676, 1599, 1512, 1449, 1373, 1259, 1028, 970, 838, 753, 702 cm^{-1}.

^{1}H NMR (600 MHz, *syn/anti* = 96/4); δ = 0.91 (t, *J* = 7.6 Hz, 2.88H), 0.92 (t, *J* = 7.5 Hz, 0.12H), 1.26 (t, *J* = 6.9 Hz, 0.96H), 1.29-1.31 (m, 0.04H), 1.75-1.99 (m, 2H), 2.86 (brs, 1H), 3.60-3.63 (m, 0.04H), 3.65 (quin, *J* = 4.6 Hz, 0.96H), 4.64-4.68 (m, 1H), 6.21-6.25 (m, 0.04H), 6.25 (dd, *J* = 6.2, 15.8 Hz, 0.96H), 6.65 (d, *J* = 15.8 Hz, 0.04H), 6.67 (d, *J* = 15.8 Hz, 0.96H), 7.22 (t, *J* = 7.6 Hz, 1H), 7.29 (dd, *J* = 7.6, 7.6 Hz, 2H), 7.31-7.34 (m, 2H), 7.45-7.50 (m, 2H), 7.56-7.61 (m, 1H), 7.90 (d, *J* = 8.5 Hz, 0.08H), 7.98 (d, *J* = 8.3 Hz, 1.92H).

^{13}C NMR (*syn*, 150 MHz); δ = 12.3, 21.0, 23.4, 52.6, 72.9, 126.5, 127.6, 128.3, 128.4, 128.5, 128.7, 129.5, 131.2, 133.4, 136.6, 137.6, 204.8.

HRMS (ESI-TOF, Pos.) calcd for $C_{19}H_{20}O_2$ ([M+Na]$^+$): 303.1356, found: 303.1346.

HPLC (Dialcel Chiralpak AS-3, ^{n}hexane/ ^{i}PrOH = 30/1, flow rate 1.0 mL/min); t_R = 27.7 min (*syn*, minor), t_R = 52.6 min (*syn*, major), t_R = 74.8 min (*anti*, minor), t_R = 99.9 min (*anti*, major).

3-Cyclohexyl-3-hydroxy-2-methyl-1-phenylpropan-1-one (**3ia**)[11]
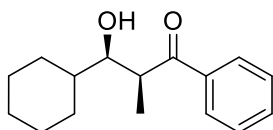
Colorless oil

^{1}H NMR (600 MHz, *syn/anti* = 95/5); δ = 0.94-1.06 (m, 2H), 1.13-1.32 (m, 6H), 1.45-1.52 (m, 1H), 1.64-1.81 (m, 4H), 2.10 (d, *J* = 13.1 Hz, 1H), 2.99-3.04 (m, 0.05H), 3.07 (brs, 0.95H), 3.56-3.59 (m, 0.10H), 3.65-3.73 (m, 1.95H), 7.48 (dd, *J* = 7.6, 8.2 Hz, 2H), 7.59 (t, *J* = 7.6 Hz, 1H), 7.94 (d, *J* = 6.9 Hz, 2H).

^{13}C NMR (*syn*, 150 MHz); δ = 10.5, 25.8, 26.1, 26.3, 29.1, 29.5, 40.1, 41.2, 75.4, 128.4, 128.7, 133.3, 135.9, 205.9.

HPLC (Dialcel Chiralcel OD-H, ^{n}hexane/ ^{i}PrOH = 9/1, flow rate 0.5 mL/min); t_R = 15.7 min (*anti*, minor), t_R = 17.6 min (*syn*, minor), t_R = 20.3 min (*syn*, major), t_R = 26.5 min (*anti*, major).

1,5-Diphenyl-3-hydroxy-2-methylpentan-1-one (**3ja**)[7]
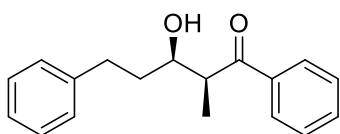
Colorless oil

^{1}H NMR (600 MHz, *syn/anti* = 94/6); δ = 1.11 (d, *J* = 6.2 Hz, 0.18H), 1.18 (d, *J* = 7.6 Hz, 2.82H), 1.59-1.65 (m, 1H), 1.82-1.90 (m, 1H), 2.59-2.65 (m, 1H), 2.78-2.84 (m, 1H), 3.05 (brs, 0.06H), 3.19 (brs, 0.94H), 3.35 (qd, *J* = 2.8, 7.5 Hz, 0.94H), 3.43-3.49 (m, 0.06H), 3.78-3.82 (m, 0.06H), 3.99 (d, *J* = 8.9 Hz, 0.94H), 7.07-7.21 (m, 5H), 7.37 (t, *J* = 7.6 Hz, 1H), 7.48 (t, *J* = 7.6 Hz, 1H), 7.82 (d, *J* = 7.6 Hz, 1H).

^{13}C NMR (*syn*, 150 MHz); δ = 11.2, 32.3, 36.0, 44.6, 70.6, 125.8, 128.3, 128.4, 128.4, 128.7, 128.7, 130.0, 133.4, 135.7, 141.8, 205.8.

HPLC (Dialcel Chiralcel OD-H, ^{n}hexane/ ^{i}PrOH = 98/2, flow rate 0.5 mL/min); t_R = 23.7 min (*syn*,

minor), t_R = 25.6 min (*anti*, minor), t_R = 45.8 min (*syn*, major), t_R = 87.9 min (*anti*, minor).

3-Hydroxy-1-(4'-methoxyphenyl)-2-methyl-3-phenylpropan-1-one (**3jb**)[12]
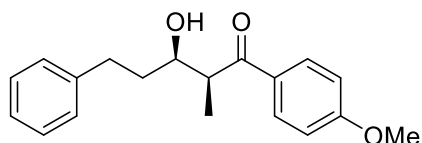
Colorless oil

^{1}H NMR (600 MHz, *syn/anti* = 95/5); δ = 1.25 (d, *J* = 7.6 Hz, 2.85H), 1.45 (d, *J* = 6.9 Hz, 0.15H), 1.65-1.71 (m, 1H), 1.80-1.85 (m, 0.05H), 1.91-1.99 (m, 0.95H), 2.70 (ddd, *J* = 6.9, 9.6, 13.7 Hz, 1H), 2.90 (ddd, *J* = 5.2, 9.6, 13.7 Hz, 1H), 3.38 (qd, *J* = 2.7, 7.2 Hz, 0.95H), 3.44 (brs, 1H), 3.46-3.52 (m, 0.05H), 3.87 (s, 2.85H), 3.89 (s, 0.15H), 4.03-4.07 (m, 0.95H), 4.12 (q, *J* = 7.2 Hz, 0.05H), 6.94 (d, *J* = 8.9 Hz, 1.90H), 6.97 (d, *J* = 8.9 Hz, 0.10H), 7.18 (t, *J* = 7.6 Hz, 1H), 7.22 (d, *J* = 6.9 Hz, 2H), 7.27 (q, *J* = 7.6 Hz, 2H), 7.92 (d, *J* = 8.9 Hz, 2H).

^{13}C NMR (*syn*, 150 MHz); δ = 11.2, 32.4, 36.0, 44.0, 55.5, 55.5, 70.6, 113.9, 114.1, 125.8, 128.4, 128.5, 128.6, 130.8, 131.0, 142.0, 163.8, 204.5.

HPLC (Dialcel Chiralpak AD-H, ^{n}hexane/ ^{i}PrOH = 30/1, flow rate 1.0 mL/min); t_R = 40.9 min (*syn*, major), t_R = 45.8 min (*syn*, minor), t_R = 52.9 min (*anti*, major), t_R = 57.5 min (*anti*, minor).

3-Hydroxy-1-(4'-chlorophenyl)-2-methyl-3-phenylpropan-1-one (**3jc**)
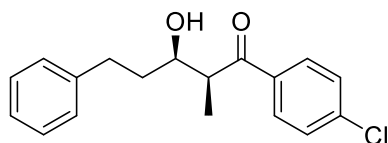
White solid; mp 94-96 ^{o}C.

IR (neat) ν = 3488, 2898, 1672, 1588, 1455, 1394, 1249, 1220, 1092, 967, 848, 697 cm^{-1}.

^{1}H NMR (600 MHz, *syn/anti* = 96/4); δ = 1.23 (d, *J* = 7.6 Hz, 2.88H), 1.42 (d, *J* = 6.9 Hz, 0.12H), 1.64-1.71 (m, 1H), 1.88-1.96 (m, 1H), 2.68 (ddd, *J* = 6.9, 9.6, 13.7 Hz, 1H), 2.87 (ddd, *J* = 5.5, 9.6, 13.7 Hz, 1H), 3.13 (brs, 1H), 3.35 (qd, *J* = 2.8, 7.2 Hz, 0.96H), 3.71-3.74 (m, 0.04H), 4.01-4.07 (m, 1H), 7.15-7.22 (m, 3H), 7.24-7.29 (m, 2H), 7.41 (d, *J* = 8.3 Hz, 1.92H), 7.45 (d, *J* = 8.7 Hz, 0.08H), 7.81 (d, *J* = 8.3 Hz, 1.92H), 7.84 (d, *J* = 8.7 Hz, 0.08H).

^{13}C NMR (*syn*, 150 MHz); δ = 11.1, 32.3, 36.0, 44.8, 44.8, 70.5, 125.9, 128.4, 128.4, 128.4, 128.4, 129.0, 129.8, 129.8, 134.0, 139.9, 141.7, 204.4.

HRMS (ESI-TOF, Pos.) calcd for $C_{18}H_{19}O_2Cl$ ([M+Na]$^+$): 325.0966, found: 325.0958.

HPLC (Dialcel Chiralpak AD-H (double), ^{n}hexane/ ^{i}PrOH = 19/1, flow rate 1.0 mL/min); t_R = 27.0 min (*anti*, major), t_R = 27.8 min (*anti*, minor), t_R = 40.7 min (*syn*, major), t_R = 46.1 min (*syn*, minor).

1,5-Diphenyl-3-hydroxy-2-ethylbutan-1-one (**3jd**)[13]
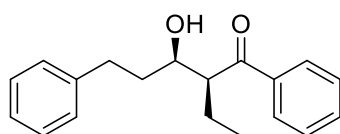
Colorless oil

^{1}H NMR (600 MHz, *syn/anti* = >99/<1); δ = 0.80 (t, *J* = 7.6 Hz, 3H), 0.85 (t, *J* = 7.3 Hz, <0.03H), 1.50-1.69 (m, <0.01H), 1.68 (dddd, *J* = 3.4, 6.6, 8.4, 15.3 Hz, 1H), 1.71-1.78 (m, 1H), 1.78-1.86 (m, 2H), 2.59 (ddd, *J* = 6.6, 9.7, 13.7 Hz, 2H), 2.74 (brs, 1H), 2.79 (ddd, *J* = 5.3, 9.6, 14.1 Hz, 1H), 3.38 (q, *J* = 4.7 Hz, 1H), 3.40-3.44 (m, <0.01H), 3.72-3.77 (m, <0.01H), 3.83-3.90 (m, 1H), 7.10 (d, *J* = 7.6 Hz, 2H), 7.15-7.20 (m, 2H), 7.39 (t, *J* = 7.6 Hz, 2H), 7.42 (t, *J* = 7.8 Hz, <0.02H), 7.50 (t, *J* = 7.6 Hz, 1H), 7.54 (t, *J* = 7.4 Hz, <0.01H), 7.85 (d, *J* = 6.9 Hz, 2H), 7.95 (d, *J* = 5.5 Hz, <0.02H).

^{13}C NMR (*syn*, 150 MHz); δ = 12.4, 20.6, 32.4, 36.6, 52.1, 71.4, 125.8, 128.4, 128.4, 128.4, 128.4, 128.4, 128.4, 128.7, 128.8, 133.4, 137.4, 141.7, 205.4.

HPLC (Dialcel Chiralcel OD-H, ^{n}hexane/ ^{i}PrOH = 19/1, flow rate 0.5 mL/min); t_R = 24.8 min (*syn*, minor), t_R = 36.2 min (*anti*), t_R = 41.2 min (*syn*, major), t_R = 49.3 min (*anti*).

4-Benzyloxy-3-hydroxy-2-methyl-1-phenylbutan-1-one (**3ka**)[14]
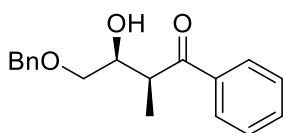
Colorless oil

^{1}H NMR (600 MHz, *syn/anti* = 99/1); δ = 1.24 (d, *J* = 7.6 Hz, 0.03H), 1.27 (d, *J* = 7.6 Hz, 2.97H), 2.98 (brs, 1H), 3.48 (dd, *J* = 5.6, 9.6 Hz, 1H), 3.54 (dd, *J* = 5.0, 9.5 Hz, 1H), 3.69-3.75 (m, 0.99H), 3.79-3.84 (m, 0.01H), 4.21 (q, *J* = 5.5 Hz, 1H), 4.48 (d, *J* = 2.8 Hz, 2H), 7.24-7.34 (m, 5H), 7.46 (t, *J* = 7.6 Hz, 2H), 7.57 (t, *J* = 7.6 Hz, 1H), 7.95 (d, *J* = 7.6 Hz, 2H).

^{13}C NMR (*syn*, 150 MHz); δ = 12.8, 42.5, 71.1, 71.5, 73.3, 127.7, 127.7, 128.3, 128.3, 128.4, 128.4, 128.6, 128.6, 133.3, 136.1, 137.8, 204.3.

HPLC (Dialcel Chiralcel OJ-H, ^{n}hexane/ ^{i}PrOH = 9/1, flow rate 1.0 mL/min); t_R = 17.7 min (*syn*, minor), t_R = 22.6 min (*syn*, major), t_R = 24.3 min (*anti*, major), t_R = 41.1 min (*anti*, minor).

3-Hydroxy-2-methyl-1-phenylpentan-1-one (**3la**)[15]
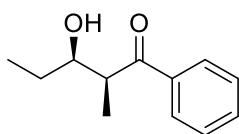
Colorless oil

^{1}H NMR (600 MHz, *syn/anti* = 94/6); δ = 0.93 (t, *J* = 7.5 Hz, 3H), 1.18 (d, *J* = 7.6 Hz, 3H), 1.36-1.46 (m, 1H), 1.50-1.58 (m, 1H), 2.88 (brs, 0.06H), 3.08 (brs, 0.94H), 3.42 (qd, *J* = 3.1, 7.2 Hz, 0.94H), 3.48-3.53 (m, 0.06H), 3.70-3.76 (m, 0.06H), 3.84-3.90 (m, 0.94H), 7.41 (dd, *J* = 7.8, 7.8 Hz, 2H), 7.51 (t, *J* = 7.2 Hz, 1H), 7.87 (d, *J* = 7.8 Hz, 2H).

^{13}C NMR (*syn*, 150 MHz); δ = 10.5, 11.0, 27.2, 44.1, 72.8, 128.4, 128.7, 133.4, 135.9, 205.8.

HRMS (ESI-TOF, Pos.) calcd for $C_{12}H_{16}O_2$ ([M+Na]$^+$): 215.1048, found: 215.1062.

HPLC (Dialcel Chiralpak AS-H, ^{n}hexane/ ^{i}PrOH = 60/1, flow rate 0.5 mL/min); t_R = 36.9 min (*syn*, minor), t_R = 40.4 min (*anti*, minor), t_R = 65.0 min (*syn*, major), t_R = 143.2 min (*anti*, major).

3-Hydroxy-1-(4'-methoxyphenyl)-2-methyl-pentan-1-one (**3lb**)[16]
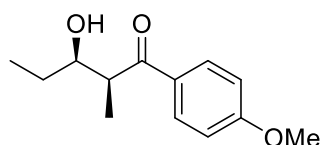
Colorless oil

^{1}H NMR (600 MHz, *syn/anti* = 95/5); δ = 0.99 (t, *J* = 7.6 Hz, 0.15H), 1.00 (t, *J* = 6.9 Hz, 2.85H), 1.24 (d, *J* = 7.6 Hz, 2.85H), 1.27 (d, *J* = 6.9 Hz, 0.15H), 1.42-1.50 (m, 1H), 1.57-1.68 (m, 1H), 3.34 (brs, 1H), 3.45 (qd, *J* = 2.9, 7.3 Hz, 0.95H), 3.50-3.55 (m, 0.05H), 3.88 (s, 2.85H), 3.89 (s, 0.15H), 6.96 (d, *J* = 8.9 Hz, 2H), 7.94 (d, *J* = 8.9 Hz, 2H).

^{13}C NMR (*syn*, 150 MHz); δ = 10.5, 11.1, 27.1, 43.4, 55.5, 72.9, 113.8, 113.9, 128.7, 130.7, 163.8, 204.5.

HRMS (ESI-TOF, Pos.) calcd for $C_{13}H_{18}O_3$ ([M+Na]$^+$): 245.1148, found: 215.1158.

HPLC (Dialcel Chiralpak AS-H, ^{n}hexane/ ^{i}PrOH = 9/1, flow rate 0.5 mL/min); t_R = 20.9 min (*syn*, minor), t_R = 34.5 min (*syn*, major), t_R = 45.9 min (*anti*), t_R = 58.0 min (*anti*).

3-Hydroxy-1-(4'-chloro)-2-methyl-pentan-1-one (**3lc**)
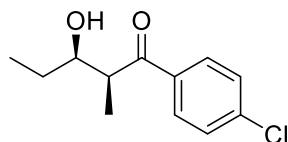
Colorless oil

IR (neat) ν = 3425, 2966, 2936, 2877, 1676, 1596, 1448, 1374, 1210, 1115, 966, 796, 707, 658 cm^{-1}.

^{1}H NMR (600 MHz, *syn/anti* = 95/5); δ = 0.98 (t, *J* = 6.9, 0.15H), 0.99 (t, *J* = 7.6 Hz, 2.85H), 1.25 (d, *J* = 6.9 Hz, 3H), 1.43-1.52 (m, 1H), 1.56-1.65 (m, 1H), 2.83 (brs, 0.05H), 3.03 (brs, 0.95H), 3.45 (qd, *J* = 3.2, 7.2 Hz, 0.95H), 3.49-3.55 (m, 0.05H), 3.88-3.99 (m, 0.95H), 5.08-5.15 (m, 0.05H), 7.45 (d, *J* = 8.8 Hz, 2H), 7.89 (d, *J* = 8.8 Hz, 2H).

^{13}C NMR (*syn*, 150 MHz); δ = 10.4, 11.1, 27.2, 44.3, 72.9, 129.0, 129.8, 134.3, 139.8, 204.3.

HRMS (ESI-TOF, Pos.) calcd for $C_{12}H_{15}O_2Cl$ ([M+Na]$^+$): 249.0653, found: 249.0658.

HPLC (Dialcel Chiralpak AS-H, ^{n}hexane/ ^{i}PrOH = 19/1, flow rate 0.4 mL/min); t_R = 24.2 min (*syn*, minor), t_R = 40.8 min (*anti*, major), t_R = 47.0 min (*syn*, major), t_R = 49.9 min (*anti*, minor).

3-Hydroxy-2-methyl-1-phenyloctan-1-one (**3ma**)[8]
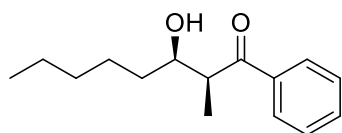
Colorless oil

^{1}H NMR (600 MHz, *syn/anti* = 95/5); δ = 0.89 (t, *J* = 6.8 Hz, 3H), 1.25 (d, *J* = 7.4 Hz, 3H), 1.28-1.62 (m, 8H), 3.16 (brs, 1H), 3.47 (qd, *J* = 3.0, 7.2 Hz, 0.95H), 3.53-3.60 (m, 0.05H), 3.84-3.90 (m, 0.05H), 4.00-4.06 (m, 0.95H), 7.48 (dd, *J* = 7.4, 7.7 Hz, 2H), 7.59 (t, *J* = 7.4 Hz, 1H), 7.91-7.98 (m, 2H).

^{13}C NMR (*syn*, 125 MHz); δ = 11.0, 14.0, 22.6, 25.7, 31.8, 34.3, 44.5, 71.3, 128.4, 128.7, 133.4, 135.9, 205.9.

HPLC (Dialcel Chiralpak AS-3+AS-H, ^{n}hexane/ ^{i}PrOH = 30/1, flow rate 0.5 mL/min); t_R = 39.2 min (*syn*, minor), t_R = 42.0 min (*anti*, minor), t_R = 59.8 min (*syn*, major), t_R = 124.4 min (*anti*, major).

3-Hydroxy-1-(4'-methoxyphenyl)-2-methyl-octan-1-one (**3mb**)
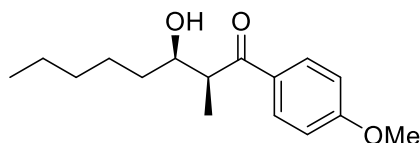
Colorless oil

IR (neat) ν = 3459, 2933, 2859, 1659, 1602, 1511, 1460, 1419, 1310, 1259, 1217, 1173, 1030, 969, 843, 766, 605 cm^{-1}.

^{1}H NMR (600 MHz, *syn/anti* = 93/7); δ = 0.89 (t, *J* = 6.9 Hz, 3H), 1.24 (d, *J* = 7.6 Hz, 3H), 1.26-1.43 (m, 6H), 1.47-1.54 (m, 1H), 1.55-1.63 (m, 1H), 3.30 (brs, 1H), 3.42 (qd, *J* = 2.8, 14.6 Hz, 0.93H), 3.47-3.53 (m, 0.07H), 3.88 (s, 3H), 3.98-4.05 (m, 0.93H), 4.12 (q, *J* = 7.15 Hz, 0.07H), 6.95 (d, *J* = 8.9 Hz, 2H), 7.94 (d, *J* = 8.9 Hz, 2H).

^{13}C NMR (*syn*, 125 MHz); δ = 11.1, 14.0, 22.6, 25.7, 31.8, 34.2, 43.9, 55.5, 71.4, 113.9, 128.8, 130.8, 163.8, 204.6.

HRMS (ESI-TOF, Pos.) calcd for C$_{16}$H$_{24}$O$_3$ ([M+Na]$^+$): 287.1618, found: 287.1630.

HPLC (Dialcel Chiralpak AS-H, ^{n}hexane/ ^{i}PrOH = 19/1, flow rate 0.8 mL/min); t_R = 17.7 min (*syn*, minor), t_R = 21.6 min (*anti*, minor), t_R = 27.3 min (*syn*, major), t_R = 68.5 min (*anti*, minor).

2-Ethyl-3-hydroxy-1-phenyloctan-1-one (**3md**)[17]
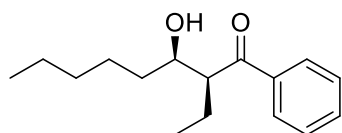
Colorless oil

^{1}H NMR (600 MHz, *syn/anti* = 91/9); δ = 0.84-0.91 (m, 6H), 1.21-1.38 (m, 4H), 1.40-1.58 (m, 4H), 1.78-1.96 (m, 2H), 2.72 (brs, 0.91H), 3.08 (brs, 0.09H), 3.48 (td, *J* = 4.4, 9.0 Hz, 1H), 3.90 (td, *J* = 4.1, 8.3 Hz, 1H), 7.49 (dd, *J* = 7.5, 7.7 Hz, 2H), 7.59 (t, *J* = 7.5 Hz, 1H), 7.95-8.00 (m, 2H).

^{13}C NMR (*syn*, 150 MHz); δ = 12.3, 14.0, 20.5, 22.5, 25.8, 31.7, 35.0, 52.2, 72.0, 128.3, 128.7, 133.3, 137.6, 205.4.

HRMS (ESI-TOF, Pos.) calcd for C$_{17}$H$_{26}$O$_2$ ([M+Na]$^+$): 271.1669, found: 271.1676.

HPLC (Dialcel Chiralpak AS-H, ^{n}hexane/ ^{i}PrOH = 40/1, flow rate 0.5 mL/min); t_R = 17.3 min (*anti*, minor), t_R = 20.9 min (*syn*, minor), t_R = 26.6 min (*syn*, major), t_R = 52.4 min (*anti*, minor).

3-Hydroxy-5-((4-methoxybenzyl)oxy)-2-methyl-1-phenylhexan-1-one (**3na**)
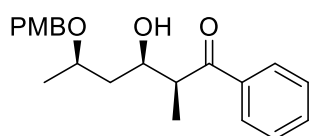
Colorless oil

IR (neat) ν = 3465, 2971, 1679, 1602, 1513, 1375, 1257, 1163, 1030, 971, 833, 772, 713, 606 cm^{-1}.
^{1}H NMR (600 MHz); δ (*syn*, 91% ee) = 1.21 (d, *J* = 6.2 Hz, 3H), 1.24 (d, *J* = 2.8 Hz, 0.12H), 1.26 (d, *J* = 6.9 Hz, 2.88H), 1.57-1.62 (m, 1H), 1.66-1.74 (m, 1H), 3.50 (q, *J* = 6.9 Hz, 0.96H), 3.53-3.58 (m, 0.04H), 3.78 (s, 3H), 3.80-3.85 (m, 1H), 4.14-4.18 (m, 1H), 4.36 (d, *J* = 11.0 Hz, 0.96H), 4.39 (d, *J* = 11.0 Hz, 0.04H), 4.57 (d, *J* = 11.0 Hz, 0.96H), 6.83-6.89 (m, 2H), 7.22-7.27 (m, 2H), 7.46 (dd, *J* = 7.1, 7.6 Hz, 2H), 7.57 (t, *J* = 7.6 Hz, 1H), 7.88 (d, *J* = 7.1 Hz, 0.08H), 7.94 (d, *J* = 7.1 Hz, 1.92H).   δ (*anti*, 91% ee) = 1.26 (d, *J* = 7.6 Hz, 2.88H), 1.29 (d, *J* = 7.6 Hz, 0.12H), 1.38 (d, *J* = 6.2 Hz, 0.12H), 1.42 (d, *J* = 6.2 Hz, 2.88H), 1.77-1.84 (m, 1H), 2.04-2.11 (m, 1H), 3.56 (qd, *J* = 3.2, 7.2 Hz, 1H), 3.85 (s, 2.88H), 3.87 (s, 0.12H), 4.21-4.26 (m, 1H), 5.33-5.39 (m, 1H), 6.89 (d, *J* = 8.8 Hz, 1.92H), 6.92 (d, *J* = 8.9 Hz, 0.08H), 7.42 (dd, *J* = 7.5, 7.9 Hz, 2H), 7.56 (t, *J* = 7.5 Hz, 1H), 7.91 (d, *J* = 7.1 Hz, 1H), 7.96 (d, *J* = 8.8 Hz, 1.92H), 8.00 (d, *J* = 8.9 Hz, 0.08H).
^{13}C NMR (150 MHz); δ (2*S*, 3*R*, 5*R*) = 13.2, 19.5, 41.4, 46.0, 55.2, 70.0, 72.1, 75.2, 113.9, 128.4, 128.6, 129.4, 130.1, 133.1, 136.5, 159.2, 204.3.   δ (2*R*, 3*S*, 5*R*) = 12.1, 19.5, 41.1, 45.2, 55.2, 68.8, 70.3, 72.1, 113.8, 128.4, 128.7, 129.4, 130.6, 133.3, 136.0, 159.1, 205.4.   δ (2*R*, 3*R*, 5*R*) = 11.1, 20.4, 40.3, 44.1, 55.4, 68.6, 69.0, 113.6, 122.9, 128.5, 128.7, 131.6, 133.5, 166.0, 205.4.
HRMS (ESI-TOF, Pos.) calcd for $C_{21}H_{26}O_4$ ([M+Na]$^{+}$): 365.1729, found: 365.1740.

3-Hydroxy-2-methyl-1-phenyl-3-(thiophen-2-yl)propan-1-one (**3oa**)[7]
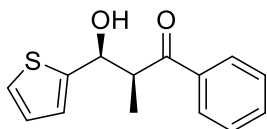
Colorless oil
^{1}H NMR (600 MHz, *syn/anti* = 98/2); δ = 1.17 (d, *J* = 6.9 Hz, 0.06H), 1.32 (d, *J* = 6.8 Hz, 2.94H), 3.59 (brs, 1H), 3.80 (qd, *J* = 4.1, 6.9 Hz, 1H), 3.85-3.91 (m, 0.02H), 5.26 (d, *J* = 7.6 Hz, 0.02H), 5.47 (d, *J* = 3.4 Hz, 0.98H), 6.96 (dd, *J* = 3.4, 4.1 Hz, 1H), 6.99 (d, *J* = 3.4 Hz, 1H), 7.22 (d, *J* = 4.1 Hz, 2H), 7.48 (dd, *J* = 7.3, 7.6 Hz, 2H), 7.59 (t, *J* = 7.3 1H), 7.94 (d, *J* = 7.6 Hz, 1.96H), 7.99 (d, *J* = 7.6 Hz, 0.04H).
^{13}C NMR (*syn*, 150 MHz); δ = 12.2, 47.7, 70.5, 123.5, 124.2, 126.6, 128.4, 128.8, 133.6, 135.5, 145.8, 204.9.
HPLC (Dialcel Chiralcel OD-H, ^{n}hexane/ ^{i}PrOH = 98/2, flow rate 0.5 mL/min); t_R = 43.8 min (*syn*, minor), t_R = 51.9 min (*syn*, major), t_R = 66.1 min (*anti*, minor), t_R = 74.0 min (*anti*, major).

3-(Furan-2-yl)-3-hydroxy-2-methyl-1-phenylpropan-1-one (**3pa**)[18]
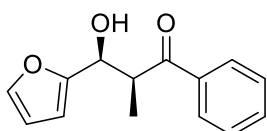
Colorless oil
^{1}H NMR (600 MHz, *syn/anti* = 99/1); δ = 1.15 (d, *J* = 7.6 Hz, 0.03H), 1.30 (d, *J* = 7.6 Hz, 2.97H), 3.37 (brs, 1H), 3.94 (qd, *J* = 4.1, 7.6 Hz, 0.99H), 4.05-4.11 (m, 0.01H), 5.02 (d, *J* = 6.9 Hz, 0.01H), 5.21 (d, *J* = 3.4 Hz, 0.99H), 6.28-6.34 (m, 2H), 7.34 (brs, 0.99H), 7.37 (brs, 0.01H), 7.48 (t, *J* = 7.6 Hz, 2H), 7.59 (t, *J* = 7.6 Hz, 1H), 7.96 (d, *J* = 6.9 Hz, 0.99H), 7.99 (d, *J* = 6.9 Hz, 0.01H).

^{13}C NMR (*syn*, 150 MHz); δ = 12.4, 44.6, 68.6, 106.6, 110.2, 128.4, 128.4, 128.7, 128.7, 133.5, 135.5, 141.6, 154.5, 204.5.

HPLC (Dialcel Chiralcel OD-H, ^{n}hexane/ ^{i}PrOH = 98/2, flow rate 0.5 mL/min); t_R = 26.1 min (*anti*), t_R = 32.1 min (*anti*), t_R = 38.8 min (*syn*, minor), t_R = 46.4 min (*syn*, major).

3-Hydroxy-2-methyl-1-phenyl-3-(pyridin-2-yl)propan-1-one (3qa)[7]
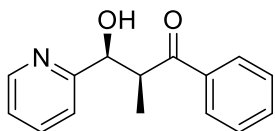
Colorless oil

^{1}H NMR (600 MHz, *syn/anti* = 36/64); δ = 1.15 (d, *J* = 6.9 Hz, 1.02H), 1.22 (d, *J* = 6.9 Hz, 1.98H), 4.08 (qd, *J* = 3.4, 7.0 Hz, 0.36H), 4.16-4.22 (m, 0.64H), 5.02 (d, *J* = 5.9 Hz, 0.64H), 5.23 (d, *J* = 3.7 Hz, 0.36H), 7.15 (td, *J* = 7.4, 4.9 Hz, 1H), 7.39-7.47 (m, 3.64H), 7.50 (d, *J* = 7.9 Hz, 0.36H), 7.63-7.68 (m, 1H), 7.94-7.98 (m, 2H), 8.51 (d, *J* = 4.5 Hz, 0.64H), 8.53 (d, *J* = 4.7 Hz, 0.36H).

^{13}C NMR (*syn*, 150 MHz); δ = 11.6, 46.2, 73.7, 121.3, 122.3, 128.6, 128.7, 133.4, 135.9, 136.6, 148.6, 160.6, 205.2, (*anti*); δ = 15.0, 46.0, 76.5, 121.6, 122.5, 128.5, 128.6, 133.2, 136.5, 136.6, 148.7, 160.9, 205.1.

HRMS (ESI-TOF, Pos.) calcd for $C_{15}H_{16}NO_2$ ([M+H]$^{+}$): 242.1181, found: 242.1188.

HPLC (Dialcel Chiralpak AS-H, ^{n}hexane/ ^{i}PrOH = 9/1, flow rate 0.5 mL/min); t_R = 19.0 min (*syn*, minor), t_R = 27.4 min (*syn*, major), t_R = 29.5 min (*anti*, minor), t_R = 34.6 min (*anti*, major).

2-Hydroxy-3-methyl-4-oxo-4-phenyl-butyric acid ethyl ester (3ra)[19]
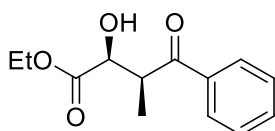
Colorless oil

^{1}H NMR (600 MHz, *syn/anti* = 82/18); δ = 1.20 (t, *J* = 7.6 Hz, 0.54H), 1.26 (t, *J* = 6.9 Hz, 2.46H), 1.30 (d, *J* = 6.9 Hz, 1.64H), 1.36 (d, *J* = 7.6 Hz, 0.36H), 3.32 (d, *J* = 4.1 Hz, 0.82H), 3.60 (d, *J* = 8.3 Hz, 0.18H), 3.93 (ddd, *J* = 4.1, 6.9, 14.4 Hz, 0.82H), 3.96-4.01 (m, 0.18H), 4.12-4.19 (m, 0.36H), 4.26 (dd, *J* = 6.9, 14.4 Hz, 1.64H), 4.39 (dd, *J* = 4.8, 8.2 Hz, 0.18H), 4.59 (t, *J* = 4.1 Hz, 0.82H), 7.47-7.52 (m, 2H), 7.59 (t, *J* = 7.6 Hz, 1H), 7.93 (d, *J* = 8.2 Hz, 1.64H), 7.96 (d, *J* = 6.9 Hz, 0.36H).

^{13}C NMR (*syn*, 150 MHz); δ (*syn*) = 12.1, 14.0, 44.0, 44.3, 61.5, 61.9, 71.6, 73.1, 128.3, 128.4, 128.7, 128.7, 133.3, 135.7, 173.1, 201.6; δ (*anti*) = 12.1, 14.1, 44.0, 44.3, 61.6, 62.0, 71.6, 73.2, 128.4, 128.4, 128.7, 128.8, 133.5, 136.0, 173.2, 201.7.

HPLC (Dialcel Chiralpak AS-H, ^{n}hexane/ ^{i}PrOH = 9/1, flow rate 0.5 mL/min); t_R = 37.3 min (*syn*, major), t_R = 41.3 min (*syn*, minor), t_R = 55.3 min (*anti*, major), t_R = 68.1 min (*anti*, minor).

2-Hydroxy-3-methyl-4-oxo-4-phenyl-butyric acid isopropyl ester (3sa)[19]
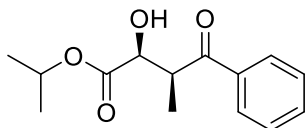
Colorless oil

^{1}H NMR (400 MHz, *syn/anti* = 89/11); δ = 3.63 (d, *J* = 3.7 Hz, 0.89H), 3.84 (d, *J* = 7.0 Hz, 0.11H), 5.05 (sep, *J* = 5.0 Hz, 0.89H), 5.10 (sep, *J* = 5.4 Hz, 0.11H), 6.95-7.01 (m, 2H), 7.03-7.09 (m, 1H), 7.31-7.37 (m, 2H).

^{13}C NMR (*syn*, 100 MHz); δ (*syn*) = 29.8, 37.3, 37.4, 55.6, 76.0, 77.4, 122.8, 123.1, 126.7, 128.8, 158.3, 181.3.

HPLC (Dialcel Chiralpak AD-H+AS, ^{n}hexane/ ^{i}PrOH = 9/1, flow rate 0.5 mL/min); t_R = 51.0 min (*syn*, major), t_R = 54.1 min (*syn*, minor), t_R = 57.4 min (*anti*, major), t_R = 86.2 min (*anti*, minor).

3-Hydroxy-2-methyl-1-phenylpropan-1-one (**3ta**)[20]
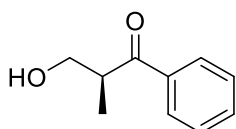
Colorless oil

^{1}H NMR (500 MHz); δ = 1.24 (d, *J* = 7.1 Hz, 3 H), 2.35 (brs, 1H), 3.68 (ddq, *J* = 4.3, 7.0, 7.1 Hz, 1H), 3.80 (dd, *J* = 4.3, 11.1 Hz, 1H), 3.94 (dd, *J* = 7.0, 11.1 Hz, 1H), 7.48 (dd, *J* = 7.3, 8.5 Hz, 2H), 7.58 (t, *J* = 7.3 Hz, 1H), 7.97 (d, *J* = 8.5 Hz, 2H).

^{13}C NMR (*syn*, 125 MHz); δ = 14.5, 42.9, 64.5, 128.4, 128.7, 133.3, 136.1, 204.4.

HPLC (Dialcel Chiralpak AD-H, ^{n}hexane/ ^{i}PrOH = 19/1, flow rate 1.0 mL/min); t_R = 17.5 min (major), t_R = 20.3 min (minor).

$[\alpha]_D^{23}$ = $-$ 41.1 (*c* = 0.90, EtOH).

3-Hydroxy-2-methyl-1-(4'-methoxyphenyl)propan-1-one (**3tb**)[20]
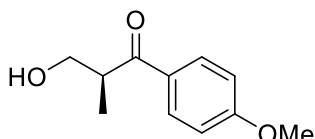
Colorless oil

^{1}H NMR (500 MHz); δ = 1.22 (d, *J* = 7.1 Hz, 3 H), 2.60 (brs, 1H), 3.62 (ddq, *J* = 4.3, 7.0, 7.1 Hz, 1H), 3.78 (dd, *J* = 4.3, 11.0 Hz, 1H), 3.87 (s, 3H), 3.91 (dd, *J* = 7.0, 11.0 Hz, 1H), 6.95 (d, *J* = 8.9 Hz, 2H), 7.95 (d, *J* = 8.9 Hz, 2H).

^{13}C NMR (*syn*, 125 MHz); δ = 14.7, 42.4, 55.4, 64.6, 113.8, 129.0, 130.7, 163.6, 202.9.

HPLC (Dialcel Chiralpak AD-H, ^{n}hexane/ ^{i}PrOH = 19/1, flow rate 1.0 mL/min); t_R = 30.7 min (major), t_R = 38.9 min (minor).

$[\alpha]_D^{24}$ = 4.2 (*c* = 1.5, CHCl$_3$).

3-Hydroxy-2-methyl-1-(4'-chlorophenyl)propan-1-one (**3tc**)[20]
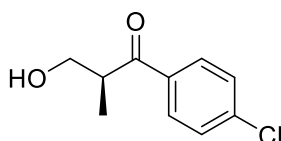
Colorless oil

^{1}H NMR (500 MHz); δ = 1.21 (d, *J* = 7.3 Hz, 3 H), 2.52 (brs, 1H), 3.62 (ddq, *J* = 4.3, 7.2, 7.3 Hz, 1H), 3.77 (dd, *J* = 4.3, 11.0 Hz, 1H), 3.87 (s, 3H), 3.93 (dd, *J* = 7.2, 11.0 Hz, 1H), 7.44 (d, *J* = 8.5 Hz, 2H), 7.90 (d, *J* = 8.5 Hz, 2H).

^{13}C NMR (*syn*, 125 MHz); δ = 14.4, 43.0, 55.4, 64.4, 129.0, 129.8, 134.4, 139.7, 203.0.

HPLC (Dialcel Chiralpak AD-H, ^{n}hexane/ ^{i}PrOH = 19/1, flow rate 1.0 mL/min); t_R = 18.6 min (major), t_R = 28.7 min (minor).

$[α]_D^{24}$ = 4.1 (*c* = 1.05, CHCl$_3$).

3-Hydroxy-2-methyl-1-phenyl-1-butanone (**3ua**)[21]
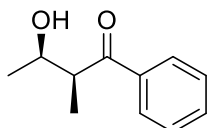
Colorless oil

^{1}H NMR (600 MHz, *syn/anti* = 98/2); δ = 1.24 (d, *J* = 6.2 Hz, 3H), 1.28 (d, *J* = 7.6 Hz, 3H), 2.93 (brs, 0.02H), 3.18 (brs, 0.98H), 3.43 (qd, *J* = 3.2, 7.6 Hz, 0.98H), 3.47-3.52 (m, 0.02H), 4.12 (q, *J* = 6.2 Hz, 0.02H), 4.25 (qd, *J* = 3.4, 6.5 Hz, 0.98H), 7.49 (dd, *J* = 7.6, 7.6 Hz, 2H), 7.59 (t, *J* = 7.2 Hz, 1H), 7.95 (d, *J* = 7.6 Hz, 2H).

^{13}C NMR (*syn*, 150 MHz); δ = 11.2, 20.3, 45.7, 67.4, 128.4, 128.7, 133.4, 135.9, 205.8.

HRMS (ESI-TOF, Pos.) calcd for C$_{12}$H$_{16}$O$_2$ ([M+Na]$^+$): 201.1148, found: 201.1158.

HPLC (Dialcel Chiralcel OD-H (double), ^{n}hexane/ ^{i}PrOH = 100/1, flow rate 0.3 mL/min); t_R = 20.9 min (*syn*, minor), t_R = 34.5 min (*syn*, major), t_R = 45.9 min (*anti*), t_R = 119.9 min (*anti*).

4-Chloro-3-hydroxy-2-methyl-1-phenyl-1-butanone (**3va**)[11]
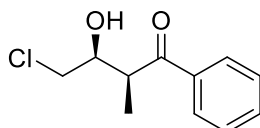
Colorless oil

^{1}H NMR (400 MHz, *syn/anti* = >99/<1); δ = 2.50 (d, *J* = 5.7 Hz, 3H), 3.91 (brs, 1H), 4.36 (d, *J* = 4.7 Hz, 2H), 4.50 (qd, *J* = 3.9, 5.7 Hz, >0.99H), 4.55-4.62 (m, <0.01H), 4.72-4.78 (m, <0.01H), 4.83-4.90 (m, >0.99H), 7.43-7.50 (m, 2H), 7.54 (t, *J* = 5.9 Hz, 1H), 7.83 (d, *J* = 5.7 Hz, 2H).

^{13}C NMR (*syn*, 100 MHz); δ = 32.2, 53.8, 57.9, 79.0, 122.9, 123.1, 123.2, 127.1, 129.0, 183.9.

The ee value was determined as acetate;

1-Chloro-3-methyl-4-oxo-4-phenylbutan-2-yl acetate
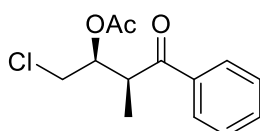
Colorless oil

IR (neat) ν = 3449, 2983, 2935, 1744, 1679, 1449, 1372, 1229, 1038, 969, 703 cm^{-1}.

^{1}H NMR (600 MHz, *syn/anti* = >99/<1); δ = 1.27 (d, *J* = 7.6 Hz, 3H), 2.11 (s, 3H), 3.72 (dd, *J* = 4.8,

11.7 Hz, 1H), 3.78 (dd, J = 3.4, 12.4 Hz, 1H), 4.06 (td, J = 7.6, 13.6 Hz, 1H), 5.39-5.42 (m, <0.01H), 5.47 (quin, J = 4.1 Hz, >0.99H), 7.50 (t, J = 7.6 Hz, 2H), 7.60 (t, J = 8.3 Hz, 1H), 7.96 (d, J = 8.3 Hz, 2H).

^{13}C NMR (*syn*, 150 MHz); δ = 14.2, 20.8, 41.6, 44.5, 73.8, 128.4, 128.8, 133.6, 135.9, 170.2, 201.3.

HRMS (ESI-TOF, Pos.) calcd for $C_{13}H_{15}O_3Cl$ ([M+H]$^+$): 255.0788, found: 255.0795.

HPLC (Dialcel Chiralpak AD-H (double), ^{n}hexane/ ^{i}PrOH = 19/1, flow rate 0.5 mL/min); t_R = 28.6 min (*syn*, minor), t_R = 30.1 min (*syn*, major), t_R = 32.9 min (*anti*, major), t_R = 35.1 min (*anti*, minor).

1-Hydroxy-2-methyl-1-phenylpentan-3-one (**3ae**)[7]
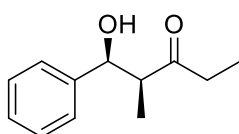
Colorless oil

IR (KBr) ν= 3527, 1685, 1590, 1469, 1365, 1296, 1029, 748 cm^{-1}.

^{1}H NMR (600 MHz, *syn/anti* = 90/10); δ = 0.94 (d, J = 7.4 Hz, 0.3H), 1.00 (t, J = 7.4 Hz, 0.3H), 1.04 (t, J = 7.2 Hz, 2.7H), 1.08 (d, J = 7.2 Hz, 2.7H), 2.31-2.59 (m, 2H), 2.84 (qd, J = 4.1, 7.2 Hz, 0.9H), 2.94 (quin, J = 7.4 Hz, 0.1H), 3.13 (brs, 1H), 4.76 (q, J = 8.2 Hz, 0.1H), 5.06 (d, J = 4.0 Hz, 0.9H), 7.24-7.38 (m, 5H).

^{13}C NMR (*syn*, 150 MHz); δ (*syn*) = 7.5, 10.6, 52.2, 73.3, 125.9, 127.4, 128.2, 141.8, 216.2.

HPLC (Dialcel Chiralcel OJ-H, ^{n}hexane/ ^{i}PrOH = 19/1, flow rate 0.4 mL/min); t_R = 33.1 min (*anti*, minor), t_R = 34.4 min (*syn*, minor), t_R = 36.2 min (*anti*, major), t_R = 40.4 min (*syn*, major).

5-Hydroxy-4-methylhexan-3-one (**3ue**)[22]
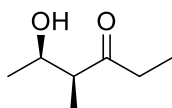
Colorless oil (isolated as 4'-bromobenzoate)

^{1}H NMR (400 MHz, *syn/anti* = 88/12); δ = 1.83 (t, J = 5.8 Hz, 3H), 1.91 (d, J = 5.8 Hz, 0.36H), 1.94 (d, J = 5.7 Hz, 2.64H), 2.06 (d, J = 5.1 Hz, 3H), 3.01 (qd, J = 3.4, 5.8 Hz, 2H), 3.30 (q, J = 5.0 Hz, 0.88H), 3.30-3.40 (m, 0.12H), 3.32 (q, J = 5.0 Hz, 1H), 7.05 (d, J = 6.8 Hz, 1.76H), 7.09 (d, J = 6.8 Hz, 0.24H), 7.28 (d, J = 6.8 Hz, 1.76H), 7.38 (d, J = 6.8 Hz, 0.24H).

^{13}C NMR (*syn*, 100 MHz); δ (*syn*) = 8.2, 12.3, 16.9, 34.6, 51.3, 72.7, 127.4, 129.1, 132.1, 131.5, 165.9, 212.1.

HPLC (Dialcel Chiralpak AD-H, ^{n}hexane/ ^{i}PrOH = 19/1, flow rate 1.0 mL/min); t_R = 7.20 min (*anti*, minor), t_R = 7.69 min (*syn*, major), t_R = 8.38 min (*syn*, minor), t_R = 9.84 min (*anti*, major).

2-(1-Hydroxy-3-phenylpropyl)-2-methyl-3,4-dihydronaphthalen-1(2H)-one (**3jg**)

Experimental Section
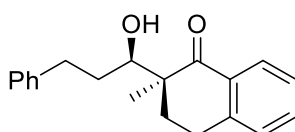
Colorless crystal; mp 86-87 °C.

IR (neat) ν = 3467, 2934, 2361, 1672, 1600, 1454, 1304, 1224, 1066, 970, 743, 700 cm^{-1}.

^{1}H NMR (600 MHz, syn/anti = 98/2); δ = 1.15 (s, 3H), 1.63-1.69 (m, 2H), 1.80-1.84 (m, 2H), 2.55-2.61 (m, 1H), 2.75 (dt, J = 4.1, 17.2 Hz, 1H), 2.88-2.98 (m, 2H), 3.83 (dd, J = 3.4, 17.9 Hz, 1H), 3.95 (brs, 1H), 7.06-7.23 (m, 7H), 7.38 (dt, J = 1.3, 7.6 Hz, 1H), 7.92 (d, J = 7.6 Hz, 2H).

^{13}C NMR (syn, 150 MHz); δ = 15.0, 24.9, 31.0, 32.5, 47.9, 60.3, 74.2, 125.7, 126.8, 128.0, 128.3, 128.5, 128.5, 131.2, 133.7, 142.4, 143.2, 205.3.

HRMS (ESI-TOF, Pos.) calcd for C$_{20}$H$_{22}$O$_2$ ([M+H]$^+$): 295.1698, found: 295.1696.

HPLC (Dialcel Chiralpak AD-H (double), ^{n}hexane/ ^{i}PrOH = 19/1, flow rate 1.0 mL/min); t$_R$ = 32.4 min (syn, minor), t$_R$ = 36.1 min (anti), t$_R$ = 38.3 min (syn, major), t$_R$ = 57.8 min (anti).

2-Hydroxy-2-(2-methyl-1-oxo-1,2,3,4-tetrahydronaphthalen-2-yl)acetic acid ethyl ester (**3rg**)[23]
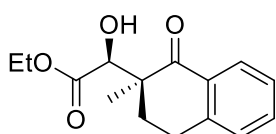
Colorless oil

^{1}H NMR (600 MHz, syn/anti = 90/10); δ = 1.08 (t, J = 7.6 Hz, 2.7H), 1.27 (t, J = 6.9 Hz, 0.3H), 1.36 (s, 2.7H), 1.40 (s, 0.3H), 1.78 (dt, J = 5.8, 13.5 Hz, 0.1H), 1.98 (dt, J = 4.7, 13.5 Hz, 0.9H), 2.03-2.11 (m, 0.9H), 2.19-2.29 (m, 0.1H), 2.92 (dt, J = 4.7, 17.1 Hz, 0.9H), 3.00-3.06 (m, 0.9H), 3.07-3.15 (m, 0.1H), 3.28 (d, J = 4.7 Hz, 0.9H), 3.35 (d, J = 7.0 Hz, 0.1H), 4.16 (q, J = 7.0 Hz, 1.8H), 4.21-4.25 (m, 0.2H), 4.55 (d, J = 7.0 Hz, 0.1H), 4.61 (d, J = 4.3 Hz, 0.9H), 7.23 (d, J = 7.7 Hz, 0.9H), 7.26 (d, J = 6.7 Hz, 0.1H), 7.32 (t, J = 7.6 Hz, 0.9H), 7.35 (t, J = 7.4 Hz, 0.1H), 7.53 (t, J = 7.5 Hz, 0.1H), 8.01 (d, J = 7.7 Hz, 0.1H), 8.03 (d, J = 7.9 Hz, 0.9H).

^{13}C NMR (syn, 150 MHz); δ (syn) = 29.8, 37.3, 37.4, 55.6, 76.0, 77.4, 122.8, 123.1, 126.7, 128.8, 158.3, 181.3.

HPLC (Dialcel Chiralpak IA, ^{n}hexane/ ^{i}PrOH = 9/1, flow rate 1.0 mL/min); t$_R$ = 51.0 min (anti, major), t$_R$ = 54.1 min (anti, minor), t$_R$ = 57.4 min (syn, minor), t$_R$ = 86.2 min (syn, major).

(S)-2-((R)-Hydroxy(phenyl)methyl)cyclohexan-1-one (**3am**)[24]
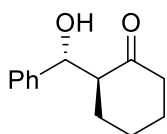
Colorless oil

IR (KBr) ν= 3486, 1698, 1605, 1464, 1329, 1296, 1209, 1039, 770 cm^{-1}.

^{1}H NMR (500 MHz, syn/anti = 21/79) δ= 1.22-1.37 (m, 1H), 1.48-1.60 (m, 2H), 1.60-1.70 (1H, m), 1.84-1.75 (m, 1H), 2.04-2.11 (m, 1H), 2.31-2.42 (m, 1H), 2.42-2.52 (m, 1H), 2.58-2.65 (m, 1H), 3.97 (d, J = 2.6 Hz, 1H), 4.79 (d, J = 8.8 Hz, 0.79H), 5.04 (d, J = 8.8 Hz, 0.21H), 7.24-7.34 (m, 5H).

^{13}C NMR (125 MHz) δ (anti) = 24.7, 27.8, 30.8, 42.6, 57.4, 74.7, 127.0, 127.9, 128.3, 140.9, 215.6.

HPLC (Daicel Chiralpak AD-H, ^{n}hexane/ ^{i}PrOH = 19/1, flow rate = 0.5 ml/min); t$_R$ = 22.3 min (syn, major), t$_R$ = 27.2 min (syn, minor), t$_R$ = 41.1 min (anti, major), t$_R$ = 42.6 min (anti, minor).

(*S*)-2-((*R*)-hydroxy(phenyl)methyl)cyclopentan-1-one (**3an**)[25]
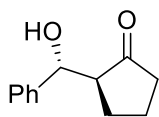
Colorless oil

IR (KBr) ν= 3522, 1700, 1596, 1462, 1335, 1295, 1029, 768 cm^{-1}.

^{1}H NMR (500 MHz, *syn/anti* = 13/87) δ= 1.22-1.37 (m, 1H), 1.48-1.60 (m, 2H), 2.04-2.11 (m, 1H), 2.31-2.42 (m, 1H), 2.42-2.52 (m, 1H), 2.58-2.65 (m, 1H), 3.97 (d, *J* = 2.6 Hz, 1H), 4.79 (d, *J* = 8.8 Hz, 0.87H), 5.04 (d, *J* = 8.8 Hz, 0.13H), 7.26-7.34 (m, 5H)

^{13}C NMR (125 MHz) δ (*anti*) = 24.7, 27.8, 30.8, 42.6, 57.4, 74.7, 127.0, 127.9, 128.3, 140.9, 215.6.

HPLC (Daicel Chiralpak AD-H, ^{n}hexane/ ^{i}PrOH = 19/1, flow rate = 0.5 ml/min); t$_R$ = 21.3 min (*syn*, major), t$_R$ = 28.2 min (*syn*, minor), t$_R$ = 45.1 min (*anti*, major), t$_R$ = 49.6 min (*anti*, minor).

(2*S*,3*R*)-*S*-(*tert*-Butyl)-3-hydroxy-2-methyl-3-phenylpropanethioate (**3ai**)[26]
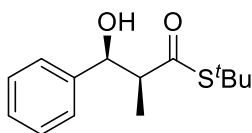
^{1}H NMR (500 MHz, *syn/anti* = 96/4) δ= 1.01 (d, 0.12H, *J* = 6.8 Hz), 1.13 (d, 2.88H, *J* = 7.2 Hz), 1.43 (s, 8.64H), 1.47 (s, 0.36H), 2.78-2.83 (m, 0.96H), 2.83-2.89 (m, 0.04H), 4.77 (d, 0.04H, *J* = 8.4 Hz), 5.08 (d, 0.96H, *J* = 4.0 Hz), 7.24-7.35 (m, 5H).

^{13}C NMR (125 MHz) δ (*syn*) = 48.3, 74.0, 126.2, 127.5, 128.3, 141.4, 205.1.

HPLC (Dialcel Chiralcel OD, ^{n}hexane/ ^{i}PrOH = 100/1, flow rate 1.0 mL/min); t$_R$ = 11.8 min (*syn*, major), t$_R$ = 14.9 min (*anti*, minor), t$_R$ = 18.4 min (*syn*, minor), t$_R$ = 25.6 min (*anti*, major).

(2*S*,3*R*)-*S*-(*tert*-Butyl)-3-hydroxy-2-methyl-5-phenylpentanethioate (**3ji**)[27]
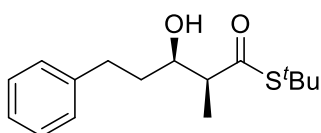
^{1}H NMR (500 MHz, *syn/anti* = 63/37) δ= 1.19 (d, 3H, *J* = 6.8 Hz), 1.42 (s, 9H), 1.61-1.67 (m, 1H), 1.68-1.83 (m, 1H), 2.55-2.69 (m, 3H), 2.81-2.89 (m, 1H), 3.90-3.94 (m, 1H), 7.16-7.22 (m, 3H), 7.25-7.31 (m, 2H).

^{13}C NMR (125 MHz) δ (*syn*) = 24.7, 27.8, 30.8, 42.6, 57.4, 74.7, 127.0, 127.9, 128.3, 140.9, 215.6.

HPLC (Dialcel Chiralpak AD-H, ^{n}hexane/ ^{i}PrOH = 100/1, flow rate 0.5 mL/min); t$_R$ = 53.7 min (*syn*, major), t$_R$ = 58.3 min (*anti*, minor), t$_R$ = 61.5 min (*syn*, minor), t$_R$ = 84.3 min (*anti*, major).

---

[1] a) K. F. Thom, *US Pat.*, 3615169, 1971; b) S. Kobayashi, *Synlett.* **1994**, 689-701.

[2] a) H. Gaspard-lloughmane, C. Le Roux, *Eur. J. Org. Chem.* **2004**, 2517-2532; b) S. Répichet, A. Zwick, L. Vendier, C. Le Roux, J. Dubac, *Tetrahedron Lett.* **2002**, *43*, 993-995.

[3] a) J. F. Hochepied, P. Bonville, M. P. Pileni, *J. Phys. Chem. B.* **2000**, *104*, 905-912; b) N. Moumen, M. P. Pileni, *J. Phys. Chem.* **1996**, *100*, 1867-1873.

[4] C. Bolm, M. Ewald, M. Felder, G. Schlingloff, *Chem, Ber.* **1992**, *125*, 1169-1190.

[5] E. M. Dipl, C. Schneider, *Chem. Eur. J.* **2007**, *13*, 2729-2741.

[6] S. Ishikawa, T. Hamada, K. Manabe, S. Kobayash, *Synthesis,* **2005**, 2176-2182.

[7] T. Hamada, K. Manabe, S. Ishikawa, S. Nagayama, M. Shiro, S. Kobayashi, *J. Am. Chem. Soc.* **2003**, *125*, 2989-2996.

[8] H. –J. Li, H. –Y. Tian, Y. –C. Wu, Y. –J. Chen, L. Liu, D. Wang, C. –J. Li, *Adv. Synth. Catal.* **2005**, *347*, 1247-1256.

[9] H. –X. Wei, R. L. Jasoni, H. Shao, J. Hu, P. W. Paré, *Tetrahedron Lett.* **2004**, *60*, 11829-11835.

[10] C. D. Smith, G. Rosocha, L. Mui, R. A. Batey, *J. Org. Chem.* **2010**, *75*, 4716-4727.

[11] S. Kobayashi, I. Hachiya, *J. Org. Chem.* **1994**, *59*, 3590-3596.

[12] T. Mukaiyama, T. Takuwa, K. Yamane, S. Imachi, *Bull. Chem. Soc. Jpn.* **2003**, *76*, 813-824.

[13] T. Inoue, T. Mukaiyama, *Bull. Chem. Soc. Jpn.* **1980**, *53*, 174-178.

[14] F. Eustache, P. I. Dalko, J. Cossy, *J. Org. Chem.* **2003**, *68*, 9994-10002.

[15] J. L. Vicario, D. Badía, E. Domínguez, M. Rodríguez, L. Carrillo, *J. Org. Chem.* **2000**, *65*, 3754-3760.

[16] N. Shinghal, A. L. Koner, P. Mal, P. Venugopalan, W. M. Nau, J. N. Moorthy, *J. Am. Chem. Soc.* **2005**, *127*, 14375-14382.

[17] A. T. Nielsen, C. Gibbons, C. A. Zimmerman, *J. Am. Chem. Soc.* **1951**, *73*, 4696-4701.

[18] A. Bartoszewicz, M. Livendahl, B. Martín-Matute, *Chem. Eur. J.* **2008**, *14*, 10547-10550.

[19] R. Matsubara, Y. Nakamura, S. Kobayashi, *Angew. Chem. Int. Ed.* **2004**, *43*, 3258-3260.

[20] S. Kobayashi, T. Ogino, H. Shimizu, S. Ishikawa, T. Hamada, K. Manabe, *Org. Lett.* **2005**, *7*, 4729-4731.

[21] H. –F. Wang, G. –H. Ma, S. –B. Yang, R. –G. Han, P. –F. Xu, *Tetrahedron: Asymmetry*, **2008**, *19*, 1630-1635.

[22] K. Mori, S. Sano, Y. Yokoyama, M. Bando, M. Kido, *Eur. J. Org. Chem.* **1998**, *6*, 1135-1142.

[23] G. Pousse, F. L. Cavelier, L. Humphreys, J. Rouden, J. Blanchet, *Org. Lett.* **2010**, *12*, 3582-3585.

[24] Z. Xu, P. Daka, H. Wang, *Chem. Commun.* **2009**, 6825-6827.

[25] T. Shiomi, T. Adachi, J. Ito, H. Nishiyama, *Org. Lett.* **2009**, *11*, 1011-1014.

[26] S. E. Denmark, B. D. Griedel, D. M. Coe, M. E. Schnute, *J. Am. Chem. Soc.* **1994**, *116*, 7026-7043.

[27] M. Hirama, S. Masamune, *Tetrahedron Lett.* **1979**, *20*, 2225-2228.

Chapter 2 : Design of the Simplest Metalloenzyme-like Catalyst System in Water

Materials and Methods

General procedure for synthesis of chiral ligands
1-bromo-11-(2-pyridyl)undecane (**5**)
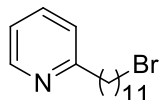
A 1.65 M solution of ^{n}BuLi (61.0 mL, 100 mmol) in hexane was added dropwise with stirring to α-picoline **4** (9.31 g, 100 mmol) in 150 mL of THF at −78 ˚C under argon atmosphere. The mixture was allowed to warm to − 20 ˚C and then re-cooled to − 40 ˚C. To a − 40 ˚C solution of 1,10-dibromodecane (33.5 mL, 150 mmol) in THF (150 mL) was added the mixture *via* canula at rate as to keep the internal reaction temperature below −20 ˚C. The resultant mixture was allowed to warm gradually to room temperature. After stirred for 10 h, the crude product was acidified to pH 1 with aqueous 1N HCl, then concentrated under reduced pressure to remove volatile solvents. The aqueous layer was washed with Et_2O, and then basified to pH 10 with aqueous 1N NaOH. After extracted with dichloromethane (50 mL, 3 times), the combined mixture was dried over anhydrous Na_2SO_4. After removal of the solvent under reduced pressure, the residue was chromatographed on neutral silica gel (elution: ^{n}hexane/AcOEt = 3/1) to afford 1-bromo-11-(2-pyridyl)undecane **5** (18.9 g, 61 %) as a slightly yellow oil.

IR (neat) ν = 3031, 1496, 1454, 1227, 1201, 756, 695 cm^{-1}.
^{1}H NMR (500 MHz); δ = 1.26-1.41 (m, 14 H), 1.68 (quin, J = 7.7 Hz, 2H), 1.80 (quin, J = 7.2 Hz, 2H), 2.73 (t, J = 7.7 Hz, 2H), 3.36 (t, J = 6.8 Hz, 2H), 7.04 (dd, J = 5.0, 7.7 Hz, 1H), 7.09 (t, J = 7.7 Hz, 1H), 7.57 (dd, J = 1.4, 7.7 Hz, 1H), 8.52 (d, J = 4.0 Hz, 1H).
^{13}C NMR (125 MHz); δ = 27.3, 28.1, 28.7, 29.1, 29.3, 29.4, 29.9, 31.5, 32.6, 38.4, 120.8, 122.6, 136.2, 149.1, 162.5.
HRMS calcd for $C_{16}H_{27}NBr$ ([M+H]$^+$): 312.1327, found: 312.1329.

11-(2-pyridyl)undecanenitrile (**6**)
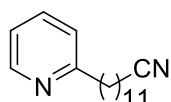
To a solution of 1-bromo-11-(2-pyridyl)undecane **5** (11.55 g, 37 mmol) in DMSO (50 mL) was added KCN (4.82 g, 74 mmol). After heating at 80 ˚C for 2 h, the mixture was quenched with 1N NaOH aqueous solution. After stirred for 2 h, the mixture was quenched with 1N NaOH solution. Purification on a silica gel column (elution: ^{n}hexane/AcOEt = 4/1 to 2/1) yielded 11-(2-pyridyl)undecanenitrile **6** (8.35 g, 87 %) as a yellow oil.

IR (neat) ν = 3035, 2252, 1603, 1498, 1455, 1078, 1031, 735, 696 cm^{-1}.

^{1}H NMR (500 MHz); δ = 1.18-1.25 (m, 14H), 1.65 (quin, *J* = 7.4 Hz, 2H), 1.72 (quin, *J* = 7.4 Hz, 2H), 2.33 (t, *J* = 7.4 Hz, 2H), 2.71 (t, *J* = 7.9 Hz, 2H), 7.09 (dd, *J* = 5.1, 7.1 Hz, 1H), 7.13 (d, *J* = 7.9 Hz, 1H), 7.58 (dt, *J* = 1.7, 7.9 Hz, 1H), 8.52 (d, *J* = 5.1 Hz, 1H).

^{13}C NMR (125 MHz); δ = 29.1, 29.4, 29.9, 38.4, 120.8, 122.7, 136.2, 149.1, 162.5, 203.5.

HRMS calcd for C$_{17}$H$_{27}$N$_2$ ([M+H]$^+$): 259.4097, found: 259.4087.

12-pyridin-2-yldodecylamine (**7**)
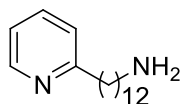
To a stirred suspension of LiAlH$_4$ (1.14 g, 30 mmol) in dry THF (10 mL) was added nitrile **6** (10.34 g, 40 mmol) dissolved in dry THF (40 mL) dropwise under an argon atmosphere. The reaction course was monitored by TLC, and once all the starting material was consumed (3h, at room temperature), the mixture was quenched with an aqueous solution of 1N NaOH (50 mL). After filtration through Celite$^®$, the filter cake rinsed well with three portions of AcOEt. The combined filtrate and washings were concentrated under reduced pressure. Purification on a silica gel column which was pre-treated with AcOEt/Et$_3$N = 19/1 (elution: AcOEt/MeOH = 1/0 to 0/1) yielded 11-(2-pyridyl)undecanenitrile **7** (9.45 g, 90 %) as a colorless oil.

IR (neat) ν = 3366, 3284, 3962, 3026, 2932, 1603, 1497, 1453, 1079, 746, 699 cm^{-1}.

^{1}H NMR (500 MHz); δ = 1.22-1.38 (m, 18H), 1.39-1.45 (m, 2H), 1.72 (t, *J* = 7.4 Hz, 2H), 2.67 (t, *J* = 7.4 Hz, 2H), 2.77 (t, *J* = 7.9 Hz, 2H), 7.08 (t, *J* = 6.2 Hz, 1H), 7.13 (d, *J* = 7.9 Hz, 1H), 7.57 (t, *J* = 7.9 Hz, 1H), 8.51 (d, *J* = 5.1 Hz, 1H).

^{13}C NMR (125 MHz); δ = 25.3, 25.4, 30.1, 46.8, 59.5, 64.7, 66.6, 126.7, 127.2, 128.0, 128.2, 128.3, 128.5, 135.6, 141.4, 175.1.

HRMS calcd for C$_{17}$H$_{31}$N$_2$ ([M+H]$^+$): 263.2487, found: 263.2441.

1,3-bis[(2*S*,2'*S*)-2-carbobenz-1-pyrrolidinyl]propane (**9**)
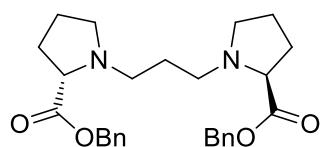
To a solution of *L*-proline benzylester **8** (2.41 g, 10 mmol) in acetonitrile (10 mL) were aadded K$_2$CO$_3$ (2.90 g, 21 mmol) and 1,3-dibromopropane (908.1 mg, 4.5 mmol). The mixture was stirred for 3 h under reflux conditions. After cooled to room temperature, the mixture was filterated through Celite$^®$ and diluted with AcOEt. The collected filtrate was concentrated under reduced pressure. The residue was chromatographed on silica gel (elution: CHCl$_3$/MeOH = 9/1) to afford 1,3-bis[(2*S*,2'*S*)-2-carbobenz-1-pyrrolidinyl]propane **9** (2.31 g, 88 %) as a slightly yellow oil.

IR (neat) ν = 3409, 3067, 2854, 1744, 1243, 1215, 768, 705 cm^{-1}.

^{1}H NMR (500 MHz); δ = 1.67-1.70 (m, 2H), 1.76-1.79 (m, 2H), 1.88-1.93 (m, 4H), 2.09-2.10 (m, 2H), 2.30-2.34 (m, 2H), 2.40-2.43 (m, 2H), 2.62-2.66 (m, 2H), 3.13-3.18 (m, 4H), 5.15 (q, *J* = 2.5,

4.6 Hz, 4H), 7.28-7.36 (m, 10H).

^{13}C NMR (125 MHz); δ = 25.3, 25.4, 30.1, 46.8, 59.5, 64.7, 66.6, 126.7, 127.2, 128.0, 128.2, 128.3, 128.5, 135.6, 141.4, 175.1.

HRMS calcd for $C_{27}H_{35}N_2O_4$ ([M+H]$^+$): 451.2552, found: 451.2541.

(2*S*,2*S*')-1,1'-trimethylenedipyrrolidine-2,2'-dicarboxylate (**10**)[1]
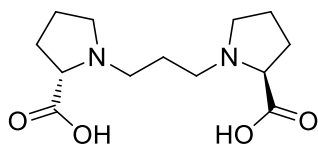
1,3-Bis[(2*S*,2'*S*)-2-carbobenz-1-pyrrolidinyl]propane **9** (5.95 g, 13 mmol) was added to a suspension of 10% Pd/C (1.23 g) in degassed EtOH (35 mL). The mixture was stirred at room temperature under H$_2$ atmosphere for 2h. The solution was filtered through Celite® to remove the Pd/C and the filtrate was evaporated to afford a white solid **10** (3.97 g, >99%). This crude product was used in the next step without further purification.

Hygroscopic white powder

IR (KBr) ν = 3409, 3058, 2904, 1625, 1618, 1380, 1215, 644 cm^{-1}.

^{1}H NMR (500 MHz in D$_2$O); δ = 1.08 (t, *J* = 1.8 Hz, 2H), 1.76-1.90 (m, 2H), 2.00-2.09 (m, 3H), 2.30-2.40 (m, 2H), 3.06-3.10 (m, 1H), 3.17-3.28 (m, 2H), 3.50-3.58 (m, 1H), 3.68-3.72 (m, 2H), 3.86-3.90 (m, 2H).

^{13}C NMR (125 MHz); δ = 25.3, 30.2, 46.8, 59.5, 66.6, 175.1.

HRMS calcd for $C_{13}H_{23}N_2O_4$ ([M+H]$^+$): 271.3327, found: 271.3341.

[To confirm the optical purity, this crude product was converted into methyl ester as follow:
1,3-bis[(2*S*,2'*S*)-2-carbomethoxy-1-pyrrolidinyl]propane
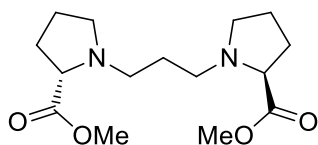
The crude diacid **7** (3.50 g, 10 mmol) in MeOH (30 mL) allowed to stir at 0 ˚C. To a 0 ˚C solution was added thionyl chloride (2.60 g, 22 mmol). The mixture was stirred under reflux conditions overnight and then all volatile solvents were removed under reduced pressure. Extraction was performed by using brine and Et$_2$O. Distillation of the crude product yielded 1,3-bis[(2*S*,2'*S*)-2-carbomethoxy-1-pyrrolidinyl]propane (2.98 g, 67%) as a colorless oil.

^{1}H NMR (500 MHz in D$_2$O); δ = 1.67-1.92 (m, 8H), 2.07-2.15 (m, 2H), 2.24-2.33 (m, 2H), 2.36-2.45 (m, 2H), 2.61-2.72 (m, 2H), 3.08-3.25 (m, 4H), 3.71 (s, 6H).

^{13}C NMR (125 MHz); δ = 23.2, 28.0, 29.4, 51.8, 53.3, 66.2, 174.8.

[α]$_D^{30}$ = –111.9 (*c* = 0.23, MeOH), *lit.*[1] [α]$_D^{20}$ = –104.4 (*c* = 4.0, H$_2$O).]

(2*S*,2'*S*)-1,1'-(propane-1,3-diyl)bis(*N*-12-(2-pyridyl)-dodecyl)pyrrolidine-2-carboxamide) (**L18'**)
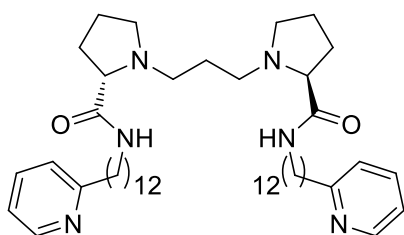
To a solution of diacid **10** (270.5 mg, 1.0 mmol) in dichloromethane (25 mL) were added triethylamine (310 μL, 2.0 mmol) and isobutyl chloroformate (280 μL, 2.2 mmol) at 0 ˚C. After stirred for 30 min, to the resultant mixture was added 12-pyridin-2-yldodecylamine **7** (581.0 mg, 2.0 mmol) in dichloromethane (3 mL), and the mixture was allowed to room temperature and stirred for 2 h. The mixture was quenched with water and extracted with AcOEt. After dried over anhydrous Na_2SO_4, the solvent was removed under reduced pressure. The residue was chromatographed on silica gel (elution: ^{n}hexane/AcOEt = 4/1 to 2/1) to afford (2*S*,2'*S*)-1,1'-(propane-1,3-diyl)bis(*N*-12-(2-pyridyl)-dodecyl)pyrrolidine-2-carboxamide) **L18'** (594 mg, 72%) as a viscous oil. The optimization of reaction conditions is shown in Table **S-1**.

IR (neat) ν = 3410, 3057, 2850, 1702, 1243, 1215, 760, 695 cm^{-1}.
^{1}H NMR (500 MHz); δ = 1.21-1.36 (m, 22H), 1.45-1.51 (m, 4H), 1.57-1.88 (m, 8H), 2.11-2.20 (m, 2H), 2.26-2.34 (m, 2H), 2.47-2.58 (m, 8H), 2.60 (t, *J* = 7.6 Hz, 4H), 2.59 (t, *J* = 7.5 Hz, 2H), 2.78 (t, *J* = 7.8 Hz, 4H), 3.15 (t, *J* = 7.0 Hz, 2H), 3.19-3.27 (dq, *J* = 1.4, 6.9 Hz, 2H), 7.09 (dt, *J* = 2.1, 6.2 Hz, 2H), 7.14 (d, *J* = 7.7 Hz, 4H), 7.58 (dt, *J* = 1.9, 7.7 Hz, 2H), 8.52 (d, *J* = 4.0 Hz, 2H), 9.23 (s, 2H).
^{13}C NMR (125 MHz); δ = 25.3, 25.4, 30.1, 46.8, 59.5, 64.7, 66.6, 126.7, 127.2, 128.0, 128.2, 128.3, 128.5, 135.6, 141.4, 175.1.
HRMS calcd for $C_{47}H_{78}N_6O_2^+$ ([M+H]$^+$): 759.6265, found: 759.6299.
$[\alpha]_D^{25}$ = − 28.8 (*c* = 0.20, MeOH).

(2*S*,2'*S*)-1,1'-(propane-1,3-diyl)bis(*N*-12-(2-pyridyl)-dodecyl)pyrrolidine-2-carboxamide)-*N*,*N*'-dioxide (**L18**)
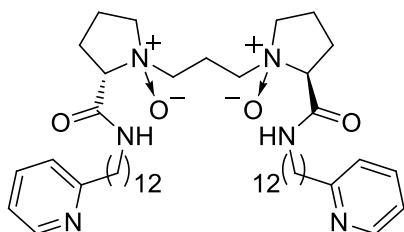
To a solution of (2*S*,2'*S*)-1,1'-(propane-1,3-diyl)bis(*N*-12-(2-pyridyl)-dodecyl)pyrrolidine-2-carboxamide) **L18'** (153 mg, 0.2 mmol) in dichloromethane (6.5 mL) was added *m*CPBA (ca. 70%, 99 mg, 0.4 mmol, see Table **S-1**) at 0 ˚C. The mixture was stirred for 2h at the same temperature. The resultant mixture was concentrated under reduced pressure. The residue was chromatographed on basic alumina (elution: AcOEt/MeOH = 1/0 to 3/1) to afford *N*,*N*'-dioxide **L18** (158 mg, 99%) as a colorless and slightly viscous oil.

IR (neat) ν = 3410, 3057, 2850, 1702, 1243, 1215, 760, 694 cm^{-1}.

^{1}H NMR; δ = 1.13-1.30 (m, 36H), 1.40-1.48 (m, 4H), 1.64 (quin, *J* = 7.9 Hz, 4H), 1.89-1.98 (m, 2H), 2.27-2.41 (m, 4H), 2.59 (quin, *J* = 7.4 Hz, 2H), 2.70 (t, *J* = 7.9 Hz, 4H), 2.77 (t, *J* = 7.6 Hz, 4H), 3.07-3.43 (m, 8H), 3.53 (quin, *J* = 9.3 Hz, 2H), 7.02 (dd, *J* = 5.1, 7.4 Hz, 2H), 7.05 (d, *J* = 7.4 Hz, 2H), 7.51 (dt, *J* = 1.7, 7.4 Hz, 2H), 8.44 (d, *J* = 4.5 Hz, 2H), 10.55 (brs, 2H).
^{13}C NMR (125 MHz); δ = 19.7, 20.0, 27.0, 27.6, 29.2, 29.3, 29.4, 29.5, 29.9, 38.4, 38.6, 64.5, 67.8, 76.7, 77.0, 77.3, 120.7, 122.6, 136.1, 149.1, 162.4, 167.2.
HRMS calcd for $C_{47}H_{78}N_6O_4^+$ ([M+H]$^+$): 791.6163, found: 791.6145.
$[\alpha]_D^{25} = -11.9$ (*c* = 0.20, MeOH).

Characterization of catalyst:

Fig. S1. Characterization of **L1** in CD_3OD

^{1}H NMR
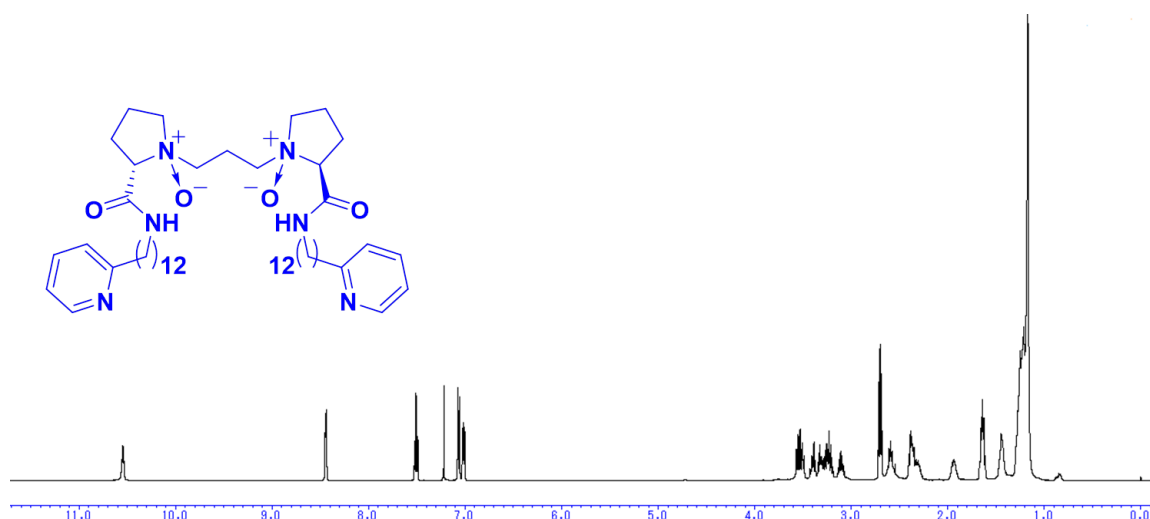
^{13}C NMR
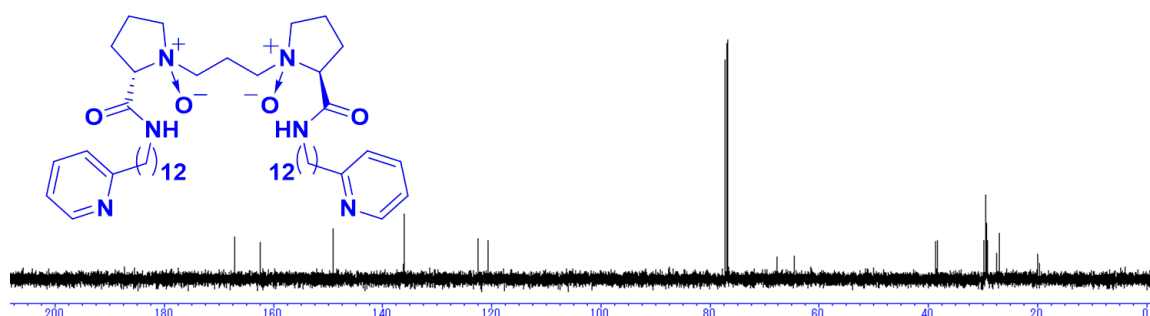
Table S-1. The effect of oxidant

Run	Oxidant	Equivalent of Oxidant	Yield (%)
1	*m*CPBA	2.2	<50

2	*m*CPBA	2.0	>99
3	Peracetic Acid	2.0	98
4	*tert*-Butyl hydroperoxide (TBHP)	2.0	N.R.
5	Cumene hydroperoxide (CHP)	2.0	N.R.

General Procedure for Synthesis of **L19-L23**

Table. S-2. Condensation and *N*-oxidation step for synthesis of **L19**-**L23**
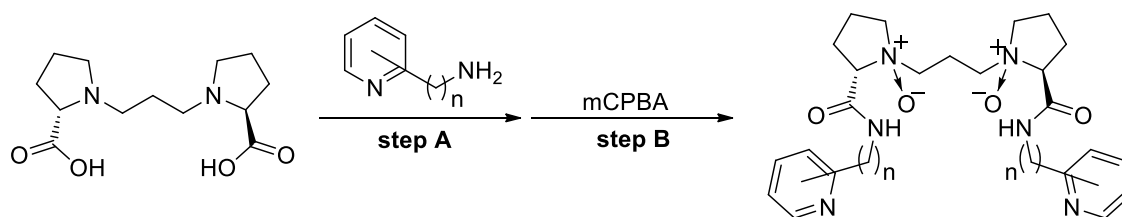
Ligand	n	Pyridine	Yield of Step A (%)	Yield of Step B (%)
L18	12	*o*-	72	Quant.
L19	12	*m*-	56	88
L20	12	*p*-	50	96
L21	14	*o*-	68	82
L22	10	*o*-	78	Quant.
L23	8	*o*-	43	Quant.

(2*S*,2'*S*)-1,1'-(propane-1,3-diyl)bis(*N*-12-(3-pyridyl)-dodecyl)pyrrolidine-2-carboxamide)-*N*,*N*'-dioxide (**L19**)
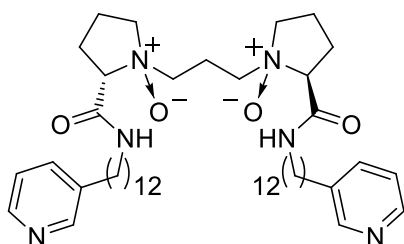
Prepared from 3-picoline.

Viscous oil.

IR (neat) ν = 3411, 3057, 2850, 1703, 1243, 1215, 761, 695 cm^{-1}.

^{1}H NMR (600 MHz); δ = 1.23-1.35 (m, 36H), 1.45-1.52 (m, 4H), 1.58-1.87 (m, 8H), 2.11-2.19 (m, 2H), 2.26-2.34 (m, 2H), 2.48-2.62 (m, 8H), 3.15-3.24 (m, 8H), 7.19 (dd, *J* = 4.8, 7.6 Hz, 2H) 7.48 (d, *J* = 8.2 Hz, 2H), 8.42 (d, *J* = 4.8, 2H), 8.43 (s, 2H), 9.80 (brs, 2H).

^{13}C NMR (150 MHz); δ = 18.3, 24.1, 26.8, 29.0, 29.1, 29.3, 29.4, 29.7, 30.5, 31.0, 32.9, 38.7, 64.5,

53.9, 67.8, 123.1, 135.7, 137.8, 147.0, 149.8, 174.5.

HRMS calcd for $C_{47}H_{78}N_6O_4^+$ ([M+H]$^+$): 791.6163, found: 791.6119.

$[\alpha]_D^{25} = -12.1$ ($c = 0.20$, MeOH).

(2*S*,2'*S*)-1,1'-(propane-1,3-diyl)bis(*N*-12-(4-pyridyl)-dodecyl)pyrrolidine-2-carboxamide)-*N*,*N*'-dioxide (**L20**)
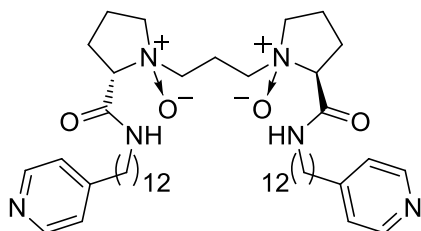
Prepared from 4-picoline.

Viscous oil.

IR (neat) ν = 3409, 3055, 2850, 1702, 1241, 1215, 761, 694 cm^{-1}.

^{1}H NMR (600 MHz); δ = 1.18-1.35 (m, 36H), 1.41-1.53 (m, 4H), 1.57-1.86 (m, 8H), 2.08-2.18 (m, 2H), 2.26-2.33 (m, 2H), 2.36-2.61 (m, 8H), 3.00-3.28 (m, 8H), 7.07-7.11 (m, 4H), 8.43-8.47 (m, 4H), 9.81 (brs, 2H).

^{13}C NMR (150 MHz); δ = 20.0, 27.0, 27.6, 28.9, 29.0, 29.1, 29.2, 29.3, 29.4, 29.5, 29.6, 30.1, 30.2, 34.3, 35.2, 38.6, 64.6, 67.8, 123.9, 125.9, 138.7, 149.5, 167.2.

HRMS calcd for $C_{47}H_{78}N_6O_4^+$ ([M+H]$^+$): 791.6163, found: 791.6160.

$[\alpha]_D^{25} = -11.6$ ($c = 0.21$, MeOH).

(2*S*,2'*S*)-1,1'-(propane-1,3-diyl)bis(*N*-14-(2-pyridyl)-dodecyl)pyrrolidine-2-carboxamide)-*N*,*N*'-dioxide (**L21**)
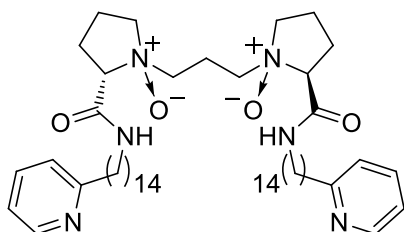
Viscous oil.

IR (neat) ν = 3411, 3058, 2851, 1703, 1243, 1216, 761, 695 cm^{-1}.

^{1}H NMR (500 MHz); δ = 1.2-1.4 (m, 32H), 1.44-1.56 (m, 2H), 1.58-1.65 (m, 4H), 1.98-2.06 (m, 2H), 2.36-2.46 (m, 4H), 2.58-2.67 (m, 4H), 3.14-3.7 (m, 10H), 8.1-8.2 (m, 2H), 8.4-8.6 (m, 2H), 10.6 (brs, 2H).

^{13}C NMR (125 MHz); δ = 20.1, 26.0, 27.0, 27.6, 29.2, 29.3, 29.4, 29.5, 29.6, 29.8, 30.4, 38.4, 38.6, 64.6, 67.9, 120.7, 122.6, 136.1, 149.1, 162.5, 167.2.

HRMS calcd for $C_{51}H_{86}N_6O_4^+$ ([M+H]$^+$): 847.6789, found: 847.6755.

$[\alpha]_D^{25} = -11.8$ ($c = 0.22$, MeOH).

(2*S*,2'*S*)-1,1'-(propane-1,3-diyl)bis(*N*-10-(2-pyridyl)-dodecyl)pyrrolidine-2-carboxamide)-*N*,*N*'-dioxide (**L22**)
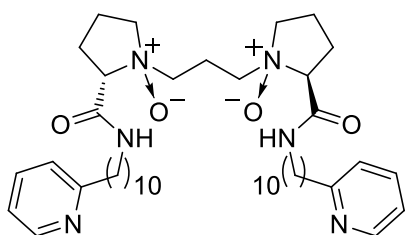
Viscous oil.

IR (neat) ν = 3410, 3057, 2850, 1702, 1243, 1216, 760, 693 cm^{-1}.

^{1}H NMR (500 MHz); δ = 1.18-1.41 (m, 28H), 1.43-1.56 (m, 4H), 1.59-1.92 (m, 8H), 2.04-2.11 (m, 2H), 2.23-2.33 (m, 2H), 2.40-2.76 (m, 8H), 2.97-3.29 (m, 8H), 6.98-7.05 (m, 2H), 7.05 (d, J = 7.3 Hz, 2H), 7.47-7.53 (m, 2H), 8.44 (d, J = 4.5 Hz, 2H), 10.51 (brs, 2H).

^{13}C NMR (125 MHz); δ = 19.8, 19.9, 27.1, 27.6, 29.3, 29.4, 29.5, 29.6, 29.9, 38.3, 38.6, 64.5, 67.9, 120.6, 122.7, 136.2, 149.3, 162.2, 167.0.

HRMS calcd for C$_{43}$H$_{70}$N$_6$O$_4^+$ ([M+H]$^+$): 735.5537, found: 735.5554.

$[α]_D^{25}$ = − 12.1 (c = 0.20, MeOH).

(2*S*,2'*S*)-1,1'-(propane-1,3-diyl)bis(*N*-8-(2-pyridyl)-dodecyl)pyrrolidine-2-carboxamide)-*N*,*N*'-dioxide (**L23**)
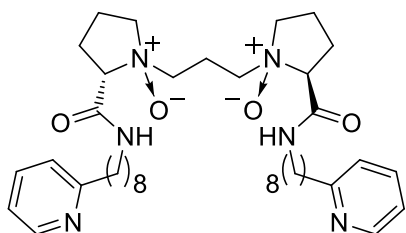
Viscous oil.

IR (neat) ν = 3410, 3056, 2851, 1701, 1242, 1215, 762, 692 cm^{-1}.

^{1}H NMR (500 MHz); δ = 1.19-1.41 (m, 20H), 1.44-1.54 (m, 4H), 1.60-1.89 (m, 8H), 2.08-2.21 (m, 2H), 2.24-2.33 (m, 2H), 2.42-2.81 (m, 8H), 2.94-3.26 (m, 8H), 7.00-7.06 (m, 2H), 7.07 (d, J = 7.4 Hz, 2H), 7.48-7.53 (m, 2H), 8.45 (d, J = 4.4 Hz, 2H), 10.53 (brs, 2H).

^{13}C NMR (125 MHz); δ = 19.9, 20.1, 27.0, 27.5, 29.2, 29.3, 29.5, 30.0, 38.3, 38.6, 64.6, 67.8, 120.8, 122.5, 136.0, 149.1, 162.5, 167.4.

HRMS calcd for C$_{39}$H$_{62}$N$_6$O$_4^+$ ([M+H]$^+$): 679.4911, found: 679.4891.

$[α]_D^{25}$ = − 11.7 (c = 0.21, MeOH).

(2*S*,2'*S*)-1,1'-(propane-1,3-diyl)bis(2-((5-undecylpyridin-2-yl)carbamoyl)pyrrolidine)-*N*,*N*'-dioxide (**L24**)
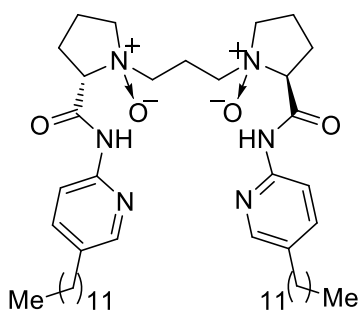
Viscous oil.

IR (neat) ν = 3410, 3057, 2850, 1702, 1243, 1215, 760, 694 cm^{-1}.

^{1}H NMR (500 MHz); δ = 0.88 (t, *J* = 6.8 Hz, 6H), 1.18-1.33 (m, 44H), 1.48-1.60 (m, 4H), 1.85-1.96 (m, 4H), 2.38-2.58 (m, 6H), 3.28-3.38 (m, 4H), 4.58-4.68 (brs, 2H), 7.41 (d, *J* = 8.5 Hz, 2H), 7.89 (d, *J* = 8.5 Hz, 2H), 8.08 (s, 2H), 10.5 (brs, 2H).

^{13}C NMR (125 MHz); δ = 14.2, 19.6, 20.3, 22.8, 27.5, 29.2, 29.4, 29.5, 29.6, 29.7, 31.3, 32.0, 32.5, 50.4, 64.2, 67.7, 76.8, 76.9, 77.2, 77.4, 114.7, 134.5, 138.3, 147.7, 148.8, 165.8.

HRMS calcd for $C_{47}H_{78}N_6O_4^+$ ([M+H]$^+$): 791.6163, found: 791.6134.

[α]$_D^{25}$ = − 28.8 (*c* = 0.20, MeOH).

(2*S*,2'*S*)-1,1'-(propane-1,3-diyl)bis(N-dodecyl)pyrrolidine-2-carboxamide)-*N,N'*-dioxide (**L25**)
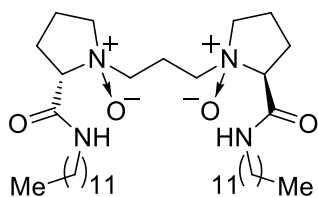
Viscous oil.

IR (neat) ν = 3412, 3055, 2861, 1702, 1432, 1204, 760 cm^{-1}.

^{1}H NMR (500 MHz); δ = 0.85-0.91 (m, 6H), 1.20-1.34 (m, 34H), 1.46-1.55 (m, 4H), 1.98-2.17 (m, 4H), 2.34-2.48 (m, 6H), 2.63-2.70 (m, 2H), 3.13-3.21 (m, 2H), 3.25-3.42 (m, 4H), 3.43-3.49 (m, 2H), 3.54-3.64 (m, 4H), 10.65 (t, *J* = 5.0 Hz, 2H).

^{13}C NMR (125 MHz); δ = 14.1, 20.4, 22.7, 27.1, 27.9, 29.3, 29.4, 29.6, 31.9, 38.8, 55.1, 71.2, 167.2.

HRMS calcd for $C_{37}H_{72}N_4O_4^+$ ([M+H]$^+$): 637.5632, found: 637.5659.

[α]$_D^{25}$ = − 12.8 (*c* = 0.21, MeOH).

(2*S*,2'*S*)-1,1'-(propane-1,3-diyl)bis(N-dodecyl)pyrrolidine-2-carboxamide)-*N,N'*-dioxide (**L26**)
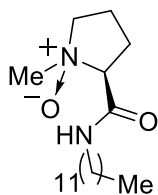
Yellow solid; mp 51-54 ^{o}C

IR (neat) ν = 3411, 3052, 2858, 1698, 1430, 1206, 759 cm^{-1}.

^{1}H NMR (500 MHz); δ = 0.87-0.89 (m, 3H), 1.22-1.36 (m, 18H), 1.50-1.60 (m, 2H), 1.81 (brs, 4H), 2.00-2.06 (m, 1H), 2.40-2.51 (m, 2H), 3.26-3.31 (m, 3H), 3.38-3.43 (m, 1H), 3.59-3.70 (m, 2H), 10.83 (brs, 1H).

^{13}C NMR (125 MHz); δ = 14.1, 20.5, 22.6, 27.1, 27.8, 29.3, 29.4, 29.5, 31.9, 38.8, 55.0, 71.2, 167.4.

HRMS calcd for $C_{18}H_{36}N_2O_2^+$ ([M+H]$^+$): 313.2855, found: 313.2895.

[α]$_D^{25}$ = − 14.9 (*c* = 0.24, MeOH).

(2*S*,2'*S*)-1,1'-(propane-1,3-diyl)bis(pyrrolidine-2-carboxamide)-*N,N'*-dioxide (**L27**)
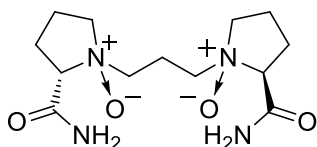
Slightly viscous oil.

IR (neat) ν = 3425, 2960, 1671, 1210, 772 cm^{-1}.

^{1}H NMR (500 MHz); δ = 1.24-1.28 (m, 1H), 1.99-2.08 (m, 3H), 2.36-2.54 (m, 5H), 2.64-2.71 (m, 2H), 3.28-3.35 (m, 1H), 3.46-3.48 (m, 1H), 3.52-3.56 (m, 3H), 3.60-3.68 (m, 3H), 4.12 (dd, J = 6.8, 14.2 Hz, 1H), 6.00-6.26 (m, 2H), 10.52 (brs, 2H).

^{13}C NMR (125 MHz); δ = 14.2, 20.0, 20.2, 21.0, 27.4, 60.4, 64.8, 68.0, 76.9, 177.4, 183.4, 197.7.

HRMS calcd for $C_{13}H_{24}N_4O_4^+$ ([M+H]$^+$): 301.1876, found: 301.1866.

$[\alpha]_D^{25}$ = $-$ 100.2 (c = 0.20, MeOH).

(2S,2'S,4R,4'R)-1,1'-(propane-1,3-diyl)bis(2-((2,6-dimethylphenyl)carbamoyl)-4-(dodecyloxy)pyrrolidine)-N,N'-dioxide (**L28**)
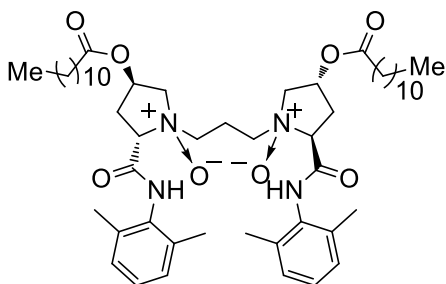
Slightly viscous oil.

IR (neat) ν = 3426, 2859, 1665, 1541, 1211, 772, 704 cm^{-1}.

^{1}H NMR (500 MHz); δ = 0.88 (t, J = 6.9 Hz, 6H), 1.21-1.34 (m, 36H), 1.58-1.64 (m, 4H), 2.18 (s, 12H), 2.64 (dd, J = 6.9, 14.3 Hz, 2H), 2.73-2.81 (m, 2H), 3.19 (ddd, J = 7.4, 13.7, 13.7 Hz, 2H), 3.45 (dd, J = 4.6, 12.1 Hz, 2H), 3.72-3.79 (m, 2H), 3.85-3.90 (m, 2H), 4.12 (dd, J = 6.3, 13.2 Hz, 2H), 4.22 (dd, J = 6.9, 13.2 Hz, 2H), 5.50-5.55 (m, 2H), 7.02-7.10 (m, 6H), 12.35 (brs, 2H).

^{13}C NMR (125 MHz); δ = 14.1, 18.9, 20.2, 22.7, 24.7, 29.1, 29.2, 29.3, 29.4, 29.6, 31.9, 34.0, 35.4, 65.8, 70.2, 74.9, 75.5, 127.0, 128.3, 133.3, 134.1, 164.2, 173.2.

HRMS calcd for $C_{53}H_{85}N_4O_8^+$ ([M+H]$^+$): 905.6367, found: 905.6360

$[\alpha]_D^{25}$ = $-$ 23.7 (c = 0.22, MeOH).

Typical Experimental Procedure for hydroxymethylation:

A mixture of Sc(OTf)$_3$ (15.7 mg, 0.032 mmol) and chiral N,N'-dioxide **L18** (15.8 mg, 0.02 mmol) in water (1.2 mL) was stirred at room temperature for 1 h.   To a resulting 16.7 mM of the catalyst solution was added a ketone **11** (55 μL, 0.4 mmol) and an aqueous solution of formaldehyde **1t** (150 μL, 35% w/w, 2.0 mmol).   After stirred for 24 h at 40 ^{o}C, the reaction mixture was quenched with sat. aqueous NaHCO$_3$ and brine.   The aqueous layer was extracted with dichloromethane (three times), and the combined organic layers were washed with brine, and dried over anhydrous Na$_2$SO$_4$. After removal of the solvents under reduced pressure, the residue was purified by preparative TLC (elution: ^{n}hexane/AcOEt = 3/1) to give the corresponding hydroxymethylated adduct **12t** (64.0 mg, 91% yield) as a white powder.

Analytical data for aldol reactions

All aldol adducts are literature-known; obtained analytical data for these compounds is in full agreement with reported data.

(*S*)-2-Hydroxymethyl-2-methyl-indan-1-one (**12t**)[2]
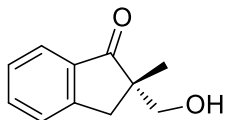
White solid; mp 67-70 ^{o}C

IR (neat): ν = 3435, 3073, 2962, 2927, 2869, 1706, 1608, 1587, 1465, 1434, 1377, 1328, 1294, 1229, 1207, 1152, 1090, 1047, 988, 872, 798, 716, 649, 579, 505, 470, 414 cm^{-1}.

^{1}H NMR (500 MHz); δ = 1.22 (s, 3H), 2.64 (t, 1H, *J* = 5.2 Hz), 2.88 (d, 1H, *J* = 17.2 Hz), 3.27 (d, 1H, *J* = 17.2 Hz), 3.61 (dd, 1H, *J* = 5.2, 10.8 Hz), 3.83 (dd, 1H, *J* = 5.2, 10.8 Hz), 7.35 (d, 1H, *J* = 7.6 Hz), 7.45 (d, 1H, *J* = 7.6 Hz), 7.60 (dd, 1H, *J* = 7.6, 8.0 Hz), 7.71 (d, 1H, *J* = 8.0 Hz).

^{13}C NMR (125 MHz); δ = 20.6, 37.9, 50.9, 67.7, 124.1, 126.6, 127.3, 135.1, 135.7, 153.3, 211.1.

HRMS calcd for C$_{11}$H$_{12}$O$_2^+$ ([M + H]$^+$): 177.0871, found 177.0850.

HPLC (Daicel Chiralpak AD-H, ^{n}hexane/ ^{i}PrOH = 19/1, flow rate = 1.0 mL min^{-1}); t_R = 17.8 min (minor), t_R = 19.7 min (major).

$[\alpha]_D^{25}$ = – 18.2 (*c* = 0.75, CHCl$_3$).

(*S*)-2-Hydroxymethyl-2-ethyl-indan-1-one[3]
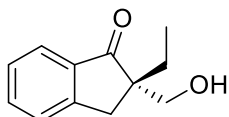
^{1}H NMR (600 MHz); δ = 0.81 (t, 3H, *J* = 7.6 Hz), 1.70 (qd, 1H, *J* = 7.6, 13.8 Hz), 1.75 (qd, 1H, *J* = 7.6, 13.8 Hz), 3.03 (d, 1H, *J* = 17.2 Hz), 3.07 (d, 1H, *J* = 17.2 Hz), 3.62 (d, *J* = 11.0 Hz, 1H), 3.86 (d, 1H, *J* = 11.0 Hz), 7.36 (t, 1H, *J* = 7.6 Hz), 7.47 (d, 1H, *J* = 7.6 Hz), 7.60 (td, 1H, *J* = 1.4, 7.6 Hz), 7.72 (d, 1H, *J* = 7.6 Hz).

^{13}C NMR (125 MHz); δ = 8.0, 24.6, 37.9, 50.9, 65.7, 124.1, 126.6, 127.2, 135.1, 135.7, 153.3, 211.0.

HPLC (Daicel Chiralpak AD-H, ^{n}hexane/ ^{i}PrOH = 19/1, flow rate = 0.5 mL min^{-1}); t_R = 36.8 min (minor), t_R = 40.8 min (major).

(*S*)-2-(Hydroxymethyl)-2,6-dimethyl-2,3-dihydro-1*H*-inden-1-one[4]
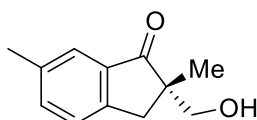
^{1}H NMR (600 MHz): δ = 1.24 (s, 3H), 2.39 (s, 2.25H, *S*), 2.40 (s, 0.75H, *R*), 2.85 (d, 1H, *J* = 17.2 Hz), 3.18 (d, 1H, *J* = 17.2 Hz), 3.62 (d, 1H, *J* = 11.0 Hz), 3.80 (d, 0.25H, *J* = 11.0 Hz, *R*), 3.81 (d, 0.75H, *J* = 11.0 Hz, *S*), 7.35 (d, 1H, *J* = 7.6 Hz), 7.43 (d, 1H, *J* = 7.6 Hz), 7.53 (d, 1H, *J* = 8.3 Hz).

^{13}C NMR (150 MHz): δ = 20.6, 21.0, 37.6, 51.1, 67.8, 124.0, 126.3, 135.8, 136.4, 137.4, 150.6, 211.2.

HPLC (Daicel Chiralpak AD-H, ^{n}hexane/ ^{i}PrOH = 19/1, flow rate = 0.5 mL min^{-1}); t_R = 34.9 min (minor), t_R = 41.1 min (major).

HRMS calcd for $C_{12}H_{15}O_2{}^+$ ([M + H]$^+$): 191.10720, found 191.10720.

(*S*)-2-Hydroxymethyl-2-methyl-3,4-dihydro-2*H*-naphthalen-1-one[3]
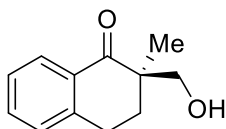
^{1}H NMR (400 MHz): δ = 1.23 (s, 3H), 1.78 (ddd, 1H, J = 3.6, 4.8, 13.2 Hz), 2.23 (ddd, 1H, J = 5.2, 12.0, 13.4 Hz), 2.89 (br, 1H), 2.94 (ddd, 1H, J = 3.6, 5.2, 17.2 Hz), 3.15 (ddd, 1H, J = 4.8, 12.0, 17.2 Hz), 3.65 (d, 1H, J = 11.2 Hz), 3.73 (d, 1H, J = 11.2 Hz), 7.24-7.33 (m, 2H), 7.47-7.51 (m, 1H), 8.01-8.03 (m, 1H).

^{13}C NMR (150 MHz): δ = 18.2, 25.0, 31.3, 46.3, 69.0, 126.7, 127.7, 128.7, 131.4, 133.6, 143.4, 204.0.

HPLC (Daicel Chiralpak AD-H, ^{n}hexane/ ^{i}PrOH = 100/1, flow rate = 1.0 mL min^{-1}); t_R = 29.3 min (minor), t_R = 34.9 min (major).

(*R*)-3-hydroxy-2-methyl-1-phenylpropan-1-one[2]
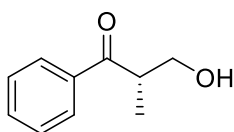
^{1}H NMR (600 MHz): δ = 1.18 (d, 3H, J = 6.9 Hz), 2.25 (br, 1H), 3.58-3.63 (m, 1H), 3.75 (d, 1H, J = 11.0 Hz), 3.86 (d, 1H, J = 7.6 Hz), 7.42 (t, 1H, J = 8.2 Hz), 7.50-7.53 (m, 1H), 7.90 (dt, 2H, J = 1.7, 8.2 Hz).

^{13}C NMR (150 MHz): δ = 14.5, 42.8, 64.5, 128.4, 128.7, 133.3, 136.0, 204.4.

HPLC (Daicel Chiralpak AD-H, ^{n}hexane/ ^{i}PrOH = 19/1, flow rate = 0.5 mL min^{-1}); t_R = 36.9 min (minor), t_R = 40.3 min (major).

HRMS calcd for $C_{10}H_{13}O_2{}^+$ ([M + H]$^+$): 165.09155, found 165.09212.

S-Ethyl (*S*)-3-hydroxy-2-methylphenylpropanethioate[2]
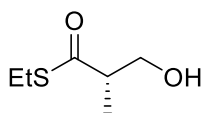
^{1}H NMR (400 MHz): δ = 1.22 (d, 3H, J = 7.2 Hz), 1.27 (t, 3H, J = 7.6 Hz), 2.82-2.95 (m, 3H), 3.71 (dd, 1H, J = 4.6, 11.0 Hz), 3.79 (dd, 1H, J = 7.2, 11.0 Hz).

^{13}C NMR (100 MHz): δ = 14.2, 14.6, 23.2, 50.4, 64.9, 203.5.

HPLC (Daicel Chiralcel OD-H, ^{n}hexane/ ^{i}PrOH = 30/1, flow rate = 0.5 mL min^{-1}); t_R = 18.9 min (minor), t_R = 21.1 min (major).

[1] X. Yang, B. Li, E. Fu, *Synthetic Communications* **2005**, *35*, 271-278.

[2] S. Ishikawa, T. Hamada, K. Manabe, S. Kobayashi, *J. Am. Chem. Soc.* **2004**, *126*, 12236–12237.

[3] T. Mahapatra, N. Jana, S. Nanda, *Tetrahedron: Asymmetry* **2008**, *19*, 1224-1232.

[4] M. Kokubo, C. Ogawa, S. Kobayashi, *Angew. Chem. Int. Ed.* **2008**, *47*, 6909–6911.

Chapter 3 : Asymmetric Boron Conjugate Additions in Water

<Reagents>

      Unless stated otherwise, commercially available reagents were used as received with the exception of the following substrates, which were prepared through reported methods.   Analytical data for these compounds are in full agreement with reported data.

(*E*)-1-(4'-methoxyphenyl)-3-phenylprop-2-en-1-one (**13d**)[1]
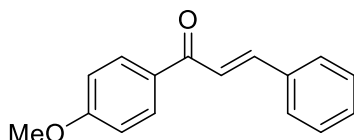
White solid
^{1}H NMR (500 MHz); δ = 3.90 (s, 3H), 6.98 (dd, *J* = 1.7 Hz, *J* = 5.2 Hz, 2H), 7.40-7.43 (m, 3H), 7.48 (d, *J* = 48.7 Hz, 1H), 7.56-7.65 (m, 2H), 7.80 (d, *J* = 48.7 Hz, 1H), 8.03-8.05 (t, *J* = 2.3 Hz, 2H).
^{13}C NMR (125 MHz); δ = 22.7, 25.6, 38.1, 129.9, 138.8, 141.1, 147.3, 150.5, 153.5, 154.0, 199.6.

(*E*)-4-Methyl-1-phenylpent-2-en-1-one (**13i**)[2]
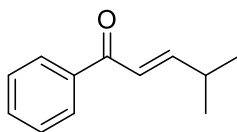
A little bit yellow liquid
^{1}H NMR (500 MHz); δ = 1.11 (d, *J* = 6.9 Hz, 6H), 2.54-2.56 (m, 1H), 6.79 (dd, *J* = 6.4 Hz, *J* = 9.2 Hz, 1H), 7.04 (dd, *J* = 6.4 Hz, *J* = 9.2 Hz, 1H), 7.42-7.52 (m, 3H), 7.89 (d, *J* = 7.6 Hz, 2H).
^{13}C NMR (125 MHz); δ = 21.4, 31.5, 123.1, 128.5, 132.5, 138.1, 156.0, 191.3.

(*E*)-4,4-Dimethyl-1-phenylpent-2-en-1-one (**13j**)[3]
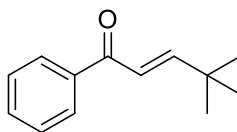
A little bit yellow liquid
^{1}H NMR (500 MHz); δ = 1.15 (s, 9H), 6.76 (d, *J* = 13.8 Hz, 1H), 7.04 (d, *J* = 13.8 Hz, 1H), 7.44-7.48 (m, 2H), 7.52-7.56 (m, 1H), 7.90 (d, *J* = 8.4 Hz, 2H).
^{13}C NMR (125 MHz); δ = 26.1, 28.8, 34.1, 121.0, 128.5, 132.5, 138.3, 159.6, 191.6.

(*E*)-1,3-Diphenyl-2-buten-1-one (**13m**)[4]
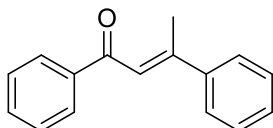
Orange oil
^{1}H NMR (500 MHz); δ = 2.62 (s, 3H), 7.15 (s, 1H), 7.42-7.89 (m, 8H), 8.02-8.05 (m, 2H).
^{13}C NMR (125 MHz); δ = 18.9, 122.2, 125.9, 128.0, 128.3, 128.4, 129.9, 132.0, 139.0, 142.3, 155.2, 199.2.

(*E*)-4-Phenylpent-3-en-2one (**13n**)[5]
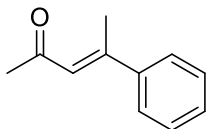
Yellow oil
^{1}H NMR (500 MHz); δ = 2.30 (d, *J* = 1.1 Hz, 3H), 2.54 (s, 3H), 6.50 (s, 1H), 7.36-7.39 (m, 3H), 7.45-7.50 (m, 2H).
^{13}C NMR (125 MHz); δ = 18.9, 31.9, 125.0, 126.4, 128.6, 129.1, 142.4, 154.0, 199.1.

Ethyl (*E*)-3-phenylbut-2-enoate (**13v**)[6]
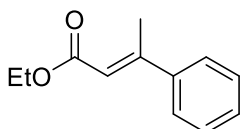
A little bit yellow liquid
^{1}H NMR (500 MHz); δ = 1.06 (t, *J* = 7.3 Hz, 3H), 2.16 (s, 3H), 3.96-4.01 (m, 2H), 5.88-5.90 (m, 1H), 7.15-7.38 (m, 5H).
^{13}C NMR (125 MHz); δ = 14.1, 26.5, 59.5, 119.2, 126.4, 127.5, 128.0, 138.2, 154.3, 169.9.

(*E*)-*N*,*N*-diethyl-3-phenylbut-2-enamide (**13y**)[7]
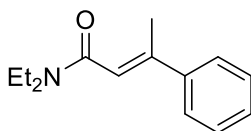
White Solid
^{1}H NMR (500 MHz); δ = 1.07 (t, *J* = 5.3 Hz, 6H), 2.19 (s, 3H), 2.59-2.62 (m, 4H), 5.72-5.73 (m, 1H), 7.19-7.41 (m, 5H).
^{13}C NMR (125 MHz); δ = 13.9, 35.2, 59.1, 117.2, 127.1, 127.6, 128.0, 140.2, 155.3, 172.1.

(2*E*, 4*E*)-1-phenylhexa-2,4-dien-1-one (**1c**)[8]
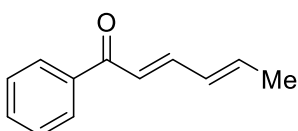
Yellow Solid
^{1}H NMR (500 MHz); δ = 1.89 (d, *J* = 6.0 Hz, 3H), 6.20-6.38 (m, 2H), 6.86 (d, *J* = 14.6 Hz, 1H), 7.35-7.59 (m, 4H), 7.88-7.96 (m, 2H).

^{13}C NMR (125 MHz); δ = 18.9, 123.6, 128.6, 130.7, 132.6, 138.5, 141.1, 145.7, 193.2.

(2*E*, 4*E*)-1-phenylocta-2,4-dien-1-one (**1d**)[9]
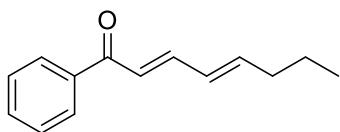
A little bit yellow oil

^{1}H NMR (500 MHz); δ = 0.91 (t, *J* = 7.5 Hz, 3H), 1.39-1.46 (m, 2H), 2.15-2.22 (m, 2H), 6.20-6.38 (m, 2H), 6.86 (d, *J* = 14.6 Hz, 1H), 7.35-7.59 (m, 4H), 7.88-7.96 (m, 2H).

^{13}C NMR (125 MHz); δ = 14.0, 23.4, 36.2, 124.1, 128.9, 131.1, 133.2, 138.5, 141.1, 145.5, 194.6.

Ethyl (2*E*, 4*E*)-5-phenylpenta-2,4-dienoate (**17c**)[10]
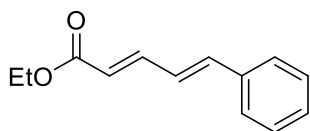
A little bit yellow liquid

^{1}H NMR (500 MHz); δ = 1.07 (t, *J* = 5.6 Hz, 3H), 3.87-3.93 (m, 2H), 6.01-6.02 (m, 1H), 6.31-6.31 (m, 1H), 6.65-6.67 (m, 1H), 6.91-6.93 (m, 1H), 7.22-7.43 (m, 5H).

^{13}C NMR (125 MHz); δ = 14.3, 26.5, 126.8, 127.4, 127.9, 129.1, 130.4, 133.2, 136.1, 148.7, 169.1.

Ethyl (2*E*, 4*E*)-3-methyl-5-phenylpenta-2,4-dienoate (**17d**)[11]
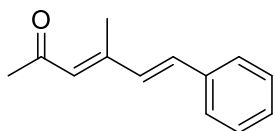
A little bit yellow solid

^{1}H NMR (500 MHz); δ = 2.24 (s, 3H), 2.36 (s, 3H), 6.24 (s, 1H), 6.75 (d, *J* = 13.4 Hz, 1H), 6.98 (d, *J* = 13.4 Hz, 1H), 7.26–7.35 (m, 3H),7.44–7.46 (m, 2H).

^{13}C NMR (125 MHz); δ = 14.1, 32.2, 127.1, 127.4, 128.7, 128.9, 132.8, 135.4, 136.4, 151.3, 200.1

(3*E*, 5*E*)-4-methyl-6-phenylhexa-3,5-dien-2-one (**17e**)[12]
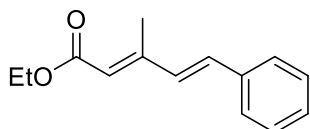
Yellow liquid

^{1}H NMR (500 MHz); δ = 1.12 (t, *J* = 5.4 Hz, 3H), 2.42 (s, 3H), 3.84-3.92 (m, 2H), 5.89-5.91 (m, 1H), 6.61-6.62 (m, 1H), 6.78-6.80 (m, 1H), 7.19-7.43 (m, 5H).

^{13}C NMR (125 MHz); δ = 14.3, 17.2, 26.5, 121.2, 126.7, 127.9, 128.4, 130.1, 134.7, 138.2, 152.3, 174.1.

(*E*)-3-styrylcyclohex-2-en-1-one (**20a**)[13]
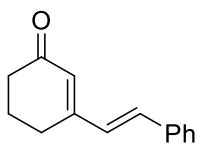
Yellow solid
^{1}H NMR (500 MHz); δ = 1.99-2.08 (m, 2H), 2.42-2.54 (m, 4H), 6.02 (s, 1H), 6.69 (d, *J* = 15.6 Hz, 1H), 6.92 (d, *J* = 15.6 Hz, 1H), 7.24-7.41 (m, 5H).
^{13}C NMR (125 MHz); δ = 23.1, 25.2, 38.0, 126.2, 127.9, 128.2, 128.6, 130.1, 134.5, 137.7, 160.2, 200.7.

(*E*)-3-(2-phenylprop-1-en-1-yl)cyclohex-2-en-1-one (**20b**)[14]
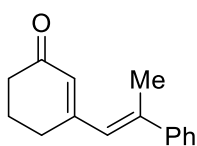
Yellow solid
^{1}H NMR (500 MHz); δ = 1.89-2.01 (m, 2H), 2.32-2.56 (m, 7H), 6.02 (s, 1H), 6.87 (s, 1H), 7.25-7.42 (m, 5H).
^{13}C NMR (125 MHz); δ = 16.7, 22.4, 24.7, 38.2, 127.1, 127.8, 128.4, 128.8, 128.9, 134.5, 137.7, 157.8, 199.9.

(*E*)-3-styrylcyclopent-2-en-1-one (**20c**)[13]
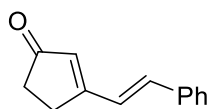
A liitle bit yellow solid
^{1}H NMR (500 MHz); δ = 2.48-2.54 (m, 2H), 2.85-2.88 (m, 2H), 6.09 (s, 1H), 7.06 (d, *J* = 17.8 Hz, 1H), 7.19 (d, *J* = 17.6 Hz, 1H), 7.29-7.41 (m, 3H), 7.48-7.53 (m, 3H).
^{13}C NMR (125 MHz); δ = 29.7, 36.5, 125.5, 126.3, 127.7, 128.3, 128.9, 131.0, 133.6, 159.2, 207.2.

(*E*)-3-styrylcyclohept-2-en-1-one (**20d**)[13]
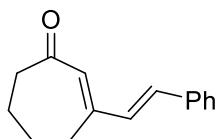
A little bit yellow solid
^{1}H NMR (500 MHz); δ = 1.78-1.91 (m, 4H), 2.59-2.63 (m, 2H), 2.70-2.72 (m, 2H), 6.13 (s, 1H), 6.81 (d, *J* = 15.6 Hz, 1H), 6.92 (d, *J* = 15.6 Hz, 1H), 7.24-7.46 (m, 5H).
^{13}C NMR (125 MHz); δ = 21.5, 25.7, 28.7, 42.3, 127.7, 128.9, 129.3, 132.1, 134.0, 134.7, 137.3, 155.6, 206.2.

(*Z*)-4-benzylidenecyclohex-2-en-1-one (**20e**)
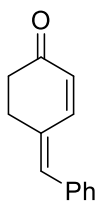
A little bit yellow solid; mp 127-130 $^{\circ}$C.

IR (neat) ν = 1189, 1607, 1664, 2762 cm^{-1}.

^{1}H NMR (500 MHz); δ = 1.69-1.79 (m, 2H), 2.65-2.68 (m, 2H), 6.06 (d, J = 13.4 Hz, 1H), 6.39 (d, J = 13.4 Hz, 1H), 7.09 (s, 1H), 7.29-7.53 (m, 5H).

^{13}C NMR (125 MHz); δ = 28.7, 39.2, 126.5, 127.2, 127.5, 128.2, 129.5, 131.2, 134.1, 150.2, 200.3.

HRMS (ESI) calcd for $C_{13}H_{12}O$ [M+H]$^+$ 184.0888, found 184.0886.

Cyclohexa-2,4-dien-1-one (**20f**)[15]
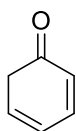
Yellow liquid

^{1}H NMR (500 MHz); δ = 3.02 (d, J = 8.2 Hz, 2H), 6.28-6.30 (m, 1H), 6.77-6.79 (m, 1H), 7.01-7.04 (m, 1H), 7.12-7.14 (m, 1H).

^{13}C NMR (125 MHz); δ = 39.9, 126.7, 129.2, 133.2, 137.9, 194.5.

7-Phenyl-4,4a,5,6-tetrahydronaphthalen-2(3H)-one (**20g**)[16]
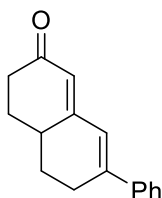
Yellow solid

^{1}H NMR (500 MHz); δ = 1.57-1.87 (m, 4H), 2.56-2.91 (m, 5H), 6.26 (s, 1H), 6.96 (s, 1H), 7.16-7.35 (m, 5H).

^{13}C NMR (125 MHz); δ = 28.0, 29.2, 29.6, 36.7, 37.6, 121.9, 123.7, 126.9, 127.7, 127.9, 136.4, 140.9, 158.6, 200.9.

3-((1*E*, 3*E*)-4-phenylbuta-1,3-dien-1-yl)cyclohex-2-en-1-one (**20h**)[17]
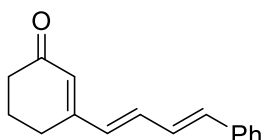
Orange solid

^{1}H NMR (500 MHz); δ = 2.06-2.09 (m, 2H), 2.44(t, J = 7.6 Hz, 2H), 2.54 (t, J = 7.6 Hz, 2H), 6.02 (s, 1H), 6.42 (d, J = 16.3 Hz, 1H), 6.72 (d, J = 16.7 Hz, 1H), 6.82 -6.84 (m, 1H), 6.92-6.95 (m, 1H), 7.29-7.43 (m, 5H).

^{13}C NMR (125 MHz); δ = 22.5, 25.0, 37.6, 127.0, 127.8, 128.5, 128.7, 129.4, 133.5, 136.0, 136.9, 137.2, 158.7, 199.9.

Synthesis of α,β-Unsaturated Imines

[General Method]

Method A: The corresponding amine (10 mmol), corresponding ketone (10 mmol), montmorillonite K10 (1 g) and molecular sieves 5A (1 g) were stirred in CH$_3$CN (10 mL) for 16 h at room temperature. The reaction mixture was filtered through celite$^®$, and the product was isolated by distillation.

Method B: A mixture of ketone (10 mmol) and benzylamine (10 mmol) in 20 mL of hexane (freshly distilled from calcium hydride) was refluxed for 15 h over molecular sieves 5A (1 g). After filtration, the crude oil was crystallized under refrigeration, and recrystallization from THF/^{n}hexane = 1/4.

(2*E*, 3*E*)-*N*-isopropyl-4-phenylbut-3-en-2-imine
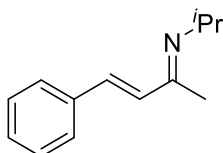
The title compound was prepared according to Method A.

Yellow oil.

^{1}H NMR (400 MHz, CDCl$_3$); δ = 1.00 (d, *J* = 5.6 Hz, 6H), 2.05 (s, 3H), 2.49-2.57 (m, 1H), 6.83 (d, *J* = 16.6 Hz, 1H), 7.32-7.59 (m, 6H).

^{13}C NMR (100 MHz, CDCl$_3$); δ = 11.6, 23.4, 67.3, 119.9, 127.8, 128.8, 128.9, 129.8, 136.2, 165.0.

HRMS (ESI) calcd for C$_{13}$H$_{18}$N [M+H]$^+$ 188.1439, found 188.1426.

(2*E*, 3*E*)-N,4-diphenylbut-3-en-2-imine423
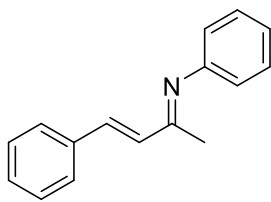
The title compound was prepared according to Method B.

White solid; mp 47-53 ^{o}C.

^{1}H NMR (500 MHz, CDCl$_3$); δ = 2.28 (s, 3H), 6.69 (d, *J* = 15.9 Hz, 1H), 7.18-7.53 (m, 11H).

^{13}C NMR (125 MHz, CDCl$_3$); δ = 13.7, 115.8, 116.6, 119.5, 120.1, 122.3, 128.1, 130.9, 136.3, 145.4, 149.1, 161.2.

(2*E*, 3*E*)-*N*-benzyl-4-phenylbut-3-en-2-imine (**30a**)[18]
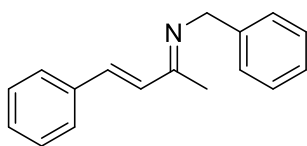
The title compound was prepared according to Method B.

Pale yellow solid; mp 61-66 °C.

^{1}H NMR (500 MHz, CDCl$_3$); δ = 2.19 (s, 3H), 4.67 (s, 1H), 4.74 (s, 1H), 6.99 (d, 1H, J = 16.4 Hz), 7.03 (d, 2H, J = 8.5 Hz), 7.26-7.53 (m, 10H).

^{13}C NMR (125 MHz, CDCl$_3$); δ = 12.2, 50.1, 124.5, 125.4, 126.0, 126.3, 126.9, 128.5, 133.4, 137.1, 139.9, 162.8.

(2*E*, 3*E*)-4-phenylbut-3-en-2-one oxime[18]
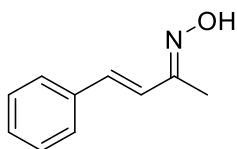
To a solution of (*E*)-4-phenylbut-3-en-2-one (1.46 g, 10 mmol) and pyridine (2.0 mL, 25 mmol) in EtOH (20 mL) was added NH$_2$OH•HCl (1.04 g, 15 mmol) in one portion and the reaction mixture was stirred at 60 °C for 12 h.   The reaction was quenched with water and extracted twice with AcOEt. The combined organic layers was washed with 1N aqueous HCl and brine, and dried over MgSO$_4$.   Volatile materials were removed under reduced pressure.

White solid; 122-124 °C.

^{1}H NMR (500 MHz, CDCl$_3$); δ = 2.15 (s, 3H), 6.87-6.93 (m, 2H), 7.28-7.35 (m, 3H), 7.46 (d, 2H, J = 7.9 Hz).

^{13}C NMR (125 MHz, CDCl$_3$); δ = 9.7, 125.7, 126.9, 128.4, 128.7, 133.4, 136.3, 156.8.

(*E*)-1-phenyl-2-((*E*)-4-phenylbut-3-en-2-ylidene)hydrazine[19]
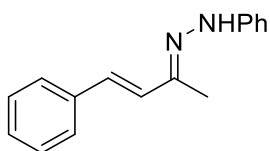
Benzalacetone (1.46 g, 10 mmol) and phenylhydrazine (1.16 g, 11 mmol) were dissolved in MeOH and AcOH (1mL) was added.   The reaction solution was stirred at room temperature.   After the completion of the reaction, the solid was collected by filtration and washed with cooled MeOH.   Then the solid was dissolved in dichloromethane, and the organic layer was washed with saturated aqueous NaHCO$_3$, brine.   After dried over Na$_2$SO$_4$, the mixture was filtered and evaporated to give the solid, which was further purified by recrystallization from AcOEt/MeOH.

Yellow solid; mp 132-135 °C.

^{1}H NMR (500 MHz, CDCl$_3$); δ = 1.96 (s, 3H), 5.40 (br s, 1H), 6.64 (d, 1H, J = 8.2 Hz), 6.89 (d, 1H, J = 8.0 Hz), 7.24-7.37 (m, 8H), 7.47-7.50 (d, 2H, J = 8.8 Hz).

^{13}C NMR (125 MHz, CDCl$_3$); δ = 14.5, 113.5, 120.5, 126.5, 127.6, 128.4, 129.3, 129.4, 130.1, 138.7, 143.0, 147.1.

(1*Z*, 2*E*)-*N*-benzyl-1,3-diphenylprop-2-en-1-imine (**30b**)[18]
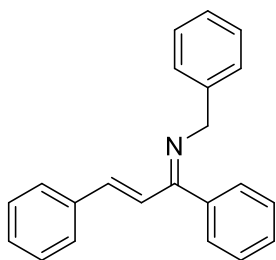
The title compound was prepared according to Method B, then recrystallized from ^{n}pentane/THF = 4/1.

White solid.

^{1}H NMR (500 MHz, CDCl$_3$); δ = 4.48 (s, 2H), 6.48 (d, 1H, J = 16.4 Hz), 7.20-7.24 (m, 3H), 7.24-7.29 (m, 4H), 7.30-7.40 (m, 6H), 7.46-7.51 (m, 3H).

^{13}C NMR (125 MHz, CDCl$_3$); δ = 57.6, 126.6, 127.3, 127.6, 127.9, 128.5, 128.6, 128.7, 128.9, 132.4, 135.8, 136.0, 139.9, 140.2, 170.4.

(1*Z*, 2*E*)-*N*-benzyl-1-phenyl-3-(*p*-tolyl)prop-2-en-1-imine (**30c**)
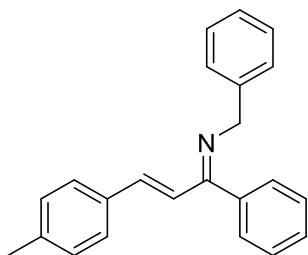
The title compound was prepared according to Method B, then recrystallized from ^{n}pentane/THF = 4/1.

^{1}H NMR (500 MHz, CDCl$_3$); δ = 2.28 (s, 3H), 4.62 (s, 1H), 4.78 (s, 1H), 6.29 (d, 1H, J =16.4 Hz), 6.57 (d, 1H, J = 16.4 Hz), 7.04-7.32 (m, 14H).

^{13}C NMR (125 MHz, CDCl$_3$); δ = 17.6, 22.5, 55.7, 57.5, 126.4, 126.8, 127.3, 127.6, 128.1, 128.7, 128.8, 132.2, 135.9, 136.0, 140.1, 140.6, 169.9.

HRMS (ESI) calcd for C$_{23}$H$_{21}$N [M+H]$^+$ 312.1752, found 312.1744.

(1*Z*, 2*E*)-N-benzyl-3-phenyl-1-(*p*-tolyl)prop-2-en-1-imine (**30d**)
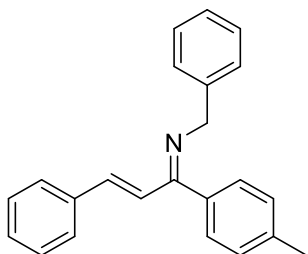
The title compound was prepared according to Method B, then recrystallized from ^{n}hexane/1,4-dioxane = 4/1.

^{1}H NMR (500 MHz, CDCl$_3$); δ = 2.40 (s, 3H), 4.29-4.61 (m, 2H), 6.39 (d, 1H, J =16.0 Hz), 6.61 (d, 1H, J = 16.0 Hz), 7.07-7.39 (m, 14H).

¹³C NMR (125 MHz, CDCl$_3$); δ = 18.7, 24.1, 56.1, 59.2, 126.5, 126.8, 127.3, 127.4, 128.1, 128.5, 129.3, 131.9, 136.2, 136.4, 139.9, 140.2, 170.8.

HRMS (ESI) calcd for C$_{23}$H$_{21}$N [M+H]$^+$ 312.1752, found 312.1761.

(1*Z*, 2*E*)-*N*-benzyl-3-(4-chlorophenyl)-1-phenylprop-2-en-1-imine (**30e**)
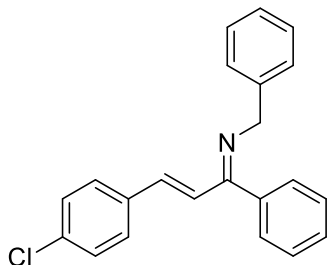
The title compound was prepared according to Method B, then recrystallized from ^{n}pentane/Et$_2$O = 4/1.

¹H NMR (500 MHz, CDCl$_3$); δ = 4.57 (s, 1H), 4.73 (s, 1H), 6.44 (d, 1H, *J* =14.5 Hz), 6.91 (d, 1H, *J* = 14.6 Hz), 7.11-7.58 (m, 12H), 7.94 (d, 2H, *J* = 7.6 Hz).

¹³C NMR (125 MHz, CDCl$_3$); δ = 60.5, 120.6, 124.5, 127.6, 127.9, 128.4, 128.7, 128.9, 129.1, 129.3, 129.7, 130.2, 132.1, 134.7, 140.3, 167.9.

HRMS (ESI) calcd for C$_{22}$H$_{18}$NCl [M+H]$^+$ 332.1206, found 332.1202.

(2*E*, 3*E*)-*N*-benzyl-4-(*p*-tolyl)but-3-en-2-imine (**30f**)
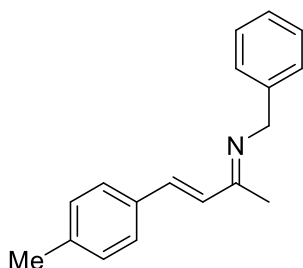
The title compound was prepared according to Method B, then recrystallized from ^{n}pentane/Et$_2$O = 4/1.

¹H NMR (500 MHz, CDCl$_3$); δ = 2.15 (s, 3H), 2.41 (s, 3H), 4.65 (s, 1H), 4.75 (s, 1H), 6.92 (d, 1H, *J* = 17.2 Hz), 7.21-7.47 (m, 10H).

¹³C NMR (125 MHz, CDCl$_3$); δ = 12.1, 23.5, 50.0, 120.0, 120.4, 127.5, 127.6, 128.7, 130.3, 130.5, 136.2, 137.8, 139.8, 159.9.

HRMS (ESI) calcd for C$_{18}$H$_{20}$N [M+H]$^+$ 250.1596, found 250.1604.

Bis(pinacolato)diboron (**14a**)[20]
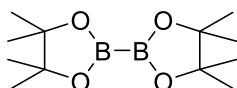
White solid

¹H NMR (500 MHz); δ = 1.26 (s, 24H).

¹³C NMR (125 MHz); δ = 25.0, 83.5.

^{11}B NMR (160 MHz); δ = 30.6 [lit[21] 30.6 ppm].

\<Metal Salts\>

Cu(OH)$_2$ was purchased from Kojundo (99.0% min. purity).

Typical Experimental Procedure for Chiral Cu(OH)$_2$-Catalyzed Enantioselective Boron Conjugate Additions to α,β-Unsaturated Carbonyl Compounds in Water (Table 5, entry 2):

To an aqueous solution (1 mL) of Cu(OH)$_2$ (2.0 mg, 5 mol%) and chiral 2,2'-bipyridine **L1** (7.9 mg, 6 mol%) was added an acetic acid solution (24 mM, 1 mL).   After stirred vigorously for 1 h at room temperature, the resultant mixture was allowed to cool to 5 ^{o}C.   Chalcone **13a** (81.9 mg, 0.4 mmol) and B$_2$(pin)$_2$ **14a** (121.8 mg, 0.48 mmol) was then added successively at the same temperature.   After stirring for 12 h, the reaction mixture was filtered and rinsed with AcOEt. The aqueous layer was extracted with AcOEt (20 mL) three times, and the combined organic layers were dried over anhydrous Na$_2$SO$_4$.   After concentrated under reduced pressure, the crude mixture was purified by preparative TLC (^{n}hexane/AcOEt = 4/1) to afford the desired product **15a** (127.9 mg, 95% yield) as a colorless oil.

(*R*)-1,3-Diphenyl-3-(4,4,5,5-tetramethyl-1,3,2-dioxaborolan-2-yl)propan-1-one (**15a**)[22]
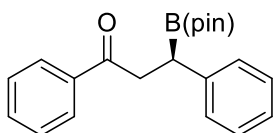
^{1}H NMR (500 MHz); δ = 1.25 (s, 12H), 2.80 (t, *J* = 6.0 Hz, 1H), 3.39 (d, *J* = 2.9 Hz, *J* = 5.8 Hz, 1H), 3.54 (d, *J* = 2.9 Hz, *J* = 5.8 Hz, 1H), 7.28-7.48 (m, 7H), 7.56-7.59 (m, 1H), 7.95 (d, *J* = 7.0 Hz, 2H).
^{13}C NMR (125 MHz); δ = 25.1, 44.4, 70.0, 83.6, 120.7, 127.5, 128.0, 128.3, 128.4, 133.6, 136.6, 143.0, 200.1.
HPLC (Dialcel Chiralpak IA, ^{n}hexane/ ^{i}PrOH = 90/10, flow rate 0.5 mL/min); t$_R$ = 9.2 min (*S*, minor), t$_R$ = 12.5 min (*R*, major).

Analytical Data for Oxidized or Substituted Compounds

Almost all adducts are literature-known; obtained analytical data for these compounds is in full agreement with reported data.   The absolute configurations of optically active compounds were determined by comparison of the order of retention time in the chiral HPLC analyses.

Typical Experimental Procedure for Oxidation Step

After the reaction of **13a** with **14a** completed, the reaction mixture was filtered and rinsed with THF (3 mL).   The excess amount of NaBO$_3$·4H$_2$O (488 mg) was then added and the mixture was stirred at room temperature for 4 h.   The aqueous layer was extracted with AcOEt (20 mL) three times, and the combined organic layers were dried over anhydrous Na$_2$SO$_4$.   After concentrated under reduced pressure, the crude mixture was purified by preparative TLC (^{n}hexane/AcOEt = 4/1) to afford the desired product **16a** (84.6 mg, Quant.) as a colorless oil.

(*R*)-3-Hydroxy-1,3-diphenylpropan-1-one (**16a**)[23]
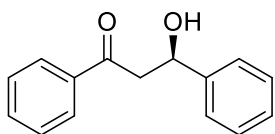
Colorless oil
^{1}H NMR (500 MHz); δ = 3.37 (d, *J* = 5.8 Hz, 2H), 5.35 (t, *J* = 6.0 Hz, 1H), 7.28-7.48 (m, 7H), 7.56-7.59 (m, 1H), 7.95 (d, *J* = 7.0 Hz, 2H).
^{13}C NMR (125 MHz); δ = 47.4, 70.0, 120.7, 127.5, 128.0, 128.3, 128.4, 133.6, 136.6, 143.0, 200.1.
HPLC (Dialcel Chiralcel OD-H, ^{n}hexane/ ^{i}PrOH = 85/15, flow rate 0.7 mL/min); t_R = 14.4 min (*S*, minor), t_R = 16.3 min (*R*, major).
$[\alpha]_D^{27}$ = + 69.3 (*c* = 0.84, CHCl$_3$).

Typical Experimental Procedure for Substitution Step[24]

After the reaction of **13a** with **14a** completed, the reaction mixture was filtered and the crude was purified by flash column chromatography and dissolved in 5 mL of DCM. Then BCl$_3$ (1.0 mmol) was added slowly to the solution. The reaction mixture was then stirred for 4 h at room temperature. After removal of the solvent and pumped off the volatiles (0.4 kPa, 1 hr), 5 mL of DCM was added and the solution was cooled down to 0 °C. Benzyl azide was then added and the reaction mixture was warmed up slowly to room temperature and continued stirring for 30 min. Finally, Et$_2$O and NaOH (1 M in H$_2$O) were added to the solution to quench the reaction. The crude was purified by PTLC (^{n}hexane/AcOEt = 1/2) to afford the desired product (95.5 mg, 81% yield) as a colorless oil.

(*R*)-3-(benzylamino)-1,3-diphenylpropan-1-one[25]
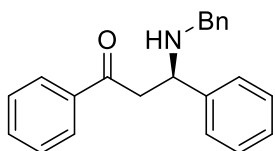
Colorless oil
^{1}H NMR (500 MHz); δ = 1.77 (s, 1H), 3.28-3.40 (m, 2H), 3.57-3.66 (m, 2H), 4.30-4.32 (m, 1H), 7.19-7.52 (m, 13H), 7.90 (d, *J* = 7.0 Hz, 2H).
^{13}C NMR (125 MHz); δ = 45.6, 47.1, 58.7, 127.2, 127.2, 127.3, 127.4, 127.7, 127.9, 128.1, 128.3, 133.4, 137.8, 140.1, 143.2, 198.6.
HPLC (Dialcel Chiralcel OD-H, ^{n}hexane/ ^{i}PrOH = 90/10, flow rate 1.0 mL/min); t_R = 14.7 min (*S*, minor), t_R = 18.9 min (*R*, major).
$[\alpha]_D^{28}$ = + 26.3 (*c* = 0.42, MeOH).

(*R*)-3-Phenyl-3-hydroxy-1-(4'-fluorophenyl)propan-1-one (**16b**)[26]
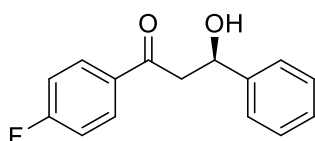
Colorless oil

^{1}H NMR (500 MHz); δ = 3.33-3.36 (m, 2H), 3.46 (d, J = 2.6 Hz, 1H), 5.33-5.35 (m, 1H), 7.10-7.14 (m, 2H), 7.28-7.44 (m, 5H), 7.99 (d, J = 7.0 Hz, 2H).

^{13}C NMR (125 MHz); δ = 47.2, 70.1, 115.8 (d, J = 4.2 Hz), 121.5, 125.7, 128.2 (d, J = 107.5 Hz), 130.9 (d, J = 9.6 Hz), 132.9, 142.9, 157.2 (d, J = 256 Hz), 198.4.

HPLC (Dialcel Chiralpak AS-H, ^{n}hexane/ ^{i}PrOH = 90/10, flow rate 1.0 mL/min); t_R = 13.2 min (S, minor), t_R = 14.2 min (R, major).

$[α]_D^{28}$ = + 53.3 (c = 0.86, CHCl$_3$).

(R)-3-(2'-Chlorophenyl)-3-hydroxy-1-(4'-fluorophenyl)propan-1-one (**16c**)[26]
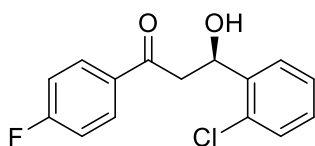
Colorless oil

^{1}H NMR (500 MHz); δ = 3.13 (dd, J = 8.7, 11.5 Hz, 1H), 3.51 (d, J = 16.3 Hz, 1H), 3.73 (s, 1H), 5.32 (d, J = 9.6 Hz, 1H), 7.10-7.15 (m, 2H), 7.22-7.26 (m, 1H), 7.31-7.36 (m, 2H), 7.70 (d, J = 7.7 Hz, 1H), 7.99-8.00 (m, 2H).

^{13}C NMR (125 MHz); δ = 45.3, 66.8, 115.8 (d, J = 4.2 Hz), 127.3 (d, J = 4.7 Hz), 128.6, 129.4, 130.9 (d, J = 9.6 Hz), 131.0, 131.2, 133.0, 140.3, 167.1, 198.5.

HPLC (Dialcel Chiralcel OD-H, ^{n}hexane/ ^{i}PrOH = 85/15, flow rate 0.7 mL/min); t_R = 13.9 min (S, minor), t_R = 16.2 min (R, major).

$[α]_D^{27}$ = + 58.2 (c = 0.85, CHCl$_3$).

(R)-3-hydroxy-1-(4'-methoxylphenyl)-3-phenylpropan-1-one (**16d**)[26]
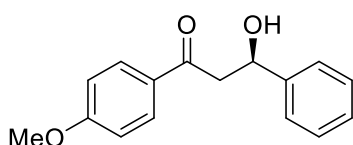
Colorless oil

^{1}H NMR (500 MHz); δ = 3.31 (d, J = 7.6 Hz, 2H), 3.72 (s, 1H), 3.86 (s, 3H), 5.32 (m, 1H), 6.91(d, J = 9.0 Hz, 2H), 7.27-7.30 (m, 1H), 7.37 (t, J = 6.0 Hz, 2H), 7.44 (d, J = 7.7 Hz, 2H), 7.93 (d, J = 9.0 Hz, 2H).

^{13}C NMR (125 MHz); δ = 46.9, 55.5, 70.2, 113.8, 113.9, 121.3, 125.7, 127.6, 128.5, 129.7, 130.5, 164.3, 198.7.

HPLC (Dialcel Chiralcel OD-H, ^{n}hexane/ ^{i}PrOH = 85/15, flow rate 1.0 mL/min); t_R = 11.2 min (S, minor), t_R = 12.8 min (R, major).

$[α]_D^{25}$ = + 37.2 (c = 0.80, CHCl$_3$).

(R)-3-(4'-Chlorophenyl)-3-hydroxy-1-phenylpropan-1-one (**16e**)[23]
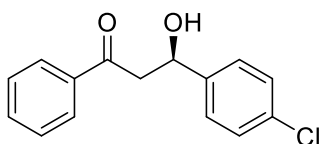
Colorless oil

^{1}H NMR (500 MHz); δ = 3.34 (d, *J* = 5.8 Hz, 2H), 3.61 (d, *J* = 8.5 Hz, 1H), 5.33 (t, *J* = 6.0 Hz, 1H), 7.33-7.39 (m, 4H), 7.47 (t, *J* = 8.1 Hz, 2H), 7.58-7.61 (m, 1H), 7.95 (d, *J* = 7.0 Hz, 2H).

^{13}C NMR (125 MHz); δ = 47.2, 69.5, 127.2, 128.1, 128.7, 128.8, 133.8, 136.5, 140.1, 141.5, 200.0.

HPLC (Dialcel Chiralpak AD-H, ^{n}hexane/ ^{i}PrOH = 90/10, flow rate 1.0 mL/min); t$_R$ = 13.6 min (*S*, minor), t$_R$ = 14.3 min (*R*, major).

[α]$_D^{26}$ = + 43.3 (*c* = 0.81, CHCl$_3$).

(*R*)-3-(4'-Methoxyphenyl)-3-hydroxy-1-phenylpropan-1-one (**16f**)[23]
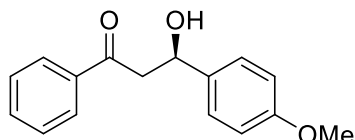
Colorless oil

^{1}H NMR (500 MHz); δ = 3.34-3.37 (m, 2H), 3.50 (d, *J* = 2.9 Hz, 1H), 3.80 (s, 3H), 5.28-5.30 (m, 1H), 6.89-6.92 (m, 2H), 7.34-7.37 (m, 2H), 7.44-7.47 (m, 2H), 7.56-7.59 (m, 1H), 7.95 (dd, *J* = 1.8, 5.2 Hz, 2H).

^{13}C NMR (125 MHz); δ = 55.3, 67.1, 74.3, 114.0, 127.0, 128.1, 128.7, 133.6, 135.2, 136.7, 159.2, 200.2.

HPLC (Dialcel Chiralpak AS-H, ^{n}hexane/ ^{i}PrOH = 80/20, flow rate 1.0 mL/min); t$_R$ = 15.2 min (*S*, minor), t$_R$ = 16.2 min (*R*, major).

[α]$_D^{25}$ = + 46.5 (*c* = 0.92, CHCl$_3$).

(*S*)-3-Hydroxy-1-phenylbutan-1-one (**16g**)[27]
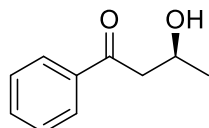
Colorless oil

^{1}H NMR (500 MHz); δ = 1.30 (d, *J* = 6.9 Hz, 3H), 3.04 (dd, *J* = 8.6, 9.2 Hz, 1H), 3.16 (dd, *J* = 3.4, 14.9 Hz, 1H), 3.30 (s, 1H), 4.41 (d, *J* = 2.3 Hz, 1H), 7.47 (t, *J* = 8.0 Hz, 2H), 7.56-7.60 (m, 1H), 7.94-7.96 (m, 2H).

^{13}C NMR (125 MHz); δ = 22.4, 46.5, 64.0, 128.0, 128.7, 133.5, 136.8, 200.8.

HPLC (Dialcel Chiralcel OD-H, ^{n}hexane/ ^{i}PrOH = 90/10, flow rate 0.7 mL/min); t$_R$ = 5.3 min (*R*, minor), t$_R$ = 7.1 min (*S*, major).

[α]$_D^{29}$ = + 68.2 (*c* = 0.93, CHCl$_3$).

(*S*)-3-Hydroxy-1-phenylpentan-1-one (**16h**)[27]
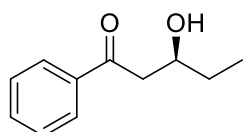
Colorless oil

^{1}H NMR (500 MHz); δ = 1.00-1.03 (m, 3H), 1.57-1.66 (m, 2H), 3.01-3.06 (m, 1H), 3.19 (dd, *J* = 2.3, 16.5 Hz, 1H), 3.28 (s, 1H), 4.15 (d, *J* = 7.5 Hz, 1H), 7.47 (t, *J* = 8.0 Hz, 2H), 7.58-7.61 (m, 1H), 7.95-7.97 (m, 2H).

^{13}C NMR (125 MHz); δ = 9.9, 29.3, 44.5, 69.1, 128.0, 128.7, 128.7, 133.5, 133.5, 136.7, 201.0.

HPLC (Dialcel Chiralcel OD-H, ^{n}hexane/ ^{i}PrOH = 90/10, flow rate 0.7 mL/min); t_R = 10.0 min (*R*, minor), t_R = 13.1 min (*S*, major).

$[\alpha]_D^{27}$ = + 62.2 (*c* = 0.79, CHCl$_3$).

(*R*)-3-Hydroxy-4-methyl-1-phenylpentan-1-one (**16i**)[28]
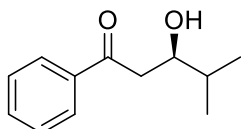
Colorless oil

^{1}H NMR (500 MHz); δ = 0.99-1.02 (m, 6H), 1.79-1.83 (m, 1H), 3.03 (dd, *J* = 8.0, 9.8 Hz, 1H), 3.14-3.18 (m, 1H), 4.00 (t, *J* = 2.5 Hz, 1H), 7.47 (t, *J* = 8.1 Hz, 2H), 7.56-7.59 (m, 1H), 7.96 (dd, *J* = 1.2, 7.5 Hz, 2H).

^{13}C NMR (125 MHz); δ = 17.8, 18.5, 33.1, 42.0, 72.4, 128.1, 128.6, 133.4, 137.0, 195.7.

HPLC (Dialcel Chiralcel OD-H, ^{n}hexane/ ^{i}PrOH = 90/10, flow rate 0.5 mL/min); t_R = 12.4 min (*S*, minor), t_R = 13.2 min (*R*, major).

$[\alpha]_D^{28}$ = + 69.9 (*c* = 0.98, CHCl$_3$).

(*R*)-3-Hydroxy-4,4-dimethyl-1-phenylpentan-1-one (**16j**)[29]
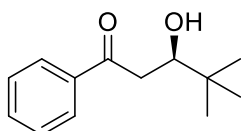
Colorless oil

^{1}H NMR (500 MHz); δ = 0.98 (s, 9H), 2.98 (dd, *J* = 7.5, 10.3 Hz, 1H), 3.07 (s, 1H), 3.18 (d, *J* = 17.2 Hz, 1H), 3.88 (d, *J* = 10.1 Hz, 1H), 7.45-7.48 (m, 2H), 7.56-7.59 (m, 1H), 7.96 (d, *J* = 8.4 Hz, 2H).

^{13}C NMR (125 MHz); δ = 25.8, 27.7, 34.4, 40.1, 75.1, 123.5, 128.1, 128.6, 133.4, 201.6.

HPLC (Dialcel Chiralcel OD-H, ^{n}hexane/ ^{i}PrOH = 85/15, flow rate 0.7 mL/min); t_R = 11.2 min (*S*, minor), t_R = 13.1 min (*R*, major).

$[\alpha]_D^{29}$ = + 70.2 (*c* = 0.87, CHCl$_3$).

(*R*)-4-Hydroxy-4-phenylbutan-2-one (**16k**)[26]
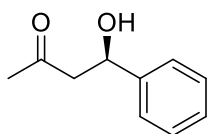
Colorless oil

^{1}H NMR (500 MHz); δ = 1.63 (s, 3H), 2.79-2.91 (m, 2H), 3.26 (d, J = 3.5 Hz, 1H), 5.15 (t, J = 2.8 Hz, 1H), 7.26-7.35 (m, 5H).

^{13}C NMR (125 MHz); δ = 30.7, 52.0, 69.9, 125.6, 127.7, 128.5, 142.8, 209.0.

HPLC (Dialcel Chiralcel AS-H, [n]hexane/ [i]PrOH = 90/10, flow rate 1.0 mL/min); t_R = 10.1 min (S, minor), t_R = 11.1 min (R, major).

$[\alpha]_D^{28}$ = + 55.5 (c = 1.06, CHCl$_3$).

(R)-3-hydroxycyclohexanone (16l)[30]
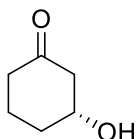
Colorless oil

^{1}H NMR (500 MHz); δ = 1.69-1.79 (m, 2H), 1.89-2.07 (m, 2H), 2.30 (dd, J = 7.0, 6.2 Hz, 2H), 2.38 (dd, J = 7.6, 14.0 Hz, 1H), 2.59 (dd, J = 4.1, 14.0 Hz, 1H), 4.07-4.19 (m, 1H).

^{13}C NMR (125 MHz); δ = 21.2, 33.4, 40.8, 50.2, 69.4, 210.2.

$[\alpha]_D^{29}$ = + 37.3 (c = 0.80, CHCl$_3$).

The ee value was determined as benzoylated compound;

To the oxidized product **16l** (ca. 0.2 mmol) in dichloromethane (2 mL) was added pyridine (31.6 mg, 0.4 mmol) and benzoyl chloride (140.6 mg, 1.0 mmol).　The mixture was stirred for 1 h at 0 °C.　The resulting mixture was quenched with water.　The obtained organic layer was extracted with brine and dried over anhydrous Na$_2$SO$_4$.　After removal of the solvent, the residue was purified by preparative TLC ([n]hexane/AcOEt = 3/1) to afford benzoylated product (41.9 mg, 96% yield in 3 steps) as a colorless oil.

(R)-3-oxocyclohexyl benzoate
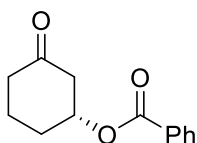
Colorless oil

^{1}H NMR (500 MHz); δ = 1.69-1.79 (m, 2H), 1.99-2.07 (m, 2H), 2.28-2.32 (m, 2H), 2.37-2.42 (m 1H), 2.60-2.66 (m, 1H), 4.83-4.87 (m, 1H), 7.45-7.48 (m, 2H), 7.56-7.59 (m, 1H), 7.96-7.99 (m, 2H).

^{13}C NMR (125 MHz); δ = 21.2, 32.4, 40.8, 50.2, 68.4, 128.0, 128.7, 133.6, 136.9, 207.3, 212.2.

HPLC (Dialcel Chiralcel OD-H, [n]hexane/ [i]PrOH = 90/10, flow rate 0.5 mL/min); t_R = 16.9 min (R, major), t_R = 18.5 min (S, minor).

(S)-3-hydroxy-1,3-diphenylbutan-1-one (16m)[31]
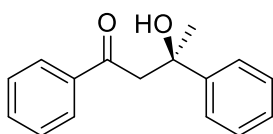
Colorless oil
^{1}H NMR (500 MHz); δ = 1.62 (s, 3H), 3.34 (d, J = 17.0 Hz, 1H), 3.79 (d, J = 17.0 Hz, 1H), 4.87 (s, 1H), 7.21 (t, J = 7.0 Hz, 1H), 7.31 (t, J = 8.0 Hz, 2H), 7.44-7.49 (m, 4H), 7.57 (t, J = 7.0 Hz, 1H), 7.95 (d, J = 8.0 Hz, 2H).
^{13}C NMR (125 MHz); δ = 30.9, 49.1, 71.2, 124.3, 126.6, 128.0, 128.2, 128.6, 133.6, 136.6, 147.5, 200.6.
HPLC (Dialcel Chiralcel OD-H, ^{n}hexane/ ^{i}PrOH = 90/10, flow rate 0.7 mL/min); t_R = 18.5 min (R, minor), t_R = 21.7 min (S, major).
$[\alpha]_D^{29}$ = + 51.2 (c = 1.21, CHCl$_3$).

(R)-4-hydroxy-4-phenylpentan-2-one (**16n**)[32]
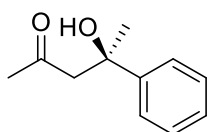
Colorless oil
^{1}H NMR (500 MHz); δ = 1.51 (s, 3H), 2.06 (s, 3H), 2.83 (d, J = 17.0 Hz, 1H), 3.10 (d, J = 17.0 Hz, 1H), 4.31 (s, 1H), 7.23-7.43 (m, 5H).
^{13}C NMR (125 MHz); δ = 30.2, 33.6, 53.9, 72.8, 124.1, 126.3, 128.4, 147.2, 208.7.
HPLC (Dialcel Chiralcel OD-H, ^{n}hexane/ ^{i}PrOH = 90/10, flow rate 0.8 mL/min); t_R = 15.0 min (R, major), t_R = 16.8 min (S, minor).
$[\alpha]_D^{28}$ = + 27.3 (c = 0.93, CHCl$_3$).

(R)-3-hydroxy-3-methylcyclohexan-1-one (**16o**)[33]
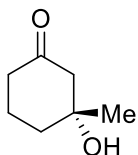
Colorless oil
^{1}H NMR (500 MHz); δ = 1.32 (s, 3H), 1.89-1.99 (m, 2H), 2.34-2.48 (m, 4H), 3.98 (m, 1H), 5.31 (s, 1H).
^{13}C NMR (125 MHz); δ = 13.8, 20.4, 29.8, 37.6, 47.9, 54.1, 64.7, 208.0.

The ee value was determined as benzoylated compound;
To the oxidized product **16o** (ca. 0.2 mmol) in dichloromethane (2 mL) was added pyridine (31.6 mg, 0.4 mmol) and benzoyl chloride (140.6 mg, 1.0 mmol). The mixture was stirred for 1 h at 0 ^{o}C. The resulting mixture was quenched with water. The obtained organic layer was extracted with brine and dried over anhydrous Na$_2$SO$_4$. After removal of the solvent, the residue was purified by preparative TLC (^{n}hexane/AcOEt = 3/1) to afford benzoylated product (41.9 mg, 88% yield in 3 steps) as a colorless oil.
(R)-1-methyl-3-oxocyclohexyl benzoate
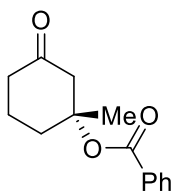
Colorless oil

^{1}H NMR (500 MHz); δ = 1.35 (s, 3H), 1.89-2.02 (m, 2H), 2.34-2.48 (m, 4H), 3.98 (m, 1H), 5.31 (s, 1H), 7.457.96 (m, 5H).

^{13}C NMR (125 MHz); δ = 13.8, 20.4, 29.8, 37.6, 47.9, 54.1, 64.7, 128.0, 128.7, 133.6, 136.9, 178.2, 208.2.

HPLC (Dialcel Chiralcel OD-H, ^{n}hexane/ ^{i}PrOH = 90/10, flow rate 0.5 mL/min); t_R = 5.1 min (*S*, minor), t_R = 6.5 min (*R*, major).

(*R*)-3-hydroxy-3-phenylcyclohexan-1-one (**16p**)[34]
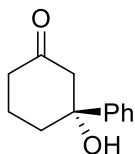
White Powder; mp 134-136 ^{o}C.

^{1}H NMR (500 MHz); δ = 1.59-1.89 (m, 2H), 2.20-2.48 (m, 5H), 2.61 (m, 1H), 2.92 (s, 1H), 7.26-7.46 (m, 5H).

^{13}C NMR (125 MHz); δ = 21.7, 36.5, 47.9, 54.1, 68.7, 124.7, 128.2, 128.2, 131.9, 131.9, 147.5, 210.0.

HPLC (Dialcel Chiralcel AD-H, ^{n}hexane/ ^{i}PrOH = 90/10, flow rate 1.0 mL/min); t_R = 10.0 min (*R*, major), t_R = 13.7 min (*S*, minor).

$[α]_D^{27}$ = + 12.2 (*c* = 0.85, CHCl$_3$).

(*R*)-3-hydroxy-3-methylcyclopentan-1-one (**16q**)[35]
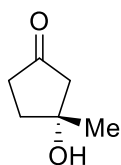
Colorless oil

^{1}H NMR (500 MHz); δ =1.55 (s, 3H), 2.21-2.23 (m, 2H), 2.68-2.69 (m, 2H), 3.01 (s, 3H), 4.17 (s, 1H).

^{13}C NMR (125 MHz); δ = 29.6, 33.7, 37.6, 52.1, 69.8, 213.9.

$[α]_D^{30}$ = + 19.1 (*c* = 0.93, CHCl$_3$).

The ee value was determined as benzoylated compound;

To the oxidized product **16q** (ca. 0.2 mmol) in dichloromethane (2 mL) was added pyridine (31.6 mg, 0.4 mmol) and benzoyl chloride (140.6 mg, 1.0 mmol).   The mixture was stirred for 1 h at 0 ^{o}C.   The resulting mixture was quenched with water.   The obtained organic layer was extracted

with brine and dried over anhydrous Na_2SO_4. After removal of the solvent, the residue was purified by preparative TLC (*n*hexane/AcOEt = 3/1) to afford benzoylated product (41.9 mg, 88% yield in 3 steps) as a colorless oil.

(*R*)-1-methyl-3-oxocyclohexyl benzoate
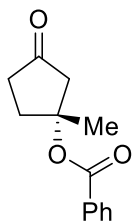
Colorless oil

^{1}H NMR (500 MHz); δ = 1.55 (s, 3H), 2.21-2.23 (m, 2H), 2.68-2.69 (m, 2H), 3.01 (s, 3H), 7.41-7.89 (m, 5H).

^{13}C NMR (125 MHz); δ = 29.6, 33.7, 37.6, 52.1, 69.8, 128.0, 128.7, 133.6, 136.9, 175.4, 205.9.

HPLC (Dialcel Chiralcel OD-H, *n*hexane/ *i*PrOH = 90/10, flow rate 0.5 mL/min); t_R = 13.9 min (*S*, minor), t_R = 16.9 min (*R*, major).

(*R*)-Methyl 3-hydroxy-3-phenylpropanoate (**16r**)[36]
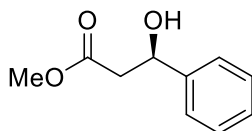
Colorless oil

^{1}H NMR (500 MHz); δ = 2.66-2.77 (m, 2H), 3.38 (s, 1H), 3.68 (s, 3H), 5.11 (d, *J* = 9.1 Hz, 1H), 7.25-7.37 (m, 5H).

^{13}C NMR (125 MHz); δ = 43.2, 51.7, 70.2, 125.6, 127.7, 128.4, 142.6, 172.6.

HPLC (Dialcel Chiralcel OD-H, *n*hexane/ *i*PrOH = 90/10, flow rate 1.0 mL/min); t_R = 12.0 min (*S*, minor), t_R = 13.3 min (*R*, major).

$[α]_D^{28}$ = + 37.9 (*c* = 0.92, CHCl$_3$).

(*R*)-Ethyl-3-hydroxy-3-phenylpropanoate (**16s**)[37]
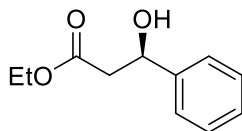
Colorless oil

^{1}H NMR (500 MHz); δ = 1.23 (t, *J* = 6.3 Hz, 3H), 2.66-2.75 (m, 2H), 3.30 (d, *J* = 2.9 Hz, 1H), 4.15 (q, *J* = 5.7 Hz, 1H), 5.09-5.12 (m, 1H), 7.23-7.36 (m, 5H).

^{13}C NMR (125 MHz); δ = 14.1, 43.3, 60.8, 70.3, 125.6, 127.7, 128.5, 142.5, 173.3.

HPLC (Dialcel Chiralcel OD-H, *n*hexane/ *i*PrOH = 90/10, flow rate 1.0 mL/min); t_R = 11.2 min (*S*, minor), t_R = 12.9 min (*R*, major).

$[α]_D^{28}$ = + 48.9 (*c* = 0.84, CHCl$_3$).

(*S*)-Ethyl-3-hydroxybutanoate (**16t**)[38]
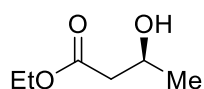
Colorless oil
^{1}H NMR (500 MHz); δ = 1.20-1.29 (m, 6H), 2.39-2.51 (m, 2H), 3.05 (s, 1H), 4.15-4.23 (m, 3H).
^{13}C NMR (125 MHz); δ = 22.4, 42.8, 60.6, 64.2, 172.8, 212.2.
$[\alpha]_D^{28}$ = + 36.2 (*c* = 0.96, CHCl$_3$).

The ee value was determined as benzoylated compound;
To the oxidized product **16t** (ca. 0.2 mmol) in dichloromethane (2 mL) was added pyridine (31.6 mg, 0.4 mmol) and benzoyl chloride (140.6 mg, 1.0 mmol).   The mixture was stirred for 1 h at 0 °C.   The resulting mixture was quenched with water.   The obtained organic layer was extracted with brine and dried over anhydrous Na$_2$SO$_4$.   After removal of the solvent, the residue was purified by preparative TLC (^{n}hexane/AcOEt = 3/1) to afford benzoylated product (37.8 mg, 80% yield in 3 steps) as a colorless oil.
(*S*)-4-ethoxy-4-oxobutan-2-yl benzoate
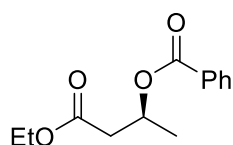
Colorless oil
^{1}H NMR (500 MHz); δ = 1.20-1.29 (m, 6H), 2.39-2.51 (m, 2H), 4.19-4.23 (m, 3H), 4.98 (s, 1H), 7.45-7.48 (m, 2H), 7.56-7.59 (m, 1H), 7.95-7.99 (m, 2H).
^{13}C NMR (125 MHz); δ = 14.0, 22.4, 42.8, 60.6, 64.2, 128.0, 128.7, 133.6, 136.9, 172.8, 212.2.
HPLC (Dialcel Chiralcel OD-H, ^{n}hexane/ ^{i}PrOH = 85/15, flow rate 0.7 mL/min); t$_R$ = 10.8 min (*S*, major), t$_R$ = 12.2 min (*R*, minor).

(*S*)-4-hydroxytetrahydro-2H-pyran-2-one (**16u**)[39]
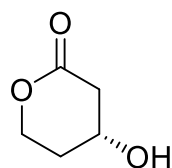
Colorless oil
^{1}H NMR (500 MHz); δ= 1.81-1.88 (m, 2H), 2.61-2.78 (m, 2H), 3.56 (m, 1H), 4.29 (m, 1H), 4.36 (m, 1H), 4.64 (m, 1H).
^{13}C NMR (125 MHz); δ = 27.1, 42.5, 59.5, 68.3, 178.2.
$[\alpha]_D^{33}$ = + 6.1 (*c* = 0.93, CHCl$_3$).

The ee value was determined as benzoylated compound;
To the oxidized product **16u** (ca. 0.2 mmol) in dichloromethane (2 mL) was added pyridine (31.6 mg, 0.4 mmol) and benzoyl chloride (140.6 mg, 1.0 mmol).   The mixture was stirred for 1 h at 0

°C. The resulting mixture was quenched with water. The obtained organic layer was extracted with brine and dried over anhydrous Na$_2$SO$_4$. After removal of the solvent, the residue was purified by preparative TLC (^{n}hexane/AcOEt = 3/1) to afford benzoylated product (41.9 mg, 96% yield in 3 steps) as a colorless oil.

(*S*)-3-oxocyclohexyl benzoate
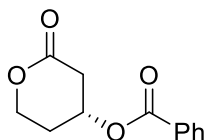
Colorless oil

^{1}H NMR (500 MHz); δ = 1.81-1.88 (m, 2H), 2.61-2.78 (m, 2H), 3.56 (m, 1H), 4.29 (m, 1H), 4.41 (m, 1H), 7.45-7.48 (m, 2H), 7.56-7.59 (m, 1H), 7.96-7.99 (m, 2H).

^{13}C NMR (125 MHz); δ = 21.2, 32.4, 40.8, 50.2, 68.4, 128.0, 128.7, 133.6, 136.9, 207.3, 212.2.

HPLC (Dialcel Chiralcel OD-H, ^{n}hexane/ ^{i}PrOH = 90/10, flow rate 0.5 mL/min); t$_R$ = 6.9 min (*R*, minor), t$_R$ = 9.5 min (*S*, major).

Ethyl (*R*)-3-hydroxy-3-phenylbutanoate (**16v**)[40]
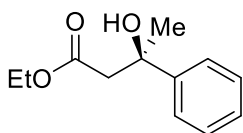
Yellow oil

^{1}H NMR (500 MHz); δ =1.18 (t, *J* = 6.8 Hz, 3H), 1.62-1.68 (m, 3H), 2.32-2.39 (m, 2H), 2.73 (d, *J* = 13.4 Hz, 1H), 3.00 (d, *J* = 13.4 Hz, 1H), 4.73 (s, 1H), 7.24 (t, *J* = 6.9 Hz, 1H), 7.32 (t, *J* = 7.5 Hz, 2H), 7.43 (d, *J* = 8.0 Hz, 2H).

^{13}C NMR (125 MHz); δ = 14.1, 28.5, 45.6, 60.8, 72.3, 127.5, 127.8, 128.5, 129.6, 182.9.

HPLC (Dialcel Chiralcel OD-H, ^{n}hexane/ ^{i}PrOH = 90/10, flow rate 0.7 mL/min); t$_R$ = 8.8 min (*S*, minor), t$_R$ = 13.2 min (*R*, major).

[α]$_D$^{21} = + 27.9 (*c* = 0.82, CHCl$_3$).

(*R*)-3-Hydroxy-*N,N*-dimethyl-3-phenylpropanamide (**16w**)[41]
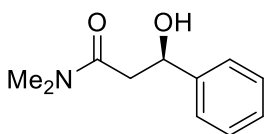
A little bit yellow oil

^{1}H NMR (500 MHz); δ = 2.59-2.71 (m, 2H), 2.90 (s, 3H), 2.94 (s, 3H), 5.12-5.15 (m, 1H), 7.28-7.29 (m, 1H), 7.34-7.40 (m, 4H).

^{13}C NMR (125 MHz); δ = 34.9, 36.8, 70.1, 125.5, 127.1, 128.1, 143.0, 172.0.

HPLC (Dialcel Chiralcel OD-H, ^{n}hexane/ ^{i}PrOH = 90/10, flow rate 1.0 mL/min); t$_R$ = 13.0 min (*S*, minor), t$_R$ = 14.6 min (*R*, major).

[α]$_D$^{26} = + 91.5 (*c* = 0.62, CHCl$_3$).

(*R*)-3-Hydroxy-*N,N*-diethyl-3-phenylpropanamide (**16x**)[42]
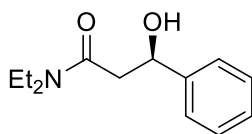
A little bit yellow oil
^{1}H NMR (500 MHz); δ = 1.07-1.12 (m, 6H), 2.55-2.67 (m, 4H), 3.15-3.24 (m, 1H), 3.31-3.42 (m, 1H), 4.99 (s, 1H), 5.34 (d, *J* = 9.3 Hz, 1H), 7.24-7.38 (m, 5H).
^{13}C NMR (125 MHz); δ = 12.9, 13.9, 40.1, 41.4, 41.8, 70.5, 125.6, 127.3, 128.3, 143.2, 171.3.
HPLC (Dialcel Chiralcel OD-H, ^{n}hexane/ ^{i}PrOH = 90/10, flow rate 1.0 mL/min); t_R = 13.7 min (*S*, minor), t_R = 14.4 min (*R*, major).
$[\alpha]_D^{27}$ = + 89.9 (*c* = 0.73, CHCl$_3$).

(*R*)-*N,N*-diethyl-3-hydroxy-3-phenylbutanamide (**16y**)[43]
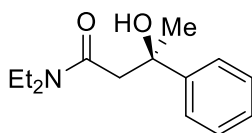
Colorless oil
^{1}H NMR (500 MHz); δ = 1.17 (t, J = 5.4 Hz, 6H), 1.64 (s, 3H), 2.55-2.67 (m, 4H), 2.84-2.99 (m, 1H), 7.28-7.47 (m, 5H).
^{13}C NMR (125 MHz); δ = 13.9, 19.2, 40.1, 42.2, 70.5, 125.6, 127.9, 130.1, 140.7, 173.5.
HPLC (Dialcel Chiralcel OD-H, ^{n}hexane/ ^{i}PrOH = 90/10, flow rate 1.0 mL/min); t_R = 13.7 min (*S*, minor), t_R = 14.4 min (*R*, major).
$[\alpha]_D^{29}$ = + 61.7 (*c* = 0.64, CHCl$_3$).

Ethyl (*R*)-3-hydroxy-3-phenylbutanoate (**16z**)[40]
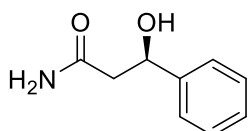
Yellow oil
^{1}H NMR (500 MHz); δ = 2.69 (m, 2H), 3.60 (s, 1H), 5.71 (s, 2H), 7.33-7.35 (m, 1H), 7.47-7.50 (m, 2H), 7.54-7.59 (m, 2H).
^{13}C NMR (125 MHz); δ = 46.5, 71.7, 125.7, 128.9, 128.9, 133.2, 133.2, 139.7, 176.0.
HPLC (Dialcel Chiralpak AD-H, ^{n}hexane/ ^{i}PrOH = 90/10, flow rate 1.0 mL/min); t_R = 12.4 min (*S*, minor), t_R = 15.9 min (*R*, major).
$[\alpha]_D^{21}$ = + 31.7 (*c* = 1.00, CH$_3$OH).

(*R*)-3-Hydroxy-3-phenylpropanenitrile (**16α**)[44]
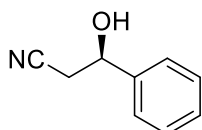
Pale yellow oil

^{1}H NMR (500 MHz); δ = 2.37 (s, 1H), 2.75-2.78 (m, 2H), 5.03 (t, J = 3.0 Hz, 1H), 7.34-7.41 (m, 5H).

^{13}C NMR (125 MHz); δ = 27.9, 70.0, 70.5, 125.4, 128.8, 133.2, 141.0.

HPLC (Dialcel Chiralcel OJ-H, ^{n}hexane/ ^{i}PrOH = 90/10, flow rate 1.0 mL/min); t_R = 23.6 min (*S*, minor), t_R = 27.4 min (*R*, major).

$[α]_D^{26}$ = + 55.3 (*c* = 0.84, CHCl$_3$).

(*R*, *E*)- 6-phenyl-4-(4,4,5,5-tetramethyl-1,3,2-dioxaborolan-2-yl)hex-5-en-2-one
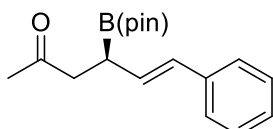
Colorless oil

^{1}H NMR (500 MHz); δ = 1.06 (s, 6H), 1.15 (s, 6H), 2.07-2.13 (m, 3H), 2.71-2.79 (m, 3H), 6.21 (d, J = 15.1 Hz, 1H), 6.64 (d, J = 15.1 Hz, 1H), 7.26-7.41 (m, 3H), 7.47 (d, J = 5.6 Hz, 2H).

^{13}C NMR (125 MHz); δ = 23.7, 30.6, 40.2, 49.8, 88.7, 127.2, 128.2, 128.9, 129.4, 130.3, 135.1, 209.4.

HPLC (Dialcel Chiralpak IA, ^{n}hexane/ ^{i}PrOH = 90/10, flow rate 0.5 mL/min); t_R = 13.2 min (*S*, minor), t_R = 14.4 min (*R*, major).

$[α]_D^{25}$ = −31.3 (*c* = 0.78, CDCl$_3$).

(*R*, *E*)-4-hydroxy-6-phenylhex-5-en-2-one (**18a**)[45]
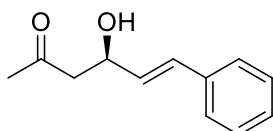
Colorless oil

^{1}H NMR (500 MHz); δ = 2.07-2.13 (m, 3H), 2.77 (m, 2H), 3.06 (brs, 1H), 4.73-4.77 (m, 1H), 6.21 (d, J = 15.1 Hz, 0.98H), 6.64 (d, J = 15.1 Hz, 0.98H), 7.29-7.38 (m, 3H), 7.47 (d, J = 5.6 Hz, 2H).

^{13}C NMR (125 MHz); δ = 30.6, 49.8, 68.4, 127.2, 128.2, 128.9, 129.4, 130.3, 135.1, 209.4.

HPLC (Dialcel Chiralcel OD-H, ^{n}hexane/ ^{i}PrOH = 90/10, flow rate 1 mL/min); t_R = 13.2 min (*S*, minor), t_R = 14.4 min (*R*, major).

$[α]_D^{25}$ = + 18.3 (*c* = 0.82, CHCl$_3$).

(*R*, *E*)-3-hydroxy-1,5-diphenylpent-4-en-1-one (**18b**)[46]
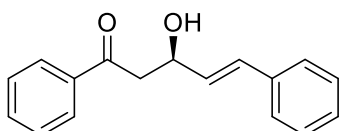
Colorless oil

^{1}H NMR (500 MHz); δ = 2.07-2.13 (m, 3H), 2.77 (m, 2H), 4.73-4.77 (m, 1H), 6.21 (d, J = 15.1 Hz, 1H), 6.64 (d, J = 15.1 Hz, 1H), 7.29-7.38 (m, 3H), 7.47 (d, J = 5.6 Hz, 2H).

^{13}C NMR (125 MHz); δ = 22.4, 25.0, 37.7, 127.2, 128.2, 128.2, 128.9, 128.9, 129.4, 129.4, 135.1, 200.1.

HPLC (Dialcel Chiralcel OD-H, ^{n}hexane/ ^{i}PrOH = 95/5, flow rate 0.5 mL/min); t_R = 19.0 min (*S*, minor), t_R = 22.5 min (*R*, major).

$[α]_D^{21}$ = + 27.9 (*c* = 0.82, CHCl$_3$)

(*R*, *E*)-3-hydroxy-1-phenylhex-4-en-1-one (**18c**)[47]
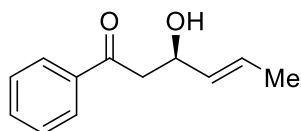
Colorless oil

^{1}H NMR (500 MHz); δ = 1.71 (d, *J* = 6.3 Hz, 3H), 3.13-3.22 (m, 3H), 4.70 (d, *J* = 5.6 Hz, 1H), 5.58-5.63 (m, 1H), 5.75-5.82 (m, 1H), 7.47 (t, *J* = 8.0 Hz, 2H), 7.56-7.59 (m, 1H), 7.96 (d, *J* = 8.5 Hz, 2H).

^{13}C NMR (125 MHz); δ = 17.7, 45.2, 68.7, 127.1, 128.1, 128.6, 132.1, 133.5, 136.7, 200.3.

HPLC (Dialcel Chiralpak AS-H, ^{n}hexane/ ^{i}PrOH = 90/10, flow rate 1.0 mL/min); t_R = 11.8 min (*S*, minor), t_R = 14.5 min (*R*, major).

$[α]_D^{29}$ = + 27.2 (*c* = 0.54, CHCl$_3$).

(*R*, *E*)-3-hydroxy-1-phenyloct-4-en-1-one (**18d**)
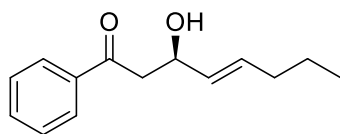
Colorless oil

IR (neat) ν = 1210, 1597, 1682, 2958, 3434 cm^{-1}.

^{1}H NMR (500 MHz); δ = 0.90 (t, *J* = 7.5 Hz, 3H), 1.38-1.45 (m, 2H), 2.00-2.05 (m, 2H), 3.13-3.22 (m, 3H), 4.71 (s, 1H), 5.58-5.63 (m, 1H), 5.75-5.82 (m, 1H), 7.47 (t, *J* = 8.0 Hz, 2H), 7.56-7.59 (m, 1H), 7.96 (d, *J* = 8.5 Hz, 2H).

^{13}C NMR (125 MHz); δ = 13.7, 22.2, 34.3, 45.3, 68.8, 128.1, 128.7, 130.9, 132.3, 133.5, 136.8, 200.3.

HPLC (Dialcel Chiralpak AS-H+AY-H, ^{n}hexane/ ^{i}PrOH = 90/10, flow rate 0.7 mL/min); t_R = 14.5 min (*S*, minor), t_R = 15.9 min (*R*, major).

HRMS (ESI) calcd for $C_{14}H_{19}O_2$ [M+H]$^+$ 219.1385, found 219.1390.

$[α]_D^{30}$ = +28.6 (*c* = 0.91, CHCl$_3$).

(*R, E*)-ethyl 3-hydroxy-5-phenylpent-4-enoate (**18e**)[48]
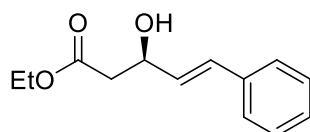
Colorless oil

^{1}H NMR (500 MHz); δ =1.28 (t, *J* = 6.8 Hz, 3H), 2.62-2.68 (m, 2H), 3.13 (s, 1H), 4.19 (dd, *J* = 6.4 Hz, *J* = 8.5 Hz, 2H), 4.73 (s, 1H), 6.22 (dd, *J* = 6.3, 9.8 Hz, 1H), 6.66 (d, *J* = 17.0 Hz), 7.24 (t, *J* = 6.9 Hz, 1H), 7.32 (t, *J* = 7.5 Hz, 2H), 7.38 (d, *J* = 8.0 Hz, 2H).

^{13}C NMR (125 MHz); δ = 14.1, 41.4, 60.8, 68.8, 126.5, 127.8, 128.5, 129.9, 130.7, 136.4, 172.2.

HPLC (Dialcel Chiralcel OD-H, ^{n}hexane/ ^{i}PrOH = 90/10, flow rate 1.0 mL/min); t_R = 14.0 min (*S*, minor), t_R = 20.8 min (*R*, major).

$[α]_D^{21}$ = + 27.9 (*c* = 0.82, CHCl$_3$).

(*R, E*)-4-hydroxy-4-methyl-6-phenylhex-5-en-2-one (**18f**)[13]
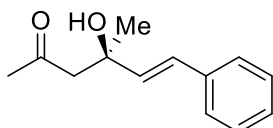
Colorless oil

^{1}H NMR (500 MHz); δ = 1.39 (s, 3H), 2.17 (s, 3H), 2.71 (d, *J* = 17.2 Hz, 1H), 2.84 (d, *J* = 17.2 Hz, 1H), 4.14 (s, 1H), 6.24 (d, *J* = 16.0 Hz, 1H), 6.58 (d, *J* = 16.0 Hz, 1H), 7.20–7.17 (m, 1H), 7.26–7.23 (m, 2H), 7.35 (d, *J* = 7.5 Hz, 2H).

^{13}C NMR (125 MHz); δ = 28.4, 32.1, 53.2, 72.0, 126.4, 127.5, 127.8, 128.6, 135.1, 136.9, 210.0.

HPLC (Dialcel Chiralcel OD-H, ^{n}hexane/ ^{i}PrOH = 95/5, flow rate 1.0 mL/min); t_R = 16.5 min (*S*, minor), t_R = 21.3 min (*R*, major).

$[α]_D^{20}$ = + 19.2 (*c* = 0.61, CHCl$_3$).

(*R, E*)-ethyl 3-hydroxy-3-methyl-5-phenylpent-4-enoate (**18g**)[49]

Colorless oil

^{1}H NMR (500 MHz); δ =1.28 (t, *J* = 6.8 Hz, 3H), 2.62-2.68 (m, 2H), 3.13 (s, 1H), 4.19 (dd, *J* = 6.4, 8.5 Hz, 2H), 4.73 (s, 1H), 6.22 (dd, *J* = 6.3, 9.8 Hz, 1H), 6.66 (d, *J* = 17.0 Hz, 1H), 7.24 (t, *J* = 6.9 Hz, 1H), 7.32 (t, *J* = 7.5 Hz, 2H), 7.38 (d, *J* = 8.0 Hz, 2H).

^{13}C NMR (125 MHz); δ = 14.1, 28.5, 45.5, 60.8, 71.3, 126.5, 127.5, 127.8, 128.5, 134.7, 136.7, 172.6.

HPLC (Dialcel Chiralcel OD-H, ^{n}hexane/ ^{i}PrOH = 90/10, flow rate 0.7 mL/min); t_R = 12.4 min (*S*, minor), t_R = 15.9 min (*R*, major).

$[α]_D^{21}$ = + 27.9 (*c* = 0.82, CHCl$_3$).

(*S, E*)-3-styryl-3-(4,4,5,5-tetramethyl-1,3,2-dioxaborolan-2-yl)cyclohexan-1-one
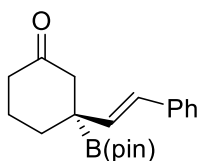
Colorless oil

^{1}H NMR (500 MHz); δ = 1.16 (s, 6H), 1.23 (s, 6H), 2.42-2.68 (m, 4H), 3.13-3.15 (m, 2H), 4.19 (dd, J = 6.4, 8.5 Hz, 2H), 6.07 (dd, J = 4.6, 9.4 Hz, 1H), 6.49 (d, J = 13.2 Hz, 1H), 7.24-7.42 (m, 5H).
^{13}C NMR (125 MHz); δ = 14.1, 23.2, 28.5, 39.6, 45.5, 60.8, 85.2, 126.5, 127.5, 127.8, 128.5, 134.7, 136.7, 172.6.
HPLC (Dialcel Chiralpak IA, ^{n}hexane/ ^{i}PrOH = 90/10, flow rate 1.0 mL/min); t_R = 14.2 min (S, minor), t_R = 19.3 min (R, major).
$[\alpha]_D^{29}$ = −16.5 (c = 0.27, CDCl$_3$).

(*R*)-3-(2-phenyl-2-(4,4,5,5-tetramethyl-1,3,2-dioxaborolan-2-yl)ethyl)cyclohex-2-en-1-one
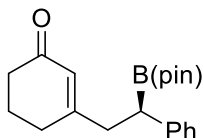
Colorless oil
^{1}H NMR (500 MHz); δ = 1.08 (s, 6H), 1.15 (s, 6H), 1.85-1.90 (m, 2H), 2.21-2.26 (m, 4H), 2.46 (dd, J = 5.4, 9.2 Hz, 1H), 2.55 (dd, J = 4.9, 8.7 Hz, 1H), 2.79-2.83 (m, 1H), 5.86 (s, 1H), 7.22-7.30 (m, 5H).
^{13}C NMR (125 MHz); δ = 22.5, 24.1, 30.0, 37.0, 37.6, 47.6, 84.2, 125.6, 127.7, 127.8, 128.5, 143.7, 163.0, 200.0.
HPLC (Dialcel Chiralpak IA, ^{n}hexane/ ^{i}PrOH = 90/10, flow rate 0.5 mL/min); t_R = 32.5 min (S, minor), t_R = 41.2 min (R, major).
$[\alpha]_D^{26}$ = −17.3 (c = 0.31, CDCl$_3$).

(*R*, *E*)-3-hydroxy-3-styrylcyclohexanone (**21a**)
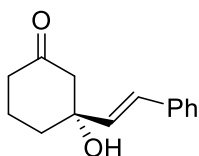
Colorless oil
IR (neat) ν = 1425, 1601, 1701, 3276 cm^{-1}.
^{1}H NMR (500 MHz); δ =0.97 (s, 1H), 2.62-2.68 (m, 2H), 3.13 (s, 1H), 4.19 (dd, J = 6.4, 8.5 Hz, 2H), 4.73 (s, 1H), 6.22 (dd, J = 6.3, 9.8 Hz, 1H), 6.66 (d, J = 17.0 Hz), 7.24 (t, J = 6.9 Hz, 1H), 7.32 (t, J = 7.5 Hz, 2H), 7.38 (d, J = 8.0 Hz, 2H).
^{13}C NMR (125 MHz); δ = 14.1, 28.5, 45.5, 60.8, 71.3, 126.5, 127.5, 127.8, 128.5, 134.7, 136.7, 172.6.
HPLC (Dialcel Chiralcel OD-H, ^{n}hexane/ ^{i}PrOH = 90/10, flow rate 0.7 mL/min); t_R = 12.4 min (S, minor), t_R = 15.9 min (R, major).
HRMS (ESI) calcd for C$_{14}$H$_{16}$O$_2$ [M+H]$^+$ 216.1150, found 216.1154.
$[\alpha]_D^{21}$ = + 19.2 (c = 0.96, CHCl$_3$).

(*R*)-3-(2-hydroxy-2-phenylethyl)cyclohex-2-enone (**22a**)
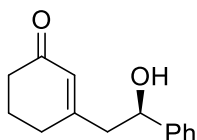
Colorless oil

IR (neat) ν = 1176, 1610, 1662, 3421 cm^{-1}.

^{1}H NMR (500 MHz); δ = 1.85-1.90 (m, 2H), 2.21-2.26 (m, 4H), 2.50 (dd, J = 4.6, 9.7 Hz, 1H), 2.60 (dd, J = 5.2, 9.2 Hz, 1H), 2.93 (s, 1H), 4.83 (s, 1H), 5.85 (t, J = 4.6 Hz, 1H), 7.22-7.30 (m, 5H).

^{13}C NMR (125 MHz); δ = 22.5, 30.0, 37.0, 47.6, 72.3, 125.6, 127.7, 127.8, 128.5, 143.7, 163.0, 200.0.

HPLC (Dialcel Chiralpak AS-H, ^{n}hexane/ ^{i}PrOH = 90/10, flow rate 1.0 mL/min); t_R = 66.5 min (S, minor), t_R = 78.3 min (R, major).

HRMS (ESI) calcd for C$_{14}$H$_{16}$O$_2$ [M+H]$^+$ 216.1150, found 216.1151.

[α]$_D^{20}$ = + 37.3 (c = 1.07, CHCl$_3$).

(*R, E*)-3-hydroxy-3-(2-phenylprop-1-en-1-yl)cyclohexan-1-one (**21b**)
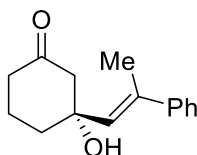
Colorless oil

IR (neat) ν = 1396, 1616, 1697, 3392 cm^{-1}.

^{1}H NMR (500 MHz); δ =1.69-1.79 (m, 2H), 1.99-2.07 (m, 2H), 2.31-2.37 (m, 2H), 2.62-2.68 (m, 2H), 4.79 (s, 1H), 5.89 (d, J = 8.3 Hz), 7.26 (t, J = 6.9 Hz, 1H), 7.33 (t, J = 7.5 Hz, 2H), 7.40 (d, J = 8.0 Hz, 2H).

^{13}C NMR (125 MHz); δ = 14.1, 18.8, 28.5, 45.5, 60.8, 71.3, 126.2, 127.0, 127.9, 129.1, 137.3, 141.0, 172.6.

HPLC (Dialcel Chiralcel OD-H, ^{n}hexane/ ^{i}PrOH = 90/10, flow rate 0.7 mL/min); t_R = 14.4 min (S, minor), t_R = 21.9 min (R, major).

HRMS (ESI) calcd for C$_{15}$H$_{18}$O$_2$ [M+H]$^+$ 230.1307, found 230.1308.

[α]$_D^{21}$ = + 26.0 (c = 0.64, CHCl$_3$).

(*R*)-3-(2-hydroxy-2-phenylpropyl)cyclohex-2-en-1-one (**22b**)
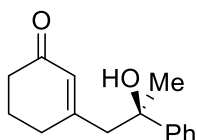
Colorless oil

IR (neat) ν = 1152, 1617, 1657, 3380 cm^{-1}.

^{1}H NMR (500 MHz); δ = 1.85-1.96 (m, 5H), 2.21-2.26 (m, 4H), 2.50 (dd, J = 4.6, 9.7 Hz, 1H), 2.60 (dd, J = 5.2, 9.2 Hz, 1H), 4.83 (s, 1H), 5.85 (t, J = 4.6 Hz, 1H), 7.21-7.34 (m, 5H).

^{13}C NMR (125 MHz); δ = 18.7, 23.1, 30.5, 36.5, 49.2, 69.8, 125.9, 127.8, 128.4, 128.8, 141.2, 158.4, 201.5.

HPLC (Dialcel Chiralpak AS-H, ^{n}hexane/ ^{i}PrOH = 90/10, flow rate 1.0 mL/min); t_R = 55.1 min (*S*, minor), t_R = 64.5 min (*R*, major).

HRMS (ESI) calcd for $C_{15}H_{18}O_2$ [M+H]$^+$ 230.1307, found 230.1304.

$[\alpha]_D^{20}$ = + 31.6 (*c* = 0.98, CHCl$_3$).

Determination of the absolute configuration of **21a** and **21b**;

The absolute configurations of **21a** and **21b** were determined to be *R* by comparison of the optical rotation and the HPLC retention time of their derivatives with those of the corresponding compounds synthesized from a literature-known compound.
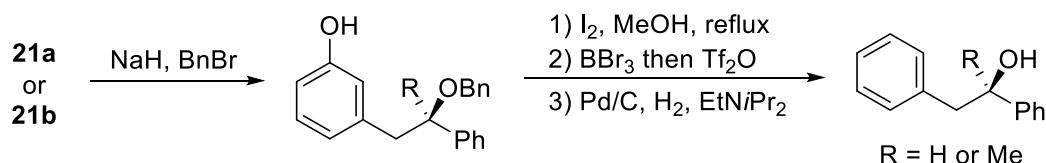
To the solution of the obtained product **21a** or **21b** (0.4 mmol) in DCM (5 mL) were added NaH (1.5 equiv., 0.6 mmol) and BnBr (1.5 equiv., 0.6 mmol) at 0 ^{o}C. After stirred at 0 ^{o}C for 2 h, the reaction solution was quenched with H$_2$O, extract with AcOEt and washed with 0.1N HCl, H$_2$O and brine. The crude mixture was purified by flash column chromatography (AcOEt/^{n}hexane = 1/2) to afford the corresponding benzyl ether (1.1812 g, 92% yield).

To the obtained ether (0.37 mmol) in MeOH (5 mL) was added I$_2$ (2.15 equiv., 0.8 mmol). The reaction mixture was refluxed for 30 min. After completion of the reaction, the resultant solution was concentrated under reduced pressure. The obtained mixture was dissolved in ^{n}hexane and washed with aqueous solution of Na$_2$S$_2$O$_3$, sat. NaHCO$_3$ *aq.* and H$_2$O. The crude was used directly in the next step without further purification. The crude mixture was dissolved in DCM (5 mL) and BBr$_3$ (0.62 mL in DCM) was added slowly. The resultant mixture was then warmed gradually up to rt and stirred for another 1.5 h. After quenched with sat. NaHCO$_3$ *aq.* at 0 ^{o}C, the reaction solution was extract with AcOEt. The crude mixture was purified by short column chromatography. (AcOEt/^{n}hexane = 1/5). To the cold solution in DCM (5 mL) and pyridine (0.4 mmol) was added Tf$_2$O (0.4 mmol) dropwise at 0 ^{o}C. The reaction mixture was stirred for 5 h at rt. After addition of sat. NaHCO$_3$ *aq.*, the resultant mixture was extracted with AcOEt and the organic layer was washed with 0.5 N HCl *aq.*, H$_2$O and brine. To 10 mL EtOH solution of the obtained mixture was added 10% Pd/C (40 mg). The reaction mixture was stirred under H$_2$ for 2 h. The crude mixture was filtered through Celite$^®$ and the volatile solvent was evaporated. The residue was purified by PTLC (AcOEt/^{n}hexane = 2/1).

(*R*)-1,2-diphenylethan-1-ol
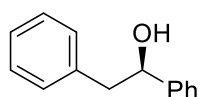
Colorless oil

^{1}H NMR (500 MHz); δ = 2.96-3.01 (m, 2H), 5.22-5.25 (m, 1H), 5.63-5.66 (m, 1H), 6.99-7.33 (m, 10H).

^{13}C NMR (125 MHz); δ = 47.6, 73.2, 126.6, 126.9, 127.6, 127.8, 128.5, 128.7, 138.1, 143.3.

HPLC (Dialcel Chiralcel OD-H, ^{n}hexane/ ^{i}PrOH = 19/1, flow rate 1.0 mL/min); t_R = 18.7 min (*R*, major), t_R = 24.3 min (*S*, minor).

$[\alpha]_D^{27}$ = –37.6 (*c* = 0.86, MeOH).

(*R*)-1,2-diphenylpropan-2-ol
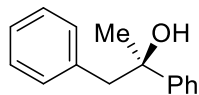
Colorless oil

^{1}H NMR (500 MHz); δ = 1.27 (s, 3H), 2.93-2.98 (m, 2H), 6.99-7.33 (m, 10H).

^{13}C NMR (125 MHz); δ = 21.2, 45.6, 71.2, 125.6, 126.5, 126.6, 127.3, 128.5, 128.7, 138.1, 143.3.

HPLC (Dialcel Chiralpak AD-H, ^{n}hexane/ ^{i}PrOH = 40/1, flow rate 1.0 mL/min); t_R = 22.5 min (*R*, major), t_R = 29.6 min (*S*, minor).

$[\alpha]_D^{29}$ = –46.6 (*c* = 1.04, MeOH).

(*R*, *E*)-3-hydroxy-3-styrylcyclopentanone (**21c**)
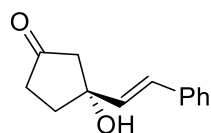
Colorless oil

IR (neat) ν = 1465, 1622, 1747, 3241 cm^{-1}.

^{1}H NMR (500 MHz); δ =2.06-2.12 (m, 2H), 2.35 (t, *J* = 6.5 Hz, 2H), 2.61 (t, *J* = 6.5 Hz, 2H), 6.07 (s, 1H), 6.87 (d, *J* = 16.1 Hz, 1H), 7.00 (d, *J* = 16.1 Hz, 1H), 7.28-7.38 (m, 3H), 7.48 (d, *J* = 7.5 Hz, 2H).

^{13}C NMR (125 MHz); δ = 30.9, 41.2, 49.6, 71.9, 126.1, 127.9, 128.1, 128.5, 143.7, 166.2, 192.1.

HPLC (Dialcel Chiralcel OD-H, ^{n}hexane/ ^{i}PrOH = 90/10, flow rate 0.7 mL/min); t_R = 45.3 min (*S*, minor), t_R = 50.5 min (*R*, major).

HRMS (ESI) calcd for $C_{13}H_{14}O_2$ [M+H]$^+$ 202.0994, found 202.0985.

$[\alpha]_D^{22}$ = + 21.1 (*c* = 0.31, CHCl$_3$).

(*R*)-3-(2-hydroxy-2-phenylethyl)cyclopent-2-enone (**22c**)
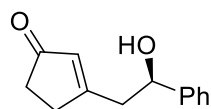
Colorless oil

IR (neat) ν = 1165, 1616, 1732, 3411 cm^{-1}.

^{1}H NMR (500 MHz); δ = 2.37-2.41 (m, 2H), 2.50 (dd, *J* = 4.6, 9.7 Hz, 1H), 2.50-2.55 (m, 2H), 2.60 (dd, *J* = 5.2, 9.2 Hz, 1H), 2.93 (s, 1H), 4.83 (s, 1H), 5.93 (s, 1H), 7.21-7.33 (m, 5H).

^{13}C NMR (125 MHz); δ = 22.5, 30.0, 37.0, 47.6, 72.3, 125.6, 127.7, 127.8, 128.5, 143.7, 163.0, 200.0.

HPLC (Dialcel Chiralpak AS-H, ^{n}hexane/ ^{i}PrOH = 90/10, flow rate 1.0 mL/min); t_R = 25.5 min (*S*, minor), t_R = 30.6 min (*R*, major).

HRMS (ESI) calcd for $C_{13}H_{14}O_2$ [M+H]$^+$ 202.0994, found 202.0992.
$[\alpha]_D^{20} = + 28.1$ ($c = 0.42$, CHCl$_3$).

(*R*, *E*)-3-hydroxy-3-styrylcycloheptanone (**21d**)
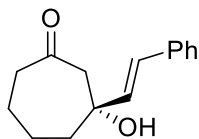
Colorless oil
IR (neat) ν = 1457, 1602, 1703, 3227 cm^{-1}.
^{1}H NMR (500 MHz); δ = 1.56–1.74 (m, 6H), 2.32–2.52 (m, 3H), 2.60 (m, 1H), 2.83 (m, 1H), 4.68 (s, 1H), 6.17 (dd, J = 6.3, 9.8 Hz, 1H), 6.63 (d, J = 17.0 Hz), 7.24-7.38 (m, 5H).
^{13}C NMR (125 MHz); δ = 24.1, 25.7, 28.5, 43.2, 59.7, 73.3, 125.9, 126.6, 127.0, 128.0, 133.9, 137.1, 207.6.
HPLC (Dialcel Chiralcel OD-H, ^{n}hexane/ ^{i}PrOH = 90/10, flow rate 0.7 mL/min); t_R = 32.4 min (*S*, minor), t_R = 35.9 min (*R*, major).
HRMS (ESI) calcd for $C_{15}H_{18}O_2$ [M+H]$^+$ 230.1307, found 230.1316.
$[\alpha]_D^{21} = + 15.9$ ($c = 0.52$, CHCl$_3$).

(*R*)-3-(2-hydroxy-2-phenylethyl)cyclohept-2-enone (**22d**)
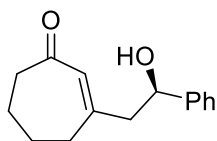
Colorless oil
IR (KBr) ν = 1227, 1601, 1711, 3412 cm^{-1}.
^{1}H NMR (500 MHz); δ = 1.92-2.05 (m, 4H) , 2.09-2.19 (m, 2H), 2.46-2.51 (m, 4H), 3.21 (t, J = 7.5 Hz, 1H), 4.83 (s, 1H), 5.91 (d, J = 4.6 Hz, 1H), 7.22-7.30 (m, 5H).
^{13}C NMR (125 MHz); δ = 25.1, 29.0, 32.2, 46.4, 72.3, 124.9, 126.1, 126.5, 129.4, 143.7, 161.8, 203.7.
HPLC (Dialcel Chiralpak AS-H, ^{n}hexane/ ^{i}PrOH = 90/10, flow rate 1.0 mL/min); t_R = 66.5 min (*S*, minor), t_R = 78.3 min (*R*, major).
HRMS (ESI) calcd for $C_{15}H_{18}O_2$ [M+H]$^+$ 230.1307, found 230.1311.
$[\alpha]_D^{23} = + 5.4$ ($c = 0.16$, CHCl$_3$).

3-((2*R*)-2-hydroxy-2-phenylethyl-1-deuterio)cyclohex-2-en-1-one (**22a-D**)
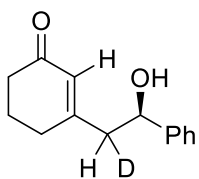
Colorless oil

¹H NMR (500 MHz); δ = 1.85-1.90 (m, 2H), 2.21-2.26 (m, 4H), 2.59 (d, *J* = 5.2 Hz, 1H), 2.93 (s, 1H), 4.83 (d, *J* = 4.6 Hz, 1H), 5.85 (s, 1H), 7.22-7.30 (m, 5H).

¹³C NMR (125 MHz); δ = 22.5, 30.0, 37.0, 47.6, 72.3, 125.6, 127.7, 127.8, 128.5, 143.7, 163.0, 200.0.

HPLC (Dialcel Chiralpak AS-H, ⁿhexane/ ⁱPrOH = 90/10, flow rate 1.0 mL/min); t_R = 66.5 min (*S*, minor), t_R = 78.3 min (*R*, major).

HRMS (ESI) calcd for $C_{14}H_{15}DO_2$ [M+H]$^+$ 217.1213, found 217.1212.

$[\alpha]_D^{20}$ = + 35.4 (*c* = 0.65, CHCl$_3$).

(*R*)-3-hydroxy-3-((1*E*, 3*E*)-4-phenylbuta-1,3-dien-1-yl)cyclohexan-1-one (**24a**)
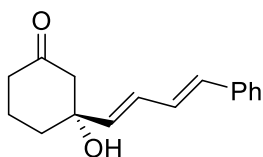
Colorless oil

IR (neat) ν = 1412, 1607, 1674, 3457 cm^{-1}.

¹H NMR (500 MHz); δ =1.67-1.76 (m, 2H), 2.01-2.08 (m, 2H), 2.30-2.37 (m, 2H), 2.60-2.67 (m, 2H), 4.43 (s, 1H), 5.86 (dd, *J* = 6.3, 9.8 Hz, 1H), 6.39 (d, *J* = 17.0 Hz), 6.54 (d, *J* = 17.0 Hz, 1H), 6.72 (dd, *J* = 6.3, 9.8 Hz, 1H), 7.26-7.40 (m, 5H).

¹³C NMR (125 MHz); δ = 21.6, 29.4, 46.7, 60.6, 70.8, 126.4, 127.6, 128.3, 128.9, 129.8, 133.4, 136.1, 137.2, 170.9.

HPLC (Dialcel Chiralcel OD-H, ⁿhexane/ ⁱPrOH = 90/10, flow rate 0.7 mL/min); t_R = 12.4 min (*S*, minor), t_R = 15.9 min (*R*, major).

HRMS (ESI) calcd for $C_{16}H_{18}O_2$ [M+H]$^+$ 242.1307, found 242.1307.

$[\alpha]_D^{21}$ = + 42.1 (*c* = 0.71, CHCl$_3$).

(*R*, *E*)-3-(2-hydroxy-4-phenylbut-3-en-1-yl)cyclohex-2-en-1-one (**25a**)
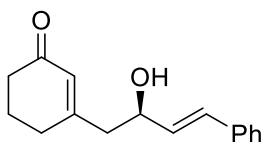
Colorless oil

IR (neat) ν = 1362, 1620, 1667, 3369 cm^{-1}.

¹H NMR (500 MHz); δ = 1.82-1.90 (m, 2H), 2.20-2.29 (m, 4H), 2.52-2.60 (m, 2H), 3.01 (s, 1H), 4.78 (s, 1H), 5.86 (s, 1H), 6.32-6.38 (m, 1H), 6.52-6.59 (m, 1H), 7.22-7.43 (m, 5H).

¹³C NMR (125 MHz); δ = 21.5, 29.7, 36.4, 47.6, 70.7, 124.9, 126.4, 127.2, 128.5, 134.5, 138.6, 141.8, 163.0, 199.6.

HPLC (Dialcel Chiralpak AS-H, ⁿhexane/ ⁱPrOH = 90/10, flow rate 1.0 mL/min); t_R = 34.5 min (*S*, minor), t_R = 48.3 min (*R*, major).

HRMS (ESI) calcd for $C_{16}H_{18}O_2$ [M+H]$^+$ 242.1307, found 242.1310.

$[\alpha]_D^{29}$ = + 36.2 (*c* = 0.55, CHCl$_3$).

(*R*, *E*)-3-(4-hydroxy-4-phenylbut-1-en-1-yl)cyclohex-2-en-1-one (**26a**)
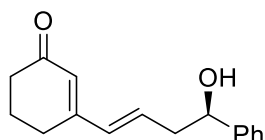
Colorless oil

^{1}H NMR (500 MHz); δ = 2.03-2.09 (m, 2H), 2.32-2.39 (m, 2H), 2.42-2.48 (m, 2H), 5.79 (s, 1H), 6.32-6.38 (m, 1H), 7.22-7.43 (m, 5H).

^{13}C NMR (125 MHz); δ = 21.5, 29.7, 36.4, 45.9, 70.7, 124.9, 126.4, 127.2, 128.5, 134.5, 138.6, 141.8, 163.0, 199.6.

HPLC (Dialcel Chiralpak AS-H, ^{n}hexane/ ^{i}PrOH = 90/10, flow rate 1.0 mL/min); t_R = 34.5 min (*S*, minor), t_R = 48.3 min (*R*, major).

HRMS (ESI) calcd for $C_{16}H_{18}O_2$ [M+H]$^+$ 242.1307, found 242.1312.

$[\alpha]_D^{23}$ = + 6.7 (*c* = 0.14, MeOH).

Determination of the absolute configuration of **26a**;

The absolute configuration of **26a** was determined to be *R* by comparison of the HPLC retention time of its derivative with those of the corresponding compound synthesized from a literature-known compound.
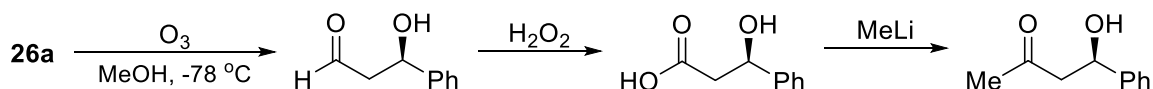
The product **26a** was dissolved in MeOH (10 mL) and was oxidized by O_3 at −78 ^{o}C. The reaction mixture was then bubbled with Ar, and rinsed with H_2O, $Na_2S_2O_3$ aqueous solution and brine. After evaporation of the solvent, 2 mL of EtOH was added to the mixture.   20% H_2O_2 *aq*. (100 μL) was then added and the reaction mixture was stirred for 1h at rt.   After addition of 1N NaOH aqueous solution (1 mL), the reaction mixture was washed with Et$_2$O.   After the subsequent addition of 1N HCl (1.5 mL), the mixture was extracted with DCM.   After removal of the volatile solvent, to the obtained mixture dissolved in DCM was added MeLi solution slowly under 0 ^{o}C. The mixture was stirred for 15 min and quenched with sat. NH$_4$Cl *aq*.   Finally, the mixture was extract with AcOEt and purified by PTLC (AcOEt/^{n}hexane = 1/4) to afford the product (66% yield, 3 steps).

(*R*, *E*)-3-(benzylimino)-1-phenylbutan-1-ol (**31a**)[18]
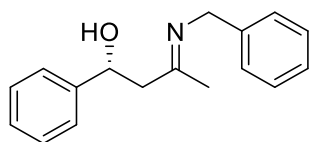
Colorless oil.

^{1}H NMR (500 MHz, CDCl$_3$); δ = 2.07 (s, 3H), 2.80-2.93 (m, 2H), 3.46 (d, 1H, *J* = 3.3 Hz), 4.66 (s, 2H), 5.11 (dd, 1H, *J* = 5.8 Hz, *J* = 3.5 Hz), 7.28-7.40 (m, 10H).

^{13}C NMR (125 MHz, CDCl$_3$); δ = 27.9, 30.7, 53.4, 70.1, 125.6, 126.5, 126.9, 127.7, 128.1, 128.5, 129.0, 139.9, 169.1.

HPLC; (Dialcel Chiralcel OD-H, ^{n}hexane/ ^{i}PrOH = 90/10, flow rate 1.0 mL/min); t_R = 10.5 min (*S*, minor), t_R = 12.4 min (*R*, major).

$[\alpha]_D^{23}$ = + 35.3 (*c* = 0.63, CDCl$_3$).

(*R*, *Z*)-3-(benzylimino)-1,3-diphenylpropan-1-ol (**31b**) [18]
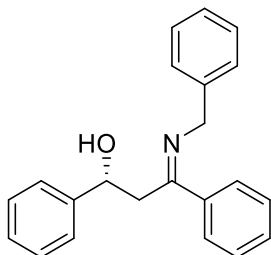
Colorless oil.

^{1}H NMR (500 MHz, CDCl$_3$); δ = 3.41 (d, 2H, *J* = 5.8 Hz), 4.32 (s, 2H), 5.39 (t, 1H, *J* = 6.5 Hz), 7.28-7.48 (m, 7H), 7.56-7.82 (m, 6H), 7.95 (d, 2H, *J* = 7.0 Hz).

^{13}C NMR (125 MHz, CDCl$_3$); δ = 47.4, 59.2, 70.2, 123.7, 127.5, 128.0, 128.3, 128.4, 128.5, 128.6, 129.1, 129.7, 133.9, 136.6, 143.2, 167.2.

HPLC; (Dialcel Chiralcel OD-H, ^{n}hexane/ ^{i}PrOH = 90/10, flow rate 0.7 mL/min); t_R = 18.1 min (*S*, minor), t_R = 20.9 min (*R*, major).

$[\alpha]_D^{21}$ = + 39.9 (*c* = 0.42, CDCl$_3$).

(*R*, *Z*)-3-(benzylimino)-3-phenyl-1-(*p*-tolyl)propan-1-ol (**31c**)
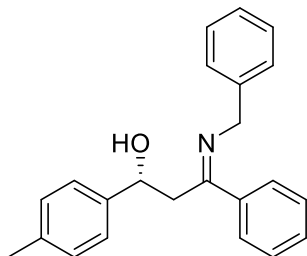
Colorless oil.

IR (KBr) ν = 1037, 1178, 1648, 2936, 3421 cm^{-1}.

^{1}H NMR (500 MHz, CDCl$_3$); δ = 2.18 (s, 3H), 3.37 (d, 2H, *J* = 8.1 Hz), 4.50 (s, 1H), 4.50 (s, 1H), 5.43 (dd, 1H, *J* = 2.9 Hz, *J* = 4.6 Hz), 7.28-7.54 (m, 12H), 7.95 (d, 2H, *J* = 8.0 Hz).

^{13}C NMR (125 MHz, CDCl$_3$); δ = 21.9, 46.8, 59.2, 69.2, 123.7, 126.7, 127.0, 127.1, 128.3, 128.5, 128.9, 129.4, 129.7, 134.4, 140.3, 143.4, 168.3.

HPLC; (Dialcel Chiralcel OD-H, ^{n}hexane/ ^{i}PrOH = 95/5, flow rate 1.0 mL/min); t_R = 17.6 min (*S*, minor), t_R = 21.5 min (*R*, major).

HRMS (ESI) calcd for C$_{23}$H$_{24}$NO [M+H]$^+$ 330.1858, found 330.1859.

$[\alpha]_D^{19}$ = + 54.2 (*c* = 0.35, CDCl$_3$).

(*R*, *Z*)-3-(benzylimino)-1-phenyl-3-(*p*-tolyl)propan-1-ol (**31d**)
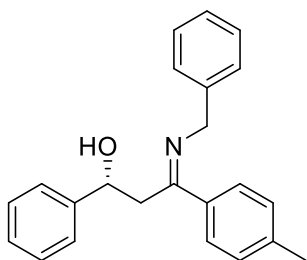
Yellow oil.

IR (KBr) ν = 1041, 1154, 1646, 2899, 3394 cm^{-1}.

^{1}H NMR (500 MHz, CDCl$_3$); δ = 2.44 (s, 3H), 3.44-3.46 (m, 2H), 4.62 (s, 1H), 4.73 (s, 1H), 5.39-5.41 (m, 1H), 7.27-7.56 (m, 12H), 7.67 (d, 2H, J = 7.5 Hz).

^{13}C NMR (125 MHz, CDCl$_3$); δ = 26.9, 55.9, 61.2, 71.1, 123.8, 125.3, 125.7, 127.6, 128.4, 128.5, 129.1, 129.5, 129.7, 130.5, 133.9, 143.3, 171.7.

HPLC; (Dialcel Chiralcel OD-H, ^{n}hexane/ ^{i}PrOH = 90/10, flow rate 0.7 mL/min); t_R = 14.2 min (*S*, minor), t_R = 16.8 min (*R*, major).

HRMS (ESI) calcd for C$_{23}$H$_{24}$NO [M+H]$^+$ 330.1858, found 330.1853.

$[\alpha]_D^{20}$ = + 39.8 (*c* = 0.47, CDCl$_3$).

(*R, E*)-3-(benzylimino)-1-(p-tolyl)butan-1-ol (**31e**)
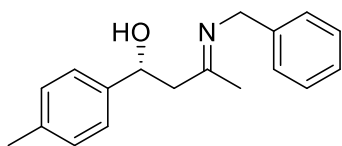
Pale yellow oil.

IR (KBr) ν = 1053, 1160, 1661, 2942, 3401 cm^{-1}.

^{1}H NMR (500 MHz, CDCl$_3$); δ = 2.12 (s, 3H), 2.59 (s, 3H), 2.70-2.84 (m, 2H), 3.51 (s, 1H), 4.77 (s, 2H), 5.12 (dd, 1H, J = 4.0 Hz, J = 9.0 Hz), 7.16-7.33 (m, 9H).

^{13}C NMR (125 MHz, CDCl$_3$); δ = 23.4, 28.6, 31.7, 53.5, 70.0, 123.1, 126.5, 126.8, 127.2, 128.4, 129.0, 138.7, 176.2.

HPLC; (Dialcel Chiralcel OD-H, ^{n}hexane/ ^{i}PrOH = 90/10, flow rate 1.0 mL/min); t_R = 9.8 min (*S*, minor), t_R = 11.8 min (*R*, major).

HRMS (ESI) calcd for C$_{18}$H$_{22}$NO [M+H]$^+$ 268.1701, found 268.1697.

$[\alpha]_D^{20}$ = + 21.6 (*c* = 0.23, CDCl$_3$).

(*R, Z*)-3-(benzylimino)-1-(4-chlorophenyl)-3-phenylpropan-1-ol (**31f**)
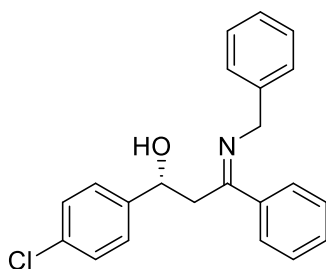
Yellow oil.

IR (KBr) ν = 1041, 1169, 1649, 2875, 3392 cm^{-1}.

^{1}H NMR (500 MHz, CDCl$_3$); δ = 2.80-2.82 (m, 2H), 3.65 (d, 1H, J = 7.8 Hz), 4.87 (d, 2H, J = 2.9 Hz), 5.37 (t, 1H, J = 7.8 Hz), 7.19-7.61 (m, 12H), 7.95 (d, 2H, J = 6.9 Hz).

^{13}C NMR (125 MHz, CDCl$_3$); δ = 31.7, 53.5, 70.0, 124.9, 125.7, 126.3, 126.6, 127.7, 127.9, 128.0, 128.5, 130.0, 131.2, 133.9, 137.5, 170.3.

HPLC; (Dialcel Chiralcel OD-H, ^{n}hexane/ ^{i}PrOH = 90/10, flow rate 1.0 mL/min); t_R = 11.4 min (*S, minor*), t_R = 13.7 min (*R, major*).

HRMS (ESI) calcd for C$_{22}$H$_{21}$ClNO [M+H]$^+$ 350.1312, found 350.1332.

$[\alpha]_D^{22}$ = + 38.6 (*c* = 0.53, CHCl$_3$).

Typical Procedure for Turnover Frequency Study

To an aqueous solution (2 mL) of Cu(OH)$_2$ (0.020 mg, 0.005 mol%) was added chiral 2,2'-bipyridine **L1** (0.079 mg, 0.006 mol%). After stirred vigorously for 15 min at room temperature, the resultant mixture was allowed to cool to 5 ^{o}C. Chalcone **13a** (83.2 mg, 0.4 mmol) and B$_2$(pin)$_2$ **14a** (121.8 mg, 0.48 mmol) was then added successively at the same temperature. After stirring for 15 min, the reaction mixture was filtered and rinsed with THF (3 mL). The excess amount of NaBO$_3$·4H$_2$O (488 mg) was then added and the mixture was stirred at room temperature for 4 h. The aqueous layer was extracted with AcOEt (20 mL) three times, and the combined organic layers were dried over anhydrous Na$_2$SO$_4$. After concentrated under reduced pressure, the crude mixture was purified by preparative TLC (^{n}hexane/AcOEt = 4/1) to afford the desired product **16a** (48.7 mg, 54 %) as a colorless oil.

Typical Procedure for Kinetic and KIE Experiments

[**Heterogeneous System**]

To an aqueous solution (2 mL) of Cu(OH)$_2$ (2.0 mg, 5 mol%) was added chiral 2,2'-bipyridine **L1** (7.9 mg, 6 mol%). After stirred vigorously for 15 min at room temperature, the resultant mixture was allowed to cool to 5 ^{o}C. Chalcone **13a** (83.2 mg, 0.4 mmol) and B$_2$(pin)$_2$ **14a** (121.8 mg, 0.48 mmol) was then added successively at the same temperature. The resultant mixture was stirred for 2, 5, 10, 15, 30 and 60 min, respectively. After stirred, the reaction mixture was filtered and rinsed with THF (3 mL). The excess amount of NaBO$_3$·4H$_2$O (488 mg) was then added and the mixture was stirred at room temperature for 4 h. The aqueous layer was extracted with AcOEt (20 mL) three times, and the combined organic layers were dried over anhydrous Na$_2$SO$_4$. After concentrated under reduced pressure, the crude mixture was purified by preparative TLC (^{n}hexane/AcOEt = 4/1) to afford the desired product **16a** as a colorless oil. The reaction was conducted 10 times and the result was calculated as an average of 8 experiments after exclusion of two outliers.

[**Homogeneous System**]

To an aqueous solution (2 mL) of Cu(OAc)$_2$ (3.2 mg, 5 mol%) was added chiral 2,2'-bipyridine **L1** (7.9 mg, 6 mol%). After stirred vigorously for 15 min at room temperature, the resultant mixture was allowed to cool to 5 ^{o}C. Chalcone **13a** (83.2 mg, 0.4 mmol) and B$_2$(pin)$_2$ **14a** (121.8 mg, 0.48 mmol) was then added successively at the same temperature. The resultant mixture was stirred for 2, 5, 7, 10, 15, 30 and 60 min, respectively. After stirred, THF (3 mL) was added. The excess

amount of NaBO$_3$·4H$_2$O (488 mg) was then added and the mixture was stirred at room temperature for 4 h. The aqueous layer was extracted with AcOEt (20 mL) three times, and the combined organic layers were dried over anhydrous Na$_2$SO$_4$. After concentrated under reduced pressure, the crude mixture was purified by preparative TLC (^{n}hexane/AcOEt = 4/1) to afford the desired product **16a** as a colorless oil. The reaction was conducted 8 times and the result was calculated as an average of 6 experiments after exclusion of two outliers.

(*R*)-3-Hydroxy-1,3-diphenyl-2-deuterio-propan-1-one (**16a-D**)
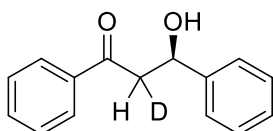
Colorless oil

^{1}H NMR (500 MHz); δ = 3.37 (m, 1H), 3.63 (s, 1H), 5.35 (t, *J* = 6.0 Hz, 1H), 7.28-7.48 (m, 7H), 7.56-7.59 (m, 1H), 7.96 (d, *J* = 7.0 Hz, 2H).

^{13}C NMR (125 MHz); δ = 47.4, 70.0, 120.7, 127.5, 128.0, 128.3, 128.4, 133.6, 136.6, 143.0, 200.1.

HPLC (Dialcel Chiralcel OD-H, ^{n}hexane/ ^{i}PrOH = 85/15, flow rate 0.7 mL/min); t$_R$ = 14.4 min (*S*, minor), t$_R$ = 16.3 min (*R*, major).

HRMS (ESI) calcd for C$_{15}$H$_{13}$DO$_2$ [M+H]$^+$ 227.1057, found 227.1060.

[α]$_D^{29}$ = + 51.3 (*c* = 1.00, CHCl$_3$).

Typical Procedure for ESI-MS Analysis

Cu(OAc)$_2$ (1.7 mg) and chiral 2,2'-bipyridine **L1** (4.0 mg) was dissolved in aqueous tetrahydrofuran (H$_2$O/THF = 4/1, 2 mL) and stirred at rt for 1 h. To the resultant homogeneous solution was added chalcone **13a** (20.8 mg) and the mixture was then stirred for another 20 min. Finally B$_2$(pin)$_2$ **14a** (30.3 mg) was added and stirred vigorously for 5 or 15 seconds. The reaction mixture was then submitted directly to ESI-MS analysis.

Typical Experimental Procedure for Catalytic Enantioselective β-Borylation in Water (Table 14, entry 1):

To a mixture of Cu(0) powder (1.9 mg, 10 mol%) and chiral 2,2'-bipyridine **L1** (8.8 mg, 12 mol%) was added degassed water (2 mL) under Ar atmosphere. After stirred vigorously for 1 h at 30 ^{o}C, chalcone **13a** (62.5 mg, 0.3 mmol) and B$_2$(pin)$_2$ **14a** (91.2 mg, 0.36 mmol) were added successively at the same temperature. After stirring for 12 h, the reaction mixture was filtered and rinsed with AcOEt. The aqueous layer was extracted with AcOEt (20 mL) three times, and the combined organic layers were dried over anhydrous Na$_2$SO$_4$. After concentrated under reduced pressure, the crude mixture was purified by preparative TLC (^{n}hexane/AcOEt = 4/1) to afford the desired product **16a** (92.9 mg, 92% yield) as a colorless oil.

Typical Procedure for Deuteration Experiments

To a mixture of Cu(0) powder (1.9 mg, 10 mol%) and chiral 2,2'-bipyridine **L1** (8.8 mg, 12 mol%) was added degassed deuterium oxide (2 mL) under Ar atmosphere. After stirred vigorously for 1 h at 30 ^{o}C, chalcone **13a** (62.5 mg, 0.3 mmol) and B$_2$(pin)$_2$ **14a** (91.2 mg, 0.36

mmol) were added successively at the same temperature. After stirring for 12 h, the reaction mixture was filtered and rinsed with THF (3 mL). The excess amount of NaBO$_3$·4H$_2$O (488 mg) was then added and the mixture was stirred at room temperature for 3 h. The aqueous layer was extracted with AcOEt (20 mL) three times, and the combined organic layers were dried over anhydrous Na$_2$SO$_4$. After concentrated under reduced pressure, the crude mixture was purified by preparative TLC (^{n}hexane/AcOEt = 4/1) to afford the desired product **16a** (62.7 mg, Quant.) as a colorless oil.

Typical Procedure for Spectrometric Investigations of Cu(0) Catalyst

Cu(0) (1.9 mg) and chiral 2,2'-bipyridine **L4** (8.8 mg) were dissolved in water and stirred at rt for 1 h. The resultant homogeneous solution was then submitted directly to spectrometric investigations.

[1] W. L. Xu, Y. G. Zhou, R. M. Wang, G. T. Wu, P. Chen, *Org. Biomol. Chem.* **2012**, *10*, 367-371.

[2] B. A. Provencher, K. J. Bartelson, Y. Liu, B. M. Foxman, L. Deng, *Angew. Chem. In.t Ed.* **2011**, *50*, 10565-10569.

[3] N. K. Rana, S. Selvakumar, V. K. Singh, *J. Org. Chem.* **2010**, *75*, 2089-2091.

[4] Y. Nishikawa, H. Yamamoto, *J. Am. Chem. Soc.*, **2011**, *133*, 8432-8435.

[5] J. A. M. Nolwenn, L. Benjamin, *J. Am. Chem. Soc.*, **2006**, *128*, 13368-13369.

[6] G. Fronza, C. Fuganti, S. Serra, *Eur. J. Org. Chem.* **2009**, *2009*, 6160-6171.

[7] M. Watanabe, S. Hisamatsu, H. Hotokezaka, S. Furukawa, *Chem. Pharm. Bull.* **1986**, *34*, 2810-2820.

[8] K. –L. Yeh, B. Liu, Y. –T. Lai, C. –W. Li, R. –S. Liu *J. Org. Chem.* **2004**, *69*, 4692-4694.

[9] K. Okuro, M. Furuune, M. Miura, M. Nomura *J. Org. Chem.* **1992**, *57*, 4754-4756.

[10] P. Wang, C. –R. Liu, X. –L. Sun, S. –S. Chen, J. –F. Li, Z. Xie, Y. Tang *Chem. Commun.* **2012**, *48*, 290-292.

[11] C. P. Lillya, A. F. Kluge *J. Org. Chem.* **1971**, *36*, 1977-1988.

[12] J. Maj, J. W. Morzycki, L. Rárová, G. Wasilewski, A. Wojtkielewicz *Tetrahedron Lett.* **2012**, *53*, 5430-5433.

[13] K. S. Lee, H. Wu, F. Haeffner, A. H. Hoveyda *Organometallics* **2012**, *31*, 7823-7826.

[14] C. Crisan, H. Normant *Bulletin de la Societe Chimique de France* **1957**, 1451-1454.

[15] M. –C. Lasne, J. –L. Ripoll, *Tetrahedron Lett.* **1980**, *21*, 463-464.

[16] K. Staub, G. A. Levina, S. Barlow, T. C. Kowalczyk, H. S. Lackritz, M. Barzoukas, A. Fort, S. R. Marder, *J. Mater. Chem.* **2003**, *13*, 825-833.

[17] M. Tissot, D. Poggiali, H. Hénon, D. Müller, L. Guénée, M. Mauduit, A. Alexakis *Chem. Eur. J.* **2012**, *18*, 8731-8747.

[18] C. Sole, E. Fernández, *Chem. Asian J.*, **2009**, *4*, 1790-1793.

[19] V. G. Desai, P. C. Satardekar, S. Polo, K. Dhumaskar, *Synth. Commun.*, **2012**, *42*, 836-842.

[20] T. Ishiyama, M. Murata, T. Ahiko, N. Miyaura *Org. Synth.* **2000**, *77*, 176-180.

[21] M. J. S. Dewar, R. Jones *J. Am. Chem. Soc.*, **1967**, *89*, 2408-2410.

[22] B. Hong, Y. Ma, L. Zhao, W. Duan, F. He, C. Song, *Tetrahedron: Asymmetry* **2011**, *22*, 1055-1062.

[23] H. Li, C. –S. Da, Y. –H. Xiao, X. Li, Y. –N. Su, *J. Org. Chem.* **2008**, *73*, 7398-7401.

[24] E. Hupe, I. Marek, P. Knochel, *Org. Lett.* **2002**, *4*, 2861-2863.

[25] J. S. Yadav, A. R. Reddy, Y. G. Rao, A. V. Narsaiah, B. V. S. Reddy, *Synlett* **2007**, 3447-3450.

[26] H. J. Xu, Y. C. Liu, Y. Fu, Y. D. Wu, *Org. Lett.* **2006**, *8*, 3449-3451.

27 K. Ahmad, S. Koul, S. C. Taneja, A. P. Singh, M. Kapoor, R. ul-Hassan, V. Verma, G. N. Qazi, *Tetrahedron Asymmetry* **2004**, *15*, 1685-1692.

28 B. M. Trost, H. Ito, *J. Am. Chem. Soc.* **2000**, *122*, 12003-12004.

29 T. Suzuki, N. Yamagiwa, Y. Matsuo, S. Sakamoto, K. Yamaguchi, M. Shibasaki, R. Noyori, *Tetrahedron Lett.* **2001**, *42*, 4669-4671.

30 C. Ghobril, C. Sabot, C. Mioskowski, R. Baati, *Eur. J. Org. Chem.* **2008**, *2008*, 4104-4108.

31 K. Hara, R. Akiyama, M. Sawamura, *Org. Lett.* **2005**, *7*, 5621-5623.

32 S. Aoki, S. Kotani, M. Sugiura, M. Nakajima, *Chem. Commun.* **2012**, *48*, 5524-5526.

33 K. –S. Lee, A. R. Zhugralin, A. H. Hoveyda, *J. Am. Chem. Soc.* **2009**, *131*, 7253-7255.

34 I. –H. Chen, L. Yin, W. Itano, M. Kanai, M. Shibasaki, *J. Am. Chem. Soc.* **2009**, *131*, 11664-11665.

35 J. Cossy, A. Bouzide, S. Ibhi, P. Aclinou, *Tetrahedron* **1991**, *47*, 7775-7782.

36 S. E. Denmark, T. Wynn, G. L. Beutner, *J. Am. Chem. Soc.* **2002**, *124*, 13405-13407.

37 S. Tang, R. H. Jin, H. S. Zhang, H. Yao, J. L. Zhuang, G. H. Liu, H. X. Li, *Chem. Commun.* **2012**, *48*, 6286-6288.

38 W. Li, X. Ma, W. Fan, X. Tao, X. Li, X. Xie, Z. Zhang, *Org. Lett.* **2011**, *13*, 3876-3879.

39 B. Loubinoux, J. –L. Sinnes, A. C. O'Sullivan, T. Winkler, *Tetrahedron* **1995**, *51*, 3549-3558.

40 N. Lin, M. –M. Chen, R. –S. Luo, Y. –Q. Deng, G. Lu, *Tetrahedron: Asymmetry* **2010**, *21*, 2816-2824.

41 D. Hirsch-Weil, K. A. Abboud, S. Hong, *Chem. Commun.* **2010**, *46*, 7525-7527.

42 M. L. Hlavinka, J. F. Greco, J. R. Hagadorn, *Chem. Commun.* **2005**, 5304-5306.

43 W. H. Puterbaugh, C. R. Hauser, *J. Am. Chem. Soc.* **1953**, *75*, 2415-2417.

44 O. Soltani, M. A. Ariger, H. Vázquez-Villa, E. M. Carreira, *Org. Lett.* **2010**, *12*, 2893-2895.

45 A. Abate, E. Brenna, A. Costantini, C. Fuganti, F. G. Gatti, L. Malpezzi, S. Serra *J. Org. Chem.* **2006**, *71*, 5228-5240.

46 C. H. Cheon, H. Yamamoto *Org. Lett.* **2010**, *12*, 2476-2479.

47 H. –X. Wei, K. Li, Q. Zhang, R. L. Jasoni, J. Hu, P. W. Pare *Helv. Chim. Acta* **2004**, *87*, 2354-2358.

48 K. Wadhwa, J. G. Verkade *J. Org. Chem.* **2009**, *74*, 4368-4371.

49 N. Lin, M. –M. Chen, R. –S. Luo, Y. –Q. Deng, G. Lu *Tetrahedron: Asymmetry* **2010**, *21*, 2816-2824.

Chapter 4 : Manipulation of Proton in Aqueous Environments

<Reagents>

Unless stated otherwise, commercially available reagents were used as received with the exception of the following substrates, which were prepared through reported methods. Analytical data for these compounds are in full agreement with reported data.

<Metal Salts>

Characterization of surfactant-combined catalysts.

Elementary analysis

$Sc(OSO_3C_{12}H_{25})_4 \cdot 5H_2O$ ($Sc(DS)_3$,white powder): Calcd C: 46.43, H: 9.20; found C: 46.91, H: 9.19.

$Sc(SO_3C_{12}H_{25})_3 \cdot 3H_2O$ (white powder): Calcd C: 51.04, H: 9.64; found C: 51.31, H: 9.40.

$Mn(OSO_2C_{12}H_{25})_2 \cdot 2H_2O$: Calcd C: 48.88, H: 9.23, S: 10.88; found C: 48.75, H: 9.34, S: 10.98.

$Fe(OSO_2C_{11}H_{23})_2 \cdot 2H_2O$: Calcd C: 46.97, H: 9.00, S: 11.22; found C: 46.97, H: 8.96, S: 11.40.

$Fe_2O(OSO_3C_{12}H_{25})_4 \cdot 5.5H_2O$: Calcd C: 44.75, H: 8.68, S: 9.96; found C: 44.72, H: 9.10, S: 9.66.

$Co(OSO_2C_{11}H_{23})_2 \cdot 4.5H_2O$: Calcd C:43.26, H: 9.08, S: 10.50; found C: 43.29, H: 9.15, S: 10.14.

$Ni(OSO_2C_{11}H_{23})_2 \cdot 6H_2O$: Calcd C: 41.29, H: 9.23, S: 10.06; found C: 41.45, H: 9.17, S: 10.06.

$Cu(OSO_2C_{12}H_{25})_2 \text{-} 4H_2O$: Calcd C: 43.17, H: 8.65, S: 9.47; found C: 43.26, H: 8.77, S: 9.62.

$Cu(OSO_2C_{10}H_{21})_2 \cdot 2H_2O$: Calcd C: 44.08, H: 8.57, S: 11.74; found C: 44.30, H: 8.55, S: 11.83.

$Cu(OSO_2C_9H_{19})_2 \cdot\text{-}2H_2O$: Calcd C: 42.05, H: 8.23, S: 12.47; found C: 41.81, H: 8.51, S: 12.72.

$Cu(OSO_2C_8H_{17})_2 \cdot 2.5H_2O$: Calcd C: 38.81, H: 7.94, S: 12.95; found C: 39.02, H: 8.01, S: 12.60.

$Zn(OSO_2C_{11}H_{23})_2 \cdot 5.5H_2O$: Calcd C: 43.46, H: 9.27, S: 9.67; found C: 43.47, H: 9.25, S: 9.85.

$AgOSO_2C_{12}H_{25}$: Calcd C: 40.34, H: 7.05, S: 8.98; found C: 40.17, H: 7.15, S: 8.89.

$Cd(OSO_2C_{11}H_{23})_2$: Calcd C: 45.76, H: 7.95, S: 11.22; found C: 45.31, H: 8.44, S: 11.00.

$In(OSO_2C_{11}H_{23})_2 \cdot H_2O$: Calcd C: 49.41, H: 9.13, S: 9.89; found C: 41.18, H:8.81, S: 10.02.

$Sn(OSO_2C_{11}H_{23})_2 \cdot H_2O$: Calcd C: 43.50, H: 7.96, S: 10.56; found C: 43.52, H: 8.07, S: 10.44.

$Yb(OSO_2C_{11}H_{23})_2 \cdot 3H_2O$: Calcd C: 42.47, H: 8.10, S: 10.31; found C: 42.70, H: 8.53, S: 10.58.

2-Benzylidene-3,4-dihydronaphthalen-1(2*H*)-one (**32a**)[1]
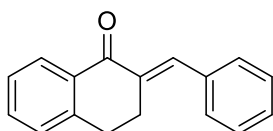
^{1}H NMR (600 MHz): δ = 2.90 (t, 2H, *J* = 6.9 Hz), 3.05-3.09(m, 2H), 7.22-7.49 (m, 8H), 7.78-7.81 (m, 1H), 8.07-8.08 (m, 1H).

^{13}C NMR (150 MHz): δ = 27.2, 28.9, 127.0, 128.1, 128.2, 128.4, 128.5, 129.8, 132.2, 135.4, 135.8, 136.7, 143.2, 187.9.

2-(4-Methoxybenzylidene)-3,4-dihydronaphthalen-1(2*H*)-one (**32b**)[1]
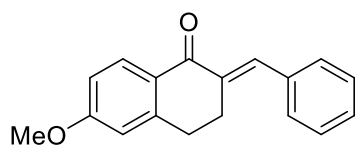
^{1}H NMR (600 MHz): δ = 2.88 (t, 2H, *J* = 6.2 Hz), 3.07 (t, 2H, *J* = 6.2 Hz), 3.78 (s, 3H), 6.88 (d, 2H, *J* = 8.9 Hz), 7.18 (d, 2H, *J* = 9.6 Hz), 7.27-7.30 (m, 1H), 7.35-7.37 (m, 2H), 7.41-7.43 (m, 1H), 7.77 (s, 1H), 8.05 (d, 1H, *J* = 7.6 Hz).
^{13}C NMR (150 MHz): δ = 27.2, 28.8, 55.3, 113.9, 126.9, 128.1, 128.4, 131.7, 133.1, 133.6, 136.7, 143.0, 159.9, 187.9.

2-(4-Chlorobenzylidene)-3,4-dihydronaphthalen-1(2*H*)-one (**32c**)[2]
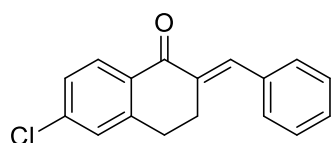
^{1}H NMR (600 MHz): δ = 2.94 (t, 2H, *J* = 6.9 Hz), 3.07 (t, 2H *J* = 6.2 Hz), 7.24 (d, 2H, *J* = 5.5 Hz), 7.34-7.38 (m, 5H), 7.46.7.49 (m, 1H), 7.77-7.788 (m, 1H), 8.10-8.12 (m, 1H).
^{13}C NMR (150 MHz): δ = 27.1, 28.7, 127.1, 128.2, 128.7, 131.1, 133.4, 134.2, 134.4, 135.2, 135.9, 143.1.

2-Benzylidene-6-methoxy-3,4-dihydronaphthalen-1(2*H*)-one (**32d**)[1]
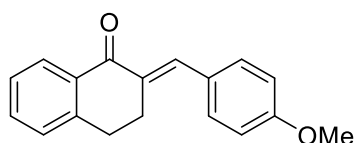
^{1}H NMR (600 MHz): δ = 2.90 (t, 2H, *J* = 6.8 Hz), 3.09 (t, 2H, *J* = 6.2 Hz), 3.86 (s, 3H), 6.68 (s, 1H), 6.85-6.87(m, 1H), 7.31-7.33 (m, 1H), 7.39-7.41 (m, 4H), 7.82 (s, 1H), 8.09-8.11 (m, 1H).
^{13}C NMR (150 MHz): δ = 27.2, 29.3, 55.4, 112.2, 113.3, 127.0, 128.3, 128.4, 129.8, 130.7, 135.6, 136.0, 145.7, 163.5, 186.8.

2-Benzylidene-2,3-dihydro-1*H*-inden-1-one (**32e**)[2]
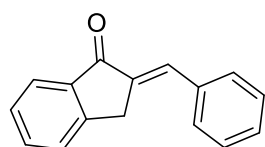
^{1}H NMR (600 MHz): δ = 4.05 (s, 2H), 7.38-7.46 (m, 4H), 7.54 (d, 1H, *J* = 7.6 Hz), 7.60 (t, 1H, *J* = 7.6 Hz), 7.66-7.67 (m, 3H), 7.90 (d, 1H, *J* = 7.6 Hz).
^{13}C NMR (150 MHz): δ = 32.4, 124.4, 126.1, 127.6, 128.9, 129.6, 130.7, 133.9, 134.6, 134.7, 135.3, 149.6, 194.3.

2-Benzylidenecyclohexanone (**32f**)[3]
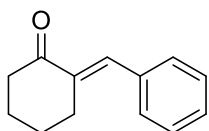
^{1}H NMR (600 MHz): δ = 1.66-1.70 (m, 2H), 1.82-1.86 (m, 2H), 2.44-2.46 (m, 2H), 2.74-2.76 (m, 2H), 7.22-7.26 (m, 1H), 7.28-7.32 (m, 4H), 7.41 (d, 1H, *J* = 2.1 Hz).
^{13}C NMR (150 MHz): δ = 23.3, 23.8, 28.9, 40.3, 128.2, 128.4, 130.2, 135.5, 136.6, 201.8.

2-Methyl-1-phenylprop-2-en-1-one (**35a**)[4]
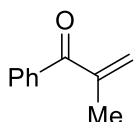
^{1}H NMR (600 MHz): δ = 2.00 (s, 3H), 5.55 (s, 1H), 5.83 (s, 1H), 7.34-7.37 (m, 2H), 7.44-7.47 (m, 1H), 7.65-7.67 (m, 1H).
^{13}C NMR (150 MHz): δ = 18.6, 127.1, 128.1, 129.3, 131.9, 137.6, 143.7, 198.4.

1,2-Diphenylprop-2-en-1-one (**35c**)[4]
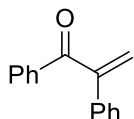
^{1}H NMR (600 MHz): δ = 5.63 (s, 1H), 6.06 (s, 1H), 7.24-7.44 (m, 7H), 7.52-7.63 (m, 1H), 7.88-7.90 (m, 2H).
^{13}C NMR (150 MHz): δ = 120.9, 127.0, 128.4, 128.5, 128.6, 128.8, 129.0, 129.2, 129.9, 133.0, 134.8, 137.0, 148.2, 197.6.

1-(4-Methoxyphenyl)-2-methylprop-2-en-1-one (**35d**)[5]
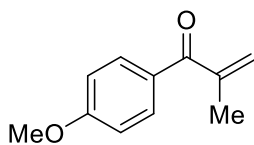
^{1}H NMR (600 MHz): δ = 1.97 (s, 3H), 3.80 (s, 3H), 5.46(s, 1H), 5.72 (s, 1H), 6.84-6.86 (m, 2H), 7.71-7.72 (m, 2H).
^{13}C NMR (150 MHz): δ = 19.0, 55.3, 113.3, 124.7, 129.9, 131.8, 143.8, 162.9, 197.1.

1-(4-Bromophenyl)-2-methylprop-2-en-1-one (**35e**)[5]
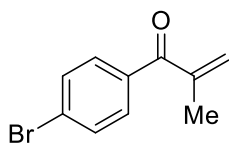
^{1}H NMR (600 MHz): δ = 2.06 (s, 3H), 5.59 (s, 1H), 5.91 (s, 1H), 7.56-7.61 (m, 4H).
^{13}C NMR (150 MHz): δ = 18.5, 126.9, 127.2, 13.9, 131.4, 136.3, 143.5, 197.1.

2-Benzyl-1-phenylprop-2-en-1-one (**35f**)[4]
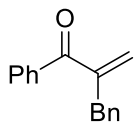
^{1}H NMR (600 MHz): δ = 3.78 (s, 2H), 5.66 (s, 1H), 5.73(s, 1H), 7.17-7.27 (m, 5H), 7.37-7.40 (m, 2H), 7.47-7.50 (m, 1H), 7.68-7.70 (m, 2H).
^{13}C NMR (150 MHz): δ = 38.3, 126.3, 126.8, 128.2, 128.5, 129.2, 129.5, 132.2, 137.7, 138.7, 147.7, 197.6.

2-Benzyl-1-(3-(trifluoromethyl)phenyl)prop-2-en-1-one (**35g**)
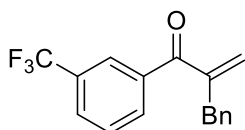
Colorless oil
^{1}H NMR (600 MHz): δ = 3.80 (s, 2H), 5.68 (s, 1H), 5.82 (s, 1H), 7.17-7.44 (m, 5H), 7.55 (t, 1H, *J* = 7.6 Hz), 7.76 (d, 1H, *J* = 7.6 Hz), 7.87 (d, 1H, *J* = 7.6 Hz), 7.95 (s, 1H). ^{13}C NMR (150 MHz): δ = 38.1, 126.1, 126.5, 127.8, 128.4, 128.6, 128.8, 129.1, 132.5, 138.2, 138.3, 147.3, 196.1.
HRMS calcd for $C_{17}H_{14}OF_3^+$ ([M + H]$^+$): 291.09967, found 291.09805.

2-Benzyl-1-(4-methoxyphenyl)prop-2-en-1-one (**35h**)
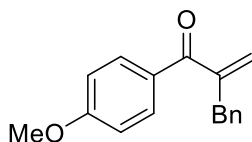
Colorless oil
^{1}H NMR (600 MHz): δ = 3.80 (s, 2H), 3.90 (s, 3H), 5.52 (s, 1H), 5.58 (s, 1H), 6.81-6.85 (m, 2H), 7.10-7.26 (m, 5H), 7.72-7.74 (m, 2H).
^{13}C NMR (150 MHz): δ = 38.7, 55.4, 113.4, 124.7, 126.3, 128.4, 129.1, 131.9, 138.6, 147.7, 163.1, 196.4.
HRMS calcd for $C_{17}H_{16}O_2^+$ ([M + H]$^+$): 253.12285, found 253.11876.

3-Methacryloyloxazolidin-2-one (**35i**)[6]
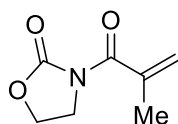
^{1}H NMR (600 MHz): δ = 1.97 (s, 3H), 3.94-3.98 (m, 2H), 4.36-4.40 (m, 2H), 5.38 (d, 2H, *J* = 16.5 Hz).
^{13}C NMR (150 MHz): δ = 19.1, 42.9, 62.2, 120.9, 139.0, 152.7, 171.0.

2-Methyl-1-(1-methyl-1*H*-imidazol-2-yl)prop-2-en-1-one (**35k**)[7]
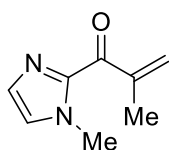
^{1}H NMR (600 MHz): δ = 1.98 (s, 3H), 3.90 (s, 3H), 5.93 (s, 1H), 6.42 (s, 1H), 6.95 (d, 1H, *J* = 11.0 Hz), 7.05 (d, 1H, *J* = 11.7 Hz).
^{13}C NMR (150 MHz): δ = 18.5, 36.0, 126.3, 128.7, 129.2, 142.8, 142.9, 186.0.

2-(Propan-2-ylidene)-3,4-dihydronaphthalen-1(2*H*)-one (**35p**)[8]
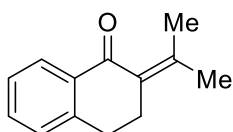
^{1}H NMR (600 MHz): δ = 1.89 (s, 3H), 2.15 (s, 3H), 2.74(t, 2H, *J* = 6.0 Hz), 2.88 (t, 2H, *J* = 6.6 Hz), 7.14 (d, 1H, *J* = 7.2 Hz), 7.22 (t, 1H, *J* = 7.2 Hz), 7.38-7.41 (m, 1H), 8.01 (d, 1H, *J* = 7.2 Hz).
^{13}C NMR (150 MHz): δ = 23.1, 23.5, 28.5, 29.9, 126.5, 127.7, 128.0, 130.3, 132.4, 134.8, 143.3, 145.8, 198.8.

2-Benzylidene-6-methoxy-3,4-dihydronaphthalen-1(2*H*)-one (**35q**)
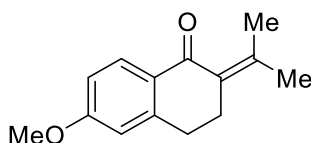
Colorless oil
^{1}H NMR (600 MHz): δ = 1.87 (s, 3H), 2.14 (s, 3H), 2.72 (t, 2H, *J* = 6.2 Hz), 2.84 (t, 2H *J* = 6.5 Hz), 3.78 (s, 3H), 6.66 (d, 1H, *J* = 2.1 Hz), 6.81-6.83 (m, 1H), 8.05 (d, 1H, *J* = 8.9 Hz).
^{13}C NMR (150 MHz): δ = 23.0, 23.3, 28.6, 30.3, 53.3, 112.0, 112.8, 128.3, 130.1, 130.3, 144.7, 145.7, 162.8, 189.9.

2-Benzylidene-2,3-dihydro-1*H*-inden-1-one (**35r**)[8]
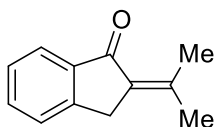
^{1}H NMR (600 MHz): δ = 1.99 (s, 3H), 2.42 (s, 3H), 3.63 (s, 2H), 7.35 (t, 1H, *J* = 7.2 Hz), 7.44 (d, 1H, *J* = 7.8 Hz), 7.53 (t, 1H, *J* = 7.2 Hz), 7.78 (d, 1H, *J* = 7.8 Hz).
^{13}C NMR (150 MHz): δ = 20.4, 24.5, 32.2, 123.8, 125.8, 127.1, 130.3, 133.6, 147.8, 149.6, 194.0.
HRMS calcd for $C_{14}H_{16}O_2^{+}$ ([M + H]$^{+}$): 217.12285, found 217.12086.

Typical Experimental Procedure for tandem sulfa-Michael reaction/enantioselective protonation in water (Table 2, entry 2):

A mixture of Sc(OTf)$_3$ (9.8 mg, 0.02 mmol) and **L1** (7.9 mg, 0.024 mmol) in water (800 µL) was stirred for 1 h at room temperature. After addition of pyridine (6.3 µL, 0.08 mmol), 2-methyl-1-phenylprop-2-en-1-one **35a** (58.5 mg, 0.4 mmol) and benzylthiol **33a** (56.3 µL, 0.48 mmol) successively, the reaction mixture was vigorously stirred for 24 h at room temperature. The resulting mixture was quenched with Water. The aqueous layer was extracted with dichloromethane (three times), and the combined organic layers were washed with CuSO$_4$ *aq*, and dried over Na$_2$SO$_4$. After filtration, the solvent was removed under reduced pressure. The residue was purified by preparative TLC (elution: chloroform/ethyl acetate = 100/1) to give the corresponding thio ethers **36aa** (99.8 mg, 92% yield). The enantiomeric excess was determined by chiral HPLC analysis.

Analytical data for sulfa-Michael addition and protonations 34aa-34fa

Absolute configuration of **34da** was determined by X-ray diffraction. Configurations of **34aa**, **34ba**, **34ca**, **34ea** and **34fa** were determined by analogy.

(*R*)-2-((*R*)-(Benzylthio)(phenyl)methyl)-3,4-dihydronaphthalen-1(2*H*)-one (**34aa**)
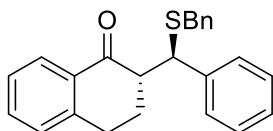
Colorless oil

IR (neat) ν = 3060, 3027, 2934, 1680, 1600, 1453, 1298, 1227, 1025 cm^{-1}.

^{1}H NMR (600 MHz, *syn/anti* = 90/10): δ = 1.62-1.69 (m, 1H), 2.26-2.31 (m, 1H), 2.83-2.90 (m, 3H), 3.44 (dd, 2H, *J* = 13.1, 51.5 Hz), 4.66 (m, 0.1 H), 4. 71 (d, 0.9 H, *J* = 4.8 Hz), 7.06-7.22 (m, 10H), 7.33 (dd, 1H, *J* = 6.2, 7.6 Hz), 7.39 (d, 2H, *J* = 7.6 Hz), 7.89 (d, 1H, *J* = 6.9 Hz).

^{13}C NMR (150 MHz): δ = 25.2, 28.8, 35.9, 47.2, 53.2, 126.5, 126.9, 127.1, 127.6, 128.0, 128.3, 128.5, 128.6, 128.8, 128.8, 129.7, 132.3, 133.2, 137.8, 138.8, 143.5, 196.5.

HPLC (Daicel Chiralcel OD-H, ^{n}hexane/ ^{i}PrOH = 100/1, flow rate = 1.0 ml/min); t_R = 13.2 min (*syn*, major), t_R = 15.5 min (*anti*, major), t_R = 16.8 min (*anti*, minor), t_R = 19.4 min (*syn*, minor).

HRMS calcd for C$_{24}$H$_{23}$OS$^+$ ([M+H]$^+$): 359.14696, found 359.14674.

(*R*)-2-((*R*)-(Benzylthio)(4-methoxyphenyl)methyl)-3,4-dihydronaphthalen-1(2*H*)-one (**34ba**)
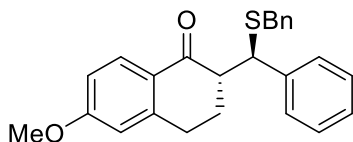
White solid (mixture)

IR (KBr): ν = 2933, 2834, 1681, 1602, 1509, 1249, 1032 cm^{-1}.

^{1}H NMR (600 MHz, *syn/anti* = 95/5): δ = 1.64-1.71 (m, 1H), 2.27-2.30 (m, 1H), 2.83-2.86 (m, 3H), 3.43 (dd, 2H, *J* = 13.1, 53.6 Hz), 3.70 (s, 3H), 4.58 (m, 0.05 H), 4.69 (m, 0.95 H), 6.73-6.75 (m, 2H), 7.06-7.21 (m, 7H), 7.30-7.34 (m, 3H), 7.89 (d, 1H, *J* = 7.6 Hz).

^{13}C NMR (150 MHz): δ = 25.1, 28.6, 35.8, 46.5, 53.3, 55.1, 113.3, 126.5, 126.9, 127.6, 128.3, 128.5, 128.8, 130.8, 133.2, 137.9, 143.5, 158.6, 196.6.

HPLC (Daicel Chiralcel OJ-H, ^{n}hexane/ ^{i}PrOH = 4/1, flow rate = 1.0 ml/min); t_R = 12.6 min (*anti*, major), t_R = 17.5 min (*anti*, minor), t_R = 19.3 min (*syn*, major), t_R = 26.0 min (*syn*, minor). HRMS calcd for $C_{25}H_{25}O_2S^+$ ([M+H]$^+$): 389.15752, found 389.15789.

(*R*)-2-((*R*)-(Benzylthio)(4-chlorophenyl)methyl)-3,4-dihydronaphthalen-1(2*H*)-one (**34ca**)
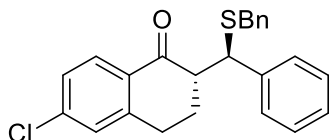
Yellow solid (mixture)

IR (KBr): ν = 2932, 1682, 1599, 1489, 1228, 1092 cm^{-1}. ^{1}H NMR (600 MHz, *syn/anti* = 94/6): δ = 1.60-1.66 (m, 1H), 2.26-2.30 (m, 1H), 2.82-2.89 (m, 3H), 3.45 (dd, 2H, *J* = 13.1, 66.3 Hz), 4.58 (m, 0.06 H), 4.73 (d, 0.94H, *J* = 4.1 Hz), 7.08- 7.24 (m, 9H), 7.28-7.37 (m, 3H), 7.86-7.88 (m, 1H). ^{13}C NMR (150 MHz): δ = 25.0, 28.8, 35.9, 46.5, 53.2, 126.6, 127.0, 127.6, 128.1, 128.4, 128.5, 128.8, 131.2, 132.2, 132.9, 133.4, 137.3, 137.5, 143.5, 196.1.

HPLC (Daicel Chiralpak AD-H, *n*-hexane/*i*-PrOH = 100/1, flow rate = 1.0 ml/min); t_R = 26.0 min (*syn*, major), t_R = 33.3 min (*syn*, minor), t_R = 40.5 min (*anti*, major), t_R = 49.1 min (*anti*, minor). HRMS calcd for $C_{24}H_{22}ClOS^+$ ([M+H]$^+$): 393.10799, found 393.10827.

(*R*)-2-((*R*)-(Benzylthio)(phenyl)methyl)-6-methoxy-3,4-dihydronaphthalen-1(2*H*)-one (**34da**)
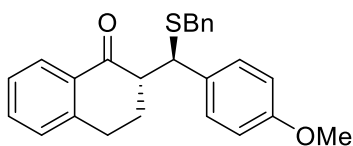
White solid; mp 99-101 ^{o}C

IR (KBr): ν = 2949, 1668, 1602, 1258, 1058 cm^{-1}.

^{1}H NMR (600 MHz, *syn/anti* = 97/3): δ = 1.65-1.71 (m, 1H), 2.29-2.33 (m, 1H), 2.83-2.90 (m, 3H), 3.49 (dd, *J* = 13.1, 48.1 Hz), 3.79 (s, 3H), 4.71 (m, 0.03 H), 4.79 (d, 0.97 H, *J* = 4.8 Hz), 6.56 (s, 1H), 6.73-6.75 (m, 1H), 7.13-7.26 (m, 9H), 7.43 (d, *J* = 8.2 Hz), 7.91 (d, 1H, *J* = 8.2 Hz).

^{13}C NMR (150 MHz): δ = 25.2, 29.0, 36.0, 47.3, 52.9, 55.3, 112.2, 113.1, 126.0, 126.9, 127.1, 128.0, 128.3, 128.9, 129.7, 130.1, 137.9, 138.9, 146.0, 163.4, 195.2.

HPLC (Daicel Chiralpak AD-H, ^{n}hexane/ ^{i}PrOH = 9/1, flow rate = 1.0 ml/min); t_R = 11.1 min (*syn*, minor), t_R = 12.3 min (*syn*, major), t_R = 14.2 min (*anti*, minor), t_R = 16.0 min (*anti*, major). HRMS calcd for $C_{25}H_{25}O_2S^+$ ([M+H]$^+$): 389.15752, found 389.15437.

(*R*)-2-((*R*)-(Benzylthio)(phenyl)methyl)-2,3-dihydro-1H-inden-1-one (**34ea**)
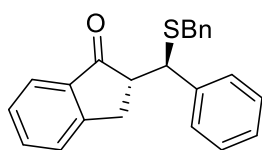
Colorless oil

IR (neat): ν = 3060, 3028, 2918, 1710, 1606, 1493, 1451, 1294, 1207, 1029 cm^{-1}.

^{1}H NMR (600 MHz, *syn/anti* = 68/32): δ = 3.0-3.2 (m, 3H), 3.43-3.60 (m, 3H), 4.55 (d, 0.68H, *J* =

2.3 Hz), 4.64 (d, 0.32H, J = 3.4 Hz), 7.11- 7.46 (m, 13H), 7.56-7.59 (m, 1H), 7.77-7.78 (m, 1H).
^{13}C NMR (150 MHz): δ = 28.74, 29.5, 35.8, 36.0, 48.6, 49.8, 52.4, 53.5, 123.8, 124.0, 126.2, 126.4, 126.9, 127.0, 127.1, 127.2, 127.3, 127.4, 128.0. 128.2. 128.3. 128.4. 128.6. 128.8. 128.9. 129.3. 134.6 134.9. 136.4. 136.7, 137.2, 137.4, 137.6, 141.4, 153.6, 204.9.
HPLC (Daicel Chiralpak AD-H, ^{n}hexane/ ^{i}PrOH = 9/1, flow rate = 1.0 ml/min); t_R = 7.8 min (*syn*, minor), t_R = 8.3 min (*syn*, major), t_R = 9.6 min (*anti*, major), t_R = 10.6 min (*anti*, minor).
HRMS calcd for $C_{23}H_{21}OS^+$ ([M+H]$^+$): 345.13131, found 345.13089.

(*R*)-2-((*R*)-(Benzylthio)(phenyl)methyl)cyclohexanone (**34fa**)
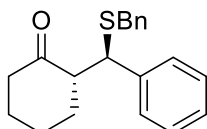
Colorless oil
IR (neat): ν = 3027, 2936, 2861, 1712, 1493, 1450, 1126, 1070 cm^{-1}.
^{1}H NMR (600 MHz, *syn*/*anti* = 62/38): δ = 1.25-1.28 (m, 1H), 1.50-1.58 (m, 1H), 1.65-1.74 (m, 2H), 1.81-1.85 (m, 1H), 1.91-1.96 (m, 0.5H), 2.16-2.19 (m, 0.5H), 2.26-2.33 (m, 2H), 2.72-2.77 (m, 1H), 3.42 (dd, 1H, J = 6.2, 13.1 Hz), 3.51 (dd, 1H, J = 13.7, 22.7 Hz), 4.12 (d, 0.5H, J = 8.9 Hz), 4.25 (d, 0.5H, J = 7.6 Hz), 7.19-7.35 (m, 9H).
^{13}C NMR (150 MHz): δ = 23.5, 24.4, 27.7, 28.0, 30.8, 31.7, 35.5, 35.7, 41.3, 42.0, 47.2, 48.4, 56.2, 56.4, 126.8, 126.9, 127.2, 128.2, 128.3, 128.5, 128.9, 129.0, 129.1, 137.9, 139.8, 141.8, 209.9, 210.7.
HPLC (Daicel Chiralpak AS-H, ^{n}hexane/ ^{i}PrOH = 9/1, flow rate = 1.0 ml/min); t_R = 15.0 min (*anti*, major), t_R = 16.1 min (*anti*, minor), t_R = 19.1 min (*syn*, minor), t_R = 25.1 min (*syn*, major).
HRMS calcd for $C_{20}H_{23}S^+$ ([M+H]$^+$): 311.14696, found 311.14676.

Analytical data for protonations 36aa–36ra

Absolute configuration of **36aa** was determined by X-ray crystallography analysis. Configurations of **36ab**-**36ae, 36ja**, and **36ka** were determined by analogy. Configuration of **36ia** was assigned by comparison of literature data[8]. The absolute configuration of **36pa** was assumed from the stereochemistry of desulfonated compound. The configurations of **36qa** and **36ra** were determined by analogy.

(*R*)-3-(benzylthio)-2-methyl-1-phenylpropan-1-one (**36aa**)
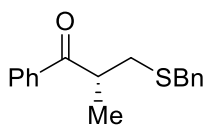
White solid; mp 54–56 °C
IR (KBr): ν = 2964, 2929, 1675, 1450, 1226, 969, 677 cm^{-1}.
^{1}H NMR (600 MHz): δ = 1.16 (d, 3H, J = 6.9 Hz), 2.47 (dd, 1H, J = 6.9, 13.1 Hz), 2.87 (q, 1H, J = 6.2 Hz), 3.48 (dd, 1H, J = 6.9, 14.4 Hz), 3.65 (s, 2H), 7.16–7.24 (m, 5H), 7.36–7.39 (m, 2H), 7.50–7.52 (m, 1H), 7.76–7.79 (m, 1H).

^{13}C NMR (150 MHz): δ = 17.7, 34.7, 37.3, 41.1, 127.0, 128.3, 128.5, 128.6, 128.8, 133.1, 136.2, 202.8.

HPLC (Daicel Chiralpak AS-H, ^{n}hexane/ ^{i}PrOH = 9/1, flow rate = 0.5 mL min^{-1}); t_R = 12.8 min (R), t_R = 16.5 min (S).

HRMS calcd for $C_{17}H_{19}OS^+$ ([M + H]$^+$): 271.11566, found 271.11381.

$[\alpha]_D^{20}$ = +30.54 (c = 1.0, CHCl$_3$).

(R)-2-((benzylthio)methyl)-1-phenylhexan-1-one (**36ba**)
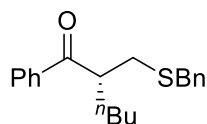
Colorless oil

IR (neat): v = 2956, 2928, 2858, 1678, 1596, 1450, 1229, 700 cm^{-1}.

^{1}H NMR (600 MHz): δ = 0.72–0.75 (m, 3H), 1.07–1.18 (m, 4H), 1.44–1.51 (m, 1H), 1.60–1.67 (m, 1H), 2.50–2.53 (m, 1H), 2.81 (dd, 1H, J = 8.25, 13.1 Hz), 3.43–3.47 (m, 1H), 3.61 (s, 2H), 7.15–7.23 (m, 5H), 7.36–7.39 (m, 2H), 7.47–7.50 (m, 1H), 7.77–7.79 (m, 2H).

^{13}C NMR (150 MHz): δ = 13.8, 22.7, 29.3, 32.3, 33.4, 37.4, 46.3, 127.0, 128.3, 128.5, 128.6, 128.9, 133.0, 137.3, 138.4, 203.0.

HPLC (Daicel Chiralcel OD-H, ^{n}hexane/ ^{i}PrOH = 100/1, flow rate = 1.0 mL min^{-1}); t_R = 10.7 min (S), t_R = 11.6 min (R).

HRMS calcd for $C_{20}H_{25}OS^+$ ([M + H]$^+$): 313.16261, found 313.16312.

$[\alpha]_D^{20}$ = +14.10 (c = 1.0, CHCl$_3$).

(R)-3-(benzylthio)-1,2-diphenylpropan-1-one (**36ca**)
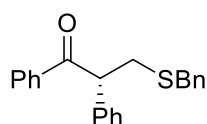
Yellow oil

IR (neat): v = 3060, 3027, 2918, 1679, 1450, 1230, 698 cm^{-1}.

^{1}H NMR (600 MHz): δ = 2.73 (dd, 1H, J = 6.2, 13.1 Hz), 3.27 (dd, 1H, J = 8.3, 13.1 Hz), 3.57 (d, 2H, J = 4.1 Hz), 4.48 (dd, 1H, J = 6.2, 8.2 Hz), 7.11–7.27 (m, 12H), 7.36–7.38 (m, 1H), 7.73–7.76 (m, 2H).

^{13}C NMR (150 MHz): δ = 35.3, 37.5, 54.2, 127.0, 127.5, 128.1, 128.4, 128.5, 128.7, 128.9, 129.0, 133.0, 136.4, 138.2, 138.7, 198.5.

HPLC (Daicel Chiralcel OD-H, ^{n}hexane/ ^{i}PrOH = 9/1, flow rate = 1.0 mL min^{-1}); t_R = 7.8 min (S), t_R = 8.8 min (R).

HRMS calcd for $C_{22}H_{21}OS^+$ ([M + H]$^+$): 333.13131, found 333.12972.

$[\alpha]_D^{20}$ = −105.61 (c = 1.0, CHCl$_3$).

(R)-3-(Benzylthio)-1-(4-methoxyphenyl)-2-methylpropan-1-one (**36da**)
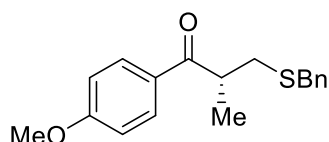
White solid; mp 91 – 94 $^\circ$C

IR (KBr): ν = 2972, 2927, 2839, 1667, 1602, 1454, 1235, 1174, 1024, 845, 700 cm^{-1}.

^{1}H NMR (600 MHz): δ = 1.13 (d, 3H, J = 6.9 Hz), 2.43-2.46 (m, 1H), 2.84-2.87 (m, 1H), 3.42 (q, 1H, J = 6.9 Hz), 3.79 (s, 2H), 6.84 (m, 2H), 7.16-7.22 (m, 5H), 7.77-7.77 (m, 1H).

^{13}C NMR (150 MHz): δ = 17.8, 34.9, 37.3, 40.6, 55.4, 113.8, 127.0, 128.5, 128.8, 129.1, 130.6, 138.5, 163.5, 201.3.

HPLC (Daicel Chiralcel OD-H, ^{n}hexane/ ^{i}PrOH = 9/1, flow rate = 1.0 mL/min); t_R = 15.7 min (*S*), t_R = 17.5 min (*R*).

HRMS calcd for C$_{18}$H$_{21}$O$_2$S$^+$ ([M+H]$^+$): 301.12622, found 301.12631.

$[\alpha]_D^{20}$ = +8.68 (*c* = 1.0, CHCl$_3$).

(*R*)-3-(Benzylthio)-1-(4-bromophenyl)-2-methylpropan-1-one (**36ea**)
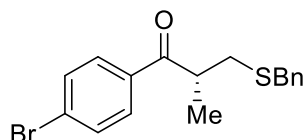
White solid; mp 70 – 73 $^\circ$C

IR (neat): ν = 2966, 2920, 1679, 1581, 1225, 833, 701 cm^{-1}.

^{1}H NMR (600 MHz): δ = 1.19 (d, 3H, J = 6.9 Hz), 2.52 (dd, 1H, J = 6.9, 13.1 Hz), 2.90 (dd, 1H, J = 6.9, 13.1 Hz), 3.43 (q, 1H, J = 6.9 Hz), 3.71 (s, 2H), 7.23-7.32 (m, 4H), 7.56-7.60 (m, 3H), 7.63-7.69 (m, 2H).

^{13}C NMR (150 MHz): δ = 17.6, 34.7, 37.3, 41.2, 127.1, 128.3, 128.6, 128.8, 129.5, 129.8, 131.8, 131.9, 134.9, 201.8.

HPLC (Daicel Chiralcel OD-H, ^{n}hexane/ ^{i}PrOH = 9/1, flow rate = 1.0 mL/min); t_R = 4.8 min (*S*), t_R = 7.6 min (*R*).

HRMS calcd for C$_{17}$H$_{18}$OSBr$^+$ ([M+H]$^+$): 349.02617, found 349.02532.

$[\alpha]_D^{20}$ = +10.53 (*c* = 1.0, CHCl$_3$).

(*R*)-2-Benzyl-3-(benzylthio)-1-phenylpropan-1-one (**36fa**)
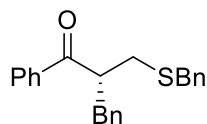
Colorless oil

IR (neat): ν = 3060, 3026, 2919, 1678, 1597, 1493, 1449, 1230, 698 cm^{-1}.

^{1}H NMR (600 MHz): δ = 2.50 (dd, 1H, J = 5.5, 13.1 Hz), 2.74 (q, 1H, J = 6.9 Hz), 2.83 (dd, 1H, J = 8.2, 13.1 Hz), 2.94 (q, 1H, J = 6.9 Hz), 3.54 (dd, 2H, J = 13.7, 17.2 Hz), 3.71-3.73 (m, 1H), 6.99-7.01 (m, 2H), 7.07-7.09 (m, 3H), 7.12-7.18 (m, 5H), 7.30-7.33 (m, 2H), 7.42-7.45 (m, 1H), 7.65-7.68 (m, 2H).

^{13}C NMR (150 MHz): δ = 32.9, 37.2, 38.3, 48.5, 126.40, 127.0, 128.3, 128.4, 128.5, 128.5, 128.8, 129.0, 133.0, 137.0, 138.4, 138.8, 202.3.

HPLC (Daicel Chiralpak AS-H, ^{n}hexane/ ^{i}PrOH = 9/1, flow rate = 1.0 mL/min); t_R = 11.9 min (*R*), t_R = 12.8 min (*S*).

HRMS calcd for $C_{23}H_{23}OS^+$ ([M+H]$^+$): 347.14696 , found 347.14757.

$[α]_D^{20}$ = −3.53 (*c* = 1.0, CHCl$_3$).

(*R*)-2-Benzyl-3-(benzylthio)-1-(3-(trifluoromethyl)phenyl) propan-1-one (**36ga**)
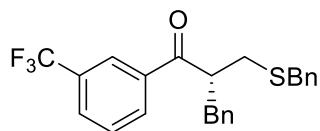
Colorless oil

IR (neat): ν = 3063, 3029, 1688, 1609, 1495, 1453, 1331, 1170, 1127, 1072, 804, 751 cm^{-1}.

^{1}H NMR (600 MHz): δ = 2.54 (dd, 1H, *J* = 5.5, 13.1 Hz), 2.76 (q, 1H, *J* = 6.9 Hz), 2.83-2.86 (m, 1H), 3.53-3.59 (m, 3H), 6.91-6.94 (m, 2H), 7.02-7.20 (m, 8H), 7.40-7.42 (m, 1H), 7.63-7.66 (m, 1H), 7.72-7.79 (m, 2H).

^{13}C NMR (150 MHz): δ = 33.2, 37.4, 38.7, 49.1, 122.7, 124.5, 125.0, 15.1, 126.6, 127.1, 128.5, 128.6, 128.8, 128.9, 129.1, 129.3, 130.9, 131.1, 131.3, 137.7, 138.2, 138.4, 201.5.

HPLC (Daicel Chiralcel OD-H, ^{n}hexane/ ^{i}PrOH = 19/1, flow rate = 0.5 mL/min); t_R = 20.6 min (*S*), t_R = 22.3 min (*R*).

HRMS calcd for $C_{24}H_{22}F_3OS^+$ ([M+H]$^+$): 415.13434, found 415.13134.

(*R*)-2-Benzyl-3-(benzylthio)-1-(4-methoxyphenyl)propan-1-one (**36ha**)
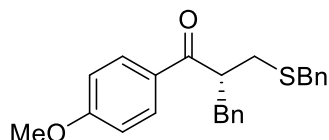
White solid; mp 97 − 100 ^{o}C

IR (KBr): ν = 3014, 2928, 1670, 1596, 1455, 1367, 1235, 1166, 1024, 931, 854, 763, 701, 605 cm^{-1}.

^{1}H NMR (600 MHz): δ = 2.50 (dd, 1H, *J* = 5.5, 13.1 Hz), 2.80 (q, 1H, *J* = 6.9 Hz), 2.88 (dd, 1H, *J* = 8.2, 13.1 Hz), 2.98-3.01 (m, 1H), 3.54 (d, 2H, *J* = 3.4 Hz), 3.70-3.75 (m, 1H), 3.85 (s, 3H), 6.78 (d, 2H, *J* = 8.9 Hz), 7.00 (d, 2H, *J* = 8.2 Hz), 7.06-7.19 (m, 8H), 7.67 (d, 2H, *J* = 8.3 Hz).

^{13}C NMR (150 MHz): δ = 33.1, 37.2, 38.4, 48.0, 56.4, 113.6, 126.3, 126.9, 128.4, 128.5, 128.8, 129.0, 130.6, 163.4, 200.6.

HPLC (Daicel Chiralcel OD-H, ^{n}hexane/ ^{i}PrOH = 9/1, flow rate = 1.0 mL/min); t_R = 12.1 min (*S*), t_R = 14.5 min (*R*).

HRMS calcd for $C_{24}H_{25}OS^+$ ([M+H]$^+$): 377.15752, found 377.15695.

$[α]_D^{20}$ = −8.47 (*c* = 1.0, CHCl$_3$).

(*R*)-3-((4-chlorobenzyl)thio)-2-methyl-1-phenylpropan-1-one (**36ab**)
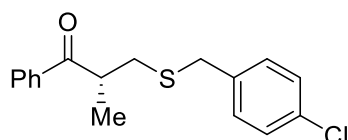
Colorless oil

IR (neat): v = 2971, 2927, 1680, 1489, 1451, 1230, 1092, 972, 700 cm^{-1}.

^{1}H NMR (600 MHz): δ = 1.15 (d, 2H, J = 6.9 Hz), 2.45 (dd, 1H, J = 6.9, 13.1 Hz), 2.84 (dd, 1H, J = 6.9, 13.1 Hz), 3.43–3.49 (m, 1H, J = 6.9), 3.59 (dd, 2H, J = 14.1, 17.5 Hz), 7.14–7.18 (m, 5H), 7.36–7.39 (m, 2H), 7.48–7.50 (m, 1H), 7.77 (m, 2H).

^{13}C NMR (150 MHz): δ = 17.7, 34.7, 36.6, 41.1, 128.2, 128.6, 128.7, 130.1, 132.8, 133.2, 136.1, 137.0, 202.6.

HPLC (Daicel Chiralcel OD-H, ^{n}hexane/ ^{i}PrOH = 100/1, flow rate = 1.0 mL min^{-1}); t_R = 15.7 min (S), t_R = 17.1 min (R).

HRMS calcd for C$_{18}$H$_{18}$OSCl$^+$ ([M + H]$^+$): 305.07669, found 305.07709.

$[\alpha]_D^{20}$ = +10.12 (c = 1.0, CHCl$_3$).

(*R*)-3-((4-methoxybenzyl)thio)-2-methyl-1-phenylpropan-1-one (**36ac**)
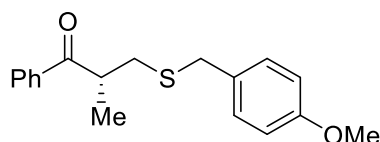
Colorless oil

IR (neat): v = 2966, 2930, 1680, 1608, 1510, 1451, 1247, 1177, 1033, 971, 701 cm^{-1}.

^{1}H NMR (600 MHz): δ = 1.5 (d, 3H, J = 6.9 Hz), 2.45 (dd, 1H, J = 7.8, 13.1 Hz), 2.84 (dd, 1H, J = 6.2, 13.1 Hz), 3.46 (q, 1H, J = 6.8), 3.60 (d, 2H, J = 2.8 Hz), 3.71 (s, 3H), 6.74 (d, 2H, J = 9 Hz), 7.12–7.14 (m, 2H), 7.35–7.38 (m, 2H), 7.46–7.49 (m, 1H), 7.76–7.78 (m, 2H).

^{13}C NMR (150 MHz): δ = 17.6, 34.6, 36.6, 41.1, 55.2, 113.9, 128.1, 128.3, 129.9, 130.3, 133.0, 136.2, 158.6, 202.8.

HPLC (Daicel Chiralcel OD-H, ^{n}hexane/ ^{i}PrOH = 9/1, flow rate = 1.0 mL min^{-1}); t_R = 8.2 min (S), t_R = 9.3 min (R).

HRMS calcd for C$_{18}$H$_{21}$O$_2$S$^+$ ([M + H]$^+$): 301.12622, found 301.12691.

$[\alpha]_D^{20}$ = +16.39 (c = 1.0, CHCl$_3$).

(*R*)-3-((4-(*tert*-butyl)benzyl)thio)-2-methyl-1-phenylpropan-1-one (**36ad**)
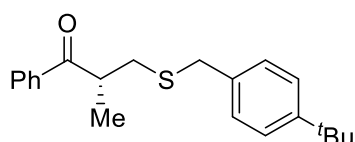
Colorless oil

IR (neat): v = 2963, 2869, 1681, 1596, 1451, 1364, 1230, 971, 701 cm^{-1}.

^{1}H NMR (600 MHz): δ = 1.15 (d, 3H, J = 6.9 Hz), 1.23 (s, 9H), 2.47 (dd, 1H, J = 6.9, 13.1 Hz), 2.88 (dd, 1H, J = 6.2, 13.1 Hz), 3.46 (q, 1H, J = 6.9 Hz), 3.62 (s, 2H), 7.14–7.17 (m, 2H), 7.23–7.24 (m, 2H), 7.35–7.37 (m, 2H), 7.46–7.48 (m, 1H), 7.77–7.78 (m, 2H).

^{13}C NMR (150 MHz): δ = 17.7, 31.3, 34.5, 34.8, 36.9, 41.1, 125.4, 128.3, 128.5, 128.6, 133.1, 135.4, 136.2, 149.9, 202.8.

HPLC (Daicel Chiralcel OD-H, ^{n}hexane/ ^{i}PrOH = 100/1, flow rate = 1.0 mL min^{-1}); t_R = 9.4 min (*S*), t_R = 11.7 min (*R*).

HRMS calcd for C$_{21}$H$_{28}$OS$^+$ ([M + H]$^+$): 327.17826, found 327.17792.

$[\alpha]_D^{20}$ = +19.23 (*c* = 1.0, CHCl$_3$).

(*R*)-3-((furan-2-ylmethyl)thio)-2-methyl-1-phenylpropan-1-one (**36ae**)
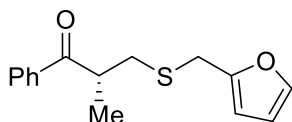
Colorless oil

IR (neat): ν = 2971, 2928, 1680, 1594, 1451, 1230, 972, 790, 701 cm^{-1}.

^{1}H NMR (600 MHz): δ = 1.17 (d, 3H, *J* = 6.9 Hz), 2.51–2.54 (m, 1H), 2.94 (dd, 1H, *J* = 6.9, 13.1 Hz), 3.52 (q, 1H, *J* = 6.9 Hz), 3.64 (dd, 2H, *J* = 9.6, 14.4 Hz), 6.09 (d, 1H, *J* = 3.4Hz), 6.22–6.22 (m, 1H), 7.26 (m, 1H), 7.37–7.40 (m, 2H), 7.47–7.50 (m, 1H), 7.83–7.84 (m, 2H).

^{13}C NMR (150 MHz): δ = 17.7, 29.1, 34.9, 41.1, 107.5, 110.4, 128.3, 128.3, 128.6, 128.6, 133.1, 136.1, 142.1, 151.6, 202.7.

HPLC (Daicel Chiralcel OJ-H, ^{n}hexane/ ^{i}PrOH = 100/1, flow rate = 1.0 mL min^{-1}); t_R = 15.3 min (*R*), t_R = 16.5 min (*S*).

HRMS calcd for C$_{15}$H$_{17}$O$_2$S$^+$ ([M + H]$^+$): 261.09492, found 261.09377.

$[\alpha]_D^{20}$ = +15.76 (*c* = 1.0, CHCl$_3$).

(*R*)-3-(3-(Benzylthio)-2-methylpropanoyl)oxazolidin-2-one (**36ia**)[49]
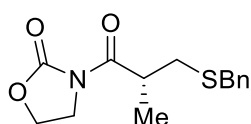
Colorless oil

IR (neat): ν = 2977, 2921, 1777, 1696, 1387, 1266, 1225, 1044, 757, 704 cm^{-1}.

^{1}H NMR (600 MHz, CDCl$_3$): δ = 1.20 (d, 3H, *J* = 6.9 Hz), 2.42-2.45 (m, 1H), 2.80-2.83 (m, 1H), 3.74 (d, 2H, *J* = 3.4 Hz), 3.99-4.13 (m, 3H), 4.41-4.44 (m, 2H), 7.22-7.33 (m, 5H).

^{13}C NMR (150 MHz, CDCl$_3$): δ = 17.4, 34.6, 36.4, 37.6, 42.7, 61.9, 126.9, 128.5, 128.9, 138.1, 153.2, 175.8.

HPLC (Daicel Chiralcel OD-H, ^{n}hexane/ ^{i}PrOH = 9/1, flow rate = 1.0 mL/min); t_R = 32.8 min (*S*), t_R = 44.6 min (*R*).

HRMS calcd for C$_{14}$H$_{18}$NO$_3$S$^+$ ([M+H]$^+$): 280.10074, found 280.09974.

$[\alpha]_D^{20}$ = +58.8 (*c* = 1.09, CHCl$_3$).

(*R*)-Methyl 3-(benzylthio)-2-methylpropanoate (**36ja**)
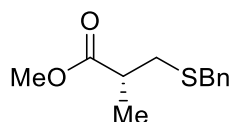
Colorless oil

IR (neat): ν = 2924, 1735, 1455, 1212, 1160, 1096, 701 cm^{-1}.

^{1}H NMR (600 MHz): δ = 1.13 (d, 3H, *J* = 6.9 Hz), 2.40 (dd, 1H, *J* = 6.9, 13.1 Hz), 2.57 (q, 1H, *J* = 6.9 Hz), 2.68 (dd, 1H, *J* = 6.9, 13.1 Hz), 3.61 (s, 3H), 3.64 (s, 2H), 7.16-7.25 (m, 5H).

^{13}C NMR (150 MHz): δ = 16.8, 34.5, 36.6, 39.8, 51.8, 127.0, 128.5, 128.8, 175.5.

HPLC: Daicel Chiralcel OD-H, ^{n}hexane/ ^{i}PrOH = 9/1, flow rate = 0.5 mL/min.: t_S = 12.8 min (*S*), t_R = 13.4 min (*R*).

HRMS calcd for C$_{12}$H$_{17}$O$_2$S$^+$ ([M+H]$^+$): 225.09492, found 225.09485.

3-(Benzylthio)-2-methyl-1-(1-methyl-1*H*-imidazol-2-yl)propan-1-one (**36ka**)
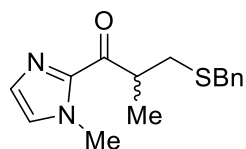
Colorless oil

IR (neat): ν = 2968, 2927, 1672, 1407, 1290, 1155, 972, 773, 702 cm^{-1}.

^{1}H NMR (600 MHz): δ = 1.26 (d, 3H, *J* = 6.9 Hz), 2.51 (dd, 1H, *J* = 6.2, 13.1 Hz), 2.84-2.88 (m, 1H), 3.74 (d, 2H, *J* = 2.1 Hz), 4.00 (s, 3H), 4.20 (dd, 1H, *J* = 6.9, 14.4 Hz), 7.04 (s, 1H), 7.16 (s, 1H), 7.20-7.31 (m, 5H).

^{13}C NMR (150 MHz): δ = 17.3, 34.1, 36.2, 40.9, 126.8, 127.2, 128.3, 128.4, 128.9, 129.1, 138.2, 138.2, 142.5, 195.1.

HPLC (Daicel Chiralpak AS-H, ^{n}hexane/ ^{i}PrOH = 9/1, flow rate = 0.5 mL/min, racemic); t_R = 19.6 min (*S*), t_R = 20.5 min (*R*).

HRMS calcd for C$_{15}$H$_{19}$N$_2$OS$^+$ ([M+H]$^+$): 275.12181, found 275.12209.

(*R*)-2-(2-(Benzylthio)propan-2-yl)-3,4-dihydronaphthalen-1(2*H*)-one (**36pa**)
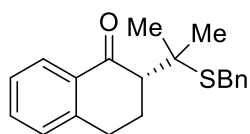
Colorless oil

IR (neat): ν = 2965, 2929, 1684, 1453, 1216, 913, 748, 711 cm^{-1}.

^{1}H NMR (600 MHz): δ = 1.36 (s, 3H), 1.73 (s, 3H), 1.91-1.99 (m, 1H), 2.49 (dd, 1H, *J* = 4.1, 13.1 Hz), 2.62-2.70 (m, 2H), 2.87-2.92 (m, 1H), 3.69 (s, 2H), 7.10-7.15 (m, 2H), 7.20-7.26 (m, 5H), 7.34-7.36 (m, 1H), 7.86 (d, 1H, *J* = 7.6 Hz).

^{13}C NMR (150 MHz): δ = 24.2, 26.5, 29.2, 29.6, 33.3, 49.2, 55.5, 126.4, 126.9, 127.7, 128.4, 128.5, 129.0, 132.9, 134.3, 138.3, 143.5, 198.7.

HPLC (Daicel Chiralcel OJ-H, ^{n}hexane/ ^{i}PrOH = 9/1, flow rate = 1.0 mL/min); t_R = 12.9 min (*S*), t_R = 14.4 min (*R*).

HRMS calcd for $C_{20}H_{23}OS^+$ ([M+H]$^+$): 311.14696, found 311.14716.

$[\alpha]_D^{20} = -5.39$ ($c = 1.0$, CHCl$_3$).

(R)-2-(2-(Benzylthio)propan-2-yl)-6-methoxy-3,4-dihydronaphthalen-1(2H)-one (**36qa**)
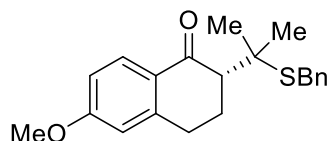
Colorless oil

IR (neat): $\nu = 2964, 1674, 1600, 1249, 1106, 1028, 1094, 711$ cm^{-1}.

^{1}H NMR (600 MHz): $\delta = 1.42$ (s, 3H), 1.81 (s, 3H), 1.98-2.04 (m, 1H), 2.48-2.51 (m, 1H), 2.64-2.73 (m, 2H), 2.91-2.95 (m, 1H), 3.76 (s, 2H), 3.84 (s, 3H), 6.62 (d, 1H, $J = 2.1$ Hz), 6.78-6.80 (m, 1H), 7.20-7.33 (m, 5H), 7.92 (d, 1H, $J = 8.9$ Hz).

^{13}C NMR (150 MHz): $\delta = 24.4, 26.5, 29.5, 29.9, 33.3, 49.4, 55.2, 55.3, 112.1, 113.0, 126.8, 127.8, 128.5, 129.0, 129.6, 138.4, 146.0, 163.2, 197.4$.

HPLC (Daicel Chiralpak AD-H, ^{n}hexane/ ^{i}PrOH = 100/1, flow rate = 1.0 mL/min); $t_R = 29.9$ min (S), $t_R = 35.0$ min (R).

HRMS calcd for $C_{21}H_{25}O_2S^+$ ([M+H]$^+$): 341.13977, found 341.14070.

(R)-2-(2-(Benzylthio)propan-2-yl)-2,3-dihydro-1H-inden-1-one (**36ra**)
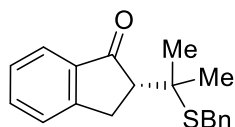
Colorless oil

IR (neat): $\nu = 2965, 2926, 1704, 1606, 1460, 1275, 1096, 752$ cm^{-1}.

^{1}H NMR (600 MHz): $\delta = 1.22$ (s, 3H), 1.67 (s, 3H), 2.71 (q, 1H, $J = 4.1$ Hz), 3.08-3.12 (m, 1H), 3.29 (dd, 1H, $J = 4.1, 17.9$ Hz), 3.69 (q, 2H, $J = 11.7$ Hz), 7.11-7.14 (m, 1H), 7.18-7.21 (m, 4H), 7.25-7.28 (m, 1H), 7.36-7.38 (m, 1H), 7.48-7.51 (m, 1H), 7.62 (d, 1H, $J = 7.6$ Hz).

^{13}C NMR (150 MHz): $\delta = 24.1, 28.8, 31.2, 33.2, 48.9, 55.6, 123.6, 126.2, 126.9, 127.2, 128.4, 128.9, 134.7, 13.6, 137.9, 153.4, 206.0$.

HPLC (Daicel Chiralcel OD-H, ^{n}hexane/ ^{i}PrOH = 9/1, flow rate = 1.0 mL/min); $t_R = 7.2$ min (S), $t_R = 7.7$ min (R).

HRMS calcd for $C_{19}H_{21}OS^+$ ([M+H]$^+$): 297.13131, found 297.13191.

Desulfurization of protonated products and determination of absolute configurations:

Raney Ni W-2 (suspension in EtOH, 2 mL) was added to a solution of protonated product **36pa** (0.1 mmol) in acetate buffer (pH 5.2, 1 mL) and 1:1 mixture of EtOH (2 mL), followed by the addition of NaPH$_2$O$_2$·H$_2$O (1.0 mmol) immediately.[9] The resultant suspension was stirred for 1h at room temperature, and the reaction mixture was filtered. Water was added to the filtrate, and the aqueous layer was then extracted with ether. The combined organic layers were successively washed with satd. NaHCO$_3$ aq. and brine, and then dried over Na$_2$SO$_4$. After filtration, the solvent was removed under reduced pressure. The residue was purified by silica gel column

chromatography (elution: ^{n}hexane/AcOEt = 10/1) to afford the desulfurized product as colorless oil.

(*S*)-2-isopropyl-3,4-dihydronaphthalen-1(2*H*)-one[10]
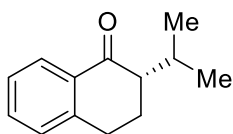
Colorless oil

^{1}H NMR (600 MHz): δ = 0.84 (d, 3H, *J* = 6.9 Hz), 0.94 (d, 3H, *J* = 7.6 Hz), 1.85-1.91 (m, 1H), 2.05-2.10 (m, 1H), 2.23-2.27 (m, 1H), 2.43-2.47 (m, 1H), 2.84-2.97 (m, 2H), 7.14-7.23 (m, 2H), 7.36-7.38 (m, 1H), 7.95 (d, 1H, *J* = 8.2 Hz).

^{13}C NMR (150 MHz): δ =18.4, 20.6, 23.4, 26.1, 28.5, 53.7, 126.5, 127.4, 128.5, 132.9, 133.0, 143.9, 199.8.

HPLC (Daicel Chiralpak AS, ^{n}hexane/ ^{i}PrOH = 100/1, flow rate = 1.0 mL/min); t_R = 8.8 min (*R*), t_R = 9.7 min (*S*).

Deuterium kinetic isotope effect experiments:

The reaction of **35a** with **33a** in D_2O was carried out as described in the typical procedure for Michael reactions. The resulting mixture was diluted with water. The aqueous layer was extracted with dichloromethane (three times), and the combined organic layers were washed with $CuSO_4$ *aq*, and dried over Na_2SO_4. After filtration, the solvent was removed under reduced pressure. The residue was purified by preparative TLC (elution: chloroform/ethyl acetate = 200/1) to afford the protonated adduct **36aa-H** and deuterated adduct **36aa-D** as a mixture. The H/D ratio of the product mixture was determined by ^{1}H NMR analysis. The enantiomeric excess was determined by chiral HPLC analysis.

Typical Experimental Procedure for tandem aza-Michael reaction/enantioselective protonation in water (Table 20, entry 2):

A mixture of $Cu(OSO_2C_9H_{19})_2$ (4.8 mg, 0.01 mmol), **L1** (3.9 mg, 0.012 mmol) and *p*-nitrobenzoic acid (3.3 mg, 0.02 mmol) in water (600 μL) was stirred for 1 h at room temperature. After addition of 2-methyl-1-phenylprop-2-en-1-one **35a** (29.7 mg, 0.2 mmol) and aniline **38a** (22.4 μL, 0.24 mmol) successively, the reaction mixture was vigorously stirred for 24 h at room temperature. The resulting mixture was quenched with $NaHCO_3$ *aq*. and brine. The aqueous layer was extracted with dichloromethane (three times), and dried over Na_2SO_4. After filtration, the solvent was removed under reduced pressure. The residue was purified by preparative TLC (elution: ^{n}hexane/AcOEt = 3/1) to give the corresponding amine **39aa** (34.9 mg, 73% yield). The enantiomeric excess was determined by chiral HPLC analysis.

(*S*)-2-Methyl-1-phenyl-3-(phenylamino)propan-1-one (**39aa**)
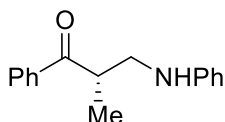
Yellow oil

IR (neat): v = 3406, 2971, 2930, 1676, 1603, 1508, 1210, 974, 750, 694 cm^{-1}.

^{1}H NMR (600 MHz): δ = 1.26 (d, 3H, J = 6.9 Hz), 3.31 (dd, 1H, J = 5.2, 13.4 Hz), 3.59 (dd, 1H, J = 7.6, 13.7 Hz), 3.85 (td, 1H, J = 6.4 13.4 Hz), 4.00 (brs, 1H), 6.59 (d, 2H, J = 8.9 Hz), 6.67-6.70 (m, 1H), 7.15 (t, 2H, J = 7.9 Hz), 7.44 (t, 2H, J = 7.9 Hz), 7.55 (t, 1H, J = 7.6 Hz), 7.92 (d, 2H, J = 8.2 Hz).
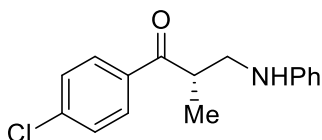
^{13}C NMR (150 MHz): δ = 16.0, 40.2, 46.4, 112.7, 117.3, 128.3, 128.6, 129.2, 133.2, 136.2, 147.7, 203.4.

HPLC (Daicel Chiralcel OJ-3, ^{n}hexane/ ^{i}PrOH = 9/1, flow rate = 0.5 mL min^{-1}); t_R = 56.6 min (*R*), t_R = 59.5 min (*S*).

HRMS calcd for C$_{16}$H$_{18}$ON$^+$ ([M + H]$^+$): 240.13884, found 240.12741.

$[\alpha]_D^{20}$ = +55.91 (*c* = 0.5, EtOH, 58% ee).

(*S*)-1-(4-Chlorophenyl)-2-methyl-3-(phenylamino)propan-1-one (**39sa**)

Yellow oil

IR (neat): v = 3408, 2972, 2931, 1677, 1603, 1589, 1508, 1208, 1092, 975, 749, 693 cm^{-1}.

^{1}H NMR (600 MHz): δ = 1.18 (d, 3H, J = 7.6 Hz), 3.24 (dd, 1H, J = 5.5, 13.7 Hz), 3.52 (dd, 1H, J = 7.9, 13.4 Hz), 3.71-3.75 (m, 1H), 3.87 (brs, 1H), 6.51 (d, 2H, J = 7.6 Hz), 6.63 (t, 1H, J = 7.2 Hz), 7.09 (t, 2H, J = 7.9 Hz), 7.34 (t, 2H, J = 8.2 Hz), 7.77-7.79 (m, 2H).

^{13}C NMR (150 MHz): δ = 15.9, 40.2, 46.4, 112.7, 117.4, 128.9, 129.3, 129.7, 134.5, 139.6, 147.5, 202.3.

HPLC (Daicel Chiralcel OD-H, ^{n}hexane/ ^{i}PrOH = 9/1, flow rate = 1.0 mL min^{-1}); t_R = 12.9 min (*S*), t_R = 20.3 min (*R*).

HRMS calcd for C$_{16}$H$_{17}$ONCl$^+$ ([M + H]$^+$): 274.09987, found 274.09353.

$[\alpha]_D^{20}$ = +62.13 (*c* = 1.0, EtOH, 75% ee).

(*R*)-*N*-(2-Methyl-3-(phenylamino)propanoyl)benzamide (**39ta**)[11]

Major configuration was assigned to be *R* by comparison of literature data.
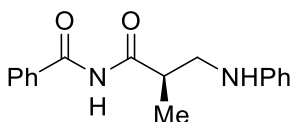
Brown oil

^{1}H NMR (600 MHz): δ = 1,31 (d, 3H, J = 6.9 Hz), 3.31 (dd, 1H, J = 4.8, 13.1 Hz), 3.53 (dd, 1H, J = 8.9, 13.1 Hz), 3.76 (brs, 1H), 6.65 (d, 2H, J = 7.6 Hz), 6.72 (t, 1H, J = 7.2 Hz), 7.16 (t, 2H, J = 7.9 Hz), 7.43 (t, 2H, J = 7.9 Hz), 7.56 (t, 1H, J = 7.6 Hz), 7.76 (d, 2H, J = 7.6 Hz), 8.90 (br, 1H).

^{13}C NMR (150 MHz): δ = 14.9, 40.3, 46.9, 113.1, 117.9, 127.6, 128.8, 129.3, 132.7, 133.1, 147.6, 165.3, 177.4.

HPLC (Daicel Chiralpak AD-H, ^{n}hexane/ ^{i}PrOH = 9/1, flow rate = 1.0 mL min^{-1}); t_R = 22.1 min (*R*), t_R = 45.0 min (*S*).

HRMS calcd for $C_{17}H_{19}N_2O_2^+$ ([M + H]$^+$): 283.14465, found 283.13444.

(*S*)-3-((4-Bromophenyl)amino)-2-methyl-1-phenylpropan-1-one (**39ab**)
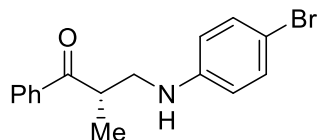
Yellow oil

IR (neat): v = 3397, 2972, 1675, 1594, 1502, 703, 469 cm^{-1}.

^{1}H NMR (600 MHz): δ = 1.27 (d, 3H, J = 6.9 Hz), 3.29 (dd, 1H, J = 4.8, 13.7 Hz), 3.58 (dd, 1H, J = 7.9, 13.4 Hz), 3.81-3.87 (m, 1H), 4.06 (brs, 1H), 6.47 (d, 2H, J = 8.9 Hz), 7.23 (d, 2H, J = 8.2 Hz), 7.47 (t, 2H, J = 7.6 Hz), 7.58 (t, 1H, J = 7.6 Hz), 7.92 (t, 2H, J = 7.6 Hz).

^{13}C NMR (150 MHz): δ = 16.0, 40.0, 46.3, 108.8, 114.3, 128.3, 128.7, 131.9, 133.3, 136.1, 146.7, 203.3.

HPLC (Daicel Chiralcel OD-H, ^{n}hexane/ ^{i}PrOH = 9/1, flow rate = 0.5 mL min^{-1}); t_R = 23.7 min (*S*), t_R = 25.3 min (*R*).

HRMS calcd for $C_{16}H_{17}ONBr^+$ ([M + H]$^+$): 318.04935, found 318.04626.

$[\alpha]_D^{20}$ = +44.76 (*c* = 1.0, EtOH, 55% ee).

3-((4-Methoxyphenyl)amino)-2-methyl-1-phenylpropan-1-one (**39ac**)
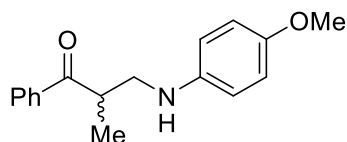
Yellow oil

IR (neat): v = 3385, 2931, 1677, 1595, 1513, 1449, 1233, 703 cm^{-1}.

^{1}H NMR (600 MHz): δ = 1.24 (d, 3H, J = 6.9 Hz), 3.23 (dd, 1H, J = 5.2, 13.4 Hz), 3.53 (q, 1H, J = 6.9 Hz), 3.72 (s, 3H), 3.80-3.84 (m, 1H), 6.55 (d, 2H, J = 8.9 Hz), 6.74 (d, 2H, J = 8.9 Hz), 7.43 (t, 2H, J = 7.6 Hz), 7.54 (t, 1H, J = 7.6 Hz), 7.89-7.90 (m, 1H).

^{13}C NMR (150 MHz): δ =16.0, 40.2, 47.7, 55.7, 114.4, 114.9, 128.3, 128.6, 133.1, 136.3, 141.8, 152.2, 203.5.

HPLC (Daicel Chiralcel OD-H, ^{n}hexane/ ^{i}PrOH = 9/1, flow rate = 0.5 mL min^{-1}); t_R = 26.4 min, t_R = 29.2 min.

HRMS calcd for $C_{17}H_{20}O_2N^+$ ([M + H]$^+$): 270.14940, found 270.14417.

(*S*)-3-((2-Methoxyphenyl)amino)-2-methyl-1-phenylpropan-1-one (**39ad**)
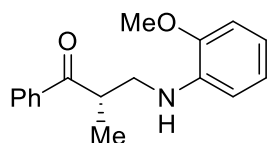
Colorless oil

IR (neat): v = 3417, 2968, 2935, 1679, 1601, 1516, 1457, 1248, 1222, 1029, 974, 738, 705 cm^{-1}.

^{1}H NMR (600 MHz): δ = 1.21 (d, 3H, J = 6.9 Hz), 3.23 (q, 1H, J = 6.4 Hz), 3.57 (q, 1H, J = 6.9 Hz), 3.69 (s, 3H), 3.77-3.83 (m, 1H), 4.42 (brs, 1H), 6.59 (t, 2H, J = 7.6 Hz), 6.66 (d, 1H, J = 6.9 Hz), 6.80 (t, 1H, J = 7.6 Hz), 7.38 (t, 2H, J = 7.9 Hz), 7.49 (t, 1H, J = 7.6 Hz), 7.86 (d, 2H, J = 6.9 Hz).
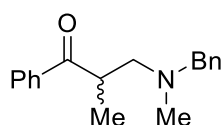
^{13}C NMR (150 MHz): δ = 15.9, 40.2, 46.3, 55.3, 109.5, 109.6, 116.4, 121.1, 128.3, 128.6, 133.0, 136.3, 137.7, 146.8, 203.3.

HPLC (Daicel Chiralcel OD-H, ^{n}hexane/ ^{i}PrOH = 9/1, flow rate = 1.0 mL min^{-1}); t_R = 15.8 min (*R*), t_R = 14.5 min (*S*).

HRMS calcd for $C_{17}H_{20}O_2N^+$ ([M + H]$^+$): 270.14940, found 270.14100.

$[\alpha]_D^{20}$ = +50.78 (*c* = 1.0, EtOH, 64%ee).

3-(Benzyl(methyl)amino)-2-methyl-1-phenylpropan-1-one (**39af**)

Yellow oil

IR (neat): v = 2973, 2936, 2840, 2792, 1682, 1451, 1227, 973, 740, 702 cm^{-1}.

^{1}H NMR (600 MHz): δ = 1.23 (d, 3H, J = 6.9 Hz), 2.21 (s, 3H), 2.52 (q, 1H, J = 6.2 Hz), 2,91 (q, 1H, J = 6,4 Hz), 3.53 (dd, 2H, J = 13.1, 19.2 Hz), 3.77 (q, 1H, J = 6.9 Hz9, 7.24 (t, 3H, J = 6.5 Hz), 7.27-7.30 (m, 2H), 7.49 (t, 2H, J = 7.9 Hz), 7.59 (t, 1H, J = 6.2 Hz), 7.57-7.60 (m, 1H), 7.98 (d, 2H, J = 7.6 Hz).

^{13}C NMR (150 MHz): δ = 16.2, 39.3, 42.7, 61.1, 62.7, 1268, 128.1, 128.2, 128.2, 128.8, 132.8, 136.9, 139.1, 203.8.

HPLC (Daicel Chiralpak AS-H, ^{n}hexane/ ^{i}PrOH = 40/1, flow rate = 0.5 mL min^{-1}); t_R = 10.8 min, t_R = 11.3 min.

HRMS calcd for $C_{18}H_{22}ON^+$ ([M + H]$^+$): 268.17014, found 268.16274.

### 3-(Dimethylamino)-2-methyl-1-phenylpropan-1-one (**39ag**)[12]
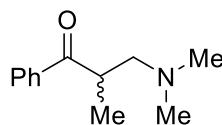
Colorless oil

^{1}H NMR (600 MHz): δ = 1.18 (d, 3H, J = 6.9 Hz), 2.21 (s, 6H), 2.32 (q, 1H, J = 6.2 Hz), 2.76 (dd, 1H, J = 7.6, 12.4 Hz), 3.67 (td, 1H, J = 6.9, 13.7 Hz), 7.44 (t, 2H, J = 7.9 Hz), 7.53 (t, 1H, J = 7.6 Hz), 7.96 (d, 2H, J = 6.9 Hz).

^{13}C NMR (150 MHz): δ = 16.5, 39.1, 45.9, 62.8, 128.2, 128.6, 132.8, 136.6, 203.4.

HPLC (Daicel Chiralcel OJ-H, ^{n}hexane/ ^{i}PrOH = 9/1, flow rate = 1.0 mL min^{-1}); t_R = 5.31 min, t_R = 7.22 min.

HRMS calcd for $C_{12}H_{18}ON^+$ ([M + H]$^+$): 192.13884, found 192.13206.

S-tert-Butyl 2-methyl-3-(phenylamino)propanethioate (**39ua**)
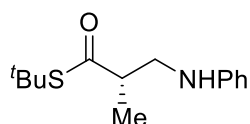
Yellow oil

^{1}H NMR (600 MHz): δ = 1.14 (d, 3H, J = 6.9 Hz), 1.39 (s, 9H), 2.83 (td, 1H, J = 6.6, 13.6 Hz), 3.10 (q, 1H, J = 6.4 Hz), 3.36 (dd, 1H, J = 7.6, 13.0 Hz), 3.85 (brs, 1H), 6.53 (d, 2H, J = 7.6 Hz), 6.63 (t, 1H, J = 7.6 Hz), 7.08-7.11 (m, 2H).

^{13}C NMR (150 MHz): δ = 15.6, 29.8, 47.1, 48.1, 48.2, 112.9, 117.5, 129.2, 147.6, 203.3.

HPLC (Daicel Chiralpak AD-H, ^{n}hexane/ ^{i}PrOH = 9/1, flow rate = 1.0 mL min^{-1}); t_R = 4.86 min (*minor*), t_R = 6.39 min (*major*).

HRMS calcd for $C_{14}H_{22}ONS^+$ ([M + H]$^+$): 252.14221, found 252.14166.

Determination of the absolute configuration of **39af**;

The absolute configuration of **39af** was determined to be *S* by comparison of the optical rotation of their derivatives with those of the corresponding compounds synthesized from a literature-known compound.

C–N bond cleavage of protonated products and determination of absolute configurations:

To a solution of **39af** was added 4 equivalent of ceric ammonium nitrate (CAN) in a 3:1 mixture of MeCN/H$_2$O at ambient temperature. After stirring for 30 min, 1M aqueous solution of NaOH was added and the resultant mixture was extracted four times with DCM. The combined organic layer was washed with brine, filtered and concentrated under reduced pressure. After di-*tert*-butyl carbonate (2 equiv.) was added, the resulting mixture was dissolved in a toluene/water biphasic system (2:1 mixture) and NaOH (1.5 equiv.) was then added. After stirred for 3 h at room temperature, the reaction mixture was diluted with water and extracted twice with AcOEt. The combined organic layer was washed with brine, dried over anhydrous Na$_2$SO$_4$, filtered and concentrated under reduced pressure. The residue was purified by flash chromatography to afford the desired product as a colorless oil.

(*S*)-*tert*-Butyl (2-methyl-3-oxo-3-phenylpropyl)carbamate[13]
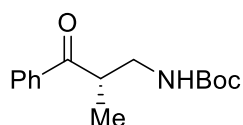
Colorless oil

^{1}H NMR (600 MHz): δ =1.13 (d, 3H, J = 6.9 Hz), 1.33 (s, 9H), 3.33 (t, 2H, J = 6.2 Hz), 3.71 (q, 1H, J = 6.6 Hz), 4.91 (brs, 1H), 7.41 (t, 2H, J = 7.9 Hz), 7.51 (t, 1H, J = 7.2 Hz), 7.90 (d, 2H, J = 7.6 Hz).

^{13}C NMR (150 MHz): δ = 15.6, 28.3, 41.2, 42.8, 79.2, 128.4, 128.7, 133.2, 136.0, 156.0, 203.6.

HRMS calcd for $C_{15}H_{22}NO_3^+$ ([M + H]$^+$): 264.15997, found 183.18598.

$[\alpha]_D^{25}$ = +45.8 (*c* = 0.56, CHCl$_3$). [lit.: $[\alpha]_D^{25}$ = −45.4 (*c* = 0.56, CHCl$_3$).]

Typical Experimental Procedure for tandem aza-Michael addition/protonation:

An aqueous solution of $Cu(OSO_2C_9H_{19})_2$ (5.1 mg, 0.01 mmol) and chiral 2,2'-bipyridine ligand **L1** (4.0 mg, 0.012 mmol) was stirred for 1 h at room tepmarature.   After addition of **35g** (29.2 mg, 0.2 mmol) and aniline **38a** (22.4 mg, 0.24 mmol) successively, the reaction mixture was vigorously stirred for 24 h at room temperature.   The resulting mixture was quenched with saturated $NaHCO_3$ *aq*. and pure water.   The aqueous layer was extracted with dichloromethane (three times), and the combined organic layers were washed with brine, and dried over anhydrous Na_2SO_4.   After filtration, the solvent was removed under reduced pressure.   The residue was purified by preparative TLC (elution: ^{n}hexane/ AcOEt = 4/1) to give the corresponding product **39ga** (40.0 mg, 83% yield).

1-phenyl-3-(phenylamino)butan-1-one (**39ga**)[14]
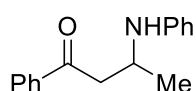
Orange oil

^{1}H NMR (500 MHz): δ = 1.32 (d, 3H, J = 6.2 Hz), 3.06 (q, 1H, J = 8.1 Hz), 3.30 (dd, 1H, J = 4.5, 16.4 Hz), 3.80 (brs, 1H), 4.13-4.18 (m, 1H), 6.63 (d, 2H, J = 7.9 Hz), 6.69 (t, 1H, J = 7.4 Hz), 7.16 (t, 2H, J = 7.9 Hz), 7.45 (t, 2H, J = 7.9 Hz), 7.55 (t, 1H, J = 7.4 Hz), 7.93 (d, 2H, J = 7.4 Hz).

^{13}C NMR (150 MHz): δ = 21.0, 44.4, 45.6, 113.5, 117.5, 128.0, 128.5, 129.3, 133.1, 137.1, 146.8, 199.2.

HPLC (Daicel Chiralpak AS-H, ^{n}hexane/ ^{i}PrOH = 9/1, flow rate = 0.5 mL min^{-1}); t_R = 20.8 min, t_R = 22.1 min.

HRMS calcd for $C_{16}H_{18}ON^+$ ([M + H]$^+$): 240.13884, found 240.13793.

1   W. Z. Xu, Z. T. Huang, Q.Y. Zheng, *J. Org. Chem.* **2008**, *73*, 5606-5608.
2   T. Ishimaru, N. Shibata, T. Horikawa, N. Yasuda, S. Nakamura, T. Toru, M. Shiro, *Angew. Chem. Int. Ed.* **2008**, *47*, 4157-4161.
3   R. Qiu, Y. Qiu, S. Yin, X. Xu, S. Luo, C. T. Au, W. Y. Wong, S. Shimada, *Adv. Synth. Catal.* **2010**, *352*, 153-162.
4   J. A. R. Rodrigues, E. P. Siqueira-Filho, M. de Mancilha, P. J. S. Moran, *Synth. Commun.* **2003**, *33*, 331-340.
5   M. M. Curzu, G. A. Pinna, *Synthesis*, **1984**, 339-342.
6   T. Poisson, Y. Yamashita, S. Kobayashi, *J. Am. Chem. Soc.* **2010**, *32*, 7890-7892.
7   M. P. Sibi, B. Gustafson, J. Coulomb, *Bull. Korean. Chem. Soc.* **2010**, *31*, 541-542.
8   K. Okamoto, T. Hayashi, *Org. Lett.* **2007**, *9*, 5067-5069.
9   a) M. Node, K. Nishide, Y. Shigeta, K. Obata, H. Shiraki, H. Kunishige, *Tetrahedron* **1997**, *53*, 12883-12894; b) K. Nishide, Y. Shigeta, K. Obata, M. Node, *Tetrahedron Lett.* **1996**, *37*, 2271-2274.
10   H. Fujiwara, K. Tomioka, *J. Chem. Soc., Perkin Trans. 1* **1999**, 2377-2381.
11   P. H. Phua, S. P. Mathew, A. J. P. White, J. G. Vries, D. G. Blackmond, K. K. M. Hii, *Chem. Eur. J.* **2007**, *13*, 4602-4613.
12   A. S. Angeloni, G. Gottarelli, M. Tramontini, *Tetrahedron* **1969**, *25*, 4147-4151.
13   R. M. Figueiredo, R. Frohlich, M. Christmann, *J. Org. Chem.* **2006**, *71*, 4147-4154.
14   Q. Kang, Y. Zhang, *Org. Biomol. Chem.* **2011**, *9*, 6715-6720.

Chapter 5 : Catalytic Construction of Hydrogen Isotope Chirality in Deuterium Oxide

<Reagents>

Unless stated otherwise, commercially available reagents were used as received with the exception of the following substrates, which were prepared through reported methods. Analytical data for these compounds are in full agreement with reported data.
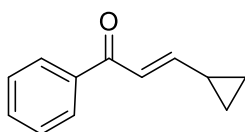
(*E*)-3-Cyclohexyl-1-phenylprop-2-en-1-one (**41d**)[1]
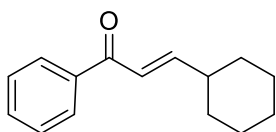
^{1}H NMR (600 MHz): δ = 1.12-1.32 (m, 5H), 1.61-1.66 (m, 1H), 1.69-1.83 (m, 4H), 2.15-2.22 (m, 1H), 6.76 (d, 1H, *J* = 15.5 Hz), 6.93 (dd, 1H, *J* = 6.5, 15.5 Hz), 7.39 (t, 2H, *J* = 7.6 Hz), 7.47 (t, 1H, *J* = 7.6 Hz), 7.85 (d, 2H, *J* = 7.6 Hz).
^{13}C NMR (150 MHz): δ = 25.8, 26.0, 31.9, 41.0, 123.5, 128.5, 132.5, 154.9, 191.4.

(*E*)-3-Cyclopropyl-1-phenylprop-2-en-1-one (**41e**)[1]

^{1}H NMR (600 MHz): δ = 0.26-0.30 (m, 2H), 0.52-0.56 (m, 2H), 1.21-1.29 (m, 1H), 6.60 (dd, 1H, *J* = 10.2, 14.7 Hz), 6.86 (d, 1H, *J* = 14.7 Hz), 7.08-7.18 (m, 3H), 7.93 (d, 2H, *J* = 8.5 Hz).
^{13}C NMR (150 MHz): δ = 8.9, 15.2, 123.1, 127.9, 128.3, 128.6, 132.2, 154.2, 188.6.

(*E*)-3-(but-2-enoyl)oxazolidin-2-one (**41k**)[2]
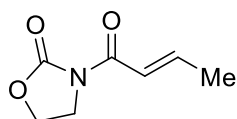
^{1}H NMR (500 MHz): δ = 1.96 (dd, 3H, *J* = 1.2, 6.9 Hz), 4.07 (t, 2H, *J* = 7.5 Hz), 4.43 (t, 2H, *J* = 7.5 Hz), 7.14-7.29 (m, 2H).
^{13}C NMR (125 MHz): δ = 18.4, 42.6, 62.0, 121.4, 146.7, 153.4, 165.1.

Typical Experimental Procedure for tandem thia-Michael addition/deuteration:
A solution of Sc(OTf)$_3$ (0.003 mmol), chiral 2,2'-bipyridine ligand **L1** (0.0036 mmol) and pyridine (0.009 mmol) in D$_2$O was stirred for 1 h at room tepmarature. After addition of **41a** (52.3 mg, 0.3 mmol) and thiol **33a** (44.7 mg, 0.36 mmol) successively, the reaction mixture was vigorously stirred for 24 h at room temperature. The resulting mixture was quenched with saturated CuSO$_4$ *aq.* and pure water. The aqueous layer was extracted with dichloromethane (three times), and the

combined organic layers were washed with brine, and dried over anhydrous Na$_2$SO$_4$. After filtration, the solvent was removed under reduced pressure. The residue was purified by preparative TLC (elution: chloroform/ethyl acetate = 200/1) to give the corresponding product (85.6 mg, 95% yield).

(2*R*,3*R*)-2-Deuterio-3-(benzylthio)-4-methyl-1-phenylpentan-1-one (**42aa** + **43aa**)
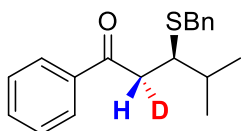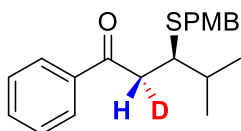

Coloerless oil
^{1}H NMR (600 MHz, in C$_6$D$_6$): δ = 0.84 (d, 3H, *J* = 6.8 Hz), 0.86 (d, 3H, *J* = 6.8 Hz), 1.81 (qd, 1H, *J* = 4.1, 6.8 Hz), 2.99-3.00 (m, 1H), 3.66 & 3.67 (s, 2H), 7.08-7.12 (m, 1H), 7.13-7.23 (m, 4H), 7.36 (t, 2H, *J* = 7.6 Hz), 7.46 (t, 1H, *J* = 7.6 Hz), 7.82 (d, 2H, *J* = 8.1 Hz).
^{13}C NMR (150 MHz, in C$_6$D$_6$): δ = 18.7, 20.0, 32.8, 37.6, 42.8 (t, *J* = 19.5 Hz), 47.8, 127.0, 128.4, 128.5, 128.6, 129.5, 132.8, 137.8, 139.3, 197.9.
^{2}H NMR (600 MHz, in C$_6$H$_6$): δ = 3.22 (br).
HPLC (Daicel Chiralcel OD-H, ^{n}hexane/ ^{i}PrOH = 9/1, flow rate = 0.5 mL min^{-1}); t_R = 10.8 min (minor), t_R = 11.4 min (major).

(2*R*,3*R*)-2-Deuterio-3-((4-methoxybenzyl)thio)-4-methyl-1-phenylpentan-1-one (**42ac** + **42ac**)
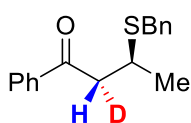

Colorless oil
^{1}H NMR (600 MHz, in C$_6$D$_6$): δ = 0.87 (d, 3H, *J* = 6.8 Hz), 0.92 (d, 3H, *J* = 6.8 Hz), 1.77-1.83 (m, 1H), 2.80 (t, 1H *J* = 2.7 Hz), 3.26 (s, 3H), 3.36-3.40 (m, 1H), 3.61 (d, 1H, *J* = 13.1 Hz), 3.69 (d, 1H, *J* = 13.1 Hz), 6.68-6.71 (m, 2H), 7.04-7.04 (m, 2H), 7.11-7.15 (m, 1H), 7.19 (d, 2H, *J* = 8.7 Hz), 7.81-7.84 (m, 2H).
^{13}C NMR (150 MHz, in C$_6$D$_6$): δ = 18.7, 20.1, 32.8, 37.0, 42.8 (t, *J* = 19.5 Hz), 47.7, 53.3, 54.7, 114.1, 128.3, 128.4, 128.6, 130.5, 131.1, 132.8, 137.9, 159.1, 198.0.
^{2}H NMR (600 MHz, in C$_6$H$_6$): δ = 3.15 (br, major).
HPLC (Daicel Chiralcel OD-H, ^{n}hexane/ ^{i}PrOH = 9/1, flow rate = 0.75 mL min^{-1}, 221 nm); t_R = 7.7 min (major), t_R = 8.2 min (minor).

(2*R*,3*S*)-2-Deuterio-3-(benzylthio)-1-phenylbutan-1-one (**42ba** + **43ba**)
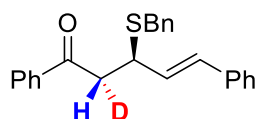

Colorless oil

^{1}H NMR (600 MHz, in C$_6$D$_6$): δ = 1.22 (d, 3H, J = 6.8 Hz), 2.68 (dt, 0.89H, J = 2.2, 8.7 Hz), 2.96-2.98 (m, 0.11H), 3.38-3.44 (m, 1H), 3.52 (d, 1H, J = 13.4 Hz), 3.58 (d, 1H, J = 13.4 Hz), 7.02 (t, 3H, J = 7.6 Hz), 7.10 (dd, 3H, J = 7.4, 14.6 Hz), 7.23 (d, 1H, J = 7.5 Hz), 7.71 (d, 2H, J = 7.3 Hz).

^{13}C NMR (150 MHz, in C$_6$D$_6$): δ = 21.5, 35.4, 35.6, 45.4-46.2 (m), 127.0, 128.1, 128.5, 128.6, 128.8, 133.1, 136.9, 138.3, 198.1.

^{2}H NMR (600 MHz, in C$_6$H$_6$): δ = 2.68 (br, minor), 2.96 (br, major).

HPLC (Daicel Chiralcel OJ-H, ^{n}hexane/ ^{i}PrOH = 9/1, flow rate = 0.5 mL min^{-1}); t_R = 7.1 min (major), t_R = 7.8 min (minor).

(2*R*,3*R*)-2-Deuterio-3-(benzylthio)-1,5-diphenylpent-4-en-1-one (**42ca** + **43ca**)
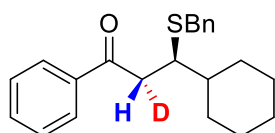

Coloreless oil

^{1}H NMR (600 MHz, in C$_6$D$_6$): δ = 2.94 (d, 0.87H, J = 7.9 Hz), 3.00-3.04 (m, 0.13H), 3.58 (d, 2H, J = 1.7 Hz), 4.13 (t, 1H, J = 8.5 Hz), 6.09 (dd, 1H, J = 9.1, 15.9 Hz), 6.39 (d, 1H, J = 15.9 Hz), 6.96-7.32 (m, 13H), 7.69 (dd, 2H, J = 1.1, 7.5 Hz).

^{13}C NMR (150 MHz, in C$_6$D$_6$): δ = 35.6, 42.8 (t, J = 20.9 Hz), 43.1, 126.6, 127.0, 127.6, 128.2, 128.4, 128.5, 128.6, 129.2, 130.0, 131.4, 132.7, 137.2, 138.5, 195.7.

HPLC (Daicel Chiralcel OD-H, ^{n}hexane/ ^{i}PrOH = 9/1, flow rate = 1.0 mL min^{-1}); t_R = 9.7 min (minor), t_R = 12.4 min (major).

(2*R*,3*R*)-2-Deuterio-3-(benzylthio)-3-cyclohexyl-1-phenylpropan-1-one (**42da** + **43da**)
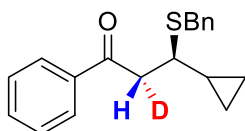

Coloerless oil

^{1}H NMR (600 MHz, in C$_6$D$_6$): δ = 1.10-1.16 (m, 4H), 1.24 (dq, 1H, J = 3.4, 12.0 Hz), 1.42-1.47 (m, 1H), 1.51-1.75 (m, 6H), 2.86-2.89 (m, 1H), 3.37 (t, 1H, J = 4.8 Hz), 3.64 (d, 1H, J = 13.1 Hz), 3.71 (d, 1H, J = 13.1 Hz), 7.01 (t, 1H, J = 7.6 Hz), 7.06-7.18 (m, 5H), 7.28 (d, 2H, J = 7.6 Hz), 7.85 (d, 2H, J = 8.3 Hz).

^{13}C NMR (150 MHz, in C$_6$D$_6$): δ = 5.51, 5.53, 17.6, 36.3, 42.8 (t, J = 20.2 Hz), 45.8, 127.0, 128.4, 128.6, 129.3, 132.8, 137.8, 139.3, 197.4.

^{2}H NMR (600 MHz, in C$_6$H$_6$): δ = 3.14 (br).

HPLC (Daicel Chiralcel OJ-H, ^{n}hexane/ ^{i}PrOH = 7/3, flow rate = 1.0 mL min^{-1}); t_R = 10.8 min (minor), t_R = 11.4 min (major).

(2*R*,3*R*)-2-Deuterio-3-(benzylthio)-3-cyclopropyl-1-phenylpropan-1-one (**42ea** + **43ea**)
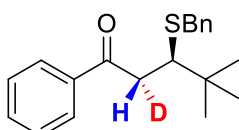
Coloerless oil

^{1}H NMR (600 MHz, in C$_6$D$_6$): δ = 0.06-0.15 (m, 2H), 0.19-0.24 (m, 1H), 0.32-0.37 (m, 1H), 0.79-0.86 (m, 1H), 2.82 (dd, 1H, J = 6.5, 9.3 Hz), 2.94-2.97 (m, 1H), 3.63 (d, 1H, J = 13.1 Hz), 3.72 (d, 1H, J = 13.1 Hz), 6.99-7.05 (m, 3H), 7.07-7.13 (m, 3H), 7.29 (d, 2H, J = 7.6 Hz), 7.78 (d, 2H, J = 7.6 Hz).

^{13}C NMR (150 MHz, in C$_6$D$_6$): δ = 18.7, 20.0, 32.8, 37.6, 42.8 (t, J = 19.5 Hz), 47.8, 127.0, 128.4, 128.5, 128.6, 129.5, 132.8, 137.8, 139.3, 197.9.

^{2}H NMR (600 MHz, in C$_6$H$_6$): δ = 3.15 (br).

HPLC (Daicel Chiralcel OJ-H, ^{n}hexane/ ^{i}PrOH = 9/1, flow rate = 1.0 mL min^{-1}); t_R = 11.6 min (minor), t_R = 12.9 min (major).

(2*R*,3*R*)-2-Deuterio-3-(benzylthio)-4,4-dimethyl-1-phenylpentan-1-one (**42fa** + **43fa**)
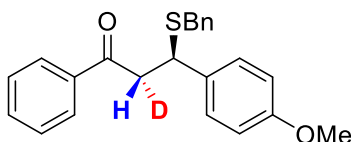

Coloerless oil

^{1}H NMR (600 MHz, in C$_6$D$_6$): δ = 0.62 (s, 9H), 2.64-2.67 (m, 1H), 3.08 (d, 1H, J = 3.5 Hz), 3.46 (d, 1H, J = 12.6 Hz), 3.50 (d, 1H, J = 12.6 Hz), 6.71 (t, 1H, J = 7.3 Hz), 6.80 (dt, 4H, J = 1.6, 7.8 Hz), 6.87 (t, 1H, J = 7.5 Hz), 7.01 (d, 2H, J = 7.3 Hz), 7.61 (d, 2H, J = 7.5 Hz).

^{13}C NMR (150 MHz, in C$_6$D$_6$): δ = 27.6, 35.2, 39.3, 42.0 (t, J = 19.5 Hz), 52.5, 127.0, 128.5, 128.7, 129.6, 132.8, 138.1, 139.2, 198.3.

^{2}H NMR (600 MHz, in C$_6$H$_6$): δ = 3.24 (br).

HPLC (Daicel Chiralcel OD-H, ^{n}hexane/ ^{i}PrOH = 9/1, flow rate = 1.0 mL min^{-1}); t_R = 4.3 min (minor), t_R = 4.8 min (major).

(2*R*,3*R*)-2-Deuterio-3-(benzylthio)-3-(4'-methoxyphenyl)-1-phenylpropan-1-one (**42ga** + **43ga**)

Coloreless oil

^{1}H NMR (600 MHz, in C$_6$D$_6$): δ = 3.21-3.23 (m, 0.14H), 3.25-3.28 (m, 3.86H), 3.43 (d, 1H, J = 13.6 Hz), 3.47 (d, 1H, J = 13.6 Hz), 6.72-6.75 (m, 2H), 6.95 (t, 2H, J = 7.6 Hz), 7.01-7.06 (m, 2H), 7.11 (t, 1H, J = 7.6 Hz), 7.22 (d, 2H, J = 7.6 Hz), 7.30-7.32 (m, 2H), 7.64-7.67 (m, 2H).

^{13}C NMR (150 MHz, in C$_6$D$_6$): δ = 36.1, 44.1, 45.3 (t, J = 19.3 Hz), 54.7, 114.1, 127.1, 128.3, 128.5, 128.6, 129.3, 129.6, 132.7, 138.6, 159.2, 196.0.

HPLC (Daicel Chiralcel OJ-H, ^{n}hexane/ ^{i}PrOH = 7/3, flow rate = 1.0 mL min^{-1}); t_R = 23.6 min (minor), t_R = 38.3 min (major).

(2*R*,3*R*)-2-Deuterio-3-(benzylthio)-3-(4'-chlorophenyl)-1-phenylpropan-1-one (**42ha** + **43ha**)
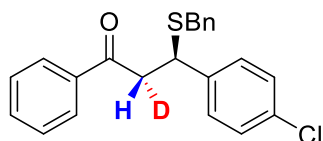
Coloreless oil

^{1}H NMR (600 MHz, in C$_6$D$_6$): δ = 3.05 (d, 0.88H, J = 8.3 Hz), 3.10-3.12 (m, 0.12H), 3.29 (d, 1H J = 13.7 Hz), 3.35 (d, 1H, J = 13.3 Hz), 6.95 (t, 2H, J = 7.6 Hz), 7.00-7.10 (m, 7H), 7.11-7.17 (m, 3H), 7.61 (d, 2H, J = 7.6 Hz).

^{13}C NMR (150 MHz, in C$_6$D$_6$): δ = 36.1, 43.7, 44.9 (t, J = 19.5 Hz), 127.2, 127.9, 128.1, 128.2, 128.3, 128.6, 128.7, 128.8, 129.2, 129.9, 133.0, 138.1, 141.1, 195.5.

^{2}H NMR (600 MHz, in C$_6$H$_6$): δ = 3.15 (br, major).

HPLC (Daicel Chiralcel OJ-H, ^{n}hexane/ ^{i}PrOH = 7/3, flow rate = 1.0 mL min^{-1}); t_R = 17.2 min (minor), t_R = 28.9 min (major).

(2*R*,3*R*)-2-Deuterio-3-(benzylthio)-1-(4'-methoxyphenyl)-3-phenylpropan-1-one (**42ia** + **43ia**)
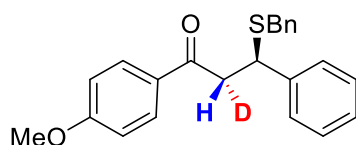
Coloreless oil

^{1}H NMR (600 MHz, in C$_6$D$_6$): δ = 3.12 (s, 3H), 3.23 (d, 0.93H, J = 8.3 Hz), 3.26-3.28 (m, 0.07H), 3.41 (d, 1H J = 13.1 Hz), 3.44 (d, 1H, J = 13.1 Hz), 4.68 (d, 1H, J = 7.6 Hz), 6.53 (d, 1H, J = 8.2 Hz), 7.02 (t, 2H, J = 7.6 Hz), 7.07-7.20 (m, 8H), 7.41 (d, 2H, J = 8.3 Hz), 7.68 (d, 1H, J = 7.6 Hz).

^{13}C NMR (150 MHz, in C$_6$D$_6$): δ = 36.2, 44.9, 53.3, 54.8, 100.3, 113.8, 127.1, 127.3, 127.9, 128.3, 128.5, 128.6, 128.7, 129.3, 130.5, 130.6, 138.5, 142.8, 163.6.

HPLC (Daicel Chiralcel OJ-H, ^{n}hexane/ ^{i}PrOH = 7/3, flow rate = 1.0 mL min^{-1}); t_R = 27.8 min (minor), t_R = 35.9 min (major).

(2*R*,3*R*)-2-Deuterio-3-(benzylthio)-3-(naphthalen-2-yl)-1-phenylpropan-1-one (**42ja** + **43ja**)
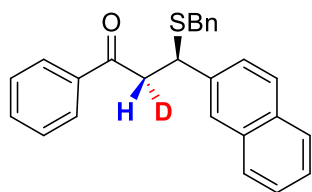
Coloreless oil

^{1}H NMR (600 MHz, in C$_6$D$_6$): δ = 3.28 (d, 0.88H, J = 7.6 Hz), 3.30-3.34 (m, 0.12H), 3.39 (d, 1H J = 13.7 Hz), 3.41 (d, 1H, J = 13.7 Hz), 4.80 (d, 1H, J = 7.6 Hz), 6.94 (t, 1H, J = 7.6 Hz), 7.00-7.10 (m, 5H), 7.21-7.27 (m, 2H), 7.57-7.67 (m, 7H), 7.74 (m, 1H).

^{13}C NMR (150 MHz, in C$_6$D$_6$): δ = 21.8, 34.9, 35.9, 62.6, 114.2, 130.3, 130.9, 159.1, 171.2.

HPLC (Daicel Chiralcel OJ-H, ^{n}hexane/ ^{i}PrOH = 7/3, flow rate = 1.5 mL min^{-1}); t_R = 16.2 min (minor), t_R = 29.7 min (major).

3-((2*R*,3*S*)-3-(benzylthio)butanoyl-2-*d*)oxazolidin-2-one (**42ka** + **43ka**)
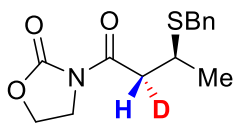
Coloerless oil

^{1}H NMR (600 MHz, in C_6D_6): δ = 6.97 (d, 3H, *J* = 6.7 Hz), 2.60-2.64 (m, 2H), 2.68-2.74 (m, 2H), 3.03 (pent, 1H, *J* = 6.9 Hz), 3.32 (d, 1H, *J* = 13.3 Hz), 3.40 (d, 1H, *J* = 13.3 Hz), 6.73 (t, 1H, *J* = 7.6 Hz), 6.83 (d, 2H, *J* = 7.7 Hz), 7.01 (d, 2H, *J* = 7.7 Hz).

^{13}C NMR (150 MHz, in C_6D_6): δ = 27.6, 35.2, 39.3, 42.0 (t, *J* = 19.5 Hz), 52.5, 127.0, 128.5, 128.7, 129.6, 132.8, 138.1, 139.2, 198.3.

^{2}H NMR (600 MHz, in CH_2Cl_2): δ = 3.06 (br, minor), 3.27 (br, major)

HPLC (Daicel Chiralcel OD-H, ^{n}hexane/ ^{i}PrOH = 7/3, flow rate = 1.0 mL min^{-1}); t_R = 15.1 min (minor), t_R = 17.8 min (major).

Typical Experimental Procedure for tandem Friedel-Crafts-type 1,4-addition/protonation:

To an aqueous solution of Sc(DS)$_3$ (6.4 mg, 0.0075 mmol) was added **L1** (3.0 mg, 0.009 mmol) and stirred for 1 h at room tepmarature. After addition of chalcone (31.3 mg, 0.15 mmol) and indole **40a** (21.2 mg, 0.18 mmol) successively, the reaction mixture was vigorously stirred for 24 h at room temperature. The resulting mixture was quenched with saturated NaHCO$_3$ *aq.* and brine. The aqueous layer was extracted with dichloromethane (three times), and the combined organic layers were washed with brine, and dried over Na$_2$SO$_4$. After filtration, the solvent was removed under reduced pressure. The residue was purified by preparative TLC (elution: chloroform/ethyl acetate = 200/1) to give the corresponding product (33.2 mg, 68% yield).

(*S*)-1-(1*H*-Indol-3-yl)-1,3-diphenylpropan-1-one (**45ha**)
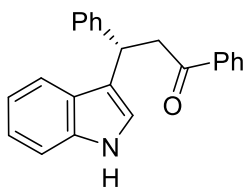
^{1}H NMR (600 MHz, CDCl$_3$): δ = 3.73 (dd, *J* = 7.6, 16.8 Hz, 1H), 3.83 (dd, *J* = 7.2, 16.8 Hz, 1H), 5.08 (t, *J* = 7.2 Hz, 1H), 6.98-7.00 (m, 1H), 7.00-7.05 (m, 1H), 7.13-7.20 (m, 2H), 7.24-7.38 (m, 5H), 7.41-7.46 (m, 3H), 7.52-7.56 (m, 1H), 7.92-7.95 (m, 2H), 7.98 (brs, 1H).

^{13}C NMR (150 MHz, CDCl$_3$): δ = 38.2, 45.2, 111.1, 119.3, 119.4, 119.5, 121.4, 122.1, 126.3, 126.6, 127.8, 128.1, 128.4, 128.5, 132.9, 136.6, 137.1, 144.2, 198.6.

HPLC: Daicel Chiralpak AD-H, ^{n}hexane/ ^{i}PrOH = 7/3, flow rate = 1.0 ml/min.: t_S = 14.9 min (*S*), t_R = 16.8 min (*R*).

A mixture of Pd(OCOCF$_3$)$_2$ (6.6 mg, 0.02 mmol), **L1** (8.0 mg, 0.024 mmol) and SDS (11.5 mg, 0.04 mmol) were stirred in water for 1 h at room tepmarature. After addition of **41b** (29.3 mg, 0.2 mmol) and indole **40a** (67.6 mg, 0.24 mmol) successively, the reaction mixture was vigorously

stirred for 24 h at room temperature. The resulting mixture was quenched with saturated NaHCO$_3$ *aq.* and brine. The aqueous layer was extracted with dichloromethane (three times), and the combined organic layers were washed with brine, and dried over anhydrous Na$_2$SO$_4$. After filtration, the solvent was removed under reduced pressure. The residue was purified by preparative TLC (elution: chloroform/ethyl acetate = 200/1) to give the corresponding product **45ba** (52.7 mg, Quant.).

(*R*)-3-(1*H*-Indol-3-yl)-1-phenylbutan-1-one (**45ba**)
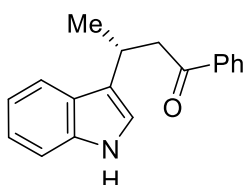
^{1}H NMR (600 MHz, CDCl$_3$): δ = 1.52 (d, *J* = 7.1 Hz, 3H), 3.31 (dd, *J* = 4.7, 18.0 Hz, 1H), 3.41 (dd, *J* = 8.0, 18.0 Hz, 1H), 3.74 (ddq, *J* = 4.7, 7.1, 8.0 Hz, 1H), 6.28 (m, 1H), 7.04 (ddd, *J* = 1.2, 7.2, 8.2 Hz, 1H), 7.11 (ddd, *J* = 1.4, 7.2, 8.0 Hz, 1H), 7.31 (dd, *J* = 0.8, 8.0 Hz, 1H), 7.44-7.48 (m, 2H), 7.52 (dd, *J* = 0.8, 7.0 Hz, 1H), 7.57 (dddd, *J* = 1.2, 1.4, 7.4, 7.4 Hz, 1H), 7.94-7.97 (m, 2H), 8.62 (brs, 1H).
^{13}C NMR (150 MHz, CDCl$_3$): δ = 19.9, 27.9, 47.0, 97.5, 110.6, 119.4, 119.8, 121.2, 128.0, 128.2, 128.6, 133.4, 135.7, 136.7, 144.2, 200.1.
HPLC: Daicel Chiralpak AD-H, ^{n}hexane/ ^{i}PrOH = 7/3, flow rate = 1.0 ml/min.: t_S = 23.3 min (*S*), t_R = 31.1 min (*R*).

[1] M. A. Ciufolini, N. E. Byrne, *J. Chem. Soc., Chem. Commun.* **1988**, 1230-1231.
[2] G. Dsimoni, G. Faita, S. Filippone, M. Mella, M. G. Zampori, M. Zema, *Tetrahedron* **2001**, *57*, 10203-10212.

Chapter 6 : Electrochemical Manipulation of Metal for Catalysis in Aqueous Environments

<Reagents>

Unless stated otherwise, commercially available reagents were used as received with the exception of the following substrates, which were prepared through reported methods. Analytical data for these compounds are in full agreement with reported data.

Typical Experimental Procedure for the preparation of LASC-SWNT catalysts:

SWNT 28 mg and LASC 0.14 mmol were combined together in 20 mL water and sonication (Hielscher, 400W maximum power, 24 kHz, in pulsed mode with 125 ms pulses) was conducted on the solution for 6 hr under 0 °C. Centrifugation was then performed for 1.5 h and the solution was carefully decanted from the pellet. The centrifugated LASC-SWNT mixture was directly used as the starting suspension before the catalyst preparations. To the resulting homogenized solution was added freshly-distilled aldoxime and α,β-unsaturated ketone.

(3*S*,4*S*,5*S*)-(3',5'-dihydroxyphenyl)(3,5-diphenylisoxazolidin-4-yl)methanone
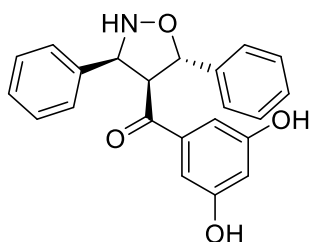
White Powder; mp 196-204 °C.

IR (neat): v = 1379, 1621, 1688, 2765, 3399 cm^{-1}.

^{1}H NMR (500 MHz); δ =3.71 (dd, J = 2.4, 8.7 Hz, 1H), 4.24 (d, J = 5.3 Hz, 1H), 5.32 (d, J = 8.5 Hz, 1H), 7.15 – 7.51 (m, 10H), 7.60 – 7.82 (m, 3H), 9.36 (brs, 2H).

^{13}C NMR (125 MHz); δ = 66.2, 69.4, 83.0, 116.8, 126.4, 126.8, 127.2, 127.5, 128.6, 130.1, 135.2, 138.7, 139.5, 147.2, 156.4, 201.9.

HPLC (Dialcel Chiralcel OD-H, ^{n}hexane/ ^{i}PrOH = 4/1, flow rate 1.0 mL/min); t_R = 34.7 min (*S*, minor), t_R = 39.0 min (*R*, major).

HRMS (ESI) calcd for C$_{22}$H$_{20}$NO$_4$ [M+H]$^+$: 362.1392, found: 362.1398.

((3*S*,4*S*,5*R*)-5-methyl-3-phenylisoxazolidin-4-yl)(phenyl)methanone
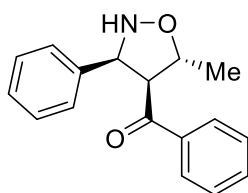
White crystal; mp 134 -137 °C.

IR (neat): v = 1412, 1607, 1674, 3457 cm^{-1}.

^{1}H NMR (500 MHz); δ = 1.60 (d, *J* = 6.6 Hz, 3H), 3.11 (dq, *J* = 1.5, 13.3 Hz, 1H), 4.01 (dd, *J* = 8.1, 10.5 Hz, 1H), 4.85 (dd, *J* = 2.3, 5.0 Hz, 1H), 7.25 – 7.64 (m, 6H), 7.93 (d, *J* = 10.2 Hz, 2H), 8.20 (d, *J* = 10.2 Hz, 2H).

^{13}C NMR (125 MHz); δ = 54.3, 63.7, 68.9, 81.2, 114.9, 126.1, 126.3, 127.2, 127.9, 128.6, 130.3, 131.1, 133.4, 138.5, 139.9, 161.2, 204.5.

HPLC (Dialcel Chiralcel OD-H, ^{n}hexane/ ^{i}PrOH = 9/1, flow rate 1.0 mL/min); t_R = 16.3 min (*S*, minor), t_R = 23.5 min (*R*, major).

HRMS (ESI) calcd for $C_{17}H_{18}NO_2$ [M+H]$^+$: 268.1338. found: 268.1341.

Acknowledgement

First and foremost I would like to express deepest sense of gratitude to my supervisor Prof. Shū Kobayashi, for his overflowing eagerness for being pathfinder, excellent guidance, caring, patience and providing me with an excellent atmosphere for research, who has always been a stimulus to me in inculcating the learning attitude towards cutting-edge research.

I have to express my appreciation to Prof. Eiichi Nakamura and Dr. Koji Harano (Department of Chemistry, School of Science, The University of Tokyo) for DLS and CV measurements, to Prof. Shigeo Maruyama and Dr. Shohei Chiashi (Department of Mechanical Engineering, Faculty of Engineering, The University of Tokyo) for Raman analysis and to Mr. Noriaki Kuramitsu for electron microscopic analysis.

No words of thanks can sum up the gratitude that I owe to many people; associate professor in our group Dr. Yasuhiro Yamashita has often bestowed upon edifying counsels and exhortation; assistant professor Dr. Masaharu Ueno has provided instruction in the rudiments to me with years of meritorious deed although I had had no pretensions to learning or ability; project assistant professor Dr. Hiroyuki Miyamura and Dr. Yoo Woo–Jin have updated me in my research task through animated discussions; previous project assistant professor Dr. Miyuki Yamaguchi (incumbent research assistant professor at School of Pharmaceutical Sciences, University of Shizuoka) has offered an immense contribution to my research as significant insight and moral support as well as technical help; GSC research associate professor Dr. Yuichiro Mori has also promoted me for academic excellence.

I should express my sense of indebtedness equally to all my colleagues who have continuously contributed to a number of significant achievements on research and sometimes provided me with encouragement for my academic pursuits. The following is a list of people whom I work with and I should appreciate: Prof. Thierry Ollevier (Université Laval), Prof. Chandan Mukherjee (Indian Institute of Technology Guwahati), Dr. Lei Zhu (Postdoctoral fellow at The University of Tokyo), Dr. Katsuaki Kawasumi (Postdoctoral fellow at Massachusetts Institute of Technology), Dr. Toshimitsu Endo (Ono Pharmaceutical Co., LTD.), Mr. Daisuke Yagyu (Showa Denko K. K.), Mr. Junpei Goto, Mr. Masaru Sakai (Yoshindo Inc.), Mr. Pengyu Xu (D1 student), Mr. Naohiro Murata (M2 student), Mr. Nobuhisa Masaki (M2 student), Mr. Isshiki Satoshi (M1 student), Mr. Yoshiaki Ohzeki (M1 student), Mr. Yuichiro Kawahara (B4 student), Mr. Masumi Miyo (B4 student) and visitors including Ms. Emilie Langlois (Escuela Superior de Cómputo). I'm deeply indebted to all people for their patience to my undependable and unenlightened guidance.

Words fail me in expressing my unquestionable gratitude to true companions of my life and cheek by jowl my bosom friends Koichiro Masuda and Tomohiro Yasukawa, who have followed the dictates of my heart and paid sincere and serious attention at my academic voyage to the top of their

bent. Their sublimity and endeavor were moonstruck during my research work, which have obliged me to burn the midnight oil.

I thank all those whose names may have escaped attention here but have in one way or the other contributed to my research.

Apart from that, I am head over heels indebted to Mr. Yoan Udagawa as one of those who have blazed the trail in 'science' in Japan.

Last but not the least, I sought inspiration and I owe a great deal to my mother and father who have unquestionably given their ears for the primrose path in my life. I would prefer to pay homage by dedicating my dissertation to my family including the deceased grandmother and grandfather under whose careful protection and tutelage I have been able to enjoy my life.

Taku Kitanosono
2014.11.30